TN
1
A5
Vol. 211
NIC

TRANSACTIONS

OF THE

AMERICAN INSTITUTE OF MINING, METALLURGICAL, AND PETROLEUM ENGINEERS

(INCORPORATED)

Volume 211

SOCIETY OF MINING ENGINEERS OF AIME

1958

Mining, Minerals Beneficiation, Coal,
Industrial Minerals, Geology,
Geophysics

THIS VOLUME IS MADE UP OF PAPERS AND DISCUSSIONS PRESENTED AT MEETINGS HELD AT NEW YORK, FEB. 20-23, 1956; NEW ORLEANS, FEB. 24-28, 1957; NEW YORK, FEB. 16-20, 1958; AND SPOKANE, APR. 17-19, 1958.

PUBLISHED BY THE INSTITUTE
AT THE OFFICE OF THE SECRETARY
29 WEST 39TH STREET
NEW YORK 18, N. Y.

COPYRIGHT, 1959, BY THE
AMERICAN INSTITUTE OF MINING, METALLURGICAL, AND PETROLEUM ENGINEERS
(INCORPORATED)
PRINTED IN THE UNITED STATES OF AMERICA

FOREWORD

This volume of the Transactions of the Society of Mining Engineers of the American Institute of Mining, Metallurgical and Petroleum Engineers is the tenth bound in this format from pages previously published in MINING ENGINEERING. It is the 211th volume of Transactions published by AIME for the mineral and petroleum engineering profession.

The present format was adopted ten years ago as a result of a twofold need. First, prompt publication of technically and scientifically valuable papers in our monthly magazine was needed to provide rapid circularization of information and ideas. Second, the bound Transactions were needed for library reference for both the proximate and distant futures. The format used serves both needs with maximum economy.

The contributions contained in this Volume 211 of the Transactions record sound development, notable achievement, and progressive thinking by the engineers in the mineral industries. This advancement in technology is, however, no more than a stepping stone toward meeting our growing mineral needs from an ever dwindling natural warehouse. Truly advanced and perhaps radical thinking is needed to develop totally new methods for finding mineral deposits, and mining, beneficiating, and reducing their crude materials to usable products. This thinking must be above and beyond our daily work of improving existing processes and products if our industry and our engineers are to do their parts in providing for future generations.

The authors, contributors to discussions, and the various committee members who made this volume possible have earned the thanks and appreciation of all the members of SME and AIME. The high standards represented by the contents of this volume should serve as a springboard and a stimulant for future contributions from the mineral engineers to their industries' growth.

Stanley D. Michaelson, *President*
Society of Mining Engineers of AIME

November 24, 1958

CONTENTS

MINING ENGINEERING was paged consecutively throughout 1958. Thus in this volume of the Mining Transactions there are 11 interruptions in the pagination. The missing pages appeared in MINING ENGINEERING. This volume consists of all the Mining Transactions for 1958.

Mining

Planning Deep Mining at Homestake. By A. H. SHOEMAKER 685
Precision Survey for Tunnel Control. By DOUGLAS D. DONALD 977
U. S. Government Support to Mineral Industries of Latin America. By SUMNER M. ANDERSON 1176
Lucky Friday Mine: History, Geology, and Development. By WILLIAM T. FOLWELL 1266

Minerals Beneficiation

Flotation of a Canadian Kyanite. By R. A. WYMAN 111
Rotobelt Filter, New Tool in Minerals Beneficiation. By C. F. CORNELL, R. C. EMMETT, and D. A. DAHLSTROM 253
Relation of Magnetic Susceptibility to Mineral Composition. By ERNEST M. SPOKES and DAVID R. MITCHELL 373
Discussion 489
Intergranular Comminution by Heating. By J. H. BROWN, A. M. GAUDIN, and C. M. LOEB, JR. 490
Fine Grinding at Supercritical Speeds. By R. T. HUKKI 581
Discussion 589, 892
Correction 892
Grinding Ball Size Selection. By F. C. BOND 592
Relative Effectiveness of Sodium Silicates of Different Silica-Soda Ratios as Gangue Depressants in Nonmetallic Flotation. By C. L. SOLLENBEGER and R. B. GREENWALT 691
Effect of Chemical Reagents on the Motion of Single Air Bubbles in Water. By D. W. FUERSTENAU and C. H. WAYMAN 694
Graphical Representation of Theoretical Soluble Losses by CCD. By R. J. WOODY 786
Distribution Curves for Sink-and-Float Separation of Iron Ores. By RUDOLPH G. WUERKER 788
Iron Oxide Slime Coatings in Flotation. By D. W. FUERSTENAU, A. M. GAUDIN, and H. L. MIAW 792
Scale-Up Relationships in Spodumene Flotation. By W. E. HORST 1182
Advances in Magnetic Separation of Ores. By L. A. ROE 1261
Magnetic Separation for Mesabi Magnetite Taconite. By J. E. FORCIEA, L. G. HENDRICKSON, and O. E. PALASVIRTA 1269

Coal

Convertol Process. By A. H. BRISSE and W. L. McMORRIS, JR. 258
COAL MINE BUMP SYMPOSIUM: Introduction 877
U. S. Bureau of Mines Investigations and Research on Bumps. By E. F. THOMAS 878
Ground Stress Investigations in Canadian Coal Mines. By A. BROWN 879
Control of Mountain Bumps in the Pocahontas No. 4 Seam. By W. G. TALMAN and J. L. SCHROEDER, JR. 892
Mountain Bumps at the Sunnyside Mines. By J. PEPERAKIS 982
Deep Coal Mining in Springhill No. 2 Mine. By W. F. CAMPBELL 986
Coal Mine Bumps Can Be Eliminated. By H. E. MAUCK 993
Causes and Control of Coal Mine Bumps. By C. T. HOLLAND 994

Industrial Minerals

Resources and Utilization of North Carolina Pyrophyllite. By JASPER L. STUCKEY 97
Instrumentation in Ideal's New Houston Cement Plant. By THOMAS B. DOUGLAS 266
Application of Electrostatics to Potash Beneficiation. By I. M. LEBARON and W. C. KNOPF 1081
Application of Electrostatics to Concentration of Coarse Pebble Phosphate. By E. NORTHCOTT and F. N. OBERG 1084
Application of Electrostatics to Feldspar Beneficiation. By E. NORTHCOTT and I. M. LEBARON 1087
The Geiger Counter as a Control Tool in Processing Potassium-Bearing Ores. By W. C. KNOPF and G. SAMSEL 1094

Geology

Porphyry Copper Deposit, Cuajone, Peru. By W. C. Lacy 104
Mineralized Cretaceous Horizons in Northeastern Mexico. By P. Sanchez-Mejorada 108
Geology of Toquepala, Peru. By Kenyon Richard and James H. Courtright 262
Discussion 699
Structural Control of Contact Metasomatic Deposits in the Peruvian Cordillera. By A. J. Terrones L. 365
Lineament Tectonics and Some Ore Districts of the Southwest. By Evans B. Mayo 1169

Geophysics

Case History of the Juniper Prospect. By S. H. Ward and R. A. Barker 100
Seismic-Refraction Method in Ground-Water Exploration. W. E. Bonini and E. A. Hickok 485
Significance of Geochemical Distribution Trends in Soil. By D. H. Yardley 781
Rubeanic Acid Field Test for Copper in Soils and Sediments. By H. V. Warren and R. E. Delavault 1186

Technical Notes

Cleaning Fine Coal with Newly Developed Jig. By E. H. Citron 489
Study of Thorium and Uranium Minerals by X-Ray Microscopy. By S. Yamaguchi 689
Improved Methods for Measuring Aeration in Flotation Cells. J. B. Gayle 796

Abstract

Interpretation of the Literature on the Mechanism of the Hall Process. By John J. Stokes, Jr. 496

Discussion of Papers Published Prior to 1958

Genesis of Titaniferous Magnetites and Associated Rocks of the Lake Sanford District, New York. By J. L. Gillson 379
Petrologic Methods for Application to Solid Fuels of the Future. By James M. Schopf 591
Mineralizing Solutions That Carry and Deposit Iron and Sulfur. By B. S. Butler 595
Filtration and Control of Moisture Content on Taconite Concentrates. By A. F. Henderson, C. F. Cornell, A. F. Dunyon, and D. A. Dahlstrom 596

Extractive Metallurgy

As many members of the Society of Mining Engineers are interested in the papers of the Extractive Metallurgy Division of The Metallurgical Society of AIME, the titles of the papers published for the Division in 1958 are listed below. These papers, and discussion, appear in *AIME Transactions* (1958) **212**, The Metallurgical Society.

Effect of Roasting on Recovery of Uranium and Vanadium from Carnotite Ores by Carbonate Leaching. By J. Halpern, F. A. Forward, and A. H. Ross 65
Interpretation of the Literature on The Mechanism of the Hall Process. By J. J. Stokes, Jr. 75
Sinter Roasting of Lead-Rich Galena Concentrates at the Electrothermic Lead Plant of the Ronnskar Works, Sweden. By S. J. Wallden, N. B. Lindvall, and K. G. Gorling 146
The Reduction of Cupric Salts in Aqueous Perchlorate and Sulfate Solutions by Molecular Hydrogen. By E. R. MacGregor and J. Halpern 244
A Kinetic Study of the Dissolution of UO_2 in Carbonate Solution. By R. L. Pearson and M. E. Wadsworth 294
A Kinetic Study of the Oxidation of Pyrite in Aqueous Suspension. By D. R. McKay and J. Halpern 301
The Electrolytic Preparation of Molybdenum from Fused Salts. V. Electrorefining Studies in the Presence of Tin, Iron, Copper, Silicon, and Nickel. By D. E. Couch and S. Senderoff 320
The Rate of Infiltration of Metals. By K. A. Semlak and F. N. Rhines 325
Density of Molten Cu-Fe Sulfide Mattes. By M. Bourgon, G. Derge, and G. M. Pound 338
The Dissolution of Sulfide Ores in Acid Chlorine Solutions: A Study of the More Common Sulfide Minerals. By K. J. Jackson and J. D. H. Strickland 373
The Effect of Additions on the Exchange of Chlorine between Calcium Chloride and Metal Oxides. By N. F. Neumann and A. W. Schlechten 445
The Improved Wheaton-Najarian Vacuum Condenser. By H. K. Najarian 493
The Determination of Hydrogen in Titanium and Its Alloys—A Critical Review. By T. D. McKinley 563
A Kinetic Study of the Dissolution of UO_2 in Sulfuric Acid. By T. L. MacKay and M. E. Wadsworth 597
Data on Copper Converter Practice in Various Countries. By F. E. Lathe and L. Hodnett 603

Gerhardt mine, Carolina Pyrophyllite Co., Staley, N. C.

Resources and Utilization of North Carolina Pyrophyllite

by Jasper L. Stuckey

PYROPHYLLITE, first identified as soapstone,[1] later as agalmatolite,[2] and finally as pyrophyllite,[3] has been known to occur in North Carolina for more than 130 years and has been produced intermittently in commercial amounts for the past 100 years. Pyrophyllite mining, however, has become a major industry in North Carolina only during the past 25 years. North Carolina and California are the chief producing states. Current annual production averages 125,000 tons, of which slightly more than 90 pct comes from North Carolina.

Distribution and Geologic Setting: All known pyrophyllite deposits in North Carolina are associated with rocks of the Carolina Slate Belt,[4] which is composed of a vast series of metamorphosed volcanic and sedimentary materials, occurring as two zones extending in a northeast-southwest direction across the state. The larger of these zones, lying in the central Piedmont region, varies from 8 to 50 miles wide. The smaller zone lies along the eastern edge of the Piedmont region and is partly covered by coastal plain sediments.

The rocks in both zones consist of a great volcanic-sedimentary series, composed of air-laid and water-laid tuffs and breccias, lava flows, and slates. On the basis of composition, they may be classed into three groups: 1) tuffs, breccias, and lava flows of acid or rhyolitic composition; 2) tuffs, breccias, and lava flows of a basic or andesitic composition; and 3) water-laid slates composed of fine grained materials derived chiefly from the acid tuffs and breccias and

J. L. STUCKEY, Member AIME, is State Geologist of North Carolina, Raleigh, N. C.

TP 4652H. Manuscript, Feb. 14, 1956. New York Meeting, February 1956.

containing varying amounts of land waste. In the order of abundance, tuffs and breccias are most important, followed by slates and flows.

Of some 15 known occurrences of pyrophyllite in North Carolina, six have been developed enough to indicate important reserves of mineable pyrophyllite. These major deposits occur near Robbins and Glendon, Moore County; near Stanley, Randolph County; near Snow Camp, Alamance County; near Hillsboro, Orange County; and near Oxford, Granville County. All these deposits, with two exceptions, occur along prominent hills or ridges. The Glendon deposit occurs in gently undulating topography, while that near Robbins occurs in a relatively flat area covered largely by a thin veneer of coastal plain sand. All the known deposits appear to occur in acid tuffs and breccias, as none have been found in the slates or basic rock types.

Structure of Deposits: A prominent feature of most pyrophyllite bodies is an irregular, oval, or lenslike form. This structure is observed along the strike and also vertically to the depth reached in mining. In nearly every deposit that has been developed enough to show the true structure, bodies and lenses of pyrophyllite are found along with lenses of tuffaceous rocks that exhibit various stages of alteration. Most pyrophyllite deposits occur as narrow bands or zones aligned with the cleavage strikes and dip of the country rock. The strike of the cleavage in both the country rock and the pyrophyllite bodies is northeast-southwest, while the dip is steeply to the northwest.

In most cases the larger mineralized zones consist of a very siliceous footwall, a well developed mineralized zone, and a highly siliceous and sericitic hanging wall.[5] Where these conditions exist, contacts between the mineralized zone and the footwall and the hanging wall are gradational. Contacts between the footwall and country rock and the hanging wall and country rocks are also gradational. When the footwall and hanging wall are absent, as they frequently are, contacts between mineralized zone and country rock are gradational.

Mineralogy: The mineralogy of the major deposits is relatively simple. Pyrophyllite, the most abundant mineral, occurs as foliated masses, massive granular bodies, and radial fibrous aggregates. The pyrophyllite in the deposits near Glendon and Robbins, Moore County, consists almost entirely of the foliated variety. That in the other major deposits consists largely of massive granular and radial fibrous forms, with occasional small amounts of the foliated variety. Quartz is abundant throughout the deposits except in the very purest pyrophyllite, occurring as large masses of a cherty or milky appearance, as stringers and veins of almost clear material, and as nodules and fine-grained particles. Sericite is often concentrated as bands or zones along the hanging wall of the pyrophyllite bodies and to a lesser extent along the footwall.[5] It is also present as finely divided scales and flakes and as zones through good pyrophyllite. One or more of the minerals diaspore, topaz, andalusite, and kyanite are present in all the deposits except those in Moore County. Andalusite is abundant in the Hillsboro deposit. In the deposit near Oxford there is considerable topaz, some blocks 1 to 2 ft long, as well as amounts of andalusite and kyanite. Chloritoid varies in amount from minor to abundant, while chlorite, pyrite, hematite, and magnetite are common but minor accessories.

Origin of Pyrophyllite: All available field and laboratory evidence suggests that the pyrophyllite bodies were formed through metasomatic replacements[1] of acid tuffs and breccias. Mineralization, however, was not a simple process and probably was accomplished in stages. Following metamorphism, there was considerable silicification along the zones where the pyrophyllite bodies were later developed. Following silicification, pyrite and chloritoid were formed, varying in amounts from minor to abundant. Pyrophyllite was next formed by replacement of the previously silicified tuffs and breccias. Sericite developed along with the pyrophyllite or immediately following. The position of the minerals diaspore, topaz, andalusite, and kyanite in the sequence is not clear, but they appear to have been formed early in the process, as they have been replaced[5] partially by pyrophyllite and sericite. The fact that the mineralizing solutions were of magmatic origin is indicated by small granitic masses that intruded the volcanic rocks, occurring as masses along the western edge of the Carolina Slate Belt.

Reserves: Sufficient evidence is not available to determine accurately the reserves of pyrophyllite in North Carolina, but there is enough information to establish fairly dependable indicated reserves. The writer stated in 1928:[4]

> Taking into consideration the mineralogy and origin of the deposits, the source of the solutions, and the relation in the distribution of the gold and pyrophyllite deposits, it seems reasonable to expect pyrophyllite in commercial amounts to a minimum depth of 500 feet. This statement does not mean that every pyrophyllite prospect can be developed into a mine at that depth. It does mean, however, that all indications point to a depth of that magnitude for the larger bodies which really show promise at the surface.

The results obtained in exploring for pyrophyllite over the intervening years have borne out this statement. Some small prospects have been explored that did not prove continuous in depth, but drillholes more than 500 ft deep have failed to reach the bottom of the major deposits drilled to that depth.

The pyrophyllite deposit occurred as irregular lenses 100 to 500 ft wide and 500 to 2000 ft long or more. The bodies of workable pyrophyllite occur near the center of the deposits and vary in width from 25 to 200 ft. Pyrophyllite has a specific gravity of 2.8 to 2.9 and weighs 175 lb per cu ft. Each 100 ft of length and depth of a pyrophyllite body 100 ft wide should yield 50,000 tons, allowing for a 60 pct recovery. Using these figures and assuming recovery to a depth of 400 to 500 ft, a reserve of some 12 to 14 million tons of pyrophyllite is indicated in North Carolina. It should be pointed out, however, that all these reserves are controlled by four companies operating in the state, and no known deposits are available for new producers.

Mining Methods: Pyrophyllite mining on a commercial basis was started in North Carolina about 1855[2] and has continued intermittently since that time. At first, prospecting and mining were carried out by pits, shallow shafts, drifts, and open cuts. As demands for larger quantities have increased and off-color material has become salable, open cuts —made possible by information from diamond drilling and by modern earth-moving machinery— have furnished most of the production. The largest pyrophyllite mine in North Carolina, the only modern

underground mine, is operated by Standard Mineral Co., at Robbins in Moore County, by a 500-ft shaft, drifts, and stopes.

Processing: Processing of pyrophyllite has changed slowly through the years as demands and uses for the mineral have increased and changed. Prior to about 1855 it was used only locally—for stove linings, fireplaces, chimneys, mantles, and gravestones —and was cut and shaped to fit the particular need. Production of pyrophyllite crayons was started about 1880, continuing until 1922. Ground pyrophyllite was first produced in North Carolina about 1855.[2] From 1855 to 1913 grinding was carried out first at Hancock's Mills and later at Glenn's Mills, both located on Deep River near the present village of Glendon, Moore County. The grinding stock was carefully selected, air dried, and crushed. It was then crushed by hand, ground with millstones, and passed through bolting cloth.

In 1902 the first plant contructed exclusively for grinding pyrophyllite was built near the deposit. This was followed in 1904 by a second plant on another deposit about a mile away. Both plants were alike in that the grinding stock was air dried and crushed. In one plant the crushed material was passed through a hammer mill, ground with millstones, fed into a ball mill, ground 8 hr, and screened. In the other mill the crushed material was ground with millstones, the fines removed by air, and the coarse material fed into a ball mill, ground, and screened. Both plants were abandoned by the end of 1921.

Before 1918 all the known pyrophyllite deposits of any importance in North Carolina were located along the north side of Deep River, in the general vicinity of Glendon, Moore County. In that year, what later proved to be the largest known deposit in the state was discovered about two miles southwest of Robbins, Moore County, when wagon wheels brought up a fine white material that proved to be pyrophyllite. The first modern grinding plant was built on this property about 1921. The process first used consisted of crushing, grinding in a hammer mill, and screening. The hammer mill did not prove satisfactory for fine grinding, and after some modifications the process was discarded. A new process was installed, consisting of crushing, grinding in a roller mill, and screening. As the ceramic market for pyrophyllite has become important, conical pebble mills for fine grinding have been installed in this plant and the other plants in the state.

At present three companies—Standard Mineral Co. at Robbins, Carolina Pyrophyllite Co. at Staley, and Glendon Pyrophyllite Co. at Glendon—are mining and processing pyrophyllite for market. A fourth company, North State Pyrophyllite Co. at Greensboro, is mining pyrophyllite and producing a variety of pyrophyllite refractories but is not selling pyrophyllite as such. None of these companies is carrying out beneficiation or true mineral dressing on crude pyrophyllite. By selective mining, blending, grinding, and screening, a wide variety of grades, standardized both as to grain size and chemical composition, is being produced for fillers and specialty products and for use in ceramic bodies and refractories.

In the processes used to date only pyrophyllite pure enough to make a salable finished product has been used. As a result much good material containing 60 to 75 pct pyrophyllite has been discarded. During recent years, as demands have increased, improved methods of grinding and screening have reclaimed much material formerly discarded. In view of the somewhat limited reserves and increasing demands, too much good material is being left in the ground or thrown on the dumps. The tonnage estimates made are based on the assumption that all material containing 40 to 50 pct pyrophyllite and not too much off-color will be used. During the past two or three years considerable research has been in progress on removal of iron, free silica, and other impurities. The North Carolina State College Minerals Research Laboratory, Asheville, has aided in this program, and a great deal of information not yet in use is being accumulated. On the basis of information now compiled and still being obtained, all indications point to new and improved pyrophyllite milling operations in North Carolina in the near future. Details of the proposed new processes are not yet obtainable, but a large tonnage of pyrophyllite, higher in quality and slightly higher in price than that now being produced, should be made available to industry as demands increase.

Uses of Pyrophyllite: Prior to about 1855 pyrophyllite was used locally for tombstones, and such stones—still well preserved—may be seen in two or more cemeteries near Glendon. Emmons[2] in 1856 described it as an excellent substitute for soapstone in stove linings, fireplaces, chimneys, and mantles. He stated that it was not suitable for paint, as it became translucent when mixed with oil, but described it as a filler that helped retain the perfume in soap and added that large quantities were ground for the New York market in 1855. He described it as suitable for antifriction powder and for use as a cosmetic and quoted Jackson to the effect that it would make a very refractory material for stoneware and crucibles.

At present pyrophyllite is used chiefly for manufacture of insecticides, rubber, ceramics, refractories, plastics, paint, and roofing paper. It has a number of minor uses for products including cosmetics, wallboard, cordage, textiles, bleaching powder, and soap. The best production figures available indicate that about one half the current annual production goes into insecticides and rubber, one third into ceramics and refractories, and the remainder into plastics, paint, roofing, and minor uses.

Uniformity of grain size and mineral content is becoming important for all uses. For ceramics, whiteware, and wall tile, where the size of the finished product must be controlled accurately, pyrophyllite is one of the best materials available, provided it is perfectly uniform in grain size and composition. For use in special refractories, such as car tops for tunnel kilns, monolithic furnace lining, and furnace lining requiring rapid temperature changes, pyrophyllite makes an excellent body that is shock-resistant.

References

[1] D. Olmsted: *Report on the Geology of North Carolina*, Part I, p 23, 1824.

[2] E. Emmons: *Geological Report of the Midland Counties of North Carolina*, pp. 52-54, 217-218. Raleigh, 1856.

[3] G. J. Brush: *American Journal of Science*, 1862, no. 34, p. 219.

[4] J. L. Stuckey: The Pyrophyllite Deposits of North Carolina. North Carolina Department of Conservation and Development *Bull. 37*, 1928.

[5] S. D. Broadhurst and R. J. Councill: High Alumina Minerals in the Volcanic-Slate Series, North Carolina. North Carolina Department of Conservation and Development *Inf. Circ. 10*, 1953.

[6] B. C. Burgess: Pyrophyllite: *Industrial Minerals*, Chap. 37, AIME, New York, 1949.

[7] A. F. Greaves-Walker and J. J. Amero: The Development of an Unfired Pyrophyllite Refractory. *North Carolina State College Record*, June 1944, p. 40.

Discussion of this paper sent (2 copies) to AIME before Feb. 28, 1958, will be published in MINING ENGINEERING.

Case History of the Juniper Prospect

by S. H. Ward and R. A. Barker

THE Juniper Prospect is in Carleton County, N. B., at approximately 46° 31′ north latitude, 67° 20′ west longitude.

During the summer of 1955 an area in west-central New Brunswick was selected for aerial electromagnetic prospecting with American Metal Co.'s helicopter-mounted equipment. Generalized, small-scale government geologic maps had suggested that this area was located along the western border of the northeast-trending granitic backbone of northwestern New Brunswick and might be underlain by the Ordovician-Silurian sediments and volcanics that are the host rocks for the recently discovered sulfide deposits of the Bathurst-Newcastle district.

S. H. WARD, Member AIME, is Geophysicist with Nucom Ltd., Toronto, Canada. R. A. BARKER is an Exploration Geologist with the American Metal Co. Ltd., Toronto.

TP 4685L. Manuscript, March 4, 1957. New Orleans Meeting, February 1957.

The helicopter electromagnetic equipment located an anomalous conductive area, coincident with a small aeromagnetic closure, about five miles west of the town of Juniper.

Subsequently 30 mining claims (total area about 6600 x 8000 ft) were staked and company personnel conducted geological, geophysical, and geochemical investigations on the property. The claims and immediately contiguous areas were mapped geologically, and an area of about 2000 x 4000 ft was soil-sampled and also surveyed by ground electromagnetic and gravity methods. Finally six diamond drillholes, totaling 3500 ft in length, were drilled to test the anomalous conditions discovered by the several exploration techniques used.

The discovery of base metal sulfides during drilling was a technical success for the exploration methods, but the quantity of sulfides was too small to be profitably exploited.

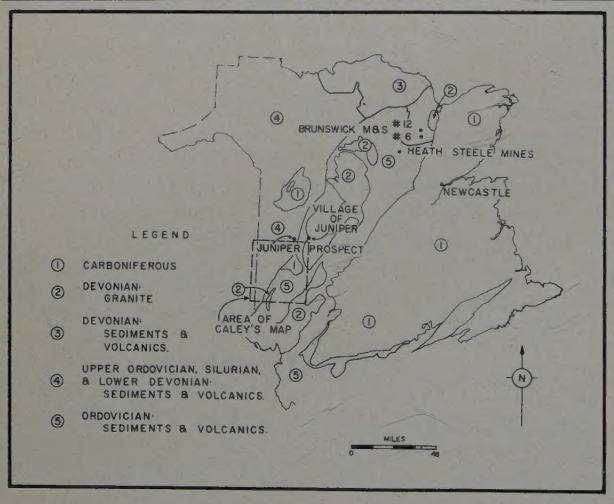

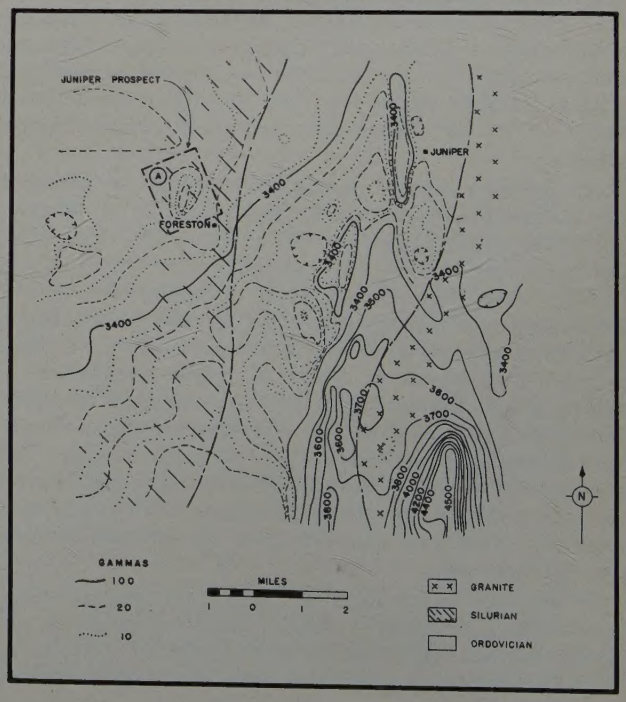

Fig. 1 (above)—Generalized geologic map of New Brunswick (after G. S. C.). Fig. 2 (right)—Map showing aeromagnetic contours with superimposed generalized geology of area near Juniper Prospect (after G. S. C.).

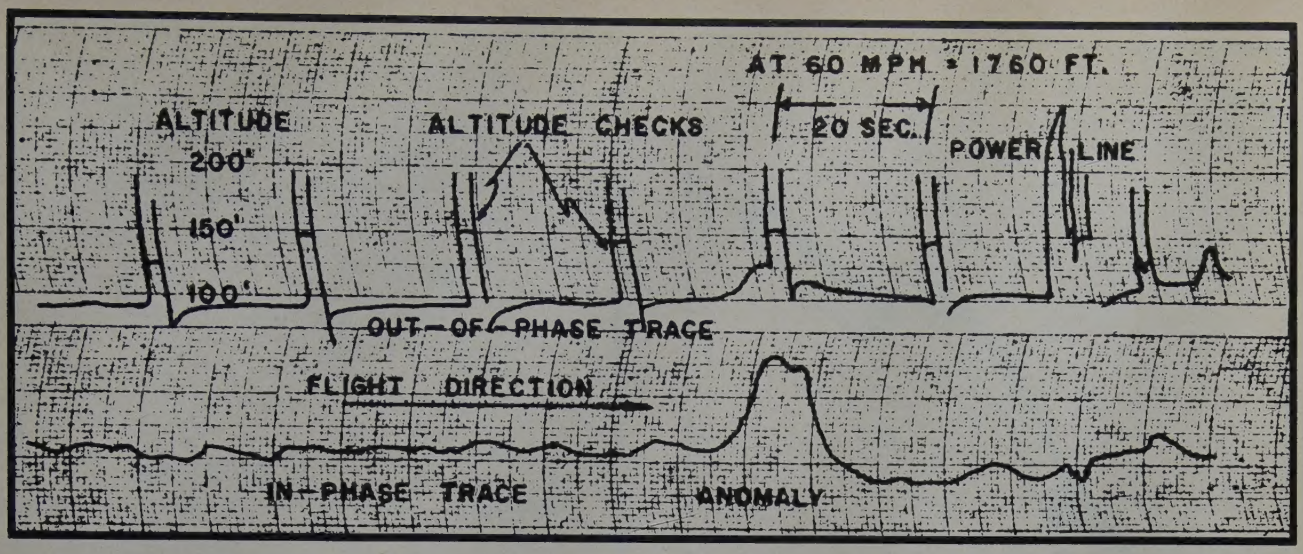

Fig. 4—Typical helicopter EM trace.

Geology: No published geologic maps of the Juniper area are available, with the exception of the Geologic Map of the Maritime Provinces (see Fig. 1) on a scale of 1 in. to 12 miles. The area immediately to the southwest has been mapped by Caley on a scale of 1 in. to 2 miles.[2] Projection of Caley's units some three or four miles northeastward suggests that the Juniper property is underlain by Silurian slates in contact with Pre-Silurian quartzites and slates to the east. The western border of the main granitic core of New Brunswick lies about five miles to the east of the Juniper Prospect.

Claim lines, streams, roads, and grid picket lines were traversed during geologic mapping, see Fig. 3. Relief on the property is not more than 50 ft and swampy areas are numerous and extensive.

Outcrops are confined to the stream that traverses the northeast corner of the property and to the road that parallels the southern boundary. Almost no outcrop was found in the central grid area, but float was considered to be representative of bedrock. Both float and outcrop indicate that the whole property is underlain by a monotonous sequence of slates and argillites varying slightly in sand content but essentially of similar composition. No structures other than bedding and cleavage or jointing were observed, although it is possible that strata may be repeated in the area by steep isoclinal folding. Strikes vary slightly about a north-east direction and both bedding and cleavage dip steeply to the east. No evidence of faulting was observed. Sulfide minerals were not seen either in float or outcrop.

Geochemistry: Approximately 1000 soil samples were collected in a grid pattern over an area 4000 x 4600 ft. Samples were taken by soil auger at a depth of about 2 ft and were spaced at 100-ft intervals along lines 200 ft apart. Samples were unobtainable at a number of places because of swamps.

All samples were analyzed for copper and zinc, using the well known dithizone colorometric method after digestion with hot nitric acid. Several scattered above-normal zinc values were recorded, but no larger anomalous areas were outlined.The geochemical results were, therefore, interpreted as being essentially uninteresting.

Helicopter and Ground Electromagnetic Data: The reconnaissance helicopter electromagnetic (HEM) survey, on flight lines spaced ¼ mile apart, located a response on one line passing directly over the aeromagnetic anomaly marked *A* in Fig. 2. Subsequently, several other flights were made at close intervals and the peaks of the HEM anomalies so registered are shown in Fig. 3. The correlation between the HEM and aeromagnetic data appears to be fairly good. A typical HEM trace over this conductor is shown in Fig. 4.

Following detailed geologic examination of the area of the combined HEM and aeromagnetic

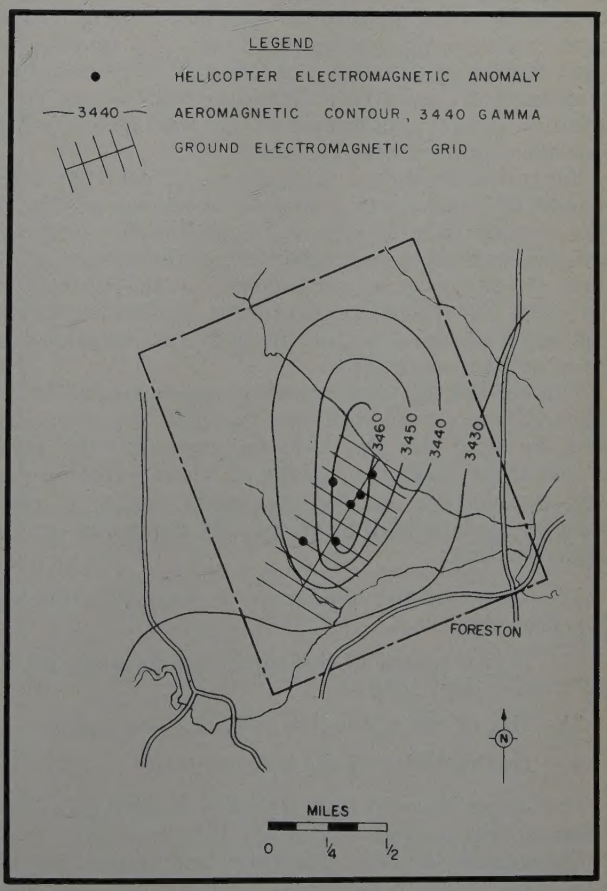

Fig. 3—Map showing aeromagnetic and helicopter EM anomalies at Juniper Prospect.

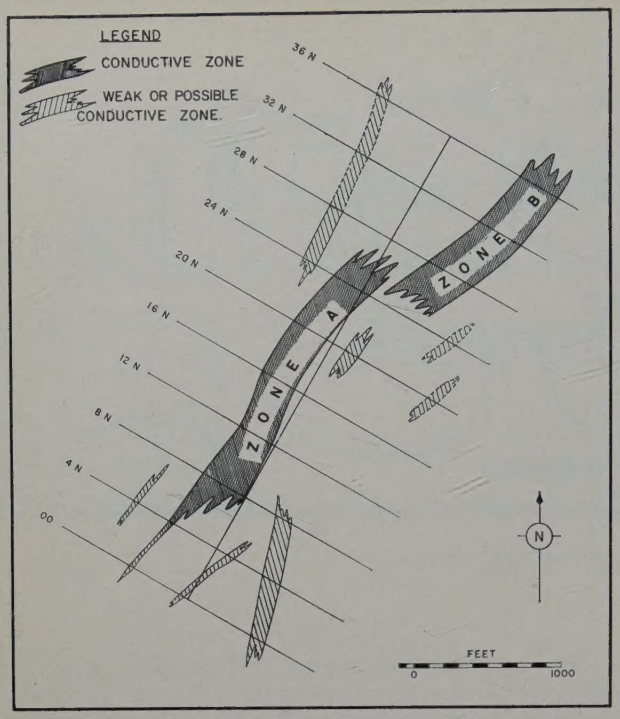

Fig. 5—Map showing conductive zones outlined by ground EM survey.

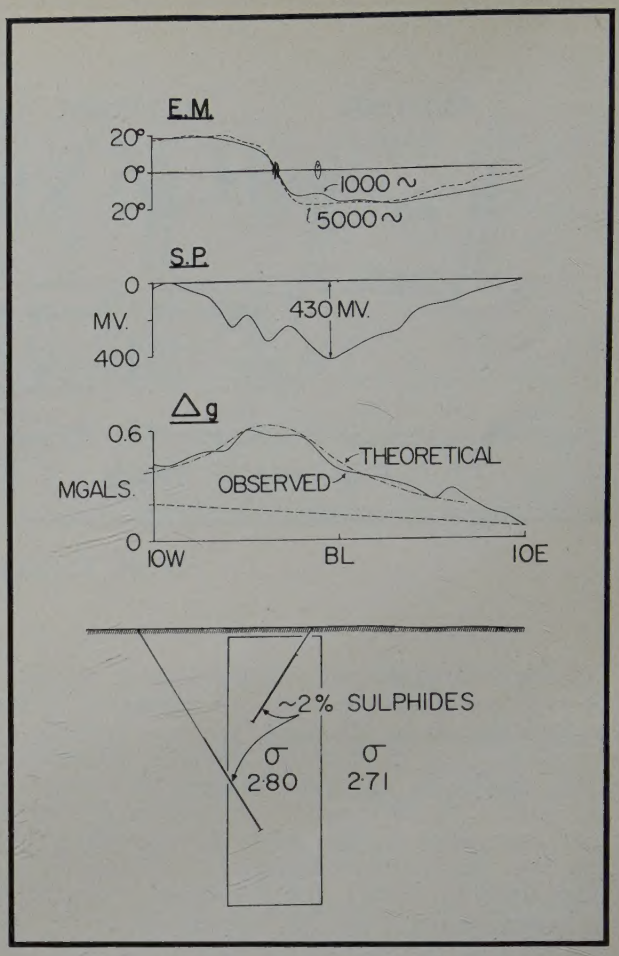

Fig. 6—Section (facing north) showing EM, SP, and gravity profiles on line 16N.

anomalies, a ground electromagnetic (EM) survey was carried out using the McPhar dual-frequency vertical coil technique. Fig. 5 indicates the conductive zones delineated by this method. One broad prominent zone parallels the geologic strike throughout the grid area and several weaker zones or possible zones exist to the east and west of it. The broad zone would appear to be offset by faulting or tight folding in the region of line 25N. This might be accounted for by a fault, striking N45°W and paralleling topographic linears in the area, but no other evidence supports this structure.

For purposes of discussion the broad zone has been subdivided into parts *A* and *B*, as shown in Fig. 5. The conductivity of zone *A* is good at the northern extreme and decreases to fair in the southern portion. Zone *B* exhibits good conductivity in the vicinity of line 24N, but this decreases to fair northward. Other conductors located within the grid area appeared to be of minor importance.

Typical EM *dip angle* profiles are shown in Fig. 6. The dashed curve indicates the 5000-cps response and the solid line the 1000-cps response; the ratio of the areas under the curves provides a measure of the conductivity of the causative body. In this instance, interpretation of the EM dip angle profile indicates that:

1) Depth of the conductor is shallow, probably less than 50 ft.

2) Depth extent of the conductor is large, probably more than 1000 ft.

3) Dip of the conductor is steeply eastward.

4) Conductivity of the body is good.

Past experience in New Brunswick with this electromagnetic survey technique indicates that most carbonaceous and/or graphitic sediments are of moderate to poor electrical conductivity, whereas most massive sulfide bodies, especially those containing pyrrhotite, are of good to excellent electrical conductivity. Exceptions to this rule have been noted, mostly where intense shearing of graphitic sediments produces good to excellent conductors. While massive sulfide bodies show good to excellent electrical conductivity, disseminated bodies range from very poor to excellent conductors depending upon the amount, type, and distribution of mineralization.

Thus the EM survey, by conductivity analysis alone, places this conductor in an interesting category. This information, together with the knowledge (derived from the aeromagnetic data) that the conductor is directly or indirectly associated with magnetic minerals, leads to the conclusion that pyrrhotite is the most logical common cause. The combined magnetic and electromagnetic anomalies might be explained, of course, by graphitic sediments interbanded with magnetic iron formation, but the limited areal extent of the aeromagnetic anomaly is against this.

Since there was no outcrop in the immediate area of the grid and no mineralized float was seen during geologic reconnaissance, completion of a gravity survey before drilling appeared to be the next logical step. The gravity survey would be expected to determine whether or not a significant amount of excess mass was directly associated with the EM conductors. A large, sharp gravity anomaly directly over the EM conductors might be interpreted as a representation of a substantial tonnage of massive sulfides.

In the course of the geophysical investigations, a self-potential profile was obtained along line

16N. For comparison, this profile is shown in Fig. 6, along with the EM and gravity profiles.

Gravity Survey Data: When a gravity survey was applied to this property, the basic assumption was made that the excess mass sought came to within about 50 ft of surface and dipped steeply. A sharp gravity feature would be expected, therefore, from any substantial tonnage of near-surface excess mass, and the gravity survey could be limited initially to a small area. Consequently the area covered was only 2000 x 2400 ft. The observed gravity contours over this area are shown in Fig. 7. A density of 2.65 gms/cc was assumed in applying the Bouguer correction. No correction was necessary for terrain.

From Fig. 7 it may be seen that the observed gravity contours create a domed surface of maximum relief 0.60 mgals over the area surveyed. The peak of this broad anomaly falls along zone *A*. Most of the anomaly may be attributed to a deep-seated source or, alternatively, to a diffuse and shallow one. It does not appear to reflect the large near-surface excess mass that was sought.

The gravity data might be explained by a deep-seated large massive sulfide body, but stringers would have to extend from such a body to surface to account for the conductors located by the EM survey. Alternatively, a small disseminated sulfide body might exist near surface.

To emphasize the near-surface effects and provide targets for drilling based on the latter alternative, a second-order surface was removed from the observed contours of Fig. 7 (least square fitting of second-order surface). The residual contours of Fig. 8 result. A small anomaly of about 0.15 mgals centered about 2+00W line 16N is the most striking feature remaining. This anomaly coincides, at least in part, with conductive zone *A*.

Although the gravity survey data tended to downgrade this prospect as an economic possibility, some drilling appeared to be warranted. Drilling was recommended to test the shallow ore possibilities and to provide a brief test of the deep ore possibilities.

Drilling Results: Of the six holes diamond drilled in the grid area, five were 300 to 600 ft long and one was 1300 ft long.

Diamond drilling confirmed the interpretation of the general geology of the prospect gained from surface mapping. All the core is composed of argillaceous sediments, varying in color from predominant gray, through green and black, to red and reddish brown. Minor variations in composition are shown by more sandy and quartzose layers. Although the black slates are doubtless carbonaceous, none are highly graphitic and therefore not conductive as proven by tests with an ohmmeter. Metamorphic grade is very low; chlorite is present but no biotite was observed in the hand specimen.

Many quartz and quartz-carbonate veinlets (averaging ⅛ to ¼ in. wide) form stockworks throughout much of the core. In a number of places there is a slight bleaching adjacent to these veinlets.

Highly contorted bedding (?) surfaces and the presence of sedimentary fragments in a similar matrix are possible evidence of primary slumping and pre-lithification deformation.

All cores contained minor disseminated pyrite and marcasite (?) especially in the darker sediments, as well as pyrite, pyrrhotite, and some chalcopyrite, sphalerite, galena, and arsenopyrite in very small ramifying veinlets, which form stockworks similar

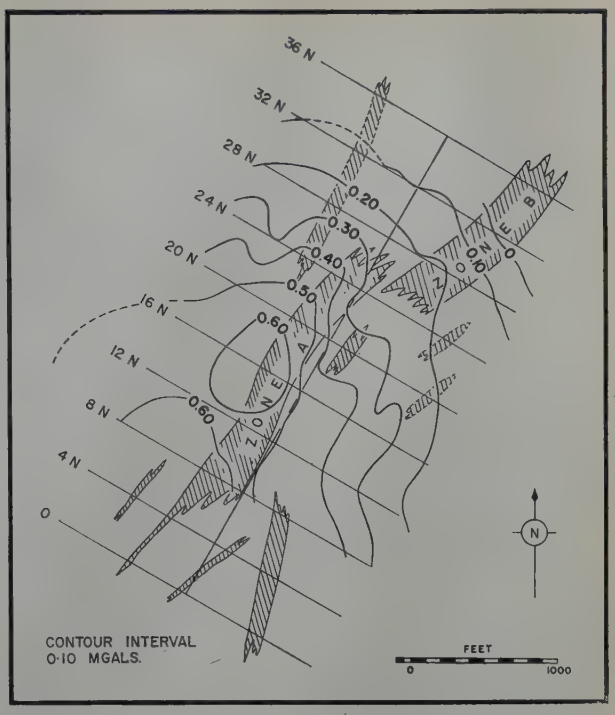

Fig. 7—Map showing observed gravity contours in relation to conductive zones.

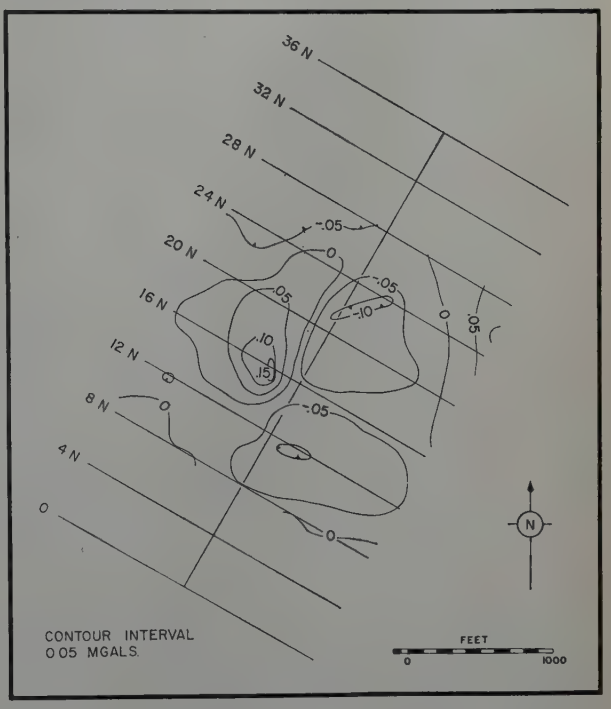

Fig. 8—Map showing second-order residual gravity contours.

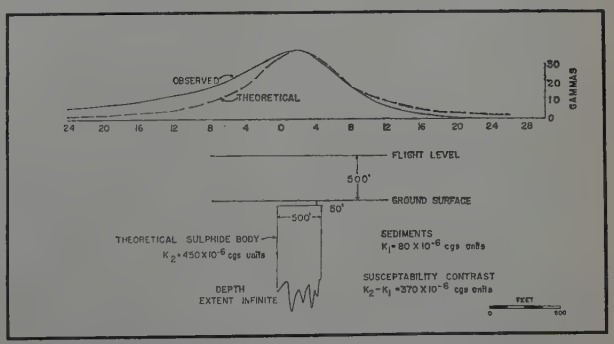

Fig. 9—Section (facing north) showing comparison of theoretical and observed aeromagnetic anomalies.

to the quartz-carbonate stockworks and in some places coinciding with them. The sulfide veinlets range from about 1/16 in. to 1 in. wide and average about ⅛ in. wide. They appear to have been emplaced along fracture or joint planes. The stockworks are confined to zones intersected in the holes, but these zones do not have noticeable stratigraphic or structural boundaries.

The quantities of base metals contained in these veinlets are insignificant from an economic viewpoint, but they appear to be an adequate explanation of all the geophysical data. The minor pyrrhotite, because it is of excellent conductivity and occurs in a stockwork, readily explains the EM data. There seems to be enough pyrrhotite mineralization to cause the small aeromagnetic anomaly and enough total sulfides to cause the gravity anomaly. Measurements on many samples of diamond drill core showed that any anomalous density or magnetic susceptibility could be directly attributed to pyrrhotite. The unmineralized argillite was found to be amazingly uniform, having a density of 2.71±.04 gms/cc and a magnetic susceptibility of 80×10^{-6} cgs units (based on measurements on 91 samples). The argillite mineralized with pyrrhotite showed densities up to 3.28 gms/cc and susceptibilities up to 6700×10^{-6} cgs units.

As a final check on the adequacy of the drillhole data as an explanation of the geophysical data, the gravity and magnetic anomalies due to masses of dimensions and characteristics shown in Figs. 6 and 9 have been computed. The comparisons of theoretical and observed anomalies suggest that the assumptions for the theoretical models are in reasonable agreement with the results obtained by drilling.

A density contrast of 0.09 gms/cc is required for the body used to compute the theoretical gravity profile. Four percent sulfide (density 5.0 gms/cc) in argillite of density 2.71 gms/cc would provide this density contract. A susceptibility contrast of 370×10^{-6} cgs units is required for the body used to compute the theoretical aeromagnetic profile. This could arise from approximately 2 pct pyrrhotite in argillite of susceptibility 80×10^{-6} cgs units, assuming a susceptibility for massive pyrrhotite of $18{,}000 \times 10^{-6}$ cgs units. The above percentages of sulfide mineral content are in good agreement with a visually estimated 2 to 4 pct total sulfides in drill core.

Conclusion

Prior to drilling, the summation of all geological and geophysical data indicated that the possibilities for commercial mineralization on this property were meager. However, a limited drilling program appeared to be warranted and was carried out. Drilling results corroborated the geological and geophysical interpretations. Consequently it is believed: 1) that enough drilling has been carried out and 2) that a commercially exploitable ore deposit is not likely to exist on the property.

Acknowledgments

The authors wish to thank the management of American Metal Co. Ltd. for permission to publish this article. Constructive criticism and encouragement from various members of the exploration division of the mining and exploration department is gratefully acknowledged.

References

[1] After Map 910A, Geological Survey of Canada, 1949.
[2] Map 380A, Geological Survey of Canada, 1935.

Discussion of this paper sent (2 copies) to AIME before Feb. 28, 1958, will be published in MINING ENGINEERING.

Porphyry Copper Deposit Cuajone, Peru

by W. C. Lacy

THE Cuajone porphyry copper deposit is the northernmost of a group of three deposits in southern Peru controlled by the Southern Peru Copper Corp.—Toquepala, Quelleveco, and Cuajone—all within a 20-mile belt.

Although small pockets of high-grade copper oxide ores were worked in the Cuajone area in the 19th century, it was not until 1939 that its potentialities as a disseminated deposit were recognized by O. C. Schmedeman. An exploratory drilling program was begun in December 1942 and continued until early 1945. The program was revived in November 1952 and completed early in 1954. Early exploration was by diamond drilling. Later exploration was predominantly churn drilling, with diamond drilling used only for wildcat holes.

Along this northwest-trending belt of deposits, which follows the western slopes of the Andean Range, quartz-monzonite has invaded earlier diorite intrusives and a series of warped and tilted Cretaceous(?) volcanic flows. Little faulting of consequence has been recognized within the mineralized areas. Sulfide minerals were introduced into all these diverse rocks, and mineralization was followed by erosion, oxidation, and enrichment. In Late Tertiary and/or Quaternary time the entire

W. C. LACY, Member AIME, formerly Chief Geologist, Cerro de Pasco Corp., is now Professor of Geology, University of Arizona, Tucson, Ariz.

TP 4642I. Manuscript, May 7, 1957. New Orleans Meeting, February 1957.

area was blanketed beneath volcanic flows, agglomerate, and ash.

Streams fed by glacial meltwater cut deep canyons through these volcanics and in the Cuajone area exposed a narrow belt of leached capping in the Chuntacala Valley and a wide halo of alteration in the Torata and Cocatea valleys (Fig. 1). Spurs between the valleys are relatively flat, westward-dipping plateaus capped by the post-ore volcanics. Outcrops of the underlying older rocks are scarce and the geology must be largely interpreted from drilling data.

The Cuajone quartz-monzonite porphyry stock is roughly 6500 ft long and 3500 ft wide. The long axis strikes northwest, and both lateral contacts dip steeply to the northeast. It invades an earlier diorite intrusive and a sequence of southwestward-dipping Cretaceous(?) volcanic flows which include: an andesite porphyry (not reached by any drillholes in the vicinity of ore mineralization); a basalt, with olivine-rich phases; an overlying rhyolite porphyry and a second andesite porphyry capping the rhyolite porphyry. These volcanics lie unconformably on Cretaceous quartzite, shale, and

Table I. Summary of Geological Events

Quaternary to recent:	Alluvium	
Tertiary to Quaternary:	Volcanics	
	Volcanic ash	
	Agglomerates	
	Vitrophyes	
	Andesite porphyry flows	
	Rhyolite porphyry flows	
Erosional unconformity. Period of oxidation and enrichment.		
Tertiary (?):	Intrusive Series	
	Breccia dikes	
	Latite porphyry dikes	
Period of sulfide mineralization. Copper introduced late.		
Tertiary (?):	Breccia pipes	
	Quartz-monzonite porphyry stocks	
	Diorite and quartz-diorite stocks	
Period of mild folding and tilting to the southwest.		
Late Cretaceous (?):	Volcanics	+ 3000 ft
	Andesite porphyry	0 to 350 ft
	*Rhyolite porphyry	± 1000 ft
	Basalt (olivine)	± 2000 ft
	Andesite porphyry	?
Cretaceous:	Sedimentary Rocks	
	Quartzite, shales, coal	?

* Probably equivalent to the Quelleveco quartz-porphyry.

coal beds exposed in valleys north of the Cuajone area. Post-ore latite porphyry dikes, and breccia dikes or breccia pipes, which appear to be genetically related to the latite porphyry, cut mineralized quartz-monzonite and the warped volcanics.

Breccia pipes and shatter pipes* belonging to an earlier generation cut the quartz-monzonite porphyry stock and Cretaceous(?) volcanics and appear to have localized ore mineralization.

* The term *breccia pipe* refers to a pipe-like body of brecciated rock in which the rock fragments have moved generally upward and have been rotated. *Shatter pipe* is used to refer to a pipe-like zone of strong shattering of the rock, but with apparently little movement of the rock fragments vertically and little rotation in place.

A possibly still earlier generation of breccia, observed along the northern portion of the Cuajone stock, was solidly cemented by quartz, tourmaline, and minor sulfides. Tourmaline is rare in the later breccias.

Shape: The principal orebody, the Chuntacala, comprised essentially of primary sulfides, is located on the southern nose of the northeastward-dipping Cuajone quartz-monzonite stock. Drilling revealed it to be roughly circular in plan, about 3000 ft diam

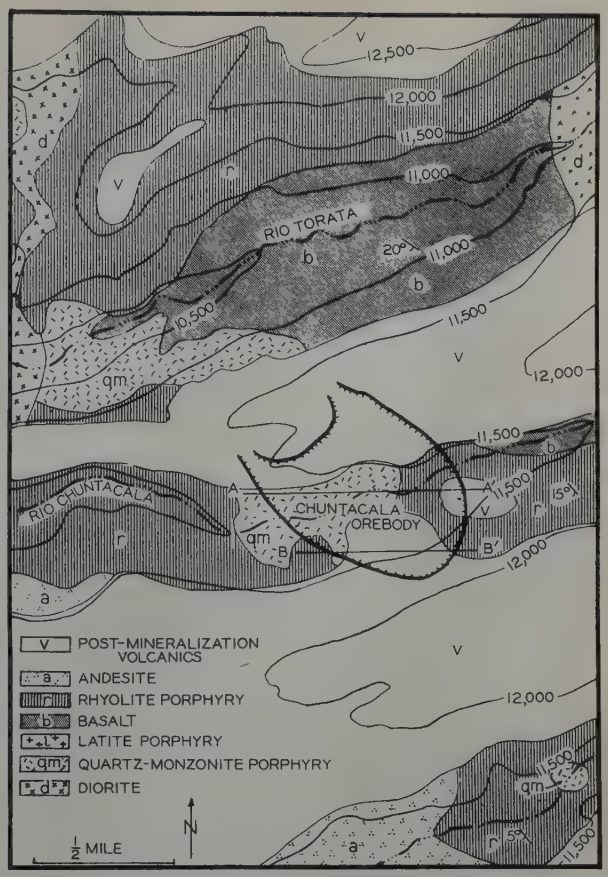

Fig. 1—Geological map of Cuajone area.

near the surface. It has two irregular horn-like extensions to the northwest, not yet explored in detail, which follow the contact between volcanics and intrusive. With depth the orebody divides into two distinct roots, shown in Figs. 2 and 3. The northern portion tapers downward as an inverted cone with an elliptical plan; at a depth of 1600 ft below the bottom of the valley it runs 650 ft in an east-west direction and 1300 ft north-south. The southern portion follows down the south contact zone of the quartz-monzonite intrusive as a tapering figure with a crescentic plan. Drillholes were stopped in primary ore at a depth of 1935 ft below the valley within these roots. The ore occurs within the quartz-monzonite and the warped volcanics.

Ore Mineralization: Sulfides within the orebody occur as small veinlets up to 2.5 in. wide but usually 0.5 in. wide or less in closely spaced array. Rock fragments between the veinlets contain disseminated sulfide grains. Pyrite is the most abundant of the sulfide minerals, chalcopyrite the principal primary ore mineral. Minor quantities of bornite, galena, sphalerite, and enargite were noted in cores and sludge samples. Molybdenite is common but spotty in its occurrence associated with quartz veinlets and as fracture coatings. Supergene enrichment processes have formed chalcocite and covellite. Chrysocolla, cuprite, tenorite and local concentrations of native copper have formed where the zone of oxidation has encroached upon enriched ore.

There appears to be a general increase in abundance of lead and zinc minerals toward the outer portions of the ore zone, but economically they are of little importance, and no quantitative data regarding their distribution was obtained. A study

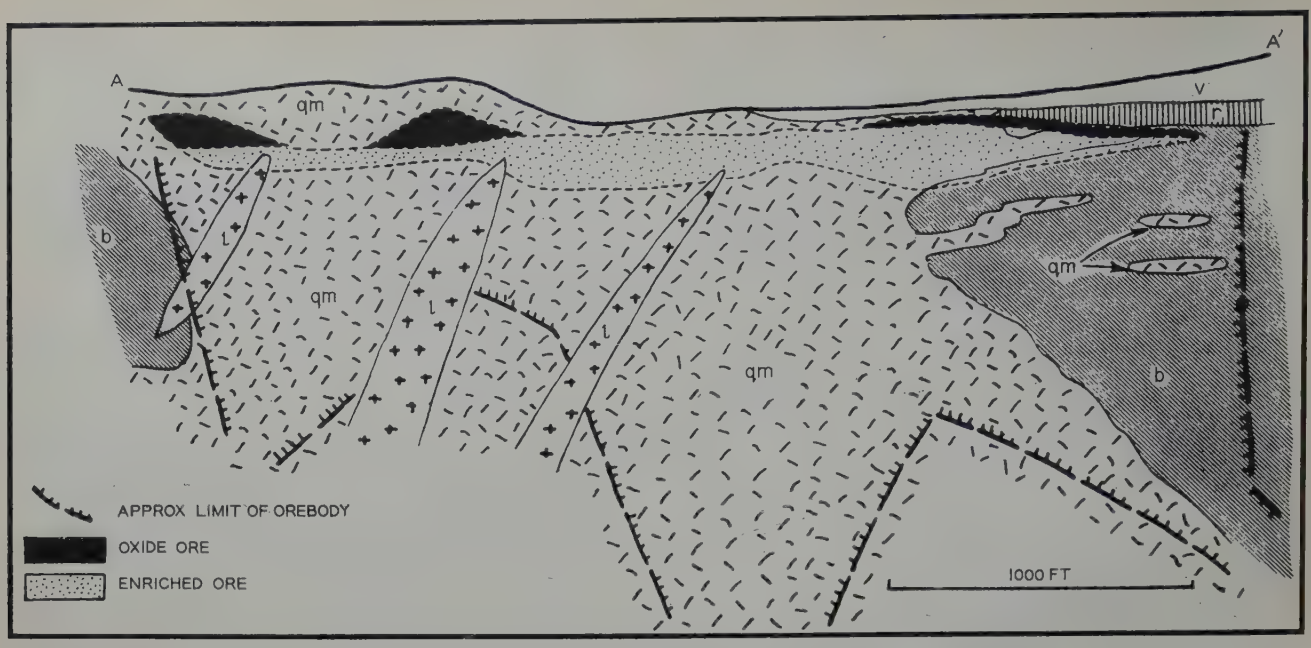

Fig. 2—Cross section through central portion of Chuntacala orebody.

indicates that in and around the Chuntacala orebody the ratio of iron to copper in the sulfides varies. Within the central pipe portion of the orebody and close to the contacts of the intrusive stock the copper/iron ratio is high and a small percentage of sulfides indicates high copper values. On the outer fringes of the mineralized area the ratio is low, and even a high percentage of sulfides does not promise ore grade. This zoning was important in interpreting geophysical results obtained using pulse methods.[1]

Wallrock Alteration: The course of chemical changes that took place in the wallrock related to the processes of ore deposition varied with the initial chemical composition of the altered rocks. However, the ultimate products of intense alteration were the same irrespective of the nature and composition of the original rock.

Wallrock alteration at Cuajone is similar to that generally described as characteristic of the porphyry-copper deposits of the western U. S. Evidence can be observed on both small and large scales for expanding fronts of alteration, each being displaced outward by a higher intensity phase emanating from fractures or channelways. On a small scale in the quartz-monzonite or rhyolite porphyry, sulfide veinlets may be flanked by zones rich in secondary quartz, grading outward through sericite and quartz into a clay-sericite mixture, and finally a broad argillized zone. The same pattern holds on a broad scale: areas of strong silicification and sericitization (intense alteration) grade outward into areas of mixed silicification, sericitization, and argillation (moderate alteration) and this in turn into a broad zone argillation (weak alteration). In basalt the alteration follows the same general pattern, but a wider variety of alteration minerals is formed in the lower intensity zones. These include serpentine, talc, chlorite, and clay minerals. Zones of intense alteration in the basalt are characterized by quartz and sericite but may also contain minor quantities of epidote.

A zone of weak to moderate intensity alteration of the rock around the Chuntacala orebody forms a halo about a mile and a half wide. Areas with high intensity alteration are generally confined to the immediate area of the orebody but only partially conform to the ore distribution pattern, as shown in Fig. 4.

Controls of Ore Localization: Future geological mapping of the open pit areas will reveal the complex nature of the structure that can only be generally surmised from drilling data. However, control of ore localization appears to be principally structural in nature, with copper values concentrated along zones of shattering or brecciation that were open at the time copper-bearing solutions were introduced. Where structures transcended rock boundaries, rock types exerted minor control as to the grade of copper values.

Within the southern portion of the quartz-monzonite porphyry stock there appears to be a cluster of breccia pipes adjacent to which the rock has been severely shattered. The number and extent of these pipes is not known. These apparently have served to localize ore values. Alteration of the wallrock in the vicinity of this supposed pipe cluster is generally only of moderate intensity.

A zone of irregular shattering and brecciation occurs adjacent to the contact area between quartz-monzonite and volcanics affecting both. This zone is best developed around the southern nose of the stock, and ore mineralization related to this feature seems to merge with that of the breccia pipe cluster

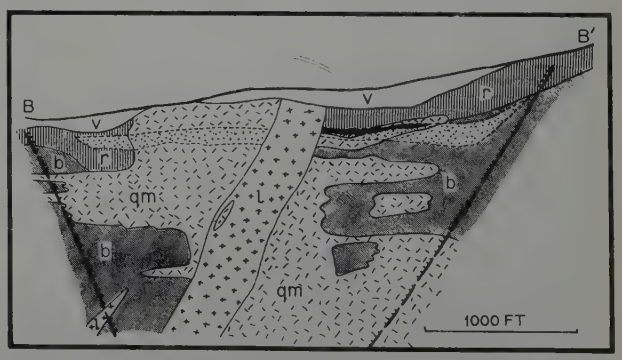

Fig. 3—Cross section through southern portion of Chuntacala orebody.

Fig. 4—Plan of Chuntacala orebody showing alteration intensity.

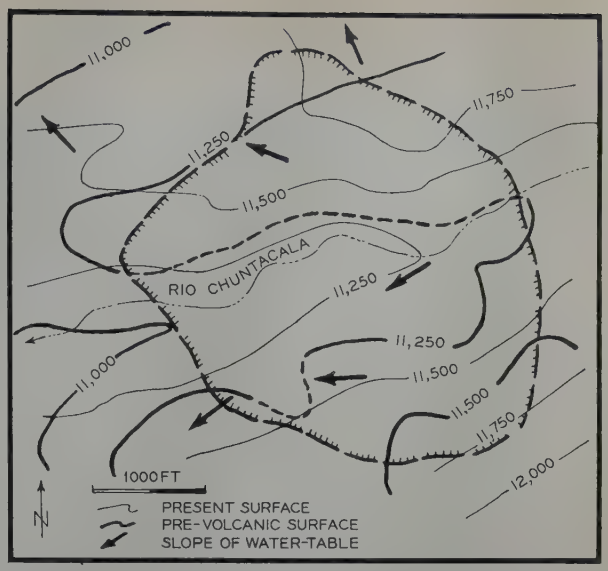

Fig. 5—Plan of Chuntacala orebody showing relations between present surface, pre-volcanic surface, and present water table.

in the upper levels. Intense wallrock alteration accompanies mineralization localized along this structure.

In places where drillholes cut down through alternating quartz-monzonite porphyry and basalt, control of ore grade by rock type is striking. Copper values are generally 0.1 to 0.2 pct higher in the basalt; in only a few instances was there no change or reversal. The rhyolite porphyry appears to react chemically in the same fashion as the quartz-monzonite porphyry.

Oxidation and Enrichment: Construction of contours, based on drillhole data, of the Pre-Tertiary—volcanics land surface, depth of oxidation, depth of enrichment, location and thickness of the oxide ores, and configuration of the present water table yielded interesting data regarding oxidation and enrichment of ores in the Chuntacala orebody.

At the time of extrusion of the Late Tertiary(?) or Quaternary flows and deposition of clastics the topography in the area of the Chuntacala orebody was one of considerable relief—approximately 600 ft in the immediate area of the Chuntacala orebody. Valley and ridge areas did not conform with present topography. This old topography appears to exert a greater influence upon present subsurface drainage and the resultant water table configuration than does the present topography. (See Fig. 5).

The top of the zone of enrichment in the southern and central portions of the Chuntacala orebody faithfully approximates this pre-volcanics erosion surface, being only a few feet below the surface in the valley areas and under about 200 ft of leached capping in the ridge areas. In the northern portion of the orebody the pattern is confused, with no apparent relation to present ore pre-volcanics erosion surfaces. Proximity to the deeply eroded Torata Valley and rapid fall-off of the water table in this direction may have resulted in deep oxidation and leaching along permeable fractured zones.

The bottom of the enriched zone is irregular and does not parallel either present or pre-volcanics erosion surfaces. Locally it extends to more than 160 ft in narrow roots; elsewhere there is no enrichment. Depth of secondary enrichment appears to be a function of rock permeability, with shattered and brecciated zones permitting deeper phreatic circulation, and is seemingly unrelated to rock type or wallrock alteration.

Oxide ores of the Chuntacala orebody are located principally upon the pre-volcanics ridges and appear to be due to encroachment of oxidation on the enriched zone in pre-volcanics time.

Acknowledgments

Many geologists have contributed to the present understanding of the Cuajone district which is briefly summarized above. Particularly important are the contributions of W. R. Bacon, J. D. Hamilton, John Livermore, G. C. Amstutz, J. R. Bogert, and P. R. Eakins. Permission to publish this article was granted by Southern Peru Copper Corp. and Cerro de Pasco Corp.

Reference

[1] A. A. Brant: The Role of Geophysical Methods in Modern Exploration Programs. *Engineering and Mining Journal*, Mining Guidebook, mid-March 1955, p. 32.

Discussion of this paper sent (2 copies) to AIME before Feb. 28, 1958, will be published in MINING ENGINEERING.

Correction

Grinding Practice at Tennessee Copper Co.'s Isabella Mill. By F. M. Lewis and J. E. Goodman. (MINING ENGINEERING, November 1957.) Page 1253, Col. 2, paragraph 1 beginning line 10 should read: "Actual costs of carrying out this plan are tabulated in column 3. It will be seen that these costs follow the estimates in column 2 very closely." Line 16 of the same paragraph should read: "operating cost in column 3." Page 1255, line 2 under Conclusions should read: "13 pct more efficient."

Mineralized Cretaceous Horizons in Northeastern Mexico

by P. Sanchez-Mejorada

GEOLOGISTS who are acquainted with the mines of northeastern Mexico realize that the most important lead-silver replacement deposits of the province are confined to a single formation. But since the formation is several hundred meters thick, the author has determined the relative position of the lead *mantos* in the belief that this information will prove useful in the search for new mines.

This article describes the stratigraphic location of lead-silver replacement deposits known in several mines situated in a region comprising part of the states of Coahuila and Nuevo Leon. The area studied extends for 200 km* (125 miles) from east to west and 70 km (45 miles) north to south.

* Conversions of metric units to English units are approximate.

Metallogenic Province: The most important metallic deposits of the region have the following common characteristics:

1) The orebodies occur as *manto* replacements of calcareous sediments.

2) The horizons that have contributed large tonnages of ore are in similar positions in the corresponding stratigraphic columns (as it will be shown later on).

3) Lead is the most important metal in the ores. Silver is commonly present in small amounts. Occurrence of zinc is dependent on the degree of oxidation of the primary sulfides.

4) A large proportion of the total production has been in the form of oxidized ores.

5) The deposits are located on anticlines.

Rocks of Cretaceous age crop out over large areas of the states of Nuevo Leon and Coahuila, forming part of a belt that extends to the south along the eastern Sierra Madre. The sediments are cut by a small number of intrusive stocks ranging in characteristics from rhyolite to diorite.

The most prominent structural feature of the region is a series of folds trending northwest-southeast. Faulting is not conspicuous in the region, although a major fault zone is found farther East.[1]

The physiography closely reflects structural features, with mountains formed by anticlines and valleys conforming with intermediate synclines. Narrow valleys have also been developed along the axes of many anticlines, where solution of limy sediments and erosion have proceeded along axial tension fractures.

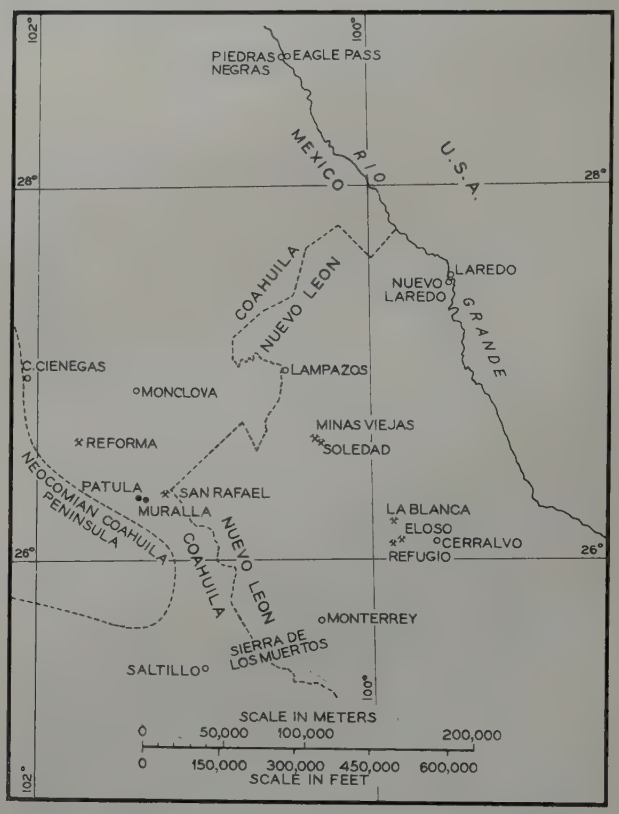

Fig. 1—Location of several lead mines in northeastern Mexico.

Stratigraphy: Rocks of the Upper Cretaceous are exposed in only a small percentage of the total area. Generally they have been eroded away from the mountains and are covered by recent talus and alluvium in the valleys.

Humphrey[2] has published an excellent paper describing the Cretaceous formations of the Sierra de los Muertos, a short distance west of Monterrey. A brief summary of these formations is given below to convey an overall picture of the stratigraphic sequence that prevails just south of the area under consideration.

Upper Cretaceous

Indidura: Essentially thin shaly sediments.

Cuesta del Cura: Limestone in thin wavy beds

P. SANCHEZ-MEJORADA, Member AIME, is a Geologist with Cia. Minera de Penoles, S. A.

TP 4680I. Manuscript, March 18, 1957. New Orleans Meeting, February 1957.

with black chert. This formation marks the transition from lower to upper Cretaceous.
Lower Cretaceous.

Aurora Limestone: Gray, massive limestone in thick to medium beds.

La Pena: Formation rich in cephalopods and composed of marls and shales interstratified with thin beds of shaly limestones and bands of black chert. Humphrey applies the term *La Pena* to only a fraction of the formation originally described under this name by Imlay.[3] Humphrey's classification is used in this article because this restricted section forms a very distinctive unit in the region.

Cupido: Medium to thick-bedded limestone with dolomitic beds that are more abundant toward the base of the formation.

Taraises: Limy-shaly sediments and thin limestone beds.

The upper portion of this stratigraphic sequence prevails without important variations throughout the region, but there are radical changes in the pre-Cupido formations.

The soft Indidura sediments are commonly found only as narrow belts along the foothills of the mountains. The Cuesta del Cura limestone is not prominent in general, and it may be absent.

The Aurora limestone forms the most extensive outcrops and the top of the formation often outlines the mountains.

The sediments of La Pena form a thin band of soft rocks that are more easily eroded than the adjoining hard limestones. This fact is reflected in the topography and the vegetation, affording an excellent marker throughout the region.

The Cupido formation is very similar to the Aurora, except for the presence of dolomite beds in the former. The dolomites are believed to be of marine origin, although some dolomitization has been recognized as being related to the mineralizing processes.

A section measured by the author in the San Lazaro canyon, along the Saltillo-Monclova highway, shows that the Cupido formation with typical dolomitic beds is 295 m (970 ft) thick, and that the lowest 45-m (150-ft) unit includes many dolomite beds and interbedded shales. This formation rests on detrital strata that correspond to the top of the *Patula Arkose.*

The *Patula Arkose,* which attains a thickness of more than 600 m (2000 ft) is composed of red, green, and gray sandstones, graywackes, and arkoses that vary from fine to very coarse grained and grade to conglomerate. Some red and green beds of fine grained sandstone and shale are found at the upper portion of the formation in the Muralla valley. Burckhardt[4] established the age of this formation as late Neocomian and early Aptian (based on studies made by C. J. Hares, L. B. Kellum, E. Boese, and O. A. Cavins).

Metalliferous Deposits in Several Mines: The following districts are shown on the accompanying map.

Reforma District: The most important active mine of the region, the Ocampo Unit of Cia. Minera de Penoles in Reforma, has produced more than 1 million tons of ore consisting of oxidized lead minerals, mostly cerussite, bearing small amounts of silver. Gangue is calcite, quartz, iron oxides, and barite.

The deposit lies on the western flank of the asymmetrical and slightly overturned anticline of Sierra

STRATIGRAPHIC COLUMN IN SIERRA DE LOS MUERTOS
NEAR MONTERREY, N.L. MEXICO
AFTER W.E. HUMPHREY

	TEXAS	EUROPEAN STAGES		SIERRA DE LOS MUERTOS		THICKNESS IN MTS
UPPER CRETACEOUS	AUSTIN	SANTONIAN		PARRAS SHALE		1400±
		CONIACIAN				
	EAGLE FORD	TURONIAN		INDIDURA FORMATION		550±
	WOODBINE	CENOMANIAN				
	WASHITA	ALBIAN	UPPER GAULT	CUESTA DEL CURA FORMATION		120 TO 150
LOWER CRETACEOUS	FREDERICKSBURG		LOWER GAULT	AURORA LIMESTONE		300 TO 450
	TRINITY		LOWER ALBIAN			
		APTIAN	GARGASIAN	LA PEÑA FORMATION		8 TO 40
			BEDOULIAN	CUPIDO FORMATION		600 TO 750
		NEOCOMIAN	BARREMIAN			
			HAUTERIVIAN	TARAISES FORMATION		260±
			VALANGINIAN			
			BERRIASIAN			
UPPER JURASSIC		TITHONIAN				
		PORTLANDIAN		LA CASITA FORMATION	UPPER MEMBER	370±
		KIMMERIDGIAN			LOWER MEMBER	300
		OXFORDIAN	ARGOVIAN	ZULOAGA LIMESTONE		90±

Fig. 2—Refer to text for brief summary of these formations.

de la Purisima, replacing dolomitic limestone beds near the base of the Cupido formation.

Commercial mineralization occurs for 1700 m (5600 ft) along the strike, and slightly more than 400 m (1300 ft) down the dip. The strata are practically vertical in the lower levels of the mine, but the upper levels are located near the top of the arch, where the beds are flattening. Secondary flexures have an important role in the structural control of individual ore shoots.

Mineralization is not confined to a particular bed, but localization of ore within the stratigraphic column varies through the mine between 8 and 60 m above the top of the Patula Arkose. The ore-replaced unit lies at an average of 150 m (500 ft) below the base of La Pena formation.

San Rafael Mine: This mine lies in a small range formed by an anticline parallel to the regional trend. A small synclinal flexure is superposed on the crest of the major fold, and a fault is located close to the axial plane of the anticline. Vertical displacement along the fault is more than 300 m (above 1000 ft).

The Indidura, Aurora, La Pena, and Cupido formations are present in San Rafael. La Pena beds are about 30 m (100 ft) thick, and the Cupido formation comprises a limestone unit 40 m (130 ft) thick resting over 150 m (500 ft) of black, sugary dolomitic limestone. This section is underlain by a unit that includes shaly limestone, shale (generally carbonaceous), sandstone, and conglomerate that marks the transition to the Patula Arkose.

Sphalerite, galena, subordinate pyrite, and small amounts of gangue are found in San Rafael replacing some members of the transition unit, 10 to 30 m (about 30 to 100 ft) below the base of the black dolomitic limestone of the Cupido formation.

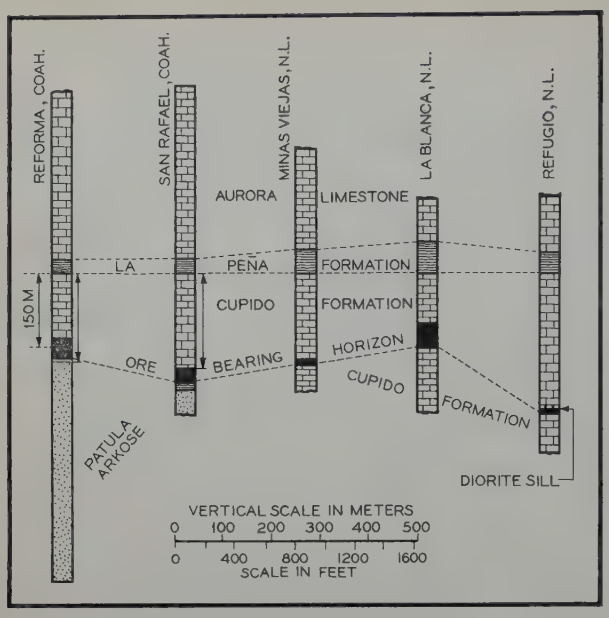

Fig. 3—Stratigraphic sections corresponding to several mines in northeastern Mexico.

Mineralizing solutions ascended along the axial fault until they reached the favorable horizon where the replacement took place, forming a pipe-like orebody. Part of the solutions leaked beyond the horizon and deposited their mineral load in small tabular bodies along the fault.

Minas Viejas: This district is located near the summit of the Iguana range, which is formed by a nearly symmetrical anticlinorium. Several monoclinal folds, minor canoe synclines, and other flexures occur in the upper part of the major structure.

These minor folds had a predominant role in the structural control of the ore deposits, and some of the largest orebodies have been found in gently dipping beds, in the vicinity of those places where the dip of the strata changes abruptly.

The mineral deposits occur as lead and zinc *mantos* replacing certain horizons of the Cupido formation. The ore is found in an advanced state of oxidation, but relict galena is not uncommon. The bulk of the production has consisted of argentiferous lead ore, while zinc has been produced in subordinate amounts.

The major ore horizon is located about 180 m (600 ft) below the base of La Pena formation, or 40 m (130 ft) below the local unit named *La Calle,* which is a very conspicuous unit and an excellent local marker. Eight dolomitic beds have been recognized under *La Calle,* and ore is often found in an 8 m (25 ft) thick horizon that includes three dolomitic beds.

La Soledad: This mine lies at the foothill of the Iguana range, in the eastern limb of the Minas Viejas fold. The Soledad deposit is similar to that of Minas Viejas, and ore occurs in about the same stratigraphic position.

La Blanca: La Blanca district is located in the northeastern limb of a very gentle anticline. The mineral deposit occurs as a practically horizontal pipe-like body of thoroughly oxidized argentiferous lead minerals, low grade zinc ore, and large amounts of iron oxides. It has been mined out over a length of 2 km (1.25 miles).

The ore horizon is part of the Cupido formation and lies within 100 to 150 m (350 to 500 ft) below the base of La Pena formation. Several thin dolomitic beds are found in the vicinity of the replaced beds, but they have no apparent effect on the orebody.

In the outskirts of La Blanca mine there are several narrow veins along which mineralizing solutions reached the impervious La Pena shaly beds and formed thin *mantos* of little importance.

Refugio—El Oso: Five diorite sills, 2 to 40 m (7 to 130 ft) thick, intrude the gently dipping Cupido strata in this area. The ore deposits are pipe-like bodies of lead, zinc, and silver sulfides replacing limestone just underneath some of the sills. Structurally, the orebodies are controlled by steep fractures, which formed channelways for mineralizing solutions, and by the damming effect of the igneous sills.

The largest body of Refugio occurs 280 m (900 ft) below La Pena formation, while the corresponding distance at El Oso is 235 m (770 ft). This last orebody is very small in cross section, but it is continuous over 1 km along the strike. The minerals of El Oso are oxidized.

Factors Responsible For Location of Favorable Horizons: Fig. 3 shows the position of the ore-bearing horizons in the stratigraphic columns of the mines that have been described. The uniformity of the position of the replacement *mantos* in all the mines is evident, except in El Refugio, where the presence of igneous sills introduced a modification that readily explains the variation.

A question arises as to the reason for such uniformity over a very large region, and why the deposits were formed in the Cupido beds in preference to other strata, such as the similar Aurora limestone.

Prescott,[5] who studied the limestone replacement deposits of central-northern Mexico, affirms that about 50 pct of all the tonnage mined out in that province was derived from a single horizon. His explanation is that "the only discernible common factor in all cases is the position of the bed at or near the base of limestones." Nevertheless, Fig. 3 shows that in the case of northeastern Mexico there is a remarkable uniformity in the location of the ore *mantos,* in spite of a marked difference in the type of the immediate underlying sediments.

Two factors are fundamentally responsible for the stratigraphic position of the mineralized bodies, i.e., depth of the formation during the metallogenic epoch, and the characteristics of the favorable beds.

The region under study remained under the sea until the Eocene,[6] when the orogenic movements started. Igneous stocks were emplaced as a result of the diastrophic deformation that continued until late in the Tertiary, and in conjunction with it. The mineralization is supposed to have been related to the igneous activity.

The period of time that elapsed between the orogenic uprising and the mineralizing activity was relatively short. It is probable, therefore, that the thickness of Upper Cretaceous and Tertiary sediments may have been more or less uniform throughout the region. Consequently, the pressure of the mineralizing solutions that were ascending through various channels in the region, in the same epoch, must have been approximately uniform at a given horizon. The sealing effect of the widespread La Pena shaly beds no doubt further increased the uniformity in the pressure of the ascending mineralizing solutions.

It is the writer's opinion that the mineralizing solutions traveled from a deep-seated source until the proper conditions of temperature and pressure for ore deposition were found and that the Cupido formation was buried at the time within the limits of that favorable vertical range. Localization of the orebodies in a particular horizon, within the Cupido formation, was due to characteristics that must be peculiar to certain beds.

Hayward and Triplett[7] have shown that dolomitic limestones play important roles in the control of many replacement deposits of northern Mexico. Their illustrations show that dolomites are favorable host rocks in some deposits and that they act as the controlling element in other cases, without any indication of preferential replacement. Fletcher[8] also states that although magnesian content is not an essential characteristic of a favorable horizon, it is "the most important index we have for favorable horizons."

The dolomitic limestones of the Cupido series are believed to be the final instrument responsible for the stratigraphic position of the orebodies. The mineral deposits are not confined to dolomitic beds in the mines described, but they undoubtedly were a controlling factor in the circulation of mineralizing solutions, offering better circulating media, in some instances, and in other cases acting as barriers to solutions.

Acknowledgments

The stratigraphic columns of the various mines described have been measured in the field by the author, who is solely responsible for the data and ideas expressed. Nevertheless, all the basic information has been obtained on behalf of Cia. Minera de Penoles, S. A., and much valuable knowledge has been derived from the study of its files.

Thanks are given to F. L. Wingfield, chief geologist, and to other officials of Cia. Minera de Penoles, for their permission to publish this article.

References

[1] R. V. Garfias and C. T. Chapin: Geologia de Mexico. *Editorial Jus*, 1949, p. 64.

[2] W. E. Humphrey: Geology of the Sierra de los Muertos Area, Mexico. *GSA Bulletin*, January 1949, vol. 60, p. 94.

[3] R. W. Imlay: Geology of the Western Part of the Sierra de Parras. *GSA Bulletin*, July 1936, vol. 47, p. 1119.

[4] C. Burckhardt: Etude Synthetique sur le Mesozoique Mexicain. *Memoires de la Societé Paleontologique Suisse*, 1930, vol. 49, pp. 144-147.

[5] B. Prescott: The Underlying Principles of the Limestone Replacement Deposits of the Mexican Province. *Engineering and Mining Journal*, 1926, vol. 122, nos. 7 and 8.

[6] L. B. Kellum, R. W. Imlay, and W. G. Kane: Evolution of the Coahuila Peninsula, Mexico, Part I. *GSA Bulletin*, 1936, vol. 47, no. 7.

[7] W. M. Hayward and W. H. Triplett: Occurrence of Lead-Zinc Ores in Dolomitic Limestones in Northern Mexico. *AIME TP 442*, 1931.

[8] A. R. Fletcher: Mexico's Lead-Silver Manto Deposits and Their Origin. *Engineering and Mining Journal*, 1929, vol. 127, no. 13, pp. 511-512.

Discussion of this paper sent (2 copies) to AIME before Feb. 28, 1958, will be published in MINING ENGINEERING.

Flotation of a Canadian Kyanite

by R. A. Wyman

Laboratory and pilot plant investigations yield successful results.

KYANITE schists in the Sudbury area have been generally described by Haw,[1] who has also given particular information on preliminary treatment of three large samples from Dryden township, Ontario.[2] Kyanite, garnet, biotite, quartz, and feldspar comprise the main ingredients of this ore. Kyanite is the valuable mineral.

About 5½ tons of −35 +200 mesh product, made by dry rod milling, screening, and separation on the Exolon magnetic separator, were available for treatment by flotation. Magnetic separation had effectively reduced garnet and biotite so that flotation feed consisted essentially of kyanite, quartz, and feldspar, the kyanite content averaging 32 pct and representing about 86 pct of the kyanite in the original ore.

Earlier work on kyanite at the Mines Branch, Ottawa, [3-5] employed an acid circuit, but to avoid production difficulties in the use of acids and at the same time take advantage of the fact that industrial minerals respond somewhat to soap flotation, it was decided first to investigate the higher pH levels.

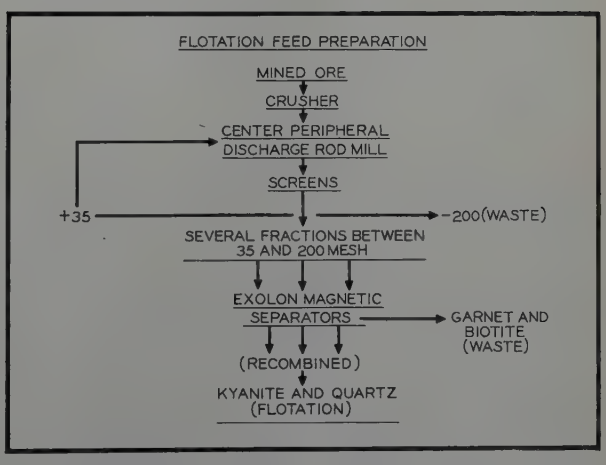

Fig. 1—Stages in preliminary treatment of flotation feed prior to pilot plant operation.

Exploratory tests using −65 +200 mesh feed ended with production of 96.6 pct kyanite concentrate rep-

R. A. WYMAN, Member AIME, is Head of the Milling Section, Department of Mines and Technical Surveys, Industrial Minerals Div., Ottawa.

TP 4510. Manuscript, Feb. 16, 1956. New York Meeting, February 1956.

resenting an 80 pct recovery. This was derived from a system employing warm distilled water, sodium silicate (for quartz depression), sodium carbonate, and oleic acid. Used to cover the coarser size feed of −35 +200 mesh, the same system recovered 76 pct at 94 pct grade. Additional laboratory testing sought to establish optimum conditions for pilot plant work.

Conditioning: Oleic acid conditioning times from 2 to 8 min were tried, but 4 min proved adequate provided pulps were kept above 30°C.

No advantage was gained through adding the oleic acid in steps, and no improvement was observed when the collector was added to cleaning stages.

Density: Up to about 20 pct solids, recovery was found to increase as density increased. At 25 pct solids, adopted for most of the tests, recoveries and grades were generally satisfactory.

Concentrations of Reagents, pH: Several tests were done with progressively smaller reagent concentrations. As reagent level dropped, less cleaning was required. Table I shows recovery and grade in relation to reagent input and number of cleaners. Density of flotation was 25.2 pct solids for each test. The most interesting result appears in D, with low sodium carbonate and sodium silicate input (1.0 and 0.2 lb per ton respectively), and with oleic acid at 2.0 lb per ton.

Table I. Recovery and Grade in Relation to Reagent Input and Number of Cleaners

	Reagents, Lb per Ton			Cleaning Stages	Recovery, Pct	Grade, Pct	pH
	Na_2SiO_3	Na_2CO_3	Oleic Acid				
A	0.8	5	2	6	78.3	97.0	10.0
B	0.4	5	2	5	72.5	97.1	10.1
C	0.2	3	2	4	78.1	96.4	9.8
D	0.2	1	2	4	87.4	95.0	9.2
E	0.2	1	1.5	3	76.6	96.5	9.2

Water Source: Early in the laboratory testing it was noted that about three times as much collector was required when tap water was used as when distilled water was used. An effort was therefore made to determine whether some form of water treatment should be employed. With the lower collector input, distilled or demineralized water gave better results than water softened with sodium ion exchange resin.

Number of Cleaning Stages: The general testing suggested that two or perhaps three cleaning stages would be sufficient.

Pilot Plant Operations

Stages of preliminary treatment of flotation feed are presented in Fig.1. The flotation pilot plant designed and assembled on the basis of laboratory study is illustrated in Fig. 2.

Froth characteristics noted in the laboratory work were sought in the pilot plant operation. Best results with fewest cleaning stages are produced with a fine, white, effervescent and apparently lightly mineralized froth on the roughers and a thick, matted, heavily mineralized froth in the cleaners. In the laboratory, appearance of rougher-type froth on the cleaners meant extra cleaning stages, and in the pilot plant insufficiently cleaned concentrate. Sodium carbonate passing into the cleaners with rougher froth was found to account for carry-over of froth type. In the laboratory, reducing sodium carbonate input had cleared the matter up. In the pilot plant, reducing the sodium carbonate input from 1.0 to 0.7 lb

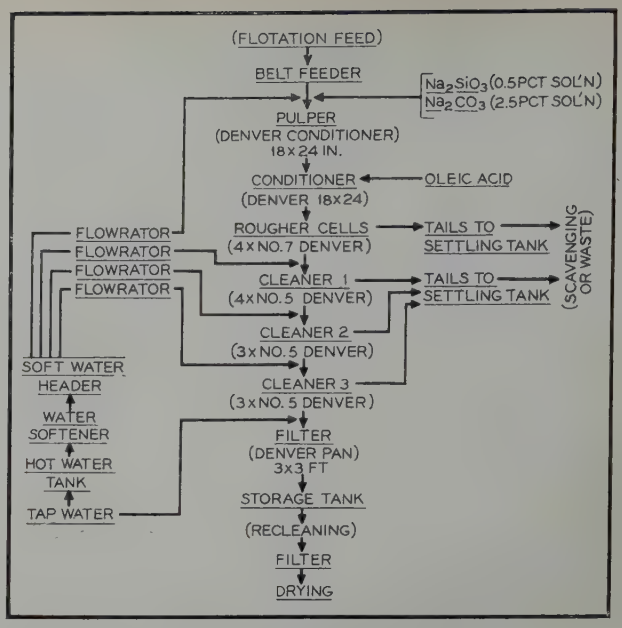

Fig. 2—Flotation circuit of pilot plant designed and assembled on the basis of laboratory study.

per ton (some sodium was picked up from water softeners) improved the froth characteristics but did not solve the cleaning problem as neatly as reduction of this reagent had in the laboratory.

Densities had been planned as 25 pct solids in roughers and 10 pct solids in cleaners, but these were modified to about 20 pct solids in all stages, and this level was continued throughout.

Grade was found to increase from 70 to 98 pct kyanite as collector input decreased from 2.5 lb per ton to 0.65 lb per ton. Correspondingly, recovery decreased from 86 to 65 pct. Under conditions approximating those used in the laboratory, recovery averaged 80 pct and grade 76 pct, with tails of 10 pct. Products were retreated in various ways to produce satisfactory overall results. For example, scavenging the tails and recleaning the concentrates produced a product grading 95 pct kyanite for a recovery of 85 pct. Tabling the tails and recleaning the concentrates gave a grade of 94 pct kyanite for a recovery of 85 pct. These figures are based on flotation feed, which itself represented 86 pct of the kyanite in ore. Indicated recovery by this system is, therefore, about 73 pct.

Acknowledgment

The author gratefully acknowledges the close cooperation of V. A. Haw throughout this investigation, particularly in providing prompt and efficient minerals separation analyses.

References

[1] V. A. Haw: Kyanite in Canada. CIM *Bulletin*, January 1954, vol. 47, p. 27. Mines Branch, Department of Mines and Technical Surveys, Ottawa, Canada.

[2] V. A. Haw: Progress Report—Investigation of Methods for Recovery of Kyanite from Samples Submitted by the Hoyle Mining Company, Limited, Sudbury, Ontario. *Industrial Minerals Report No. 295*, November 1954. Mines Branch, Department of Mines and Technical Surveys, Ottawa, Canada.

[3] H. L. Beer: Concentration of Kyanite Ore from the Hoyle Mining Company, Sudbury, Ontario. *IMR No. 161*, February 1953. Mines Branch, Department of Mines and Technical Surveys, Ottawa, Canada.

[4] H. L. Beer: Batch Concentration Tests on Kyanite Ore from Kyanite Corporation of Canada, Mattawa, Ontario. *IMR No. 163*, March 1953.

[5] H. L. Beer: Flotation Concentration of a Sample of Kyanite Ore from the Property of Strategic Metals Limited, Clarendon, Ontario. *IMD No. 206*, October 1953.

Discussion of this paper sent (2 copies) to AIME before Feb. 28, 1958, will be published in MINING ENGINEERING.

The Rotobelt Filter

New Tool in Minerals Beneficiation

by C. F. Cornell, R. C. Emmett, and D. A. Dahlstrom

FOR many years the disk-type and cloth-covered drum filters have found widest application in liquid-solids separation, which uses continuous filters. The disk type is less expensive, occupies less floor space per square foot of filtration area, and requires negligible down time for filter media changing. However, because filter cloth is billowed out by the blowback in the cake discharge, it is very short-lived if the scraper blades are set too close. Consequently cake weight is very important in assisting cake discharge, which normally necessitates a minimum cake thickness of ⅜ to ½ in. Also, the vertical position of the disks eliminates the possibility of efficient cake washing for removal of soluble values. The disk-type filter is generally limited, therefore, to applications that require no cake washing and form relatively thick cakes within the normal range of filter cycle times.

The conventional cloth-covered drum filter is a more flexible unit, permitting wider variation in the percentage of cycle time devoted to cake formation, dewatering, or washing, as required by the application. Thinner filter cakes can be discharged because a horizontal line across the filter medium at the location of the scraper blade is equidistant from the edge of the blade at all points. The scraper blade therefore may be set a short distance from the filter medium or, where wire winding is not used, a floating scraper can be utilized so that the contour of the cloth can be followed. The drum filter is generally employed when there are difficult filtering slurries with resultant thin cakes or when cake washing to recover soluble values must be practiced.

Difficulties sometimes encountered in continuous filter operation can be summarized in the following four categories:

1) Low filtration and/or washing rates due to blinding of the filter medium.

2) Poor cake discharge resulting from sticky cakes, filter medium blinding, or too thin a cake for the particular type of filter.

3) High filter media costs caused by short life and frequent down times for cloth changing. This results from blinding or from abrasion by the scraper blade when cakes are thin.

4) Blowback of filtrate at cake discharge because not enough air passes through the cake to purge the drainage area and filtrate lines during dewatering.

To reduce or eliminate blinding tendencies several modifications have been tried, for example, cover-cleaning showers, blowback under the feed slurry, and snap-blow cake discharge. In many cases, however, this simply retards the rate of blinding, since the filter medium is kept clean at its outer surface only by these methods. As blinding usually occurs within or on the back of the medium, the operator is finally forced either to remove the cloth and scrub the medium intensively with a cleaning solution or acid-rinse it on the filter—all resulting in down time, short cloth life, and additional costs.

C. F. CORNELL and R. C. EMMETT, Members AIME, are Research and Development Engineers, Eimco Corp., Palatine, Ill. D. A. DAHLSTROM, Member AIME, is Director of Research and Development.

TP 4500B. Manuscript, April 8, 1957. New Orleans Meeting, February 1957.

This page of Mining Transactions AIME follows p. 112. The intervening non-Transactions pages appeared in MINING ENGINEERING.

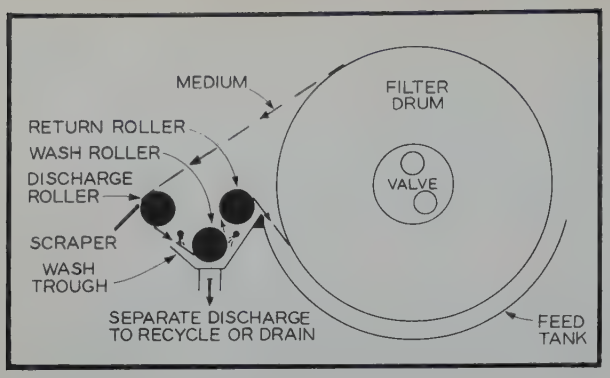

Fig. 1—Basic Rotobelt mechanism.

Improved cake discharge has been obtained in some applications by use of the roller or string discharge drum filter. Use of the roller is limited to a very tacky cake that readily sticks to itself, such as clay; it is not suited to many applications. The string discharge presents a difficult operation if the strings have a tendency to pull through the cake upon lifting it from the drum surface. In many metallurgical applications string maintenance becomes costly because the solids are abrasive.

Blowback of filtrate can be eliminated by a purge system that pulls atmospheric air under the filter medium to sweep out the drainage decking and internal piping. This modification adds to the initial cost, but it is easily justified when soluble values must be recovered or when cake moisture is critical. The roller and string discharge can also eliminate blowback, although subject to the limitations already mentioned.

From this brief discussion it is apparent that filter operations, particularly the more difficult applications, would be greatly improved if it were possible to maintain a clean filter medium, discharge thin cakes easily, eliminate blowback, and use either a permanent medium or one that could be changed with a minimum of down time.

Even with these improvements, it would be essential to preserve in any new filter the operating advantages of the present disk and drum-type filter: 1) flexibility of operation, 2) maximum practical vacuum or pressure drop across the cake to achieve maximum filtration and washing rate and to minimize cake moisture content, and 3) lowest solids content of the filtrate consistent with the type of filter medium employed. Any modification that did not retain these advantages would be a distinct handicap to the operation.

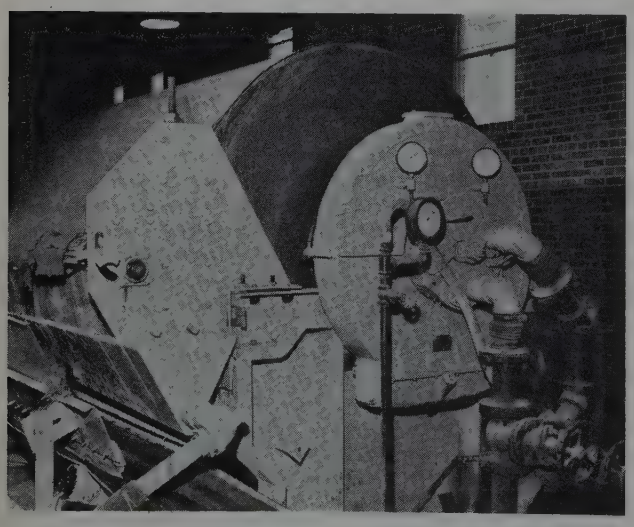

Fig. 2—The 6-ft diam x 8-ft face Rotobelt filter in operation. Permanent stainless steel filter medium belt.

The need for filtration equipment incorporating these improvements has been greatly accelerated by recent developments in extractive metallurgy and by advances in physical ore dressing techniques. In extractive metallurgy, with leaching processes treating valuable elements and low grade ores, efficient recovery of solute must be maintained. In both cases, owing to the creation of larger amounts of colloidal slimes or difficult filtering material, thin cakes and/or poor cake discharging characteristics are encountered that may increase blinding tendencies of the filter media. Longer media life is imperative, moreover, since filters are usually made of costly synthetic fabrics.

Theory and Design of the Rotobelt Filter: To prevent blinding, it would be advantageous to wash both front and back surfaces of the filter medium. This would mean removing the filter medium constantly so that high velocity liquid sprays could be made to impinge on it. A series of small diameter rolls would also be required to return the filter to the drum. There would be several other advantages. In assuming different radii of curvature as it passes over the rolls the filter material flexes, changing the position of the individual strands in relation to each other. Accordingly, solids deposited within the filter medium would loosen or work free and thereby maintain permeability. At the same time the cake would break more cleanly from the filter medium as it assumed a small radius of curvature (although slightly larger than the medium) when it reached the discharge roll. Thin cakes could therefore be discharged easily as a complete sheet.

Fig. 1 illustrates the basic mechanism of the Eimco Rotobelt filter. The endless belt passes over a discharge roll, and as the filter medium reaches the first point of a small radius of curvature, the cake is removed. A scraper blade set slightly away from the medium conducts the cake away in a continuous sheet. The small diameter roll allows the blade to be set very close to the surface without contact, since a horizontal line across the roll at the location of the scraper is equidistant from the scraper at all points as the roll rotates.

The medium is conducted under a wash roller that is partially submerged in a wash trough. A spray wash on either side of the medium permits thorough cleaning of each surface and any solids removed are recovered together with the wash fluid in the wash trough. In cases where the solids or the soluble material washed from the medium are valuable, effluent from the wash trough can be recycled to a convenient point upstream in the flowsheet. The blinding tendency of the solids or liquor with the particular medium employed will dictate the extent of spray washing required. In many cases only a periodic rinse is needed.

A return roller places the medium back on the drum. It has been found that the roller alignment system increases the percentage of drum area that can be employed for cake formation, washing and dewatering, thereby increasing effective area. On large diameter drum filters, it is possible to leave one half to one entire additional sector of the drum

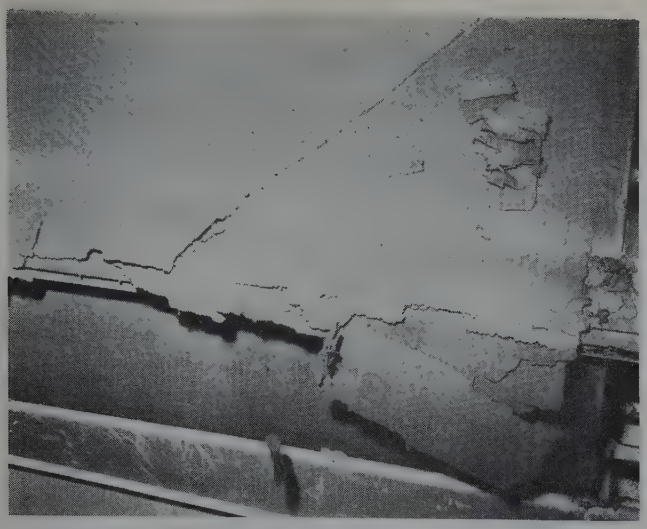

Fig. 3—Close-up of cake discharge from 6-ft diam x 8-ft face Rotobelt filter. Note cleanness of medium after discharge.

under vacuum, thereby reducing cake moistures to a minimum at faster cycle times.

Both the discharge and return roller have self-aligning features so that the medium is normally maintained in proper alignment on the drum. One roller is equipped with take-up screws at each end to correct for gradual belt stretching during operation. Any required adjustment is made very rapidly and without stopping filtration.

To maintain vacuum on the filter, obtain isolation between drum sectors, and prevent leakage, each division strip is fitted with a soft rubber insert that is slightly higher than the filter deck surface. Soft rubber inserts are also applied in the groove on each end of the drum. Finally, about 2 in. of the medium at each edge is impregnated with a sealing compound. This 2-in. band is kept in alignment with the rubber inserts on the drum ends so that a perfect seal is obtained. By this construction, each drum sector is completely sealed both from the atmospheric pressure side and the adjacent sectors. Thus regulation of drying vacuum, separation of strong and wash filtrates, or any other operation performed on a conventional drum filter can also be achieved with the Rotobelt filter.

As compared with conventional drum filters, the Rotobelt offers the following advantages:

1) A clean, non-blinded medium at all times to achieve maximum filtration rate.

2) Ease of complete cake discharge, even with thin filter cakes, so that fast drum cycles can be employed to increase filtration rates further.

3) Elimination of filtrate blowback.

4) Reduction of filter cloth wear to a minimum, as scraper blade does not contact medium.

5) Increase in effective area of the filter due to greater percentage of time under vacuum.

6) Decrease in down time for changing filter media as no calking or wire winding is employed.

7) Easy access to filter deck for cleaning if necessary, as it is always exposed between the take-off and return point of the medium.

8) Maintenance of as high a vacuum level as desired by sealing method that prevents leakage.

An operating 6-ft diam x 8-ft face Rotobelt unit is shown in Fig. 2. The traverse of the medium to the wash trough is clearly visible. It will be noted that a high vacuum is being maintained. The cake normally comes off as a blanket but it has been broken away to show the medium return to the wash trough.

Fig. 3 is a close-up of the discharge point to illustrate the completeness of discharge obtained. The medium is seen to be completely clear of solids on the surface after leaving the point of discharge. A portion of the cake has been scraped away preceding the knife to show the flexing action on the cake and the slight separation between knife and medium.

In the initial development of the Rotobelt filter, a specially constructed stainless steel belt such as is shown in Figs. 2 and 3 was used as filter medium. This medium is so constructed that there is no flexing of the individual strands to cause eventual fatigue of the metal. However, in passing over the rollers, the strands will change position so that any embedded solids tend to work out and maintain the medium permeability. The metal belt was employed originally because it offered dimensional stability, lateral stiffness, and a permanent medium. These characteristics simplify the automatic self-alignment of the belt without unnecessary stretching.

Pilot plant studies have demonstrated that cloth medias are superior to conventional cloth-covered drum filters, but because they lack dimensional stability and lateral stiffness, the alignment system must be modified. Full-scale tests are being conducted with cloth media to prove the required roller design. With the application of cloth media, it will be possible to handle any filtration problem that can be treated with continuous filtration.

Rotobelt Filter in Metallurgical Applications: To determine the advantages of using the Rotobelt filter type of operation on many different industrial problems, a complete pilot plant was assembled on a flat-bed trailer as shown in Fig. 4. An 18-in. diam x 12-in. face Rotobelt filter was chosen which could be operated with either the stainless steel

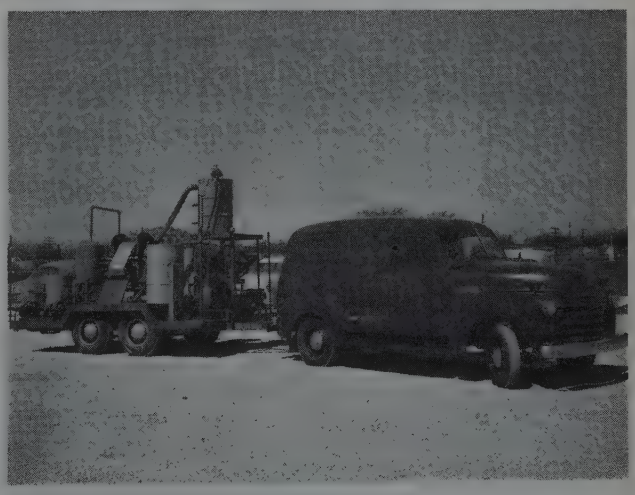

Fig. 4—Portable pilot plant Rotobelt filter unit complete with 18-ft diam x 12-ft face Rotobelt filter and all auxiliaries for pumping, flocculating, and filtering any slurry.

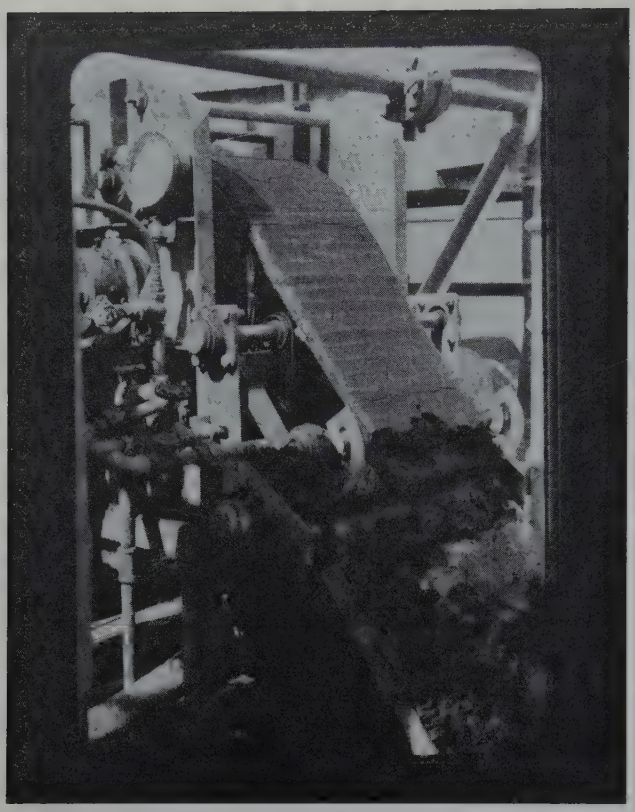

Fig. 5—Close-up of cake discharge from portable pilot plant Rotobelt filter unit. Filtration of barium sulfide solution from tailings.

belt or any cloth medium. Filtrate pumps, wet-type vacuum pump, mix tank, chemical feed pumps, flocculator, and other accessory equipment were all included on the trailer. The only additional requirements for operation were a power source, water for the vacuum pump, and a feed slurry. During these filtration studies many industrial plants, including several metallurgical installations, were visited in all parts of the country and in Canada.

At one plant visited, large cloth-covered drum filters separate gangue solids from a liquor containing dissolved lithium oxide following leaching of the ore. While it is relatively easy to filter the solids there have been blinding problems with these filters owing to the presence of slimes. The pilot plant Rotobelt filter was used to handle the same feed slurry as the plant filter.

Results are indicated in Table I. It is immediately apparent that the clean medium offered by the Rotobelt filter resulted in a much higher filtration rate, 4.6 times that of the cloth-covered drum filters. Approximately the same cake thickness was obtained in a cycle time only 13 pct of the time required for the plant filters. Undoubtedly this was due to the complete cake discharge obtained with the Rotobelt unit together with the removal of slimes from the filter medium surface by the wash sprays.

In this application, the non-blinding filter medium would have additional advantages. As the cake is spray-washed with water to remove soluble values of lithium oxide, the clean medium would permit greater permeability to wash fluid so that the proper wash displacement could be more easily attained. Also, in order to prevent complete blinding of the cloth medium in plant operation, the cloth must be acid-washed for 3 hr every one or two weeks, and cloth life averages only six to eight weeks. It is evident that the Rotobelt could greatly reduce media expense.

Table I. Separation of Lithium Oxide Solution from Leached Gangue

	Plant Cloth-Covered Drum Filters	Pilot Plant Roto-belt Filter
Filter media	Polyethylene	Stainless Steel Belt
Filter cycle time, minutes per revolution	9.5	1.25
Vacuum, Hg-In.		
Form	24	19
Dry	20	19
Feed solids concentrate, wt pct	47.2	47.5
Cake thickness, in.	1 to 1¼	1¼
Cake moisture, wt pct	21.9	22.4
Filtration rate, pounds dry solids per hour per square foot	66	302.7

At a second plant, soluble barium sulfide was removed from waste solids by a three-stage countercurrent decantation system. Underflow from the final stage is passed through a liquid cyclone, and underflow from the cyclone is sent to waste. The cyclone underflow contains 2 pct barium sulfide, which should be recovered if possible. However, blinding of filter media by slimes was anticipated because of results observed in other phases of the flowsheet. Thickener underflow temperature was 90°C, which would also promote the blinding due to crystallization within the filter medium when vacuum is applied.

The pilot plant Rotobelt filter was tested on both thickener and cyclone underflow with very satisfactory results. Fig. 5 illustrates operation and cake discharge obtained during the test work. It will be noted that a very even and homogenous cake was obtained, with a corresponding complete discharge.

Fig. 6 is a plot of filtration rate expressed as dry pounds per hour per square foot and cake weight percent moisture content as functions of filter cycle time for thickener underflow feed. Increasing cycle time to 2.0 min per revolution would achieve a low moisture of 48 pct at a filtration rate of 78 lb of dry solids per hour per square foot. Cake discharge was still complete at a filter cycle time of only 0.92 min per revolution, even though a ¼-in. cake was obtained. Filtration rate increased to 92.7 dry lb per hr per ft^2, or an increase of 19 pct. Moisture content, on the other hand, was raised only 1.8 pct. Occasional peak tonnages could be handled at only a slight change in cake moisture content merely by lowering filter cycle time with the variable speed drive.

Barium sulfide content of the wet cake was always 1 pct or less, representing a saving of better than 71 pct of the barium sulfide presently lost. If cake washing were practiced, recovery could be increased to better than 90 pct of the amount now being discarded.

Considerably higher filtration rates of 343 lb of dry solids per hr per ft^2 were obtained with the cyclone underflow, but this was possible owing to the much coarser feed solids. It was considered preferable to design full-scale operation to treat the thickener underflow, as this would eliminate recycling excessive amounts of slimes found in the cyclone overflow with the present system. Settling rates would be improved in all thickeners and the

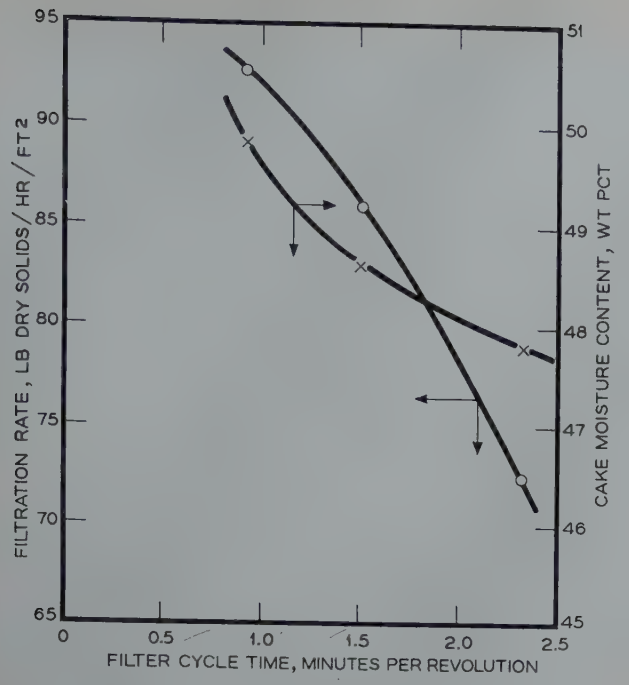

Fig. 6—Filtration rate and cake moisture content as a function of filter cycle time. Pilot plant Rotobelt filtration of barium sulfide slurry. Thickener underflow feed slurry at 22.9 wt pct solids.

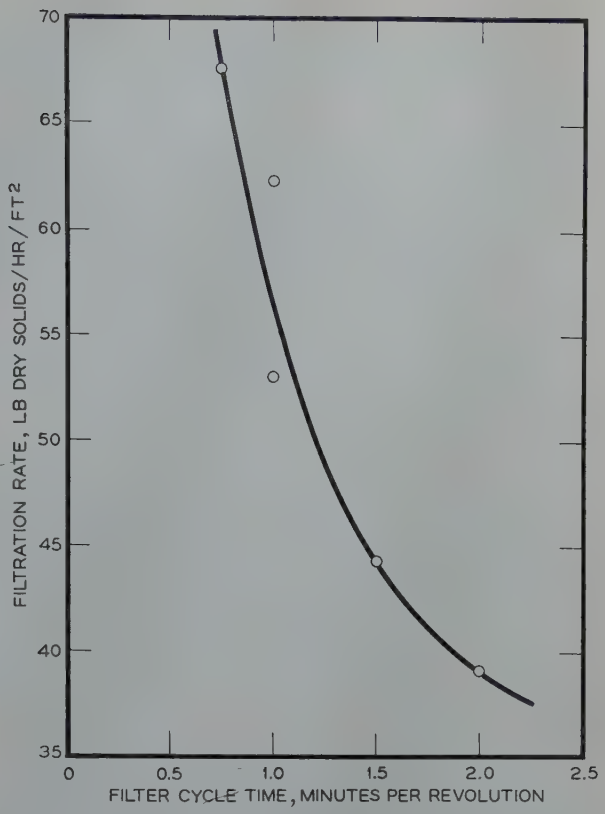

Fig. 7—Filtration rate as a function of filter cycle time. Dewatering of iron ore slimes on the Rotobelt filter. Feed solids concentration = 50 to 55 wt pct and vacuum level = 23 Hg-In. Nylon filter medium belt. Twenty percent drum submergence.

pumping and maintenance costs of the cyclone eliminated.

At one iron ore property, all material less than ¼ in. was to be processed in a wet beneficiation plant. Material finer than 100 mesh was sent to a thickener, which produced a slurry of 50 to 55 pct solids. Filtration of the underflow was attempted with a disk-type filter, but a very thin cake was formed that could not be discharged properly from the disks. Owing to colloidal slimes and incomplete discharge, the filter medium was blinded after a short period of operation.

The pilot plant Rotobelt filter employing the stainless steel belt was first tried, but the cake could not be properly formed. Owing to the relatively large effective mesh size of the belt, the solids would not bridge the openings. When a nylon belt was tested, cake formation was perfect. Fig. 7 plots filtration rate expressed as dry solids per hour per square foot as a function of filter cycle time. Filtration rate ranged from 39 dry lb per hr per ft² at 2 min per revolution to 67.5 dry lb per hr per ft² at 0.75 min per revolution. Cake moisture contents were 33.9 and 35.7 wt pct, respectively. It should be emphasized that cake thicknesses varied from only 3/16 to ¼ in. even with the use of flocculating reagents and would be too thin to permit using a disk-type filter. Also, because of the colloidal slimes present, complete cake discharge is essential to prevent blinding the filter medium.

Complete discharge was always obtained with the Rotobelt filter, even with cakes as thin as 1/8 in. It is therefore possible to operate the filter at relatively high drum speeds to take advantage of the greatly increased filtration rates illustrated in Fig. 7. Filtrate clarity was very good, even with colloidal slimes in the feed, averaging only 0.7 wt pct solids. It should also be emphasized that a continuous spray cleaning of the cloth was not necessary. Washing the cloth every 20 min maintained the filtration rate at its maximum value for any particular cycle time.

Summary

The Eimco Rotobelt filter was developed to permit continuous or periodic cleaning of both sides of the filter medium without stopping the filter operation. An endless belt filter medium passes over an initial roller for cake discharge. The sharp change in the radius of curvature permits the cake to break loose readily from the medium and discharge completely in the form of a blanket. After the discharge roller, the medium passes down to a wash roller located in a wash trough, which is kept separate from the filter tank. To maintain maximum permeability both sides of the medium can be washed with high velocity sprays as required by the operation. The belt is then returned to the drum by a final roll. Both the discharge and return rollers are self-aligning, automatically maintaining the belt in constant alignment. All drum sectors contain soft rubber inserts in the division strips and in the end grooves on the drum. Both edges of the belt are impregnated with a rubber sealing compound for 2 in., sealing off leakage between adjoining sectors and leakage from the atmospheric pressure side. Consequently, high operating vacuums can be maintained at all times if desired.

In all cases cited in the text, the Rotobelt filter either obtained complete filtration or achieved substantially better performance than conventional drum and disk-type filters. Severe blinding problems were eliminated and/or very thin cakes could be discharged completely without difficulty.

Convertol Process

Efficient method removes usable coal from high ash slurries.

by A. H. Brisse and W. L. McMorris, Jr.

IN the last several years the coal industry has intensified its effort to solve the growing problem of cleaning and recovering fine mesh coals. On one hand there has been increasing civic pressure for cleaner streams, and on the other hand there has been increasing production of fine mesh coal, resulting directly from adoption of the modern mining methods so essential to the economy of the coal mining industry.

Cleaning fine coal with the same precision possible with coarser coals is a difficult task, and for coals finer than 200 mesh it has been impractical. Furthermore, the inclusion of —200 mesh material in the final product markedly increases costs of dewatering and thermal drying, which are necessary steps if coal is to meet market requirements. Consequently these extreme fines have generally been wasted. As a result, problems have been created in many districts because there has not been enough area for adequate settling basins.

Wasting of coal in the —200 mesh slimes may account for a loss in washer yield equivalent to 2.0 to 2.5 pct of the raw coal input. With rising mining costs the value of such a loss is constantly increasing and a need for a better solution to the fines problem becomes more pressing every day. From an operating viewpoint, also, continuous removal of extreme fines from the washing plant circuit permits good water clarification practice, improving significantly the overall cleaning efficiency.

The obvious desirability of recovering a commercially acceptable coal from washery slimes prompted U. S. Steel Corp. to investigate the merits of the Convertol process developed in Germany.*

* U. S. Pat. 2,769,537. Other patents pending.

Although this process has been used commercially in Europe for some time, little if any consideration has been given to its possible adoption in the U. S. until very recently.

Fundamentals of the Convertol Process: In the Convertol process, droplets of dispersed oil are brought into intimate contact with the solids suspended in the coal slurry to be treated. This contact causes oil to displace the water on the surface of the coal by preferential wetting, or phase inversion, after which the coal particles are allowed to agglomerate in a manner permitting their removal from the slurry by centrifugal filtration. The clay and other particles of mineral matter suspended in the slurry do not have the affinity for oil the coal particles have. Consequently the oil treatment is preferential to coal to the extent that more than 95 pct of the oil used reports with the clean coal recovered.

Figs. 1 through 3 will clarify the steps involved in the process. Fig. 1 shows the suspended material in the slurry to be treated, which is a thickened product containing 40 to 45 pct solids. Oil is now injected into the slurry under vigorous agitation to produce good oil to coal contact conditions, which result in preferential oiling of the coal particles. These coal particles are then permitted to agglomerate by gentle stirring in a conditioner to form flocs, as shown in Fig. 2. At this point in the process the agglomerated oiled coal can be washed and partially dewatered on a vibrating screen, as shown in Fig. 3. Finally, the washed flocculate can be further dewatered in a high-speed screen basket centrifuge or in a solid bowl centrifuge.

Commercial Application of the Convertol Process in Germany: The original Convertol process was developed by Bergwerksverband zur Verwertung von Schutzrechten der Kohlentechnik, G.m.b.H., a German research organization controlled by the Coal Operators Assn. of the Ruhr Valley. The process as reduced to commercial practice in Germany[1] is shown in Fig. 4. In this process a thickened slurry (40 to 45 pct solids) mixed with a predetermined percentage of oil is fed from a surge tank to the phase inversion mill. After the phase inversion step, the slurry is usually discharged directly to a high-speed screen centrifuge. From 3 to 10 pct oil is used, depending on type of oil, size consist of coal to be recovered, and operating temperature.

The top size of fine coal cleaned in Germany by the Convertol process is limited by the size of the openings in the centrifuge screen basket. Any mineral matter coarser than the basket opening, which is generally 60 to 80 mesh, must remain with the oiled coal. If the coal fines have been effectively cleaned down to about 80 mesh, the cleaning performance of the process is practically unaffected by the presence of coarse coal particles. However, since recovery of coal much coarser than 80 mesh is more economical by conventional methods, it normally becomes more costly to allow substantial percentages of this coarse coal in Convertol process feed. Where the general plant layout does not permit effective cleaning of coal sizes down to 80 mesh or lower, there is some justification for a coarser Con-

A. H. BRISSE and W. L. McMORRIS, JR., Members AIME, are, respectively, Chief Research Engineer and General Manager, Coal Preparation and Distribution, U. S. Steel Corp., Pittsburgh.

TP 4698F. Manuscript, May 13, 1957. New Orleans Meeting, February 1957.

vertol feed. For example, in one of the German plants visited, the Convertol process was in use for cleaning of —28 mesh coal that had been screened from a ½ x 0-in. jig washed coal. In the slurry fed to the phase inversion unit, the material in the 28 to 80-mesh range still contained some free mineral matter which the Convertol process in its simplest form of application could not remove. In this particular plant, therefore, three flotation cells were added to the circuit between the phase inversion process and the centrifuge. Frothing air was eliminated, but the mass of oiled coal was floated away, as is done in a bulk oil process, while the coarser mineral grains settled out as tailings. The float product from the cells was then fed to the basket centrifuge for dewatering. This added flotation step was included in the circuit in such a way that it could be used or not, depending on market specifications of the coal being produced at the time.

The phase inversion mills used in the German applications of the Convertol process, manufactured by Ludwig Pallmann A. G. or by the Eirich Co., resemble the rotary plate type of grinders available in the U. S. The chief difference is that the German Convertol mill, so-called, is carefully machined to provide extremely close clearances in the rotating mixing chamber, wheras the American-made rotary plate grinder makes use of cast grinding plates without particular attention to close clearances. Fig. 5 is a view of the interior of the Pallmann phase inversion mill as used in the pilot plant.

The high-speed centrifuges employed in Germany for dewatering the Convertol product are centrifugal filters in which the bowl is slotted and backed up by a very fine mesh screen. Fig. 6 shows a unit with the hood removed. In general, they resemble scaled-down models of the CMI or Rheinevelt centrifugal driers common in the U. S. In the German units the conical slotted bowl, which is about 14 in. diam at the base and 7 in. diam at the top, is driven at approximately 2800 rpm. Capacity of these units is 3 to 4 tph of dewatered product. The most successful screen cloths currently used are made of electrolytically deposited sheet nickel 0.013 in. thick, in which formed round conical (nonblinding) holes about 0.01 in. diam are spaced in a rectangular pattern of 10 holes per cm. The life of such screens varies from 40 to 100 hr, depending on throughput and quality of the finished Convertol product. With high percentages of pyrite and refuse in this product, screen life is relatively low.

Although work is actively under way in Germany to develop larger high-speed basket centrifuges, to the authors' knowledge such units have not been put into commercial use.

Most German Convertol installations are processing a thickened slurry of 40 to 50 pct solids analyzing 15 to 18 pct ash (dry basis), containing 55 to 65 pct —200 mesh material with a top size of about 100 mesh. The recovered product usually contains 5 to 6 pct ash and 6 to 10 pct oil (dry basis). Moisture of the product is 15 to 20 pct and ash content of the dry refuse 60 to 70 pct.

Recent improvements in the German process aroused interest in this country, and there were several inspections of German installations. As a result a Convertol pilot plant capable of recovering 3 to 5 tph fine coal from a slurry containing 35 to 45 pct solids was placed in operation late in 1955 at the central cleaning plant of U. S. Steel Corp. at Gary, W. Va. This experimental unit was a duplicate of the Convertol plants as used in Germany. The phase inversion mill was manufactured by the Ludwig Pallmann A. G. and the screen basket centrifuge was supplied by Siebtechnick Co., also in Germany.

For the first several months of operation the process steps and equipment were similar to those used in Germany, with the addition of a Denver conditioner inserted in the process sequence between the Pallmann phase inversion mill and the super centrifuge as shown in Fig. 7. Results obtained were highly satisfactory. Initial slurry feed consisted of 40 pct —200 mesh and 30 pct +100 mesh with a small percentage of material above 48 mesh. This feed material, containing 14 to 16 pct ash and 0.70 pct sulfur (on a dry basis), was obtained from the thickener underflow as shown in Fig. 7. About 80 pct of this material was recovered as coal containing approximately 9.5 pct ash, 0.70 pct sulfur, and about 20 pct moisture. Such a recovery required 3 to 5 pct oil (based on total dry solids in the feed) depending on viscosity of the oil. Maintaining a slurry feed rate of 35 gpm, the amount of coal recovered varied between 3 and 4 tph of dry product. The product was a fluffy, easily handled material from which no moisture could be removed by hand squeezing.

Under the above conditions, it was found possible to operate the centrifuge with a given screen to recover about 100 tons of product without any undue change in recovery percentage. Operation beyond

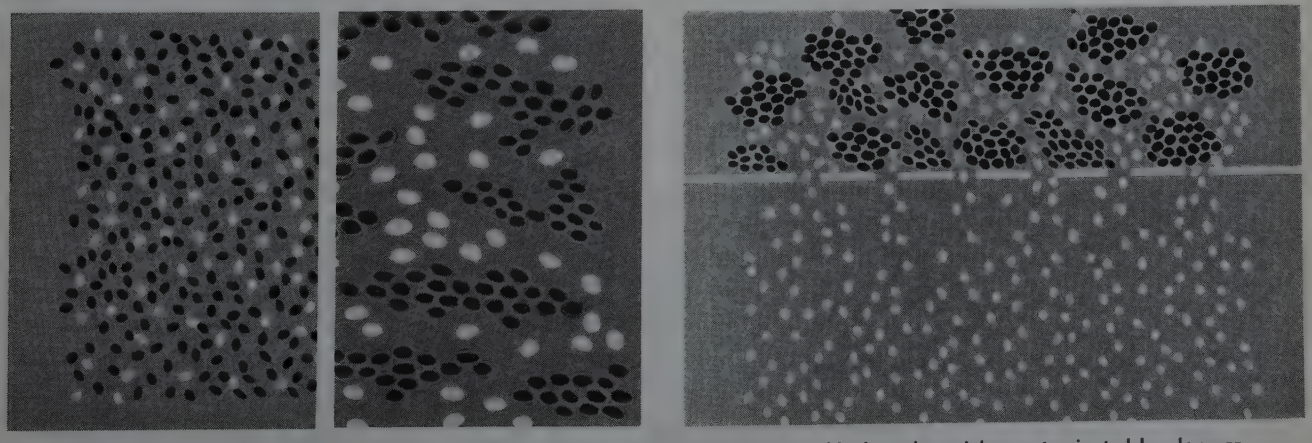

Fig. 1 (left)—Thickened slurry feed to Convertol process. Shown in proportion are black coal particles contaminated by clay particles (white) in suspension in plant water. Fig. 2 (center)—Oiled coal particles agglomerate in flocs. Sketch shows flocculated coal as it is gently stirred in conditioner. Fig. 3 (right)—Flocculated oiled coal being washed on vibrating screen. Under ideal conditions coal agglomerates are retained on screen cloth while clay particles (white) are washed away.

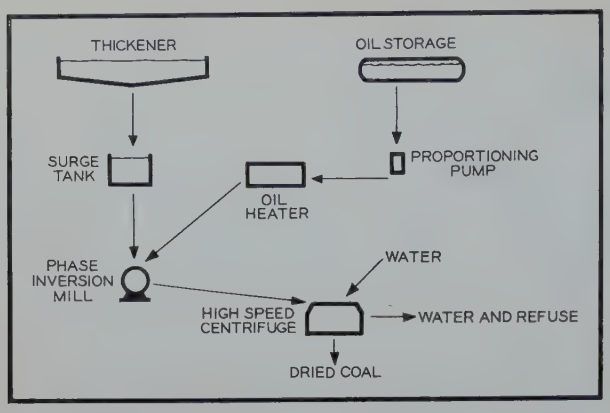

Fig. 4—Typical German Convertol plant.

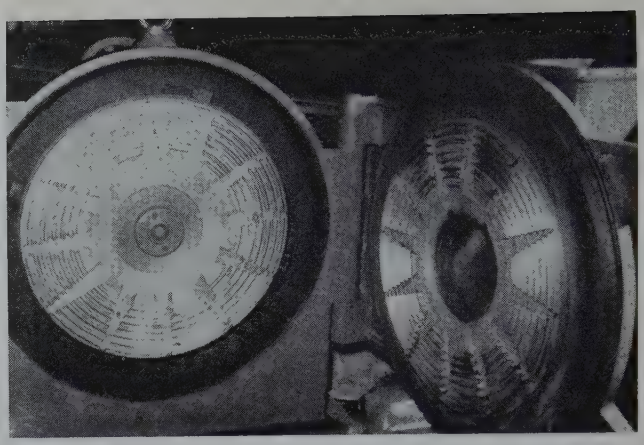

Fig. 5—Interior view of Pallmann phase inversion mill. Feed opening can be seen in center of fixed disk at right. Disk at left is driven.

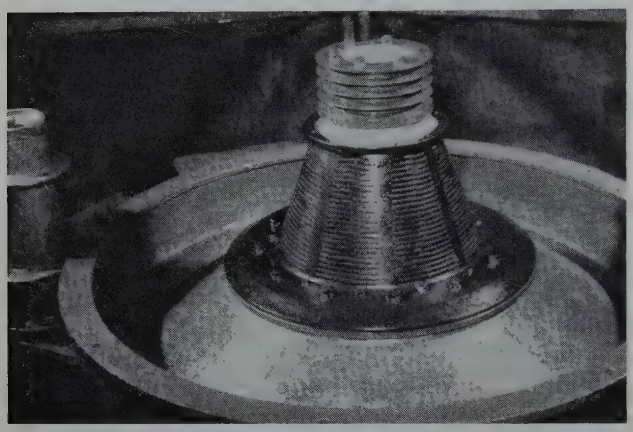

Fig. 6—High-speed screen centrifuge with hood removed. Conical section below belt pulley is the slotted bowl into which screen is fitted. Unit is fed through center of pulley.

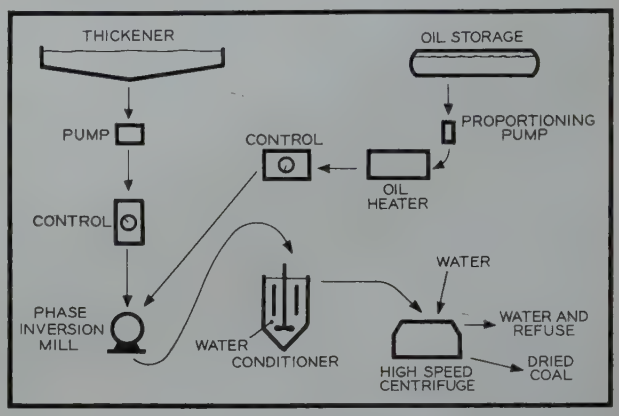

Fig. 7—Original Convertol pilot plant, Gary, W. Va.

this point resulted in a rapidly decreasing rate of recovery, as shown in Fig. 8. This loss in recovery was caused by the gradual increase in the size of the screen perforations due to wear, and it is evident from Fig. 8 that these perforations reach a critical size after approximately 100 tons of throughput. At this point in the life of the screen, the flocculated coal particles appear to pass freely through the basket. The frequency with which it becomes necessary to change these basket screens and their relatively high cost were two important factors that led to investigation of other methods of dewatering the product.

After several months of operation, the plant water circuit was modified to permit partial classification of thickener feed. This change eliminated much of the coarser material that previously found its way into the feed to the pilot plant. The size consist of the solids in the new feed now revealed 60 to 65 pct material smaller than 200 mesh, with 20 to 25 pct +100 mesh and a negligible percentage of material above 48 mesh. Ash content in the feed solids now leveled off at about 19 pct. As a result of these changes, operating characteristics of the unit were materially changed. Although the product remained fluffy and relatively dry, its ash content was noted to rise to about 10.5 pct and its moisture content to 25 pct. Oil requirements rose to a range of 6 to 8 pct of the dry solids input. This rise in oil requirement was expected in view of the great increase in specific surface of the solids to be oil-coated, as reviewed in Fig. 9. In the size range under consideration, it can be seen that specific area increases rapidly with decreasing particle size.

Whereas formerly material from the conditioner was of firm consistency, the changes in feed conditions noted above resulted in a material that was thinner and more fluid as discharged from that unit. This change was accented by further modification of the washing plant water circuits which eliminated nearly all the +100 mesh material from the thickener feed. This last change further reduced feed particle size and increased the dewatering burden on the high-speed screen centrifuge. The strain on this unit was almost immediately made apparent by continual plugging of the perforated screen and accompanying increase in replacement frequency. At this stage of the project it was decided to investigate alternate ways to dewater the Convertol product.

The process sequence was then modified by substituting for the screen centrifuge a vibrating screen followed by a solid bowl centrifuge, as shown in Fig. 10. In this sequence the oiled coal agglomerate is washed with fresh water to remove as much clay and mineral matter as possible prior to its centrifugation in the solid bowl unit.*

* Patent applied for.

At the time this new process sequence was placed in operation, the slurry feed contained over 80 pct −200 mesh material analyzing 24 pct ash and 0.70 pct sulfur (on a dry basis). However, use of the solid bowl centrifuge eliminated the costly down time due to changing screens in the original centrifuge. Further, output of the pilot plant has been raised from 3 to 4 tph to about 7 tph dry product. The material recovered contains approximately 11 pct ash, 0.70 pct sulfur, and 25 pct moisture. Product

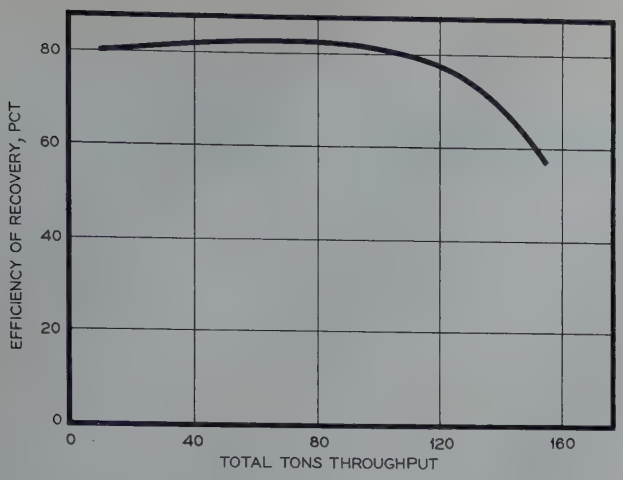

Fig. 8—Typical screen performance for Convertol process.

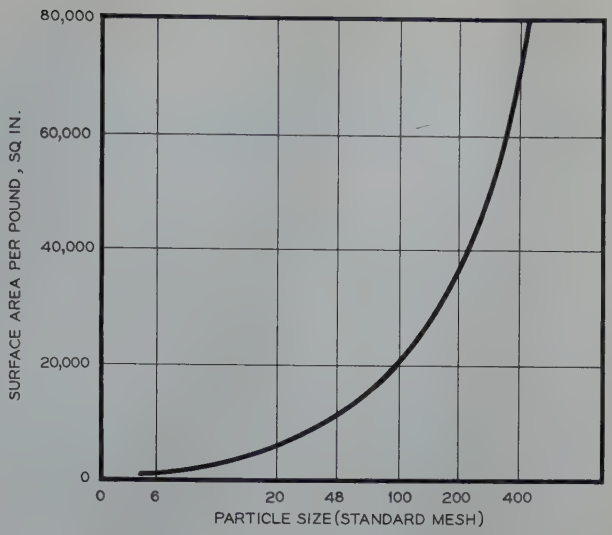

Fig. 9—Particle size vs surface area of coal.

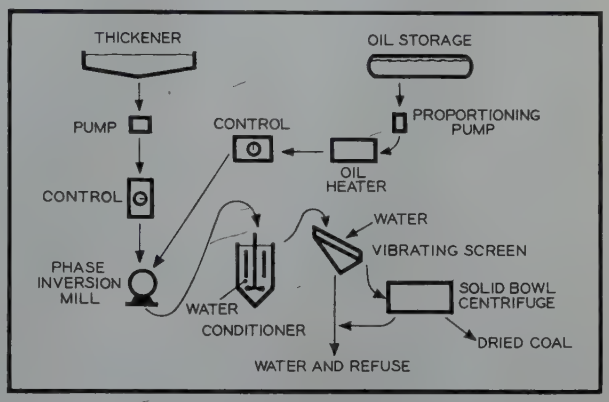

Fig. 10—Modified Convertol pilot plant, Gary, W. Va.

recovery is about 80 pct. This recovery requires injection of oil in the amount of 5 to 8 pct of dry solids input, again varying with the type of oil used.

Experience to date indicates that oils vary considerably in the effectiveness with which they can be used in the Convertol process. For example, kerosene will effect phase inversion very rapidly when present in small percentages (2 to 6 pct of the product) at room temperature, whereas the heavy oils such as Bunker C and other petroleum residues will effect phase inversion at much slower rates and only when present in higher percentages (8 to 10 pct) and heated to relatively high temperatures (200 to 250°F). The rate of phase inversion obtained with these oils appears to be principally a function of oil viscosity, which explains the general effect of temperature on phase inversion rate exhibited by the heavier petroleum oils. However, it appears that these heavier oils yield a product that is somewhat more strongly agglomerated than is the case when the lighter petroleum oils are used. These stronger agglomerates can obviously be washed and otherwise processed more vigorously than the weak ones and are thus more desirable as an end product.

The more common tar oils have not been found very satisfactory in the Convertol process. Their limited use has indicated the needed percentages to be excessive (over 20 pct of the product) and recovery of coal to be most unsatisfactory. Work with these oils is now in progress in the hope that further data may point to conditions that will permit their use economically.

On the basis of results obtained with the process as described above, a second unit is being installed at the washing plant of the Robena mining operations of U. S. Steel Corp. in Greensboro, Pa. All equipment used at Robena is American-made. It is hoped to obtain experience with this newer unit using slurries typical of those currently produced during washing of coals found in that district. It will also be possible to make a good unit-by-unit comparison between the American and German equipment available to construct Convertol plants.

In any consideration of the economics of using Convertol, it must be recognized that the cost of producing enough raw coal to supply an additional ton of washed product may sometimes compete with the cost of a ton of coal recovered by the Convertol process. Nevertheless, the Convertol process permits maximum extraction of usable coal from existing reserves. In the long run, this factor is extremely important. Further, where settling pond areas are inadequate, recovery of 60 to 80 pct of the solids normally wasted in such ponds is of economic value because it conserves usable ground space.

It should also be pointed out that oil present in the Convertol product has a greater value to the coke plant operator than is indicated by its heating value alone. Because this oil is reformed into organic chemicals, similar to those normally recovered from the coking process,[1] its use to recover coal for metallurgical purposes is economically sound. When the coal product is destined for markets other than metallurgical coke-making, the economic feasibility of the Convertol process must obviously be considered in terms of the factors involved.

In general, the Convertol process has been found extremely effective for removing usable coal from high ash slurries. The product obtained is fluffy and non-dusting and therefore easily mixed with the plant washed product. Certain refinements must still be made in control of the process to permit maintenance of high recoveries with minimum oil consumption under all conditions, including occasional washing plant operating emergencies. It must be stressed, however, that since oil consumption is primarily a function of feed size consist and oil type, the most economic mode of operation of the Convertol process is obviously related to the conditions under which it is to be used.

Reference

[1] K. Lemke: The Cleaning and Dewatering of Slurries by the Convertol Process. Second International Coal Preparation Congress, Essen, 1954.

Discussion of this paper sent (2 copies) to AIME before March 31, 1958, will be published in MINING ENGINEERING.

Geology of Toquepala, Peru

by Kenyon Richard and James H. Courtright

TOQUEPALA is a porphyry copper deposit in which mineralization is localized by a large breccia pipe formed in close genetic relation to intrusive rocks. The deposit is in southern Peru, 55 airline miles north of the small city of Tacna and the same distance inland from the port of Ilo. Quellaveco and Cuajone, geologically similar deposits, lie 12 and 19 miles north of Toquepala. Chuquicamata is 400 miles to the south.

The deposit is high on the southwestern slope about 20 miles from the crest of the Cordillera Occidental of the Andes Chain. It lies in a mountainous desert where the steep southwesterly slope of the Andes is dissected by a succession of rapidly downcutting, deep canyons. Local topography is moderately rugged with a dendritic drainage pattern and an elevation of 8000 to 14,000 ft. Volcanic peaks along the crest of the Cordillera rise over 19,000 ft.

Local precipitation, including a little snow, amounts to about 10 in. during January and February, but general runoff in the region is slight. Throughout southern Peru the springs and streams are widely separated. Crude canals irrigate small farms on terraced slopes along the streams and provide sparse subsistence to the semi-nomadic inhabitants.

During the past decade, engineering and geological explorations of the region, as well as the mineral deposits themselves, have required construction of a network of several hundred miles of roads. Before this, roads extended only a few miles inland. Many areas still can be reached only by trail.

Toquepala was briefly described in 19th century geographical literature as a copper deposit, and it received desultory attention from Chilean prospectors early in the present century. It was first recognized as a mineralized zone of possible real importance by geologist O.C. Schmedeman during an exploration trip for Cerro de Paso Copper Corp. in 1937. The discovery was late as compared to earlier recognition of Chuquicamata, Potrerillos, and Braden of Chile and Cerro Verde of southern Peru. This was due partly to the region's difficult accessibility but principally to the obscure character of the outcrop evidence of copper.

From 1938 until 1942 Cerro de Pasco Copper Corp. partially explored the deposit by adits and diamond drillholes. This campaign was supplied by a 60-mule pack train continuously shuttling over a 30-mile trail. Northern Peru Mining & Smelting Co., a wholly owned subsidiary of American Smelting & Refining Co., undertook regional engineering studies in 1945 and drill exploration in 1949. According to published data[1] the deposit contains 400 million tons of open pit ore averaging a little over 1 pct Cu. It is currently undergoing large-scale development by Southern Peru Copper Corp., which is owned by American Smelting & Refining, Phelps Dodge, Cerro de Pasco, and Newmont Mining.

K. RICHARD and J. H. COURTRIGHT, Members AIME, are Geologists with American Smelting & Refining Co., Tucson, Ariz.
TP 4643I. Manuscript, June 7, 1957. New Orleans Meeting, February 1957.

Summary of Geology: The deposit is situated in a terrane composed of Mesozoic(?) and Tertiary volcanic rocks intruded by dioritic apophyses of the Andean Batholith. These formations are exposed in a northwesterly trending belt about 15 miles wide. Along the northeast they are unconformably overlain by Plio-Pleistocene pyroclastic rocks, which occupy much of the crest of the Andes, and along the southwest they are covered by the Moquegua formation of Pliocene(?) age.

The mineralized area, oblong in shape and about 2 miles long, has been a locus of intense igneous activity. Several small intrusive bodies having irregular forms occur within and adjacent to a centrally located, large breccia pipe. The mushroom-shaped orebody consists of a flat-lying enriched zone of predominant chalcocite with a stem-like extension of hypogene chalcopyrite ore in depth within and around the pipe.

This breccia pipe is relatively large and has been formed by repeated episodes of brecciation. Small satellitic pipes occur at random within a 2-mile radius of this central pipe. These too were individual sourceways of mineralization, although not always of ore grade. Within and around the zone of breccia pipes and mineralization there are a few faults and veins, but these are discontinuous random structures of minor significance. There are no regional or local systems of faults or other planar structures recognized which could account either for the mechanical development of the breccia pipes or for their localization as a group or as individuals.

Hydrothermal alteration is pervasive in the zone of mineralization. Clay minerals appear to be abundant in places, but their percentages are undetermined. Quartz and sericite are the principal alteration products, and in many instances original rock textures are obliterated. The principal sulfides, hypogene pyrite and chalcopyrite and supergene chalcocite, occur mainly as vug fillings in the breccia and as small discrete grains scattered through all the altered rocks. Sulfide veinlets are relatively scarce. Sulfides are more abundant and alteration is more intense in certain rock units, such as the diorite and most of the breccias.

Although the Toquepala mineral deposit is similar in most respects to the porphyry copper deposits of southwestern U. S., it most closely resembles the Braden deposit of Chile, as described by Lindgren

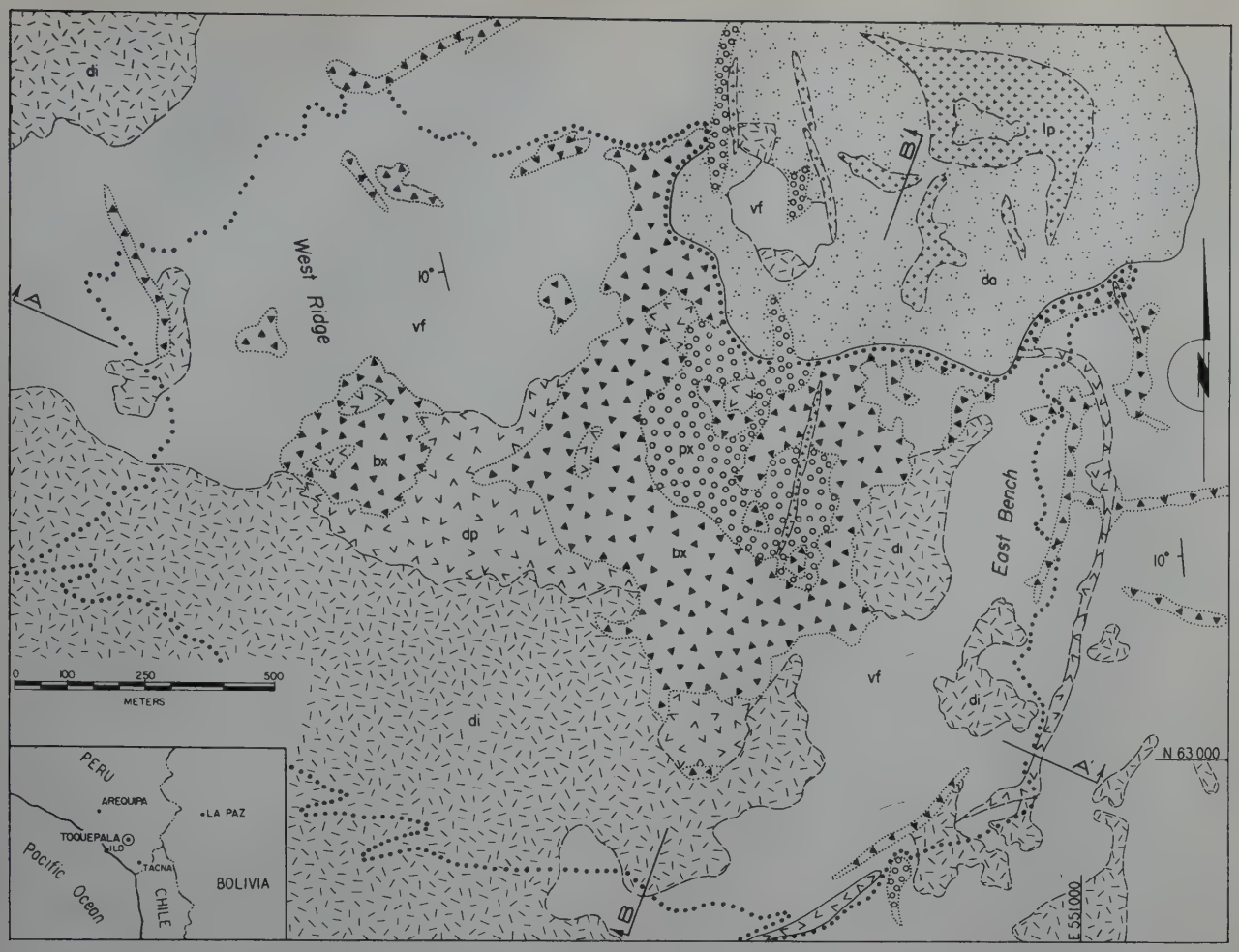

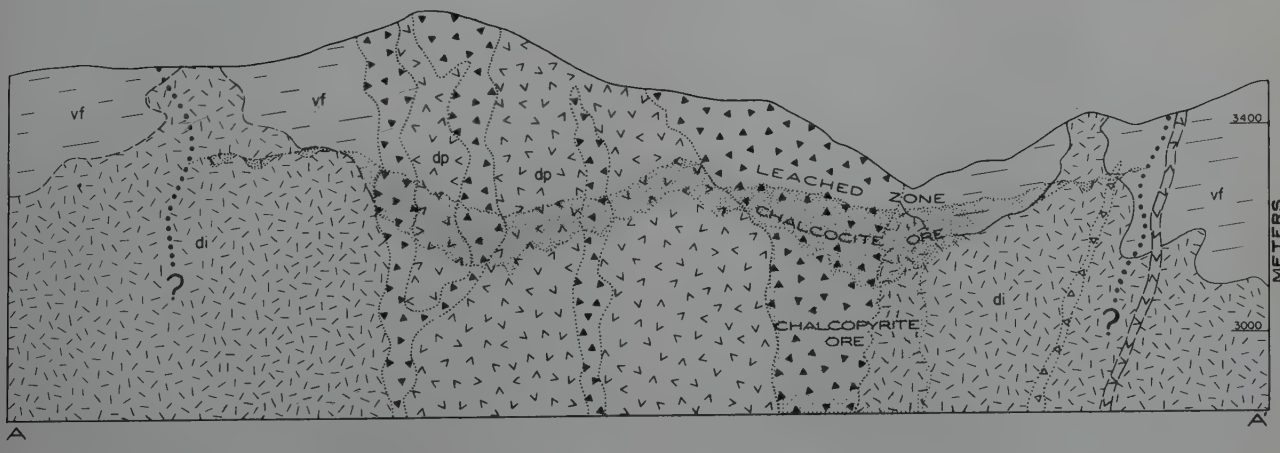

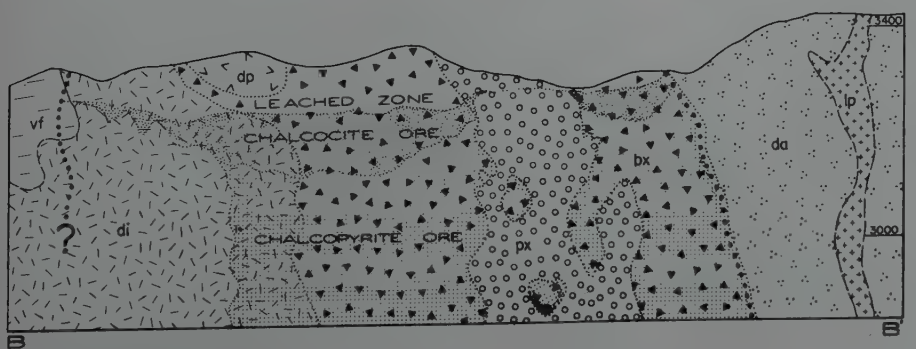

LEGEND

- LATITE PORPHYRY
- PEBBLE BRECCIA
- DACITE AGGLOMERATE
- ORE BRECCIA
- DACITE PORPHYRY
- DIORITE
- VOLCANIC FLOWS
- OUTLINE OF HYDROTHERMAL ALTERATION ZONE

TOQUEPALA GEOLOGIC MAP AND SECTIONS

and Bastin.[2] Judging from their statements on the forms and textures of the breccias and their postulations of age relationships, the intrusives, the breccias, and the mineralization of Braden have many counterparts at Toquepala.

Rock Units and Structure: Layered volcanics having a total thickness of more than 5000 ft are the oldest rocks in the area. The lowermost unit is a massive, rhyolitic flow with an exposed thickness of 500 ft, locally named the Quellaveco formation. Its base has not been observed. Lithologically and structurally this formation is similar to the rhyolite porphyry at Cuajone, which Lacy[3] has tentatively assigned to Late Cretaceous. The volcanic sequence, with the various field names assigned, is as follows:

Name	Thickness, Ft	Character
Alta series	3000+	Mainly pyroclastics and ignimbrites
Toquepala series	1500+	Mainly rhyolite and andesite flows (?)
Major Unconformity	—	—
Quellaveco quartz Porphyry	500+	Rhyolite porphyry flow

Gentle folds occasionally are seen, but regional dips of 5° to 10° SW are persistent. Lenticularity of certain horizons has been noted within the Alta and, more particularly, the Toquepala series. This is explained by minor erosional disconformities. On structural and lithologic grounds the Alta and Toquepala series may correspond to the Tacaza volcanics (Tertiary) of Jenks[4] and Newell.[5] These men have recognized the erosional interval between the Sillapaca and older Tacaza volcanics as an important one in southern Peru and a correlative of McLaughlin's *Puna* surface.[6] This surface is described as "late mature" or "old age."[4] High accordant summits representing this surface are seen a few miles north of Toquepala. Projected to Toquepala this surface may have existed only a couple of hundred feet above the present highest point of the modern surface over the orebody. This *Puna* surface is believed to have played an important part in the enrichment history at Toquepala.

In the Toquepala region apophyses of the diorite batholith of the Andes intrude the Quellaveco, Toquepala, and Alta volcanics and comprise half the surface exposures within a radius of several miles of the mine. Contacts with the flow rocks are discordant and usually sharp but sometimes gradational. There are small-scale irregularities in the shape of the contact, but dikes of diorite are not seen. Composition of the diorite varies somewhat, but a consistent border facies is not apparent. The volcanics seldom show any special, well-defined contact effects, due either to metamorphism or structural disturbance, although throughout they have undergone a very low grade, uniform metamorphism. It is inferred that the diorite batholith underlies the entire locality and that it was implaced mostly by assimilation rather than injection.

Within the zone of hydrothermal alteration, the volcanics and diorite are intruded by small stocks and dikes of dacite porphyry. This formation is not found elsewhere in the region. The stocks are steep-sided and notably irregular in shape, although one dike forms an even quarter-ring near the southeast edge of the alteration zone. The form, composition, and spatial connection with the disseminated copper mineralization suggests correlation between this formation and the monzonites of the porphyry copper deposits of western U. S.

A rock termed *dacite agglomerate,* with the same composition and texture of matrix as the dacite porphyry, intrudes a large volcanic neck and marks the north edge of the ore zone. This intrusive contains abundant small inclusions of dacite porphyry and other material and a few large sunken blocks. The writers class this rock unit as an agglomerate and not a breccia.

The youngest intrusive formation is a group of aphanitic porphyries ranging in composition from andesite to latite and named *latite* porphyry. They are post-mineral in age. They sometimes occur as small stocks, but mainly as steep dikes. Although most of these intrusive bodies are found within the neck of dacite agglomerate, a small swarm of thin latite porphyry dikes extends southward into the ore zone.

Fractures: Numerous small faults and quartz-tourmaline-sulfide veinlets of random orientation are scattered through the orebody, but these are appreciably less abundant than in most deposits of this type. Sulfide veins more than 3 in. wide are rare. In only one locality—the southern and southeastern area lying inside the dacite ring dike—is a system of parallel fractures evident. This system of close-spaced veinlets has a trend parallel to the ring dike, being arranged concentrically around the main breccia pipe and dipping steeply toward it.

A few post-mineral faults are present, but these are only minor features in the structural pattern. Displacements of a few feet were noted on two faults cutting layered volcanics along the west edge of the zone of alteration. Elsewhere fault planes with a few inches of gouge were occasionally observed, but nowhere in the district do relationships indicate displacements of consequence. This lack of major faulting is clearly evidenced by the undisturbed continuity of marker flows in the region.

Breccias: The writers restrict the term *breccia* to formations composed *entirely* of fragmental material in which the fragments have been rotated and displaced, in contrast to rock that has been merely intricately jointed, and also to rock that was emplaced in a fused condition.

As shown on the geologic map and sections, there are two main types of pipe breccia, termed *ore* and *pebble* breccia, which are texturally distinct and have somewhat different modes of formation. The pebble breccia is characterized by rounded fragments, whereas the ore breccia is made up essentially of angular fragments. The matrix of the ore breccia is largely composed of quartz, tourmaline, and sulfides, whereas that of the pebble breccia is a sandy, mud-like material with disseminated rather than vuggy mineralization. In texture and color the pebble breccia closely resembles a freshly broken surface of sidewalk concrete.

Commonly the ore breccia fragments are all of the same rock type, corresponding to whatever formation lies immediately adjacent, but the main breccia mass contains a large central portion that is characterized by heterogeneity of rock type. Apparently this core of mixed rock fragments represents the conduit within which the most violent disturbances took place, and the surrounding breccia represents the shattered periphery of the pipe, although rotation of fragments is evident in the shattered zone as well as within the central conduit. The outer margins of the breccias in places are indistinct, suggesting that there was a gradual transition to undisturbed rock.

As evidenced by textural features, ore-type brec-

ciation took place in a number of episodes, both before and after intrusion of the dacite porphyry.

The mechanics of formation of the Toquepala ore breccia are uncertain, as is the case with most mineralized breccia pipes. However, the occurrence of large masses of angular, mixed fragments without evidence of melting and in an environment essentially free of faulting indicates an origin related to gaseous explosion. Evidence suggests that the process was episodic. First, there may have been a leak of gas to the ground surface, possibly along a joint system. This leak may have triggered an explosion that evacuated a small tube—a diatreme. Then the tube was filled by avalanching of the walls. Repeated explosion, partial evacuation, and avalanching could then have increased the horizontal dimensions of the pipe to its present large diameter.

Since the pebble breccia consists of hard pebbles in a matrix of rock flour, it would seem to have been produced by a milling action in which the rock fragments were semi-suspended in an actively circulating medium such as water or gas. In this state this pebble breccia may have had *instrusive* mobility, although portions of it may also have been formed more or less in place.

Although appearing on the map as a single unit cutting all formations except latite porphyry, pebble breccia actually consists of *intrusions* of at least two, and possibly three ages. The mapped outline marks, for the most part, a young pebble breccia. The pebble dikes cutting the dacite agglomerate may be still younger. Existence of an earlier breccia of the pebbly type is indicated by inclusions of a pebble breccia with a mud-like matrix *in* ore breccia. Because hybrid ore breccia has indistinctive textures and because its distribution is not accurately known, it has not been differentiated from typical ore breccia on the geologic map. It occurs around the pebble pipe, possibly in large masses, and it may constitute deeper portions of the pebble pipe itself.

Late in the sequence of brecciations, a large explosion vent was formed and filled with intrusive dacite agglomerate containing large sunken masses of older flow rocks and diorite. This activity removed a large portion of the main breccia pipe.

Alteration-Mineralization: The mineral deposit is areally defined by hydrothermal alteration of all rocks, except latite porphyry, within an elliptical zone enclosing the orebody, as shown on the geologic map and sections. The transition to unaltered rock around the margins is gradational rather than sharp, and several small areas of alteration occur outside the main zone. In contrast to most porphyry copper orebodies, which are surrounded by large alteration zones, the Toquepala zone is only slightly larger than the orebody.

The hydrothermal alteration products—chiefly assemblages of quartz, sericite, and clay—are those characterizing most deposits of the porphyry copper type. Sulfides impregnate all altered, unleached rocks. A major portion of the alteration zone of Toquepala is considered to be *strongly* altered and is characterized by almost complete conversion to quartz and sericite-clay and partial to complete destruction of original rock textures.

Weaker alteration facies occur mostly near the edges of the deposit away from the breccias. Prior to leaching and enrichment, the areas of stronger alteration contained more sulfides in general and more chalcopyrite in particular.

The most pronounced alteration effect is found in the diorite. The fresh rock is composed of feldspar, ferromagnesian minerals, and minor quartz with a medium granotoid texture, whereas the altered rock consists of a sugary mosaic of quartz and sericite. In contrast, the dacite porphyry usually retains remnants of original texture, the alteration products being more argillic.

As in many deposits of this type, the principal hypogene sulfides are pyrite and chalcopyrite, with very minor amounts of such minerals as bornite, molybdenite, and sphalerite. The history of mineralization-alteration at Toquepala, however, is more complex than the average. Earliest mineralization consisted of abundant tourmaline and quartz with minor sulfides. Later, but prior to the intrusion of dacite porphyry, deposition of sulfides and quartz with minor tourmaline began. This continued, with successive interruptions by periods of brecciation and by intrusions. Late in this sequence the formation of the dacite agglomerate-filled vent removed the northeast portion of the ore zone. Subsequent alteration-mineralization was weak, as shown by the feeble nature of its effect on agglomerate.

Irrespective of rock types involved, the ore breccia contains the strongest mineralization. The hybrid ore breccia is somewhat weaker in hypogene copper content, probably due to its mud-like, less permeable matrix. The pebble breccias are still weaker, for the same reason, but contain about the same amount of hypogene copper as does the average protore outside the breccia zone. Among the unbrecciated rocks, diorite was the most receptive and the flow rocks the least. A portion of the dacite porphyry is well mineralized, but elsewhere—particularly around the southwest side of the main breccia pipe—it is low in copper.

Enrichment: The chalcocite zone, a major part of the open pit orebody, ranges from 500 ft in thickness in the interior to only a few feet on the fringes. Although irregular in detail its upper surface has a generally flat-lying, sharp contact with the leached zone above. The lower limit is indistinct, the transition to clean primary mineralization being almost imperceptible, except in a few instances where the chalcocite terminates abruptly against a gouge slip or a post-ore dike. The highest grade chalcocite ore was formed by enrichment of the zone of stronger primary mineralization, the surrounding protore being overlain by chalcocite ore of moderate grade.

As indicated on Section *B* of the accompanying map, only a negligible amount of enrichment occurred in the pebble breccia. The relative impermeability to supergene solutions is evident in the rise in the base of oxidation and the abrupt pinching of the chalcocite zone at the periphery of the pebble pipe.

The leached outcrops at Toquepala are similar in many respects to those found over other porphyry copper orebodies. Certain anomalous features exist, however. Limonite-after-chalcocite with characteristic color and texture is present, but its distribution in the outcrops reflects only in part the amount of chalcocite below. The most abundant development of this limonite occurs high on canyon walls and along ridge crests 600 to 1000 ft above the top of the chalcocite zone. The leached rock intervening, in drillholes as well as in outcrops, appears originally to have contained little other than low grade primary mineralization—ex-

cepting the main breccia pipe, which for the most part shows outcrop evidence of strong primary mineralization. The high-lying horizon may represent a relatively ancient chalcocite zone—one that formed below the water table of a pre-existing, mature erosion surface. It is suggested that this may have been the *Puna* surface.

Over most of the ore area the leached zone contains only about 0.10 pct Cu in an unidentified form. This zone represents essentially complete leaching down to the sharp-line contact with the top of the chalcocite zone. There is no *mixed* zone of copper silicates, oxides, and sulfides. However, minor amounts of copper silicates are seen in surface outcrops in some of the less strongly altered areas, particularly near the fringe of the zone of alteration.

In most enriched copper deposits, the supergene chalcocite blanket seems to have migrated downward to its present position through progressive stages of leaching and precipitation, leaving behind a more or less continuous record of diagnostic limonites. At Toquepala the paucity of such limonites in several hundred feet of leached capping above the base of oxidation can best be explained by assuming a relatively rapid and *permanent* drop in the water table to somewhere near its present level just above the present base of oxidation. Under such conditions the copper derived by leaching of the ancient chalcocite blanket, and the primary chalcopyrite immediately underlying it, would have been carried down in solution until it reached the reducing environment at the water table. Here accumulation of the present chalcocite orebody took place. Subsequently erosion cut deeply into the capping, forming the modern topography without modification of the chalcocite orebody.

Acknowledgments

Thanks are due the Southern Peru Copper Corp. and the American Smelting & Refining Co. for permission to publish this article.

References

[1] *Mining World*, February 1955, p. 71.
[2] W. Lindgren and E. S. Bastin: The Braden copper deposit, Rancagua, Chile, in *Copper Resources of the World*, 16th International Congress, 1935, vol. 2, p. 459.
[3] W. C. Lacy: Personal communication.
[4] W. F. Jenks (Editor, *Handbook of South American Geology*): *GSA Memoir 75*, 1956.
[5] N. D. Newell: Geology of the Lake Titicaca Region, Peru and Bolivia. *GSA Memoir 36*, 1949.
[6] D. H. McLaughlin: Geology and Physiography of the Peruvian Cordillera, Department of Junin and Lima. *GSA Bull. 35*, 1924.

Discussion of this paper sent (2 copies) to AIME before March 31, 1958, will be published in MINING ENGINEERING.

Instrumentation in Ideal's New Houston Cement Plant

by Thomas B. Douglas

INSTRUMENTATION in the process industries can no longer be regarded as a convenience, but rather an absolute necessity. Although many chemical processes must already be conducted with instruments, every properly designed application of automatic process control will improve operation: 1) the product will be more uniform and of higher quality; 2) the manual labor saved will reduce cost; 3) uniformity of flow and uniform control of process will increase production; and 4) surges will be eliminated, making it possible to operate equipment near ultimate capacity at all times.

Industrial instruments fall into two general classifications—those that measure and those that measure and control. The cement industry has been using instruments for a number of years, particularly in the burning process, primarily for indicating and recording. Automatic process control makes additional use of these instruments, and others, to control variables. Assisted by the instrument manufacturers, engineers at Ideal Cement Co. achieved considerable progress in determining how well the usual recording instruments could be made to control various phases of cement-making. The results of these experiments were used to make the new plant at Houston as wholly automatic as possible.

The original Houston plant, built in 1937 by Gulf Portland Cement Co., consisted of only one 8 x 220-ft kiln and the necessary grinding mills and accessory equipment and had a capacity of 900 bbl per day (300,000 bbl annually). Ideal Cement Co. purchased this plant in 1940 and almost immediately started plans to increase its production. In 1941 a 9 x 220-ft kiln was installed and grinding and storage capacity were increased. The growing demand for cement in the Houston area necessitated a third kiln (9 ft 6 in. x 250 ft) in 1947. This brought the plant up to its present capacity of about 1.3 million bbl per year. Calcium silicates in cement are produced in a burning operation at high temperatures from raw mix of argillaceous and calcareous materials that have been crushed, mixed, and ground to a fine powder. The composition of this mixture must be kept consistent within narrow limits. Raw mixing and grinding may be done either wet or dry, but in both instances the materials must be correctly proportioned, finely ground, and thoroughly intermixed before entering the kiln. As the raw mix passes through a long horizontal rotary

T. B. DOUGLAS, Member AIME, is Vice President in charge of Operations, Ideal Cement Co., Denver.

TP 4684H. Manuscript, Jan. 24, 1957. New Orleans Meeting, February 1957.

kiln, first water and then carbon dioxide are driven off. As the temperature increases, calcium silicates are formed by the chemical reactions. The clinker produced in the kiln is cooled and mixed with a carefully controlled amount of gypsum and ground to a very fine powder. This is Portland cement.

Flowsheet of the New Plant: For the calcareous constituent of the mix the Houston plant uses oyster shells hydraulically dredged in Galveston Bay and delivered to the dock in barges carrying about 2500 tons each. As received, these shells contain 95 to 97 pct calcium carbonate. At the new plant the shells are unloaded by a crawler crane with a 4-yd clamshell bucket and dumped into hoppers for transportation to raw mill feed bins or to a storage area. The argillaceous constituent, a clay found nearby, is loaded onto barges by a dragline crane and unloaded with the crawler crane. Since the wet process is used at this plant, the clay, which consists of fine grained particles and thus requires no particular grinding, is merely mixed with water in a wash mill to form a clay slip. Oyster shells and clay slip are proportioned to give a mix containing about 77 pct calcium carbonate and fed into one of two 11 x 32-ft two-compartment ball mills. These mills are driven by 2000-hp motors—to the writer's knowledge the first motors of this size used in a cement plant. Small amounts of other raw materials, such as silica sand or iron ore, are sometimes added at this point to obtain the desired chemical composition. These materials are mixed and ground in the mills to 85 pct passing 200 mesh. The resulting slurry contains about 41 pct water. Slurry is pumped to one of three large tanks, 55 ft diam and 45 ft high, each holding enough slurry for 24-hr operation of the two kilns. From these tanks the slurry is pumped to the feed end of the kilns, into which it is fed at a predetermined rate by a ferris wheel feeder. The kilns are 12 ft diam and 450 ft long and have a slope of ⅜ in. per ft; their top speed is 80 rph and capacity is 4250 bbl per day (360 lb per bbl). Natural gas is used for fuel—about 1.15 million Btu's per bbl. During the 6 hr the raw mix passes through the kilns it is heated gradually to a maximum of 2750°F. As the clinker leaves the kilns it drops into air-quenching coolers 6 ft wide by 100 ft long from which it is discharged at about 100°F. The kilns are equipped with electrostatic precipitators of 99 pct efficiency; thus only 0.06 grains of dust per cubic foot of gas are discharged into the atmosphere. Cooler stacks are equipped with cyclone dust collectors.

Clinker from the coolers is conveyed to one of eight concrete clinker storage silos that also serve as the finish mill feed bins. The interstice bins are used to store gypsum. The clinker and gypsum are proportioned automatically and fed to the finish grinding mills, which are also 11 x 32-ft two-compartment ball mills driven by 2000-hp motors. Each of these mills is close-circuited with two 16-ft air separators. Dust collectors are used in conjunction with these separators to aid in cooling the cement as well as for general dust collection. The finished cement, or fines from the separators, is conveyed to the storage silos by one of two 9-in. Fuller-Kinyon pumps.

Cement is stored in a battery of 21 concrete silos 26 ft diam and 93 ft high and in 12 interstice bins having a total capacity of 216,000 bbl. In the packhouse next to the storage silos there are three packing machines for loading sacked cement in rail cars or on trucks. Facilities are also available for loading bulk rail cars or trucks and for loading barges or boats at the waterfront.

Instrumentation at the Houston Plant: Since the heart of the cement-making process is the kiln, the entire manufacturing process is designed to obtain maximum production through the kilns. At the discharge end of the kilns there is a burner floor where the kiln operations are ordinarily watched visually and with the aid of indicating and recording instruments. Just above the burner floor a central control room has been installed from which the entire process can be controlled, from the raw mills to the finished cement silos. The equipment running lights eliminated from the main control panel have been replaced by a continuous monitor, indicating, and alarm system detecting error signals. Almost all equipment pieces are sequence-operated from a minimum of push buttons at the control panel.

In the raw grinding department the principal variables to be controlled are: 1) proportion of shell to clay, 2) optimum production rate to produce a slurry of the desired fineness, and 3) water content. Continuous sampling of the raw mill product is analyzed hourly to check chemical composition and fineness of the slurry, and the proportion of shell to clay is regulated to maintain the composition within the desired limits. Weighing belt feeders are used for the shell and a ferris wheel feeder for the clay slip. Once the desired ratio is set manually, it is maintained automatically.

After experimentation has determined the optimum feed rate to the mill, the rate will be controlled by a Hardinge electric ear.

At this stage of the process water is added, and the raw grinding is done wet. As the water content has a marked effect on the burning operations and fuel efficiency, it is important that for proper pumpability it be maintained as low as possible and held constant. About three fourths of the water is added at the feed end of the mill—this includes the water in the clay slip—and more water to maintain a constant slurry moisture is added at the discharge end of the mill and automatically controlled by an Ohmart specific gravity meter. Attached to the slurry pipeline, this meter measures the specific gravity of the slurry continuously by detecting the difference in the radiation of gamma rays, emanating from a small sample of caesium, through the slurry. A recorder for the water content is located at the main control panel.

As the slurry is pumped to one of the three kiln feed tanks, the proportion of shell to clay, as determined from the hourly analyses, is changed as necessary so that when the tank is full the slurry will be of the proper chemical composition. The usual blending tanks have been eliminated. At the central control panel there are liquid level indicators for the clay slip tank at the raw mill, as well as for the three kiln feed tanks, so the operator will know at all times just how much clay slip or slurry is in each tank. All slurry pumps and valves are operated from the central control room. There are automatic pressure controllers in front of each slurry pump so that these will operate most efficiently and without unsightly leakage.

Many variables must be controlled in the burning process, but they resolve themselves principally into maintaining the desired burning temperature to produce the greatest amount of high quality clinker at the best fuel efficiency. Too low a temperature

will result in *underburned* clinker in which the chemical reactions have not been completed, and too high a temperature will cause unnecessary damage to the kiln refractory lining.

At the feed end of the kiln the draft, exit gas temperature, and oxygen content of the exit gas are controlled. The desired amount of draft is maintained by a pressure controller that automatically positions a damper in the ductwork to the induced draft fan. The set point of this controller is electrically adjusted by the exit gas temperature recorder-controller within fixed upper and lower draft limits. Better fuel economy is obtained as the back end temperature is reduced, since less heat is being lost into the atmosphere. This temperature is maintained at about 600°F.

Experience has shown that it is best to maintain a slightly oxidizing condition in the kiln and keep the oxygen content of the exit gas about 1 pct. Oxygen contents above this amount show that too much air is being used for combustion, reducing fuel efficiency. Lower oxygen contents indicate the possibility of incomplete combustion. A Hays Magno Therm continuous oxygen recorder has therefore been installed. If the oxygen content falls below 0.75 pct, control is exerted to close the fuel valve proportionally.

Chromel-alumel thermocouples have been installed in the kiln at a point where the temperature is about 2000°F. This is a few feet ahead of the burning zone, where the temperature reaches about 2750°F and where the final chemical reactions take place. The thermocouple output is picked up by a trolley wire system outside the kiln. From this instrument fuel flow to the burner can be controlled. If the oxygen content becomes too low or the firing end too hot the control will be augmented by the instruments measuring these quantities. A Rayotube radiation pyrometer records the temperature in the burning zone. This will be used as a controller only in extreme cases, to sound an alarm and automatically close the fuel valve if the temperature reaches 2900°F.

A draft recorder and controller holds the draft in the firing hood under a slightly negative pressure. This is controlled by remotely positioning the cooler stack fan damper.

Rate of fuel flow is also recorded and there is an automatic shut-off valve and flame failure protection on the gas line.

In addition to these recorders and controllers, all of which are mounted in the central control room, a 10-point monitor recorder charts on one strip the following variables:

1) Kiln feeder speed.
2) Kiln speed.
3) Rate of fuel flow.
4) Exit gas temperature.
5) Feed end draft.
6) Load temperature.
7) Rayotube temperature.
8) Percent oxygen in exit gas.
9) Secondary air temperature.
10) Clinker temperature at cooler discharge.

A view of the kiln interior is necessary for inspection of the load and flame and the kiln lining.

One of the latest innovations in the Houston plant is the television camera and monitor for observation of the burning process. The monitors are mounted in the central control room so that the operator can observe the inside of the kilns by means of television and still have the benefit of the recorders. With a pan and tilt control the operator is able to position the camera remotely. He can also adjust the camera operation by means of iris and lens controls.

The principle of the air-quenching cooler is to force cool air through the bed of hot clinker. This not only cools the clinker but also supplies combustion air to the kiln. Hot air in excess of that which can be used in the kiln advantageously is discharged into the atmosphere. Variables that can be controlled include: 1) grate speed to control thickness of the clinker bed, 2) amount of air forced into the cooler, and 3) proportion of usable to wasted hot air. The following instruments are installed on each of these coolers:

1) A clinker temperature recorder for the clinker at the cooler discharge.
2) A recorder for the air temperature at the entrance to the kiln hood.
3) A recorder and controller in conjunction with a Rayotube sighted on the clinker bed under the overgrate baffle. These instruments will maintain a constant clinker temperature at this point by controlling the cooler fan damper rather than by regulating the grate speed, which has been the usual practice. The overgrate baffle is used to direct all of the recuperated air required to the kiln and the balance to the cooler stack.
4) An indicator for pressure at the suction side of the cooler fan.
5) An indicator for the pressure under the cooler grates.
6) A recorder for the cooler stack gas temperature.
7) An indicator for the pressure in the cooler stack.

The clinker from the coolers is conveyed to the storage bins by a system of natural frequency conveyors, elevators, and belt conveyors. Belt scales (Transportometers) continuously weigh and total clinker from each kiln. Tellevel indicators show when each clinker storage bin is full. Controls on a finish mill are simply the proper ratio of gypsum to clinker and the maximum production rate to produce cement of the required fineness, which is about 95 pct passing 325 mesh. The clinker and gypsum are proportioned automatically by belt feeders and feed rate to the finish mills is regulated by Hardinge electric ears.

A common pipeline runs from finish mills to storage silos, branching into three feeding lines to alleviator-airslide systems for each of the three rows of silos. Flow of cement can be changed from one silo to another by selector switches in the main control room. These silos are also equipped with Tellevel indicators.

When the conveying systems are properly interlocked withdrawal of cement from these storage silos is essentially automatic. At each of the three packing machines there is a control panel. When the operator sets the selector switch for the silo from which he wishes to pack cement and pushes the starter button, the equipment starts in the proper sequence. Bulk loading for trucks and for rail, as well as for loading barges at the waterfront, is handled by similar control panels.

Discussion of this paper sent (2 copies) to AIME before March 31, 1958, will be published in MINING ENGINEERING.

Structural Control of Contact Metasomatic Deposits in the Peruvian Cordillera

by Alberto J. Terrones L.

THE classical papers on contact metasomatic deposits by Lindgren on the Clifton-Morenci district,[1] by Barrell on Marysville, Mont.,[2] and by Goldschmitt on the Oslo district, Norway,[3] laid the foundation for understanding of the importance of separating the metamorphic process from the subsequent metasomatic stage. Knopf[4] made a big step forward by recognizing that sulfide ore minerals are invariably younger than silicates and by further stressing the importance of structural control[5] in ore finding. Some years later Harrison Schmitt[6] fought the idea that contact metasomatic deposits are erratic, irregular, bunchy, economically marginal, and of small size, concluding that these descriptions have little factual basis. He emphasized the importance of detail mapping and careful geological study as fundamental requirements for a better understanding of these deposits.

This article presents a comparative description of the structural features at the Magistral, Antamina, Morococha, Vilca, Ferrobamba, Katanga (Quibio), Tintaya, and Huarca contact deposits (Fig. 1). Further, it will describe how these structural features controlled the emplacement of the intrusives, their shape, distribution of metamorphic and metasomatic halos, and sulfide deposition in post-skarn structural channelways. Finally, the modifications introduced by a superimposed hydrothermal stage recognized at some localities will be discussed.

Primary exploration and careful sampling of recognized structural targets were instrumental in outlining the copper ore potential at the Antamina and Tintaya districts, thus proving the benefits and reward of careful geological examinations in this type of deposit.

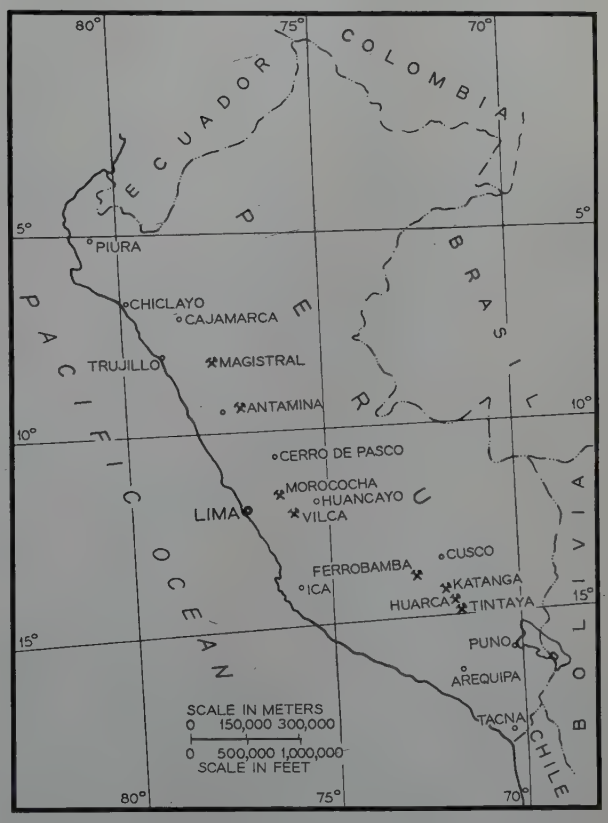

Fig. 1—Location map of Peruvian contact metasomatic deposits.

The Magistral District: This district lies in the Province of Pallasca, Department of Ancash, in northern Peru, at 8° 16′ S and 77° 47′ W. High to medium grade copper orebodies in garnetite, bordering a quartz monzonite stock, are exposed at the bottom of a glaciated valley in the western slope of the Andes at 4250 m (14,000 ft)* elevation.

A. J. TERRONES, Member AIME, is Exploration Geologist, Cananea Consolidated Copper Co., S. A., Mexico City.

TP4705I. Manuscript, Sept. 19, 1957. New Orleans Meeting February 1957.

* Conversions of metric units to English units are approximate.

This page of Mining Transactions AIME follows p. 268. The intervening non-Transactions pages appeared in MINING ENGINEERING.

A quartz monzonite stock, elliptical in plan (Fig. 2), cuts across the middle Cretaceous (Machay) limestone on the southwest flank of a northwest-trending (N 40°-45° W) anticline. A major southwest-dipping reverse fault, striking parallel to the folding, is exposed several hundred meters west from the center of the intrusion. Marble and porcellanite (pyroxene rock) are the products of the metamorphic stage. The writer noticed that the porcellanite layers selectively metamorphosed the more shaly members of the sedimentary sequence and extend much farther away from the intrusive contacts than does the marble.

Garnet replaces marble and pyroxene rock forming a metasomatic aureole 120 to more than 200 m (450 to 650 ft) wide around the stock and along branching dikes or sills. In general the garnetite is medium grained, but locally it is distinctly coarse, with individual crystals up to 2.0 to 2.5 cm (0.8 to 1.0 in.). The author observed that lenses of coarse grained garnet selectively replaced marble beds, whereas felsitic garnet appears to be more frequently associated with porcelainized (pyroxene rock) beds. This strongly suggests that during replacement the garnet preserved the original metamorphic texture of the rocks (formed during the metamorphic stage). This effect seems to be more pronounced in the outlying borders of the garnetite than close to the intrusive contacts.

Chalcopyrite and pyrrhotite are the most abundant sulfide minerals, with pyrite, molybdenite, sphalerite, and galena in subordinate amounts. Magnetite is locally abundant. In addition, D. H. McLaughlin[7] reports arsenopyrite, native arsenic, jamesonite, tethahedrite, and veinlets of supergene chalcocite. Most of the oxidized sulfide bodies were eroded by glacier action. Secondary enrichment is negligible.

Sulfide mineralization, essentially post-garnetite, forms either lenticular high grade copper ore concentrations along post-garnet fractures or medium to low grade disseminations controlled by minor fractures and the more pervious coarse garnetite layers. Ore mineralization is more restricted to zones at the border zones of garnet, either along the monzonite contact or following the outlying marble and porcellanite contacts. A few irregular occurrences are localized in the heart of the garnetite zone.

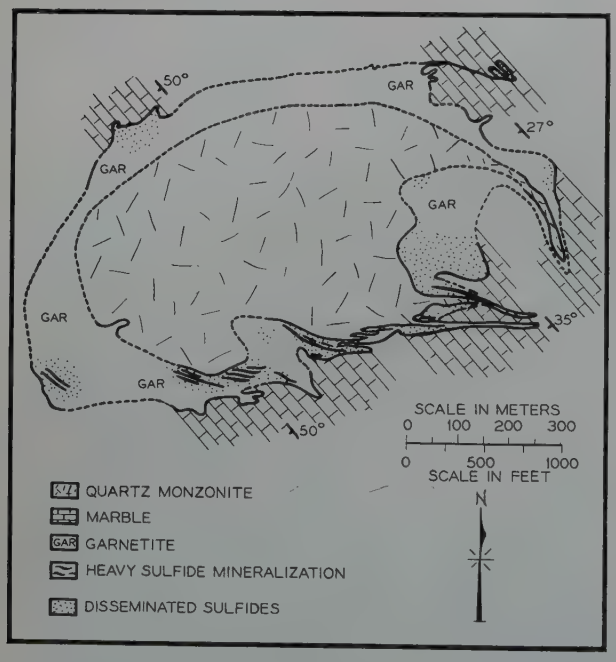

Fig. 2—Surface geology of the Magistral district, Peru. (After map by D. H. McLaughlin, modified from field notes by A. J. Terrones.)

The width of the high grade vein-like lenticular bodies varies from a fraction of a meter to 6.0 m (1 to 20 ft). Their strike length is 25 to 50 m (80 to 160 ft). The high grade lenses are not isolated; they are linked bodies surrounded by sulfide disseminations (Fig. 2) forming continuous zones of milling grade ore. Small sulfide bodies also occur along branching dikes and sills.

The writer observed that disseminated sulfides occur mainly as filling the interstices between coarser garnet crystals. After microscopic investigations McLaughlin reached the same conclusion,[7] stating that sulfides "occur as irregular grains in the garnetite moulded about and corroding silicates...." This proves that ore mineralization is definitely later than garnetite.

Moderate argillic alteration, exposed at some of the branching dikes, is the only evidence of hydrothermal activity. Except for local pyritization with sparse chalcopyrite, the quartz monzonite stock is practically fresh.

The Antamina District: The Antamina district is located in the Province of Huari, Department of Ancash, in the northern part of Peru, at 9° 32′ S and 77° 04′ W, with elevations ranging from 4200 to 4500 m.

An irregular quartz monzonite intrusive, in part concordant with bedding and in part cross-cutting as an irregular dike feeder, intruded a dome of middle Cretaceous limestone (Jumasha limestone according to Bodenlos and Ericksen).[8] Dikes and sills branch out from this irregular intrusion or occur as seemingly isolated bodies probably connected to a buried stock. The main quartz monzonite intrusive, covering an area of more than half a square kilometer, is exposed at the bottom and eastern side of a northeast-trending glacial valley. Andesite porphyry dikes, outcropping near the southeast corner of the district, very likely represent offsprings of a more basic differentiate (diorite) at depth.

The northwest portion of the Antamina dome is offset 350 m (1150 ft) northwest by an unexposed northeast-trending pre-intrusive fault known as Valley fault (Fig. 3). A strong reverse fault striking parallel to the trend of folding (N 40° W) and dipping to the southwest, outcrops 500 m (1650 ft) west of the nearest mineralized showings.

Detailed surface geological mapping and diamond drilling indicates that the main quartz monzonite intrusive is sill-shaped or semi-laccolithic, branching off from an irregular northeast-trending feeder dike 100 to 300 m (350 to 1000 ft) wide (Fig. 4). This feeder was probably emplaced along the Valley fault zone (Fig. 4).

Shaly beds were selectively metamorphosed to porcellanite (diopside rock) extending several hundred meters out from the marble and garnet contacts. Garnet is the dominant contact silicate. According to G. C. Amstutz its average index of refraction (higher than 1.79) suggests an intermediate composition between grossularite and andradite. The main garnetite body at the Antamina dome is exposed around the southern half of the intrusive (Fig. 3) as an elliptical arch 1700 m long. The thick-

ness of the garnet above the laccolithic intrusive (Fig. 4) is 200 to 350 m (650 to 1150 ft). At present very little is known about the extension and thickness of garnetite underneath this concordant intrusive body. However, there are evidences that garnetization continues south, outside the Antamina dome, along the dike feeder that follows the trend of the Valley fault zone. Nearly 1500 m (5000 ft) southwest of the center of the Antamina dome, an irregular garnetite zone (the Usupallares area) is exposed. This zone is related to narrow quartz monzonite porphyry dikes and sills that might be also connected to the main dike along the Valley fault.

Wollastonite is next after garnet in order of abundance but is earlier than the garnetization. Actinolite and tremolite are of local occurrence. Scapolite crystals are rare. Magnetite is contemporaneous to slightly later than garnet but earlier than the sulfides. Pyrite, chalcopyrite, and sphalerite are the most abundant sulfide minerals within the garnetite. Molybdenite, galena, and scheelite are present in subordinate amounts.

The filling of open spaces with slight replacement of garnet (Fig. 5) controlled the sulfide deposition. Post-garnet fracturing and coarse grained garnetite guided the distribution of sulfides. For instance, the largest high grade orebody so far disclosed by exploration is a chimney-shaped body localized at the intersection of strong sheeting, striking N 75° to 80° W and dipping 65° to 75° S, with a belt of coarsely crystallized garnet striking N 40° W and dipping 70° to 75° NE. In plan (Fig. 6), the orebody is elongated along the strike of sheeting, but in sections its plunge is nearly parallel to the dip of the coarse garnet belt. Since the coarse grained belt corresponds in position to the projection of the axial plane of an overturned secondary anticline exposed immediately above the garnetite contact (Fig. 3), the writer believes that this belt probably represents an inherited structure, namely, pre-existing shattering along the axial zone of the secondary anticline.

A subsequent hydrothermal stage introduced further complications. Quartz, calcite, and a second generation of pyrite filled fractures accompanied by chlorite, epidote, and the albite alteration of the garnetite. Certain areas were strongly chloritized and pyritized, but it has been found that these areas are generally lean. Moderate quartz-sericite-chlorite alteration, with pyrite and small amounts of chalcopyrite mineralization, occur in the main quartz monzonite intrusive. Pyrite, galena, sphalerite, tetrahedrite, some chalcopyrite, quartz, fluorite, and rhodocrosite fill fractures within sericitized quartz monzonite dikes or sills in the outlying areas of the district. Sulfides also occur in fractures following the contacts of these minor intrusives with marmorized and slightly silicated and silicified limestone. Sulfide mineralization, associated with hydrothermal alteration in fringing intrusives, is tentatively regarded as mesothermal.

The Morococha District: This district lies in central Peru, in the Province of Yauli, Department of Junin, at 11° 35′ S 76° 11′ W, and close to the Continental Divide at elevations ranging from 4500 to 5000 m (15,000 to 16,600 ft).

The petrology of contact metamorphism and metasomatism and the modifications introduced by

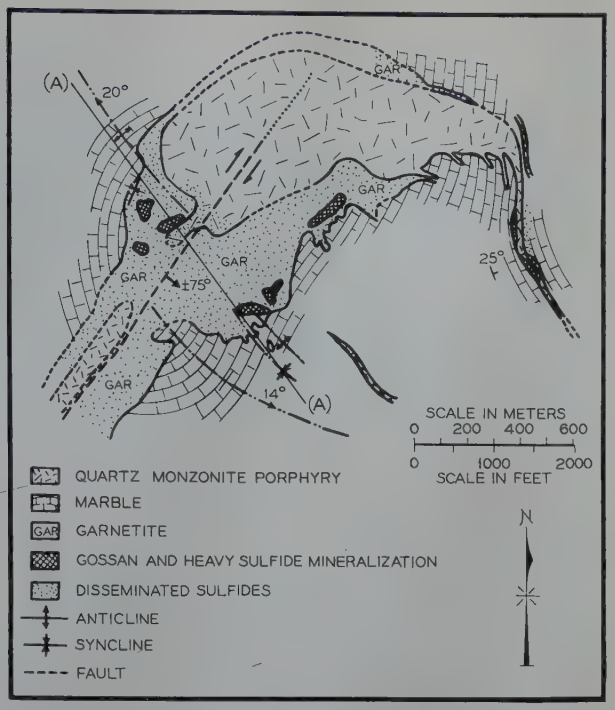

Fig. 3—Surface geology of the Antamina district, Peru. (After A. J. Terrones and U. Petersen.)

subsequent hydrothermal activity at Morococha were first recognized and studied in detail a number of years ago.[9]

The intrusive stage at Morococha started with the injection of a large diorite stock, oval-shaped in plan, elongated in the N 25° W direction. Its longer axis is nearly 6 km (3.5 miles) and the minor axis measures about 4 km (2.5 miles). After the diorite smaller stocks of granodiorite to quartz monzonite composition were intruded.

Marble, with little or no silicates, is the prevailing contact effect around the diorite intrusion. This is in sharp contrast with the extensive tactite belt of anhydrous silicates surrounding the comparatively smaller quartz monzonite stocks. Stratigraphic control of the distribution of marble and contact silicates is marked. The author[10] recognized on the surface the following horizons, from top to bottom, of the Potosi limestone (Jurassic, Lias) which surrounds these stocks. The sedimentary characteristics and corresponding contact effects are:

1) Horizon *D*: 62 to 108 m (205 to 355 ft) of thin-bedded, limy, and sandy shales grading down the column to purplish, mottled, sandy, and limy shales alternating with chert layers. This horizon is entirely silicated to porcellanite up to 1100 or 1300 m (3500 to 4500 ft) away from intrusive contacts (Fig. 7). From there on, only the uppermost calcareous portion remains silicated for 1000 m (3000 ft) more, until silification practically fades out at 2500 m (8000 ft) outward from the monzonitic intrusions.

2) Laura Horizon: 110 m (360 ft) of dolomitic limestone with chert nodules and a few shaly and sandy beds including a 5-m (16-ft) thick trachyte flow. Fresh limestone begins to grade into marble 300 to 350 m (1000 to 1150 ft) from the nearest intrusive contact. Cherty nodules and shaly layers are selectively silicated to diopside rock. Garnet and

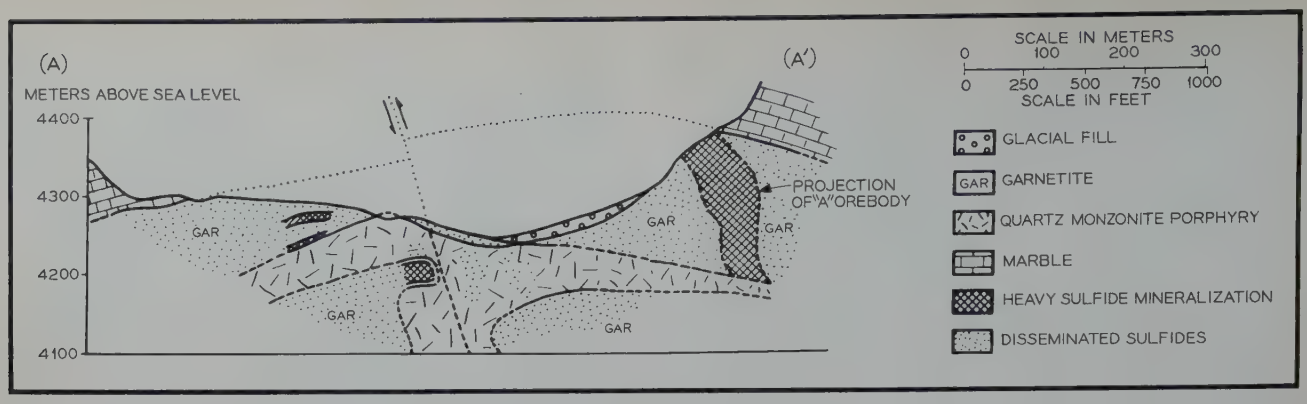

Fig. 4—Cross section (A-A'), looking northeast, Antamina district, Peru. (After A. J. Terrones and U. Petersen.)

tremolite occur only within 150 m (500 ft) of the intrusives. Magnetite occurrences are restricted to hydrated garnet-tremolite layers within the marble horizons, tending to disappear 200 m (650 ft) from the monzonite contact.

3) Horizon *E*: 26 m (85 ft) of medium to coarse grained sandstone and shaly beds with an interbedded fossiliferous dolomitic limestone bed with chert nodules. The entire horizon is thoroughly silicated within 150 m (500 ft) of the intrusive contacts, with garnet lenses replacing porcelainized beds. Only the sandy, shaly, and cherty members are selectively silicated more than 1000 m (3000 ft) away from the intrusive. The dolomitic limestone remains marmorized up to 300 m (1000 ft) from the quartz monzonite contacts.

Widespread and intense hydrothermal activity masked, and at places completely obliterated, the products of contact metasomatism. Only after detail mapping was it possible to recognize aggregates of grossularite and tremolite containing fair amounts of pyrite, pyrrhotite, sphalerite, chalcopyrite, and molybdenite as disseminated grains, blebs, and minor stringers which escaped the flooding of hydrothermal solutions. Outside these remnants it is very difficult to differentiate original contact metasomatic ore from ore mineralization deposited during the overlapping hydrothermal stage. While this latter process was under way, large volumes of contact silicates were altered (hydrated) to serpentine, chlorite, and talc. Apparently serpentine is earlier than the chlorite-talc alteration. Talc seems to be closely related to the deposition of sulfides belonging to the hydrothermal stage.

Serpentine shows a preference to replace the layers of diopside (porcellanite) rock, thus forming layered ore structures. Haapala concludes[11] that the underlying serpentine is almost contemporaneous with magnetite. The writer doubts this and believes that magnetite is a residual product from the much earlier contact metasomatic stage.

The Vilca Prospect: Small bodies of oxidized lead-zinc-silver ore occur along seven garnetized beds of Machay limestone (Middle Cretaceous), alternating with porcellanite and marble beds in an overturned anticline. This small prospect, near Vilca in Central Peru (12° 08′ S, 75° 08′ W), is of interest because of the remarkable selectivity of garnetization along porcellanite beds and because of the localization of ore pockets within the garnetite beds in the axial zone of the anticline.

A large diorite stock intruding a major anticline is exposed 2 km (1.25 miles) south but a quartz diorite porphyry sill nearly 1000 m (3000 ft) southeast is the nearest intrusion. Neither intrusive shows important garnetite. Each limb of the anticline is cut by a steep, nearly east-west trending fault. It is postulated that an underlying monzonitic body, intruded along the downward extensions of the east-west faults, is responsible for the garnetization and sulfide minerlization.

Disseminated pyrite and galena, with minor amounts of tetrahedrite and sphalerite, form small pockets of low grade ore in the shattered garnetite beds at the apex of the fold. Detail mapping shows that this mineralization follows fractures parallel to the bedding, preferably along the contacts with bordering porcellanite beds (Fig. 8). Some of these mineralized fractures cut across the silicated beds and form small replacement bodies in the marble layers. Fracturing or shattering of the more brittle porcelainized beds probably favored the selective replacement by garnet and sulfides.

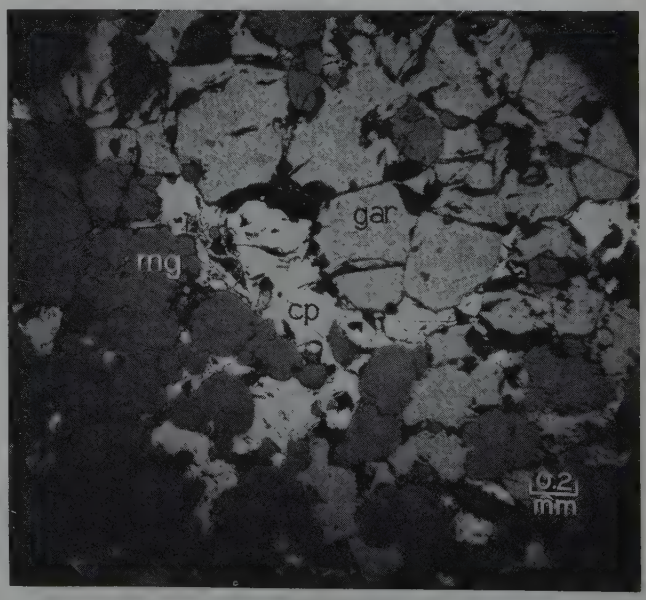

Fig. 5—Chalcopyrite (white) filling interstitial spaces between earlier garnet (gray) and magnetite (black) at the Antamina copper deposit, Peru. X40.

The Ferrobamba District: The Ferrobamba, Charcas, Chalcobamba, and Sulfobamba deposits comprise this district, which extends 13 km (8 miles) along an east-west trending belt with center 14° 04′ S 72° 22′ W, 83 km (5.5 air miles) southwest of Cusco in the Department of Apurimac.

Regional investigations by W. F. Jenks[12] showed that the lower half of the Cretaceous Ferrobamba limestone was intruded by stocks of granodiorite, monzonite, quartz monzonite, and diorite. Larger dioritic stocks appear to be elongated along major axis of structural deformation.

Coarse marble is the dominant contact effect in practically all types of intrusives. Garnet, epidote, and wollastonite are restricted to the more acidic intrusions. F. C. Kruger[13] reported that magnetite and coarse specularite occur invariably interlayered with contact silicates. Chalcopyrite is more abundant than pyrrhotite and bornite, occurring as blebs, pods, or layers along relict bedding planes or disseminated in massive magnetite. It became evident, from mapping, that chalcopyrite mineralization is intimately associated with impure banded mixtures of contact silicates rather than with purer garnet or epidote. At Charcas, Kruger[13] noticed that chalcopyrite-pyrrhotite mineralization is in general concordant with bedding, but at the other deposits in the district it cuts across stratification following joints or irregular fractures. Sulfides at this locality were found to be in part contemporaneous and in part later than magnetite. The reported occurrence of chlorite at Chalcobamba suggests the existence of an incipient hydrothermal stage.

Jenks[12] summarizes the major factors controlling the location of copper orebodies in the Ferrobamba region as follows:

1. The presence of the Ferrobamba limestone, particularly the basal half of the formation.

2. The presence of monzonite or quartz monzonite in contract with the limestone and occurring as small stock or apophyses within or from large diorite masses. (Monzonite dikes or small monzonite stocks, not directly associated with large diorite intrusives, do not seem to have brought in copper values or even formed appreciable amounts of garnet.)

3. The presence of cross folds at high angle to regional trends and apparently due to crumpling at culminations and depressions of plunging folds.

The Katanga (Quibio) Prospect: At this prospect, 82 km (51 miles) southeast of Ferrobamba, hornblende diorite and quartz diorite porphyry stocks intruded dark gray, finely banded, mottled Ferrobamba limestone beds that alternate with thin-bedded shales and sandstones. Coarse marble selectively follows the limestone horizons, whereas contact silicates (mainly pyroxene) replace the more shaly members. Lenticular masses of hematite-magnetite up to 25 m (80 ft) thick occur only around the hornblende diorite stock (Quibio hill).

Garnet-tremolite lenses with magnetite, specularite, pyrite, and oxidized chalcopyrite mineralization occur as elongated endomorphic replacements in quartz diorite porphyry along fractures or zones of brecciation parallel to the intrusive contact. Outside the porphyry, steep plunging lenticular bodies with the same mineral composition are localized between quartz diorite and marble containing chloritized silicates. These lenses essentially follow the attitude of bedding.

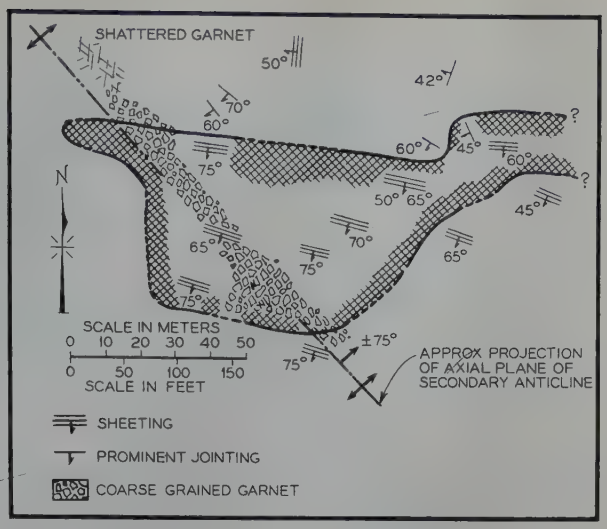

Fig. 6—Structural map of the A orebody on level A, Antamina district, Peru.

No garnet-tremolite and associated sulfides were noticed along the hornblende diorite contacts. Slight quartz-sericite alteration in the quartz porphyry, as well as chloritization of contact silicates, indicates a mild, post-ore hydrothermal activity.

The Tintaya District: The Tintaya district lies in the province of Espinar, Cusco Department, at 14° 47′ S, 71° 20′ W, and 4000 m (13,000 ft) above sea level.

An augite diorite stock and a later monzonite porphyry differentiate intruded Jurrassic (Portlandian) quartzites and middle Cretaceous (Cenomanian) limestone beds. The diorite is the largest intrusive in the district, about 9x5 km (5.5x3 miles), showing a definite elongation in the NW-SE direction, parallel to the major tectonic axis. The monzonite porphyry stock is much smaller—more than 2 km (1.2 miles) long by 1 to 2 km (0.6 to 1.2 miles) wide—and was emplaced at the northern extremity of the diorite stock. Numerous dikes and sills protrude from the southern border of the monzonite, cutting across an intervening block of limestone 300 to 500 m (1000 to 1650 ft) wide, which separates both stocks. Some of these dikes cut across the earlier diorite intrusive.

Cross folds and faults trending northeast or east-northeast, nearly at right angles to lines of structural deformation, were mapped in the outskirts of the district. A northeast-trending fault is tangent to the southeast border of the monzonite stock. It is interesting to note that the southern portion of this stock and major branching dikes (Fig. 9) are elongated parallel to the trend of east-northeast cross structures. No cross folding is recognized at this particular locality. Bedding strikes persistently N 50° W and dips 30° to 45° SW (Fig. 9). Therefore cross faulting and related fracturing must have guided the emplacement of monzonite.

Coarse to fine marble, and very locally diopside rock, are the only products of contact metamorphism occurring around diorite. Garnet, magnetite, and sulfides, as the products of the metasomatic stage, were exclusively developed along monzonite contacts where coarse to fine marble occurs also.

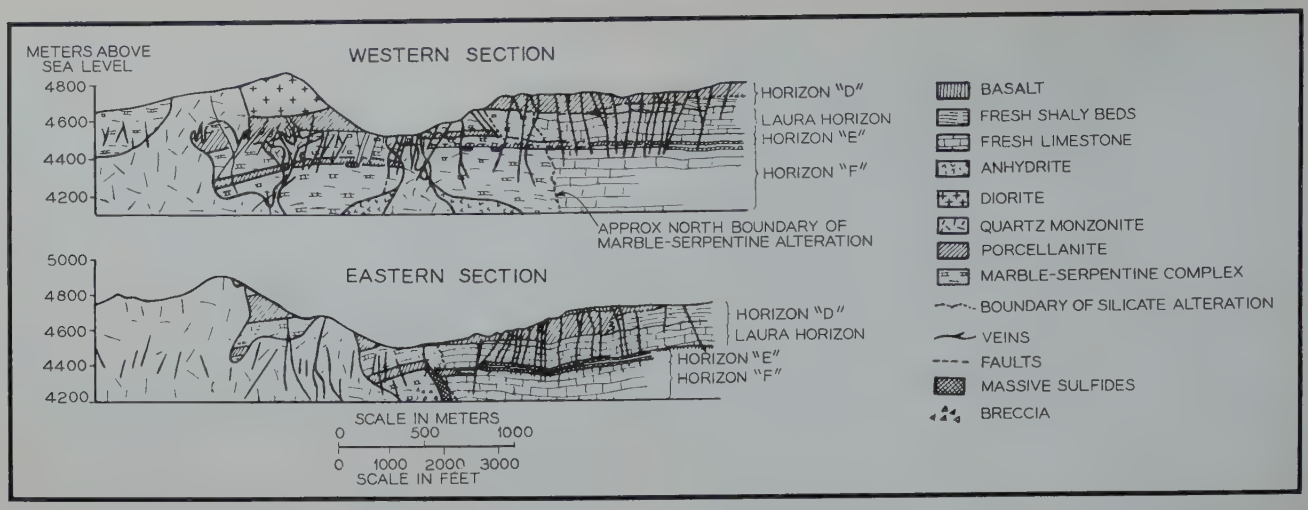

Fig. 7—North-south sections, looking west, through the north-central Morococha district, Peru, showing contact silicate alteration in relation to stratigraphy and structure.

The distribution and the shape of the garnetite are mainly controlled by the shape of the monzonite intrusive (Fig. 8) and very possibly, although to a minor extent, by the grain size in the marble. Coarse grained and wholly recrystallized limestone was more favorable for contact silicate replacement than dense and tighter, partly recrystallized, gray-black limestone.

F. de las Casas[14] describes the Tintaya garnet as an isomorphic mixture of andradite and grossularite. He also found that copper mineralization was almost invariably associated with grossularite, and concluded that this mineral "represents the last phase of garnetization when ferric iron was not available in the (replacing) solution. . . ."

Magnetite and hematite are somewhat contemporaneous and slightly later than garnet, but definitely earlier than quartz and sulfides. Quartz fills fractures in garnet and selectively replaced garnet along crystal boundaries and certain internal layers formed by crystal zoning (Fig. 10). Bornite is earlier and much less abundant than chalcopyrite,

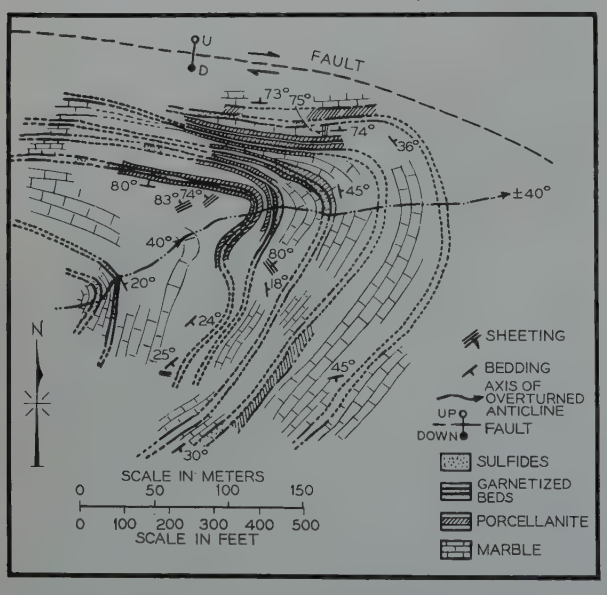

Fig. 8—Structural of map, Vilca prospect, Peru, showing selective garnetization along porcelainized beds. (After J. A. Cabieses, modified by A. J. Terrones.)

which is the main ore mineral in the sulfide zone. Sulfides were deposited in quartz stringers, filled interstitial cavities (Fig. 10), were associated with calcite veinlets, and filled tiny crystal fractures. In general, ore mineralization is more evenly distributed within garnetite than at other Peruvian deposits. However, there are indications that post-garnet shattering along monzonite and marble contacts, as well as formation of coarse grained grossularite garnet, served to concentrate copper mineralization with leaner ore localized at impervious dense garnet. Observations seem to confirm that coarse grained garnet was inherited after coarse marble beds.

The orebodies are predominantly manto-like, although along dikes they occur as tabular or lenticular bodies cutting across bedding. Sulfides were oxidized *in situ* with little or no supergene enrichment. Chrysocolla and brochantite are the dominant oxide minerals.

Chloritization and subordinate serpentinization are locally moderate to intense, forming soft powdery material that at places collapsed to originate post-ore slump breccias. Hydration of garnet, accompanied by moderate to slight quartz-sericite-clay alteration in the monzonite intrusives, attests the existence of a mild, but barren, post-ore hydrothermal stage.

The Huarca Prospect: At this prospect, lying 10 km (6 miles) southwest of Tintaya, an irregular vein-like garnetite body, with banded oxidized chalcopyrite-bornite mineralization, is localized along a small quartz-monzonite porphyry stock.

The garnet, which replaced marble and monzonite along the contact (Fig. 11), was subsequently fractured and replaced by lenses of magnetite and cut by veins of chalcopyrite-bornite-pyrite stringers lying nearly parallel to the contact zone, producing a banded structure very much like a vein deposit. Fine grained garnetized beds, with disseminated sulfides in stringers and small grains, branch out from the contact zone along minor dikes.

The main ore zone is 1 to 10 m (3 to 30 ft) wide and is oxidized to 20 m (65 ft) below the surface. Main oxide minerals are copper carbonates, chrysocolla, and cuprite. Small amounts of supergene chalcocite are mixed with sulfide and oxide min-

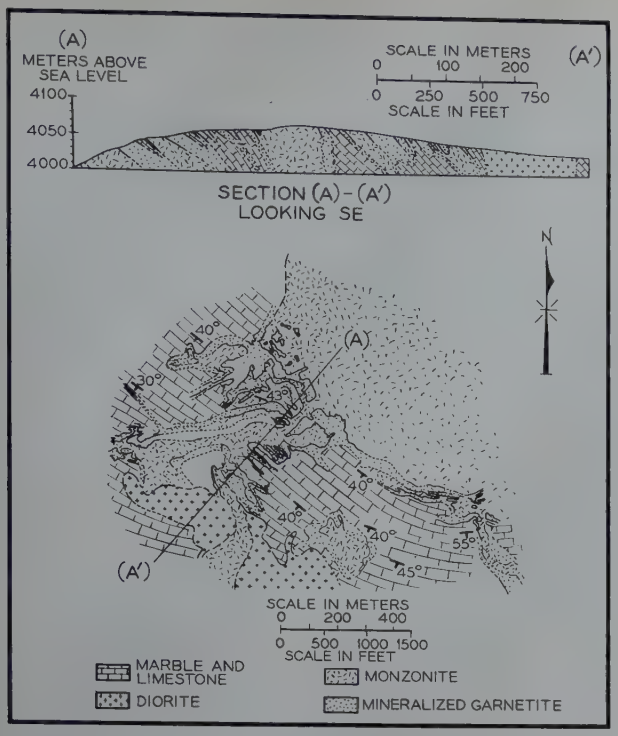

Fig. 9—Structural control of mineralized garnetite along monzonite dikes and sills, emplaced along east-northeast fracturing and northwest-trending bedding, at southwest Tintaya district, Peru.

erals. Garnet was locally chloritized by subsequent hydrothermal alteration.

Conclusions

An orderly, continuous, and to a certain extent overlapping sequence of events is visualized in the evolution of geological processes that originated the contact metasomatic deposits in the Peruvian Cordillera. The entire process can be subdivided in four stages: 1) intrusive stage, 2) metamorphic stage, 3) metasomatic stage, and 4) hydrothermal stage.

Without any attempt to minimize the importance of physico-chemical controls, it is concluded that structure played a role of considerable significance throughout all four stages in determining the distribution, shape, size, concentration, and subsequent modifications of ore mineralization. Proper understanding and evaluation of the relative importance

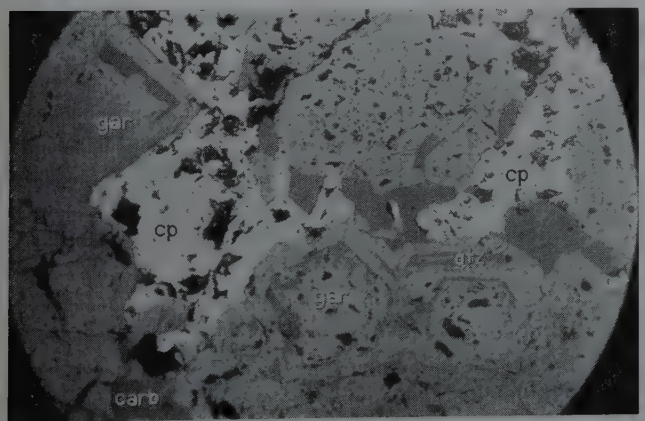

Fig. 10—Quartz (dark gray), replacing garnet crystals (light gray), following grain boundaries, small fractures, or crystal zoning. Chalcopyrite (white) fills interstitial spaces and partly replaces garnet and quartz. Tintaya copper deposit, Peru. X72.

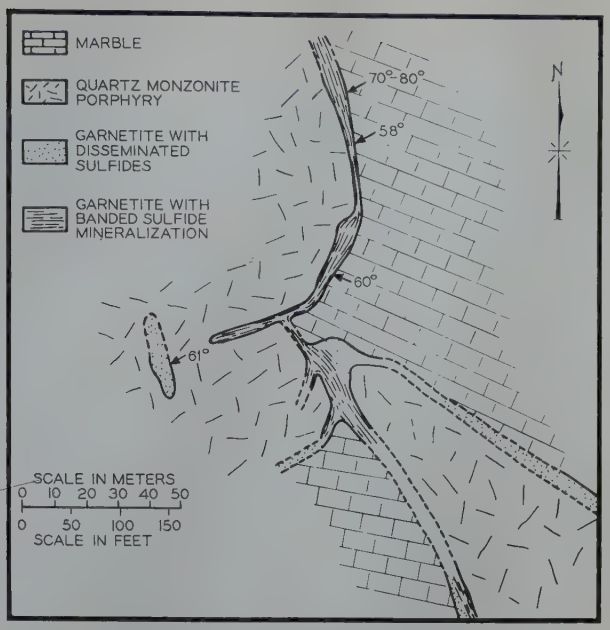

Fig. 11—Vein-like garnetite deposit along fractured quartz monzonite-marble contract at Huarca prospect, southern Peru. (After A. J. Terrones and R. H. Kimball, Jr.)

of structural features, developed and modified during the evolution of these four stages, are critical in planning intelligent exploration and mine development.

Intrusive Stage: Magmatic differentiation from diorite to quartz monzonite or to granodiorite was essential. Garnetization and sulfide mineralization are invariably related to the intrusion of later and more acidic differentiates. This condition is well illustrated at Morococha, Ferrobamba, Katanga (Quibio), and Tintaya. No basic intrusive is exposed at Magistral, but the andesite porphyry dikes at Antamina probably represent branches of a buried diorite stock. At Vilca a large diorite stock outcrops near the ore showings, but the acidic intrusive is concealed under silicated and marmorized limestone. W. C. Lacy[15] recognized that the same process of magmatitic differentiation operated at other important mining districts in Central Peru (Cerro de Pasco, Yauricocha, Raura, and Julcani) besides Morococha and concluded that ore solutions escaped during the quartz monzonite phase.

Pre-intrusion structures determined, to a certain extent, the final shape of stocks and minor intrusive bodies. Earlier diorite stocks at Morococha, Ferrobamba, and Tintaya are elongated parallel to major tectonic axes, whereas the emplacement of later monzonitic intrusives seemed to prefer cross folding or fracturing at right angles to this direction. The east-northeast elongation of the Magistral quartz monzonite stock, the intrusion of the quartz monzonite dike feeder at Antamina along the northeast-trending Valley fault, the monzonitic intrusions along cross folding at Ferrobamba, and the east-northeast elongation of the southern portion of the Tintaya monzonite stock and dikes are evidences pointing to a predominance of cross-trending structural control in the intrusion of acidic differentiates. This structural preference is explained by:

1) Pre-existing minor cross folds, shears and fractures, oriented nearly at right angles to regional tensional stresses, caused by the stretching of longitudinal folds under active northeast-southwest

compression. These cross structures were the loci of least resistance at the surge of the intrusive stage.

2) Arching or bending of folded structures, caused by the vertical upward stresses of intruding diorite stocks, which reactivated tensional stresses perpendicular to the east-northeast direction, forced apart pre-existing lines of least resistance. Tension fractures and northeast-trending shears were opened while shattering or brecciation occurred along the axial planes of cross folds.

3) Injection of acidic differentiates into well prepared ground, dominantly along weaker east-northeast trending belts.

Metamorphic Stage: Marble and porcellanite were developed under rising temperature conditions. Their distribution and shape were guided by stratigraphy and by pre-existent structure. Marble is controlled by the position of limestone beds, whereas porcellanite (diopside rock) follows the more shaly and siliceous beds.

Porcellanite persists much farther away from intrusive contacts than marble. This is clearly shown at Magistral, Antamina, and Morococha.

Metasomatic Stage: Garnet is superimposed over marble and porcellanite and is the dominant silicate mineral within the tactite zone surrounding acidic intrusives. Wollastonite was proved to be earlier than garnet at Antamina and Morococha. Fair amounts of epidote were noticed at Ferrobamba. Tremolite occurs everywhere in subordinate amounts and scapolite is rare. Garnet, replacing marble beds, tends to produce granular textures, whereas felsitic or dense garnet predominates along porcellanite beds. There are evidences at Morococha and Vilca that fracturing in porcellanite contributed to localize garnetization in silicated beds.

Magnetite overlaps garnet but appears to be earlier than quartz and introduced calcite. Fairly large bodies of hematite-magnetite border the diorite intrusives at Ferrobamba, Katanga (Quibio), and Tintaya. Sulfides overlap quartz and appear to be definitely later than magnetite.

Distribution of highly pervious coarse garnet and post-garnet fracturing controlled the shape and size of both massive and disseminated sulfide orebodies. Distribution of coarse garnet, which provided ore-solution channelways, was caused by:

1) Selective metasomatic replacement of coarser marble beds (Magistral, Antamina, Morococha, and Ferrobamba). In this case the garnet inherited the original grain size of marble beds.

2) Free crystal growth at open cavities in strongly shattered, brecciated, or fractured marble and porcellanite. The attitude of some of the more regular bodies of coarse grained garnet might reflect the trend of pre-skarn structural features (Magistral, Antamina, Vilca, Katanga and Tintaya), such as shattering or brecciation along projections of tight folds (Antamina), or of prominent fracturing.

Chalcopyrite is the dominant sulfide mineral. Pyrrhotite, bornite, pyrite, sphalerite (marmatitic), and galena come next in order of abundance. Molybdenite is locally important (Antamina) and scheelite forms only spotty concentrations near marble contacts (Antamina and Morococha).

Sulfides occupy interstitial cavities between garnet crystals or fill fractures ranging in size from tiny crystal cracks to wide fracture zones, most of them located near or at the garnetite contacts. At Antamina and Tintaya, sulfides occur throughout the entire volume of garnetite. At Magistral, Vilca, Katanga (Quibio), and Huarca the sulfide mineralization tends to be more localized by fracturing along the garnetite borders.

Hydrothermal Stage: There are evidences that hydrothermal activity followed the pneumatolitic stage that caused the contact metasomatic silicate-oxide-sulfide replacements. The degree of intensity of this last stage is variable, ranging from very slight at Magistral to highly intense at Morococha.

Sulfide deposition usually accompanied the hydrothermal stage. It may have been minor, but in some cases new and important commercial orebodies orginated, superimposed upon older contact metasomatic ore mineralization. Best examples of this overlapping condition are found at Antamina and at north-central Morococha. The recognition of both types of ore mineralization requires detailed and careful geological mapping in conjunction with systematic petrographic investigation.

The hydrothermal stage might completely obliterate the original structure of contact metasomatic orebodies, and even careful mapping would be entirely ineffective in an attempt to reconstruct the original contact metasomatic ore structures. Fortunately it seems that this happened only in extreme cases, and detailed mapping of anhydrous and hydrated silicates usually reveals the original pattern of contact metasomatic mineralization. Even mild cases of superimposed hydrothermal alteration may locally introduce a different structural setting at contact metasomatic orebodies, such as the post-ore slumping and brecciation, recognized at Tintaya, caused by local weakening of garnetite after hydrothermal alteration.

Acknowledgments

The author is greatly indebted to Cerro de Pasco Corp. for granting permission to publish certain information contained in this article. He also acknowledges the kindness of Juan M. Velasco from Lima, Peru, for allowing the publication of information on the Katanga (Quibio) and Huarca properties.

The comments and additional information reported in personal communications by D. H. McLaughlin; F. N. Spencer, Jr.; W. F. Jenks; F. C. Kruger; and F. de las Casas are gratefully acknowledged.

References

[1] W. Lindgren: *Mineral Deposits*, pp. 695-745. McGraw-Hill Book Co. Inc., New York, 1933.
[2] J. Barrell: Geology of the Marysville Mining District, Montana. *USGS Prof. Paper*, pp. 116-150, 1905.
[3] V. M. Goldschmidt: *Die Kontactmetamorphose in Kristianiagebiet*, 1911. (Reference from Lindgren, p. 705).
[4] A. Knopf: Ore Deposits of the Western States: Lindgren volume, 1942, *AIME*, pp. 537-557.
[5] A. Knopf: *Ore Deposits as Related to Structural Features*. Edited by W. H. Newhouse, Princeton University Press, 1942.
[6] H. Schmitt: The Contact Pyrometasomatic Aureoles. *AIME TP 2357*, 1948.
[7] D. H. McLaughlin: Personal communication.
[8] A. J. Bodenlos and G. E. Ericksen: Lead-Zinc Deposits Cordillera Blanca and Northern Cordillera Huayhuash, Peru: *USGS Bull.* 1017, pp. 89-100, 1955.
[9] T. G. Moore: The Geology and Ore Deposits of Morococha, Peru. Doctoral dessertation, Harvard University, 1936.
[10] A. J. Terrones: Estratigrafia del distrito o miner de Morococha. Sociedad Geologica del Peru, *Volumen Jubilar*, XXV Aniversario, Parte II, Faciculo 8, pp. 8-9, 1949.
[11] P. S. Haapala: *Morococha Anhydrite. Boletin de la Sociedad Geologica del Peru*, 1953, vol. 26 (Broggi Volume), pp. 21-32.
[12] W. F. Jenks: Personal communication.
[13] F. C. Kruger: Personal communication.
[14] F. de las Casas: Personal communication.
[15] W. C. Lacy: Differentiation of Igneous Rocks and Its Relation to Ore Deposition in Central Peru. *Boletin de la Sociedad Geologica del Peru*, 1953, vol. 26 (Broggi volume), pp. 121-134.

Discussion of this paper sent (2 copies) to AIME before April 30, 1958, will be published in MINING ENGINEERING.

Relation of Magnetic Susceptibility to Mineral Composition

There is evidence that study of minerals now considered to have susceptibilities too low for magnetic separation should be continued. Present concepts may be false.

by Ernest M. Spokes and David R. Mitchell

INFORMATION on magnetic properties of minerals other than magnetite is scanty and sometimes erroneous. Often there is no information at all. W. R. Crane's table of tractive forces published in 1901 is still the best guide in the field, but Crane's data can be used as a guide only, since he ignored such important factors as impurities in the minerals, size, and packing effect. During the 1930's work by the U. S. Bureau of Mines added greatly to knowledge of the behavior of certain minerals in a magnetic field. The USBM bulletin gave for the first time complete magnetic characteristics for magnetite and fragmentary data for a few other minerals.

The work reported here covers a study of the magnetic-susceptibility relationships of the wolframite series of minerals and sphalerites as related to their chemical compositions. Theories are proposed to explain divergences found from commonly accepted beliefs.

Gouy Method for Determining Magnetic Susceptibility: The Gouy principle has been adequately described in the literature[1-3] and applied in various ways.[4-6] It may be summarized by stating that a body of material (gas, liquid, solid, or powder mixed with gas or liquid) of cylindrical shape changes in apparent weight if suspended with one end in a zone of higher magnetic field strength than is found in that portion of the field surrounding the other end of the cylinder. This may be expressed as

$$\frac{K_2 - K_1}{2} A(H^2 - H_0^2) = mg. \qquad [1]$$

E. M. SPOKES and D. R. MITCHELL, Members AIME, are, respectively, Professor of Mining Engineering, University of Kentucky, Lexington, Ky., and Professor of Mining Engineering, The Pennsylvania State University, University Park, Pa.

TP 4700B. Manuscript, Oct. 19, 1957. New York Meeting, February 1958.

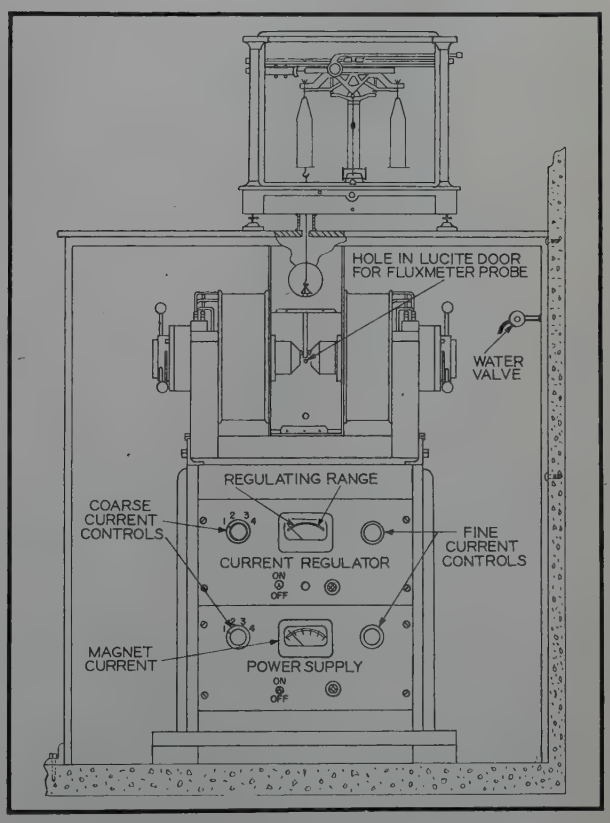

Fig. 1—Arrangement of balance and magnet.

In determining the susceptibility of mineral specimens by the Gouy method, the mineral is reduced to a fine powder and packed in a glass weighing tube. Precise measurement of the bore and depth of the tube is made unnecessary by a calibration procedure. Using the basic expression of Eq. 1, Hoare[6]

Definition of Terms Used in Equations

A : cross-sectional area of test cylinder.
H : higher value of the field strength at cylinder ends.
H_0: lower value of the field strength at cylinder ends.
m: weight change of a test cylinder, in grams.
g : acceleration of gravity.
C : a constant, equal to $\frac{1}{2g}$.
W: weight of water in a weighing tube.
c : weight of water in the meniscus in a tube.
L : length of column of water below the meniscus.
L': length of a weighing tube.
d : density of water at ambient temperature.
f_1 : a constant for a given field strength, pertaining to specimens in weighing tubes, nominally equal to $1 - \frac{H_0^2}{H^2}$
f_2 : a similar constant pertaining to the weighing tubes themselves.
N : a constant applying to the space occupied by a sample in a given weighing tube, defined in Eq. 5.
P : a constant applying to the tube itself, defined in Eq. 9.
S : weight of sample in weighing tube.
s : density of corresponding mineral.
T : weight of a glass weighing tube.
t : density of the glass.
$\delta W, \delta S, \delta T$: changes in the corresponding weights when observed in a magnetic field.
K : the volume susceptibility of a substance, equal to the intensity, I, of magnetism in the substance divided by the strength of the field producing that magnetism. The substance is identified by subscripts:
1. medium surrounding a sample
2. material being tested
w. water
a. air
s. a sample
t. the glass of a weighing tube.

derived Eq. 2 for the calibration of weighing tubes with water as a standard:

$$\delta W = \frac{C(W-c)}{dL}(K_w - K_a)\ (H^2 - H_0^2). \qquad [2]$$

At any given field strength, for a fixed value of L,

$$H^2 - H_c^2 = H^2\left(1 - \frac{H_0^2}{H^2}\right) = f_1 H^2. \qquad [3]$$

Substituting Eq. 3 in Eq. 2 obtains

$$\delta W = \frac{C(W-c)}{dL}(K_w - K_a)\ f_1 H^2. \qquad [4]$$

The calibration characteristic of the tube is now defined:

$$N = \frac{C}{L} = \frac{\delta W}{(W-c)}\frac{d}{f_1 H^2\ (K_w - K_a)}. \qquad [5]$$

Hoare's equation for finding the susceptibility of a salt (or other powdered material) may be expressed as

$$\delta S = \frac{C(H^2 - H_0^2)}{L}\frac{S}{s}(K_s - K_a). \qquad [6]$$

From this it is evident that

$$K_s = K_a + \frac{\delta S}{f_1 H^2}\frac{s}{NS}. \qquad [7]$$

Since the glass of the weighing tubes has a volume susceptibility different from that of the surrounding air, application of the magnetic field causes a weight change in the tube as well as in the contents. By analogy, then, the following equations are established from Eqs. 2 and 5:

$$\delta T = \frac{C'T}{tL'}(K_t - K_a)\ (H^2 - H_0^2). \qquad [8]$$

The constant P is used during calibration of the equipment to assist in averaging the values of f_2 and δT. It is defined by

$$P = \frac{CT}{tL'}(K_t - K_a) \qquad [9]$$

and is obtained by using the relationship

$$P = \frac{\delta T}{f_2 H^2}. \qquad [10]$$

The constants f_1 and f_2 are determined experimentally by methods described later. Any instrumental error in the field strength measurement is absorbed in the values of these constants when they are determined for the different values of H. It should be noted that since L' is greater than L, H_0 does not bear the same relationship to H in f_1 as it does in f_2, and so these two constants are not the same numerically.

The specific susceptibility is calculated from Eq. 11:

$$X_s = \frac{K_s}{s} \qquad [11]$$

Magnetic Balance and Accessory Equipment: For the magnet, a Varian Model V-4004 4-in. electromagnet, water cooled, with V-2300 power supply and V-2301 current regulator was used. Pole pieces tapered to 2-in. diam were selected because they gave a larger field strength than untapered poles or those tapered to 3 in.; the advantage, as compared with pointed poles or poles having 1-in. diam faces, was a field of uniform strength for enough distance from the magnet axis to allow for minor discrepancies in positioning the test samples and to provide space for the probe of a Rawson Lush Fluxmeter for measuring and monitoring the strength of the magnetic field.

An Ainsworth Type TY semi-micro analytical balance with magnetic damper was used for the weighings. It was modified at the factory for weighing suspended loads and was mounted over the magnet as shown in Fig. 1.

For magnet weighings a piece of gold locket-chain, with a ring at the upper end and a hook at the lower, was hung from the left pan. A support disk of thin aluminum was attached to the hook.

A piece of pyrex glass tubing, 8 mm OD by 14.8 cm long, was used for each weighing tube. One end was closed and the other flared so that it resembled a test tube. The flaring was carefully positioned so that the tube, when placed in the slot in the aluminum disk, would hang with the inside of the bottom at the axis of the magnet poles. After flaring, the tops were ground flat and loosely fitting aluminum stoppers were made. Each tube was inscribed at 10, 11, and 12-cm depth (only the last depth was actually used), and each tube and corresponding stopper was lettered to match.

Specimen Preparation and Handling: Specimens were identified by place of origin whenever this was known. To obtain the most precise values possible, careful preparation of the specimens was required. With one exception (Climax wolframite), each sample was hand-picked to remove excess waste after being broken to about ¼ in. It was then crushed to pass a 48 mesh screen. The Climax sample, a concentrate of about 100 pct −65 mesh, was treated in the same manner as the other specimens from this point. The material was then screened to +100, 100 to 200, 200 to 270, and −270 mesh fractions. The smallest fraction was discarded as being too fine for effective concentration by the magnetic and gravity processes that followed.

An Isodynamic separator, Model L1, was used to eliminate highly magnetic minerals such as magnetite from all specimens, and, from the wolframite series and the magnetic sphalerites, the gangue of low attractability. A special technique was developed for preparation of small quantities of concentrate of higher purity.

The wolframite group was next cleaned with acid to remove soluble gangue minerals, including sulfides and carbonates.* After 4 cc of concentrated nitric acid per gram of sample were added to the mineral, it was held at a low boil in a hood for 10 min, the acid was decanted immediately, and the remaining solids were washed several times with distilled water and dried. From this point on, all specimens were treated alike.

The dry mineral was next screened on the following Tyler sieves: 65, 100, 115, 150, 170, 200, 250, and 270 mesh. Each size fraction was then further cleaned separately in a free-settling classifier. The rising current was adjusted to cause a small part of the material to overflow while the bulk settled in the column. The settled product was examined on the petrographic microscope for remaining gangue, and it was recleaned if there appeared to be an excessive quantity.

The density of each specimen was measured by taking up to 18 g of the largest size particles—usually larger than 100 mesh—and making at least two determinations with a pycnometer. An agreement within 1 pct was sought.

The cleaned specimens were ground in a mullite mortar on a Fisher mortar grinder until all would pass through a 270 mesh sieve. The ground sample

* Although Dana[7] states that wolframite is insoluble in acids, some solubility in hydrochloric acid was noted and is possibly a function of composition.

Table I. Magnetic Characteristics and Chemical Composition of Minerals in the Wolframite Series

Origin	Susceptibility*		Density	Chemical Analysis, Pct			Spectrographic Analysis, Pct**				
	Specific	Volume		Fe	Mn	W	Co	Ni	Al	Ba	Be
Huebnerites: iron to manganese atomic equivalent ratio less than 1:4											
North Carolina	36.83±0.11	261.3	7.096	0.34	17.25	58.68	—	0.03	0.04	—	—
Mexico	35.87±0.17	251.5	7.012	0.53	16.67	55.46	0.06	0.045	0.17	—	—
Wolframites: iron to manganese atomic equivalent ratio from 1:4 to 4:1											
Korea	36.50±0.17	261.3	7.161	4.08	11.19	58.47	—	0.04	0.04	0.02	—
Climax	35.94±0.13	249.3	6.937	5.82	11.17	59.04	—	0.04	0.2	0.02	—
Silverton	35.60±0.73	257.4	7.231	5.96	10.71	56.57	—	0.03	0.04	—	—
China	35.57±0.20	258.5	7.266	9.10	8.05	58.49	<0.008	0.035	0.02	0.02	—
Sweden	34.27±0.06	242.4	7.074	9.89	7.62	58.30	—	0.04	0.035	0.02	0.00017
England	35.66±0.16	256.8	7.200	10.63	6.58	55.79	—	0.035	0.025	0.02	0.00011
France	35.00±0.25	247.3	7.065	12.79	5.22	59.26	—	0.035	0.16	0.02	—
Unknown	31.75±0.21	217.1	6.838	13.53	3.96	56.45	—	0.03	0.14	0.02	0.0007
Ferberites: iron to manganese atomic equivalent ratio greater than 4:1											
Peru	33.33±0.23	242.7	7.284	15.74	2.20	56.55	—	0.035	0.02	0.08	—
Malaya	35.25±0.23	253.1	7.180	17.22	1.64	59.37	—	0.035	0.018	0.025	—
Nederland—A	32.92±0.10	210.3	6.388	17.70	0.75	56.95	0.02	0.035	0.25	0.04	—
Nederland—B	33.39±0.08	212.4	6.360	16.83	0.40	57.68	—	0.03	0.1	0.02	—

Origin	Spectrographic Analysis, Pct**											
	Ca	Cr	Cu	Mg	Pb	Si	Sn	Sr	Ti	V	Zn	Zr
Huebnerites: iron to manganese atomic equivalent ratio less than 1:4												
North Carolina	—	—	—	0.035	—	<0.05	—	—	0.011	—	—	<0.001
Mexico	0.35	—	0.04	0.1	0.025	—	0.14	—	0.02	—	—	<0.002
Wolframites: iron to manganese atomic equivalent ratio from 1:4 to 4:1												
Korea	0.2	<0.001	0.008	0.045	0.1	—	—	—	0.055	—	—	0.0055
Climax	0.18	0.002	0.018	0.12	0.25	0.4	—	—	0.25	—	0.055	0.025
Silverton	<0.18	—	0.007	0.013	—	0.08	<0.04	—	0.008	—	<0.03	<0.003
China	0.19	0.002	0.013	0.01	0.09	—	<0.04	—	<0.004	—	0.07	0.012
Sweden	0.4	0.0014	0.014	0.20	0.11	—	0.05	—	0.013	—	0.09	0.015
England	0.3	0.0035	0.035	0.035	—	0.08	—	0.006	0.014	—	<0.001	0.011
France	0.35	<0.002	0.04	0.05	0.045	0.55	—	—	0.015	—	0.045	0.01
Unknown	0.3	<0.002	6.	0.013	0.03	0.25	0.045	—	0.014	—	<0.006	0.007
Ferberites: iron to manganese atomic equivalent ratio greater than 4:1												
Peru	0.35	0.008	0.06	0.12	2.5	<0.05	—	0.006	0.05	0.095	1.	0.016
Malaya	0.35	0.005	0.013	0.075	0.04	—	0.055	—	0.05	—	—	0.013
Nederland—A	0.5	0.005	0.1	0.055	0.13	3.	0.06	0.006	0.05	0.095	0.1	0.013
Nederland—B	0.5	0.007	0.005	0.035	0.04	3.	0.045	0.006	0.05	0.095	0.035	0.016

* Susceptibility is in cgsm units x 10^6. Susceptibility values are an average of observations at 10,000, 15,000, 19,000, and 21,000 oersteds.
** As and Mo were not detected in any specimens. Ag was not found except 0.005 pct in the Peruvian wolframite; Nederland *A* contained 0.085 pct Sb, not observed in the others.
Dashes indicate that an element was not detected in concentrations within the sensitivity of the method used and the line observed.

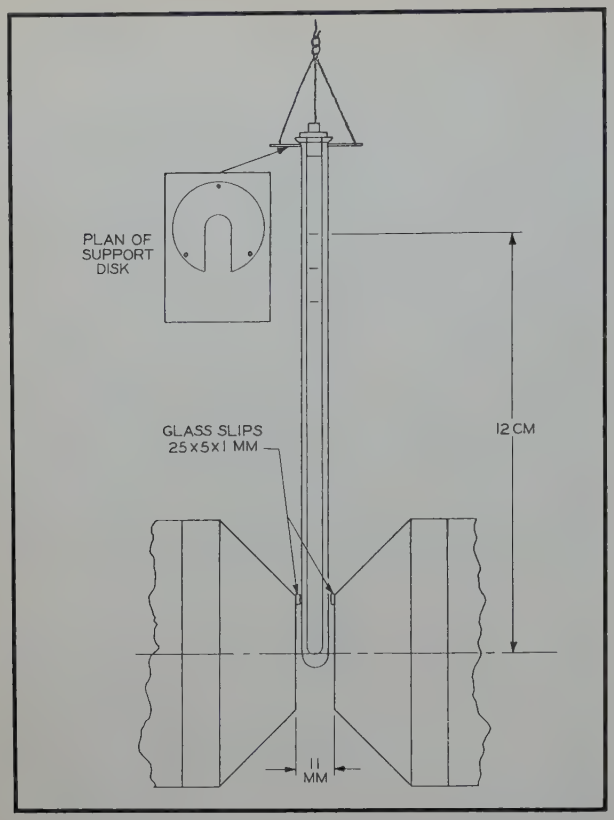

Fig. 2—Weighing tube suspension details.

was placed in a plastic vial 1 in. diam by 2 in. long, with a glass baffle 11/16 in. wide, 3/16 in. thick, and 1 15/16 in. long fastened in the cap. It was then placed in a large-mouthed jar on rotating rollers and mixed for a minimum of 4 hr.

The mineral powder was transferred from storage vial to weighing tube in a pyrex tube. The powder was added to the weighing tube in small increments and tamped solidly with a pyrex rod.

Operation of Magnetic Balance: Four calibrated weighing tubes were filled with a given specimen and weighed at null-field and at each of four field strengths. From the corrected $\delta(T + S)$ the appropriate value of δt was subtracted algebraically, leaving δS.

For convenience in calculation, Eq. 7 may be rewritten

$$\frac{K_s - K_a}{s} = \frac{\delta S}{f_1 H^2 N S}. \qquad [12]$$

The function $(K_s - K_a) \div s$ was computed for all specimens in the wolframite group

At this point a pattern that was reasonably consistent across all samples was observed in the values of the function: for any sample the figures calculated for 10,000 oersteds were the smallest, with successive increases in magnitude to those for 21,000 oersteds. This was attributed to errors in determining f_1, possibly owing to the small number of observations on which those computations were based. It is possible that the pattern was caused by a slight ferromagnetic characteristic of the mineral.

To eliminate the error, the sum of the determinations of the function for a given specimen at one field strength was divided by the average of all determinations on that specimen. All of the quotients so found for a given field strength were added together and divided by the number of individual weighings at that field. This gave factors that corrected the original f_1's when multiplied by them. The functions from Eq. 8 were adjusted accordingly.

A second pattern, related to individual weighing tubes, was next observed. This was eliminated by a similar process to correct N for each tube. The function $(K_s - K_a) \div s$ was again adjusted and was analyzed statistically for each specimen to eliminate highly divergent units. Of the 242 original weighings of wolframite group minerals, only 8 were discarded by this operation.

After elimination of the anomalous original weights, the entire calculation was repeated and the probable error determined. Multiplication by s gave $K_s - K_a$; to this K_a was added; and, finally, this last sum was divided by s to obtain X, the specific susceptibility.

In the case of the sphalerite specimens it was found that a ferromagnetic characteristic caused a variation in susceptibility with field strength. The corrected values of f_1 and N obtained in the wolframite study were used to compute $(K_s - K_a) \div s$ for each weighing, and the average of the four values at each field strength was used to determine K_s and X.

Removed from weighing tubes, the samples were analyzed by wet methods for major constituents and spectrographically for minor components. Iron, manganese, and tungsten in the wolframite group—designated as (Fe, Mn) WO_4—and zinc, sulfur, and iron in the sphalerites were considered to be major.

Wolframite Series Minerals: Data for the wolframite group are given in Table I. The iron-to-manganese atomic equivalent ratio varies from 1:52 in the huebnerite from North Carolina to 41:1 in one of the ferberites from the Nederland district in Colorado.

It may be noted that the sum of the iron and manganese in the Malayan ferberite exceeds that possible if the formula is (Fe, Mn)WO_4. Dana[8] suggested that ferberite did not exist as $FeWO_4$, but rather as a combination of $FeWO_4$ with FeO.

Crystallographic theory developed since Dana expressed his solution of the problem has demonstrated the impossibility of such a compound, and FeO has not been identified as a naturally occurring substance.

The latest edition of Dana[9] suggests instead: "The departure from (Mn, Fe): $W = 1$ shown by some analyses of ferberite and other members of the series apparently is due to analytical error." Although this is an easy explanation of composition difficulties, and although it is recognized that the accuracy of analyses of wolframite by the best procedures now known is always subject to question, it is believed that lack of agreement between the iron-plus-manganese content and the tungsten assay in various cases may be attributed to the presence of oxides of iron.

It is not proposed, of course, that these oxides are compounded with the wolframite in contradiction of crystallographic principles, but rather that there is an intimate mixture of wolframite, ilmenite, magnetite, and possible hematite crystals of submicroscopic size; there may also be other minerals in the mixture. The presence of titanium, as revealed by the spectrograph, indicates ilmenite, and both ilmenite and magnetite could be among the minerals removed by the Isodynamic separator during the cleaning process when it was operated at low magnetic intensity. The fact that strongly

magnetic minerals were present in larger sizes supports the contention that they could be locked in the supposedly pure wolframite samples used in this investigation and others.

The presence of hematite or one of its modifications was suggested by the gangue associated with the Nederland *A* ferberite, which had the general appearance of ferruginous chert under the microscope.

The relationship found between iron content and specific susceptibility in the wolframite family is shown in Fig. 3. The linear relationship between X^2 and the percentage of iron may be expressed by Eq. 13:

$$X^2 = 1347 - 13.1\,\text{Fe}. \qquad [13]$$

The correlation coefficient of the linear data is —0.762; the odds against a chance occurrence of such a correlation are greater than 500 to 1. It is recognized that this correlation and the equation are sensitive to small variations in the specific susceptibility and in the iron assay; they are presented to show that there is a dependence of susceptibility upon iron content and that the susceptibility decreases, rather than increases, with larger amounts of iron in the mineral.

The positions of the points for the Malayan and the unknown samples are worthy of comment. None of the x-ray patterns for these samples indicated the principal magnetite lattice spacing,* but a number gave indications of the secondary spacing. A particularly strong response from the Malayan sample suggested magnetite in the specimen. Since a percentage of magnetite too small to be detected by x-ray procedures could have a noticeable effect on susceptibility, it is considered that failure of this technique to give a positive indication of magnetite does not rule out its presence. The unknown specimen gave no unusual spacings in its x-ray pattern; the 6 pct Cu revealed by spectrographic analysis could have had a strong depressing effect on the susceptibility, as that element and its sulfides are theoretically diamagnetic.

Most significant is the fact that correlation of magnetic susceptibility with iron content is negative, and therefore positive with reference to manganese. Although manganese has the strongest response of the paramagnetic elements other than oxygen, it would not normally be expected to have a stronger effect than a ferromagnetic element such as iron. The explanation is to be found in studying the ionic susceptibilities of manganese and iron.

Iron in the metallic state is ferromagnetic, and thus its susceptibility varies with field strength. In the combined form, however, the ions have paramagnetic susceptibilities. The value for Fe^{+++} is the same as that for manganese, whereas for Fe^{++} it ranges from 89 to 94 pct of the amount for the ferric ion. Consequently when iron replaces manganese in the compound (Fe, Mn)WO_4, the net paramagnetic susceptibility is reduced.

When iron occurs with both valences in the same compound, as in magnetite, Fe_3O_4 or $Fe_2O_3 \cdot FeO$, or pyrrhotite, $Fe_{z-1}S_z$, the ion has a ferrimagnetic nature, and high susceptibilities that vary with field strength are observed.

* A spacing ranging from 2.46 to 2.497A on the wolframite group may have concealed it.

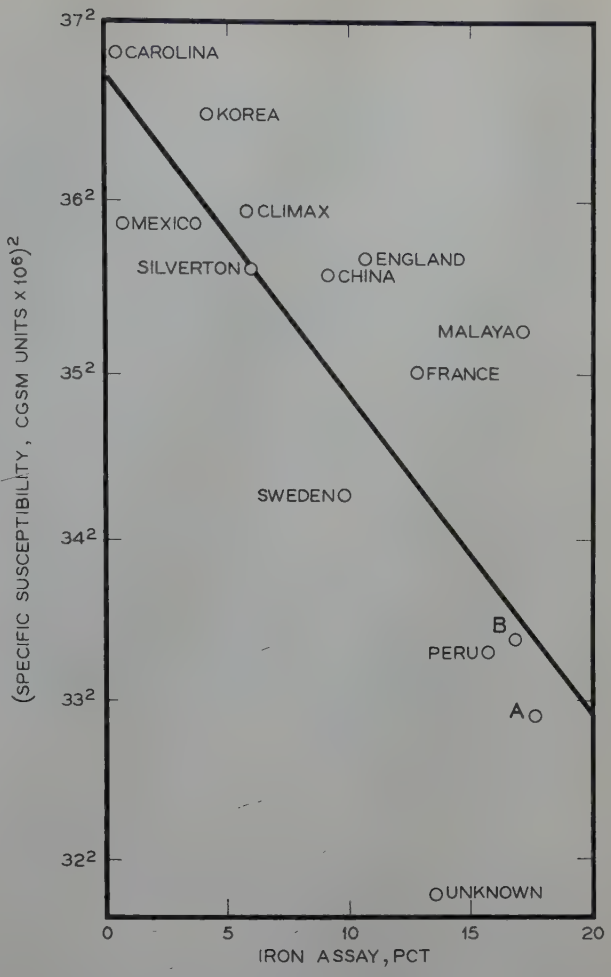

Fig. 3—Correlation of magnetic susceptibility with iron content in minerals of the wolframite group.

Sphalerites: Table II presents the data on sphalerite. It will be seen that each specimen has a different susceptibility for each field strength; this is due to the presence in the mineral of some substance that is either ferromagnetic or ferrimagnetic. The fact that iron is in the mineral, almost certainly in the form of a sulfide, is evidence that this characteristic is caused by the ferrimagnetic sulfide, pyrrhotite. The x-ray patterns of the various specimens did not differ significantly from each other with respect to the various sulfides of iron; however, only the Gilman sample contained enough iron for the sulfide to be detected by this technique.

Another noteworthy feature in Table II is that neither the susceptibility at a given field nor the rate of decline of that characteristic with increasing field strength is closely related to the iron content; the difference in rate of decline is strikingly indicated by the crossing lines in the bottom portion of Fig. 4.

The spectrographic record of higher nickel content in the Lockport sample is the most likely explanation of the greater slope, indicating stronger ferromagnetism, and the higher susceptibility at lower field strength, where ferromagnetism is more effective. It will be noted that the decline of the Lockport susceptibility places the values in a more normal relationship in fields greater than 19 kiloersteds.

The lower susceptibility of the Chester sample compared to the Bucks may be explained by the higher copper content of the Chester sample.

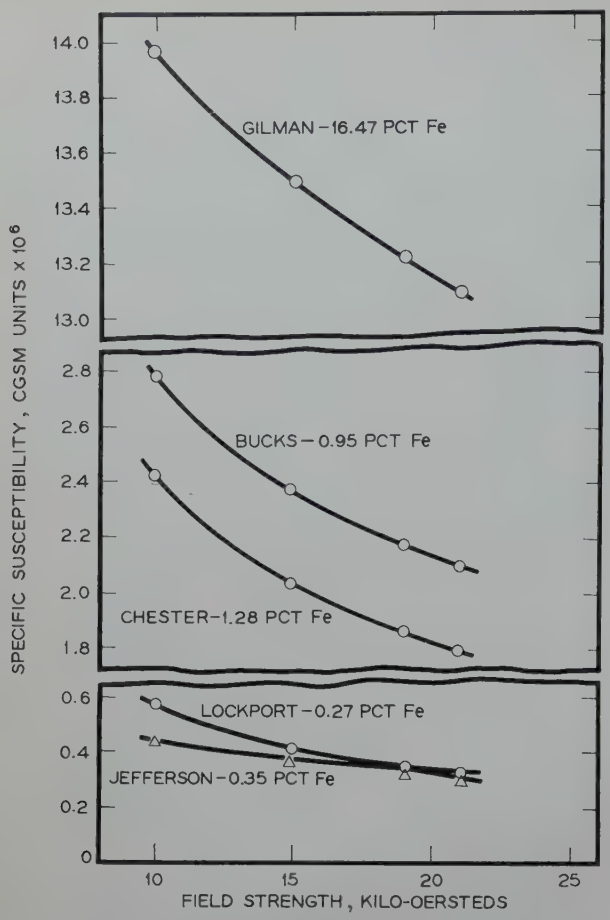
GILMAN – 16.47 PCT Fe
BUCKS – 0.95 PCT Fe
CHESTER – 1.28 PCT Fe
LOCKPORT – 0.27 PCT Fe
JEFFERSON – 0.35 PCT Fe
SPECIFIC SUSCEPTIBILITY, CGSM UNITS x 10⁶
FIELD STRENGTH, KILO-OERSTEDS

Fig. 4—Relationships between iron content, field strength, and magnetic susceptibility of sphalerite.

Correlation between iron content and magnetic response appears again to be parabolic, expressed at 10,000 oersteds by Eq. 14:

$$X^2 = 12.13\ \text{Fe} - 5.07 \qquad [14]$$

The correlation coefficient for the five values was +0.9995, with less than one chance in 1000 of fortuitous occurrence. In this case, of course, correlation is positive with respect to iron. It will be noted that susceptibility should be zero when the iron assay drops to 0.42 pct; the Lockport and Jefferson samples would be expected to have negative rather than positive values. More extensive investigation of this mineral should give a regression line intercepting the iron axis farther to the left.

The equation indicates that iron-free sphalerite should have a susceptibility of −2.57, which would not be possible. (Bismuth, the most diamagnetic of the solid elements, has a susceptibility of −1.35; the hydrogen has −1.97). The value of −0.264 for sphalerite reported by Voigt and Kinoshita[10] doubtless indicates the direction the line should take.

With the exceptions mentioned, the minor constituents or trace elements observed were not considered to have a significant effect upon the susceptibilities in either group of minerals.

Conclusions

The primary dependence of magnetic susceptibility upon iron-containing minerals was established, with the unexpected postulate that in minerals where iron in the ferrous state has a substitution relationship with manganese, there may be an inversion of the correlation of susceptibility with iron content. It was observed that susceptibility varied as the square root of the iron content, either directly, as in sphalerite, or inversely, as in wolframite.

The negative correlation of susceptibility with iron content in the wolframite series appears to be in direct conflict with a commonly accepted concept that the wolframite minerals are nonmagnetic with the exception of ferberite. This has been stated: "The high-iron members of the series are weakly magnetic."[9] Further conflict with this statement is found in Table I, which indicates a range in specific susceptibility of 31.7 to 36.8 x 10^{-6} cgsm units. This variation of some 15 pct between high and low values is hardly enough to justify a distinction between weakly magnetic and nonmagnetic members of the series, particularly when the nonuniformity of the magnets found in most laboratories is taken into consideration. It must be concluded that any ferberite that is unusually magnetic owes this property not to the high percentage of iron in the form of the tungstate, but to the presence of additional iron as magnetite, intimately locked with the ferberite so that it cannot be distinguished from the ferberite.

Because the concept that the ferberites are more highly magnetic is faulty, any attempt to improve

Table II. Magnetic Characteristics and Chemical Composition of Sphalerites, Susceptibility in Cgsm units x 10^6

Origin	Specific Susceptibility				Volume Susceptibility				Density	Chemical Analysis, Pct		
	H = 10,000	15,000	19,000	21,000	10,000	15,000	19,000	21,000		Zn	Fe	S
Gilman	13.962	13.493	13.220	13.088	56.71	54.81	53.70	53.16	4.062	42.05	16.47	33.75
Chester	2.4333	2.0438	1.8592	1.7912	9.960	8.365	7.610	7.331	4.093	63.15	1.28	32.18
Bucks	2.7809	2.3748	2.1748	2.0981	11.117	9.493	8.694	8.387	3.998	61.98	0.95	30.46
Jefferson	0.4508	0.3816	0.3499	0.3376	1.757	1.487	1.364	1.316	3.898	59.60	0.36	29.72
Lockport	0.5697	0.4120	0.3386	0.3130	2.314	1.673	1.375	1.271	4.062	61.19	0.27	31.13

Origin	Spectrographic Analysis, Pct*													
	Co	Mn	Ni	Ag	Al	Ba	Ca	Cu	Mg	Pb	Si	Ti	W	Zr
Gilman	—	0.14	0.02	0.006	0.045	<0.02	0.15	0.3	0.06	0.5	—	0.02	3.5	0.012
Chester	0.013	—	0.035	0.004	0.02	0.03	0.15	2.	—	0.17	1.1	<0.002	—	<0.004
Bucks	<0.01	0.15	<0.007	—	0.065	—	0.3	0.018	0.18	0.5	3.	0.01	0.7	0.002
Jefferson	—	—	<0.001	0.0013	0.08	<0.02	0.4	0.019	0.35	0.025	1.	0.018	2.5	0.005
Lockport	—	—	<0.008	—	0.02	—	0.19	0.1	0.073	0.45	0.8	0.006	—	<0.001

Probable error is not indicated for the specific susceptibility of the sphalerite specimens because each value was based on only four observations.

* As, Be, Mo, Sb, Sn, and Sr were undetected. Cr (<0.003 pct) and V (<0.008 pct) were found only in the Gilman specimen.

grade and recovery of tungsten in this mineral by finer grinding to increase liberation of ferberite will probably give a magnetite concentrate and reject most of the tungsten with the types of concentrators now in use. Improvement should be sought by regrinding the present concentrates and removing the magnetite at low field intensity.

Since even the least magnetic of the wolframite samples was concentrated on the Isodynamic separator in the cleaning process, it is obvious that any mineral of this series which can be liberated from the accompanying gangue of low susceptibility without excessive grinding can be concentrated by a high intensity magnetic separator of proper design.

Sphalerite was found to possess the ferromagnetic characteristic of variation of susceptibility with field strength; from 10,000 to 21,000 oersteds that relationship was negative, with as much as 45 pct decline over that range. By contrast, the wolframites had susceptibilities more than twice that of the strongest sphalerite observed, with no ferromagnetic decline in strong fields.

The results indicate that the study of minerals now considered to have susceptibilities too low for magnetic separation should be continued, as present concepts may be erroneous. The study of minerals falling above and below this group in susceptibility should be carried out to give a complete picture of the magnetic properties of minerals.

Acknowledgment

This work was made possible by a fellowship grant of the National Science Foundation. It is reported in detail in a doctoral dissertation by Ernest Melvern Spokes entitled *The Relation of Magnetic Susceptibility to Composition in Minerals of the Wolframite Group and in Sphalerites,* The Pennsylvania State University, August 1956.

References

[1] L. G. Gouy: C. R. Academy of Science, Paris, 1889, vol. 109, p. 935.
[2] P. Pascal: C. R. Academy of Science, Paris, 1910, vol. 150, p. 1054.
[3] L. F. Bates: *Modern Magnetism,* 3rd ed., p. 115. Cambridge, 1951.
[4] S. Freed: *Journal of the American Chemical Society,* 1930, vol. 52, p. 2702.
[5] P. W. Selwood: *Journal of the American Chemical Society,* 1933, vol. 55, p. 3161.
[6] F. E. Hoare: *Proceedings of the Royal Society,* 1934, vol. 147, p. 88.
[7] J. D. Dana, et al.: *Manual of Mineralogy,* 16th ed., p. 311. John Wiley & Sons, New York, 1952.
[8] J. D. Dana, et al.: *The System of Mineralogy,* 6th ed., p. 985. John Wiley & Sons, New York, 1892.
[9] J. D. Dana, et al.: *The System of Mineralogy,* 7th ed., vol. 2, pp. 1066, 1067. John Wiley & Sons, New York, 1951.
[10] National Research Council of the U. S. A.: International Critical Tables, vol. 6, p. 364. McGraw-Hill Book Co., New York, 1929.

Discussion of this paper sent (2 copies) to AIME before April 30, 1958, will be published in MINING ENGINEERING.

Discussion

Genesis of Titaniferous Magnetites and Associated Rocks of the Lake Sanford District, New York

by J. L. Gillson

(MINING ENGINEERING, March 1956; AIME Trans., vol. 205)

Andre Hubaux: In the writer's opinion, more stress should be put on field and microscope observations, as J. L. Gillson does. His discovery of relics of big labradorite feldspars from the Marcy anorthosite in all the other rocks is proof enough that previous field observations have been inadequate.

The writer's field experience with anorthositic massifs is limited to the Egersund-Sogndal district in southern Norway; however, this is a very large and well exposed area. It seems to have so many points in common with the Adirondack region that a detailed comparison should be beneficial. This comparison was not possible 20 years ago, owing to the scarcity of geological data, at least for Norway. Both regions are now far better known—the Norway district because of the work of Professors Bugge and Barth[33–35] and especially because of the extensive field and microscopic research of P. Michot,[36–46] who introduced me in the field to the problems of that region.

In a particular unit of the Egersund district, a sodification of the plagioclase, very similar to what Gillson calls "andesinization," has taken place.[43] The percentage of anorthite in the plagioclase has dropped from 42 to 43 pct in the original norite down to 27 pct, but never below that level. This metasomatical transformation is a part of a whole series of processes of migmatitization which have produced, above the level of granitization, concentrations of Mg, Fe, and Ti and among them, patches and parallel bands of ilmenite and magnetite.

Thus both regions present somewhat comparable features and the theories to explain them have several points in common. However, as there seem to be differences between some American conceptions and the views commonly accepted at the University of Liege, I would like to make some comments about J. L. Gillson's article.

The author speaks of the garnet as being an antistress mineral. However, garnet may be found in schists, where its helicitic texture, when present, demonstrates its formation during differential movement. Furthermore, the whole concept of stress and anti-

stress minerals is no longer considered valid by European geologists, since it has been demonstrated that all supposed anti-stress minerals could be formed under nonhydrostatic pressure, and vice-versa.

The author describes and shows with photographs reaction rims of garnet which are "so characteristic of the gabbro and gabbroic ore" (p. 301) and which express a chemical disequilibrium between the feldspar and the ferromagnesian solutions responsible for the formation of these rocks. Later solutions formed the magnetite, ilmenite, etc., which are the ore minerals. But these minerals are presented as being later than the garnets. Must we then believe that these last solutions, in opposition to the first, did not react with the feldspar—that they were in chemical equilibrium with that mineral? This important difference between the activity of the first and last solutions is astonishing and should be explained.

Whatever hypothesis is put forward concerning these garnet reaction rims it should be noted that they do not exist in the Egersund district. There, many kinds of ores[47] are in contact with plagioclase, with which they seem to be in perfect chemical equilibrium.

All the problems dealing with anorthosite and related rocks are so difficult that as many observations as possible should be found to give us a hint concerning the origin of the different units. Along that line I suggest the following:

Among the norites and leuconorites of the Egersund district, some undoubtedly have a magmatic origin, whereas others, on the contrary, are formed by recrystallization in the solid state. P. Michot has demonstrated that the hypersthene in the magmatic norites has a *poikilitic interstitial texture*. The writer has found that in the same rocks the ilmenite[47] and the magnetite have the same texture. In such rocks, when they are examined in the field, the ferromagnesian minerals are evenly distributed and seem to have the same granularity as the plagioclase, and all minerals seem to have a diameter of about 1 mm. However, seen under the microscope, the grains of hypersthene, ilmenite, and magnetite are in fact much larger than those of the feldspar.

All the grains of one mineral have the same optical orientation within an area more than 2 cm in diam. This means that the grains of that mineral in this area belong to the same crystal that envelopes the plagioclases. This is readily seen for the hypersthene and the ilmenite, respectively in thin section and in polished section. When the nicols are crossed, and the stage is rotated, many *grains* of the mineral visible in the field show simultaneously the same color, since those *grains* all are parts of the same crystal. For the magnetite, one must rely on the parallelism of spinel and ilmenite grains formed by ex-solution to visualize the continuity of the crystals. Descriptively, this can be compared to big calcite crystals that are sometimes formed in sandstone, one individual of calcite enveloping and containing numerous grains and aggregates of sand. More correctly it can be compared with the ophitic texture, but it differs from it by the equidimensional aspect of the plagioclase and the very disseminated character of the enclosing mineral.

This is the poikilitic interstitial texture; it does not exist in norites and leuconorites which have recrystallized. In those rocks, on the contrary, the hypersthene, the ilmenite, and the magnetite are still interstitial, but they are much more equidimensional, and separated grains do not have the same orientation. Thus this aspect—this poikilitic interstitial texture—is very useful in the Egersund district to distinguish between norites of simple magmatic origin and norites in which recrystallization with or without introduction of new substances has taken place. It would be valuable to know whether this same criterion holds good for the rocks of the Adirondack region. If this is proved to be the case, then it could be used to identify the rocks that Gillson presents as meta-gabbro and distinguish them from those that other authors have called true gabbros of magmatic origin.

J. L. Gillson *(author's reply)*—Hubaux believes that he has developed diagnostic criteria for distinguishing recrystallized norites (or gabbro) from those of magmatic origin. Those rocks which are of magmatic origin have a poikilitic texture in which the hypersthenes, ilmenites, and magnetites are larger than the feldspars and include feldspar grains. No such observation was made in the Adirondack rock. If this texture is truly lacking, then the gabbros of the Adirondack are due to recrystallization as postulated in the original article. Obviously many observations of similar rocks must be made to establish the validity of this feature as a diagnostic one.

Hubaux also questions the conclusion that garnet is an anti-stress mineral. In the Adirondack rock the andesine grains show no strain, and the garnet which is later can be presumed to be an anti-stress mineral.

Garnet reaction rims are very characteristic of the Adirondack rocks and are not confined to the ilmenite-magnetite ores but are seen in some gabbros intrusive (?) into gneisses. Also admittedly they are not found in other anorthosite and gabbro rocks containing ilmenite-magnetite or ilmenite-hematite ores, like the deposits of the San Gabriel Mountains in California, at St. Urban, and at Allard Lake in Quebec. The garnet reaction rims indicate a period of unequilibrium that was characteristic of Adirondack conditions but was not a universal condition in rocks of this type. The reaction rims do, however, indicate recrystallization, and that was the point to be made.

Hubaux is to be commended for his additional information and observations in regard to these interesting rock types.

References

[33] T. F. W. Barth: The Large Pre-Cambrian Intrusive Bodies in the Southern Part of Norway. *International Geological Congress*, 1933, vol. 16, pp. 297-309.

[34] T. F. W. Barth: Litt om Sorlandets anorthositer. *Norsk geologisk tideskrift*, 1941, vol. 21, nos. 2 and 3, 1941, pp. 186-191.

[35] T. F. W. Barth: Geological map of the western Sorland. *Norsk geologisk tideskrift*, 1945, vol. 25, pp. 1-9.

[36] R. Michot: La série rubanée norite-granitique du massif anorthositique d'Egersund. *Annales de la Société Geologique de Belgique*, 1939, vol. 62, pp. 632-546.

[37] P. Michot: La couronne d'anorthosite hypersthenifère feuilletée et rubanée du massif anorthesitique d'Egersund. *Annales de la Société Geologique de Belgique*, vol. 62, pp. 547-551.

[38] P. Michot: Les anorthosites de la region d'Egersund. *Acad. Boy. de Belg. Bull. Classe des Sciences*, 1939, 5th ser., vol. 25, pp. 491-503.

[39] P. Michot: Le problème des textures dans les roches éruptives du massif anorthositique d'Egersund. *Ass. franc. p. avanc. des sciences, Liege*, 1939, pp. 524-528.

[40] P. Michot: Essai sur la geologie de la catazone (first note). *Acad. Roy. de Belg. Bull. Classe des Sciences*, 5th ser., 1951, vol. 37, pp. 260-276.

[41] P. Michot: Essai sur la geologie de la catazone (second note). *Acad. Boy. de Belg. Bull. Classe des Sciences*, 1952, 5th ser., vol. 38, pp. 495-500.

[42] P. Michot and J. Michot: Enclaves dans les anorthosites de la region d'Egersund. *Annales de la Société Geologique de Belgique*, 1953, vol. 76, pp. 239-247.

[43] P. Michot: Anorthosites et anorthosites. *Acad. Roy. de Belgique, Bull. Classe des Sciences*, 1955, 5th ser., vol. 41, pp. 275-294.

[44] P. Michot: L'anatexie leuconoritique. *Acad. Roy. de Belg. Bull. Classe des Sciences*, 1955, 5th ser., vol. 41, pp. 374-385.

[45] P. Michot: Structures tectoniques dans la catazone norvegienne. *Acad. Boy. de Belg. Bull. Classe des Sciences*, 1956, 5th ser., vol. 42, pp. 209-227.

[46] P. Michot: Les gisements de minerals noirs de la region d'Egersund. *Annales de la Société Geologique de Belgique*, 1956, vol. 79, pp. 183-202.

[47] A. Hubaux: Différents types de minerals noirs de la région d'Egersund. *Annales de la Société Geologique de Belgique*, 1956, vol. 79, pp. 203-215.

[48] J. Michot: Le phénomène magmatique au sein du massif anorthositique de Haaland, Egersund, Norvége. *Annales de la Société Geologique de Belgique*, 1955, vol. 78, pp. 247-266.

Collected Discussion of

Energy-Size Reduction Relationships In Comminution

(MINING ENGINEERING, page 80, January 1957, AIME Trans., vol. 208)

by R. J. Charles

Discussers
- F. C. Bond
- D. W. Fuerstenau
- J. A. Holmes
- A. J. Lynch

F. C. Bond: This is an outstanding paper on comminution theory and represents a considerable advance in mathematical formulation. It clears the way for a discussion that should ultimately decide whether the work index should be considered as a parameter according to the Third Theory or as a constant.

In the empirical differential equation

$$dE = -C\,dx/x^n \qquad [1]$$

either C or n must be treated as a variable to satisfy known crushing and grinding conditions. The author has chosen the exponent n as the variable, with C as a constant.

According to the Third Theory, in the general case n is a constant equal to 3/2, and C is a variable related to the work index Wi. If x is placed equal to P (the size in microns which 80 pct of the product passes) and F is the size 80 pct of the feed passes, then C equals 5 Wi, and

$$\int_0^W dE = \int_F^P -5\,Wi\,dx/x^{1.5} =$$

$$W = \frac{10\,Wi}{\sqrt{P}} - \frac{10\,Wi}{\sqrt{F}}$$

which is the basic equation of the Third Theory.

It is apparent that this integration involves the error of treating the parameter Wi as a constant, just as the author's treatment involves the error of integrating his variable n as a constant. These errors are probably relatively unimportant, considering the small range of the variables. When more is known about the factors contained in the work index, Eq. 1 can be revised as a partial differential equation.

The Third Theory exponent of 1/2, or $n = 3/2$ in the Charles' differential equation (Eq. 1), was not chosen primarily because it is the average between the Kick and Rittinger exponents; this may be merely fortuitous, since it is illogical to define truth as the average between two errors. It was first discovered from the study of a large mass of crushing and grinding data and confirmed by laboratory testing. The general correspondence of the Third Theory equation to actual crushing and grinding results over the entire size reduction range argues strongly that a fundamental phenomenon is involved.

The *a posteriori* theoretical explanation of the constant Third Theory exponent is that the work done in breaking rock is proportional to the length of the crack tips formed. Compressive force applied to the rock results in deformation and strain energy. When this locally exceeds the breaking strength a crack tip forms, the surrounding strain energy flows to the crack tip and extends it to split the rock, with release of the energy as heat. Under rapid impact the crack tip may form before the strain has reached equilibrium, resulting in less energy expenditure and probably a coarser product. In any case, the elastic limit of a brittle material is practically the same as its breaking strength, and the work necessary to form the crack tip is the work required to break.

The crack length of a ton of broken rock cannot be measured directly. However, the particle shapes of feed and product are similar, and the crack length is considered equal to the square root of one half of the new surface area formed. It is, therefore, proportional to $1/\sqrt{D}$, where D is the equivalent product particle diameter. This is the basis of the Third Theory equation.

Many secondary factors can be imposed upon the crack length breakage. These may cause the Third Theory work index to increase or decrease somewhat as the product size becomes finer. The work index is properly a parameter rather than a constant, making it an increasingly valuable practical criterion of the work input required in crushing and grinding.

This page of Mining Transactions AIME follows p. 380. The intervening non-Transactions pages appeared in MINING ENGINEERING.

The product size distribution is an important function of the work index, but does not completely control it. Many factors affect the work index by changing the product size distribution and otherwise. The existence of flaws or incipient cracks, bedding planes, natural grain sizes, and crystals are some structural factors affecting the work index. Dynamic factors include: amount and velocity of impact breakage, circulating loads, dilution, ball and rod sizes, mill speeds, etc.

Any analysis of the many factors affecting comminution becomes exceedingly complex and can only be done piecemeal. The point to be made here is that the Third Theory work index is the most nearly constant quantity available, as well as the most readily obtainable, and in the writer's opinion the most acceptable theoretically; therefore, the analysis of any factor is most accurately made by treating it as a function of the work index. Use of the variable exponent proposed by Charles would abandon the first approximation already available and would permit much larger errors.

The author's treatment is based on the assumption that the Schuhmann size distribution slope α remains constant as the product size decreases. Experience has shown that when the natural fines are not removed the slope normally decreases with the product size. When 80 pct of an average material passes 1 in. or more the slope approaches unity, where 80 pct passes 48 mesh it is approximately one half, and when 80 pct passes 325 mesh it is 0.4.

Charles selected the Schuhmann power law size distribution rather than the Rosin-Rammler exponential type or the log-probability plot. None are entirely satisfactory, although theoretical considerations seem to favor the exponential law.

He offers four experimental tests of the variability of the exponent n. Each of these tests involves a special case, with feed particles all of one size or closely sized between the three screen sizes from ⅜ in. to 6 mesh. According to the Third Theory n remains constant for the general case when the feed contains particles of all sizes in their natural weight distribution down to the grind limit.

It is probable that the value of n increases as the fines are artificially removed from the feed. When the fines are removed n also increases as the reduction ratio decreases. This explains the tests confirming the Rittinger theory in which a closely sized feed was used. The Third Theory equation requires an empirical correction in the feed size parameter when fines are removed from the feed.

The work index can continue essentially constant for different materials independently of whether the characteristic Schuhmann slope α is large or small. This is illustrated in the laboratory ball mill grindability test results tabulated beow:

Ore Copper	Anaconda		Utah	
Specific Gravity	3.22		2.86	
Grind. Test No.	1477A		938A	
Circulating Load, Pct	250		250	
Mesh Size Tested	α	**Wi**	α	**Wi**
28	0.715	12.2	0.615	12.8
35	0.710	12.0	0.610	10.8
48	0.695	10.9	0.610	10.5
65	0.680	11.0	—	10.6
100	—	12.5	—	10.6
150	—	12.4	—	10.2
200	—	—	—	11.7
Average	0.700	11.71	0.612	11.03
Standard deviation, pct	—	6.32	—	8.82

There can be no doubt that the work index criterion is more practical.

The Third Theory equation permits the rapid calculation of required work input when only one size parameter is known—the size 80 pct passes. Variations in size distribution slope are automatically reflected in the Wi value, and complete screen analyses are not required. On the other hand, use of the exponent n as the sole variable would require size distribution information that is often not available and would greatly restrict work input calculations.

The evidence appears to favor Charles' choice of n as a variable to correct for artificial adjustment of the feed size distribution, usually by screening out fines. When a natural feed is used, n appears to remain constant at 3/2, and the work index Wi varies, both with the material being tested and the machine operation. Standard laboratory tests define Wi for any particular material. Changes in machines, impact velocities, circulating loads, and other operating factors cause changes in both the product 80 pct passing size and the size distribution parameters, resulting in work index variations and consequent changes in mechanical efficiency. Much experimental work remains to be done before these factors can be evaluated.

R. J. Charles *(author's reply)*—The author appreciates F. C. Bond's interest in the work under discussion and would like to comment on his several points.

The Third Theory equation, written in its general form, is as follows:

$$W = \frac{10W_i}{\sqrt{P}} - \frac{10W_i}{\sqrt{F}} \text{ where } W_i = f(F,P) \qquad [19]$$

The equation can be generalized no further, since the function f, which defines the parameter W_i, can only be determined experimentally for each specific case to which the whole equation is applied. Thus, in general, when all boundary conditions are set the term W_i varies with product and feed size. In this writer's opinion an equation of the type

$$W = K\left[\frac{1}{k_P{}^{\gamma}} - \frac{1}{k_F{}^{\gamma}}\right] \qquad [20]$$

where k_P and k_F are size moduli solves the above difficulty of a varying constant, for when the constants K and γ are chosen correctly there is no necessity of bringing in a parameter to adjust the equation to fit experimental evidence. As a consequence, since it is a constant, it may be integrated and is not subject to the criticism in paragraph four of the discussion. Similarly, on the above basis, this writer objects to the statement: "The Third Theory work index is the most nearly constant quantity available, as well as the most readily obtainable."

The derivation of the general energy-size reduction equation was not predicated on any specific type of size distribution. The Schuhmann power law distribution was used only as an example that is apparently applicable to a number of experimental cases. Further, this writer is not aware of any theoretical considerations that favor any specific type of size distribution for a ground product.

With respect to the tabulated data in the above discussion the W_i values appear to be relatively constant. As a consequence the n value for both sets of data would be approximately 1.5. No stipulations would be placed on the corresponding a values except that they be greater than 0.5, which is apparently the case.

It is difficult to draw comparisons of practicality of something that has been in use for a relatively extended period of time and something that has not been tested. The Third Theory has been used with great success for many industrial problems and in many cases this writer advocates its continued use. He feels, however, that it is an inadequate mathematical description of the physical process of size reduction and as a consequence is likely to hinder further advancements of the scientific aspects of the problem.

D. W. Fuerstenau: The article by Charles has put considerable light on some of the problems of comminution, yet one important factor in his article appears to have been neglected. The question arises as to how the theory given can account for the effect of changes

of feed size in a comminution process on the energy required for a specific size reduction. In the derivation of the specific energy-size reduction relationship, used to correlate experimental results, the influence of feed size has been neglected by an approximation. Also in the experimental results all tests were performed from a constant and usually sized feed material. Any theory that can satisfactorily describe the comminution process must account for both the initial and final sizes of the particles involved, and for the work in question the reasons for dropping the terms that account for feed size in the derived equation must be explored more deeply.

R. J. Charles *(author's reply)*—Fuerstenau brings up an important point that still requires experimental investigation. The approximation referred to is, of course, only valid if the size reduction is large. If this is not the case then the feed size term should re-enter the general equation even though a relatively complicated procedure must then be followed to solve for the necessary constants. For the most general case, where the feed and product size distributions are similar, the general energy-size reduction equation leads, as indicated in the article, to the following:

$$E = \frac{C\,\alpha}{(n-1)\,(\alpha-n+1)}\left[k_p^{1-n} - k_f^{1-n}\right] \qquad [21]$$

where k_p, k_f = size moduli of product and feed; C, α, n = constants; and E = energy.

The above equation may state the case correctly; however, it is possible that a large change in feed size may alter operating conditions and therefore the equation could not be expected to hold. Unexpectedly, the above equation provides a key for testing whether or not the feed size term can be neglected. If the term $(\alpha - n + 1)$ appears negative then the approximation is not valid.

J. A. Holmes: The importance of the excellent article by Charles in stimulating a new and more flexible attitude towards size reduction problems cannot be over-emphasized. The tendency in the past has been to accept one or another of the dogmatic principles with which studies of this subject have been plagued and to pay insufficient attention to the really important characteristics of a crushing or grinding operation, namely, the properties of the material undergoing fracture and the conditions under which stresses are applied. The author of the article has indicated the true academic nature of the so-called laws of comminution and has shown that they have no direct application to crushing and grinding problems in which the quantity of useful product obtained per unit of energy input to a more or less inefficient machine is the important criterion of operation.

It is evident from Charles' results and from those obtained by the writer[16] that for any one grinding machine the value of n is determined by the properties of the material and by the variation of the efficiency of the machine in treating different sizes of particle. However, there remain these questions—what effects do different material properties and different conditions of reduction have on the efficiency of different machines, and how are these effects reflected in the general equation developed independently by Charles and by the writer. In this respect Charles' consideration of the following comments would be of interest.

It is claimed in the article that for quartz ground in a ball mill the same value of n was maintained down to very fine sizes, the finest products being assessed by measurement of surface areas. One would perhaps expect some change in n to occur as grinding progressed due to a change in the efficiency characteristic of the ball mill as the material became very fine. Since no such change was measured it would be interesting to know more about the conditions of grinding and the fineness of grind achieved in these tests. It is well known that assessments of ground products by surface area measurements are critically dependent on the method of measurement used, so that Charles' opinion on the krypton gas adsorption method in relation to grinding problems of this sort would also be of interest.

For the tests on the rod mill and ball mill it was assumed that the energy input was proportional to the grinding time. It would be interesting to know whether this assumption was supported by measurements over the whole range of reduction achieved, since it seems possible that, as the material became finer, changes in the coefficients of friction between the grinding surfaces and in the viscosity of the pulp might result in changes in the configuration of the ball or rod charge.

Charles finds that for pyrex, quartz, fluorite, and cement rock the expression $\alpha - n + 1$ tends to zero. Other materials showing well developed cleavage did not obey this rule, and since distributions of these materials deviate most markedly from the Schuhmann equation, so that α can have little significance, these exceptions are not unexpected. However, tests on quartz performed by the writer[16] in a dry grinding laboratory ball mill gave values for n and α of 1.77 and 1.07, respectively, as compared with 1.88 and 0.91 obtained by Charles in a wet grinding mill. For the dry grinding test $\alpha - n + 1 = 0.30$, as compared with 0.03 for wet grinding. Relatively large values of this expression were obtained for other inhomogeneous ores tested by the writer, even though the size distributions followed the Schuhmann law reasonably closely. It would seem, therefore, that the value of $\alpha - n + 1$ is not necessarily close to zero but is dependent on the properties of the material and on the conditions of reduction. This seems a more acceptable conclusion for two further reasons: 1) the Schuhmann law is, at best, only an approximation of the true size distribution, so that any fundamental relation between α and n seems unlikely, 2) because as $\alpha - n + 1 \to 0$, Charles' constant $A \to \infty$.

If this conclusion is correct it follows that Charles' comments on Kick's law require revision, for as n tends to the value 1 no implicit limitation is then imposed on the value of α. However, the writer agrees that the tendency is for α to decrease as n decreases and that Kick's law may be applicable for reduction of material of such fineness that its resistance to reduction becomes independent of particle size.

It is clear from Eq. 15 that the elegant graphical method of determination of n cannot be used when x_m is not large compared with k. Since this is often the case in large-scale milling practice, where stage grinding through relatively small reduction ratios may be employed, it would be of value to know how Charles would treat such a problem. Also it is not normal grinding practice to feed particles of one size, the case for which Eq 15 was derived. The writer has recently formulated a similar equation:

$$E = K\left[\frac{1}{P^r} - \frac{1}{F^r}\right] \qquad [22]$$

where r = the Kick's law deviation exponent, $= n - 1$. This equation refers to reduction of one Schuhmann distribution with an 80 pct passing size F, to a similar distribution with an 80 pct passing size P and differs from Eq. 15 in that the factors of $\frac{1}{Fr}$ and $\frac{1}{Pr}$ are the same. Charles refers briefly in his article to the treatment of unsized feeds, but in view of the above difference his more detailed comments would be of interest.

Reference has been made to results obtained in dry grinding tests on quartz in a laboratory ball mill. These results are compared in Table II with those obtained from Bond's tests under the same conditions and with those reported in the present discussion.

Although more precise details of the structural properties of the quartz and of the conditions of reduction are necessary for a complete understanding of the observed variations in n and α, these figures serve to illustrate the importance of these properties and con-

Table II. Comparison of Values of n and α for Quartz

Author	Machine	Material	Location	α	n
Charles	Rod mill, 10-in. diam (wet)	Quartz	Not given	0.91	1.90
Charles	Ball mill, 10-in. diam (wet)	Quartz	Not given	0.91	1.86
Hukki	Frictionless crusher	Quartz	Not given	0.93	1.88
Bond[17]	Ball mill, 12-in. diam (dry)	Quartz	California	—	1.79
Holmes[16]	Ball mill, 7½-ft diam (wet)	Quartz	California	—	1.70*
Holmes[16]	Ball mill, 12-ft diam (dry)	Quartz	Cornwall, U. K.	1.07	1.77
Holmes[16]	Ball mill, 7½-ft diam (wet)	Quartz	Cornwall, U. K.	—	1.68*

* Calculated figure.

ditions in determining the behavior of any one material.

R. J. Charles *(author's reply)*—Holmes' comments are especially appreciated in view of the fact that, simultaneously with this work, he has presented similar arguments, reasoned from a more fundamental basis, for the variable exponent concept of energy-size reduction. The interested reader is urged to study Holmes' work,[16] for in this writer's opinion it contains a complete solution for a long-standing problem in comminution.

With reference to the comment on fine grinding of a variety of quartz the experimental results show a possible trend (see Fig. 10) to increased resistance at the finest sizes, ($k_p \approx 5\mu$). Gas adsorption surface area measurements, while reproducible to 2 or 3 pct, are generally considered to give values within 10 pct of absolute and thus the above slight deviation from linearity, if real, could not be clearly delineated. Continuous torque measurements were not made during the investigation; however, particular attention was paid to mill design in that lifter bars were installed to aid in maintaining constant ball and rod configuration. Wattmeter readings, which give only rough indications of power actually consumed by small mills, remained essentially constant during the tests. On the assumption that the size distributions in these tests remained similar it must be concluded that the efficiency characteristics of the mill remained relatively constant.

Since the variable exponent n is limited by the value of α and since experiments conducted by both Holmes and this writer on a number of materials show that there is a marked tendency for n to decrease as α decreases, the possibility that n and α are related should not be discounted. The relationship may be only a consequence of the assumptions used in describing size distributions, but in any event it is worthy of study. The constant A does not approach infinity because the term $(\alpha - n + 1)$ approaches zero but because the term $(n - 1)$ approaches zero. In the statement regarding Kick's law the term $(\alpha - n + 1)$ was considered small, positive, and finite.

If the feed size is not large compared to the product size then the approximation referred to is, of course, not valid and the feed size term must re-enter the equations. For the case of similar feed and product size distributions integration of the general energy-size reduction equation leads to the same equation cited by Holmes. For different feed and product size distributions a slightly different equation is obtained. In any case, experimental determination of the constants required is still most easily made by testing in the range where product size is far removed from feed size. Once n is determined the feed size term can be introduced for a complete solution.

A. J. Lynch: This method of determining energy-size reduction relationships in comminution is a refinement of the general method of such determinations which has been used in various forms by Rittinger,[2] Kick,[3] Bond and Jen Tung Wang,[18] and Bond.[7] As such it is open to the same errors as these others, especially where heterogeneous ores, as defined by Gaudin,[13] are concerned.

The article is based on the Schuhmann equation for size distribution and is applicable only to solids which, after comminution, have a sizing analysis that may be defined by that equation. However, it was pointed out by Roller that this equation rarely applied to more than the finest 15 pct by weight of the particles and that in many cases the size distribution is not, in fact, a straight line but a smooth curve.

It is obvious from an inspection of Figs. 2, 4, 5, 8, and 10 that the actual product sizing analysis may differ markedly from the interpolated sizing analysis and the actual 100 pct passing size may vary greatly from the interpolated value. However, no attempt has been made to account for these variations in the calculated relationship.

The grindability is regarded as the power required for a given reduction of the solid under standardized conditions or the reduction of the solid achieved by the expenditure of a given amount of power under standardized conditions. In effect the constant n, which is a measure of the energy required to reduce the solid from some interpolated 100 pct passing size to another, is a direct function of the grindability in the same manner that the work index used in the Third Theory is a direct function of it.

The theory proposed by Charles is, in essence, similar to the Third Theory except that the criterion of size is an interpolated 100 pct passing size instead of an actual 80 pct passing size. However, the possible errors inherent in it appear to be smaller than those in the Third Theory because the measure of grindability used takes into account the full size range and is less influenced by abnormal conditions at any particular size range and is therefore more accurate.

R. J. Charles *(author's reply)*—The author appreciates the comments by A. J. Lynch and is pleased to offer the following reply. The general energy-size reduction equation, given in the article, is not based on any specific size distribution and the Schuhmann equation was used only as an illustration of how the general equation may be applied. A complex size distribution makes integration of the general equation difficult, but in principle it can be done. To avoid carrying out individual graphical integrations for specific cases, accuracy is sacrificed, for the sake of generalization, by use of an approximation. Further, it is the author's opinion that even a serious deviation from the Schuhmann equation can be tolerated in the specific procedure outlined, since all that is required is that the theoretical size modulus k be a measure of the lateral shift of similar size distribution plots.

The constant n is not analogous to the work index used in the Third Theory, for the work index is a proportionality parameter similar to the generalized constant A in the present work. The main difference between the Third Theory and the present work is that a variable exponent, dependent on material and means of processing, is advocated rather than a fixed exponent.

References

[16] J. A. Holmes: *Trans.*, Institute of Chemical Engineering, vol. 35.
[17] F. C. Bond: *AIME, Trans.*, 1949, vol. 183, p. 313.
[18] F. C. Bond and J. T. Wang: A New Theory of Comminution, *AIME Trans.*, 1950, vol. 187, p. 871.
[19] P. S. Roller: Discussion of TP 1358, *AIME Trans.*, 1941.

Seismic-Refraction Method in Ground-Water Exploration

by William E. Bonini and Eugene A. Hickok

IN the course of an investigation directed toward expanding ground-water facilities in Essex and Morris counties, New Jersey, the Board of Water Commissioners of the city of East Orange authorized a seismic-refraction survey[1] for the purpose of delineating bedrock topography below unconsolidated overburden. Results of the survey were highly satisfactory and led to the preparation of a comparatively detailed bedrock contour map. Knowledge of the bedrock depth and configuration was an important aid in selection of sites for test drilling.

The portion of the East Orange Water Reserve under consideration is in the flood plain of the Passaic River about 10 miles west of Newark, N. J. The flood plain is about 175 ft above mean sea level and is bordered by low hills rising to elevations of approximately 250 ft. The bedrock underlying the Water Reserve consists of sandstone and shale of the Triassic Brunswick formation and is covered everywhere by deposits of unconsolidated glacial outwash sand and gravel, lacustrine clay, and recent river silt as much as 150 ft thick. Yield of wells in the sandstone and shale averages 100 to 200 gpm. Since production wells constructed in the sand and gravel aquifer in the buried river valley shown on the contour map (Fig. 1) yield 300 to 1400 gpm, it was proposed to locate additional production wells in this buried valley, where the yields per well would be maximum.

In 1939 and 1946 the East Orange Water Dept. had electrical-resistivity surveys made to determine depths to bedrock. From the resistivity data the exploration company prepared a bedrock contour map. A well field expansion program begun in 1955 utilized this information to locate sites for test wells along a predicted northward extension of the buried valley in which existing production wells are located. After several test wells (wells 201-205) had been drilled, it became apparent that the resistivity information was unreliable.* For example, test well 201 recorded bedrock at a depth of 72 ft, whereas the resistivity depth determination was 130 ft. As a consequence, the test drilling program was temporarily suspended and a seismic survey was undertaken to determine the topography and extent of the buried valley known from well records to underlie the existing well field.

In the first phase of this study, several seismic shot point locations were placed at sites where well logs had been obtained previously. This procedure is necessary in a new area to determine whether the seismic method is applicable and what degree of accuracy is to be expected. At the East Orange Water Reserve, depths obtained from the shot points near test wells 202, 203, and 204 were within 8 to 11 pct of the depths logged (Table I). With this assurance that accurate results could be obtained, additional seismic spreads were located on the Water Reserve.

Using a portable refraction seismograph, in the fall of 1955 a crew of four men shot a total of 29 reversed seismic spreads in a period equivalent to six field days. Charges as heavy as 3 lb of 40 pct dynamite were necessary at a few places to overcome ground vibrations caused by traffic on nearby highways. At most other sites, a 1-lb charge was sufficient.

Travel-time plots were made for all spreads, and depths and true velocities were calculated according to formulas for multiple sloping layers by Ewing, Woollard, and Vine.[2] The plot of spread 7 (Fig. 2) is typical of the short spreads in which bedrock was shallow—about 50 ft in this case. Where there were not enough arrivals through the bedrock to define the high velocity bedrock line, the spreads were lengthened. This was done by placing shots on line several hundred feet away from each end of the line of geophones. It was then possible to construct complete reverse plots for both short and extended shot points (see spread 27, Fig. 3). Four individual depths were calculated from each extended spread.

Three and in some cases four seismic layers were observed. The surficial layer had a velocity range of 900 to 1200 fps, the lowest velocity recorded. This seismic layer is above the water table and is interpreted as recent river silt. The bedrock had the highest velocities, which ranged from 10,600 to 16,400 fps.

Intermediate velocities ranged from 4500 to 6800 fps. In every case the intermediate layer was within

W. E. BONINI is Assistant Professor, Department of Geological Engineering, Princeton University, Princeton, N. J. E. A. HICKOK is Consulting Ground-Water Geologist with Geraghty, Miller & Hickok, New York, N. Y.

TP 4717L. Manuscript, June 17, 1957.

* Details of the resistivity surveys were not available to the writers, so it was not possible to analyze these data to determine why the method, successful in other areas, gave poor results in this case.

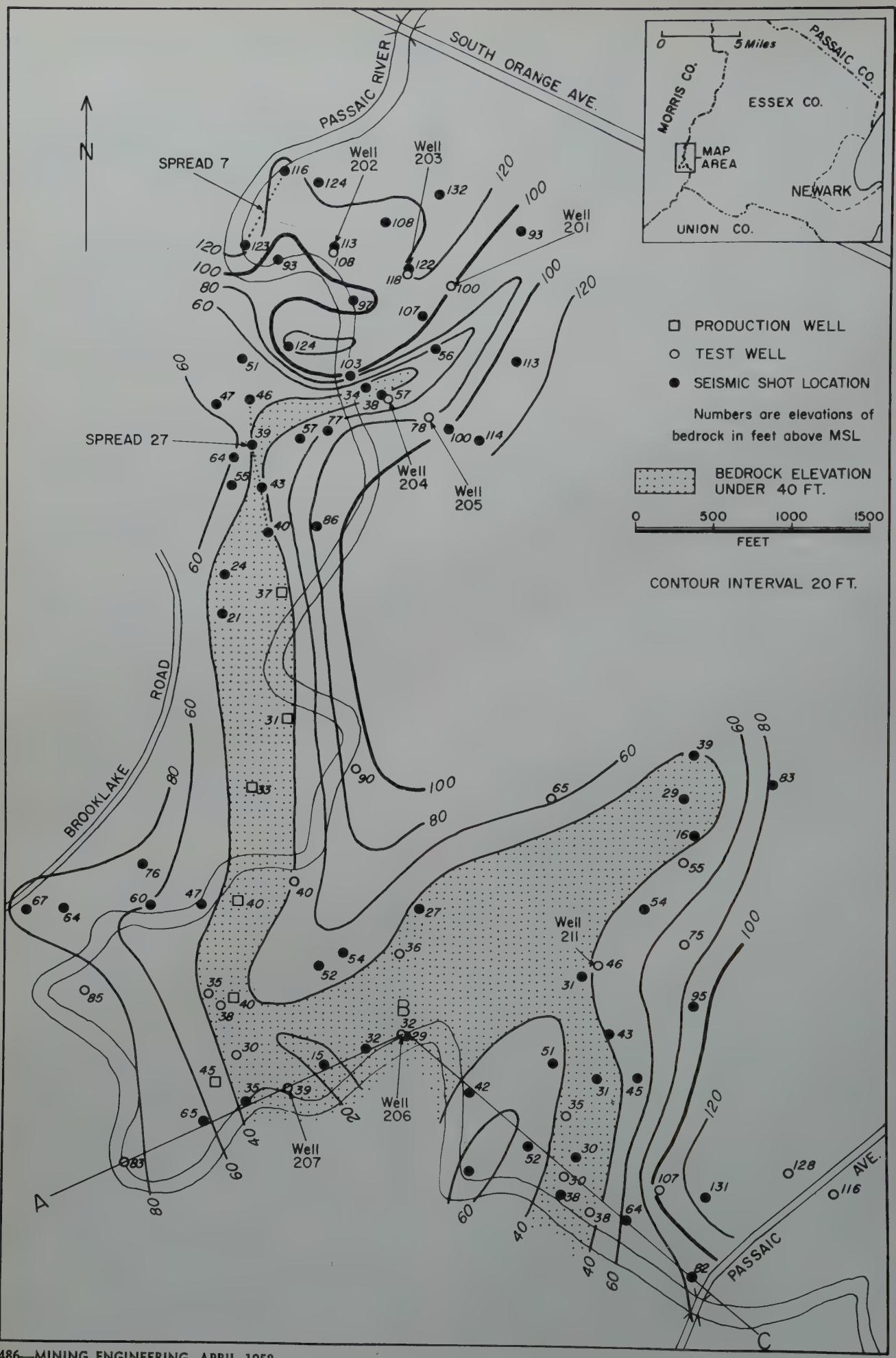
PASSAIC RIVER
SOUTH ORANGE AVE.
N
SPREAD 7
SPREAD 27
Well 202
Well 203
Well 201
Well 204
Well 205
Well 206
Well 207
Well 211
BROOKLAKE ROAD
PASSAIC AVE.
A
B
C
0 5 Miles
PASSAIC CO.
MORRIS CO.
ESSEX CO.
MAP AREA
NEWARK
UNION CO.
PRODUCTION WELL
TEST WELL
SEISMIC SHOT LOCATION
Numbers are elevations of bedrock in feet above MSL
BEDROCK ELEVATION UNDER 40 FT.
0 500 1000 1500
FEET
CONTOUR INTERVAL 20 FT.

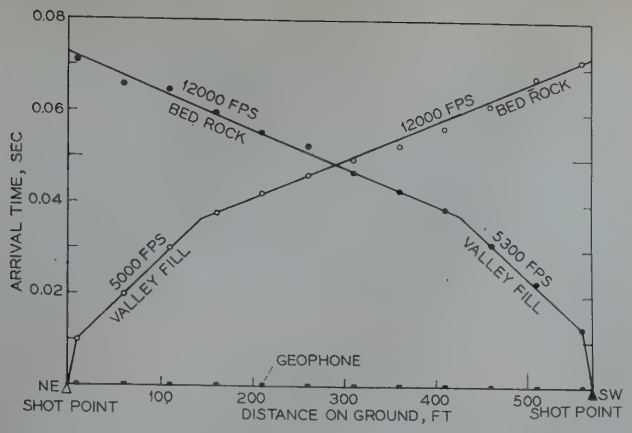

Fig. 2—Travel-time plot for seismic spread 7.

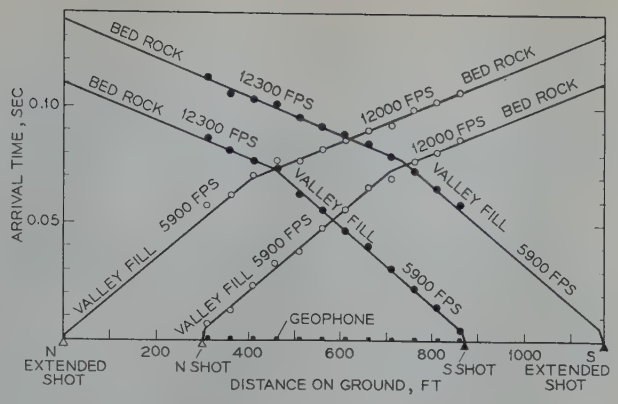

Fig. 3—Travel-time plot for seismic spread 27 with extended shot data.

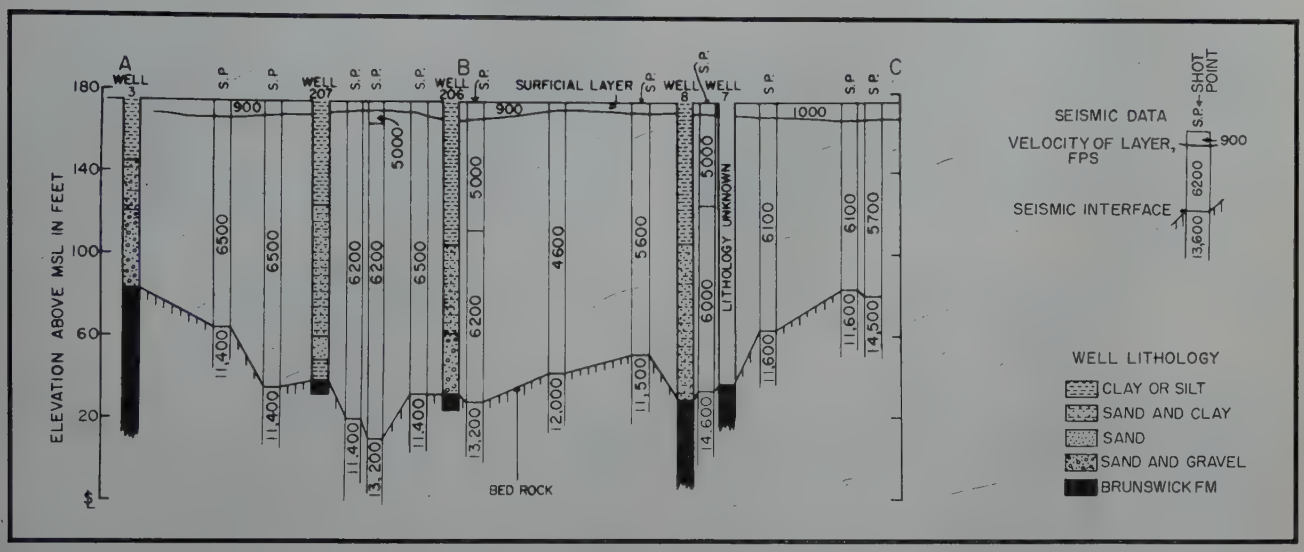

Fig. 4—Cross section A-B-C showing close comparison between well data and seismic-predicted bedrock elevations.

10 ft of surface and is correlated with unconsolidated valley fill below the water table. In five of the spreads two intermediate velocities were recorded. There are not enough data to correlate definitely the higher of these velocities with lithology. However, the log of test well 206 (Fig. 4) located near a shot point indicated a change from predominantly silt to inter-stratified *sand and clay* at a depth very near the velocity interface. Similarly, two other spreads near well 205 recorded velocities of 4500 and 6100 fps in one case and 4700 and 6800 fps in the other. The log of well 205 shows a change in lithology from gray clay to fine-to-medium gravel within 5 ft of the depth of velocity transition.

As can be seen, there is a very favorable velocity contrast between the unconsolidated valley fill and the bedrock in this area. The thickness of material above bedrock ranged from a minimum of 37 ft to a maximum of 159 ft.

Contours on the bedrock have been drawn (Fig. 1) on the basis of the seismic information and from well data. The main buried valley, in which the existing production wells are located, narrows and branches to the north. In the south the valley widens considerably where it is joined by a tributary buried valley entering from the northeast. Cross section A-B-C (Fig. 4) shows the close agreement between seismic and well-log data. Wells 206 and 207 were drilled at two locations indicated by the seismic work to be in the main valley. Wells 3, 7, and 8 existed prior to the seismic work.

A pumping test conducted at test well 206 indicated that a permanent production well at this site would be as good as any of the existing production wells or better. A new production well is scheduled for this location. Well 207 was drilled 800 ft west of well 206 toward an existing production well. However, the aquifer material at this site was too thin to warrant construction of a production well. The northeast branch valley was not explored in detail since it has been observed that maximum yields are obtained from wells located near the Passaic River. A single test well drilled in the area (well 211) did not encounter good aquifer material.

Table I lists actual bedrock depths determined from six test wells, with bedrock depths predicted by nearby seismic work. The predicted seismic depths given in the table for each well site were projected from nearby seismic data. At well 206,

Fig. 1 (left)—Contour map of Triassic bedrock surface in part of the East Orange Water Reserve. Well and seismic control are indicated.

drilled at the exact site of one of the seismic depth determinations, bedrock was encountered within 3 ft of the predicted depth. Maximum error determined was 11 pct; mean error was about 7 pct.

Table I. Comparison of Actual Depths to Bedrock Determined by Test Drilling with Those Predicted by Seismic Survey

Well No.	Actual Bedrock Depth, Ft	Predicted Seismic Depth, Ft	Percentage Error
8	140	137	— 2
202	60	55	— 8
203	51	47	— 8
204	110	122	+11
206	138	141	+ 2
211	121	131	+ 8

Conclusions

The satisfactory results of the seismic survey made in the East Orange Water Reserve show the desirability of conducting a seismic survey in any ground-water exploration program where determination of the thickness of unconsolidated water-bearing deposits is important. In the studies described above, considerable expense and time were saved by the seismic survey. An average of five seismic spreads and from 10 to 16 depth determinations were made each day. By contrast, drilling a 6-in., 100-ft cable-tool test hole took from two to five days and provided only a single depth determination. It is estimated that the cost of the 69 seismic depth determinations was comparable with the expense of drilling a single 100-ft test well. The seismic survey did not eliminate the need for all test wells but did define the most favorable areas in which to drill test wells to obtain critical aquifer information.

Acknowledgments

The writers wish to thank Charles G. Bourgin, engineer and general manager, East Orange Water Dept., and Leggette, Brashears & Graham, Consulting Ground-Water Geologists, for permission to use the information contained in this report.

References

[1] D. Linehan: Seismology Applied to Shallow Zone Research. American Society for Testing Materials, *Spec. Pub. 122*, pp. 156-170.

[2] M. Ewing, G. P. Woollard, and A. C. Vine: Geophysical Investigation in the Emerged and Submerged Atlantic Coastal Plain, Part III—Barnegat Bay, New Jersey Section. *GSA Bull.*, 1939, vol. 50, pp. 257-296.

Discussion of this paper sent (2 copies) to Aime before April 30, 1958, will be published in MINING ENGINEERING.

Technical Note

Cleaning Fine Coal with Newly Developed Jig

by E. H. Citron

CLEANING fine coal in jigs is not new in Europe, where the feldspar jig is being used almost exclusively for this purpose.

A feldspar jig operates with an artificial bed made up generally of feldspar or other hard rock material. Dimensions and specific gravity of this material must be of suitable values for good bedding qualities. For good efficiency, the size should range between 1x2 in. and 2x2x½ in. thick.

The disadvantage of an artificial bed is that it is not mobile and must be replaced every so often with new material to obtain good cleavage characteristics. A semi-mobile bed has been developed to retain only a part of the feldspar on the sieve screen—the other part is drawn off with the refuse material, from which it is reclaimed and returned to the jig feed. Recirculating this feldspar rock offers definite advantages. However, in time it will lose its original shape because of wear, and new bed material must be added to the jig feed.

The latest feldspar jigs are generally air-pulsated, Baum-type jigs, although more than 70 pct of the feldspar jigs operating in Continental Europe are still of the piston type. These jigs are very popular in Europe, but they do require a great deal of time and attention.

New Theory to Eliminate Artificial Bedding: At the preparation plants of Pittsburg & Midway Coal Mining Co. it has always been the contention that a small piston-type jig could be developed to clean fine ¼x0-in. coal down to 28 to 60 mesh efficiently by obtaining and admitting bedding material from the present plant refuse circuit to the jig feed. This eliminates use of artificial bedding materials. The jig should incorporate these essential adjustable features as follows:

Adjustable Sieve Screen

A screen that can be raised and lowered to increase or decrease washing compartment depth. The sieve screen also can be set on an incline level, or decline.

Adjustable Plunger Eccentric

Length of stroke can be adjusted to increase or decrease pulsion and suction.

Variable Plunger Speed

Variable speed reducer for decreasing and increasing the number of strokes per minute.

Water Distribution

Adjustable baffle plate separating the plunger and sieve compartment so the water can be distributed uniformly over the entire sieve screen area.

Refuse Ejector

Special unique rubber-type refuse ejector gate operated by air and electrically controlled (as a conventional jig).

Automatic Control

Conventional float that measures the specific gravity of the coal-water refuse medium in the jig is of the submerged type. The float is mounted on a vertical stem held in position by two parallel arms. A movable weight regulates the effective specific gravity of the float. The float stem can be raised and lowered, having a graduated scale to indicate the depth of bed for the setting of the float.

Hutch Drawoff

Hutch material is drawn from the cell compartment to the elevator compartment by gravity.

The first one-cell experimental jig incorporating all these features was built in January 1955 by Ore

E. H. CITRON, Member AIME, is Preparation and Mechanical Engineer, Pittsburg & Midway Coal Mining Co., Pittsburg, Kans.

TN 475F. Manuscript, March 12, 1957.

Reclamation Co. of Picher, Okla., under the direction of Pittsburg & Midway Coal Mining Co. The experimental jig was installed at the Pittsburg & Midway mine No. 19 preparation plant in Kansas, where it was set up to handle from 20 to 22 tph of material consisting of underflow from the five 14-in. cyclones and the refuse from the Rheolaveur ⅛x 0-in. fine coal washer. These two combined materials contained 45 to 55 pct of −28 mesh material, 50 pct of which floated at 1.40 sp gr, with a dry ash content of 10.2 pct. The total raw feed contained a 38.2 pct dry ash.

Results obtained from this experimental jig were above expectation. With respect to size, the jig performed most efficiently on all the sizes above 35 mesh—these sizes respresented 75 to 80 pct of total jig product.

Experimental Jig: The company experimented with several combinations of number of strokes per minute and length of stroke, ranging from 200 to 50 strokes per min with length of strokes ranging from 2 to ¾ in. Best results were obtained with the jig operating at 70 strokes per min, having a stroke length of 1 in. This combination of number of strokes per minute and length of stroke does not agree with theories presented in technical papers on fine coal jigging or with authorities on jigging. For treating ⅛x0-in. coal with a plunger-type jig, the revised formula would be as follows:

T = total travel of plunger
S = strokes per minute
L = length of stroke in inches
$T = (2 \times S) \times L = 140$

For example:

If 70 strokes per min are made, the travel of the plunger per revolution of the eccentric will be 140 + 70 = 2 in., and the stroke will be 2 + 2 = 1-in. stroke.

Length of stroke:

The amplitude of pulsation is expressed by the following formula, attributed to Rittinger:

$$V = NA\frac{3.14}{60} \qquad A = V \times N + 60 \times 3.14$$

Table I. Performance Data for New Fine Coal Jig

Test No. 1

Jig Feed: ½ mm x 0, consisting of underflow from seven 14-in. cyclones together with ⅛x0-in. refuse from Rheolaveur fine coal washery.
55 pct 1.40-sp gr float in feed
ash of 1.40-sp gr float
capacity, 22.0 tph
raw ash, 38.3 pct
dry ash, 7.5 pct

Jig Product Analysis:

Mesh	Wt, Pct	Dry Ash	Accumulated Ash
+6	2.2	5.1	5.1
6 x 8	3.4	5.3	5.2
8 x 10	2.4	5.7	5.3
10 x 18	19.1	6.2	5.9
18 x 35	44.8	8.1	7.2
35 x 60	24.2	17.0	9.7
60 x 100	3.4	26.0	10.2
−100	0.5	34.6	10.4

Jig Refuse: 10 pct 1.40-sp gr float; dry ash on float, 8.5 pct

Test No. 2

Jig Feed: same as for Test No. 1
56.5 pct 1.40-sp gr float in feed
30.4 pct raw ash
10.21 pct dry ash on 1.40-sp gr float
capacity 24.0 tph

Jig Product Analysis:

Mesh	Wt, Pct	Dry Ash	Accumulated Ash
+6	2.6	8.55	8.55
6 x 8	3.8	9.27	8.90
8 x 10	2.5	9.38	9.20
10 x 18	19.3	10.11	9.8
18 x 35	42.9	11.2	10.6
35 x 60	14.7	16.28	11.6
60 x 100	12.9	22.7	13.0
−100	1.4	30.05	13.3

Jig Refuse: 11.6 pct 1.40-sp gr float; refuse contained 11.23 pct ash on 1. 40 float; refuse raw ash, 45.93 pct

Discussion

Relation of Magnetic Susceptibility to Mineral Composition

by Ernest M. Spokes and David R. Mitchell

(MINING ENGINEERING, page 373, March 1958, vol. 211)

S. C. Sun: This article by Spokes and Mitchell deserves high commendation. For many years mineral dressers have been at a loss to explain the variation in magnetic susceptibility of the same mineral species obtained from different localities. In fact, they do not even have a list of accurately measured data on the specific magnetic susceptibility of weakly magnetic minerals to consult. Experience as a university teacher has firmly convinced me that the average student has more difficulty in acquiring a satisfactory knowledge of magnetism than of any other branch of mineral dressing. This is almost entirely because the subject has been treated far too much from a strict practical standpoint and far too little from a fundamental one. It is no exaggeration to state that almost all the published theoretical discussions are based on the experimental results of manufactured chemicals and alloys, but not of naturally occurring minerals. In an attempt to remedy this state of affairs, the author of this article not only set up a new magnetic balance in the Department of Mineral Preparation of The Pennsylvania State University, but also performed work of fundamental value, thus pointing the way to further research. This is evidenced by the fact that an investigation of the magnetic susceptibilities of manganese minerals was recently completed by S. G. Watt under the direction of David R. Mitchell, now acting dean of the College of Mineral Industries of the Pennsylvania State University. D. J. Cook is studying the magnetic susceptibility of titanium minerals under my supervision. It is hoped that our research program can be continued for several years and that similar investigations will be initiated at other universities and research institutions.

Ernest M. Spokes *(author's reply)*: The discusser has touched the heart of a pedagogical problem in the field of minerals beneficiation—students do not understand magnetism and, as a result, neither do the graduate engineers. Only recently has the average course in engineering physics started teaching the fundamentals of magnetism, as they are understood in modern physics, in addition to the classical treatment of the mathematical aspects of magnetic phenomena. It is to be hoped that this increasing instruction in fundamentals will improve our understanding and inspire research to determine more of the basic magnetic data that are essential if we are to see improved methods of separation by magnetism.

Intergranular Comminution by Heating

by J. H. Brown, A. M. Gaudin, and C. M. Loeb, Jr.

THE object of most size reduction operations in the mineral industry is to liberate the grains of valuable minerals in the ore from those of the gangue. This is usually accomplished by crushing and grinding the entire mass of ore until there is only a small probability that any single particle contains more than one mineral. During this size reduction only limited control exists over size or composition of the particles exposed to the breaking action, and there is no control over the paths followed by cracks generated during the operation. This lack of control usually results in overgrinding and in production of large quantities of very fine material. The first detriment, overgrinding, is costly in itself, but when combined with the second factor it is doubly so. Not only is the fracture of a free particle unnecessary—the fracture of these particles may also make subsequent separation operations difficult, inefficient, and wasteful.

It has been pointed out[1] that if the object of size reduction is to liberate the valuable mineral component of the ore then, ideally, fracture should follow intergranular paths to the exclusion of transgranular ones. This would result in liberation of the valuable minerals with as little size reduction as possible. This ideal comminution operation is referred to as *intergranular comminution,* and it was the object of the investigation to determine the extent to which it could be developed by heat treatments.

There are many indications in the literature that heating rocks prior to crushing may be favorable. Reports by Holman,[2] Yates[3] and Myers[4] are pertinent. These investigators showed that heating certain rocks prior to crushing them did, in fact, improve their crushing characteristics in that fewer fines were produced, although the fact that intergranular comminution was being effected apparently was overlooked.

In addition, Sosman noted that if there is appreciable anisotropism in the thermal coefficients of expansion of even a pure mineral, then considerable permanent separation of the grains of the rock can be expected as a result of heating the rock to a high temperature.[5] By the same token, if there are appreciable differences in the thermal expansion coefficients of the various minerals of a multi-component rock, similar results should be obtained by heating this rock. This has been tested, partially, by Brenner,[6] who obtained patents covering the heat treatment of some pegmatitic rocks in order to facilitate comminution of these materials. It has also been demonstrated that this may occur in taconite.[12]

Also, the possibility of causing decomposition of one mineral in a rock as a means of promoting intergranular fracture has been considered. Seigle[7] and Schiffman et al.[8] have obtained patents on such processes as applied to calcareous iron ores.

These reports all indicate that heat treatments prior to crushing may contribute materially to intergranular comminution, but they also indicate that no organized attempt has been made to determine the controlling factors of the method or to determine its applicability in general. The present article is a report on the initial phase of such an investigation. The authors have reviewed the claims of prior investigators and have attempted, also, to establish the factors that might determine the applicability of heat treatments in the mineral industry.

In this work 2000-g samples of various rocks were heated in a small laboratory furnace and crushing and sizing operations were carried out in standard laboratory equipment. All samples of each rock were as nearly identical as possible in particle size, grain size, and composition and contained only lumps coarse enough to contain many grains each.

Tests on Granite

A number of tests were made on a coarse grained Finnish granite obtained in the form of coarse chips from a local monument yard. This rock exhibited little variation from piece to piece in either composition or grain size. The minerals contained were quartz, orthoclase, small amounts of hornblende, and minute quantities of mica. Grain size ranged from about 1 mm to about 3 mm.

Temperature of the Heat Treatment: In some cases the granite was heated to a particular temperature and crushed, hot, immediately upon withdrawal from the furnace—in others the rock was allowed to cool before crushing, but without quenching to room temperature after heating. In most tests on granite the heating period was about 2 hr with the furnace at the highest temperature for about 1 hr. Cases in which these periods were varied greatly will be presented separately.

J. H. BROWN is Assistant Professor of Mineral Engineering and A. M. GAUDIN, Member AIME, Richards Professor of Mineral Engineering, Massachusetts Institute of Technology, Cambridge, Mass. C. M. LOEB, JR., is President, Lubri-Case Inc., New York, N. Y.

TP 4731B. Manuscript, Oct. 15, 1957.

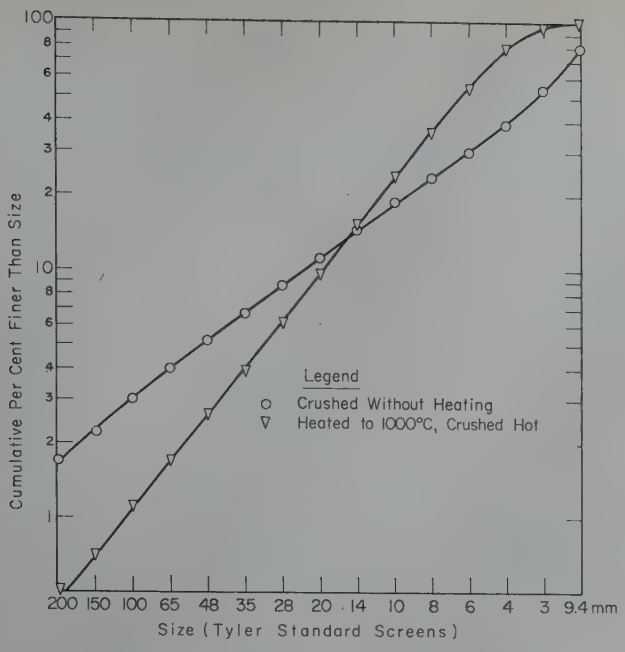
Cumulative Per Cent Finer Than Size
Legend
Crushed Without Heating
Heated to 1000°C, Crushed Hot
200 150 100 65 48 35 28 20 14 10 8 6 4 3 9.4mm
Size (Tyler Standard Screens)

Fig. 1—Size distribution data for granite tests as Schuhmann plots.

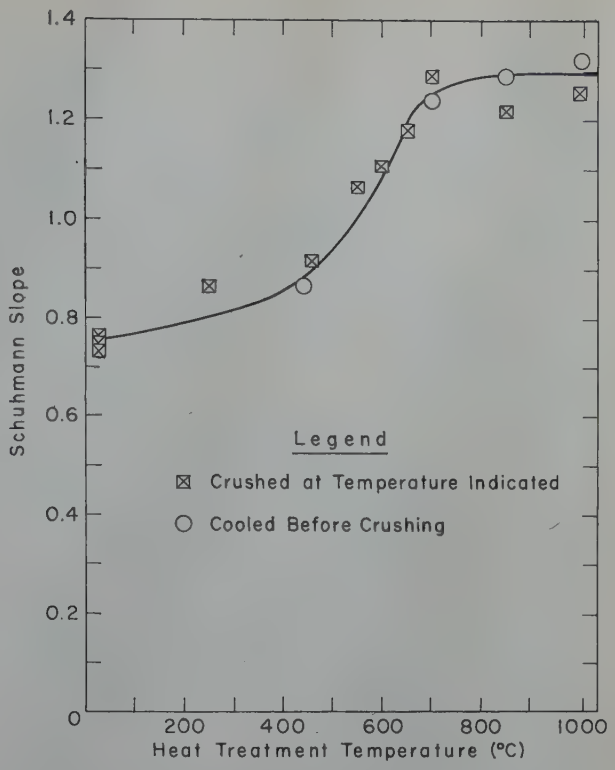

Fig. 2—Slope of Schuhmann curve vs heat treatment temperature for granite tests.

The screen analyses of the various tests were plotted in different ways, but the method illustrated in Fig. 1 was adopted as most suitable for these tests. In this figure the size distribution data for a sample crushed at room temperature and with no heat treatment in a laboratory jaw crusher are plotted as suggested by Schuhmann[9] with similar data for a sample that was heated to 1000°C and crushed at that temperature in the same crusher included for comparison. The difference in slopes of the two distribution curves is striking. The slope of the lines, in their straight portion, is a measure of the dispersion of the crushed product throughout the various size ranges. A high slope corresponds to a product showing little dispersion as in a closely sized product, and a low slope corresponds to a product with a scatter of particles in all sizes. In this case the bulk of the product from tests which had involved heating prior to crushing seemed to concentrate in the size ranges corresponding to the natural grain size of the rock. This was taken as an indication that intergranular fracture was occurring and the slope value was adopted as being indicative of the extent to which such fracture had occurred.

Fig. 2 shows the slope values obtained from plots of size distribution data as a function of the maximum temperature of the heat treatment. The figure shows that a marked change in the size distributions resulted from the heat treatments and that the change due to heating increased with increasing temperature up to a temperature of at least about 700°C. At temperatures above 700°C little further change occurred.

Temperature during Crushing: The data of Fig. 2 are divided into two sets. One series of points represents data obtained when the sample was crushed at elevated temperatures; the other represents that obtained on samples cooled before crushing. It will be noted that while there may be a tendency for samples crushed after cooling to show a different size distribution than those crushed hot (other conditions being the same) the difference appears to be of the same order as the experimental accuracy and is not consistent in its direction.

Tests for Fragility: Two samples of granite, one heated and the other not heated, were crushed in the laboratory jaw crusher set at ⅜ in. and then ground through 20 revolutions of a laboratory ball mill. Size analyses were then made on the products. The data are shown as weight frequency plots on logarithmic scales in Fig. 3. Data for parallel tests that were not ground are included for comparison. The curves show that even the very short grind affected the heated material appreciably, but that the unheated material was almost unchanged except for some production of very fine slimes. The curves show that whereas grinding the heated rock resulted primarily in the breakdown of coarse particles, grinding the raw granite resulted only in production of very fine material without major change in the coarse fractions.

Feldspar Liberation Analysis: The amount of free feldspar in the fraction of each product coarser than 35 mesh is shown in Fig. 4 as a function of the heat treatment temperature. These results were obtained by fractionating each product in a heavy liquid of specific gravity 2.580 ± 0.004. In such a liquid free feldspar particles (of the composition that prevailed in the granite under test) were the only particles that would float; locked particles and free particles of other minerals sank. These data show a large increase in liberation as a result of the heat treatment. Further, the important factor is the heat treatment temperature, not the temperature at which crushing was carried out.

Controlled Atmosphere Tests: One test was run with a nitrogen furnace atmosphere. The gas was passed into the furnace during both the heating and the subsequent cooling steps so that the charge attained a temperature of 1000°C and then cooled without the usual contact with oxygen. The product obtained under these conditions was almost identical to that obtained by heating to the same tem-

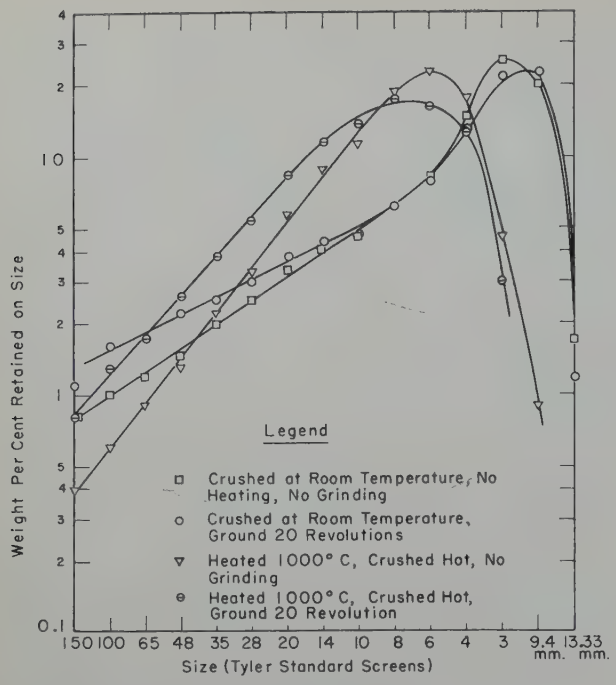
Weight Per Cent Retained on Size
Size (Tyler Standard Screens)
150 100 65 48 35 28 20 14 10 8 6 4 3 9.4 mm. 13.33 mm.
Legend
Crushed at Room Temperature, No Heating, No Grinding
Crushed at Room Temperature, Ground 20 Revolutions
Heated 1000° C, Crushed Hot, No Grinding
Heated 1000° C, Crushed Hot, Ground 20 Revolution

Fig. 3—Frequency plots of size distribution data for tests for fragility of granite after heating.

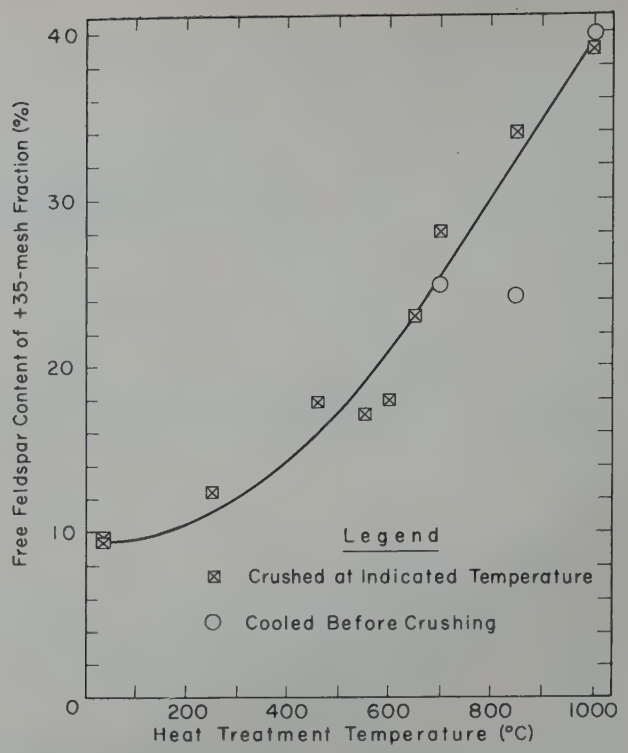

Fig. 4—Free feldspar content of 35-mesh material vs heat treatment temperature tested for granite tests.

perature in air. This similarity indicates that the substitution of nitrogen for air had no effect and that the cause of the disintegration probably was not an oxidation reaction.

Long Heating Tests: In previous tests the charges were merely heated in the furnace for about 1 hr. Two additional tests were made, therefore, to determine whether longer heating at lower temperatures could be equivalent to a higher temperature treatment. Test details are indicated in Table I. Data for tests at shorter heating times are included for comparison.

Table I. Operating Conditions and Results for Long Heating Tests

Treatment Temperature, °C	Time at Temperature, Hr	Size Distribution Slope
450°	6	1.03
500°	6	1.09
460°	1 (approx)	0.92
700°	1	1.25

Temperature control during the heating period was considered satisfactory with an estimated maximum variation of ±25°C.

Slope value in the 6-hr test at 450°C is slightly higher than that obtained for the parallel 1-hr tests, but the difference is of the same order as the experimental accuracy. Also, the slope for the 6-hr test at 500°C did not approach the value for the 1-hr 700°C test.

Grindability Test: The grindability of an ore is evaluated customarily by determining the amount of material finer than a given size which is produced by a reproducible standard grinding operation under steady state conditions. For the granite used in these tests 48 mesh was selected as the splitting size, since it was believed that this was the coarsest size at which the unheated and ground granite would be completely liberated. For this work, therefore, grindability was defined as the steady state amount of −48 mesh material produced during 100 revolutions of the mill.

The test on heated rock was made as follows:

1) Several charges were heated to 1000°C and cooled before crushing.

2) One crushed product (2000 g) was ground in a laboratory ball mill through 100 revolutions of the mill.

3) After the entire ground product was sized, the −48-mesh fraction was set aside, replaced by an equal weight of heated and crushed but not ground product, and thoroughly mixed.

4) The remixed material from step 3 was ground through another 100 revolutions of the mill.

5) Steps 3 and 4 were repeated until the amount of −48 mesh material set aside reached a constant value.

A second test was run in the same manner as this first one except that no heat treatment was used on either the original or make-up material. Only four grinds were made in this case, since the pattern of the first test indicated that a satisfactory measure of the grindability had been obtained by them. The results of the two tests are given in Table II. The data indicate grindabilities of about 340 g per 100 revolutions for the heat-treated granite and about 170 g per 100 revolutions for the raw granite. As indicated in the table there was no tendency for the slope values for the tests on the two different materials to approach the same value as the grinding treatments continued. The coarse fractions of the heated rock continued to break with relatively fewer fines than unheated rock.

It is fair to call attention to the fact that the grindability tests that were made actually penalize the quality of the grinding following heat treatment. In spite of this penalty the grindability after heat treatment showed to great advantage, as already indicated. The penalty consists in this, that the

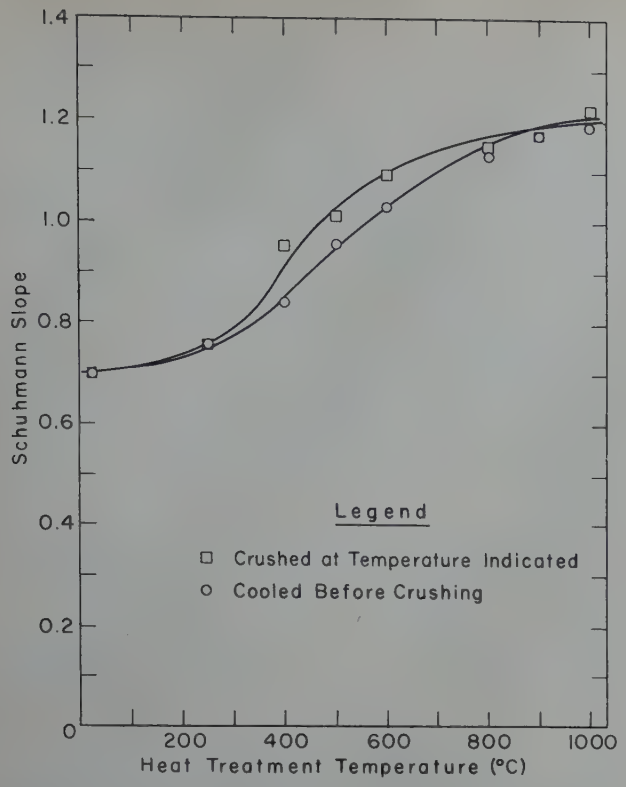

Fig. 5—Slope of Schuhmann curve vs heat treatment temperature for syenite tests.

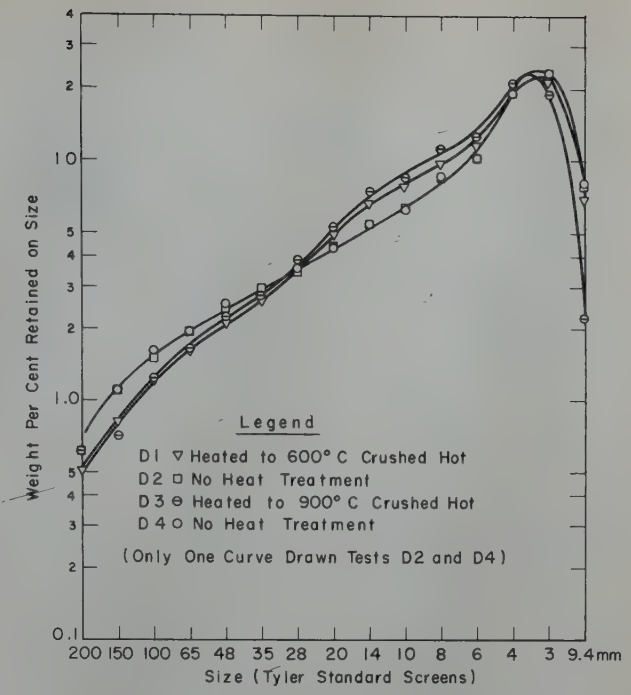
Weight Per Cent Retained on Size
Size (Tyler Standard Screens)
Legend
D1 ▽ Heated to 600° C Crushed Hot
D2 □ No Heat Treatment
D3 ⊖ Heated to 900° C Crushed Hot
D4 ○ No Heat Treatment
(Only One Curve Drawn Tests D2 and D4)

Fig. 6—Frequency plots for size distribution data of tests on franklinite.

selection of 48 mesh as the size to which the grindability was assessed, while suitable from the standpoint of the unheated rock, is unsuitable from the standpoint of the heated rock, since most of the grains have been freed by crushing after heating at a size substantially coarser than 48 mesh. Had the assessment size of the grindability been, say, 10 mesh, the writers are convinced that the ratio of the grindabilities of heated and unheated rock would have been much greater than 2:1. Even such a comparison would not have been appropriate. What really is called for is a comparison of the grindabilities of heated rock at, say, 10 mesh with unheated rock at 48 mesh. There the ratio of the grindabilities might easily have exceeded 10:1.

Table II. Experimental Data for Grindability Tests on Granite

Test Material	Grind No.	Product Grams of −48 Mesh	Slope Value of Product
Heated Granite	1	296	0.86
	2	303	1.03
	3	321	1.12
	4	331	1.18
	5	340	1.19
	6	343	1.20
	7	351	1.20
Raw Granite	1	290	0.73
	2	197	0.84
	3	184	0.87
	4	171	0.86

Tests on Syenite

It was considered that the presence of quartz in granite might have been directly responsible for its crushing behavior after heating, and that this in turn was due to the alpha-beta phase transformation of quartz which occurs at about 575°C. A syenite was chosen for testing as a material close to granite in composition and texture but containing very little quartz.

Approximately 200 lb of syenite were obtained from the Mt. Ascutney area of Vermont. This material exhibited a constant grain size of about 1.5 mm and contained orthoclase, plagioclase, hornblende, nepheline, and small amounts of magnetite and quartz.

The tests made on syenite involved heating samples to various temperatures and subsequently crushing them with the jaw crusher set to a minimum opening of 9 mm. In all heat treatments the charges were in the furnace approximately 2 hr, and as with the granite tests, half this time was spent in raising the furnace to temperature and about half in allowing the charges to remain at that temperature. In some cases the heated rock was crushed hot and in others it was allowed to cool before crushing.

Data from all size analyses were plotted in the same way as with granite, and the slope values were determined from these plots. In Fig. 5 the slope value for each test is plotted as the ordinate against the heat treatment temperature as abscissa. The curves so obtained show that the heat treatment brought about changes in size distribution comparable to the changes observed with granite. In addition, it appears that the slope values for products crushed after cooling lie slightly lower than those obtained for products crushed at elevated temperatures.

The significant conclusion to be drawn from Fig. 5 in relation to the purpose of this work is that the presence of quartz is not needed for heat treatment to produce a marked favorable effect on crushing.

Tests on an Isotropic Mineral

Among the ores and rocks on hand there appeared to be only one that was suitable for heating tests and consisted primarily of one isotropic mineral. This was a rich ore from Franklin, N. J., the major

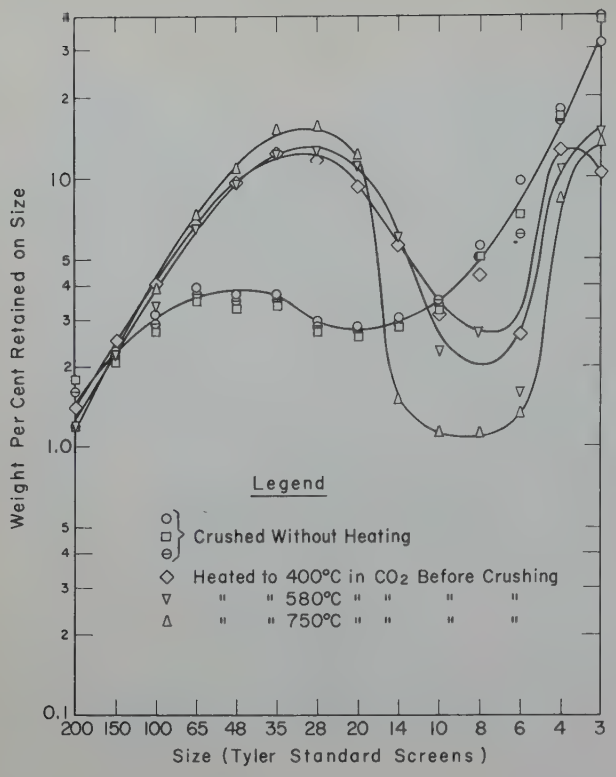
Weight Per Cent Retained on Size
Size (Tyler Standard Screens)
200 150 100 65 48 35 28 20 14 10 8 6 4 3
Legend
Crushed Without Heating
Heated to 400°C in CO_2 Before Crushing
" " 580°C " " " "
" " 750°C " " " "

Fig. 7—Frequency plots for size distribution data of marble tests.

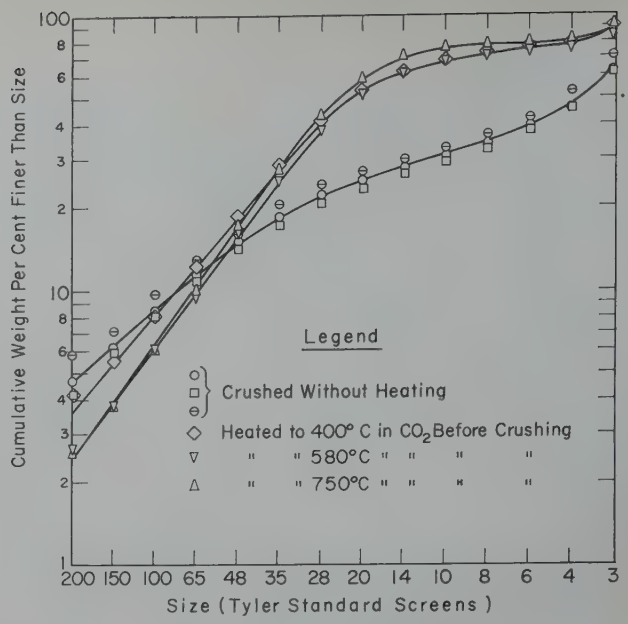
Cumulative Weight Per Cent Finer Than Size
Size (Tyler Standard Screens)
200 150 100 65 48 35 28 20 14 10 8 6 4 3
Legend
Crushed Without Heating
Heated to 400° C in CO_2 Before Crushing
" " 580°C " " " "
" " 750°C " " " "

Fig. 8—Size distribution data for marble tests as Schuhmann plots.

constituent of which was the isotropic mineral franklinite. Only enough of this ore was available to provide four 1500-g charges of −35-mm + 12-mm material. These samples contained about 5 pct calcite as small veins in the bulk material. Grain size ranged between 0.3 and 0.5 mm.

Two of the charges were crushed at room temperature without any heat treatment, one was crushed at 600°C, and one was crushed at 900°C. The size distribution data are shown as frequency plots on logarithmic scales in Fig. 6. This method of plotting the data was used in this case, since it makes small differences in the distributions more obvious than does a cumulative plot. From these curves it appears that the heat treatment had only a small effect on the size distribution of the material. Since some calcite was included in the Franklin ore there can be no assurance that this was not responsible for the small differences.

Tests on Taconite

Since it was desirable to supplement this work on special systems with tests on systems of practical interest, a sample of a magnetic taconite was obtained from Pickands, Mather & Co. Examination of a polished section and hand specimens of the taconite indicated that much of the iron mineral was present in veins up to about 10 mm in thickness, but that a considerable amount was present as very fine grains ranging down to 0.1 mm and finer, imbedded in the siliceous gangue. This fine grain size indicated that if a difference in the liberation were to be detected the screen analyses would need to be done with the utmost care.

Of the four tests made on this taconite, two samples were heated and crushed at 1000°C and two were crushed without any heat treatment. The jaw crusher was set to a minimum aperture of 2.5 mm.

The size distribution data of the products, when plotted as frequency plots, showed only slight differences in the amounts retained on sizes between 48 mesh and 200 mesh, with slightly more material reporting in these sizes in the heat-treated materials. The differences, however, did not warrant further testing of the rock at this stage of the investigation.

A brief microscopic examination of the fine sizes in the products showed that the liberation was essentially complete at about 150 mesh. It was also apparent that much of the gangue in this ore was optically anisotropic.

Tests on Marble

Marble was selected for testing as a mineral exhibiting strong thermomechanical anistropism. A sample of Danby marble, obtained from the Vermarco Lime Co., consisted of pure white stone exhibiting a regular grain size of about 0.5 mm. It contained 95 pct or more of carbonate mineral.

Table III. Equilibrium Conditions for $CaCO_3$ Decomposition

Temperature, °C	Equilibrium CO_2 Pressure, Atm
550°	0.0057
700°	0.029
800°	0.22
900°	1.0
937°	1.77

Since marble decomposes at high temperatures to give lime and carbon dioxide, heat treatments were restricted in their scope. Published data[18] on the equilibrium decomposition conditions are reproduced in Table III.

From these data it appeared that if marble were heated in a CO_2 amosphere, temperatures to about 900°C should be possible without risk of decomposition. Tests were made, therefore, with the furnace continually flushed with CO_2 during heating and cooling. The charges were heated to temperatures of 400°C, 580°C, and 750°C, and the heated and cooled

products were crushed with the jaws set to a minimum aperture of 6 mm.

The size distribution data for these crushed products are given in Fig. 7 as frequency plots and in Fig. 8 as cumulative plots. These two figures demonstrate the values of the two methods of plotting very well. It will be noted that the heated marble assumed a distribution far different from that which would be expected in a normal homogeneous material. This departure from normality is strikingly shown in the frequency plot but is not so apparent in the cumulative plot. The curves in Figs. 7 and 8 show that the heat treatment had two very marked effects on the size distribution. First, there is a remarkable similarity between the several heat treated products. Since heating to 400°C was almost as effective as heating to 750°C it seems possible that even raising the temperature by 100°C might give a noticeable effect, but this matter was not pursued. Second, it appears that much of the products from tests on heated marble concentrated in size ranges corresponding to the grain size of the rock (20 to 35 mesh). This indicates that much more intergranular fracturing occurred during crushing and screening of the heated rock than with unheated material. It was also noted that it was possible to crush lumps of heated marble to a sugary product merely by pressing between the fingers.

As a check on the extent to which chemical change might have taken place during heating, the −200-mesh fractions of the various products were pulped with distilled water and the pH of the water was then measured. If dissociation had occurred during heating then the CaO so formed should have given a higher pH to a pulp containing heated marble than to one containing unheated marble. Since none of the pulps showed a pH above 9, it is unlikely that decomposition took place during any of the heat treatments. Furthermore, tests at 700°C without atmosphere control yielded pulp pH's of 11.5 whether crushed hot or cold but still yielded almost the same screen analyses as already reported for the test at 750°C. Clearly, the intergranular fracturing of this marble sample was not primarily due to intergranular corrosion but to some other factor.

Discussion

The results of this investigation may be examined with respect to the various mechanisms by which the heating may have affected the rock. The possibility that heating rocks prior to crushing them merely amounts to introducing the energy required for fracturing as heat rather than as mechanical energy can be eliminated on the basis of data obtained. For this mechanism to be responsible the temperature of the rock during crushing should be very significant and the effects might be expected to be independent of the material being tested. Furthermore, if heating merely supplies comminution energy then only parallel translation of the size distribution curves toward the finer sizes without changes in their shapes should result from heating. Since the data do not support any of these requirements, it is logical to assume that the fracture process under investigation here is not the same as that which results when unheated rocks are crushed.

When a metal piece is broken at elevated temperatures or when the fracture is induced by a slow rate of loading, fracture will usually occur intergranularly. Conversely, with a high rate of loading or relatively lower temperatures the fracture will be transgranular and heterogeneous.[10,11] It might be supposed that a similar relation could exist in rocks, but no conclusive evidence was obtained to support this hypothesis. The temperature during crushing was not particularly significant, although it was shown that heating the rock had a marked effect in some cases. The syenite tests did indicate a slight advantage in crushing hot over crushing cold, but this was a small improvement over the improvement due to the prior temperature change.

It was noted in the tests on granite that the effect of heating became large in the vicinity of the quartz alpha-beta transformation (about 575°C). Since this transformation involves a large volume change in the quartz, it appeared possible that that mineral was literally forcing the rock apart by its sudden expansion. With most of the expansive strain focused on the grain boundaries the intergranular nature of the fracture seemed logical. The test on syenite almost duplicated those on granite, however, indicating that while the quartz transformation might have been effective to some extent it certainly was not the only factor. The tests on marble which showed that rock to be markedly affected by heating further reduced the possibility that the quartz transformation plays a dominant part.

The tests on marble were also related to another suggestion. It had been proposed in at least one patent that decomposition of calcite in an ore by heating would promote intergranular fracture of that mineral. If heating of marble were carried out only so far as to weaken intergranular bonds by causing decomposition between the grains, a logical place to expect decomposition to begin, then intergranular corrosion would be achieved. Tests in which the marble was heated with the furnace atmosphere containing more than enough CO_2 to prevent such decomposition did not prevent its breakdown, however, indicating that this intergranular corrosion was not a necessary feature of the heat effect.

It could be argued that a chemical change, for example, oxidation of ferrous iron to ferric iron, was in some way responsible for the different size distributions of the crushed products, but when granite was heated in a nitrogen atmosphere, no change in the heated crushed product could be detected. In addition, it was believed that no chemical change took place in the syenite on heating and it was shown by pH determinations that neither wholesale nor intergranular decomposition of marble had occurred in tests on that mineral. Thus, it seems unlikely that a chemical change in the rock was responsible for the effectiveness of heat treatment.

At least two other possible mechanisms could not be so completely resolved on the basis of the data obtained. The possibility that anisotropism of some of the constituent minerals of the rock was necessary was not proved by the tests on Franklin ore. A small effect was noted in this material when crushing it after heating, but that could have been due to the small calcite content of the rock. Furthermore, the taconite contained an anisotropic siliceous gangue and yet only a very small heat effect could be shown.

If unequal expansion of the individual grains in the grain aggregate were effectively tearing the aggregate apart along grain boundaries, both the intergranular nature of the fracture and the dependence of the fracture on the maximum temperature attained would be expected. Unfortu-

nately, the tests do not permit evaluation of this suggestion, for essentially identical results might have been obtained if the effects noted were due to spalling because of different heat transfer rates through the various grains of the rock. It does appear probable that one or both of these methods contribute to the process, but much work must be done to define their respective roles. In addition, the effect of such features as the grain size and porosity of the rock might bear investigation.

Conclusions

It has been shown that heating a rock prior to crushing it may result in marked improvements in its friability and in the size distribution of the crushed product. The effects noted were of the nature to be expected if intergranular fracture were occurring as a result of heating. The mechanism by which this is accomplished can not be stated with any certainty, but it appears to be more dependent on physical changes in the rock at elevated temperatures than on chemical changes.

The potential value of these treatments appears sufficient to warrant further investigations. In particular, it is the authors' hope that not only will the mechanism by which heating is effective be determined but also that a contribution can be made to the understanding of intercrystalline bonding in brittle materials.

Acknowledgments

The work presented in this article was benefited by association with a project on comminution in course at Massachusetts Institute of Technology. That project is sponsored by the Engineering Foundation, American Iron and Steel Institute, Allis-Chalmers Mfg. Co., the Atomic Energy Commission, Norton Co., International Nickel Co., and Carborundum Co. The assistance and encouragement of these organizations is gratefully acknowledged.

References

[1] J. H. Brown and A. M. Gaudin: Intergranular Comminution. Presented at Pittsburgh Regional Technical Meeting, A.I.S.I. Nov. 28, 1956.

[2] B. W. Holman: Heat Treatment as an Agent in (Quartz) Rock Breaking. *Transactions*, Institute of Mining and Metallurgy, 1927, vol. 36, pp. 219-262.

[3] A. Yates: Effect of Heating and Heating and Quenching Cornish Tin Ores. *Transactions*, Institute of Mining and Metallurgy, 1919, vol. 28, p. 41.

[4] W. M. Myers: Calcining as an Aid to Grinding. *Journal of the American Ceramics Society*, 1925, vol. 8, p. 839.

[5] R. B. Sosman: The Properties of Silica. *American Chemical Society Monograph Series*, no. 37, pp. 388-389. Chemical Catalog Co. Inc., 1927.

[6] R. F. Brenner: U. S. Patents, 2,368,194 (June 11, 1941) and 2,387,561 (March 26, 1943).

[7] J. Seigle: French Patent No. 718,751, (June 17, 1931).

[8] L. E. Schiffman, C. S. Lawson, and J. T. Blakemore: U. S. Patent 2,240,718 (Aug. 13, 1938).

[9] R. Schuhmann, Jr.: Laboratory Sizing. *Powder Metallurgy*. American Society for Metals, Cleveland, Ohio.

[10] C. S. Barrett: *Structure of Metals*, p. 391. McGraw-Hill Book Co. Inc., New York, 1952.

[11] H. C. Chang and N. J. Grant: Mechanism of Intercrystalline Fracture. *AIME Trans.*, 1956, vol. 206, p. 544.

[12] W. Mitchell, Jr., C. L. Sollenberger, and F. F. Miskell: Factors in the Economics of Heat-Treated Taconites. *AIME Trans.*, 1952, vol. 193, p. 962.

[13] *International Critical Tables of Numerical Data, Physics, Chemistry and Technology*. McGraw-Hill Book Co. Inc., New York, 1933.

Abstract

Interpretation of the Literature on the Mechanism of the Hall Process

by John J. Stokes, Jr.

(TP 4589D, Transactions of the Metallurgical Society of AIME, page 75, February 1958, vol. 212, no. 1)

Literature on the electrolysis of aluminum from cryolite melts and on the structure of these melts is surveyed critically. Data on density, freezing point, and other properties are reviewed. Theories of the electrolysis are examined in the light of these data. Two theories are presented which account equally well for the observations.

* * * *

In the early days, the process was thought of as a simple one. The actual mechanisms must be tremendously more complex. This paper is devoted to a rather narrow part of the whole subject, namely, what ions are present in the bath, and by what mechanism the current is carried.

* * * *

Using cryoscopic data, Rolin has determined the following composition for molten cryolite.

$$Na_3AlF_6 \rightarrow 3Na^+ + 3F^- + AlF_3. \qquad [1]$$

He postulates the following equation for the ionization of alumina at low concentrations

$$Al_2O_3 \rightleftarrows Al^{+++} + AlO_2^- + O^=. \qquad [2]$$

At concentrations above 0.025M he supposes the ionization of alumina to proceed as follows

$$Al_2O_3 \rightleftarrows AlO^+ + AlO_2^-. \qquad [3]$$

Rolin's mechanism of electrolysis for the more concentrated solution in Eq. 3 is as follows. The AlO^+ ion migrates to the cathode, where it is discharged, giving metallic aluminum and $O^=$ ions which migrate to the anode. The AlO_2^- ion migrates to the anode, where it is discharged, giving Al^{+++} ions and oxygen which reacts with carbon to form CO_2.

In the case of the extremely dilute solution in Eq. 2 the Al^{+++} ion migrates to the cathode and the AlO_2^- and $O^=$ migrate to the anode as before.

* * * *

Another possible mechanism for the electrolysis follows.

Ionization of Cryolite

$$Na_3AlF_6 \rightleftarrows 2Na^+ + 2F^- + NaAlF_4$$

$$Na^+ + \underset{\downarrow}{AlF_4^-} \underset{\uparrow}{\rightleftarrows} AlF_3 + Na^+ + F^-. \qquad [4]$$

Addition of Alumina

$$2Na_3AlF_6 + 2Al_2O_3 \rightleftarrows 6Na^+ + 3Al_2O_3F_4^= \qquad [5a]$$

$$Al_2O_2F_4^= \rightleftarrows 2AlOF_2^-. \qquad [5b]$$

Cathode Process

$$AlF_4^- + 3e \rightarrow 4F^- + Al. \qquad [6]$$

Anode Process

$$AlOF_2^- + 2F^- \rightleftarrows AlF_4^- + 1/2O_2 + 2e$$

or

$$Al_2O_2F_4^= + 4F^- \rightleftarrows 2AlF_4^- + O_2 + 4e. \qquad [7]$$

* * * *

Although both Rolin's and the present mechanism of the Hall process may be qualitatively satisfactory, present data are not adequate for quantitative tests of the theories.

Fine Grinding at Supercritical Speed

by R. T. Hukki

IT is no great exaggeration to say that present grinding practice and economics are largely determined by lining design. A record of outstanding liner wear can be achieved with any liner surface pattern that will positively lock the outer layer or layers of grinding media. With no slippage, lining wear is bound to be slight. At the same time, popular practice calls for tumbling loads of about 50 pct of mill volume to obtain maximum grinding capacity. Innumerable parallel grinding investigations have verified that optimum speed for such a mill lies within 70 to 85 pct of theoretical critical speed. If the mill is speeded up to 100 pct of critical, little or no grinding can be accomplished.

Earlier Work on Supercritical Grinding: First investigations concerning grinding at supercritical speeds seem to be very old. Remarkable work on the subject has been performed by White,[1] and his experiments have been described and summarized by Richards.[1] White's contributions seem to have passed unnoticed by Fahrenwald,[2,3] whose extensive experiments have been well presented, yet apparently very little appreciated. Additional work on grinding at supercritical speed has been reported, e.g., by Lewenson and Tscherny,[4] USSR; Anselm[5] and Grunder,[6] Germany; and Rose and Evans,[6] Great Britain.

Subcritical and Supercritical Speeds: In the formula of the critical speed given in the textbooks of mineral dressing, no factor indicating the coefficient of friction is generally included. If this factor = 1.0, which is equivalent to grinding conditions in a mill provided with heavily ribbed lining, the formula of the critical speed holds as such and grinding is possible at subcritical speeds only. In a mill equipped with a smooth or relatively smooth lining, the numerical value of the friction factor in the denominator of the formula becomes <1.0, indicating that grinding at supercritical speeds should be possible in such mills. It has been recently shown by the author[7] that a wide supercritical speed range will become available for grinding—and especially for fine grinding—if the basic conditions within the mill have been selected properly. Mathematical analysis of mill dynamics at supercritical speeds[7] has indicated that the mill speed may be increased if:

1) total mass of grinding medium decreases,
2) mass of the individual grinding piece increases, and
3) the coefficient of friction between the outer layer of medium and the mill lining decreases.

It is obvious that the mass of the individual grinding piece will be affected by its shape and by its specific gravity. The coefficient of friction decreases with:

1) increasing smoothness of liner surface,
2) increasing roundness of the grinding piece,
3) increasing fineness of material to be ground,
4) decreasing pulp density, and
5) decreasing hardness (abrasiveness) of the mineral to be ground.

In a mill equipped with heavily ribbed lining, practically no size reduction will take place between the lining and the outer layer of tumbling medium, because slippage is prevented. In the overwhelming majority of today's mills the grinding accomplished is by virtue of cataracting and/or cascading media with some action within the tumbling charge. Subcritical speeds only can be applied.

In grate-type or peripheral discharge mills equipped with a smooth lining a tumbling load of any kind of common medium occupying about 50 pct of mill volume will behave in such a way that practically no slippage will take place. This has been verified in experiments run by the author in the laboratory and in pilot plant mills[7] equipped with smooth lining. Again, the operation is limited to the subcritical range.

In a mill with a smooth lining, grinding will be possible either at subcritical speeds or within a wide supercritical speed range as soon as the basic requirements for a desired speed are fulfilled.

In a mill operated at supercritical speed, any point on the liner surface proceeds at a speed greater than that indicated by the formula of the critical speed, while any grinding piece situated in the outer layer of the medium against the lining proceeds in the same direction at a speed less than that indicated by the critical speed. This speed difference produces a very effective attrition grinding zone between the liner surface and the outer layer of the medium. The share of attrition grinding of the total grinding accomplished increases rapidly with increasing speed in the supercritical speed range.

The smooth surface of the mill lining may be well illustrated by the surface of a bucking board. The outer ball layer may be similarly represented by the lower surface of a muller. If the bucking board, the material to be ground, and the muller all proceed in the same direction at the same speed, no grinding will result. This is the general situation in the mills of today. If, however, the muller is pulled with respect to the board, moving or stationary, grinding will be accomplished effectively. Although grinding in today's mills is primarily the result of cataracting and/or cascading media, the principal place of grinding at high supercritical speeds will be the attrition zone.[1]

In the mineral dressing laboratory of the State Institute for Technical Research, Helsinki, Finland, large quantities of different ores have been ground in a pilot plant ball mill (3x3 ft) at a top speed about 230 pct of the critical. With the same mill, theoretical investigations concerning the grinding characteristics of ball mills equipped with a smooth lining have been carried out up to the speed of 313 pct[7] of the critical. With a smaller mill, the grinding characteristics with a variety of grinding media have been investigated at speeds up to 2000 pct of the

R. T. HUKKI, Member AIME, is Professor of Mineral Dressing, Finland Institute of Technology, Helsinki, Finland.
TP 4744B. Manuscript, Dec. 4, 1957.

This page of Mining Transactions AIME follows p. 496. The intervening non-Transactions pages appeared in MINING ENGINEERING.

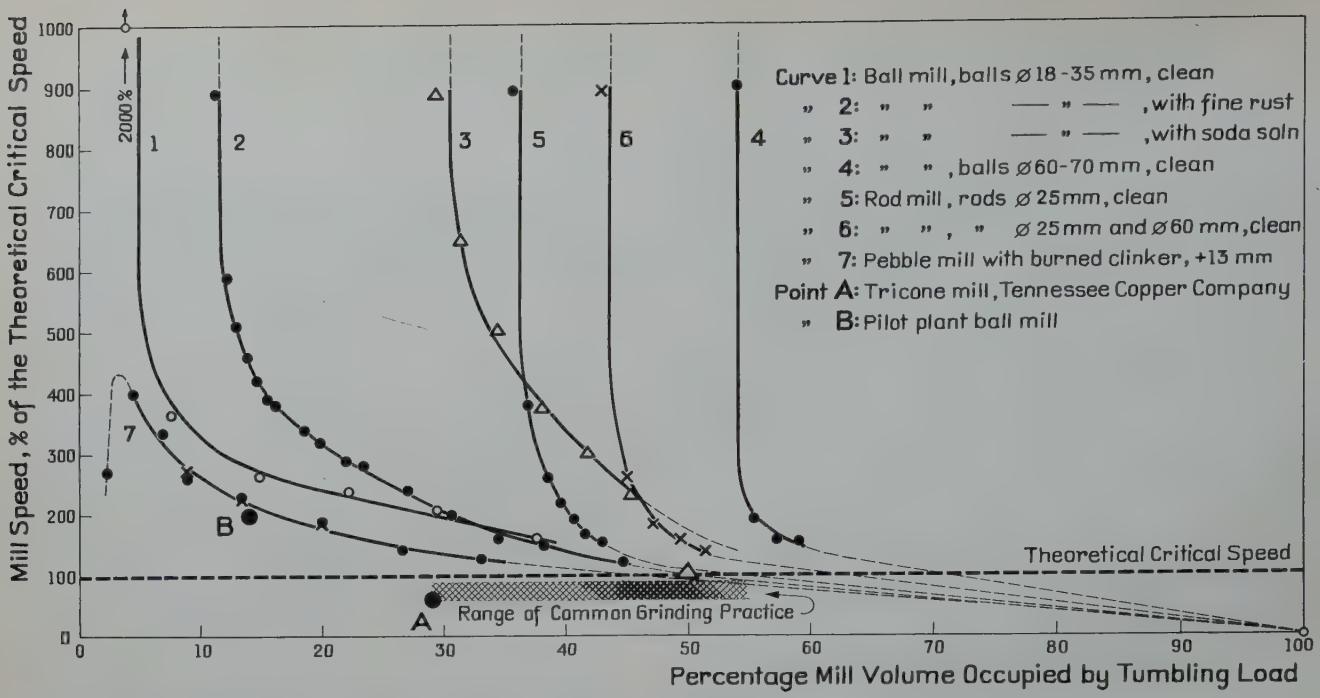
Mill Speed, % of the Theoretical Critical Speed
Percentage Mill Volume Occupied by Tumbling Load
2000%
Curve 1: Ball mill, balls ø18-35 mm, clean
" 2: " " —— " —— ,with fine rust
" 3: " " —— " —— ,with soda soln
" 4: " " ,balls ø60-70 mm, clean
" 5: Rod mill, rods ø25mm, clean
" 6: " " , " ø25mm and ø60 mm, clean
" 7: Pebble mill with burned clinker, +13 mm
Point A: Tricone mill, Tennessee Copper Company
" B: Pilot plant ball mill
Theoretical Critical Speed
Range of Common Grinding Practice
A
B

Fig. 1—Mill characteristics at supercritical speeds. Tests were made without feed in a smooth laboratory mill equipped with a variable speed drive. Actual speed of the mill at 2000 pct of the critical was 1550 rpm.

theoretical critical. The results of a series of such experiments are shown in Fig. 1. The points plotted represent experimental boundary conditions at speeds at which the medium was not caught by the mill within 1 min so as to make the medium centrifuge. Thus grinding should be at least theoretically possible at any point over an area between the axes and the respective curve obtained. All tests shown were made without any feed in the mill.

Relationship between Mill Capacity and Specific Gravity of the Medium: In general it may be stated that the grinding capacity of the tumbling medium increases directly as the specific gravity of the medium corrected by the buoyant effect of the pulp or of the bed of solids surrounding the medium.[7] To decrease the buoyant effect to the minimum and thereby increase the effective mass of the medium to its maximum, the mill should be a low-discharge grate mill or a peripheral discharge mill. Fig. 2 illustrates not only the great effect the specific gravity of the medium has on mill capacity, but also the basic influence of the buoyant effect. Fig. 2 has been constructed as follows:

In three similar high-discharge ball mills, all operated at 70 pct of critical speed, ore of 3.0 sp gr is being ground in such a way that one of the mills is loaded with crushed ore pebbles of the same specific gravity, one with steel balls, and one with tungsten carbide balls. The pulp discharged from the mill is supposed to carry 60 pct of solids and the pulp remaining in the mills an average 70 pct of solids, representing a 1.87 sp gr of the pulp. The original specific gravities of the respective media are 3.0, 7.8, and 13.1; the corrected values of effective specific gravities 1.13, 5.93, and 11.23, respectively. If the steel ball mill is given the reference capacity value of 10 tph (point *B*), the tungsten carbide mill should grind about 19.0 tph (point *C*) and the ore pebble mill only 1.9 tph (point *A*).

If the original mills were now to be replaced by three grate mills of the same effective size as the overflow mills, the pulp baths would be largely eliminated. As an extreme situation, it might be assumed that the pulp remaining in the mill is so small in volume that its buoyant effect becomes negligible. Without a great error, the maximum capacities of the three mills will thus be increased to figures directly proportional to the specific gravity values of the media—3.0, 7.8, and 13.1, whereby the tonnages will become 5.06, 13.2, and 22.1 tph, respectively.

From what has been said, it should be clear that to obtain any reasonable capacity in autogenous grinding with crushed ore pebbles of low specific gravity, the mill must be a low-discharge mill. The higher the specific gravity of the medium, the less the percentage difference in capacities of a grate mill vs overflow mill, although the differences in ground tonnages remain constant under the conditions explained.

If the specific gravity of the crushed ore pebbles to be used as a grinding medium can be increased by proper preconcentration such as magnetic separation, sink-float, or other methods, such practice should be encouraged. Also, it should be clear that addition of any medium of higher specific gravity to a charge of lower specific gravity will always increase capacity.

Relationship between Mill Speed and Capacity: In general, it is believed that capacity of a tumbling mill is directly proportional to mill speed, other things remaining constant.[8] In the Sullivan concentrator, the data provided by Banks[9] indicate that the capacity of the large rod mill has increased as a power function of the speed,[10] the exponent being about 1.5. The speed range covered by tests was 50 to 85 pct of critical.

At Outokumpu, Finland,[11] large-scale grinding experiments have been carried out in 9x12-ft autogenous overflow mills equipped with relatively smooth lining, within a speed range of 57.6 to 104 pct of critical. It has been established that the capacity of such a mill, expressed in new tons of —0.2-mm material produced, increases as a power function of the speed, the exponent being 1.4. At present this is probably the only example that can be found

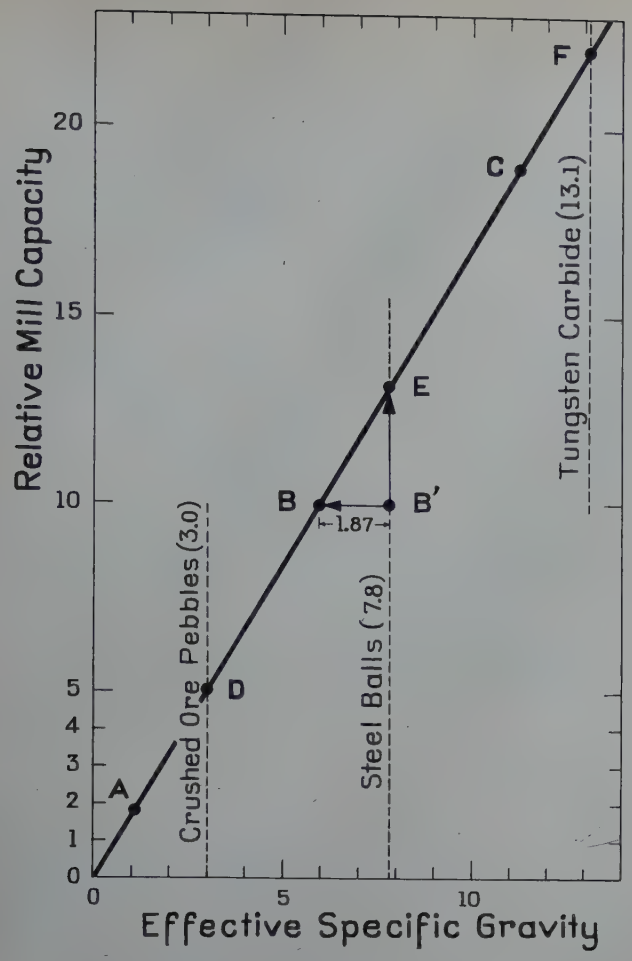

Fig. 2—Relationship between mill capacity and effective specific gravity of grinding media.

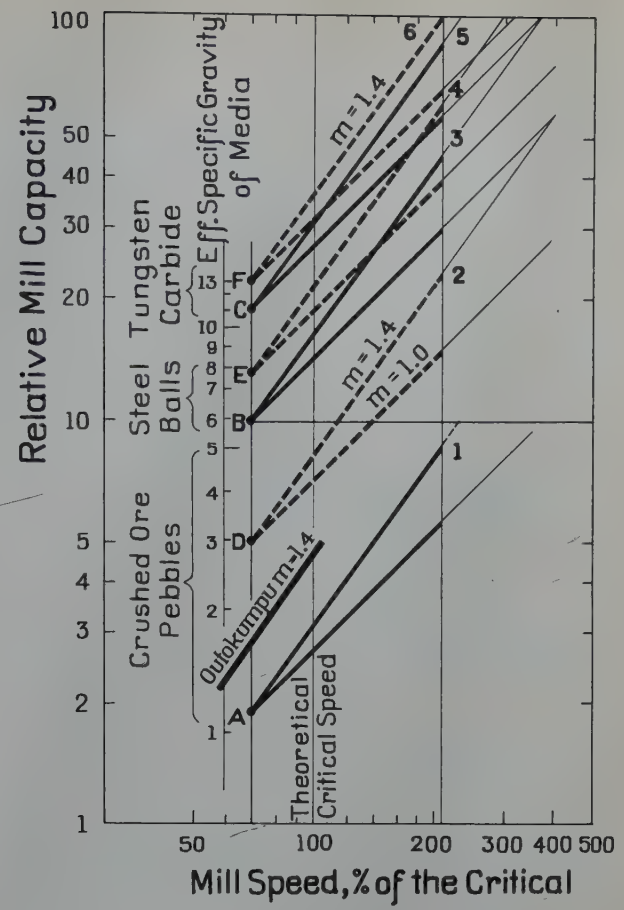

Fig. 3—Relationship between mill capacity and speed shown on logarithmic paper for different grinding media in overflow and grate mills.

anywhere of dependable mill data including the wide subcritical speed range and extending into the low supercritical range. The speed of Outokumpu mills cannot be further increased without a major alteration of the entire circuit, because of the limiting factor imposed by the mill scoop, the tip of which is already rotating at 129 pct of the theoretical critical at a mill speed of 104 pct.

On logarithmic paper, with mill speed on the abscissa and mill capacity on the ordinate, results obtained at Outokumpu give a straight line with a slope of $m = 1.4$ (see Fig. 3).

So far there is only limited experimental evidence for the speed range between 100 and 200 pct of critical, but interesting phenomena can already be predicted to take place in a mill speeded through that range. As an example, the overflow mills and the grate mills described earlier—grinding with crushed ore pebbles, steel balls, and tungsten carbide balls—will be analyzed again.

As shown in Fig. 3, basic capacities of the three overflow mills at a speed 70 pct of critical were found to be 1.9, 10, and 19 tph, respectively, corresponding to points *A*, *B*, and *C* in Figs. 2 and 3. The respective grate mill capacities of 5.06, 13.2, and 22.1 are shown by points *D*, *E*, and *F* in Figs. 2 and 3.

Through each point, two straight lines are drawn in Fig. 3, one at a slope of 1.0, the other at a slope of 1.4. The former line on the logarithmic paper represents the capacity-speed function as generally accepted, the latter the same function based on the evidence obtained at Outokumpu. The following question is now inescapable:

What would be the capacities of these mills if they were speeded, for example, from 70 pct to 210 pct of critical, representing a threefold increase in the speed?

As indicated by Fig. 3, capacity of the grate-discharge tungsten carbide mill should reach 65 to 100 tph at 210 pct. One such super-mill would thus replace 6 to 10 ordinary overflow mills of the same size grinding with steel balls at a speed of 70 pct. Even if the tungsten carbide mill were of the overflow type, its capacity should be 5.5 to 8.5 times that of the reference mill (case *B*). Naturally, the capacity of the reference mill would increase at 210 pct to a figure 3 to 4.6 times that at 70 pct.

Regarding the pebble mills, interesting features are apparent. As seen from Fig. 3, any ordinary overflow ball mill—after being changed to a grate mill and speeded from 70 pct up to 115 to 140 pct—should be able to grind the same tonnage with ore pebbles of 3.0 sp gr as the reference mill with steel balls. However, the starting capacity of a high-discharge overflow mill grinding with ore pebbles (point *A*) would be so low that it might or might not be possible to reach the original reference capacity of 10 tph.

Autogenous grinding may also be performed, of course, with a reasonable success in an overflow type of mill as done at Outokumpu, but obviously at a reduced capacity.

It should be emphasized that the speed range considered above includes only the low supercritical range up to 210 pct. The author has found in pilot plant experiments that such speeds, although

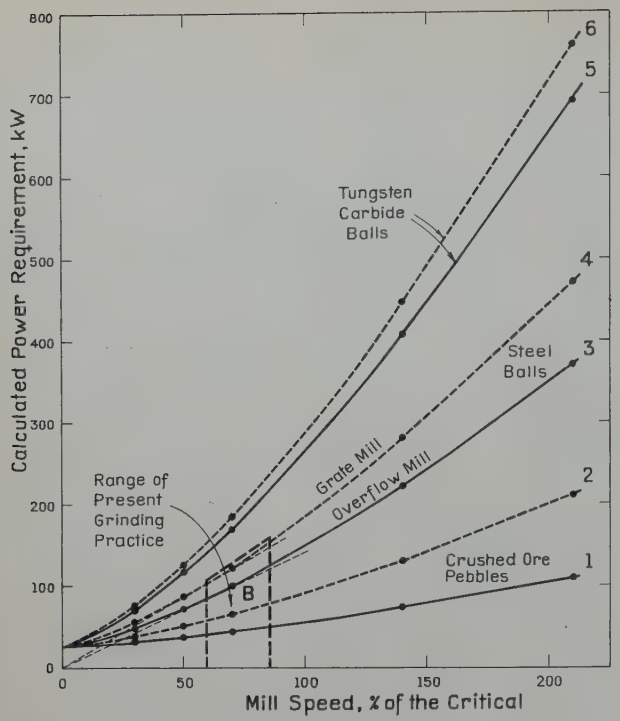

Fig. 4—Relationship between mill capacity and speed on arithmetic paper.

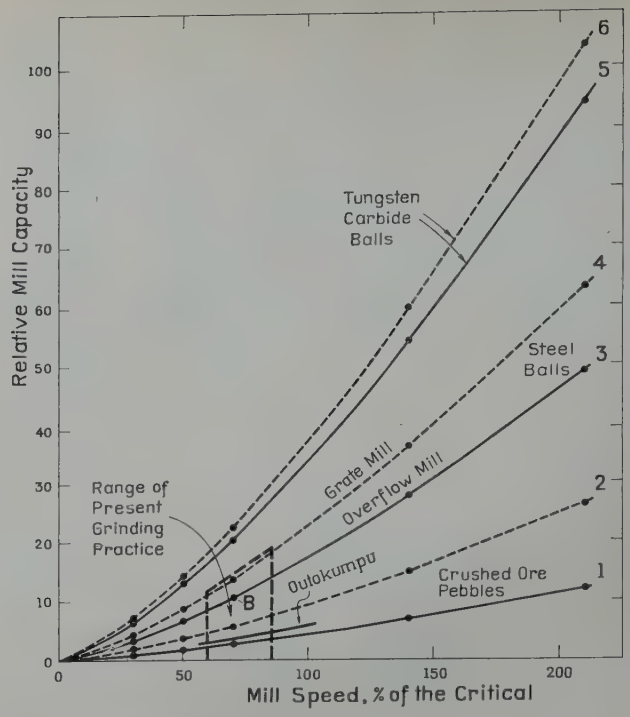

Fig. 5—Relationship between total power consumption and speed.

frightening when compared with the present gentle speeds, are by no means prohibitive. Even at these speeds, the predicted capacity figures seem phenomenal.

In cases where full capacity is not obtained from a mill by its present method of operation, relatively speaking, top capacities under optimum grinding conditions would be still higher than those indicated above.

As the logarithmic method of plotting may not give a clear enough picture of the effect of increasing mill speed on capacity, Fig. 4 is included to show on an arithmetic paper the same data as Fig. 3. Fig. 4 shows also the remarkably small area covered by the present grinding practice, an area illustrating at the same time the extent of the knowledge up to the present time in the field of the science of grinding.

From Fig. 3 it is also apparent that the overflow type of mill equipped with tungsten carbide balls should grind the same tonnage at a speed of about 80 pct of the critical as a grate mill of the same size at a speed of 70 pct. The respective figures for the two types of steel ball mills seem to be 85 to 93 pct vs 70 pct; and for the two types of pebble mills 140 to 190 pct vs 70 pct. In the case of the tungsten carbide medium, the benefit obtained with the grate-type mill construction should thus be very easily compensated by only a slight increase in speed. Even in the case of ordinary steel ball grinding, the moderate increase of speed might turn out to be more economical than the extra expense and care required by the grates. However, the less the specific gravity of the pebbles, the more pronounced will be the favorable effect of low discharge operation on grinding capacity.

The preceding discussion indicates that with increasing speed the capacity of a fine grinding mill might be increased to startling figures. A mill operated under a specified set of conditions must finally reach its grinding limit. No knowledge of this limit exists at present. A slight excess over the maximum digesting capacity of the mill will stop grinding within a very short time by flooding the mill. As all but very few of the fine grinding mills of the world are run at subcritical speeds, and even those very few have barely passed the 100 pct mark, it should be obvious that only a fraction of the total grinding capacity of the large number of mills is in effective use today. Fine grinding at subcritical speeds is analogous to operation at substandard capacity.

Energy Consumption and Importance of Idling Power: In the pilot plant ball mill the idling power (the power required to rotate an empty mill) has been found to be about 30 pct of the power value required to run the mill charged with 50 pct steel ball load at a speed of 70 pct of the critical. When the mill was speeded up to 210 pct, the idling power figure in kilowatts was found to be about 1.6 times as high as at 70 pct. The following numerical example will illustrate qualitatively the important role played by the idling power in the energy consumption in grinding.

Three similar overflow mills all use 30 kw for idling at a speed 70 pct of critical. One of the mills after being charged with iron balls draws a total of 100 kw. The difference between the two figures shows the power required to tumble the ball load. In the second mill the ball load is replaced by a crushed ore pebble load of 3.0 sp gr. The specific gravity of the pulp within the mills is assumed to be 1.87, the same as in the example described earlier. As a first approximation, the power required to tumble the pebble load would decrease in the ratio of the effective specific gravities of the two media (1.13:5.93) or to 13.3 kw. Similarly, the power required to tumble a load of tungsten carbide balls occupying the same volume in the third mill would increase in the ratio of 11.23:5.93 or to 133 kw.

As a first approximation, the grinding capacities of the three mills are assumed to be directly proportional to the effective specific gravities of the three media. Thus if the capacity of the mill equipped with steel balls is taken as 10 tph, the pebble mill will grind 1.9 tph and the tungsten car-

bide mill 19.0 tph as was shown earlier. The general situation may now be summarized as follows:

Factor	Pebble Mill	Ball Mill	Tungsten Carbide Mill
Idling power	30 kw	30 kw	30 kw
Tumbling power	13.3 kw	70 kw	133 kw
Total power	43.3 kw	100 kw	163 kw
Capacity	1.9 tph	10 tph	19.0 tph
Energy used	22.7 kw-hr per ton	10 kw-hr per ton	8.6 kw-hr per ton

This example leads to the following statement:

In a mill operated at constant speed, the energy consumption expressed in kilowatt hours per ton should decrease with increasing specific gravity of the medium, or more broadly, with increasing mass of the medium.

If the mills are now speeded up to 210 pct of critical, it should not be unreasonable to expect that, as a first approximation, the *tumbling* powers and the tonnages may increase to figures 4.6 times ($3^{1.4}$) as high as those given above, respectively. The idling power, however, will increase only 1.6 times. The total power drawn calculated for the various cases is shown in Fig. 5. The energy values are now as follows:

Factor	Pebble Mill	Ball Mill	Tungsten Carbide Mill
Idling power	48 kw	48 kw	48 kw
Tumbling power	61 kw	322 kw	610 kw
Total power	109 kw	370 kw	658 kw
Capacity	8.7 tph	46 tph	87 tph
Energy used	12.5 kw-hr per ton	8.1 kw-hr per ton	7.55 kw-hr per ton

Qualitatively, the following statement should be justified:

With increasing speed, the share of idling power in the final energy consumption figure decreases. As a result, final energy consumption should also decrease.

In the two sets of figures, the idling power does not include a possible correction originating from the fact that the weight of the tumbling load is different from mill to mill. Naturally, the increasing weight of the medium tends to reduce the difference in results obtained in the above calculations. For a comparison it might be mentioned that a figure of 23 pct for the idling power at a speed of 80 pct of critical has been reported by Gow and Guggenheim[12] for a 6 x 4-ft mill when the normal ball load was packed around the axis.

Fig. 6 is based on numerical data obtained by the technique outlined above. It includes also the results of the two sets of examples just presented. At near zero speeds the idling power drawn by the motor divided by the infinitesimal capacity figures leads to very high energy values, which, of course, have no practical significance.

If the idling power could be reduced to zero, the ideal energy-speed relationship would be represented by a horizontal line. The resulting energy value would depend primarily on characteristics of the ore and objectives of the operation but would be independent of the type of the mill (overflow or grate mill), specific gravity of the medium, and mill speed.

The examples as given should be qualitatively sound. The high idling power consumption shown in the case considered, however, may represent rather bad operating conditions. In the pilot plant

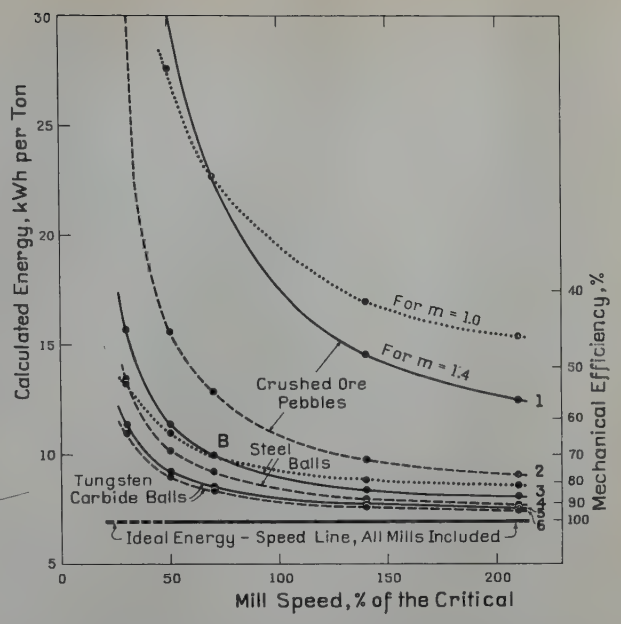

Fig. 6—Relationship between energy consumption and speed for different types of mills, based on the pilot plant ball mill data.

mill the substantial power loss can be largely credited to the speed regulator. A well designed modern mill can perform at very much better mechanical efficiency. As a result, the differences between the separate curves in Fig. 6 will be reduced. The higher the mechanical efficiency, the more the curves approach each other and finally a constant value. It might be mentioned here that the energy consumption at Outokumpu[11] remained very sharply at a constant value in autogenous grinding between speed limits of 57.6 and 104 pct. Both power consumption and capacity went up as a power function of the speed with an exponent 1.4.

Bond[8] has made a statement that, according to the general opinion, the mechanical efficiency of large-diameter mills is greater than that of small-diameter mills. In other words, the kilowatt-hour per ton figure decreases with increasing mill size. To find an explanation for this, the author has plotted on a logarithmic paper capacities of rod and overflow ball mills of different sizes against the mill weights as indicated in a catalog published by Allis-Chalmers.[13] As shown by Fig. 7, rod mill capacity seems to be a power function of mill weight, the exponent being 1.30; for the ball mill it has the value of 1.43. In the case of the smallest rod mill included, 5520 lb of mill weight are needed for each hourly ton of capacity, whereas only 2016 lb are required per ton of capacity with the largest rod mill. The respective figures for the ball mills are 15,000 and 3600 lb per ton.

As a first approximation it may be assumed that the idling power of a mill is a linear function of the weight of the mill at the same percentage value of the critical speed. Accordingly, the percentage of power available for actual grinding of the total power drawn by the motor should increase with increasing mill size.

The idling powers drawn by grinding units operating in industry have seldom been evaluated. As mechanical efficiency of mills must be based on idling power consumption, it should be of primary interest to every operator to know this basic factor as well as possible. It should also be the responsi-

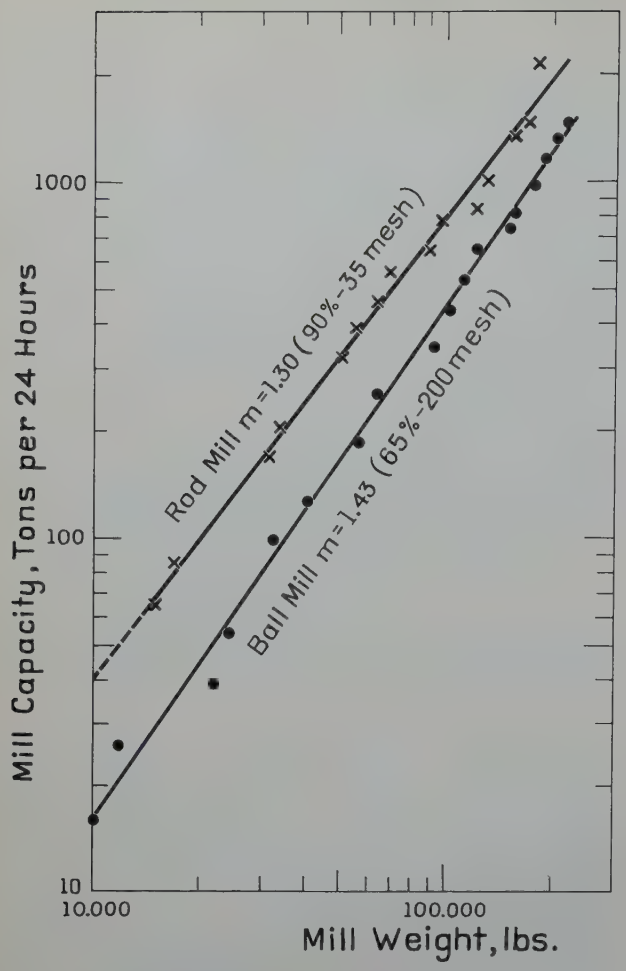

Fig. 7—Relationship between mill capacity and mill weight presented on logarithmic paper.

bility of grinding mill manufacturers to supply their customers dependable data concerning it.

Power Input With and Without Feed: Bond[14] has reported that the power input to a wet grinding ball mill is practically the same with and without feed to the mill. Accurate measurements, according to Bond, have shown that slightly more power is drawn without feed, a fact he explains as resulting from a certain lubricating action by the pulp in the mill. Bond's observations are basically correct. However, the speed range within which they apply is the normal narrow speed range of subcritical grinding. It has been explained by the author of this article that the smaller power input with feed is primarily the result of the buoyant effect of the pulp in an ordinary high discharge mill operated at low speed.[7] The effective mass of the charge is thereby lowered. With increasing speed, the medium will be more and more pulled out of the pulp body. Tests made in the pilot plant *rod mill* (3 x 4 ft) have shown that the crossing point of the two lines (one indicating the power-speed function with feed, the other the same function without feed) was located at about 60 pct of the critical in one series of grinding experiments.[7] Beyond that more power was drawn with feed than without. The difference in total power input increased linearly from the crossing point up to 135 pct of critical, the top speed at which the mill could be operated because of its shallow wave liners. At 135 pct the power input with feed was already 27 pct higher than the respective figure without feed. At present, the author has no dependable figures to show this same difference for ball mills operating at supercritical speeds. All indications are that the difference between the two power values will continue to grow (linearly or as a power function) with speed.

Relationship between Tumbling Charge and Speed: The tests shown in Fig. 1, although run in a laboratory-size mill, should qualitatively at least indicate the relationship between the tumbling charge and the speed for grate or peripheral discharge mills. The most important case to consider here is the fact that the threshold speeds for different loads of pebbles was found to be less than the respective speed values for a steel ball mill. This is shown by curves 2 and 4, respectively, in Fig. 8.

As it has not been possible for the author to run actual experiments to demonstrate to what extent the situation might change if the mill were an overflow type with a pulp bath, the corresponding cases were roughly evaluated by assuming that the friction between mill lining and tumbling charge varies directly as the effective mass of the medium and that the mill speed could be increased at the same rate the friction decreases from the basic values given by curves 2 and 4. Thus the steel ball curve 4 would be represented by curve 3 in the case of an overflow-type mill with pulp of 1.87 sp gr. Similarly, curve 2 would be represented by curve 1.

To test the correctness of the procedure, the 3x3-ft pilot plant ball mill was charged with 48 pct load of limestone pebbles and run in a closed circuit with a mechanical classifier. Limestone was fed to the circuit at about 1 tph through an open circuit 3x4-ft rod mill. At first, the maximum speed that could be used in the pebble mill was about 180 pct of critical. After the pebbles had become somewhat worn, the mill operated smoothly at a speed of 230 pct. This is shown by point *P* in Fig. 8. As indicated, the point agrees well with the calculated threshold curve despite the fact that the problem setting is not comparable in every respect. As very little is known so far about the behavior of different media in various types of mills operated at supercritical speeds, interesting and surprising phenomena are bound to be discovered in further studies.

Autogenous vs Steel Ball Grinding: Like the case history of grinding at supercritical speed, autogenous grinding also dates back many decades. One early reference from 1908 has been given by Hardinge.[15] Considerable work on the subject seems to have been done especially in South Africa as well as in the U.S. A well known modern application of auto-

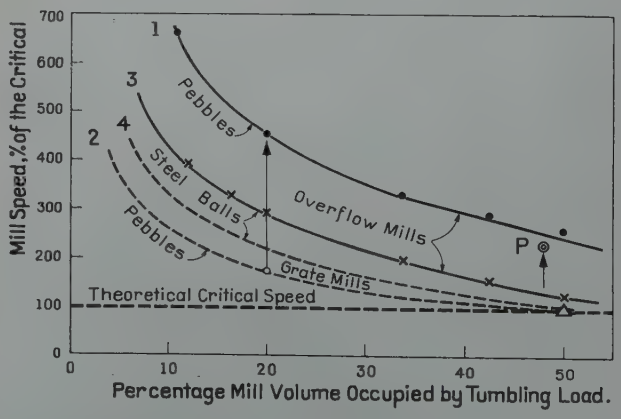

Fig. 8—Relationship between maximum mill speed and percent tumbling load for overflow and grate mills operating with balls and pebbles.

genous fine grinding within the subcritical speed range has been investigated and described by Crocker.[16]

In order to test experimentally whether or not it would be possible to replace steel balls in an ordinary overflow-type ball mill with crushed ore pebbles and to recover the loss of capacity by speeding the mill, the tests shown in Table I were carried out. In these tests limestone was ground in the pilot plant ball mill operating in closed circuit with a mechanical classifier as explained above. The mill had smooth liners. In test 1 it was run at the usual speed of 70 pct of the critical with a 24 pct load of steel balls. Under these circumstances the mill should have included all the refined features of the well known Copper Hill tricone mill grinding of the Tennessee Copper Co. In other words, the example selected for a comparison should represent a very efficient grinding circuit according to the present standards.

At first it was expected that after the balls had been replaced with limestone pebbles, a power draft comparable to that in test 1 could be used as a guide for subsequent tests. This resulted in complete failure. Only after the curves of Fig. 5 had been established could it be realized that equal energy consumption in overflow-type mills between the two types of tests is absolutely impossible. After that more pebbles were added to the mill and the mill was speeded finally up to its top speed of 230 pct. Test 2 shows a case of a smooth, steady state operation run for several hours.

The following data may be used to compare the results of test 1 and 2:

Specific gravity of limestone = 2.8
Assumed pulp density in the mill = 65 pct solids
Specific gravity of the pulp = 1.72
Effective specific gravity of steel balls = 6.08
Effective specific gravity of limestone pebbles = 1.08
Reference capacity of the steel ball mill at 70 pct speed = 1 tph
Calculated capacity of the pebble mill at 70 pct = 0.178 tph
Calculated capacity of the pebble mill at 230 pct = 0.94 tph
(based on exponent $m = 1.4$)

According to the analysis shown above, the expected capacity of the high-speed limestone pebble mill should be 94 pct of that of the low-speed ball mill.

In Table I the new tons of −x mesh material produced in the fine grinding circuit have been evaluated. It will be found that the capacity of the pebble mill when compared with the respective figures for the ball mill will be about:

92 pct for −48 mesh material ($m = 1.38$)
91.8 pct for −65 mesh material ($m = 1.38$)
83.5 pct for −100 mesh material ($m = 1.30$)
81.2 pct for −150 mesh material ($m = 1.27$)
80.5 pct for −200 mesh material ($m = 1.26$)

As the Outokumpu exponent $m = 1.4$ is based on −0.2-mm material (65 mesh), the example given here checks well with the evidence obtained at Outokumpu. Had the true exponent been the value of $m = 1.0$ as accepted today, the result obtained in test 2 would have been absolutely impossible.

Although no great accuracy can be claimed for the samples and for the figures of the screen analyses of the tests described, they do give the first real evidence that it is possible to install high-speed autogenous mills to compete in capacity and in performance with low-speed steel ball mills. The limestone pebble mill in the example given has actually presented almost the worst possibility in practice regarding the specific gravity, and at the same time the wrong type of mill (overflow mill).

In an earlier test the idling power to run the ball mill motor and speed regulator without operating the mill itself was found to be 2.7 kw at 70 pct speed and 3.9 kw at 230 pct. The respective idling power figures with the mill weighing about 800 kg were measured as 3.1 and 5.3 kw. No idling power figures

Table I. Steel Ball Vs Autogenous Grinding

	Test 1		Test 2	
	Rods	Steel Balls	Rods	Limestone Pebbles
Load, pct		24		48
Mill speed, pct		70		230
Circulating load, pct		180		225
Power, kw		6.5		9.7
Capacity, kg per hr		955		955
Product	**Feed**	**Classifier Overflow**	**Feed**	**Classifier Overflow**
−35 mesh	77.5	100.0	79.4	99.9
−48 mesh	64.8	99.6	67.6	99.6
−65 mesh	53.3	97.4	55.7	96.2
−100 mesh	45.5	91.3	46.6	84.6
−150 mesh	34.3	73.2	36.2	67.8
−200 mesh	27.7	58.8	29.1	54.1
New Kg per Hr of				
−48 mesh material		332		305
−65 mesh material		421		387
−100 mesh material		437		365
−150 mesh material		372		302
−200 mesh material		297		239

are available for the loaded mills. If the weight of the charge (medium plus pulp) is given a round figure of 1000 kg in both cases, and the increase in idling power for the increased weight grows at about the same rate as in the two cases explained above, the idling power figures for the two tests may be assumed to be 3.6 and 7.05 kw.

In test 1 the total power drawn was 6.5 kw. The share of the tumbling power is 2.9 kw. If the tumbling powers developed are in direct ratio to the effective specific gravities of the media, the tumbling power for the limestone pebble mill run at 70 pct would be 0.515 kw, and at 230 pct 2.73 kw. As the idling power for the pebble mill was estimated to be 7.05 kw at 230 pct, the total power should be about 9.78 kw. As seen from Table I, it was actually found to be 9.7 kw.

Although the result of this analysis may look to be a tailor-made figure, it was found in the first trial. It should give some confidence in the method of reasoning outlined here.

If the energy consumption figures in test 1 and 2 are studied on the basis of curves drawn in Fig. 5, showing the mill characteristics under different circumstances for this same pilot plant ball mill, the agreement is excellent.

Basic Equations of Fine Grinding: The grinding capacity of a unit-size mill 1 ft ID and 1 ft long may be written as follows:

$$T = c_1(\delta - \delta') \text{ tph} \qquad [1]$$

where δ = specific gravity of the grinding medium
δ' = average specific gravity of the pulp or of bed of solids within the mill
c_1 = a constant related with the characteristics of the ore, fineness of grinding, etc.

As shown by Fig. 3, the capacity of a mill is a

function of the percentage critical speed (n_p) raised to power m.
Thus:

$$T = c_2(\delta - \delta')\ n_p^m \text{ tph} \quad [2]$$

Indicating that

$$n_c = 76.63 \frac{1}{\sqrt{D}} \text{ rpm} \quad [3]$$

$$n_p = \frac{n}{n_c} 100 \text{ pct} \quad [4]$$

$$n_p = \frac{n\sqrt{D}}{0.7663} \text{ pct} \quad [5]$$

where n = actual mill speed, rpm
n_c = calculated critical speed, rpm
n_p = calculated percentage critical speed
D = inside diameter of the mill, in feet.
Eq. 2 may be rewritten as follows:

$$T = c_3(\delta - \delta')\ n^m\ (\sqrt{D})^m \text{ tph} \quad [6]$$

Eq. 6 was derived for a unit-size mill 1 ft ID. In a mill D ft ID the mass of a similar tumbling charge occupying the same percentage volume as before is a function of D^2. Accordingly, capacity of the mill should be written as

$$T = c_4(\delta - \delta')n^m\ (\sqrt{D})^m\ D^2 \text{ tph} \quad [7]$$

It is generally accepted that capacity of a mill is directly proportional to its length. If length is L ft, capacity becomes

$$T = c_4(\delta - \delta')\ n^m\ D^{(2+m/2)}L \text{ tph} \quad [8]$$

Eq. 8 is the basic equation of mill capacity in a general form. If $m = 1.4$ as at Outokumpu, capacity is expressed as

$$T = c_4(\delta - \delta')\ n^{1.4}\ D^{2.9}\ L \text{ tph} \quad [9]$$

As a first approximation, power consumption in grinding may be assumed to equal the sum of the idling power and the tumbling power. The idling power required should increase with increasing mill weight (size) and with increasing speed. At near zero speed it always has a definite base value. If this value for the unit mill is equal to P_0, its value for a mill of a different weight would be $k\ P_0\ (W/W_0)$, where k is a constant, W weight of the mill, and W_0 weight of the unit mill. Factor k shows the relationship between the idling power and mill weight at a constant speed. It is not known whether this relationship is linear or exponential.

For relatively low speeds (up to 200 pct of critical) the idling power may be assumed to increase linearly with increasing speed. At a speed n, the idling power may be written as

$$P_i = k\ P_0\ (W/W_0) + q\ n \text{ kw} \quad [10]$$

where q is a constant.

The tumbling power should be proportional to the force created in the mill. As the grinding capacity of the mill is also proportional to this same force, an expression which follows the law of Rittinger, the tumbling power may be written as

$$P_t = c_5(\delta - \delta')\ n^m\ D^{(2+m/2)}\ L \text{ kw} \quad [11]$$

The total power drawn by the motor will be

$$P = P_i + P_t \text{ kw} \quad [12]$$

The energy used in grinding a unit weight (a ton) of ore is obtained by dividing Eq. 12 by Eq. 8:

$$E = \frac{k\ P_0(W/W_0) + q\ n}{c_4(\delta - \delta')\ n^m\ D^{(2+m/2)}L} + \text{constant kw-hr per ton} \quad [13]$$

which is the final general expression for energy consumption. From Eq. 13 it is apparent that the energy consumption in grinding expressed in kilowatt-hours per ton should decrease with:

1) Decreasing idling power of the mill.
2) Increasing specific gravity of the grinding medium.
3) Decreasing buoyant effect of the pulp or of bed of solids.
4) Increasing speed of the mill.
5) Increasing diameter of the mill (raised to power $2 + m/2$).
6) Increasing length of the mill.
7) Decreasing relative weight of the mill itself.

It should be emphasized that the variable part in Eq. 13 may amount in a modern mill to 5 to 15 pct of the total power consumption for normal speed grinding operations with steel media. In a poorly designed mill its share might go up to 30 pct or more.

Shape of Grinding Media in Mills Operated at Supercritical Speeds: It is not coincidence, but the result of a long experience, that the working surface of the muller referred to earlier has been made cylindrical. It is not coincidence that the seasoned crushed ore pebbles in the large Outokumpu mills operated at low supercritical speeds are elliptically shaped. While the shape of a rod is basically better than that of a ball in supercritical fine grinding, the best overall surface for the medium might be obtained by introducing into the mill media that already have the shape resembling the average in a seasoned charge.

Should extremely high speeds become desirable, a rod mill in general may be run at a higher speed than a ball mill under otherwise parallel conditions.[7] It has been stated before that mill speed increases with increasing mass of the individual grinding piece. Of any useful shape of the media, a rod always has the highest mass.

Wear: It has been the author's experience that in all discussion of supercritical grinding, criticism has been focused on the question of wear.

In the present method of fine grinding, the heaviest cost item is usually the grinding medium, the steel balls. In many, if not in all grinding plants, it would be most desirable to replace the expensive steel with the inexpensive ore pebbles. The unavoidable reduction in capacity can be partially, fully, or more than fully recovered by increasing mill speed, as was shown earlier. The resulting moderate or even heavy medium wear might turn out to be an economical success rather than a source of concern as the worn out material reports in a final product.

Thus in the case of autogenous grinding the question of wear can be reduced to include the liners only. The following cases should be taken into consideration:

1) In some grinding operations the abrasive qualities of the material to be ground are so light as to be of no concern even at substantial supercritical speeds. Smooth liners of Ni-hard, for example, would give good service. This is the situation with many dry grinding operations.

2) In cases where liner wear may be a delicate problem, a compromise should be made between expense of liners, speed, and type of mill (grate vs

overflow). Grate-type mills will always favor capacity at a more moderate speed.

3) There may be a number of fine grinding problems that can be handled more economically at subcritical speeds with the present standard procedure rather than at supercritical speeds.

4) At supercritical speeds, autogenous lining of the mill by pieces of tumbling medium becomes a possibility as soon as the mill is provided with proper breaking bars that will prevent the sliding of one or several outermost layers of medium. Attrition grinding will naturally now take place in the zone between the fixed layer and the movable layer of medium opposite.[7]

The whole question of mill liners should be turned over to the metallurgists for a new basic study. Substantial improvements will no doubt be possible. Ni-hard and tungsten carbide should form a good reference pair of materials either in use at present or at least within the possibilities of being used. Once the metallurgists can produce an alloy of 10 to 100 times better wearing characteristics than the best at present, the whole unit operation of grinding will face a revolution.

At present autogenous supercritical grinding appears to face the most promising future. In plants where steel consumption is high or plants far from steel centers, the combination of inexpensive local grinding medium and sufficient mill speed should turn out a highly successful economical undertaking. The experience obtained at Outokumpu in industrial scale offers proof beyond all doubt.

It often happens that the grinding section is the bottleneck of the entire operation of a mine plant. From what has been said it should be obvious that the capacity of almost every fine grinding mill may be increased by increasing the speed. Even if direct grinding costs per unit of ore treated should go up, it might be economically sound to go to higher speeds. The economics of a mining operation should not be based on figures indicating ball wear or liner wear or any other single item of costs, but on the overall result of the whole undertaking from mine to finished product. With increasing scale of operations unit costs usually go down.

New Grinding Circuit: The wet fine grinding circuit of today consists essentially of a grinding unit and a mechanical classification unit placed side by side and operated in a closed system. The shape of the classifier is determined to some extent by the transportation problem involved.

In a few new installations mechanical classifiers have been replaced by cyclones. The pulp motion is affected by a pump and the sands (cyclone underflows) are returned by gravity.

If fine grinding is to be accomplished in mills operated at supercritical speeds certain major changes in circuit structure will be necessary—1) elimination of the mill scoop, 2) feeding medium, ore and sands by gravity, 3) placing the mechanical classifier on a higher level, and 4) pumping the mill discharge to classifier.

As soon as this principle is accepted, the shape of the classifier becomes of minor importance. As a matter of opinion, supercritical grinding should turn out to be a major incentive for new developments in the field of classification.

Investigations carried out in South Africa[17] have shown that it takes more power to operate a mill scoop in a closed grinding circuit than to pump the mill discharge into a classifier placed above the mill and return the sands by gravity. If this is correct in a general case, there is every reason to abandon present concepts regarding the architecture of fine grinding circuits.

Conclusions

The possibility of grinding at supercritical speeds has been known for more than 50 years. Time after time it has been rediscovered in a number of countries. It seems, however, that none of the investigators really grasped the simplicity of the basic principles involved. Even laboratory experiments have always been discontinued without convincing success.

In the present technical world grinding is one of the few fields of engineering where low-speed operation has been universally accepted. Today, however, grinding at supercritical speeds is already an established fact and an economic success on an industrial scale.

A number of the basic ideas of grinding at supercritical speeds, partly or fully described in this article, have been covered by patents pending.

References

[1] H. A. White: Theory of Tube-Mill Action. *Journal of the Chemical, Metallurgical, and Mining Society of South Africa*, 1905, vol. 5, p. 290. Summarized by R. H. Richards: *Ore Dressing*, vol. 3, pp. 1336-1340, McGraw-Hill, New York, 1909.

[2] A. W. Fahrenwald and H. E. Lee: *Ball Mill Studies. AIME TP 375*, 1931, pp. 3-53.

[3] A. W. Fahrenwald: Some Fine-Grinding Fundamentals. *AIME Trans.*, 1934, vol. 112, pp. 88-115.

[4] W. A. Perow and W. J. Brand: Feinmahlen der Erze. *Verlag Technik*, Berlin, 1954, p. 86.

[5] W. Anselm: *Die Zementherstellung*. Berlin, 1941.

[6] H. E. Rose and R. M. E. Sullivan: *Ball, Tube and Rod Mills*, p. 42. Constable, London, 1958.

[7] R. T. Hukki: Grinding at Supercritical Speeds in Rod and Ball Mills. International Mineral Dressing Congress, pp. 1-25. Stockholm, 1957.

[8] F. C. Bond: Mathematics of Crushing and Grinding. In *Recent Developments in Mineral Dressing*, pp. 101-115. Institution of Mining and Metallurgy, London, 1953.

[9] H. R. Banks: The Rod Mill in the Sullivan Flow. *Trans.*, Canadian Institute of Mining and Metallurgy, 1952, vol. 55, pp. 255-261.

[10] R. T. Hukki: Tumbling Mill Capacity and Power Consumption as Related to Mill Speed. *AIME Trans.*, 1954, vol. 199, pp. 728-730.

[11] H. Tanner and T. Heikkinen: Crushing and Grinding at Outokumpu. International Mineral Dressing Congress, pp. 1-14, Stockholm, 1957.

[12] A. M. Gow and M. Guggenheim: Dead-Load Ball-Mill Power Consumption. *Engineering and Mining Journal*, 1932, vol. 133, p. 652.

[13] Allis-Chalmers: *Grinding Mills*. (Catalog, 1951.)

[14] Forum on Ball Milling. *Canadian Mining and Metallurgical Bulletin*, August 1957, vol. 50, p. 515.

[15] H. Hardinge: Making Rock Grind Itself. *Engineering and Mining Journal*, June 1955, pp. 84-90.

[16] B. S. Crocker: Screened Ore Used for Fine Grinding at Lake Shore Mines. *AIME Trans.*, 1952, vol. 193, pp. 499-508.

[17] W. B. Stephenson: Private communication.

Discussion

Fred C. Bond *(Consulting Engineer, Allis-Chalmers Mfg. Co.)*—This article is interesting because it deals with the fundamentals of grinding in a novel manner. However, it is somewhat reminiscent of Mark Twain's famous evaluation of science as the production of pounds of conjecture from ounces of fact. Extrapolations abound, and some cases they are treated with a seriousness that is undeserved.

Tests should undoubtedly be made of wet grinding at supercritical speeds, using smooth mill lining and mill charges of large grinding balls as well as pebbles. However, the performance predicted in the article needs more qualification than it has received.

The author starts out by stating that the wet mill capacity varies as the effective specific gravity of the grinding medium in the pulp, with the corollary: 1) that in overflow the medium behaves as if it were completely immersed in the pulp, and 2) that in grate dis-

charge mills its gravity is unaffected by the pulp; however, he implies that its grinding efficiency is unaffected by the absence of pulp.

He continues with the statement that mill capacity varies approximately as the mill speed. This is commonly accepted throughout the usual grinding range, but Hukki extends it to beyond 200 pct of critical speed. Finally, he quotes data from Outokumpu on a wet overflow pebble mill (autogenous grinding) ranging from 58 to 104 pct of critical speed and extends this to beyond 200 pct. The weight of the proper ball charge for this high extrapolated speed receives little or no attention.

Figs. 2, 3, and 4 result directly from these extrapolations. They involve several questionable assumptions, but the most serious seems to be disregard of the decreased amount of grinding media necessary to operate mills at these high speeds without centrifuging. A decrease in amount of grinding media in this range should reduce grinding capacity.

The importance of idling power to energy consumption in kilowatt hours per ton is evidently exaggerated by the high power required to run the pilot mill on tires and rollers. The proportion of the full load power required to rotate a large empty ball mill with properly lubricated trunnion bearings is far less than 30 pct, so that its curves would be much flatter than those shown in Fig. 6.

It is true that the mechanical efficiency of conventional mills increases with mill diameter; a fair exponent of the mill diameter is 0.2. However, Fig. 7 may be misleading because the listed weights of the empty mills are not directly proportional to their internal volumes. This is apparent when the listed weights of the 40 pct ball charges are compared with the listed weights of the empty mills.

Fig. 8 shows the maximum possible percentage medium load at different speeds without pulp in the mill. The behavior with pulp is highly conjectural, particularly with steel grinding balls.

The work index is calculated from the equation

$$Wi = W \Big/ \left(\frac{10}{\sqrt{P}} - \frac{10}{\sqrt{F}} \right)$$

The last column gives the corrected work index for the standard mill 8 ft ID, considering that efficiency varies as the inside mill diameter to the power 0.20. Tests on 173 limestone samples in the Allis-Chalmers laboratory gave an average work index of 12.85.

The equivalent work index of 11.3 for a 24 pct charge of steel balls at 70 pct of critical speed compares with 19.1 for a 48 pct charge of limestone pebbles at 230 pct of critical speed. Thus the low-speed mill required only 59 pct of the energy input required per ton in the high-speed mill for the same grind and gives slightly less than the average limestone work index.

The capacity of the slow-speed ball mill with a ball charge of only 24 pct is much less than it would be with a full ball charge, so that the high-speed pebble mill capacity is considerably less than that of conventional ball mill.

The author's "Basic Equations of Fine Grinding" contain no term for the amount of the grinding charge. He states that the capacity of a mill is directly proportional to its length but that according to his equation the kilowatt-hours per ton should decrease with increasing length of the mill.

Hukki largely avoids the crucial question of metal wear in high-speed ball and rod mills. He does not even state whether the wear per ton ground will be higher or lower than in mills of conventional speeds. In this respect he seems to abandon his case for high-speed ball and rod mills and suggests changing to autogenous grinding.

Grinding is accomplished in a conventional tumbling mill by a combination of impacting, rolling, and sliding contacts. The amount of metal wear in sliding or rubbing contacts is greater than that in impacting or rolling. At supercritical speeds with reduced ball or rod charges and a smooth lining, a large proportion of the total work done is accomplished by the medium charge sliding on the mill lining. The liner wear should be increased, and the medium wear in pounds per ton ground is probably increased. The necessary reduction in the amount of medium present reduces the mill capacity and more or less balances the increased capacity resulting from higher speed. Additional tests are necessary to determine which effect will predominate.

A tumbling mill can apparently carry a larger load of pebbles or rock at high speeds than steel balls or rods. Autogenous grinding at high speeds appears to be more promising than grinding with steel media, because of decreased metal wear costs, even though the mill capacity may be decreased. The data in Table I indicate that the power cost will be much higher, but this should be confirmed by additional tests.

R. T. Hukki *(author's reply)*—The author is grateful to F. C. Bond for his discussion because it brings out a number of points that need clarification.

Several remarks raised by Bond seem to be focused on the amount of grinding medium, especially of balls, in the mill. It is apparent that Bond does not accept the results obtained at the Tennessee Copper Co. as a valid basis for the analysis presented, whereas the author does. This seems to be the primary reason for the controversy.

It has been shown at Tennessee Copper Co. that a reduction of the ball load from 45 to 29 pct of the mill volume has increased the fine grinding capacity of the tricone mill.[18] According to a later report,[19] the ball load was further reduced to 20 pct. As the pilot plant ball mill used for investigations reported resembles closely in shape the tricone mill at Tennessee Copper, the fact that a 24 pct steel ball load was used in the test instead of the 48 pct load as in the case of limestone pebbles should have given the balls a very favorable basis for comparison, as was clearly indicated in the article. The author admits that the figures might have been more convincing if a 48 pct ball load actually had been used.

If the Tennessee practice is further accepted as a sound basis of fine grinding with steel balls, the percentage ball load may remain constant over a wide speed range. Accordingly, it has been possible to operate our pilot plant ball mill with the 24 pct ball load indicated at speeds of 50 to 230 pct without any change in the amount of medium. The capacity of the mill under these conditions seems to follow the 1.4 relationship as indicated up to at least 140 pct of the critical. Beyond that, however, the auxiliary equipment available in our laboratory could not handle the large volume of pulp. For example, if one classifier had been used at a speed 70 pct of the critical, 4 to 5 similar classifiers

Data from Table I

Test No.	Media	Speed, Percent of Critical	Load, Percent of Volume	Short Tons per Hr	W Kw-Hr per Ton	Feed 80 Pct—μ	Product 80 Pct—μ	Wi Work Index	Wi Standard Mill
						(F)	(P)		
1	Steel Balls	70	24	1.053	6.18	450	120	14.0	11.3
2	Limestone Pebbles	230	48	1.053	9.21	420	135	24.7	19.1

would have been necessary at 210 pct to obtain equal classification conditions.

The work index according to Bond's basic definition calls for conditions of the *same relative mechanical efficiency*. In the paper the author has clearly shown how the mechanical efficiency of the pilot plant mill varies widely depending on the media used and on the mill speed. It is therefore surprising that Bond himself forgets his own definition of the work index and uses the data reported in Table I to calculate indices with which he intends to show the inefficiency of the high-speed operation. As a result he has demonstrated one of the common errors in the usual method of evaluation of the work index.

The equations presented must naturally be corrected as soon as dependable evidence becomes available. Regarding the effect of mill length on energy consumption, Bond has apparently misunderstood Eq. 13. The mill length appears a minor factor in connection with the variable part of the equation. The tumbling power consumption and the capacity still remain directly proportional to the mill length.

Regarding the wear of media and mill lining it should be clear that with increased speed the wear will increase and will probably increase even in terms of pounds per ton of material ground. Exact figures, whatever they may be, must be obtained in actual field practice.

The author is fully aware of the existence of many unsolved details in this study of grinding at supercritical speeds. The article is not a report of exhaustive experimental investigations—a task of dimensions far beyond our reach. Rather, it is a simplified analysis of some of the most evident variables in grinding, partly supported by experimental evidence, partly not. Of one thing the author is fully confident—independently of the stand or fall of the ideas presented in the exposing light of future critical investigations, the science of grinding will thereafter rest on much more solid foundations than today.

References

[18] Anon: The Remarkable Case of the Copperhill Ball Mill. *Engineering and Mining Journal*, 1953, vol. 154, pp. 86-89.

[19] F. M. Lewis, and J. E. Goodman: Grinding Practice at Tennessee Copper Co.'s Isabella Mill. *AIME Trans.*, 1957, vol. 208, pp. 1253-1255.

Further discussion of this paper sent (2 copies) to AIME before June 30, 1958, will be published in MINING ENGINEERING.

Discussion

Petrologic Methods for Application to Solid Fuels of the Future

by James M. Schopf

(MINING ENGINEERING, page 629, June 1956, AIME Trans., vol. 205)

Gilbert H. Cady *(Senior Geologist, Head of Coal Division Emeritus, Illinois State Geological Survey, Urbana)*—Those coal mining and preparation engineers and operators who read this article will probably be most concerned with those parts which deal with the applied aspects of coal petrology in the fields of mining and technology. Actually the two categories overlap to such a degree that they are essentially one.

The article appears to suggest that there are two points of veiw in the field of applied coal petrology. From one viewpoint the interest is in the attributes of the various macerals (Fig. 4)—vitrinite, exinite, and inertinite—in terms of utilization (when the coal is burned, coked, gasified, hydrogenated, etc.). From the other point of view, assuming that the macerals do possess individuality in behavior, interest attaches to the possibility that coal of a particular type (maceral composition) can be prepared by discriminating methods of preparation and blending. Most of the 29 items listed for mining and technology can be assigned to one or the other of these two categories.

Somewhat the same simplicity that resides in the items of the proximate chemical analysis is desirable for the petrologic analysis. This simplicity appears to be fairly well achieved by the group maceral device provided mineral matter is also included. At present, without fully adequate experimental substantiation, the three types of material represented by the group macerals vitrinite, exinite, and inertinite are regarded as sufficiently different in composition and properties so that the preponderance of any one type gives the coal distinctive properties provided it is not too high in rank. This appears to be increasingly true with coals of decreasing rank from medium volatile bituminous coals downward.

The article reflects the great emphasis placed on the technique of descriptive coal petrology in America. Such description has resulted in a good understanding of the nature of the fundamental variability in the physical composition of bituminous coals. Such understanding has been attained very largely by the thin section technique used in coal bed profile analysis introduced by R. Thiessen after the manner suggested by the data assembled in Table II.

In contrast, the group maceral concept of coal analysis in terms of the categories indicated on the left hand side of Fig. 4 is particularly useful for broken coal analysis and applied coal petrology, in which evaluation is largely based on quantitative concepts. It is inadequately emphasized in this article that although the Thiessen procedure is suitable for the purpose of petrologic description in which texture and orientation are of critical importance, it is less well adapted to the technological uses of applied coal petrology.

No doubt those persons whose interest may have been aroused in the possibilities of more refined coal preparation by this and other recent contributions to the literature of coal petrology will understand that certain technical aspects of coal petrology, particularly in the field of descriptive petrology, are still a matter of some controversy among the coal petrologists, but they will also appreciate that Schopf has made an important contribution to the field of coal petrology in America by pointing out that such petrology requires consideration of disoriented or broken coal samples and that results are expressed less in descriptive terms than in quantitative values with respect to the four types of material composing coal—vitrinite, exinite, inertinite, and mineral matter. Unfortunately because so much American coal petrology has been descriptive of the coal in the bed there is a dearth of literature on applied coal petrology. Research and experimental data in this field are greatly needed.

Grinding Ball Size Selection

by Fred C. Bond

SIZE of grinding media is one of the principal factors affecting efficiency and capacity of tumbling-type grinding mills. It is best determined for any particular installation by lengthy plant tests with carefully kept records. However, a method of calculating the proper sizes, based on correct theoretical principles and tested by experience, can be very helpful, both for new installations and for guiding existing operations.

As a general principle, the proper size of the make-up grinding balls added to an operating mill is the size that will just break the largest feed particles. If the balls are too large the number of breaking contacts will be reduced and grinding capacity will suffer. Moreover, the amount of extreme fines produced by each contact will be increased, and size distribution of the ground product may be adversely affected.

If the balls added are too small, grinding efficiency is decreased by wasted contacts that are too weak to break the particles nipped; these largest particles are gradually worn down in the mill by the progressive breakage of corners and edges.

Ball rationing is the regular addition of make-up balls of more than one size. The largest balls added are aimed at the largest and hardest particles. However, the contacts are governed entirely by chance, and the probability of inefficient contacts of large balls with small particles, and of small balls with large particles, is as great as the desired contact of large balls with large particles. Ball rationing should be considered an adjunct or secondary modification of the principle of selecting the make-up ball size to break the largest particle present.

Empirical Equation

In 1952[1,2] the author presented the following empirical equation for the make-up ball size:

$$B = \sqrt{\frac{F\,Wi}{K\,Cs}\quad\sqrt{\frac{S}{\sqrt{D}}}} \qquad [1]$$

where

B = ball, rod, or pebble diameter in inches.
F = size in microns 80 pct of new feed passes.
Wi = work index at the feed size F.
Cs = percentage of mill critical speed.
S = specific gravity of material being ground.
D = mill diameter in feet inside liners.
K = 200 for balls, 300 for rods, 100 for silica pebbles.

Eq. 1 was derived by selecting the factors that apparently should influence make-up ball size selection and by considering plant experience with each factor. Even though Eq. 1 is completely empirical, it has been generally successful in selecting the proper size of make-up balls for specific operations. But an equation based on theoretical considerations should be used with more confidence and have wider application. The theoretical influence of each of the governing factors listed under Eq. 1 was accordingly considered in detail, as described below, and a theoretical equation for make-up ball sizes was derived.

F. C. BOND, Member AIME, is a Consulting Engineer with the Processing Machinery Dept., Allis-Chalmers Mfg. Co., Milwaukee.
TP 4728B. Manuscript, Oct. 10, 1957. Tampa Meeting, October 1957.

Derivation of Theoretical Equation

Ball Size and Feed Size: The basis of this analysis is that the largest ball in a mill should be just sufficient to break the largest feed particle into several pieces, excluding occasional pieces of tramp oversize. In this article the size F which 80 pct passes is considered the criterion of the effective maximum particle feed size. The smallest dimension of the largest particles present controls their breaking strength. This dimension is approximately equal to F.

As a starting point for the analysis it is assumed that a 1-in. steel ball will effectively grind material with 80 pct passing 1 mm, or with $F = 1000\mu$ or about 16 mesh. The breaking force exerted by a ball varies with its weight, or as the cube of its diameter B. The force in pounds per square inch required to break a particle varies as its cross-sectional area, or as its diameter squared. It follows that when a 1-in. ball breaks a 1-mm particle, a 2-in. ball will break a 4-mm particle, and a 3-in. ball a 9-mm particle. This is in accordance with practical experience, as well as being theoretically correct.

Confirmation of this reasoning is supplied by the Third Theory of Comminution,[3] which states that the work necessary to break a particle of diameter F varies as $F^{1/2}$. Since work equals force times distance, and the distance of deformation before breakage varies as F, it follows that the breaking force should vary as $F^{1/2}$. These relationships are expressed in Table I, with a 1-in. ball representing one unit of force and breaking a 1-mm particle.

Table I. Factors Relating Ball Size and Feed Size

Balls		Particles Broken		
Size, B Inches	Force, (Weight) B^3 Units	Size, F Millimeters	Size, Inches	Force, $F^{3/2}$ Units
½	⅛	¼	0.00985	⅛
1	1	1	0.0394	1
2	8	4	0.157	8
3	27	9	0.354	27
4	64	16	0.630	64
5	125	25	0.985	125

This establishes theoretically the general rule used in Eq. 1 that the ball size should vary as the square root of the particle size to be broken.

Ball Size and Work Index: The work input W required per ton[3] varies as the work index Wi, and the

work input per particle of any size F also varies as Wi. Work equals force times distance (of deformation), and the distance does not necessarily or regularly vary with Wi. It follows that the breaking force varies as Wi. Since the force varies as B^3, and B^3 varies as Wi, the conclusion is that the ball diameter B varies as the cube root of the work index.

This does not agree with empirical Eq. 1, which states that B varies as $\sqrt{Wi}$.

Ball Size and Material Specific Gravity: Since the work input required per ton varies as the work index Wi and is independent of the specific gravity S, and since the number of particles per ton varies as $1/S$, it follows that at a constant Wi the work required per particle of any size F varies directly as the specific gravity S. The distance of deformation does not necessarily or regularly vary with S, so that the breaking force must vary as S. Since the force varies as B^3, it follows that B^3 varies as S. The conclusion is that the ball diameter B varies as the cube root of S.

This does not agree with empirical Eq. 1 which states that B varies as $S^{1/4}$.

Ball Size and Percent of Critical Speed: It is commonly accepted that within the practical operating speed range the work input to a mill is proportional to the percentage Cs of the critical mill speed. Since the work input per ball is proportional to B^3, at a constant work input B^3 is inversely proportional to Cs. It follows that the ball diameter B is proportional to the cube root of $1/Cs$.

This does not agree with empirical Eq. 1, which states that B varies as $\sqrt{1/Cs}$.

Ball Size and Mill Diameter: As the mill diameter D in feet inside the mill lining increases, at a constant percentage Cs of the critical speed the linear speed increases as $\sqrt{D}$ while the centrifugal force remains constant.

When the volume of the ball charge is maintained at a constant percentage of the mill volume, the weight of the ball charge increases as D^2, and the linear shell velocity increases as $\sqrt{D}$; it follows that the work input theoretically varies as $D^{5/2}$.

The number of balls of any size B varies as D^2, so that the work input per ball varies as $\sqrt{D}$, or as the linear speed of the mill. Since it has been shown that the work input per ball varies as B^3, it follows that the ball diameter B is proportional to the cube root of $\sqrt{1/D}$, or to $(1/D)^{1/6}$.

This does not agree with empirical Eq. 1, which states that B varies as $(1/D)^{1/8}$.

The above analysis neglects the special case of large diameter mills using small balls. When the make-up ball diameter B becomes less than about 1 pct of the mill diameter $12D$ in inches, a *slump factor* appears, and the work input increase with diameter falls below $D^{5/2}$. It apparently approaches $D^{3/2}$ as a limit; under these limiting conditions the effective work input is confined by ball slippage to a zone near the mill lining, and the active ball zone thus becomes proportional to D rather than D^2. The work input thus approaches $D \times \sqrt{D}$, or $D^{3/2}$, as a limit. However, the limiting number of active balls of any size B varies as D instead of D^2, so that the proper ball diameter B remains proportional to the cube root of $\sqrt{1/D}$, as in the above analysis.

Theoretical Ball Size Equation: As a result of the above factor analysis, the following theoretical equation, Eq. 2, can now be written for the proper make-up ball size B, using $1/K$ as the proportionality constant as in empirical Eq. 1:

$$B = \left(\frac{F}{K}\right)^{1/2} \left(\frac{S\,Wi}{Cs\sqrt{D}}\right)^{1/8} \qquad [2]$$

Selected average values of the proportionality constant K have been determined empirically and are listed in Table II.

Table II. Tumbling Mills

Grinding Media	Steel or C.I. Balls K	Silica Pebbles K
Wet—Overflow—Open Circuit	350	—
Wet—Overflow—Closed Circuit	350	—
Wet—Diaphragm—Open Circuit	330	170
Wet—Diaphragm—Closed Circuit	330	170
Dry—Diaphragm—Open Circuit	335	175
Dry—Diaphragm—Closed Circuit	335	175

Selection of Proper Size of Make-Up Balls

After the ball diameter B in inches has been calculated from Eqs. 1 and 2, the nearest commercial ball size is selected to be fed to the mill in sufficient amount to compensate for ball wear. However, when the value of B is 1 in. or smaller, somewhat larger balls may be preferable for the following reasons:

1) Since the small balls cost more per ton, the total grinding cost per ton may be decreased by using slightly larger balls, even though they are mechanically less efficient.

2) When the small balls are to be used in a large diameter mill, slightly larger balls will increase the power drawn by the mill and may increase the mill capacity.

3) In diaphragm discharge mills the small balls may tend to blind the grate openings and may increase ball wear per ton ground by discharging at too large a size.

Eq. 2 is preferred to Eq. 1 because of its theoretical derivation. However, in most instances both equations will probably indicate the same commercial ball size selection. This is shown in Table III,

Table III. Ball Size Calculations

Factors					Eq. 1	Eq. 2
F	Wi	S	Cs	D	B	B
500	12	2.7	76	9.0	0.613	0.625
1000	15	3.0	75	10.0	0.990	0.973
2000	10	3.3	65	12.0	1.229	1.265
5000	13	2.9	77	8.0	2.07	2.11
10000	11	2.8	70	11.0	2.69	2.73

where B values are calculated from both equations for several values of the controlling factors for wet overflow ball mills.

Rod Size Selection

Since each rod in a rod mill makes an indeterminate number of particle contacts, no theoretical derivation of the equation for proper rod sizes was attempted. The make-up rod size selection should be based on empirical Eq. 1, using the constant K equal to 300.

Ball and Rod Weights and Surface Areas

The weight, volume, surface area, and number of grinding balls or feet of grinding rods, of diameter

Table IV. Ball and Rod Data

Balls, No., or Rods, Ft	Pounds	Cubic Feet	Surface Area, Sq In.
One ball	$0.148B^3$	—	$3.142B^2$
13,500/B^3 balls	2000	6.89	42,500/B
1960/B^3 balls	290	One	6160/B
Equilibrium charge fed with B balls	2000	6.89	57,500/B
1-ft rod	$2.67B^2$	—	$37.8B$
750/B^2-ft rods	2000	5.13	28,400/B
146/B^2-ft rods	390	One	5510/B
Equilibrium charge fed with B rods	2000	5.13	30,000/B (approx)

B inches, can be calculated from Table IV. The pounds per cubic foot of grinding balls range from fewer than 280 for rough cast iron balls to 300 for well-rounded forged steel balls.

Start-Up Grinding Media Charges

When a grinding mill operates for several months with a constant size of make-up media added and a constant size of worn media discharged, an equilibrium size distribution of the grinding media is established which will continue indefinitely. This equilibrium is established more quickly in wet mills than in dry mills because of the greater media consumption per ton ground in wet mills.

The equilibrium depends on the generally accepted rule of equal film wear in equal grinding time. A film of equal thickness will be removed from all sizes of balls or rods in a mill during any grinding period, excluding ball or rod breakage.

According to this rule, when the ball or rod diameter is plotted as abscissa, and the percent weight passing that diameter is plotted as ordinate on log-log paper, the equilibrium size distribution will be represented by a straight line with a slope m of 3.84 for grinding balls and 3.01 for grinding rods.

It is desirable, particularly in wet grinding mills, that the initial ball or rod charge used in starting up a new mill should be similar to the equilibrium charge, in order that grinding results at the start-up will be about the same as those when the circuit has reached continuing equilibrium. The initial charge cannot be precisely the same as the equilibrium charge, since it is made up of only a few sizes of balls or rods, but the relative weight of each size can be selected so that it approximates the equilibrium charge. The proper proportions are determined as shown in Table V.

A straight line is drawn on log-log plotting paper starting at 100 pct passing the known make-up size at the top of the sheet, with a slope of 3.84 for balls and 3.01 for rods. Vertical lines are drawn representing the mid-points between the ball or rod sizes available. The intersections of these lines with the equilibrium distribution line determine the percent weight of each size to be used in the initial charge.

Tables V and VI, opposite, show initial ball and rod charges to be used when make-up balls or rods of the designated size are to be fed. When two or more make-up media sizes are to be used in a fixed proportion for ball rationing, each portion of the initial charge is calculated from its own make-up ball or rod size.

The situation is somewhat different in dry-grinding single-compartment ball mills, particularly when they are grinding soft materials such as limestone or cement raw material, or materials such as cement clinker, in which the larger particles have a lower work index. Here the ball wear is only one fifth to one tenth that in wet grinding, and two or three years may be required to reach equilibrium.

Table V. Start-Up Equilibria Grinding Ball Charges, Percent Weight

Make-Up Balls Fed Sizes, In.—B	4½ In.	4 In.	3½ In.	3 In.	2½ In.	2 In.	1½ In.
4½	23.0						
4	31.0	23.0					
3½	18.0	34.0	24.0				
3	15.0	21.0	38.0	31			
2½	7.0	12.0	20.5	39	34		
2	3.8	6.5	11.5	19	43	40	
1½	1.7	2.5	4.5	8	17	45	51
1	0.5	1.0	1.5	3	6	15	49
Total, pct	100.0	100.0	100.0	100	100	100	100

Table VI. Start-Up Equilibria Grinding Rod Charges, Percent Weight

Make-Up Rods Fed Sizes, In.—B	5 In.	4½ In.	4 In.	3½ In.	3 In.	2½ In.
5	18					
4½	22	20				
4	19	23	20			
3½	14	20	27	20		
3	11	15	21	33	31	
2½	7	10	15	21	39	34
2	9	12	17	26	30	66
Total, pct	100	100	100	100	100	100

In these cases the initial charge should contain a larger proportion of small balls than the equilibria charges listed above, and this proportion should be maintained by adding a rationed charge of make-up balls. The exact proportion depends on the size distribution and composition of the material fed, and no general rule has been established, except that at least half the make-up balls added should be smaller than the size B calculated from Eq. 1 or Eq. 2.

In dry grinding mills of two or more compartments, each compartment is considered a separate mill, and the make-up ball size B for each compartment is calculated from Eq. 1 or Eq. 2. The size F of the feed entering each compartment can be calculated from the fraction of the total power input drawn by the preceding compartments.

Amount of Make-Up Grinding Media Required

The amount of make-up grinding media that must be added regularly to a mill to maintain a constant volume of grinding charge and a constant power input will vary with the character of the metal and the abrasiveness of the material being ground.

Table VII. Ball and Rod Wear Replacement

	Wet		Dry	
	Kw-hr Pound	Lb Day 100 Hp	Kw-hr Pound	Lb Day 100 Hp
Grinding balls	6	300	35	50
Grinding rods	5.5	325	30	60

However, it is primarily dependent on the power input to the mill, and estimates of the amount required for new installations should be based upon the power.

Table VII lists the average kilowatt-hours per pound of metal worn away and discharged and the average pounds of make-up balls and rods required per 24-hr day for each 100 hp drawn by the mill, when it is grinding silicious materials. Dry grinding of limestone will require perhaps half the amounts listed for silicious materials. Because of the wide variations in materials and metals these values should be used for rough estimating purposes only.

Summary

Empirical and theoretical equations are given for calculating the proper sizes of balls and rods to be added regularly to tumbling grinding mills. Both equations give similar results.

A convenient table of ball and rod weights, volumes, and surface areas is given, and tables of the proper ball and rod size distribution for starting up a mill are included. Rough estimating figures for ball and rod wear are given.

References

[1] F. C. Bond: Mathematics of Crushing and Grinding. In *Recent Developments in Mineral Dressing.* Published by Institute of Mining and Metallurgy, Salisbury House, London, 1953.

[2] F. C. Bond: Crushing and Grinding Calculations. *Canadian Mining and Metallurgical Bulletin,* vol. 47, no. 507, July 1954, *Trans.,* vol. LVII, 1954, pp. 286-292.

[3] F. C. Bond: Third Theory of Comminution. *AIME Trans.,* 1952, vol. 193, pp. 484.

Discussion of this paper sent (2 copies) to AIME before May 30, 1958, will be published in MINING ENGINEERING.

Discussion

Mineralizing Solutions That Carry and Deposit Iron and Sulfur

by B. S. Butler

(MINING ENGINEERING, page 1012, October 1956, AIME Trans., vol. 205)

A. D. Mutch *(Falconbridge Nickel Mines Ltd., Onaping, Ontario)*—This contribution is prompted by the fact that the writer has recently published an article[29] which has in part the same general conclusions as B. S. Butler's, namely, the form of the standard mineral paragenesis in hypogene deposits and the parallel transition from early high temperature acid to late low temperature alkaline or neutral solutions. Since the writer also recognizes that he is not fully qualified to discuss the formation of ore deposits as a chemical problem, this discussion will be limited to summarizing other observations and will suggest how Butler's Table II might be made more effective.

The form of Butler's table is not unlike that widely used by European geologists[30] in which the various minerals are related to the types of ore fluids—pegmatitic, pneumatolic and hydrothermal. Thus the decrease in temperature and change in pH of the ore-bearing fluids as recognized by Butler may also be paralleled by perhaps even greater changes in composition, density, and character.

W. H. Newhouse's article[31] on the sequence of hypogene ore mineral deposition is still one of the most complete analyses of the problem. In it he makes four major observations:

1) The order of O, S, As, Sb is the same as their increasing atomic weights and the same as their melting points.

2) The order of the metallic elements is the same as the Schuermann series.

3) The general mineralogical order is paralleled by decreasing heats of formation.

4) The order is generally in decreasing hardness, higher metal content, and higher specific gravity.

The order of O, S, As, and Bi is also the same as their relative abundance. Another point worth mentioning about this series is that As, Sb, Bi, when abundant, often substitute for sulfur in the early pyrite-like minerals, whereas later in the sequence these elements appear to act more like metals. This behavior may be a further indication of the acid character of the early fluids.

C. J. Sullivan[32] has attempted to show that the sequence of the metallic elements is related to the order of their melting points and has discussed the interrelationship of the different types of bonding of sulfophile and oxiphile elements in minerals.

Items 3 and 4 might best be summarized by saying that bonding of the minerals in the series appears to be from ionic to covalent to metallic, the early minerals being light in weight, hard, and near-transparent; the intermediate minerals of intermediate weight, semi-transparent, and semi-conducting; and the end minerals heavy, soft, and malleable, opaque and good conductors.

A rapid fall in temperature has been assumed to be the cause of ore deposition in many deposits. Perhaps this in turn is the effect of a rapid release of energy in the form of pressure release and change of volume, the first minerals to form being those with the highest heats of formation which absorb the released energy the most rapidly.

Butler's Table II could probably be streamlined and made more effective if the listed compounds were assembled as mineralogical groups as in Dana.[33] Thus the sulfides, arsenides, antimonides, bismuthides, and sulfa salts could be arranged in AX_2, AX, A_2X_3, etc. groups. Since these are continuous substitution series, in which the fields of stability and the heats of formation of the various individual minerals can be fairly regarded as similar, this should be accomplished with no loss of clarity. The occurrence of the individual minerals and the precise sequence of the mineral deposition in any one deposit is probably more dependent on the concentration and relative abundance of the component elements.

The assembling of geological data in tabular form such as Butler's Table II will continue to be a very effective method of studying geological phenomena. The importance of this particular problem has been pointed out by C. F. Park,[34] who concludes that understanding of mechanisms of the standard paragenesis and interrelated problems of mineral zoning in space and time is one of the major keys to classification of ore deposits.

References

[29] A. D. Mutch: A Critical Evaluation of the Classifications of Ore Deposits of Magmatic Affiliations. *Economic Geology,* 1956, vol. 51, pp. 665-685.

[30] P. Niggli: *Ore Deposits of Magmatic Origin* (trans. H. C. Boydell). Thomas Murby, London, 1929.

[31] W. H. Newhouse: The Time Sequence of Hypogene Ore Mineral Deposition. *Economic Geology,* 1928, vol. 23, pp. 647-659.

[32] C. J. Sullivan: Metallic Melting Point and Ore Deposition. *Economic Geology,* 1954, vol. 49, pp. 555-574.

[33] C. Palache, H. Berman, and C. Frondel: Dana's *System of Mineralogy,* vol. 1. John Wiley & Sons Inc., New York, 1944.

[34] C. F. Park, Jr.: Zonal Theory of Ore Deposits. *Economic Geology,* 1955, 50th Anniversary Volume, pp. 227-248.

The Daniel C. Jackling Lecture

An annual invitation address by an outstanding man in mining, geology, or geophysics who has contributed significantly to the progress of technology in these fields.

The Citation for the Award:

For leadership in efficient mine operation, resulting in profits under a fixed gold price in spite of inflationary costs, and for his Lecture, "Planning for Deep Mining at Homestake."

The Award Committee:

Clark L. Wilson, Chairman

R. V. Pierce
H. V. W. Donohoo
E. A. Jones
D. M. Fraser

The combined hoisting capacity of these two shafts from lower levels is in the order of 6000 tpd. The Ross shaft lies to the west of known ore zones, the Yates to the east. The horizontal distance via the drives from these shafts to the point where Homestake ore plunged below the 5000 level is about 6400 ft.

Ventilation to the 4100 level was entirely adequate for the mine above that level, but insufficient to do more than furnish enough air for the initial development to the 5000 level. Homestake was faced, therefore, not only with the problem of providing ventilation for deepening the mine, but with furnishing adequate additional air for a substantial percentage of the developed ore reserves. The mining system, which will be described very briefly below, left sufficient ore tied up in pillars in the upper levels so that the present volumes of air serving upper levels could not be diverted to lower levels for many years.

Shrinkage stopes 60 ft in width in the direction of the plunge, with intervening pillars 40 ft wide mined by panel square setting, furnished the entire production.

In the 1930's Homestake had developed an underground distribution system for hydraulic fill. The sand fraction of the sand-slime split only was used for fill. An effective method of fill for any mining system was therefore already in operation.

New Development Shaft

Since both the Ross and Yates shafts had reached their ultimate depth, there was no other available method of getting below the developed bottom of the mine than to sink an interior shaft. Positioning the new shaft near either the Ross or Yates would have required excessively long drives to reach the ore areas, and would have eliminated the use of one of the shafts for the hoisting of transferred ore. Therefore the site of the new interior shaft was chosen some 6400 ft south of the Yates shaft, near the point where the Homestake formation plunged below the 4850 level.

The possibility that the interior shaft sinking could be postponed until a drilling campaign could give assurance of sufficient reserves to justify the larger expenditure of this deep level program was studied.

Because of the low angle plunge of the orebodies, such a drilling program would have required a very extensive development pattern on the lowest level. These drifts and crosscuts would have served no other purpose than access to chosen drilling sites.

Past experience had shown that only flat holes at right angles to the planes of schistosity had any chance of reaching a predetermined target. Because every hole ultimately became normal to the dip of the schists there was no chance of reaching more than 300 ft vertically below the collar elevation of any hole. Steep holes had been tried on several occasions and had been very carefully surveyed. Their courses were so erratic that any thought of getting reliable information from steep holes had to be abandoned.

Furthermore, these structures cannot be projected with precise accuracy even one level interval, let alone hundreds of feet. Therefore nothing less than a close interval drilling pattern over very large areas would give reliable information on ore occurrence. The cost of such a program would be excessive.

This left no choice but the early sinking of the interior shaft. Its size was chosen to allow a minimum 3000-tpd capacity. Its caging capacity was sufficient to permit initial development on several levels without installation of an ore hoist. Choice of size of the ore hoist could then be deferred until significant ore reserve information was available.

Equipment Development

Since a major transfer level was a necessity, the question naturally arose as to whether or not a change in size of equipment, track gage, and drifts would be feasible. Because Homestake was a very old mine the track gage was 18 in. and locomotives and cars were small.

Practically all of the development openings from the 5000 level up were 7 x 7 ft. Crosscut turnouts were on 20-ft radius curves. A very cursory glance at the problem of revamping the active part of the mine for a wider gage showed its impracticability.

The use of broader-gage larger equipment would then have been limited to the 5000 level and below. Since no reserves were proven below the 5000, this high initial re-equipment cost would have had to be borne without any assurance of its repayment.

A very effective 60-cu ft Granby car to replace the old 20-cu ft cars had been placed in service prior to the war. Battery locomotive manufacturers came up with an 18-in. gage locomotive capable of delivering 1000 tpd from stoping areas to shaft pockets on the longest haul level and still able to negotiate Homestake's short-radius curves. Scheduling of ore production showed that such a capacity was adequate for any foreseeable mining rate.

The small mucking machines in use were inadequate and the proper size was dangerously unstable on an 18-in. gage track. This problem was solved by building outriggers on the larger mucker, preventing any overturn.

Since adequate haulage capacity could clearly be demonstrated without gage change, the thought of a differently equipped lower mine section was given up.

By 1952 stoping had progressed downward to the point where a considerable tonnage had to be mined below the 3650 level. One of the first large shrinkage stopes driven from the 3800 to the 3650

Diamond drill station at Homestake.

level gave quite definite evidence that rock pressures were sufficient to make continuation of shrinkage stoping below the 3650 unwise, for within a period of several weeks the back began to spall wherever it was convex downward.

Panel square setting, the method used to extract the pillars between shrinks, was a high cost system, particularly since the introduction of hydraulic fill, which required the preparation of each panel on every side to hold the fill by the use of S4S 3 x 12-in. tongue and groove lumber. Also the increasing weight on the pillars made sizable rock falls more probable. Since no fill could be introduced until the completion of a panel 75 ft high, the danger of losing an entire panel was increasing.

Coupled with the physical conditions described above was the fact that the outline of the orebodies in the deeper levels was much more irregular than in the upper levels. This greater irregularity was causing difficulty in recovering ore from shrinkage stopes. It was necessary at times to set up slushers in the shrinks as they were being pulled to remove ore from flat benches.

Because most shrinks were bottomed between levels, numerous drawpoints were economically impossible. This situation resulted in large conical holes in the muck pile when *relief* was drawn, thus severely limiting the back areas that could be drilled at one time. This forced a miner to drill a pattern of diverging holes from any one possible set-up. The result upon blasting was a great deal of oversize rock, which had to be blockholed. Also some of the oversize which landed near the bottom of the draw cone could not be drilled, creating a difficult chute drawing and blasting problem.

The indirect costs—such as wear on cars and skips, adverse effect on dust concentration caused by excessive chute blasting, the occasional tonnage of unrecovered ore when bad back or wall conditions made full clean-up impossible—led to the belief that there was an appreciable margin in favor of some other system not revealed by direct cost comparisons.

Need for New Stoping Method

Changing mining methods in a mine that had developed a standardized procedure with which miners were thoroughly familiar was a serious step. However, for the lower level ore reserves, there was no choice. The only area of choice was in whether or not one selected change for deeper level ore could be applied to all ore with an increase in efficiency over the old procedures.

No method could be given serious consideration if any appreciable grade reduction would result. Any sublevel caving system was inapplicable because of the extremely irregular ore outlines, coupled with the toughness of the rock and its characteristic of breaking in large sizes. Also because of labor shortage any method requiring large advance stope development ahead of production would have curtailed output.

Open cut and fill stoping seemed to meet Homestake's requirements better than any other method studied. By this method a more effective grade control is possible than with any other, not excepting square setting. Irregular ore can be followed, no matter where it leads. Any sizable waste areas within the outside ore limits can be left unbroken in the stope. The completed cut can be quickly sampled with jackleg drills and thus any variations of ore distribution in the succeeding cut can be known in advance and properly planned for.

One of the most serious problems of shrinkage stoping at Homestake, that of dilution from infolded waste pendants near the top of the stoping section, can be handled readily by dividing the section in two parts. As soon as the cut is sand-filled the waste is then firmly supported, thus safely securing the waste inclusion. Such an occurrence in a shrinkage stope was always a worrisome hazard.

The amount of stope preparation work could be reduced materially, as cut and fill sections longer than 150 ft can be easily handled. The former method required two crosscuts each 100 ft. Raising was proportionately reduced.

There is a distinct disadvantage in that this development pattern gives less reliable grade information from initial development. Thus far there has been no difficulty in determining whether or not a block is or is not of commercial grade, but the production grade will not check the estimated grade with the former accuracy. On occasion it is very probable that additional development, not required for extraction, will be necessary to determine the feasibility of mining certain areas.

Any system which Homestake hoped to apply to the deep levels with their increasing rock pressures and eventual appearance of rock burst conditions had to eliminate pillars, as the reduction of a block of ground in the rock burst zone to remnant pillars is inviting violent failure with the consequent loss of ore and, in addition, a hazard to mine personnel. It also had to permit a reduction in the size of the stope opening whenever experience might dictate the necessity of smaller ones.

Conversion to New System

As the conversion to cut and fill progressed it became necessary to limit the length of stoping section. When this is done a single timber deadline is built to retain the sand fill when the adjacent panel is mined later. Scrap timber and outside log cuts are used for this purpose. Thus far when the next stoping section is kept 20 ft vertically below the upper section, there has been no spill-through when the upper cut is being filled.

Since gravity could no longer be used for ore removal, the ore had either to be slushed or handled with trackless equipment. Because of the difficulty of getting trackless equipment into the stopes, the necessity of repair and maintenance *in situ* unless dismantled, the great difficulty of storing while filling, and the high cost of each unit compared to slushers, slushing was chosen as the means of removal.

The size of slushers chosen is a compromise between optimum size and easy mobility. The manufacturers have been very helpful in that they have designed higher-horsepower motors for application to the smaller hoist frames. Homestake has, then, an adequate unit light enough for stope crews to move it without special rigging, saving the lost time and extra expense of a special bull gang.

Homestake's department has designed a control unit mounted in one weatherproof case, which is installed out of the stope near the manway raise. The only control in the stope is a stop-and-start pushbutton switch. The power cable running from control box to the slusher in the stope is long enough to permit moving the hoist to any desired position in the stope without relocating the control panel. By this set-up electrical work can be limited strictly to authorized electricians.

Securing the slusher hoist proved difficult in sand-filled open stopes. The mine department came up with the answer—screw bits into the sand fastened to the frame.

By use of jacklegs a closer, uniform spacing of holes was possible with a consequent marked improvement in fragmentation. Also the chute openings in the stopes were grizzlied, causing a marked decrease in chute blasting.

Conversion of an uncompleted shrinkage stope to cut and fill was an easy procedure. As soon as a shrink reached the level it could be drawn empty, and sand-filled, and cut and fill stoping started above the level. Also the intervening pillar could then be included in the cut and fill section, eliminating high-cost timber stoping.

One of the important advantages of shrinkage stoping was lost by this conversion, namely, the maintenance of a large broken ore reserve which made uniform production possible during periods of labor shortage. Compared to shrinkage, cut and fill increased timber consumption for flooring by one board foot per ton.

To make up for this broken reserve cushion an additional ball mill was installed, together with extra vat capacity so that higher tonnages could be handled in the winter to compensate for summer labor shortages. Fortunately since 1953 Homestake's labor force has been quite stable; it has been possible, therefore, to increase overall production rather than merely compensate for times of labor shortage.

Panel square setting was abandoned as soon as stopes could be filled and timbered cut and fill stoping substituted. Only one working floor is kept open. This permits securing the back as the stope is timbered, eliminating many spills and greatly simplifying repairs when they occur, as damage to timber is limited to one floor. The size of timber was successfully reduced from 12 x 12 in. to 10 x 10 in., with an important cost saving. Also, by this method it was necessary only to lace around chute and manway to contain the sand fill.

At the start of these changes certain key contract crews were chosen to demonstrate their effectiveness. To minimize *heel dragging* the crews were guaranteed previous earnings. Contract earnings early in the game increased materially and no serious resistance from contract crews ever developed. Without such preliminary guarantees it is very doubtful that such a painless conversion would have been possible.

The geothermal gradient at Homestake is high, particularly so for rocks of great geological age. The range is from a low of 44°F on the 300 level, which is the mean annual temperature, to 103.1°F on the 5600—an average of 1.1° per 100-ft increase in depth. This is not a straight line curve. From the 2300 to the 3500 level the average is only 0.77°F per

100 ft. From the 3500 to the 4850 the increase is 1.6°F per 100 ft. From the 4850 to the 5600 the curve flattens again to 1.2°F per 100 ft. Projecting the average increase from 3500 to 5600, rock temperatures in excess of 130°F are anticipated for the 7500 level. It is of interest that in the ore zone rock temperatures are encountered that are several degrees higher than in waste rock.

It is extremely difficult to predict at what vertical depth the economic limit of mining will be reached. The tenor of the ore to be found in depth, ground behavior, actual rock temperatures as contrasted to those predicted, coupled with the unknowns of labor and supply costs and price of product in years hence, make only a guess possible. Yet some guess had to be made, for the production limits imposed by the choice of ventilation capacities made at this time probably would be controlling, regardless of the outcome of development at the bottom limit imposed by the choice.

The decision was that this lower work should be capable of being extended to the 7500 level, and that adequate volumes of air should be provided to stope simultaneously on three levels and do preliminary work on two others. Probable stoping layouts on a typical level were made and the requirements of that layout were multiplied by the factors given above. The capacity to be provided as determined by this estimating came to 350,000 cfm.

Since the distance to the nearest part of the new area to be developed was a mile and a quarter, the furnishing of this additional ventilation capacity from existing openings required transferring that distance through a drift with rock temperatures approaching 100°F. Humidity would have approached saturation. The existing openings were too small to accommodate the required volumes. Increasing velocities to deliver an adequate volume would have made working conditions intolerable and would have increased power consumption fantastically.

It was obvious that the proper solution was a new vertical shaft connecting directly to the 4850 level close to the collar of the interior shaft. Air at approximately the humidity of the surface air could then be delivered to the 4850 and only the lower 1300 ft of the shaft would be in the rock temperature zone of plus 80°F. Under such conditions the introduction of cooling could be deferred several years.

Should orebodies persist several thousand feet below the developed part of the mine, it is a certainty that cooling will eventually be necessary. That possibility was taken into account in the plans for the new ventilation shaft. Ample water is available and the Lead area has sufficiently low humidities to make a closed high pressure loop with surface evaporative cooling practical.

An 18-ft diam circular shaft with a permanent hoist, manway, and pipe compartment on one side met the requirements noted above. During sinking of the shaft the necessary stations will be cut to provide expansion loops in the high pressure system when installed.

This plan called for the introduction of some 350,000 cfm, for which exhaust capacity had to be provided. The only solution which did not cost a prohibitive amount was the enlargement of the Oro Hondo shaft (the present main exhaust shaft) and the driving of a large cross section drift from the new air shaft to it.

Cost studies indicated that crosscuts at four levels could be driven to the air shaft location and pilot raises driven to within 1100 ft of surface, cheaper than to sink the entire distance. With these intermediate connections available, it then became possible to shut down the Oro Hondo and enlarge it while temporarily exhausting via these intermediate crosscuts through the new air shaft. After the completion of the Oro Hondo stripping the new shaft will then become downcast.

These maneuvers called for an accurate scheduling of stoping requirements by levels, so that the whole program could be completed before important tonnages had to be mined from below the 4100 level—the last adequately ventilated level.

The estimated cost of ventilating the 4100 to 5000 level interval for the mining of already developed reserves by refrigeration units showed that a third and probabaly more of the cost of a new air shaft could properly be charged against developed reserves, bringing the cost of ventilation to permit a thorough deep exploration program within reasonable limits, considering the size of the speculative target.

It is believed that Homestake has provided a flexible mining system and an adequate hoisting and ventilation system that will care for the needs of the mine for years to come, certainly beyond the time when the staff responsible for this plan will be concerned about any adverse comments made by future younger operators.

Discussion of this article sent (2 copies) to AIME before July 31, 1958, will be published in MINING ENGINEERING.

Technical Note

Study of Thorium and Uranium Minerals by X-Ray Microscopy

by S. Yamaguchi

S. YAMAGUCHI is with the Scientific Research Institute Ltd., Tokyo, Japan.

TN 459 H. Manuscript, Feb. 19, 1957.

IN this study of thorium and uranium minerals an x-ray shadow microscope of the Cosslett type[1] was used. A flux of electrons driven with a voltage

of about 10 kv was focused onto a target film of tungsten (thickness, about 1μ) by electron microscopy. The rather soft x-rays (wavelengths, 1 to 2 Å) were emitted from a point source prepared in the target film. Distance between an object plane and the target film was 2 mm, and that between the object and a photographic screen was 30 mm. Therefore, direct magnification of 15X was obtainable. The negatives were optically enlarged about seven times, bringing magnification of the final positives to about 100X.

A powder composed of thorium oxide and quartz was observed under the x-ray shadow microscope. In the micrograph obtained, Fig. 1, the dark and the semi-transparent particles correspond to ThO_2 and SiO_2, respectively. The former crystallites containing the atoms of high atomic number (90) completely absorbed the x-rays. On the other hand, the quartz particles composed of light elements were semi-transparent against the rays. An integrated area of the dark particles is proportional to the content of ThO_2 as compared with that of SiO_2. It is possible, therefore, from an x-ray shadow micrograph, to make a rough estimate of the heavy element in a powdered specimen.

Fig. 2 was observed from a mixture composed of ThO_2 and NiO crystallites (50:50 by weight). The NiO crystallites contain the rather heavy atoms. Nevertheless, the two types of particles can be discerned in this micrograph.

Figs. 3 and 4 were taken from a pulverized sample of natural monazite and a pulverized sample of uranium mineral, respectively. According to the results of chemical analysis, the sample shown in Fig. 3 and that of Fig. 4 contain about 50 pct monazite ($ThSiO_4(Ce,Y)PO_4$) and about 3 pct U_3O_8, respectively. As a matter of fact, the amount of the dark particles found in Fig. 3 is comparable with that in Fig. 2. In this way a qualitative and quantitative analysis of actinide elements found in powdered samples can be carried out by means of x-ray shadow microscopy.

Reference

[1] V. E. Cosslett and W. C. Nixon: *Journal of Applied Physics*, 1953, vol. 24, p. 616.

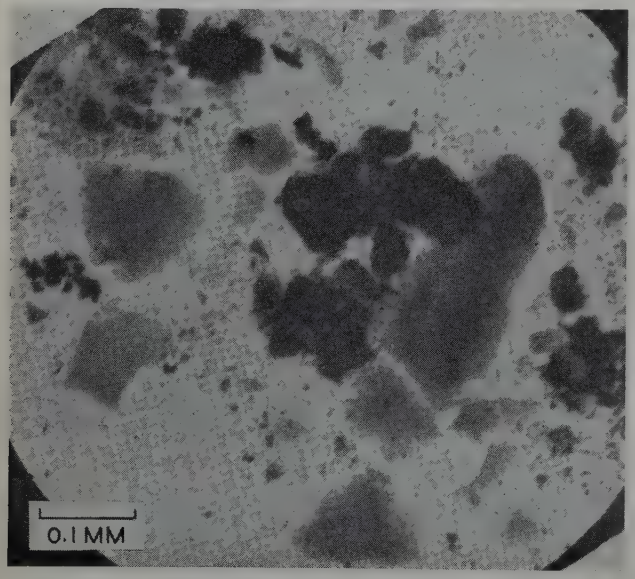

Fig. 1—X-ray shadow micrograph of ThO_2-SiO_2. Dark particles, ThO_2. Semi-transparent particles, SiO_2.

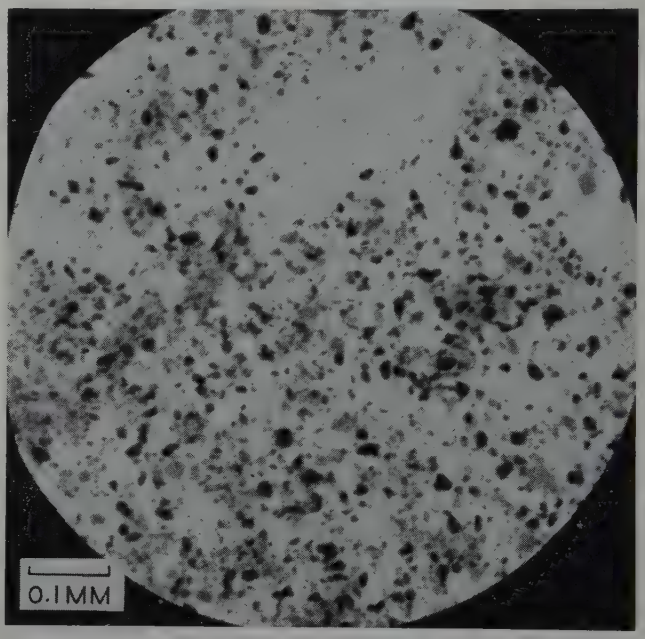

Fig. 2—Powder of ThO_2-NiO. ThO_2:NiO = 50:50 by weight.

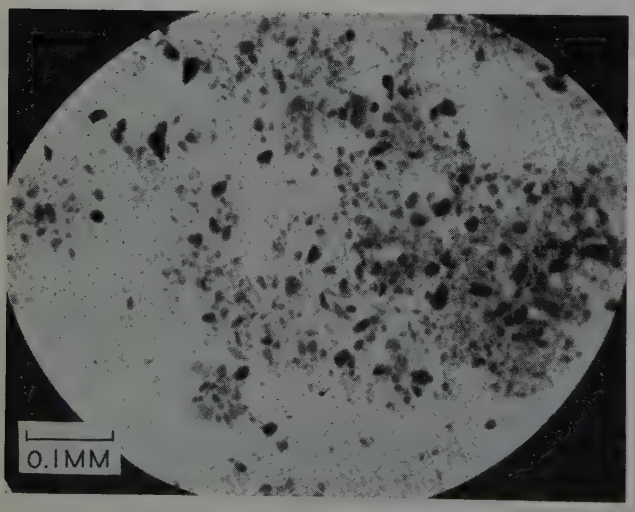

Fig. 3—Powder of natural monazite.

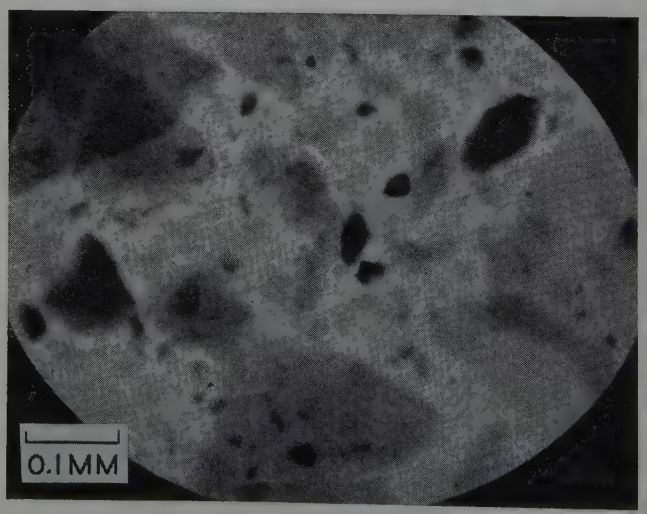

Fig. 4—Powder of uranium mineral.

Relative Effectiveness of Sodium Silicates of Different Silica-Soda Ratios as Gangue Depressants in Nonmetallic Flotation

by C. L. Sollenberger and R. B. Greenwalt

PERHAPS the most widely used dispersants or gangue depressants in nonmetallic flotation are sodium silicates, which vary in silica-to-soda ratio from 1 to 3.75. Typical manufactured silicates in order of decreasing solubility and increasing amounts of silica are *Metso,* silica-to-soda ratio of 1.00; *D,* 2.00; *RU,* 2.40; *K,* 2.90; *N,* 3.22; and *S-35,* 3.75.*

References in flotation literature[1, 2] to the use of sodium silicates are often weak because they fail to mention the type of silicate used. *Metso* and silicate *N* have occasionally been mentioned, but when the type of silicate is not mentioned, it is usually assumed to be *N,* the cheapest of the soluble silicates and the one recommended by sodium silicate manufacturers as a flotation agent.

In the Allis-Chalmers Research Laboratories a systematic study was made of the effect of different alkali-silica ratios on the concentration by flotation of two scheelite ores. One of these was a high grade ore from the Sang Dong mine in Korea. The effect of such factors as pH; addition agents; and conditioning time, temperature, and pulp density on the flotation efficiency of this ore have been described previously.[3] The other ore was a low grade ore from Getchell Mines Inc., Nevada. The mineralogy and techniques of concentrating this ore have been described by Kunze.[4] Hereafter these ores will be referred to as the Korean and Nevada ores. Experiments were made with both to determine the effect of three factors—type of silicate, concentration of silicate, and pH of the pulp—on recovery and grade of tungsten in a rougher concentrate.

Average WO_3 content of the Korean ore was 1.50 pct and of the Nevada ore 0.27 pct. The predominant tungsten mineral in both ores was scheelite, which was accompanied by a small amount of powellite. The powellite and scheelite were finely disseminated through both ores and required a —200 mesh grind for liberation. Major gangue minerals in the Korean ore, in decreasing order of abundance, were amphiboles, quartz, biotite, garnet, fluorite, and calcite. Bulk sulfides composed about 3 pct of the total weight. Gangue in the Nevada ore, in descending order of abundance, was garnet, alpha quartz, calcite, phlogopite, wollastonite, and amphiboles. Sulfide minerals were 3 to 4 pct of total weight.

Batch flotation experiments were made with 500-g samples of ore, each sample wet-ground to 90 pct passing 200 mesh. The finely ground ore was floated in a Fagergren batch cell at 25 pct solids. The natural pH of the Nevada ore was 8.9 and of the Korean ore, 8.5.

The *D, RU, K, N,* and *S-35* sodium silicates were obtained in colloidal dispersions with varying amounts of water. The most alkaline, *Metso,* was in dry powdered form. For convenience in addition, 5 pct solutions by weight were prepared from each of the silicates, on the basis of dry sodium silicate dissolved in the correct amount of distilled water. Chemical analyses of the various silicates are given in Table I, together with the pH of the 5 pct solutions.

A preliminary bulk sulfide float was made with secondary butyl xanthate as the collector and pine oil as the frother. The WO_3 analysis of the sulfide concentrate was nearly 1 pct for the Korean ore and about 0.1 pct for the Nevada ore. The tungsten contained in the sulfide concentrate constituted about 3 pct of the total tungsten in each ore. No effort was made to recover these tungsten values. The scheelite was floated with oleic acid. Adjustments in pH were made with sulfuric acid or sodium carbonate. A 1 pct solution of 85 pct Aerosol OT was sprayed on the froth and sides of the cell during the scheelite float to aid in dispersing the minerals and to decrease the entrapment of gangue particles.

Six tests were planned for each of the six types of silicate in which concentrations of 1, 2, and 4 lb of silicate per ton of dry ore were investigated at both 6.5 and 10 pH. All tests were made at room temperature. The performance of each silicate was judged from the grade and recovery of WO_3 in the scheelite rougher concentrate. Tungsten recovery was calculated on the basis of the scheelite remaining in the ore after the preliminary sulfide float. Testing of each silicate at three levels of concentration and two levels of pH required 36 tests with each scheelite ore. Variance analyses were performed on the concentrate grades and recoveries to determine whether or not the type of sodium silicate, the concentration of sodium silicate, or the pH significantly affected recovery or grade.

Results

Concentrate Grade: A variance analysis of the concentrate grades for the Korean ore showed that concentration of the silicate and pH of the ore pulp were major factors in producing a high grade concentrate. Also, the silica-to-soda ratio was important as an interaction with pH. The concentrate grade vs silica-to-soda ratio is plotted in Fig. 1. The curves show that the concentrate grade improved with an increase in concentration of sodium silicate and also

C. L. SOLLENBERGER, Member AIME, is Supervisor of Mechanical and Process Research, Research Laboratories, Allis-Chalmers Mfg. Co., Milwaukee. R. B. GREENWALT, formerly with the Allis-Chalmers Research Laboratories, is now with Arthur G. McKee & Co., Cleveland, Ohio.

TP 4745B. Manuscript, March 20, 1957. New Orleans Meeting, February 1957.

* All registered trade marks of the Philadelphia Quartz Co.

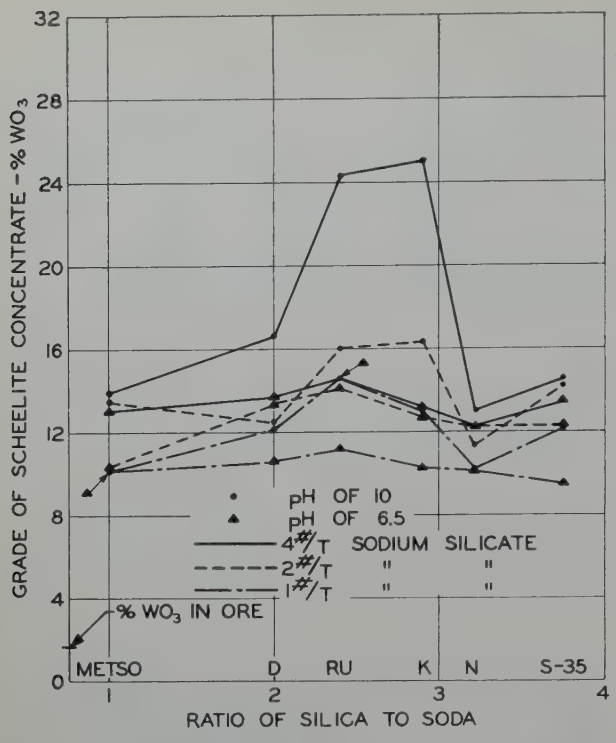

Fig. 1—Korean ore concentrate grade vs silica-to-soda ratio.

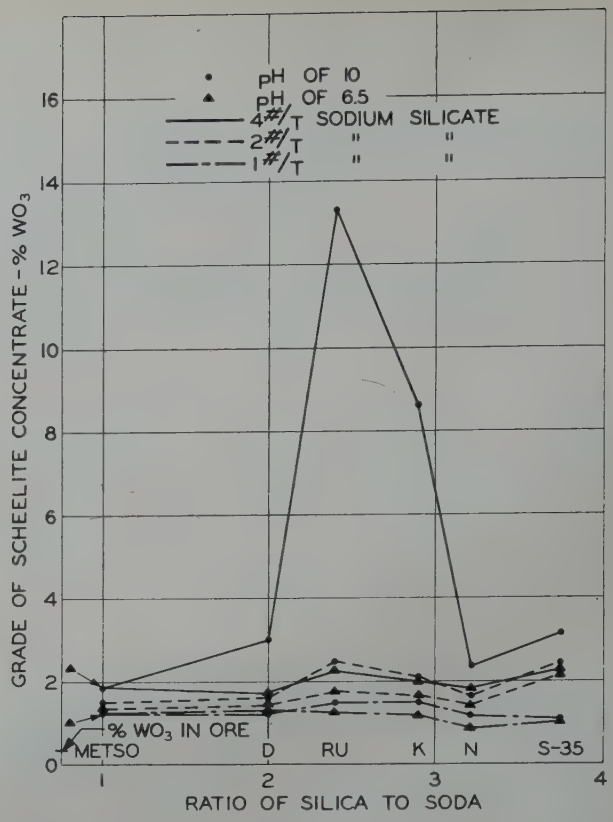

Fig. 2—Nevada ore concentrate grade vs silica-to-soda ratio.

with an increase in pH. The silica-to-soda ratio significantly affected concentrate grade only at pH 10. At this pH the sodium silicates of ratios 2.40 and 2.90 (*RU* and *K*) performed much better than the other silicates. At a concentration of 4 lb per ton, concentrate grades with these silicates were much superior to those obtained with the other silicates. The grades were respectively 24.3 and 25.0 pct WO_3 as compared to 13.0 pct WO_3 obtained with *N* sodium silicate with the same conditions of silicate concentration and pH.

The variance analysis of the grades for the Nevada ore showed that only the concentration of the silicate significantly affected the rougher concentrate grade at all levels of the other variables (the only significant main effect). However, in this analysis the residual was large, indicating either a large experimental error or a significant second order interaction (interaction of all three variables—silica-to-soda ratio, concentration, and pH). The grades are plotted vs silica-to-soda ratio in Fig. 2. The effect of concentration of the silicate can be seen on these curves. The grade increased as the concentration of sodium silicate increased, as before. Fig. 2 shows a remarkable increase in grade with silicates *RU* and *K* at pH 10 and a concentration of 4 lb per ton. These were the conditions at which maximum grades were also obtained with the Korean ore. With the Nevada ore, the grades with the *RU* and *K* silicates were 13.3 and 8.66 pct WO_3, respectively. With sodium silicate *N* and identical conditions, concentrate grade for the Nevada ore was 2.36 WO_3. Apparently the second order interaction was highly significant. Replication of the six tests at pH 10 and 4 lb per ton and a variance analysis of the replicated tests showed the silica-to-soda ratio to be highly significant at this particular pH and silicate concentration.

Recovery: Recoveries for all tests were above 88 pct and for most of them were greater than 95 pct of the contained WO_3. The high grade rougher concentrates produced with the *RU* and *K* sodium silicates contained 99 pct of the WO_3 in the Korean ore and 93 to 94 pct of the WO_3 in the Nevada ore. Recoveries of 90 pct from the Korean ore and 93 pct from the Nevada ore were obtained with sodium silicate *N* at the identical silicate concentration and pH. Apparently the great improvements in grade were obtained at no loss in recovery.

Additional Experiments

The superiority of the *RU* and *K* silicates over the other silicates in obtaining a high grade WO_3 con-

Table I. Chemical Analyses of the Sodium Silicates*

Brand of Sodium Silicate	Percent by Weight		Approximate Ratio of SiO_2 to Na_2O	Condition as Received	Price per 100 Lb of Dry Silicate, $**	pH of 5 pct Solution
	Na_2O	SiO_2				
Metso Granular	29.1	28.7	1	dry powder	7.10	12.0
D	15.1	30.2	2	colloidal dispersion	5.08	11.5
RU	13.8	33.1	2.40	colloidal dispersion	4.91	11.2
K	11.0	31.9	2.90	colloidal dispersion	4.55	11.0
N	8.9	28.7	3.22	colloidal dispersion	3.59	10.8
S-35	6.8	25.3	3.75	colloidal dispersion	5.45	10.7

* Furnished by Philadelphia Quartz Co.
** May 1955.

centrate implied that an intermediate silica-to-soda ratio or a combination of the two silicates might lead to even better results. Several additional experiments were made with a 1:1 mixture of *RU* and *K* as the gangue depressant. The mixture had an average silica-to-soda ratio of 2.65. The pulp pH was maintained at 10, but the mixture was added in amounts of 1, 2, 3, and 4 lb per ton. The experiments were run with both ores. In Fig. 3 plots of concentrate grade vs sodium silicate concentration are compared with the previous results for *RU*, *K*, and *N* silicates. A continuous increase in grade was obtained with all silicates as concentration increased. The curves show that the *RU* and *K* mixture was superior to *N* and better than either *RU* or *K* alone. The highest concentrate grades from the two ores were obtained with the 2.65 ratio at a concentration of 4 lb per ton. These grades were 28.5 and 15.7 pct WO_3 respectively for the Korean and Nevada ores. Corresponding recoveries were 89.4 and 96.4 pct. All data were obtained with a single-stage rougher float. Undoubtedly these grades could be improved with successive cleaner floats.

To determine whether or not the improvement in concentrate grade achieved with the *RU* and *K* mixture could be obtained with ores other than scheelite, additional experiments were made with two ores amenable to an oleic acid-sodium silicate float, a specular hematite ore, and a uranium ore. Several floats were made with each ore with the *RU* and *K* mixture to find conditions that produced a good concentrate. The best experiment was repeated with silicate *N* substituted for the *RU* and *K* combination. The hematite concentrate with the *RU* and *K* mixture analyzed 56 pct acid-soluble iron (head analysis 36.6 pct) and contained 89 pct of the iron in the feed. With silicate *N* the grade was 50.5 pct Fe and recovery 87 pct. The uranium ore concentrate with the *RU* and *K* mixture analyzed 0.56 pct equivalent U_3O_8 (head analysis 0.13 pct) and recovery was 71.0 pct. With silicate *N* the concentrate grade was 0.38 pct equivalent U_3O_8 and recovery 67 pct. Many more floats would have to be made for the above comparisons to be made at the proper silicate concentration and pH, but the results indicate that an improvement in concentrate grade can be obtained with the *RU* and *K* mixtures with these ores.

Cost of the Silicates

Prices in Table I show that with the exception of *S-35* the price per pound of dry silicate increases as the silicate becomes more alkaline, silicate *N* being the cheapest. Silicates *K* and *RU*, however, are next to *N* in order of increasing cost per pound.

Conclusions

1) In the rougher flotation of two scheelite ores, remarkably high concentrate grades and ratios of concentration can be obtained by selecting the proper sodium silicate, concentration of silicate, and pH.

2) Silicates having silica-to-soda ratios of 2.40 and 2.90 (*RU* and *K*) at a silicate concentration of 4 lb per ton and a pH of 10 produced the highest grades and ratios of concentration.

3) Even better results were obtained when a 1:1 mixture of these two silicates was used at the same concentration and pH. With the mixture, concentrate grade and ratio of concentration for the Nevada ore were six times greater than when silicate *N* was used, and for the Korean ore two times greater than when *N* was used.

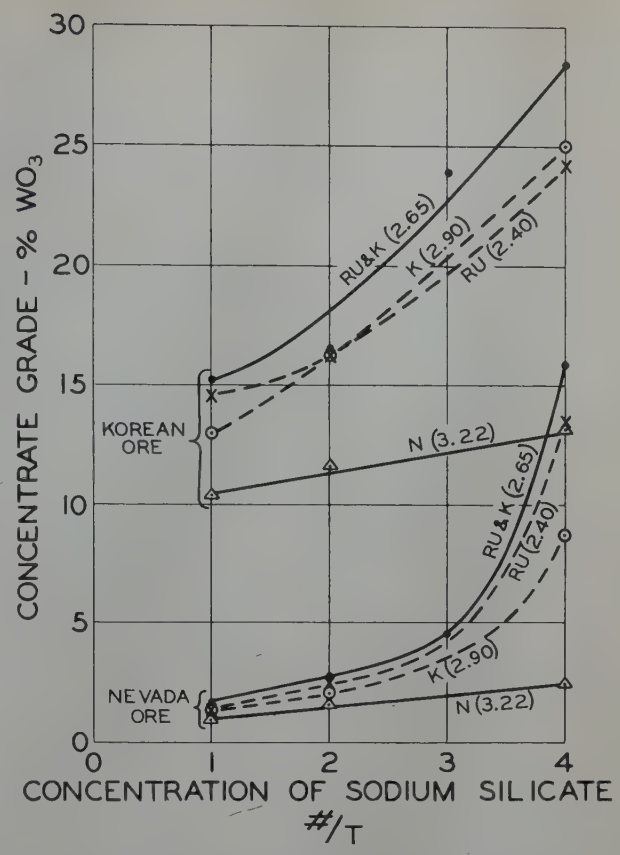

Fig. 3—Concentrate grade vs sodium silicate concentration for various sodium silicates. Numbers are ratio of SiO_2 to Na_2O.

4) These improvements were obtained with no loss in recovery.

5) At lower concentrations or at 6.5 pH, the silica-to-soda ratio had either no significant effect on concentrate grade or the improvement was much less remarkable. This indicates the necessity of determining the proper operating pH as well as the right combination of alkali-silica and the proper concentration.

6) Similar improvements in grade were found when the *RU-K* silicate mixture was used with specular hematite and uranium ores.

No effort has been made here to predict the reactions occurring in the pulp which allow much better elimination of siliceous gangue from the rougher concentrate when silicates *RU* and *K* are used at the proper concentration of silicate and pH. The chemistry of the soluble silicates is complex. Perhaps the *RU* and *K* silicates more effectively disperse the gangue or more effectively wash the slimes from the tungsten minerals, or perhaps the molecular cross section of the silicates is important in blocking the oleic acid collector from the gangue mineral. In any event, the type of silicate can be of great importance and the optimum ratio should be investigated along with the silicate concentration and pH when a flotation study is conducted.

References

[1] J. C. Vail: *Soluble Silicates*, vol. 2, p. 118. Reinhold Publishing Co., New York, 1952.

[2] *Silicate P's and Q's*, vol. 19, no. 11, 1939. Published by Philadelphia Quartz Co., Philadelphia, Pa.

[3] W. Mitchell, Jr., C. L. Sollenberger, and T. G. Kirkland: Flotation Tests on Korean Scheelite Ore. *AIME Trans.*, 1951, vol. 190.

[4] K. Kunze: Milling Tungsten Ores at the Getchell Mines. *Mining Congress Journal*, 1953, vol. 39, p. 31.

Discussion of this paper sent (2 copies) to AIME before July 31, 1958, will be published in MINING ENGINEERING.

Effect of Chemical Reagents on the Motion of Single Air Bubbles in Water

The effect of bubble size and concentration of certain reagents on the terminal velocity, shape, path, and drag coefficients of single air bubbles in distilled water has been investigated. Bubbles of a certain size range rise considerably faster than Reynolds number—drag coefficient relationships predict, whereas a small amount of frothing agent reduces their terminal velocity. The rapid velocity at which bubbles rise in distilled water appears to result from slip at the boundary and from circulation within the bubbles. Surface-active agents retard bubble motion through prevention of both circulation and slip at the boundary. A surface tension concentration gradient helps maintain bubble sphericity.

by D. W. Fuerstenau and C. H. Wayman

THE gas phase is one of the indispensible ingredients in flotation operations. Flotation depends on the collision of an air bubble and a mineral particle in a pulp and their ability to remain in contact long enough for adherence to take place. Before it is possible to understand the mechanics of air bubble-mineral particle encounter, it is necessary to learn more about the nature of bubbles themselves before collision with a mineral particle has taken place. To date, little work has been done on air bubbles in flotation systems. In 1945 Fahrenwald[1] presented a study of the role of frothers on air bubbles and on aeration in flotation, and recently Wark and Sutherland[2] discussed the work of Rosenberg[3] in relation to flotation. The research reported in this present article was undertaken to investigate systematically the effect of bubble size and the concentration of certain reagents on the terminal velocity, shape, path, and drag coefficient of single bubbles in distilled water. Most of the work is concerned with the effect of α-terpineol on bubble motion in water, but studies were made with potassium chloride, potassium hydroxide, potassium ethyl xanthate, and potassium amyl xanthate.

Experimental Method and Materials: To obtain free bubble rise and reduce wall and surface effects, the investigators used a tank of 5½x5½x30-in. internal dimensions, filled with water to within 4½ in. of the top.[4] The tank was made of acrylic plastic so that the walls would have good optical properties.

Distilled water, which was re-distilled in a block tin still and saturated with air before each test, was used in all the experiments. All solutions were made with reagent-grade chemicals. During each experiment the water was at room temperature, and during the course of an experiment the temperature did not fluctuate more than 0.5°C. Since the experiments were performed over a period of six months, the temperature varied between 25° and 27°C. The temperature at which each series of experiments was conducted is recorded with the data.

The experimental apparatus is presented diagrammatically in Fig. 1. Individual air bubbles were generated from purified compressed air through a capillary of 0.003-cm internal diameter at a rate

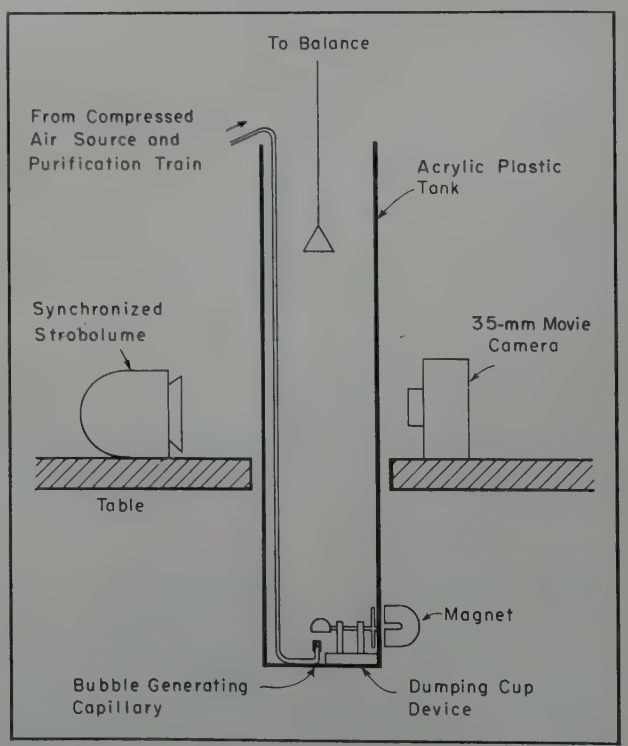

Fig. 1—Experimental apparatus for measuring terminal velocities of air bubbles in water.

D. W. FUERSTENAU, Junior Member AIME, formerly Assistant Professor, Department of Metallurgy, Massachusetts Institute of Technology, is with the Metals Research Laboratories, Electro Metallurgical Co., Niagara Falls, N. Y. C. H. WAYMAN, Junior Member AIME, is Research Assistant, Department of Metallurgy, Massachusetts Institute of Technology, Cambridge, Mass.

TP 4746B. Manuscript, Aug. 20, 1956.

that kept the individual bubbles about 2 ft apart. Under these conditions the bubbles always had a radius of 0.049 cm, not only in distilled water but also in solutions containing terpineol. Bubble sizes were determined in two different manners: 1) by measuring directly from a photograph and 2) by coalescing a hundred bubbles or more and weighing the resultant large bubble in a submerged cup. It might be added that coalescing the bubbles in solutions containing 22 mg of terpineol per liter was a difficult job. All bubbles larger than 0.049-cm equivalent radius were formed by coalescing a given number of the 0.049-cm bubbles and calculating the size. Each large bubble was formed in a small glass cup that could be dumped with a magnet. Proper positioning of the cup insured that the path of the bubble was in focus on the film in the camera. Smaller bubbles were formed by moving the capillary sideways to shear off small bubbles, one of which would be caught under the cup. The size of this bubble was measured directly from the film.

Bubbles which were photographed about 15 in. from their point of release were found to be at their terminal velocity. Shape, velocity, and path of the bubbles were determined photographically with a 35-mm movie camera, using an average speed of about 35 frames per sec. Film speeds were measured with a small neon light that flashed onto the film at a known rate through a pinhole in the back of the camera. A glass rod photographed in the plane of the rising bubbles provided a means to calibrate distance and bubble size on the film. Light for taking the pictures came from a General Radio type 1532-B Strobolume that was synchronized with the camera.

To ascertain bubble velocity, the vertical displacement of the bubble on the film was measured. Bubble speeds were calculated from the vertical displacement, scale factor, and film speed. In certain instances, bubbles spiral to the surface. Under these conditions, actual velocity might be somewhat greater than the measured vertical velocity.

Experimental Results

In describing the dimensions of a solid sphere, it is convenient to use its radius. However, to describe a fluid body that is constantly changing shape, it is convenient to use a parameter based on volume, namely, the equivalent radius, r_e, which is the radius of a sphere of a volume equal to that of the fluid body.

$$r_e = \sqrt[3]{\frac{\text{volume}}{\frac{4}{3}\pi}} \qquad [1]$$

For bubbles rising at their terminal velocity, v_t, the drag coefficient, C_D, can be written as

$$C_D = \frac{(8/3)\ g\ r_e\ (\rho_1 - \rho_2)}{v_t^2} \qquad [2]$$

and the Reynolds number, N_R, can be written as

$$N_R = \frac{2\ r_e\ v_t\ \rho_1}{\eta_1} \qquad [3]$$

where ρ_1 is the density of the fluid (1 g per cc for water), ρ_2 is the density of the fluid bubble (0.0013 g per cc for air), η_1 is the viscosity of water.

Terminal Velocity of Single Bubbles: The terminal velocities of single bubbles were measured to ascertain how the presence of a frothing agent may affect the motion of a bubble. In these experiments terminal velocities were measured as a function of bubble size and frother concentration. Within a certain size range (see Table II) bubbles rise in a wobbling, helical manner, and actual bubble velocity may be somewhat higher than the vertical velocity measured by the present techniques. Bubble sizes were varied from 0.019 to 0.94-cm equivalent radius, and the concentration of terpineol was maintained at four different concentrations (0, 3.7, 7.3, and 22 mg of terpineol per liter of distilled water). The experiments with solutions containing 3.7 mg terpineol per liter were run at 26.5 ± 0.5°C and the remainder were run at 25 ± 0.5°C. In Fig. 2, terminal velocity is plotted logarithmically as a function of equivalent radius. It can be seen from Fig. 2 that the terminal velocity of bubbles in conductivity water increases sharply to about 35 cm per sec as the bubble size is increased to 0.065-cm radius. Further increase in bubble size reduces the terminal velocity somewhat until bubbles with an equivalent radius of 0.30 cm have a terminal velocity of only 23 cm per sec before the velocity again increases with bubble size.

The presence of only 3.7 mg of terpineol per liter reduces the terminal velocity of bubbles in the size range between 0.03 and about 0.4-cm equivalent radius. Bubbles with a radius of 0.065 cm, at which size the velocity reduction is greatest, rise 18.5 cm per sec in solutions of 3.7 mg of terpineol per liter. In solutions containing 7.3 and 22 mg terpineol per

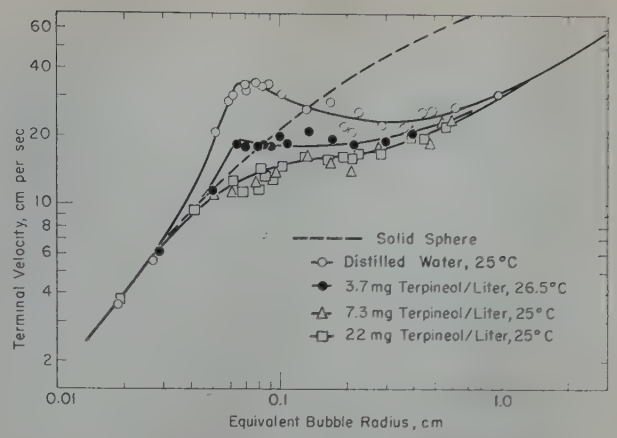

Fig. 2—Terminal velocity of single air bubbles in conductivity water and aqueous terpineol solutions as a function of bubble size.

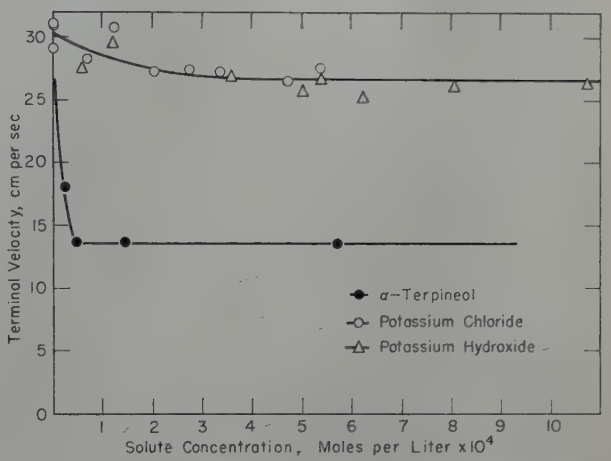

Fig. 3—Terminal velocity of a bubble of 0.082-cm equivalent radius in aqueous solutions of various reagents.

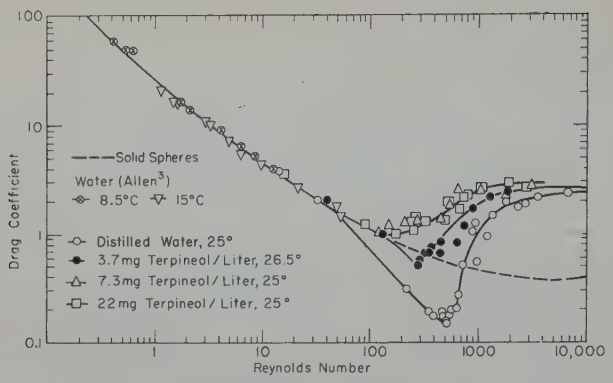

Fig. 4—Drag coefficient as a function of Reynolds number for air bubbles rising at their terminal velocity in water and in aqueous solutions of α-terpineol.

liter, a bubble of 0.065-cm radius rises at 12.5 cm per sec, which is only 36 pct of a bubble's velocity in distilled water.

To study the differences in behavior of single bubbles in aqueous solutions of heteropolar reagents and inorganic electrolytes, the terminal velocity of a bubble of 0.082-cm equivalent radius was measured as a function of the concentration of KCl, α-terpineol, and KOH. This bubble size was chosen because it was intermediate and because a bubble of this particular size not only rises at nearly maximum velocity but also is an oblate spheroid in distilled water. KCl was chosen as a reagent because it represents a typical inorganic electrolyte, but KOH was chosen because air bubbles are reputed to be negatively charged in water[5] and only adsorption of hydroxyl ions at the surface could account for this. If hydroxyl ions play a role in the surface properties of air bubbles, the addition of KOH to the system might affect their movement. Observation of the experimental data presented in Fig. 3 will show that terpineol markedly reduces the terminal velocity of 0.082-cm radius bubbles about 55 pct, whereas KCl and KOH reduce the velocity only about 10 pct. There is no significant difference between the effect of KOH and KCl. In each case, velocity reaches a certain minimum and is reduced no further.

Non-Dimensional Presentation of Data for Single Bubbles: In Fig. 4 the data are presented non-dimensionally, the drag coefficient C_D being plotted as a function of the Reynolds number, N_R, of the bubble. For comparative purposes, Allen's[6] experimental data for very small bubbles and the curve for solid spheres are plotted in Fig. 4 also. In distilled water, air bubbles behave as solid spheres when the Reynolds number is less than 40 even though bubbles remain spherical up to Reynolds numbers of 400. However, in the presence of a small amount of frother, air bubbles behave as solid objects until the Reynolds number exceeds 130. The drag coefficient of bubbles in conductivity water becomes less than that for solid spheres as the Reynolds number increases from 40 to 500, reaching a minimum of 0.15. Upon further increase in the Reynolds number, the drag coefficient increases sharply and approaches a constant value of about 2.6.[3] In solutions containing 3.7 mg of terpineol per liter of water, the drag coefficient has a minimum value at a Reynolds number of 300, this minimum being only slightly lower than that for solid spheres. In the presence of more terpineol, the drag coefficient is equal to that of solid spheres up to Reynolds numbers of 130 but is always greater than that for solid spheres when the Reynolds number exceeds 130. The drag coefficient for single bubbles approaches a constant value of about 2.6, independent of the terpineol concentration.

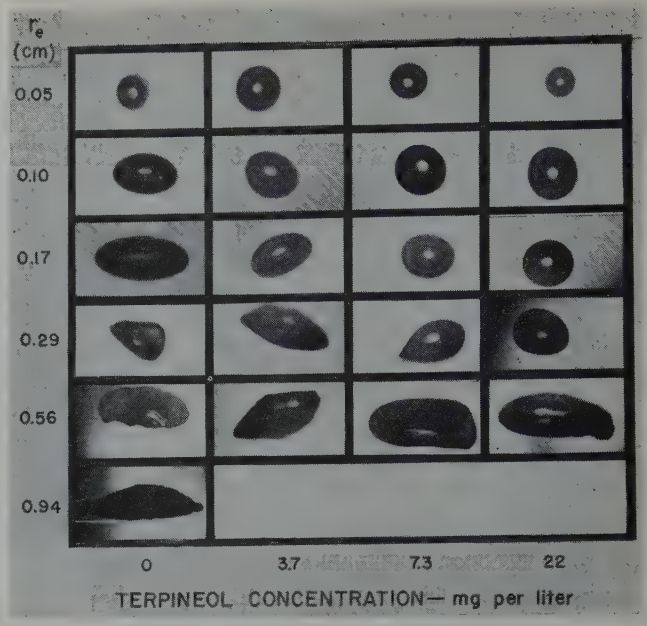

Fig. 5—Effect of terpineol concentration and bubble size on bubble shape. (Photographs made at various magnifications.)

Bubble Shapes: Small bubbles are spherical, but as the size increases, the bubbles become increasingly flattened and change to oblate spheroids. The size at which bubbles change to oblate spheroids depends on the concentration of frothing agent. Upon further increase in size, the bubbles become increasingly flattened and begin to oscillate. When the shape begins to fluctuate rapidly, the bubbles appear to be distorted oblate spheroids with jagged corners and edges. The size at which bubbles change to distorted oblate spheroids does not depend greatly on terpineol concentration. Table I presents, for the different concentrations of terpineol in distilled water, the sizes at which bubbles flatten into oblate spheroids and begin to fluctuate, forming distorted oblate spheroids. As bubbles continue to increase in size, they become increasingly distorted, fluctuating violently in shape until pressure gradients cause them to assume the shape of so-called spherical caps at an equivalent radius of about 0.9 cm.[8] The upper surface of such bubbles is essentially spherical, whereas the lower surface varies from a highly irregular surface for liquids of low viscosity to a smooth surface in very viscous fluids.[4] Spherical cap bubbles retain their shape as they rise. Bubbles considerably larger than spherical caps be-

Table I. Effect of Terpineol Concentration on Size and Reynolds Number at which Air Bubbles Distort

Concentration of Terpineol, Mg per Liter	Conditions at which Bubbles Begin to Flatten into Oblate Spheroids		Conditions at which Bubbles Become Distorted Oblate Spheroids	
	Radius, Cm	Reynolds Number	Radius, Cm	Reynolds Number
0	0.065	400	0.20	950
3.7	0.065	300	0.20	800
7.3	0.12	400	0.29	800
22	0.20	500	0.29	1100

ome doughnut-shaped, and exceedingly large bubles break up.

The photographs of bubbles presented in Fig. 5 illustrate the effect of bubble size and frother concentration on bubble shapes. It should be pointed out that the magnification of bubbles in each of the pictures presented in Fig. 5 was not held constant in making the photographs. Bubbles of five different sizes were selected for comparison in solutions containing the different terpineol concentrations. One large bubble (0.94-cm equivalent radius) in distilled water is shown to illustrate the spherical cap. In Fig. 6 three successive pictures of three different bubbles are presented (0.22, 0.56, and 0.94-cm equivalent radius) to illustrate how distorted bubbles change shape rapidly. Each picture is about 1/35 sec apart. The spherical cap essentially maintains its shape, whereas the distorted oblate spheroids change shape rapidly. Small bubbles are not shown because they do not change shape while rising.

Bubble Paths: Bubbles were found to rise with three different paths or motions: 1) rectilinear path, 2) helical or spiraling path, and 3) rectilinear rocking motion. As the bubble size increases, there is a change from a rectilinear path to a helical path. This change is not accompanied by a change in bubble shape. Spiraling begins and increases in amplitude and frequency until a maximum is reached.

Table II. Motions with which Bubbles of Different Sizes Rise in Aqueous Solutions of Terpineol

Motion or Path of Rising Air Bubbles	Size Range (Equivalent Radius, Cm) in which Bubbles Rise in Given Path for Different Concentrations of Terpineol, Mg per Liter			
	0	3.7	7.3	22
Rectilinear	<0.08	<0.07	<0.06	<0.06
Helical	0.08 to 0.20	0.07 to 0.20	0.06 to 0.09	0.06 to 0.09
Wobbling helical	Absent	Absent	0.09 to 0.21	0.09 to 0.22
Rocking rectilinear	0.20 to 0.8	0.20 to 0.8	0.21 to 0.8	0.22 to 0.8
Rectilinear	>0.8	>0.8	>0.8	>0.8

Bubbles rising with a small amplitude and high frequency of spinning often rise in a large spiral. Such motion has been termed *wobbling helical motion.* When bubbles are large enough to become distorted oblate spheroids, they rise in a rectilinear path, but the rapid change in bubble shape causes the motion to appear as rocking rectilinear. By the time bubbles form spherical caps, they do not change shape and appear to rise in a rectilinear path. In solutions containing terpineol, the largest bubble was 0.60-cm equivalent radius; however, it seems that spherical caps in such solutions will rise in the same manner as they do in distilled water. Table II gives the size range (equivalent radius in centimeters) in which the bubbles rise—with the different types of motion—for solutions containing 0, 3.7, 7.3, and 22 mg of terpineol per liter of distilled water.

Effect of Different Reagents on Shape and Terminal Velocity of Single Bubbles: In part of this investigation, the effect of potassium chloride, potassium hydroxide, terpineol, potassium ethyl xanthate, potassium amyl xanthate, and mixtures of terpineol and xanthate on the shape and terminal velocity of bubbles of 0.082-cm equivalent radius was studied. The data are presented in Table III.

Observation of Table III reveals that any molecule or ion with a long enough hydrocarbon chain

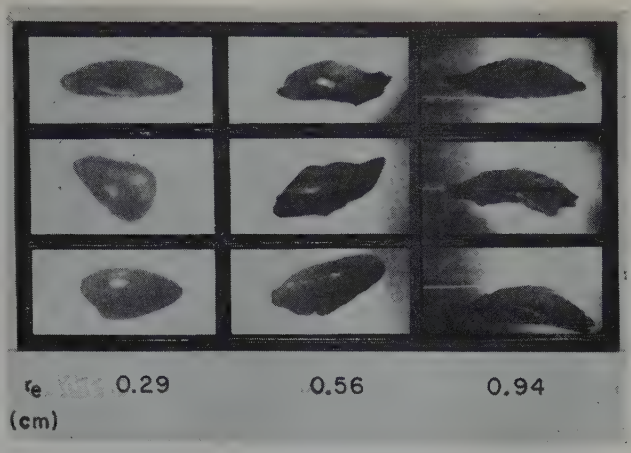

Fig. 6—Illustration of the rapid distortion of rising bubbles in conductivity water. Film speed, about 35 frames per sec.

can affect the shape and terminal velocity with which an air bubble rises in water.

Discussion of Results

The unusual behavior of bubbles in distilled water in the presence or absence of a small amount of surface-active agent must depend on gas-liquid interfacial phenomena, since those surface-active reagents which affect bubble motion are known to be strongly adsorbed at the gas-liquid interface.[4,7,8] The strong interaction of water molecules with each other probably contributes to the unusually rapid velocity of rising air bubbles in distilled water.

For fluid spheres at Reynolds numbers less than 1, Hadamard[9] and Rybczynski[10] have shown theoretically that fluid spheres moving through another fluid will circulate in the form of a vortex ring. The existence of circulation in drops has vividly been demonstrated by Garner.[11] The Hadamard-Rybczynski correction to Stokes' law states that a fluid sphere of low viscosity moving in a fluid of high viscosity should move 1.5 times as fast as a solid sphere because of internal circulation, but these concepts do not seem to apply to small air bubbles, which rise in distilled water at the velocity predicted by Stokes' law. Furthermore, they behave as solid spheres up to a Reynolds number of about 40, or a bubble radius of 0.025 cm. But the terminal velocity of bubbles larger than 0.025 cm in radius increases rapidly over that of a solid sphere until at the maximum, where bubbles begin to flatten, the terminal velocity is 2.3 times that of a solid sphere. In their derivations, Hadamard and Rybczynski assumed no slip to exist at the boundary. Since water molecules are strongly attracted to each other within the liquid through dipole interactions (the energy of association of water dipoles in the liquid state being about 6 kcal per mole[13]) but are attracted only weakly to the bubble, water molecules would have such an affinity for themselves that they would tend not to travel with the bubble in distilled water. Consequently, the existence of slip at the air-distilled water interface seems reasonable.[3,4,12] In the case of nearly all solids, water molecules are strongly held to the surface and shear must take place within the liquid during movement of the solid.

If a heteropolar organic compound is dissolved in the water, adsorption of these molecules takes place at the air-liquid interface in such a way that the hydrocarbon chain sticks into the gaseous phase, the

polar head remaining in the water. Thus, when an air bubble moves through a dilute aqueous solution of terpineol, the terpineol molecules move with the bubble (in a manner similar to the movement of a sailboat on water). Since water molecules are held to the polar group of the surface-active reagent, they travel with the bubble and movement of a bubble in a dilute aqueous solution containing the surface-active agent would be similar to the movement of a solid sphere through water because water molecules now travel with the bubble. Before a surface-active agent can affect bubble motion, its hydrocarbon chain must be long enough for adsorption and desorption to take place relatively slowly. For example, amyl xanthate ions retard bubble rise, whereas ethyl xanthate ions do not affect it appreciably (Table III).

Table III. Effect of Various Reagents on Shape and Terminal Velocity of Bubbles with an Equivalent Radius of 0.082 Cm

Aqueous Solution	Bubble Shape	Terminal Velocity, Cm per Sec
Distilled water	Oblate spheroid	31
KOH, 7 mg per liter	Oblate spheroid	29
20 to 60 mg per liter	Oblate spheroid	27
KCl, 9 mg per liter	Oblate spheroid	30
15 to 40 mg per liter	Oblate spheroid	27
Terpineol, 3.7 mg per liter	Slightly flattened spheroid	18
7 to 88 mg per liter	Spheroid	14
Potassium ethyl xanthate, 20 mg per liter	Oblate spheroid	27
Potassium amyl xanthate, 25 mg per liter	Oblate spheroid	21
20 mg of potassium ethyl xanthate plus 3.7 mg terpineol per liter	Slightly flattened oblate spheroid	16
25 mg of potassium amyl xanthate plus 3.7 mg terpineol per liter	Spheroid	14

If a bubble rising in a dilute aqueous solution of terpineol is to rise no faster than a solid sphere, both slip at the boundary and circulation must be diminished. Following the concepts of Frumkin and Levich,[18] Sutherland and Linton[14] have recently showed how surface-active agents prevent internal circulation in fluid drops, which are similar to air bubbles. If there is no slip at the boundary between a bubble and the liquid, the surface of a rising bubble experiences a tangential force τ_0 that is proportional to the viscosity of the liquid η and to the velocity gradient normal to the surface:

$$\tau_0 = \eta \left(\frac{\partial v}{\partial y}\right)_{y=0} \qquad [4]$$

This tangential force is responsible for circulation. If an air bubble behaves as a solid sphere, it is possible to calculate the maximum stress at the surface. On a solid sphere the stress varies from zero at the front of the sphere to a maximum at 57° and falls to zero behind its equator.[15] The maximum stress is

$$\tau_0 = 2.21\, v_t^{3/2}\, (\eta\rho/d)^{1/2} \qquad [5]$$

where ρ is the density of the continuous phase, d the diameter of the sphere, and v_t the terminal velocity of the sphere. Bubbles of 0.065-cm radius rising at a terminal velocity of 12 cm per sec in an aqueous solution containing 7 mg or more of terpineol per liter ($\eta = 0.01$ poise and $\rho = 1$ g per cm^2) have a maximum stress of 26 dynes per cm^2. Prevention of internal circulation in a bubble can arise only through the existence of a force that opposes the shear stress. Such an opposing force might result from the surface-tension gradient, which can be produced in solutions of a surface-active reagent. The mechanism by which a surface-tension gradient might arise is the streaming of frother molecules towards the bottom of a rising bubble. The higher surface pressure of the compressed layer of adsorbed molecules at the rear of a rising bubble will try to spread the molecules back again and will consequently oppose flow along the surface. Adsorption at the front of the bubble and desorption at the rear will have to be slow, however, in order to maintain the surface-tension gradient. The surface stress that opposes the tangential frictional stress is determined by the surface-pressure gradient $\frac{\partial \pi}{\partial S}$, where π is the difference in surface tension between the back of the bubble where the layer of adsorbed terpineol molecules is compressed and the front of the bubble where the surface concentration is reduced, or may even approach zero, at a circumferential distance S.

For the bubble described above, an average tangential stress of about 20 dynes per cm^2 might be expected if circulation is to be prevented.[17, 18] Therefore the surface pressure must vary by about 20 dynes per cm per centimeter of circumferential distance. For the above bubble, the circumferential distance from the front to the point of flow separation, which is about 110° from the front of the bubble,[16] is 0.11 cm. Hence a surface pressure difference of 2.2 dynes per cm would be necessary to prevent circulation. Use of the Gibbs equation to calculate adsorption densitites from a surface tension-concentration curve shows that $2\text{x}10^{-11}$ mole of terpineol is adsorbed per square centimeter of surface from solutions containing 7.3 mg terpineol per liter. To produce the requisite value of π, the terpineol molecules toward the rear of the bubble need be crowded only until the adsorption density is $8\text{x}10^{-11}$ mole per cm^2 if the front of the bubble is devoid of terpineol molecules.

Bubbles flatten, and consequently slow down, because the mechanical forces acting on the bubble overcome the effect of surface tension, which tends to keep the bubble spherical. However, a surface tension-concentration gradient can assist in maintaining a bubble's spherical shape by counteracting the surface stress as outlined in the previous paragraph. By increasing the concentration of terpineol in solution, the magnitude of the possible surface-tension gradient is increased. Furthermore, if bubbles are momentarily distorted as they rise, the surface stretches and forms fresh surface devoid of terpineol molecules. Hence, the new surface momentarily has a slightly higher surface tension, which acts like a spring parallel to the surface, tending to pull the bubble back into spherical shape. Stretching the bubble in distilled water does not give rise to a concentration gradient at the surface, and hence no such *spring* works, because the surface tension remains constant. For this spring effect to take place, adsorption of the surface-active agent must be slow. Once the external forces attempting to flatten the bubble become too great, circulation within the bubble sets in and the bubble begins to distort and oscillate violently.

From a molecular point of view, it seems as though all bubbles circulate in distilled water in the

absence of a surface-active agent. However, at Reynolds numbers below 40, bubbles act as solid spheres even in distilled water. This phenomenon has not yet been reconciled.[4]

Air Bubbles in Flotation: Using a 1-cu ft Massco-Fahrenwald flotation machine, Fahrenwald[1] found the average bubble radius to be 0.2, 0.11, and 0.07 cm in solutions containing 0, 3.1, and 4.6 mg of terpineol per liter. Sutherland[16] found the average radius to be 0.09, 0.07, and 0.03 cm, considering a weighted volumetric average in a 2000-g Denver subaeration flotation machine containing 2.5, 5, and 10 mg of terpineol per liter of water. There certainly will be a difference in bubble size depending on conditions within flotation machines, but the size range appears to be in the range wherein the terminal velocity of bubbles is markedly affected by frother concentration. Since bubbles rise more slowly in solutions containing surface-active agents, there will be two or three times as many chances for bubble-particle collision in the presence of a frother. Furthermore, bubbles are smaller in the presence of a surface-active agent (because small bubbles do not coalesce during their formation), and this means that the large distorted bubbles which oscillate violently should be absent in a subaeration flotation machine. The rapid oscillations of bubbles would probably repel any impinging mineral particle from the bubble surface. To find out the properties of bubbles in systems more similar to flotation conditions, work is under way to study the motion of bubbles in swarms.

Acknowledgment

This investigation was carried out in the Richards Mineral Engineering Laboratories, Massachusetts Institute of Technology, under the sponsorship of the U. S. Atomic Energy Commission. The authors wish to acknowledge the assistance of A. M. Gaudin, R. J. Charles, and K. L. Sutherland.

References

[1] A. W. Fahrenwald: *Engineering and Mining Journal*, October 1945, vol. 146, p. 94.
[2] K. L. Sutherland and I. W. Wark: *Principles of Flotation*, Institute of Mining and Metallurgy, Melbourne, Australia, 1955.
[3] B. Rosenberg: The Drag and Shape of Air Bubbles Moving in Liquids. Navy Department, The David W. Taylor Model Basin, *Report 727*, 1950.
[4] W. L. Haberman and R. K. Morton: An Experimental Investigation of the Drag and Shape of Air Bubbles Rising in Various Liquids. Navy Department, The David W. Taylor Model Basin, *Report 802*, 1953.
[5] W. A. Gortner: *Outlines of Biochemistry*. John Wiley & Sons, New York, 1949.
[6] H. S. Allen: *Philosophical Magazine*, 1900, vol. 50, pp. 323, 519.
[7] A. Gorodetskaya: *Journal of Physical Chemistry* (U.S.S.R.), 1949, vol. 23, p. 71.
[8] B. Stuke: *Die Naturwissenschaften*, 1953, vol. 39, p. 325.
[9] J. Hadamard: *Comptes Rendus*, Academy of Science, Paris, 1911, vol. 152, p. 1735.
[10] W. Rybczynski: *Bull. Acad. Sci. Cracovie.*, 1911, vol. 1, p. 40.
[11] F. H. Garner: *Trans.*, Institute of Chemical Engineers, 1950, vol. 28, p. 88.
[12] M. P. O'Brien and J. E. Gosline: *Industrial and Engineering Chemistry*, 1935, vol. 27, p. 1436.
[13] C. A. Coulson: *Valence*, p. 298. Oxford University Press, London, 1952.
[14] M. Linton and K. L. Sutherland: Dynamic Surface Forces, Drop Circulation and Liquid-Liquid Mass Transfer. Second World Congress on Surface Chemistry.
[15] H. Schlichting: *Boundary Layer Theory*, McGraw-Hill Book Co. Inc., 1955.
[16] K. L. Sutherland: *Journal of Physical Chemistry*, 1948, vol. 52, p. 394.
[17] V. G. Levich: *Journal of Electro-Technical Physics* (USSR), 1949, vol. 19, no. 1.
[18] A. N. Frumkin and V. G. Levich: *Journal of Physical Chemistry* (USSR), 1947, vol. 21, p. 1183.

Discussion of this paper sent (2 copies) to AIME before July 31, 1958, will be published in MINING ENGINEERING.

Discussion

Geology of Toquepala, Peru

by Kenyon Richard and James H. Courtright

(MINING ENGINEERING, page 262, February 1958, AIME Trans., vol. 211)

L. H. Hart *(Chief Geologist, American Smelting & Refining Co.)*— Because of a widely recognized association between breccia pipes of one form or another and many important copper deposits, conditions under which breccia pipes develop have been of great scientific interest for many years. Since these phenomena first attracted attention, many theories have been advanced to explain their origin. This is not unexpected, since it is likely that they have been formed by and under a wide range of conditions. Moreover, the entire subject is confused by the fact that the term *breccia pipe* is applied to a wide variety of occurrences. To discuss any part of the subject intelligently, therefore, it is necessary to start with definitions of the terms used.

In their discussion of the Toquepala deposit, Richard and Courtright have carefully defined the terms they have used in their presentation of a very logical geological history of Toquepala breccias. This is a real contribution, as there is no reference in the literature known to the writer where the history of a series of breccia pipe epochs, confined essentially within one channelway, may be read with the degree of certainty that appears to be possible at Toquepala.

Although the following comments are intended primarily to emphasize points brought out in the article by Richard and Courtright, certan subsequent detailed mapping by Hollister and Houston[7] within the main central mineralized area of the Toquepala deposits not only supports most of Richard's and Courtright's conclusions but also contributes additional facts that strengthen and broaden the whole concept of the origin of the Toquepala breccia pipes.

In detailed mapping by Hollister and Houston,[7] the most significant feature disclosed is a well developed system of concentric fracturing in rocks peripheral to the main breccia pipe throughout an arc of 300°, interrupted only by the late dacite agglomerate in the north quadrant. Although Richard and Courtright noted that such fractures were developed in the southern and southeastern areas, continuity in the east and west quadrants is established by consistent orientation of the stronger set of fractures and joints. The existence of these structural weakness trends is emphasized by the emplacement of dike-like phenomena in and along members of this fracture system.

Richard and Courtright described one of these dikes in the southeast quadrant. They referred to it as a ring-dike, composed of dacite porphyry. This suggests an apparent structural control of at least a part of the dacite porphyry intrusion by features related to the Toquepala breccia pipe center. This raises a perplexing question, since the dacite porphyry intrusion had been presumed to antedate breccia pipe activity. However, if this ring-dike is related to the breccia pipe center, it may indicate that some part of the dacite porphyry intrusion advanced in a manner resulting in an intensely localized stress center, which produced the concentrically arranged fracture system. The ring-dike would then appear to be evidence strongly sug-

gesting that emplacement of the final stage of the dacite porphyry intrusion was influenced by these pre-existing fractures and had accommodated itself to them. In this way, one prong of the dacite porphyry intrusion may have determined the position of the breccia pipe conduit and thereby prepared the way for the subsequent events that took place therein, including the introduction of mineralization. It is possible to visualize that this dacite porphyry prong may even have constituted the first pipe *break-through,* although no factual evidence supporting this has been observed. While the general hypothesis outlined above suggests that much of the fracturing of rocks peripheral to the pipe conduit was accomplished by stresses set up during the advance of the dacite porphyry, there is also much evidence that extensive fracturing and shattering of these rocks occurred later during the breccia injection period.

The sequence of events after the dacite porphyry intrusion is quite clearly defined and includes, first, a series of injections through the pipe-like conduit, which Richard and Courtright call *ore breccia.* They classify the second distinct breccia series *pebble breccia* and designate the final series *dacite agglomerate.* There is strong evidence that surges of activity of the first two classifications overlap and it is also likely that the dying phase of the pebble breccia epoch, postdated early dacite agglomerate. It is proposed that each of these series of events was intrusive in character. The history begins with the older classification, which Richard and Courtright call *ore breccia,* but which this writer prefers to subdivide into two groups: 1) pipe breccia and 2) peripheral shatter breccia. When these two components are carefully separated, as Hollister and Houston[7] have done in their detailed mapping, it is possible to establish the relationship of one to the other and thereby it is clear that the pipe breccia exhibits intrusive characteristics, because small outlying centers of this material are noted at considerable distances from the central pipe within the peripheral rocks. These small outliers are related to mappable structural weaknesses, often with dike-like characteristics conforming to the concentric fracture system. One of these, in the northeast quadrant, is about 60 meters distant from the main contact between the pipe breccia and the shatter breccia. This outlier is approximately 20 meters in width and traceable for a distance of about 120 meters, in a direction nearly parallel to the contact. It is also observed that close to the contact, material of pipe breccia type occurs in cracks and breaks within the intruded, shatter-brecciated rocks. However, the degree of penetration of this material diminishes rapidly away from the contact, and even near the contact it is surprisingly limited. This corresponds to a progressive decrease in the intensity of shattering and fracturing away from the pipe contact.

Many small inclusions and a few large inclusions or xenoliths of intruded rocks are observed within the pipe breccia center. In general, these appear to correspond to the adjacent, intruded rocks, and for this reason, at the surface where mapping is possible, they are largely dacite porphyry along the west border of the intrusive center and quartz diorite along the east side. This suggests only slight migration of entrapped inclusions, either upwards or downwards, but it seems certain that the isolated satellitic occurrences of pipe breccia could not have been emplaced by collapse, relaxational settling, or any means other than injection.

At some time, near the close of the activity of the pipe breccia injection, the first surge of the pebble breccia may have occurred, since there are a few cases described by Richard and Courtright where inclusions of pebble breccia are noted within their *ore breccia.* It is not entirely certain, in this writer's interpretation of this relationship, that the pebble breccia series became active before the close of the pipe breccia cycle. The occurrences of supposed inclusions in the *ore breccia* might be outliers from the pebble breccia center which have been injected—through cracks or other small openings by some media, at least simulating hydraulic or intrusive characteristics. All of these occur within a few meters of the pebble breccia contact.

Detailed mapping by Hollister and Houston[7] confirms Richard's and Courtright's conclusion that late pebble breccia dikes cut all of the rocks noted in the area, except latite dikes. One particular pebble-dike, which follows a pre-existing fault, is traceable for more than 200 meters and passes from east to west through quartz diorite, Quellaveco quartz porphyry, into pipe breccia. Also, there are countless inclusions and a few xenoliths of pipe breccia suspended within the pebble breccia center. There is one xenolith of dacite porphyry, with a diameter greater than 100 meters, within which a fairly large inclusion of pipe breccia (outlier) has been mapped. Thus the preponderance of evidence suggests that most, if not all of the pebble breccia, postdates the end of the pipe breccia cycle.

No comments herein apply to the dacite agglomerate, since subsequent studies have yielded no information suggesting any additions or modifications in the interpretations proposed by Richard and Courtright.

In summary, the writer proposes that some part of the dacite porphyry intrusion at Toquepala set up stresses that produced a system of concentrically oriented fractures, and then, in its final stage of advance, accommodated itself to zones of structural weakness so produced. Three series of later breccia injections traversed the Toquepala pipe or conduit, which, either by cause or effect, appears to have been an integral part of the concentric fracture system described.

Kenyon Richard and J. H. Courtright *(authors' reply)*—L. H. Hart's lucid amplification of certain aspects of Toquepala geology is much appreciated. Our comments on certain of his points follow.

The fractures which guided the emplacement of the dacite porphyry ring-dike are quite likely related to the breccia pipe center, but the possibility suggested by Hart that a dacite porphyry prong constituted the first pipe "break-through" is considered unlikely in view of field evidence that breccia formation began prior to the intrusion of the dacite porphyry, i.e., inclusions of ore breccia were found in dacite porphyry, as indicated in the writers' fourth paragraph under *Breccias* (page 264). To go further, inclusions of an earlier quartz-tourmaline breccia are found *within* ore breccia. Thus at least one, and possibly two, periods of brecciation preceded emplacement of dacite porphyry.

In the matter of ore and pebble breccia age relationships, there is little doubt as to the younger age of the main pebble breccia pipe and the dikes; however, evidence of an earlier intrusion of pebble breccia, which subsequently was incorporated in ore breccia, is clearly displayed in a road cut near the south margin of the main pebble breccia pipe. There, the ore breccia contains numerous inclusions of pebble breccia and is also cut by a dike of pebble breccia—demonstrating rather conclusively that at least two generations of pebble breccia are present. (The term *inclusions* is used strictly in a xenolithic sense, which precludes the alternative of small, attenuated intrusive bodies suggested in Hart's eight paragraph.)

The ore breccia can be subdivided into two units: 1) pipe breccia and 2) peripheral shatter breccia, as proposed by Hart. This distinction was recognized by the writers (third paragraph under *Breccias*) but was not mapped in detail.

As pit mining progresses there will be much better opportunities to observe age relationships. The writers anticipate that the brecciation-intrusion-mineralization sequences will be found to be even more complex than is presently recognized.

Reference

[7] V. F. Hollister and P. K. Houston, Geological Dept., American Smelting & Refining Co., November 1955.

Significance of Geochemical Distribution Trends in Soil

by D. H. Yardley

GEOCHEMICAL investigation of trace elements in surface materials was begun near Ely, Minn., in 1953 along the basal contact of Duluth gabbro with Giants Range granite (Fig. 1). This article presents data on the distribution of copper and nickel in till and in stream sediments in the area and proposes an explanation for the types of distribution found.

The Duluth gabbro, one of the world's largest basic intrusives, intrudes rocks which range in age from Keewatin to middle Keweenawan. Within the test area the gabbro is in contact with granite except for short sections where it is in contact with remnants of iron formation. Sulfide mineralization occurs within the gabbro, near and parallel to the basal contact for a distance of several miles. Schwartz and Davidson[1] have described the geologic setting of the mineralization.

The sulfides, believed to be syngenetic, include chalcopyrite, cubanite, pentlandite, pyrrhotite, and minor amounts of bornite. They occur disseminated in the silicates and as small interstitial masses. The ratio of copper to nickel is about 3.8:1, based on 66 chemical analyses of rock samples from various outcrops (Ref. 1, p. 702, and Ref. 2).

Test Procedures: With specified exceptions, all nickel and copper tests were made by the chromograph method,[3] which measures the intensity of a colored spot formed by a reaction between the metal being determined and special reagent paper. The intensity is then compared to the intensity of spots prepared from samples of known metal content. Details of the test procedure are outlined in another article (Ref. 4, pp. 77,78).

All soil samples tested in this investigation to date have been weighed on an analytical balance. However, a volumetric scoop designed to provide about 0.1 g of soil adds to the speed and ease of testing and has been found to give satisfactory results (Ref. 5, p. 531, and Ref. 19). The size of the samples used for the tests was 0.1 g. Whenever such small samples are used there is some question as to whether they are representative of the several grams in the field sample. Many repeat tests of the samples used in this investigation demonstrated that results can be reproduced within the limits of accuracy of the method without formal mixing beyond that inherent in screening the soil fractions. Furthermore, the 0.1 g is probably as representative of the field sample as the field sample is of its area of influence. Hawkes and Lakin (Ref. 6, p. 291), who considered the general problem, compared ground and quartered bulk samples of 500 g with 5-g grab samples. They concluded that "there is no significant loss in accuracy of data by substituting grab samples for bulk samples."

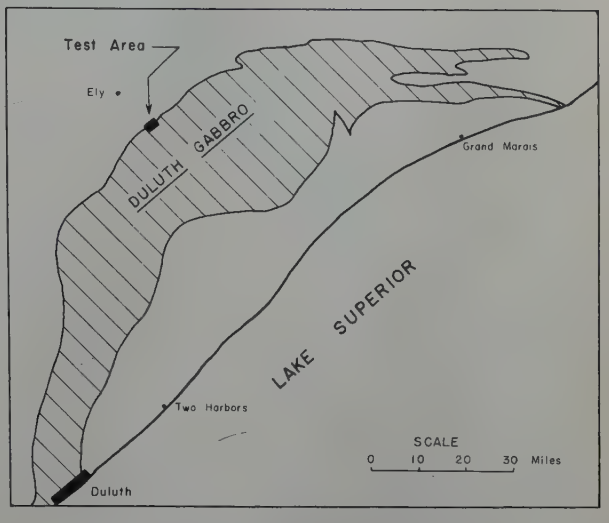

Fig. 1—Index map and outline of Duluth gabbro.

The term *soil* implies somewhat different things to the geologist, engineer, and soil scientist.[7] For convenience the term as used in this article refers to unconsolidated material (the mantle) overlying bed rock.

Sampling Procedure: Samples were taken at 100-ft intervals along north-south traverse lines across the gabbro-granite contact. The soil (till) samples were taken at an average depth of 1 ft, which was below the high-humus surface layer and into clean till. Samples taken at 1-ft intervals down to ledge showed as high a metal content at 1 ft below the air-surface as at greater depths and in two instances were slightly higher. The till at 1-ft depth did not appear to differ from material at greater depths. Total depth to bedrock has been tested at only a few points and where measured varied from 1 to 10 ft.

Aerial Distribution Contours and Profiles: Plotting of copper, nickel, and cobalt content in contour form (Fig. 2) shows that anomalous amounts of these metal ions occur in till over and closely adjacent to mineralized areas of the gabbro. Contouring nickel content alone, or the copper content, outlines the same target area. Contours of the copper content provide a more distinct anomaly than nickel because of the higher copper concentration. The traverses are rather widely spread for interpolation; however, drilling has confirmed the target area essentially as shown.

D. H. YARDLEY, Member AIME, is Associate Professor of Mining, School of Mineral and Metallurgical Engineering, University of Minnesota, Minneapolis, Minn.

TP 4765I. Manuscript, Sept. 1, 1957. New York Meeting, February 1958.

This page of Mining Transactions AIME follows p. 700. The intervening non-Transactions pages appeared in MINING ENGINEERING.

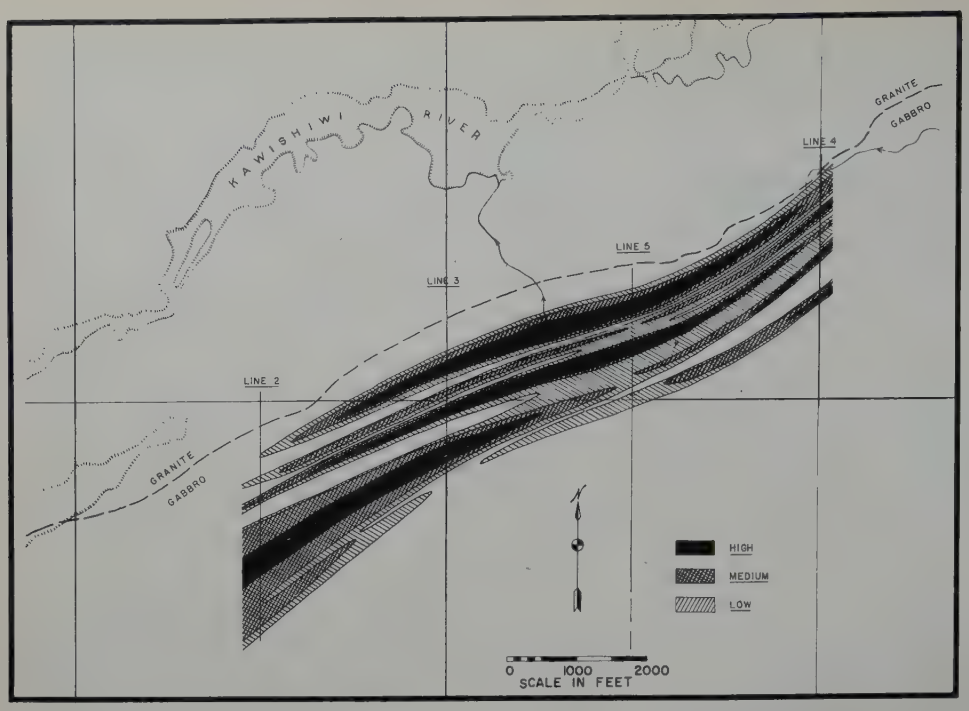

Fig. 2—Contour map of copper, nickel, and cobalt content in glacial till. Ely district, Minnesota.

The position of the northern boundary of the anomaly implies that the mineralization is parallel to, but not quite at the base of the gabbro. This is confirmed by three USBM drillholes.

Distribution by Soil Size: Testing of soil samples for any geochemical campaign involves a decision as to whether the sample should be screened and what soil fraction should be selected for testing if screening is used.

The glacial overburden in the area displays a wide range of particle size. For this reason it was necessary to select the soil fraction most likely to represent the true heavy metal content. The finer soil fractions generally are to be preferred in soil sampling, because sulfides would tend to weather to finer size (Ref. 5, p. 530).

Exceptions to this general rule do occur. Sergeev (Ref. 8, p. 46), comparing the tin, tungsten, and chromium contents of —1 mm fraction with 5 mm and coarser sizes in the part of the geochemical halo nearest the deposit, states: "The content of the valuable elements is approximately the same in both. In places, however, the coarser fraction contains somewhat more of the valuable element. Lean samples (a remote or the train part of the halo) have a lower content of the valuable element (down to zero) in the coarser fraction, although its concentration is stable in the finer fraction. It may be concluded that dispersion takes place chiefly at the expense of the finer materials." And also: "Remembering that halos of saline genesis are characterized by secondary compounds less directly related to the massive rock, the advantages of observing the halos in the fine deluvial fraction become evident. Such samples provide a reliable expression of the dispersion halo in its largest spatial development."

The example cited by Sergeev refers to elements that are resistant to chemical weathering and dominantly residual in nature. Ground-up coarse fractions that contain one or more large pieces of ore mineral would test high in metal, but even those elements which occur in resistant mineral conform to the general rule in the train part of a halo.

A factor that also favors selection of the fine soil fraction, in addition to the tendency of sulfides to weather to finer sizes, is the probability that transportation of heavy metals by capillary solutions may be important in the formation of some geochemical halos, and capillarity would be less effective in coarser materials. Bischoff (Ref. 9, p. 58) provides some indirect support for this view: "Gravel and coarse sand on the contrary proved very unfavorable, probably because of rapid drainage. . . . The depth of favorable overburden through which ground water would bring appreciable quantities of heavy metals to surface was surprising. The practical maximum overburden is now considered to be 30 to 50 feet for clay and 20 to 30 feet for fine sand." Bischoff also noted a blanketing or masking effect of sand and gravel ridges.

Distribution in Soil Fractions: The far greater number of soil particles in a unit weight of fine materials would be much more likely to include some particles of mechanically derived ore mineral than would the coarser fractions. The finer sizes also provide a much larger total surface area and so could absorb more metal ions from percolating soil solutions. Thus the finer materials would tend to *fix* relatively larger amounts of metal ions; it might be said that they have a larger total adsorption capacity and so would be much more likely than the coarse fractions to reflect the presence of anomalous concentrations of trace elements.

Samples were sieved through stainless steel screens to avoid possible contamination by abrasion. All screens used were Tyler screen scale. The +9 mesh material was crushed in an agate mortar before fusion.

Table I compares the metal content of the +9 mesh and —80 mesh fractions from ten samples of till. From these data it can be concluded that for all practical purposes the heavy metals do not occur in the +9 mesh soil size, at least for the concentration ranges shown.

Table II is a comparison of the nickel content of —9+80 mesh and —800 mesh soil fractions. Although the —9+80 mesh fraction contains less nickel, about two thirds as much as the —80 fraction, the anomaly would not be missed by testing only the —9+80 mesh fraction.

Comparison of the nickel content for 30 samples on a parallel traverse showed that the −9+80 fraction averaged 62 pct as high as the −80 fraction. Again the anomaly was obvious using either soil size. It seems reasonable to conclude that mixture of the two sizes (all the −9 mesh material) will give dependable results for many field comparisons.

The preceding figures demonstrate that for most field work the finer soil sizes are more indicative of geochemical anomalies. To confirm this view a study was made of samples of till known to contain appreciable quantities of copper and nickel. The samples were screened to six products and five chromographic analyses were made for nickel and five for copper. Agreement of analytic results was particularly good in the finer size samples. The +9 and −9+32 mesh fractions were crushed in an agate mortar before fusion in both this and later tests. Fig. 3 illustrates the distribution trend.

The notable feature is that there is an increase of metal content with decreasing soil size in the materials coarser than 80 mesh, but for the finer fractions the metal content remains about equal.

Table I. Comparison of Metal Content of +9 Mesh and −80 Mesh Fractions from Ten Samples of Till

	Nickel, Ppm		Copper, Ppm	
	+9 Mesh	−80 Mesh	+9 Mesh	−80 Mesh
	0	0	30	5
	0	5	0	7
	0	15	10	25
	0	250	5	375
	0	100	5	250
	10	100	5	300
	0	120	25	400
	50	160	50	350
	0	70	5	250
	10	10	5	15
Total	70	830	140	1977

Approximately 8 pct Ni and 7 pct Cu detected in +9 mesh fraction (compared to −80 mesh fraction).

The only exception to the trend was one sample of rubble-like material consisting of more than 50 pct of +32 mesh size. In this case the +9 mesh material tested substantially higher than the −9+32 size, but even here the normal trend applied for the fractions smaller than 32 mesh.

Certain general conclusions may be drawn from these tests on till:

1) The −9 mesh material would be satisfactory for most field work, but samples of only −80 mesh material will give more reliable results and are to be preferred where anomalies of small magnitude may be expected.

2) The leveling off of metal content in the sizes smaller than −80 mesh shows that nothing is gained by any attempt to screen to a size finer than 80 mesh.

3) There is no general direct distribution relationship between metal content and available surface area of the finer particles of till. This is significant in any consideration of the processes by which trace elements move and are fixed in soils.

Discussion of Distribution Curve in Till: The amount of metal ion in various soil sizes, if held there by adsorption, should show some relation in its distribution to the total amount of soil-particle surface area available. While this might not be a direct

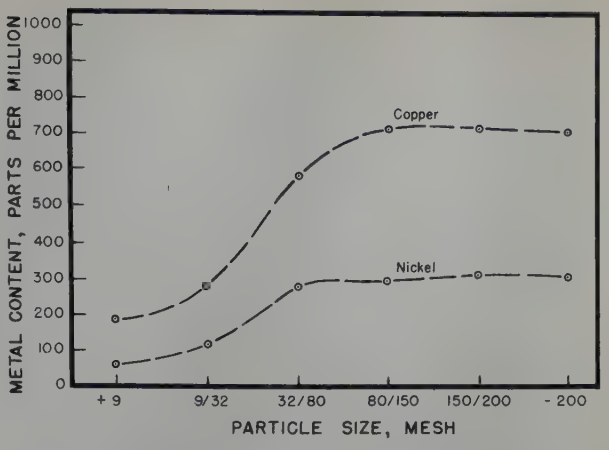

Fig. 3—Copper and nickel distribution trends in soil fractions of till. (Each point on curve represents the arithmetic mean of 28 analyses.)

linear relationship, at least there should be some increase in ion content with the increase in surface area. This reasoning should apply to heavy metals introduced (epigenetic trace elements) into the soil as ions in infiltrating soil solutions. The total content would also include similar ions derived from the nearby source area by mechanical processes (syngenetic trace elements). Here again there should be some increase of the ion in the finer sizes because of the lesser physical resistance of sulfides. Also, later chemical attack by soil solutions on such sulfide particles should help distribute a greater proportion of metal ions where the adsorption capacity is highest.

Theoretically the heavy metal content should increase as the surface area capable of fixing ions increases. The till samples, however, do not show such an increase for material finer than about 80 mesh. Either the reasoning that postulates a continued increase of ion in the finer sizes is incorrect, or some factor or combination of factors interferes with the full development of a theoretical type of distribution. If the reasoning is essentially correct, then soils where the interfering factors are absent should have metal ion contents that do increase as total soil-particle surface increases.

Table II. Comparison of Nickel Content, Ppm, of −80 Mesh Soil Fraction and −9+80 Mesh Fraction, 100-Ft Sample Spacing

−9+80 Mesh	−80 Mesh
0	0
10	20
0	0
0	0
10	0
300	400
250	500
300	300
75	100
350	400
100	150
70	150
400	700
0	75
Total 1865	2795

The following explanation is proposed for the till distribution trend of Fig. 3:

A volume of till made up of some combination of particle sizes has incomplete sorting. It is necessary to visualize a non-homogeneous sample, in which there are portions or zones of dominantly coarse

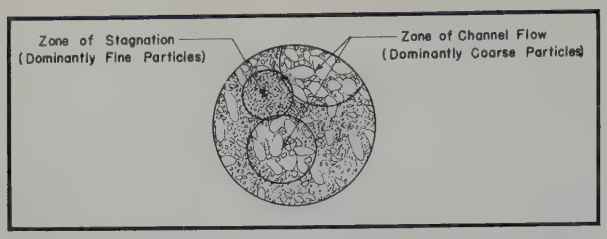

Fig. 4—Diagrammatic representation of zones of channel flow and stagnation.

particles and other portions of dominantly fine particles. Within such zones permeability and interspace sizes will depend directly on the degree of dominance of particular particle sizes, and porosity may depend on it. Assume an instant of time when the postulated mix has just been formed by glacial action. Two extremes of saturation by soil water are possible: 1) complete saturation, probably by water of low trace element content, as time and the chemical environment would hardly favor strong solution effects, and 2) complete absence of soil water, an unlikely situation. In either case the fixed trace elements present at this point would be primarily a product of mechanical weathering.

Next visualize complete or fairly complete saturation of the mix by soil water. Any metal ions present in this water can now be fixed through adsorption by the nearby particle surfaces. There will not be enough metal ions present at this stage to use up the full adsorption capacity of the particles. If stagnant conditions were to prevail at this point the only additional changes in ion distribution would be in the near vicinity of any sulfide particle which could provide ions to the soil solutions and which could migrate locally by various types of diffusion until fixed.

The next stage would be introduction of ion from a nearby source—the epigenetic component of the total heavy metal concentration. It is possible to visualize movement of soil water carrying metal ion in solution. How would a solution move through the mix? The solution would not move as a pervasive migration but would tend to *channel* through the zones of greatest permeability and to bypass zones or volumes of low permeability. Channel flow is a path of preferred flow—a path of higher permeability than the surrounding regions (Fig. 4).

Thus the introduction of additional ions to the mix as solute would be uneven. The soil particles in and adjoining the zones of channelized movement would have access to migrating ions and would be able to make use of their surface adsorption capacity. The soil volumes bypassed by the channelized flow will be those of dominantly finer sizes, of smaller interspaces, of greater resistance to fluid flow. Here conditions would be essentially those of stagnation and the particles within these zones would not have complete access to additional ions. Thus even though the zones of dominantly finer sizes have the greater total surface area and hence the greater adsorption capacity, they are unable to make use of their full potential. As migrating water is introduced into the system it follows a tortuous but continuous channel through the larger interspaces; then smaller channels form as smaller interspaces are invaded. Eventually, an equilibrium will be attained and additional channels will cease to develop. Around and between the channels of flow will be bypassed zones in which original fluid remains unaffected by the migrating soil water. Although the finer particles have the greater adsorption capacity, only a small percent of that capacity is used, while the larger particles with lesser surface capacity use a large percentage of that capacity. The final result is that the soil-fraction distribution of ions within unsorted till does not show a direct relationship to available surface area. Studies made in the Stanolind Oil & Gas Co. laboratories show that movement of solutions through oil sands does channel and that zones of stagnation exist.[10] This laboratory work provides a strong foundation for believing that movement of soil solutions will be similar in nature. It is also important to keep in mind the probability of occurrence of the events described.

The distributional curve (Fig. 3) of till samples begins to flatten at about the 80 mesh soil size. The preceding discussion can account for the flattened portion of the curve. The question arises as to why the curve ceases to rise at that particular size range. Apparently the size near 0.175 mm is a critical size. It is believed that particles below the critical size were largely in the zones of stagnation and those above the critical size were largely in the zones of solution movement. The critical size is the one where the interspaces of the soil mix are so small that they impeded flow of solution. They provide a lower limit of channel flow.

To recapitulate, below a critical particle size (and so of interspace size) the particles are able to use only a small proportion of their large adsorption capacity. Above the critical size the particles use a large proportion of their relatively small adsorption capacity. The curve can thus be explained in terms of the accessability to ions, which in turn is a reflection of the origin and geologic history of the sampled material.

The total content of heavy metal will be made up of ions of mechanical origin and ions introduced later by other processes. The adsorbed metal ions will consist of introduced material from the mineralized source and of redistributed metal ion from local reactions between soil solutions and soil particles containing metal ions. The slope of the distribution curve will depend on the amounts of heavy metal supplied in each way and on the environmental history of the mix. Where zones of fluid migration contain a higher proportion of finer particles the fine soil fractions should have a higher proportion of adsorbed metal ion. The proportion of metal ion of mechanical origin to that of later origin in a particular soil fraction will also affect the curve

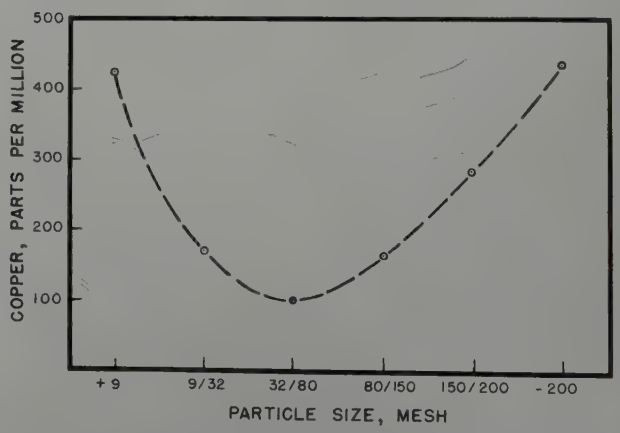

Fig. 5—Copper distribution trend in soil fractions of active stream sediments. (Each point on curve represents the arithmetic mean of 28 analyses.)

slope. It is the interplay of these variables that influences the slope of a distribution curve.

Distribution in Stream Sediments: Any explanation of the distribution curve for till which relates trace elements content to geologic history implies that material that has had a different geologic history should display a somewhat different type of distribution curve. It is known that stream sediments are very useful in geochemical exploration.[11] Stream sediments, if transported by waters containing heavy metals, should contain significant amounts of the metal. The material has had a different geologic history than till because of the exposure to a period of water transport.

The waters of streams draining mineralized terrane may contain several times as much heavy metal as other streams. All soil particles in stream sediment have had a high probability of access to metal ion during their transport as discrete particles. Individual particles of all sizes should have been able to exercise their adsorption capacity to a high degree and should display an increased concentration of ion with increase of available surface area. Some data presented by Hawkes (Ref. 11, p. 1125) suggest that this is actually the case.

Samples of active stream sediments were collected in Fillson Creek near Ely in November 1956 from locations where the stream bed overlies the mineralized zone. The waters of the creek where it crosses the mineralized zone (Fig. 2) contain about 0.025 ppm of heavy metals, as compared to 0.005 ppm in other streams of the district. The samples were dried and screened, and tests were run for copper by the biquinoline method[12] and for both copper and nickel with the chromograph. Composite results of the tests are given in Figs. 5 and 6.

The distribution curve for stream sediments is quite different from that for till. The heavy metal content does not decrease for particle sizes smaller than 80 mesh; it continues to increase. The slope of that part of the distribution curve is of the form predicated from consideration of the channel flow hypothesis presented above.

What appears at first to be a new complication is that the metal content of the coarser particles is also higher than that of the intermediate sizes. Consideration of the particular nature of the samples suggests the following explanation:

Much of the stream bed material is of local origin, particles broken off by glacial action and reworked to some extent by water action. The larger particles in the sample have a low surface to volume ratio and so have not been greatly affected by chemical weathering. Because many of these particles are derived from the mineralized zone, some contain metal as sulfides and in the silicate structures. Fusion and analyses of such samples result in high tests. The intermediate and fine size particles have a higher surface to volume ratio and so are much more subject to attack and breakdown through chemical action. This would be especially true of the sulfides. As the sulfide particles react and disintegrate they supply metal ion to the water. Adsorption of some portion of the heavy metal can now occur and the finer sediment particles would adsorb the greater proportion. Thus the intermediate size particles are impoverished relative to the coarser, while the finer particles increase in heavy metal ion content because of their high adsorption capacity.

The distribution curve of the stream sediments reflects ions of two kinds, largely mechanically derived ions in the coarser fractions and adsorbed in the finer. The total curve slopes reflect a composite of the two origins. The work of Sergeev and the till sample noted earlier support this explanation.

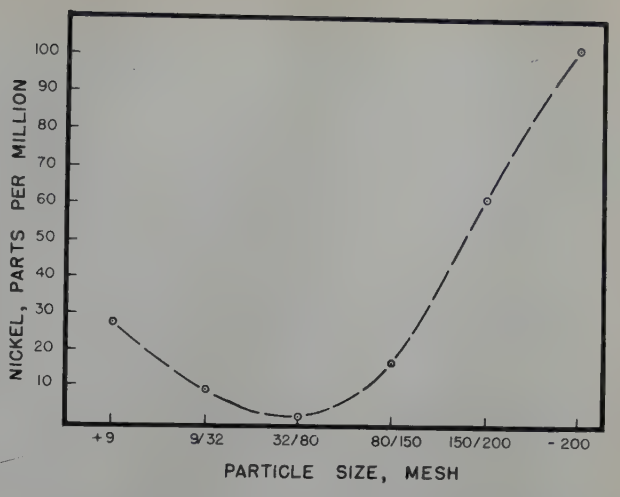

Fig. 6—Nickel distribution trend in soil fractions of active stream sediments. (Each point on curve represents the arithmetic mean of 28 analyses.)

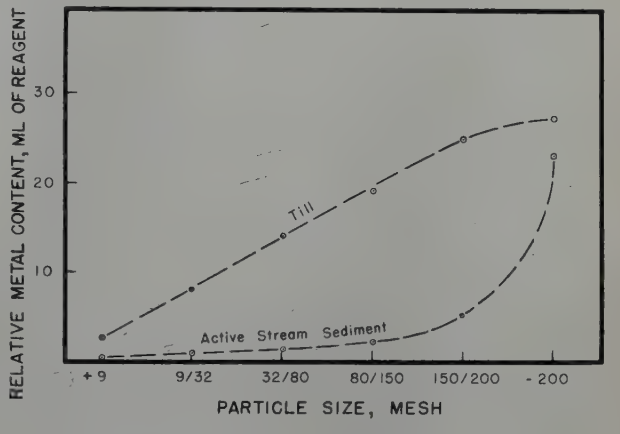

Fig. 7—Heavy metal present as exchangeable ion in till and active stream sediments. (Each point on till curve represents 20 analyses. Each point on stream sediment curve represents 36 analyses.)

To test the proposed explanation, the stream sediment samples were analyzed by a cold acetate extraction technique. This method extracts the exchangeable ion[11] but does not extract heavy metals present in mechanically derived particles nor those fixed by surface coatings such as iron oxides.[4]

The distribution of exchangeable ion content of the samples is shown in Fig. 7. The metal content of the soil particles increases in the finer fractions, as would be expected, but is very low in the coarser particles.

This decrease of exchangeable heavy metal content in the coarser particles supports the conclusion that the distribution curve for the coarse sizes (Figs. 5 and 6) results largely from particles of mechanical origin. Again it can be said the distribution curve reflects the geologic history of the material sampled.

Some additional support for the above interpretation is provided by tests of active stream sediments from Minnesota's St. Croix State Park area, which is underlain by Keweenawan volcanics. A few of the thinner flows contain native copper. Because of scarcity of outcrops little is known of the detailed spatial relation of sample points to possible zones

of native copper. However, it was believed that if twelve samples were selected from nine separate streams that cut across the strike of the flows, and five samples from the Kettle River, most of the sample points would not overlie or be very close to a copper zone. One sample (No. 7) was collected 200 ft downstream from an exposure of native copper in the Kettle River.

The results of chromograph tests of size fractions are given in Table III.

Table III. Copper Content, Ppm, in Size Fractions of Active Stream Sediments, St. Croix Park Area, Minnesota

Mesh	Average of 12 Stream Samples	Average of 4 River Samples	Sample No. 7 River Sample
−9	8	5	300
−9+32	3	0	50
−32+80	3.5	0	0
−80+150	14	6	10
−150+200	109	56	20
−200	370	240	150

Sample No. 7 and the samples from Fillson Creek (Fig. 5) are similar both in copper distribution and nearness to a mineralized source. The other St. Croix Park samples display a different distribution in that the coarser fractions are very low in copper. This is interpreted as an expression of an additional factor in the geologic history of the material, the effect of transport to a greater distance from the metal source.

Conclusion

Heavy metal distribution data for soil fractions of till and for active stream sediments show that the soil size fraction containing the highest proportion of heavy metals may differ in materials of different geologic history. A channel-flow hypothesis can explain the distribution curve of heavy metals in till. It is suggested that the distribution curve of heavy metals is a result of the geologic history of the sampled material, and it follows that a distribution curve indicates something of the geologic history of the soil.

Understanding of the heavy metal distribution trends is a useful guide in selection of sample material in geochemical reconnaissance work. A great deal more data will be needed before it is possible to make reliable predictions of the type of distribution a certain soil sample might have. It is hoped that this article will stimulate further investigation in materials of various origins.

Acknowledgment

The introductory part of this article and data on distribution in till was presented by the author to the Institute on Lake Superior Geology at Houghton, Mich., May 1956. Permission to include it here is gratefully acknowledged. Funds for the study have been provided by the Graduate School of the University of Minnesota and the Minnesota Institute of Research.

References

[1] G. M. Schwartz and D. M. Davidson: Geologic Setting of the Copper-Nickel Prospect in the Duluth Gabbro Near Ely, Minnesota. *AIME Trans.*, 1952, vol. 193, pp. 699-702.

[2] G. M. Schwartz and J. M. Harris: Notes on Field Work in the Copper-Nickel Prospect Area, Lake County, Minnesota. Minnesota Geological Survey, *Summary Report No. 6*, 1952.

[3] R. E. Stevens and H. W. Lakin: The Chromograph, a New Analytical Tool for Laboratory and Field Use. *USGS Circ. 63*, 1949.

[4] M. L. White: Occurrence of Zinc in Soil. *Economic Geology*, 1957, vol. 52, pp. 645-651.

[5] L. C. Huff: A Sensitive Field Test for Detecting Heavy Metals in Soil or Sediment. *Economic Geology*, 1951, vol. 46, pp. 524-540.

[6] H. E. Hawkes and H. W. Lakin: Vestigial Zinc in Surface Residuum Associated with Primary Zinc Ore in East Tennessee. *Economic Geology*, 1949, vol. 44, pp. 286-295.

[7] H. A. Warren and R. E. Delavault: *Soils in Geochemical Prospecting.* MINING ENGINEERING, October 1956, pp. 992-996.

[8] E. A. Sergeev: Geochemical Method of Prospecting for Ore Deposits, 1941. *Selected Russian Papers on Geochemical Prospecting for Ores*, p. 46. Translated by V. P. Sokoloff and H. E. Hawkes, USGS, 1950.

[9] C. T. Bischoff: Testing for Copper and Zinc in Canadian Glacial Soils. *AIME Trans.*, 1954, pp. 57-61.

[10] Pan American Petroleum Corp. film and brochure: *Fluid Distribution in Porous Systems*, 1954.

[11] H. E. Hawkes and H. Bloom: Heavy Metals in Stream Sediment Used as Exploration Guides. *AIME Trans.*, 1956, pp. 1121-1127.

[12] H. Almond: Rapid Field and Laboratory Method for the Determination of Copper in Soil and Rocks. *USGS Bull. 1036A*, 1955.

[13] H. Bloom: A Field Method for the Determination of Ammonium Citrate-Soluble Heavy Metals in Soils and Alluvium. *Economic Geology*, vol. 50, pp. 533-541.

[14] H. T. S. Britten: *Hydrogen Ions*, p. 79. Chapman and Hall Ltd., London, 1942.

[15] W. A. Grosh, J. W. Pennington, P. A. Wasson, and S. R. B. Cooke: Investigation of Copper-Nickel Mineralization in Kawishiwi River Area, Lake County, Minn. *USBM R. I. 5177*, 1955.

[16] F. F. Grout: The Lopolith, an Igneous Form Exemplified by the Duluth Gabbro. *American Journal of Science*, 1918, vol. 46, pp. 516-522.

[17] P. Leach: Simple Chemical Tests to Aid Prospectors. *Engineering and Mining Journal*, 1947, vol. 148, p. 79.

[18] T. S. Lovering, L. C. Huff, and H. Almond: Dispersion of Copper from the San Manuel Copper Deposit, Pinal County, Arizona. *Economic Geology*, 1950, vol. 45, pp. 493-514.

[19] M. Salmi: Prospecting for Bog-Covered Ore by Means of Peat Investigations. *Bulletin de la Commission, Geologique de Finlande*, 1955, No. 169.

[20] D. H. Yardley: Distribution of Trace Elements in Soil Fractions. *Proc.*, Institute on Lake Superior Geology, 1956.

Discussion of this article sent (2 copies) to AIME before Aug. 31, 1958, will be published in MINING ENGINEERING.

Graphical Representation of Theoretical Soluble Losses by CCD

by R. J. Woody

DESIGN of the most economic continuous countercurrent decantation (CCD) circuit is based on selection of the number of stages and the wash volume that will give the minimum summation of the following items:

1) Capital and operating costs of the CCD circuit.

2) Capital and operating costs of the precipitation circuit.

3) Value of the dissolved product lost.

R. J. WOODY, Member AIME, is Manager, Raw Materials Development Laboratory of National Lead Co. Inc., Winchester, Mass.

TP 4758B. Manuscript, March 6, 1958. New York Meeting, February 1958.

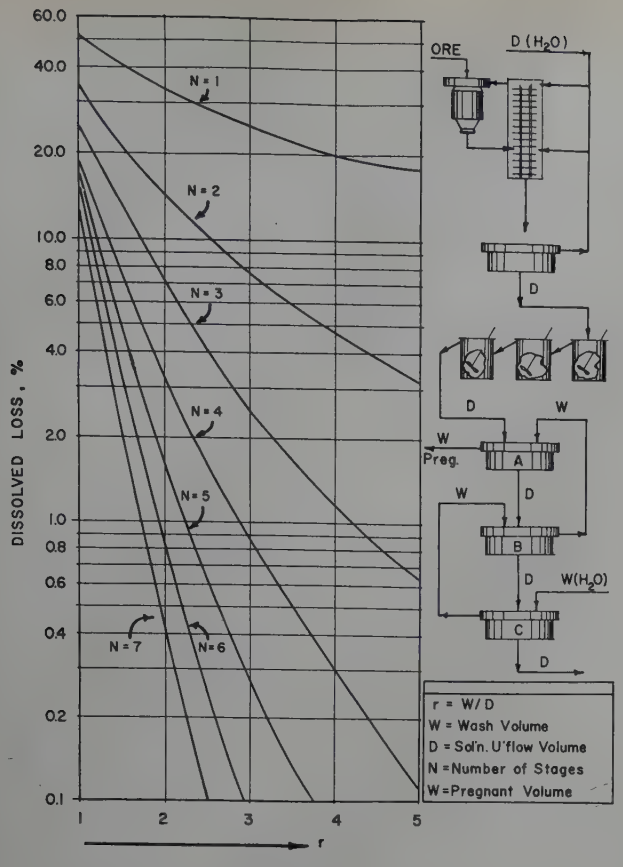

Fig. 1—Straight CCD after water grind.

Items 1 and 2 are fairly straightforward problems of estimating from ore testing data.

Item 3 involves what is commonly referred to as the theoretical soluble loss, and its value is essential in comparing like installations. Once the type of flowsheet is established and the practical operating level of the thickener underflow dilution is determined from the test data, the theoretical loss can be calculated. However, the number of stages and the wash volume must be fixed for each computation, and determination of the optimum layout for CCD and precipitation by this method becomes extremely laborious.

The charts (Figs. 1 and 2) presented here were prepared at the Winchester Laboratory to expedite the study of uranium ores with respect to the possible application of CCD. The flowsheets for which soluble losses are plotted in Figs. 1 and 2 are the two most common for straight CCD washing. A broad practical range of conditions with respect to number of stages and wash ratios is covered in the curves accompanying the flowsheets.

The soluble loss is expressed as a percentage of the desired product that is in solution in the feed to the CCD circuit.

The symbols D and W of Fig. 1 are liquid volumes in thickener underflow and overflow respectively and are assumed to remain constant at all stages. These quantities are commonly expressed as volume tons (32 cu ft) per ton of ore treated. D is determined by laboratory or pilot plant testing and represents the volume of solution per unit of dry solids in the pulp at or near its terminal density. In the determination of washing efficiency, the ratio of W to D is the controlling factor, rather than the size of either quantity, and values of W/D (r) constitute the horizontal axes of the charts.

The following example illustrates a method of using the chart in Fig. 1:

Problem: Find the combinations of number of stages (N) and pregnant solution volumes ($W = rD$) that will yield a theoretical soluble loss of 0.2 pct if the thickener spigot dilution is 0.8 volume tons per ton of ore. The essential numbers may be quickly found and tabulated (Table I).

Derivation of Soluble Loss Formulas

Water Grind Flowsheet (Fig. 1)

Let x = valuable product that was dissolved in the agitator circuit and lost in the last CCD thickener underflow in pounds per ton of ore.

And, let $W/D = r$

C underflow, $C_u = x$

C overflow, $C_o = rx$

From product balance at thickener C:

$B_u = C_u + C_o$ — zero $= x(r + 1)$, and

$B_o = r\,B_u = x(r^2 + r)$.

From product balance at thickener B:

$A_u = B_u + B_o - C_o = x(r^2 + r + 1)$, and

$A_o = r\,A_u = x(r^3 + r^2 + r)$.

From the overall product balance:

Total dissolved in CCD feed $= C_u + A_o$

Percentage loss for three stages is,

$$\frac{100\,C_u}{A_o + C_u} = \frac{100\,x}{x(r^3 + r^2 + r + 1)}$$

The general formula for N stages is, therefore:

$$\text{Soluble loss, pct} = \frac{100}{r^N + r^{N-1} + r^{N-2} + \ldots . r^{N-N}}$$

Table I. Combinations for 0.2 Pct Soluble Loss (D — 0.8)

Stages	7	6	5	4
r	2.3	2.6	3.2	4.4
Preg (rD)	1.8	2.1	2.6	3.5

It is readily apparent that information of this type is useful in estimating the combined costs of CCD and precipitation. If cost plus soluble losses is compared at enough loss levels the optimum layout with respect to number of stages and size of precipitation circuit can be established. The optimum theoretical soluble loss can also be determined.

The curves in Fig. 2 differ from those in Fig. 1 because the flowsheets are different. In the flowsheet represented by Fig. 1 water enters the feed end of the mill in volume equivalent to D, and wash volume (W) is applied at the last stage of thickening. In the flowsheet for Fig. 2 wash volume W, applied to the last thickener, is the only water added, and the water required in the grinding circuit is taken from the second stage of CCD. This solution re-enters the CCD circuit at stage 1 via the leached pulp. This type of flowsheet is very common in cyanidation. Fig. 2 also applies to acid leaching and CCD following a dry grind.

Although r in Fig. 2 is also W/D, the volume of pregnant solution per ton of ore is W minus D. Total water required in Fig. 2 is W, whereas in Fig. 1 it is W plus D. Evaporation losses are of course neglected in the estimation of theoretical soluble losses.

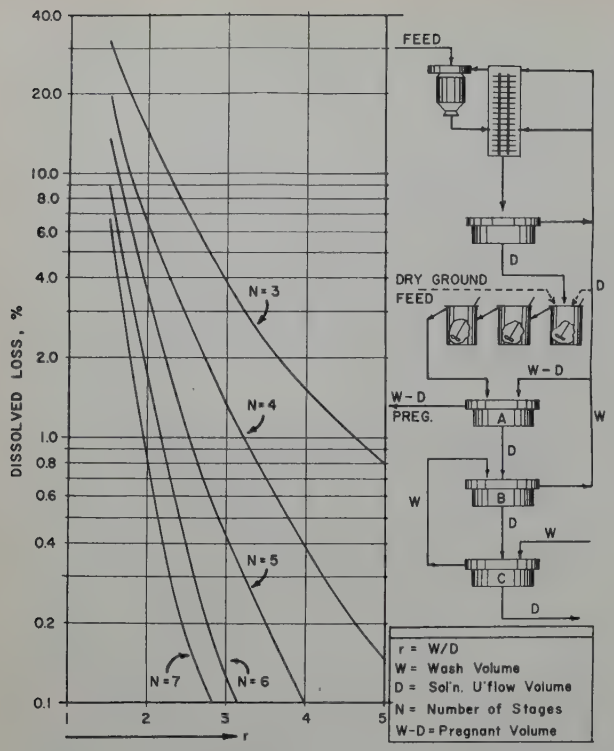

Fig. 2—Straight CCD after grinding dry or in solution.

The curves in each of these charts are the result of substitution in formulas developed for the particular flowsheets. The derivation of these formulas is presented here.

Figs. 1 and 2, and perhaps other charts like them, could be extremely useful to the design engineer for determining the most efficient system to recover products dissolved from ores and similar raw materials. Such charts are also useful for comparison of actual and theoretical washing efficiency of existing plants.

Derivation of Soluble Loss Formulas

Solution on Dry Grind Flowsheet (Fig. 2)

According to the same nomenclature used in the derivation for Fig. 1:

$C_u = x$, and
$C_0 = r\,x$.

From product balance at thickener C:

$B_u = C_u + C_0 -$ zero $= x(r+1)$, and
$B_0 = r\,B_u = x(r^2+r)$.

From product balance at thickener B:

$A_u = B_u + B_0 - C_0 = x(r^2+r+1)$, and

$$A_0 = \frac{W-D}{D} A_u = (r-1)\,A_u$$
$$= x(r^3-1).$$

From the overall balance:

Total dissolved $= C_u + A_0$
$= x + (xr^3 - x)$
$= x\,r^3$

Percentage loss for three stages:

$$\text{Soluble loss, pct,} = \frac{100x}{xr^3}$$

For N stages:

$$\text{Soluble loss, pct} = \frac{100}{r^N} = 100\left(\frac{D}{W}\right)^N$$

Acknowledgment

This work was performed for the U. S. Atomic Energy Commission under Contract No. AT (49-6)-924.

Reference

T. B. Counselman: Continuous Countercurrent Decantation Calculations. *AIME Trans.*, vol. 187, p. 223.

Discussion of this article sent (2 copies) to AIME before Aug. 31, 1958, will appear in MINING ENGINEERING.

Distribution Curves for Sink-and-Float Separation of Iron Ores

by Rudolph G. Wuerker

WITH the growing complexity of ore dressing processes and the diversity of equipment, efficiency control has become increasingly important in beneficiation. In the case of iron ore dressing, there have been sporadic attempts[1-3] to establish the optimum separation for various ores so that grade and recovery would be readily predictable. But no rigorous statistical analysis and graphical presentation of such tests could be found in the literature of this country.

R. G. WUERKER, Member AIME, is Associate Professor, Department of Mining and Metallurgical Engineering, University of Illinois, Urbana, Ill.

TP 4759B. Manuscript, Jan. 23, 1957. Tampa Meeting, October 1957.

Tests Made with Iron Ores

Expanding upon existing methods of plant supervision and efficiency control, an investigation was started in the ore dressing laboratory at the University of Illinois on the applicability of distribution analysis to iron ores. A sample of crude ore was obtained from the Ohio mine of Cleveland-Cliffs Iron Co. at Ishpeming, Mich., consisting mostly of alternating bands of hematite and siliceous gangue, both about ¼ in. wide. The ore was heavily coated with limonite, which often filled the cracks.

For the sink-and-float tests the ore was screened to the following sizes (inches): −1.05 +0.742; −0.742 +0.525; −0.525 +0.371, and −0.371 +0.185. The screened ore was then pre-soaked and subjected to heavy liquid sorting. The highest specific gravity, 3.59, obtained in the tests was reached in an aqueous solution of thallous formate and thallous malonate. At 3.29 sp gr, methylene iodide was employed. This was easily diluted with benzene to obtain lower densities.

At 2.96 sp gr the investigators used acetylene tetrabromide, which could be diluted with carbon tetrachloride to lower the specific gravity to about 2.73. Tests were stopped here, as this value is about the density of quartz or gangue.

The various fractions were set aside and the heavy liquids washed off; the ore was air-dried, crushed, and sampled for chemical analysis. Following the procedure outlined in a U. S. Steel publication,[4] assay was made for iron and for insoluble material, assuming that the latter was representative of quartz in the ore. Determination was made only for iron and insoluble, as these constituents influence the price of ore most, but any other constituent such as phosphorus and sulfur might be the object of a distribution analysis.

Calculations: The laboratory data in columns 1, 2, and 4 of Table I are followed by the calculations made in constructing distribution curves. Column 3 gives the percent weight of sink based on the total weight. Column 4 is the percentage of iron for each layer of separation as determined by separate analysis. Column 5 is the weighted product of percent weight of sink times its respective percent of iron, often referred to as *iron units*. Its dimension is percent times percent, equal to 1/10,000; however, it is customary to express the products in whole numbers. Column 6 is the cumulative percent weight of sink for each specific gravity separation, that is, the total percent that would sink at each specific gravity range. It is found by adding percent weights from column 3. Column 7 is cumulative percent iron in percent weight found by adding percents in column 5. Column 8, the cumulative percent iron in sink, is found by dividing column 7 by column 6. Column 9 is the cumulative percent weight of float for each specific gravity range. It is determined by assuming that 100 pct of the sample will float at the highest specific gravity and then subtracting the total or cumulative percent weight of sink for succeeding specific gravity ranges from 100 pct. Column 10, the cumulative percent product of the float, is derived by making additions in column 5, working from the bottom up. Column 11, the cumulative percent iron in the float, is calculated by dividing column 10 by column 9. Column 12 is the Fe-Distribution Ordinate for the sample. Each number in this column is obtained by adding half the corresponding number in column 3 to the sum of the preceding numbers in column 3.

Similar steps are necessary to prepare data showing distribution of the insoluble or any other constituent in the various gravity layers.

Plots of Distribution Curves: Plots of measured and computed data in the form of distribution curves provide a means of quick interpretation. The shape of a curve tells at a glance whether a feed is easy to clean, or whether it cannot be improved by cleaning processes, such as used in the present investigation.

Of all the plots possible, only the four most important will be discussed here. They are shown in Figs. 1 and 2 and in the most general terms are designated as:

1)	Fe-distribution curve	(*D*)
2)	Cumulative concentrated (sink)	(*A*)
3)	Cumulative tailings (float)	(*R*)
4)	Specific gravity curve	(Sp.Gr.)

Curve *D* is plotted using the midpoint of each successive layer as an ordinate and the corresponding content of the constituent the investigator is most interested in as abscissa. In the present case this is Fe. Curve *D* is the plot of the values in column 12 vs column 4 of Table I. Curve *A* is the plot of column 6 vs 8; curve *R* the plot of column 9 vs 11. The specific gravity curve uses weight percentages as ordinates and specific gravities as abscissas (column 1 vs 6). It gives the specific gravity required to effect any desired separation.

Interpretation of Distribution Curves: Idealized distribution curves for sink-and-float tests are given in Fig. 3a. The general arrangement is similar to the well known washability curves used in coal preparation (or in more general terms, in a float-and-sink process) except that the coordinate system has been turned through 180° and, of course, *sink* and *float* have been interchanged on the ordinates. This graphical representation suggests itself because it is based on the principle of reversibility of the two cases of distribution analysis in gravity separation. In Fig. 3a an imaginary iron ore, easily cleaned, and another one that is difficult to clean are condensed into one diagram. Here a sharp break of the Fe-distribution curve *D* shows the ease of cleaning, while a diagonal trend indicates the presence of a considerable middling problem, as *D* approaches the dotted line *R* in position and direction.

It is evident that the iron ore tested follows this pattern from the plot of experimental data in Table I (size +0.742 −1.05). Fig. 1 shows the Fe-distribution ordinate of this size and also its cumulative concentrate (sink) and cumulative tailings (float) curves. Theoretical recovery at various densities can be graphed from them. An attempt to separate the +0.742 −1.05 size (Table I and Fig. 1) at 2.8 sp gr would obtain, theoretically, 73 wt pct of concentrates with an iron content of 50.2 pct and 27 wt pct of tailings with 11.5 pct Fe. The Fe-distribution curve has a diagonal trend, indicating a definite middling problem. However, in the case of the +0.371 −0.525 size (Fig. 2) the ore had been crushed to a higher degree of liberation and a higher ratio of concentration was attained. A second attempt to separate at 2.8 sp gr would obtain, theoretically, 85.5 wt pct of concentrates with an iron content of 53.5 pct and 14.5 wt pct tailings with 19 pct Fe. It can be seen from Fig. 2 that 2.8 sp gr is not the optimum point and that higher ratios of concentration could be obtained with lower densities.

Besides the foregoing interpretations, the distribution curves with the necessary data can show:

1) Amount and distribution of impurities (silica and sulfur in the case of iron ore) in the different specific gravity fractions.

2) The degree to which a feed can be improved by gravity methods, with amount and kind of products to be expected.

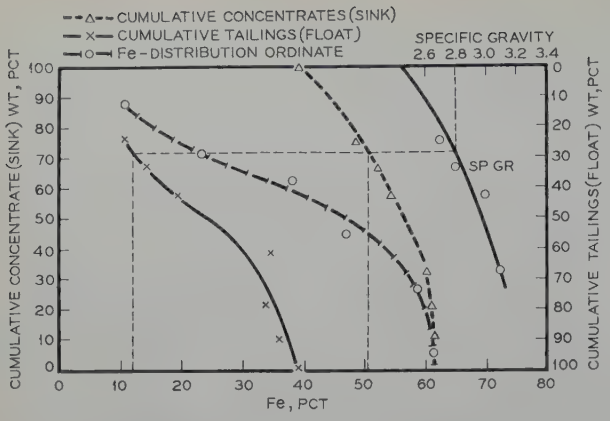

Fig. 1—Distribution curves (series 1) of Ohio mine ore, size +0.742—1.05.

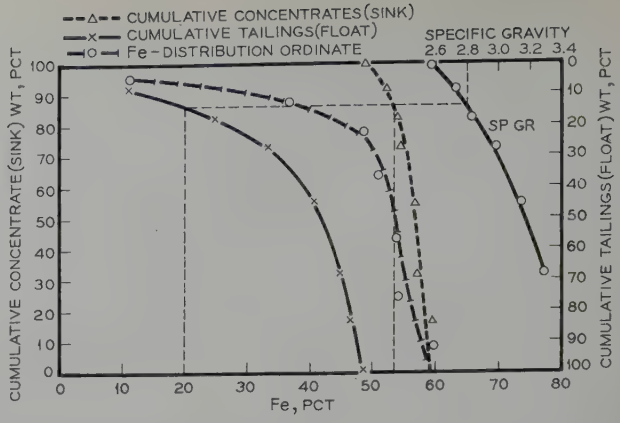

Fig. 2—Distribution curves (series 3) of Ohio mine ore, size +0.371—0.525.

3) A suggestion as to the best type of cleaning plant for the mineral under investigation.

4) An indication as to whether the feed will be easy or hard to clean.

5) An indication as to whether a certain high purity product can ever be obtained from a mineral.[6,7] The minimum percentages of deleterious ingredients can be obtained, with recoveries. Inherent impurities can be determined for the purest product of any particular size.

6) Nature and amount of the impurities in any size.

7) Occurrence of impurities as to whether free or locked in the different fractions. This will indicate whether middlings should be recrused and further treated.

8) Efficiency of existing gravity preparation plants.

Relation Between Washability Tests of Coal and Distribution Analysis of Ores

Heavy media preparation is a branch of gravity concentration that was first developed and brought to widespread application in coal preparation.[5,6] The ore dresser, especially the beneficiation engineer on the Iron Range, faced some difficulties in applying this process to his products.

In the *laboratory,* in heavy media separation the particles of lower specific gravity float, and those of higher specific gravity sink, irrespective of particle size or shape. While the preparation of a heavy medium in the case of coal separation (1.2 sp gr) from slate (2.5 sp gr) was relatively easy, the required specific gravity being 1.3 to 1.5, much higher densities were needed to separate, for example, quartz (2.75 sp gr) from iron ore (Fe_2O_3 4.9 sp gr). Heavy solutions or suspensions were needed, having in this case a specific gravity of 2.8 to 3.4. In this high density range solutions can be used economically in laboratory work only. The preparation of suspensions became a prerequisite for economic application of the process in the *plant.* However, the clean separation achieved in the laboratory is unobtainable in this case. At high separating gravities, where viscosity becomes an important factor, particle shape can definitely have a bearing on the position a particle will take. This is particularly true where currents are present. The combination of a current and a flat particle shape may well influence separation. Ferro-silicon (85 pct Fe and 15 pct Si, ground to —48 mesh) seems now to be the most commonly used suspensoid, not only in treatment of iron ores but also in separation of other ores such as zinc, fluorspar, magnesite, and garnet.

In the case of coal the valuable product is in the float, and the sink is discarded, while in most cases of ore dressing the values (concentrates) are in the sink and the float goes to waste. It can be said that in principle the float process is the reverse of the former. According to recent custom, the coal preparation engineer calls his process *float-and-sink* and the ore dresser speaks of his methods as *sink-and-float,* each one indicating that the object of his preparation process is in the first named word.

Following this assumption, all methods and techniques used in connection with heavy media preparation of coal should be applicable to sink-and-float processes for ores. Furthermore, the float-and-sink process is not restricted to coal preparation. It is

Table I. Observed and Computed Data for Distribution Curves of Ohio Mine Iron Ore, Size +0.742—1.05.

1	2	3	4	5	6	7	8	9	10	11	12
					(Sink) Cumulative Concentrates			(Float) Cumulative Tailings			
Sp Gr	Sink Wt, Grams	Sink Wt, Pct	Iron, Pct, Assay of Fraction	Fe-Units in Fraction Col. 3x4 (x10⁻⁴)	Wt, Pct	Products (x10⁻⁴)	Iron, Pct Col. 7:6	Wt, Pct	Products (x10⁻⁴)	Iron, Pct Col. 10:9	Fe-Distribution Ordinate, Pct
3.51	167.7	10.9	61.20	668	10.9	668	61.2	100.0	3949	39.5	5.5
3.29	149.0	9.7	60.31	586	20.6	1254	60.9	89.1	3281	36.9	15.7
3.14	178.0	11.6	58.77	681	32.2	1935	60.2	79.4	2695	33.9	26.4
2.95	390.0	25.4	46.96	1192	57.6	3127	54.3	67.8	2014	29.6	44.9
2.83	142.0	9.3	38.26	356	66.9	3483	52.2	42.4	822	19.4	62.2
2.73	137.0	8.9	23.27	207	75.8	3690	48.7	33.1	466	14.2	71.3
<2.73	371.0	24.2	10.70	259	100.0	3949	39.49	24.2	259	10.7	87.9
Totals	1534.7	100.0									

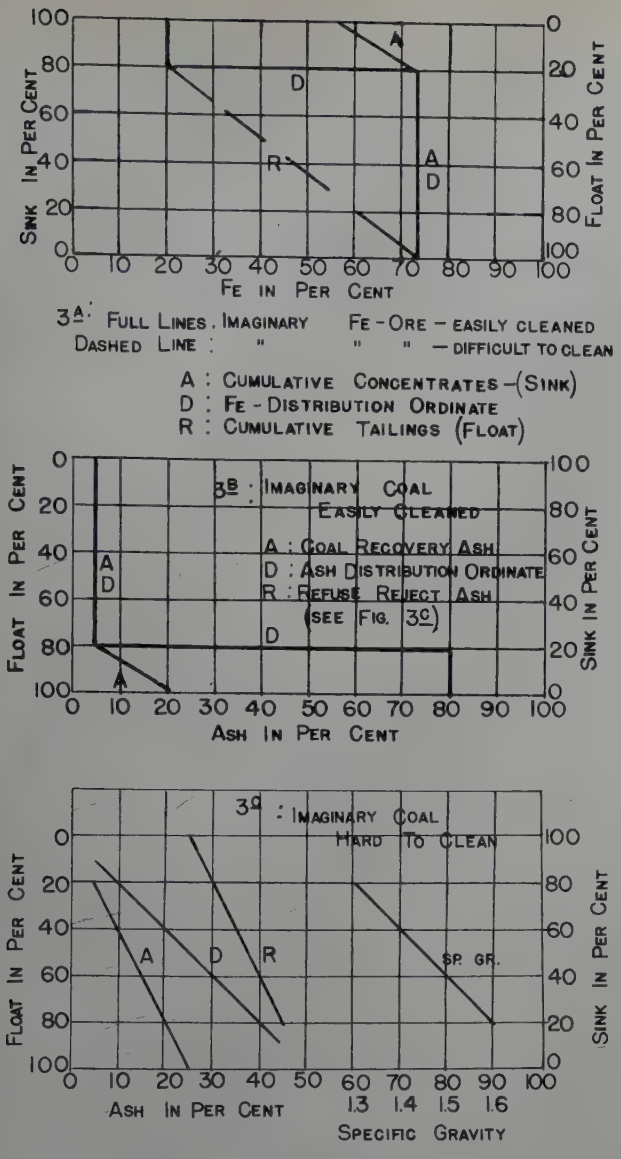
SINK IN PER CENT
FLOAT IN PER CENT
FE IN PER CENT
3A: FULL LINES, IMAGINARY FE-ORE - EASILY CLEANED
DASHED LINE: " " " - DIFFICULT TO CLEAN
A: CUMULATIVE CONCENTRATES -(SINK)
D: FE-DISTRIBUTION ORDINATE
R: CUMULATIVE TAILINGS (FLOAT)
3B: IMAGINARY COAL EASILY CLEANED
A: COAL RECOVERY ASH
D: ASH DISTRIBUTION ORDINATE
R: REFUSE REJECT ASH
(SEE FIG. 3C)
ASH IN PER CENT
3C: IMAGINARY COAL HARD TO CLEAN
SP. GR.
SPECIFIC GRAVITY

Fig. 3a (above)—Idealized distribution curves of iron ore. Fig. 3b (center)—Idealized distribution curves of coal, easily cleaned. Fig. 3c (below)—Idealized distribution curves of coal, hard to clean.

merely the best known example of a separation where the float is recovered. Likewise, the use of iron ore as a prototype for a sink-and-float process does not limit the application to this one type of ore. It is merely the most important one in terms of tonnage and it is the ore used in the present investigation.

This reversibility, together with the terms most commonly used by the ore dresser and coal preparation engineer, respectively, is presented in Figs. 3a-3c. If a distribution analysis is made of various sizes of a feed, the curve with the sharpest break shows the size at which the highest degree of liberation will be obtained. The method used here to plot the curves of an iron ore distribution analysis seems the logical way of indicating that they are the reverse of the washability curves of coal and that both result from the statistical process of distribution analysis.

Further Evaluations of Results of Distribution Analysis

Having pointed out the applicability of heavy media testing to float-and-sink as well as to sink-and-float types of feed, it is reasonable to assume that other common interpretations of coal washability curves, such as the ±0.10-sp gr curve and the Tromp curve, could be used with benefit by the ore dresser.

Since distribution analysis is universally valid, physical properties other than specific gravity can be used to check both the amenability of ores to preparation processes and the efficiency of plant performance. These are: 1) differences in magnetic force, 2) differences in electric fields, and 3) differences in properties related to froth flotation.

In the case of magnetic separation, an actual investigation is on record.[8,9] Low grade iron ores were tested in heavy media as well as with magnetic separation, and distribution curves were plotted. However, a coordinate system different from the one in the present article was used. C. C. Dell[10] used properties related to froth flotation for distribution analysis.* H. Heidenreich's book[11] lists numerous possibilities of expanding the three basic distribution curves.

* In the discussion following presentation of Dell's paper it was observed that this was merely a modification of the float-and-sink test used in coal washing.

Summary

A method has been developed for establishing a standard to determine the theoretical optimum of a beneficiation process for plant supervision and efficiency control. It has been proved that the distribution curves in heavy media testing of iron ores (sink-and-float) are merely the reverse of the washability curves in heavy media testing of coal (float-and-sink) and that both result from the statistical process of distribution analysis. Implications of this principle of reversibility are discussed, and possible applications to other processes of ore dressing are suggested.

Acknowledgments

The writer expresses appreciation to G. T. Hollett and L. J. Erck, Cleveland-Cliffs Iron Co., for securing the ore sample. Credit is due G. R. Eadie for valuable assistance in the experimental phases of the work. R. A. Henn made the analytical determinations. K. E. Merklin, Pickands Mather & Co., reviewed the manuscript.

References

[1] S. M. Marshall: Discussion of: W. H. Coghill: Degree of Liberation of Minerals in the Alabama Low-Grade Red Iron Ores after Grinding. *AIME Trans.*, 1927, vol. 75, p. 147.

[2] F. D. DeVaney and S. D. Shelton: Properties of Suspension Mediums for Float-and-Sink Concentration. USBM *R.I. 3469-R*, 1940.

[3] E. C. Bitzer: Finding a Way to Handle the HMS Middling Problem. *Engineering and Mining Journal*, November 1951, vol. 152, p. 91.

[4] U. S. Steel Corp.: *Methods of the Chemist for Analysis of Iron and Manganese Ores.*

[5] A. C. Callen and D. R. Mitchell: Washability Tests of Illinois Coal. University of Illionis, Engineering Experiment Station, *Bull. 217*, 1930.

[6] D. R. Mitchell and L. C. McCabe: Washability Characteristics of Illinois Coal Screenings. Illinois State Geological Survey *R.I.48*, 1937.

[7] T. Fraser, W. L. Crentz, and O. T. Barrett: Preparation Characteristics of Some Coals Available for the Synthetic Liquid Fuels Industry. USBM *Bull. 495*, 1950.

[8] W. Luyken and E. Bierbrauer: Ueber Rechnerische und Graphische Verfahren zur Erfassung des Aufbereitungserfolges. (Calculations and Graphical Methods for Control of Ore Dressing.) *Mitteilungen Kaiser Wilhelm Institut fuer Eisenforschung*, 1925, vol. 7, pp. 17-23.

[9] W. Luyken: Ueber Aufbereitungsversuche mit Erzen des Salzgitterer Hoehenzuges. (Tests to Determine the Dressability of Ores from Salzgitter.) *Mitteilungen Kaiser Wilhelm Institut fuer Eisenforschung*, 1925, vol. 7, pp. 25-41.

[10] C. C. Dell: Release Analysis, New Tool for Ore Dressing Research. In *Recent Development in Mineral Dressing*, p. 75. The Institution of Mining and Metallurgy, London, 1953.

[11] H. Heidenreich: Die Erfolgsrechnung in Aufbereitungsbetrieb. (Efficiency Control in Mineral Separation), *Verlag Glueckauf, GmbH.*, Essen, 1954.

Discussion of this article sent (2 copies) to AIME before Aug. 31, 1958, will be published in MINING ENGINEERING.

Iron Oxide Slime Coatings in Flotation

by D .W. Fuerstenau, A. M. Gaudin, and H. L. Miaw

A quantitative method for evaluating density of slime coatings has been developed and applied to formation of iron oxide slime coatings on quartz and on corundum. Slime coating density is related to flotation recovery and to properties of the electrical double layer at mineral surfaces.

IN spite of considerable study,[1-5] the nature of slime coatings in flotation is still not completely understood. However, phenomena that control flocculation and dispersion of colloidal systems are now interpreted in terms of electrical double layers.[6,7] Colloids will flocculate even though the particles carry the same charge, but when two dispersed colloids of opposite charge are mixed, flocculation ensues even more rapidly. Analogous phenomena seem responsible for slime coating on minerals in flotation systems.

To shed new light on the issue it was considered desirable to devise a tool that would measure slime coatings. The usual method has been to examine photographs of presumably representative surfaces, after an intervening washing in running water. But such an examination is non-quantitative, and the changes in chemical environment represented by the washing may have removed the slime coatings that existed during flotation. To provide the possibility for a correlation with electrical double layer phenomena, the experiments were made with quartz, corundum, and iron oxide, for which electrokinetic data are available.[8-12] Since the properties of the electrical double layers of these oxides depend on the pH of the solution, pH will be the most important variable. Furthermore, because the zero point of charge for silica, iron oxide, and alumina occurs at pH 3.7, 8, and 9.5, respectively, the relative charge on the slime and mineral can be changed over wide ranges. Because of its practical importance in quartz flotation, iron oxide powder was chosen as the slime. Also, its uniform composition, contrasting color, and ease of analysis make experimentation simple.

In this investigation, correlation was sought between the effect on flotation recovery of slime addition and slime coating density.

Materials and Methods

Details are available in a thesis by Miaw.[11] The quartz was selected from pure Brazilian crystalline quartz, crushed, sized (65/150 mesh) acid-cleaned, washed, and stored in conductivity water. The corundum (synthetic alumina of high purity prepared by Linde Co., Chicago) was crushed, sized (65/100 mesh) deslimed, boiled in nitric acid, washed, and stored in conductivity water. The iron oxide slime, reagent-grade ferric oxide (—400 mesh) from Allied Chemical & Dye Corp., was heated to 160°C, cooled, and stored in a vacuum desiccator. In the electron microscope the slime particles appeared to be about 0.3μ in size, but their large specific surface (87,900 cm^2 per g, by gas-adsorption method, using krypton) suggests that the actual particles are smaller than 0.3μ. Had they been perfect nonporous spheres, they would have had a diameter of 0.13μ.

D. W. FUERSTENAU, Member AIME, is Research Engineer, Electro Metallurgical Co., Niagara Falls, N. Y. A. M. GAUDIN, Member AIME, is Professor of Mineral Engineering, Massachusetts Institute of Technology, Cambridge, Mass. H. MIAW was formerly a Graduate Student, Massachusetts Institute of Technology.

TP 4767B. Manuscript, Jan. 6, 1958. New York Meeting, February 1958.

The flotation tests were made in a modified Hallimond micro-float cell[6,13] in which nitrogen gas was introduced at the rate of 0.3 ml per sec for 1 min following a 10-min conditioning period without gas. Sized mineral, very coarse compared to slime yet fine enough to offer no obstacle to flotation, was mixed in aqueous suspension with iron oxide slime, then floated at the predetermined and controlled rate. The dried float was weighed and the recovery was calculated. Quartz flotation tests were made with 1 g of 65/150-mesh quartz in 100 ml of water containing 25 mg per liter of purified dodecylammonium acetate. Corundum flotation tests were made with 1.4 g of 65/100-mesh corundum in 100 ml of water containing 12.5 mg per liter of purified sodium dodecyl sulfate. Adjustment of pH was made with HCl or NaOH.

Quantitative slime-coating studies were made by conditioning 2 g of mineral in 100 ml of solution with slime, with or without flotation reagents as desired.

Preliminary experiments were made to find out whether the time of agitation of the mineral with the slimy liquor had any effect. It was found that the slime coating increased with time up to 10 min, thereafter remaining substantially independent of time.[11] Accordingly, a 10-min agitation period was adopted for the rest of this work, even though it was realized that the time required for slime-coating formation may vary with the prevailing chemical conditions and with the system under study. After conditioning, a mineral charge was elutriated with a liquor having the composition of the flotation liquor prior to the addition thereto of mineral and slime. The ascending rate in the elutriator was adjusted to retain the mineral with adherent slime and overflow the non-adherent slime. The mineral was then leached with acid to dissolve the slime, and the iron was determined spectrophotometrically.[14] The light absorbance of the solution was measured in a Beckman Model DU spectrophotometer.

Flotation Results

Quartz-Slime System: A small amount of iron oxide slime in the system has a marked effect on flotation of quartz in that recovery is 85, 50, 6, and 2 pct in the presence of 0, 10, 20, and 40 mg slime per liter of water, respectively. Consequently pH-recovery curves were made at different slime concentrations. In the absence of iron oxide slime the recovery-pH curve is as shown in Fig. 1, curve *A*. The recovery is not affected by pH changes from 5.5 to 12. Below pH 5.5 the recovery decreases, first gradually, then rapidly, from 85 pct at pH 5.5 to 13 pct at pH 2.6.

In the presence of 25 mg per liter of ferric oxide slime, recovery begins to drop at pH 9 and becomes zero at pH 6 (Fig. 1, curve *B*). Increasing the slime content shifts the recovery curve increasingly toward the right. With 1 g per liter of slime (curve *D*) the floatability is greatly inhibited below pH 10.5.*

Corundum-Slime System: A similar study was made with corundum instead of quartz and sodium dodecyl sulfate in place of dodecylammonium acetate. The results shown in Fig. 2 suggest a mirror-image relationship for quartz and corundum.

Amount of Ferric Oxide Slime Coating

Quartz-Slime System: Using the slime elutriation technique, two series of tests were made on quartz without collector, one with a slime concentration of 1 g per liter and the other 2 g per liter. The results, presented in Fig. 3, show that maximum coatings of 10 mg and 12 mg of slime per gram of quartz, respectively, occur at about pH 8.

Three sets of tests with collector were made, each with pH as the independent variable. In sets *A* and *B*, the mineral was conditioned with slime and collector simultaneously for 10 min (*A*: 1 g per liter of slime, 25 mg per liter of dodecylammonium acetate; *B*: 1 g per liter of slime, 50 mg per liter of collector). In set *C* the mineral was conditioned first for 5 min with collector (25 mg per liter) and then slime was added for a second 5-min conditioning to give a slime concentration of 1 g per liter. Thus the total additions in sets *C* and *A* were the same, but the sequence was different. Results obtained are shown in Fig. 4, *A*, *B*, and *C*, respectively.

Comparison of the slime coating with and without collector shows that the collector in general reduces the slime coating except within a sharply delineated pH band between pH 9 and 10.

Corundum-Slime System: Fig. 5, curve *A*, shows results obtained with 1 g per liter of slime and no collector, at various pH values. Maximum coating, which is much less than that found for quartz, occurred at pH 8, and the coating decreased similarly on both sides of the peak.

Two sets of tests were made with collector, one with 12.5 mg per liter of sodium dodecyl sulfate, the other with 30 mg per liter. Results obtained are shown in Fig. 5, curves *B* and *C*, respectively. The peak of curve *B* (2.6 mg per g corundum) occurred at about pH 7, and the peak of curve *C* (5 mg per g corundum) at about pH 8. Thus, increasing collector concentration increases the coating.

Slime Coating Density

On the assumption of perfect cubes or spheres of average size, the calculated surface of the quartz used is 153 cm^2 per g. The measured surface (BET method, krypton) was 271 cm^2 per g, indicating a surface factor of 1.77. This is in line with the measurements of Hukki[15,16] and Yavasca[17,18] for a comminuted material in a size range displaying only a very small proportion of internal surface. It will be assumed that the *external* surface of the quartz used was 250 cm^2 per g.

The calculated surface of the alumina, on the assumption of perfect cubes or spheres of average size, is 86 cm^2 per g and the measured surface 276 cm^2 per g. In view of the sintered nature of the product and the small specific surface, it is believed that most of the measured surface is external surface, the large surface factor (3.2) being accounted for by the elongated habit of the particles. It will be assumed that in this case the specific external surface was 200 cm^2 per g.

The slime had a specific surface (BET, krypton) of 87,900 cm^2 per g corresponding to spheres 0.13 μ in diam. The appearance of the slime particles under low-power electron microscopy suggested an average size not over 0.3 μ. It will be assumed that the slime was of such a size that a complete con-

* For comparison, quartz was floated with dodecylammonium acetate in the presence of alumina, calcium fluoride, and kaolinite slimes. The adverse effect of alumina slime is similar to that of ferric oxide slime, whereas that of the two other slimes is different. Neither calcium fluoride nor clay inhibit the floatability above pH 7; however, in acid circuits clay slime seems to be less effective as a depressant than calcium fluoride slime.

tinuous monolayer would have been 0.2 μ thick, or weighed 0.10 mg per cm^2.

When these evaluations of mineral surface and slime-particle size are applied to the data of Figs. 3, 4, and 5 the following consequences emerge:

1) Maximal coating obtained on quartz, without collector, was 40 pct and 50 pct complete for the two slime additions tested.

2) Maximal coating on quartz, with collector, was about 45 pct (Fig. 4).

3) Maximal coating on corundum, without collector, was 7 pct (Fig. 5, *A*).

4) Maximal coating on corundum, with collector, was 25 pct (Fig. 5, *C*).

It is interesting to observe that the slime coating colored the mineral faintly in some cases, distinctly in most. In the case of corundum, without collector, just the coloring due to slime was noticeable across the central pH range. In all the other systems the coloring was much more intense.

Correlation between Slime Coating Density and Flotation Recovery

Since flotation follows the formation of partly complete collector monolayers 20Å in thickness, and since slime coatings have now been shown to be partly complete monolayers about 2000Å in thickness, it is interesting to examine their interplay.

First, it is possible that the slime consumes the collector. In the quartz-iron oxide slime-dodecylammonium acetate system, the data of Morrow[10] suggest that the collector consumed by the slime is but a very small percentage (3 pct) of the collector added.[11] For the corundum-iron oxide slime-sodium dodecyl sulfate no such estimation can be made, as adsorption data are lacking.

In the quartz system, therefore, the effect of slime coating on flotation, which is so great (Fig. 1), must be sought not along chemical lines but rather along mechanical or hydrodynamic lines. The authors are inclined to the view that a slime-studded mineral surface has a much smaller probability of making fertile contact with an air bubble than a clean surface.

Fig. 6 brings together data from floatability and from slime-coating density for the quartz system. *A* is the pH recovery curve in the absence of slime, *B* the pH recovery curve with slime present, and *C* the slime-coating density vs pH curve. The relationship between slime coating and decreased recovery is plainly seen.

Role of the Electrical Double Layer on Slime Coatings

The nature of the electrical double layers that surround both the slime particles and the coarser mineral particles has several effects on slime coating phenomena.

In this investigation the maximum slime-coating density was found to be about 50 pct coverage. Possibly this constitutes complete coverage, because the interaction of the double layers about two slime particles will prevent these particles from contacting each other. Under the conditions used in the authors' experiments, the electrical double layers are about 0.1 μ thick; hence the effective diameter of a slime particle will be 0.5 μ and not 0.3 μ.

The potential in the Stern plane, the zeta potential, is important in flocculation and dispersion, but since this potential varies with distance between particles whose double layers are interacting,[17] measurement of ξ will not yield the correct answers under flocculating conditions. Thus electrokinetic experiments in slime coating studies are valuable mostly for finding the identity of the potential-determining ions and for locating the zero point of charge, although the experiments may *indicate* the magnitude of the potential in the Stern plane under flocculating conditions. The charge at the surface of the three oxide minerals used in this investigation is controlled by the pH of the solution. Silica, iron oxide, and alumina are negatively charged at pH values greater than 3.7, 8, and 9.5, respectively, and are positively charged at pH values lower than these values.[9,11,12] The slime coating would be expected to be heaviest under conditions in which the slime is uncharged or is charged oppositely to mineral. Thus the densest coating of iron oxide slime on quartz should occur in solutions near neutral pH and the coating density should decrease as the pH becomes acid or basic. This is just what occurs (Fig. 3). Also, the densest iron oxide slime coating on corundum should occur at pH values where the minerals are oppositely charged, that is, between 8 and 9, but since the isoelectric points of iron oxide and alumina differ by only 1.5 pH units, the coating should be less than that on silica. This again fits the facts.

Summary

A new method has been developed to study quantitatively the slime coatings formed in flotation. It has been applied to a few simple systems. Correlation between coating density and decreased recovery is shown. Correlation between coating formation and surface charge is an inviting subject for further study.

Acknowledgment

The work was conducted at Massachusetts Institute of Technology under the sponsorship of the U. S. Atomic Energy Commission Research Division. The authors also express appreciation to P. L. de Bruyn and their other associates for an opportunity to discuss this work.

References

[1] S. G. Bankoff: *AIME Trans.*, 1943, vol. 153, p. 473.
[2] G. R. M. Del Guidice: *AIME Trans.*, 1934, vol. 112, p. 398.
[3] A. C. Dorenfeld: *Engineering and Mining Journal*, 1953, vol. 154, no. 5, p. 87.
[4] C. R. Ince: *AIME Trans.*, 1930, vol. 87, p. 261.
[5] S. C. Sun: *AIME Trans.*, 1943, vol. 153, p. 479.
[6] A. M. Gaudin: *Flotation*, p. 418. McGraw-Hill Book Co. Inc., New York, 1957.
[7] W. D. Harkins: *The Physical Chemistry of Surface Films*, chap. 6. Reinhold Publishing Co., New York, 1952.
[8] D. W. Fuerstenau: *Journal of Physical Chemistry*, 1956, vol. 60, p. 981.
[9] A. M. Gaudin and D. W. Fuerstenau: *AIME Trans.*, 1955, vol. 202, p. 66.
[10] A. M. Gaudin and D. W. Fuerstenau: *AIME Trans.*, vol. 202, p. 958.
[11] H. L. Miaw: *The Effect of Iron Oxide Slime Coatings on Flotation of Quartz and Other Minerals.* Master's thesis, Massachusetts Institute of Technology, 1957.
[12] H. J. Modi and D. W. Fuerstenau: *Journal of Physical Chemistry*, 1957, vol. 61, p. 640.
[13] D. W. Fuerstenau, P. H. Metzger, and G. D. Seele: *Engineering and Mining Journal*, 1957, vol. 158, no. 3, p. 93.
[14] G. M. Mellon: *Quantitative Analysis*, p. 529. Thomas Y. Crowell Co., New York, 1956.
[15] A. M. Gaudin and R. T. Hukki: *AIME TP 1779*, 1944.
[16] R. T. Hukki: *An Experimental Study of the Principles of Comminution.* Doctor of Science thesis, Massachusetts Institute of Technology, 1943.
[17] A. M. Gaudin and S. S. Yavasca: *AIME TP 1817*, 1945.
[18] S. S. Yavasca: *Surface Distribution in Comminution of Certain Materials.* Master's thesis, Massachusetts Institute of Technology, 1944.
[19] A. M. Gaudin and J. B. Morrow: *AIME Trans.*, 1954, vol. 199, p. 1196.

Discussion of this article sent (2 copies) to AIME before Aug. 31, 1958, will be published in MINING ENGINEERING.

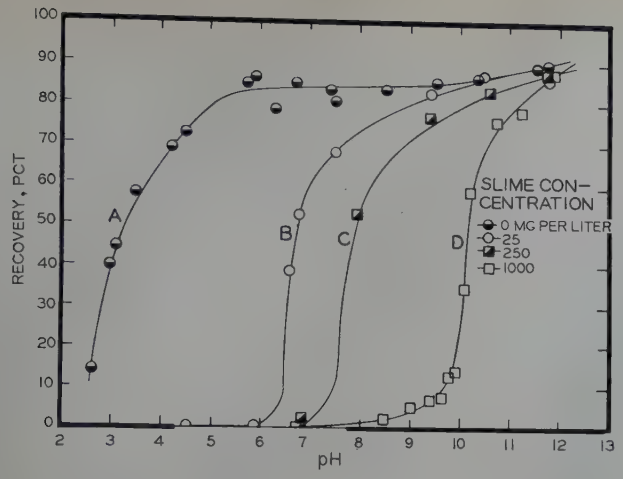

Fig. 1—Effect of ferric oxide slime on flotation of quartz as a function of pH. Test conditions: quartz, 1.0 g; water, 100 ml; DAA, 25 mg per liter; conditioning time, 10 min; flotation time, 1 min; gas flow, 0.3 ml per sec.

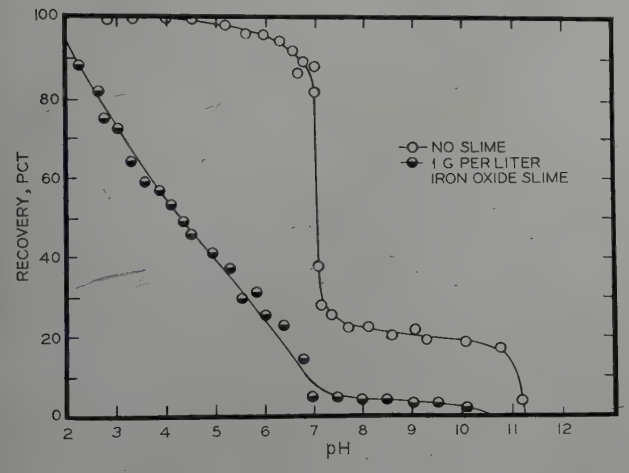

Fig. 2—Effect of ferric oxide slime on flotation of corundum as a function of pH. Test conditions: corundum, 1.4 g; water, 100 ml; SDS, 12.5 mg per liter; conditioning time, 10 min; flotation time, 1 min; gas flow, 0.3 ml per sec.

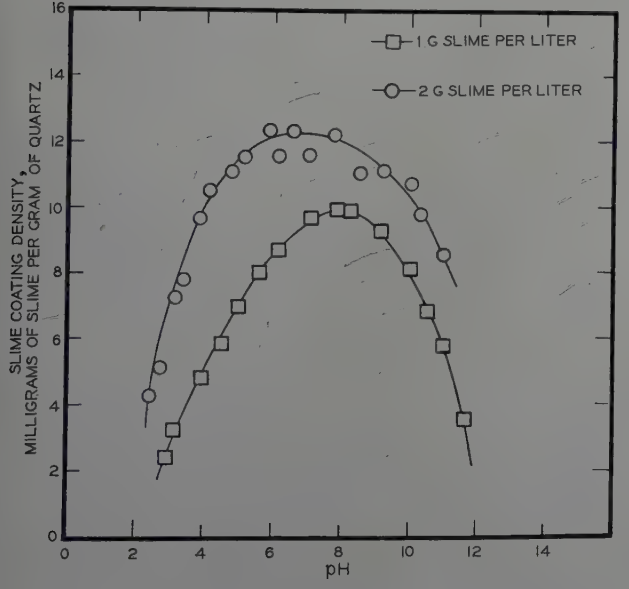

Fig. 3—Effect of slime concentration and pH on the ferric oxide slime coating density on quartz in the absence of collector.

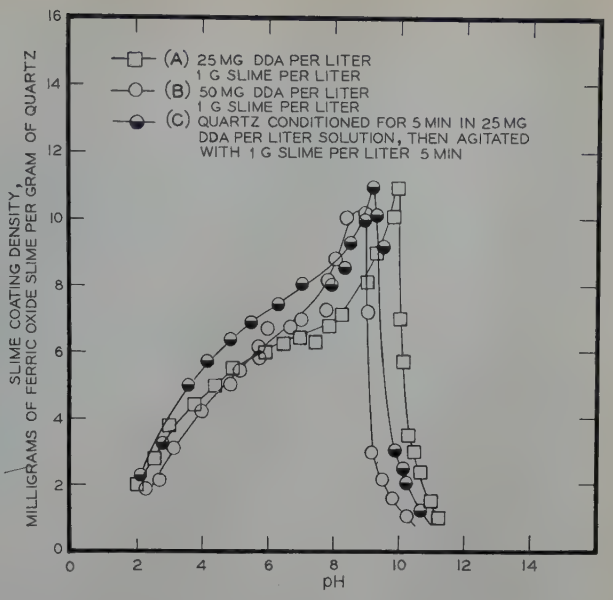
SLIME COATING DENSITY, MILLIGRAMS OF FERRIC OXIDE SLIME PER GRAM OF QUARTZ
pH
(A) 25 MG DDA PER LITER
1 G SLIME PER LITER
(B) 50 MG DDA PER LITER
1 G SLIME PER LITER
(C) QUARTZ CONDITIONED FOR 5 MIN IN 25 MG DDA PER LITER SOLUTION, THEN AGITATED WITH 1 G SLIME PER LITER 5 MIN

Fig. 4—Effect of conditioning and collector concentration of ferric oxide slime coating density on quartz.

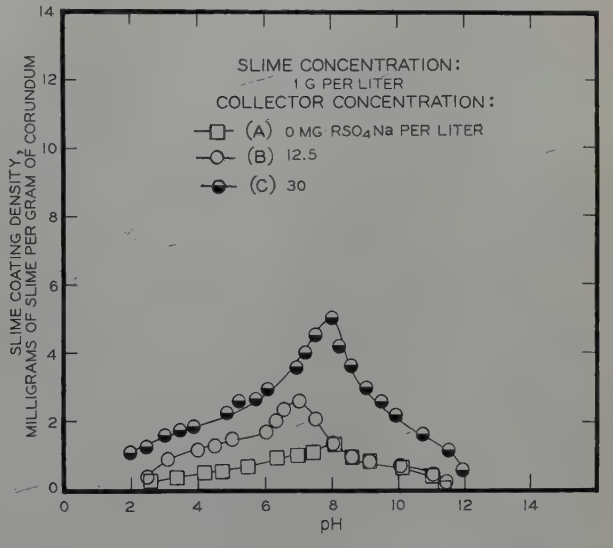

Fig. 5—Effect of collector addition on ferric oxide slime coating density on corundum.

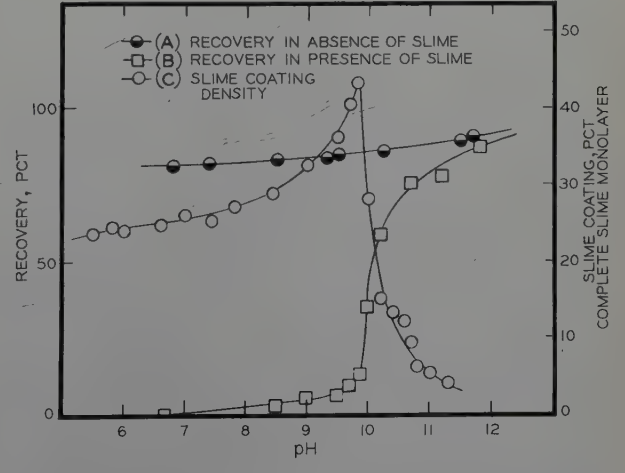
RECOVERY, PCT
SLIME COATING, PCT COMPLETE SLIME MONOLAYER
pH
(A) RECOVERY IN ABSENCE OF SLIME
(B) RECOVERY IN PRESENCE OF SLIME
(C) SLIME COATING DENSITY

Fig. 6—Relationship of recovery to slime coating density for quartz and 1 g per liter of iron oxide slime with 25 mg per liter dodecylammonium acetate as collector.

Technical Note

Improved Method for Measuring Aeration in Flotation Cells

by John B. Gayle

PRESENT flotation processes depend almost entirely on the buoyant properties of air bubbles to effect separations of mineral and gangue, but there is no convenient method for measuring aeration in flotation cells. Consequently the relation between aeration and cell performance has not been definitely established.

In connection with a comparative study of kerosene and froth flotation processes, a modification of the displacement method[1] was developed in which air escaping from the cell surface is measured with a wet-test meter. The arrangement shown in Fig. 1 is satisfactory for use with a number of cells and is not critical, except that care must be taken to use connections and tubing large enough to avoid excessive back pressures. Attempts to use smaller tubing resulted in back pressures that caused displacement of the liquid level in the receiver, so that some air was lost around the sides, an occurrence readily visible when measurements were taken with only water passing through the cell. With the arrangement shown, the manometer indicated an average reading of about ½-in. water pressure. No loss of air was evident.

Fig. 2 presents typical data for a standard Denver sub-A 24x24-in. unit cell operated at impeller speeds from 0 to 710 rpm. Each plotted point represents the average for five readings distributed over the entire cell surface. Readings were taken with only water passing through the cell. Results of this type have been used in a study of the influence of operating variables on cell performance and in detecting inherent differences in the operating characteristics of cells of various kinds.

Although the information presented in Fig. 2 resulted only with water passing through the cell, the apparatus is suitable for use during flotation of coal when various reagents are present. Possible modifications that might prove convenient under special circumstances include varying the size and shape of the receiver and substituting a calibrated, inverted, water-filled carboy or other gas-measuring device for the wet-test meter. If such modifications result in excessive back pressures, some form of draft should be applied at the discharge end of the measuring system.

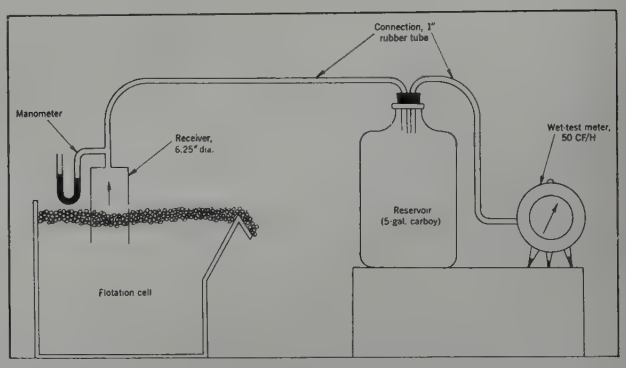

Fig. 1—Apparatus for measuring aeration in flotation cells.

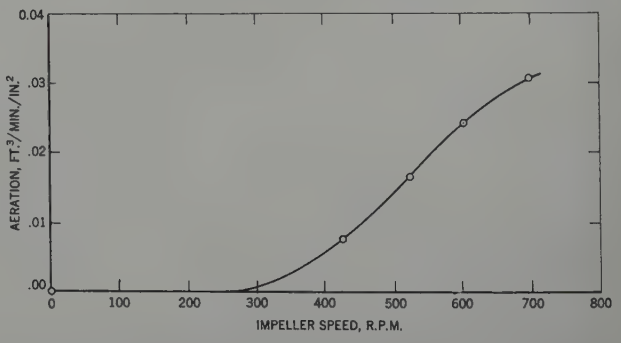

Fig. 2—Typical aeration data for semi-commercial flotation cell.

Reference

[1] Denver Equipment Co.: *Handbook*, 1954, p. 610.

J. B. GAYLE is Chief, Coal Laboratory, Southern Experiment Station, Tuscaloosa, Ala., Region V, U. S. Bureau of Mines.
TN 460B. Manuscript, April 28, 1958.

Bump Symposium

Progress in Control

Bump damage at Sunnyside Mines, December 1957.

This issue presents the first of several articles making up the Bump Symposium, which was held at the 1958 Annual Meeting of AIME. Other Symposium papers will appear in the September issue of MINING ENGINEERING.

THE term *mountain bump* describes the sudden rupture of one or more coal pillars under excessive stress. These bursts occur with varying degrees of violence and sometimes include adjacent strata, especially the bottom rock. Many failures do not develop enough violence to be dangerous and are regarded as an aid to coal production, but severe occurrences are accompanied by tons of flying coal, dense clouds of dust, and excessive gas emission. Such bursts sometimes throw heavy machinery several feet. Major factors to be considered in the problem are the nature of the strata above and below the seam and the depth of cover.

Bumps are classified as to their nature, extent of damage, and point of occurrence, e. g., *face bump, coal bump, high side bump, low side pavement bump,* and *district bump.*

The problem is extremely complex, and it cannot be over-emphasized that preventive measures, if they are to be successful, must be based on a thorough study of conditions in the individual mine. In western Canada, for example, the McGillivray mine, operating in a 9-ft seam at 2000 ft, has experienced severe bumps, but there have been no occurrences in the International mine, which operates in the same coal seam at 2400 ft, where the coal averages 17 ft thick. Differences in conditions governing the operation of these two mines are described in one of the following articles (see page 883). Again, most bumps in coal mines take place along pillar extraction lines, but at the Sunnyside mine in Utah they also occur a long way from active workings and sometimes in virgin territory. It is usual, too, for such failures to occur under fairly deep cover. But at Sunnyside, to cite only one instance, there have been disturbances along the main fault zone under less than 500 ft of cover.

All too often conditions favorable to bumps are revealed only by actual mining—at Springhill No. 2 mine, drilling in roof and pavement strata disclosed a 60-ft sandstone bed after operations had started—and where extraction has advanced too far for preventive measures to be incorporated in the mining plan, districts have had to be abandoned. But in an era when premium ores are being rapidly depleted in the face of rising demands, abandonment is not easily justified. There must be systematic planning to eliminate coal mine bumps, insofar as this is possible. As in the Gary district of West Virginia (see page 888) much has been accomplished by planned operations based on known factors in bump control. But even this is not enough. Precise instrumentation is needed to indicate where bumps are likely to occur, and in both the U. S. and Canada stress analysis studies are being carried out with this object in view. These pages reveal the progress being made.

In this issue:

U. S. Bureau of Mines Investigations and Research on Bumps
Edward Thomas
Ground Stress Investigations in Canadian Coal Mines
A. Brown
Control of Mountain Bumps in the Pocahontas No. 4 Seam
Woods G. Talman and John L. Schroder, Jr.

Next month:

Mountain Bumps at the Sunnyside Mines
John Peperakis
Deep Coal Mining in Springhill No. 2 Mine
W. F. Campbell
Coal Mine Bumps Can Be Eliminated
H. E. Mauck
Causes and Control of Coal Mine Bumps
Charles T. Holland

This page of Mining Transactions AIME follows p. 796. The intervening non-Transactions pages appeared in MINING ENGINEERING.

U. S. Bureau of Mines Investigations and Research on Bumps

by Edward Thomas

THE late George S. Rice was active in the investigation of bumps, particularly in the last ten years of his career as chief mining engineer of the U. S. Bureau of Mines. Since most of his investigation was carried out in Great Britain, continental Europe, and—to a lesser extent—Canada, his thinking on prevention was influenced considerably by the experience of those countries. It is not surprising, therefore, that when he was called upon a few years before his retirement to investigate bumps in the U. S. and suggest ways to prevent them, he turned to longwall mining. A longwall method had been most successful in combating the bump hazard in mining coal under deep cover, especially in Great Britain, but the prevailing method there at the time was advancing longwall mining, which he knew was uneconomical under U. S. mining conditions. For this reason he proposed a modified retreating longwall system that he believed included the best features of the advancing method.

As brought out by Rice,[1] if the cover is 2000 ft and 50 pct of the coal is extracted, the static load on the remaining pillars will be about 4000 psi, which exceeds the ultimate crushing strength[2] in most instances. If the pillar coal is overloaded before a pillar line is established, then the abutment zone preceding a line of extraction is no place to split pillars or extract them by any method other than an open-end system. Rice therefore advocated open-end mining, preferably by longwall, but he was willing to compromise with long-face mining if the longwall method was not acceptable.

Rice's system was put into operation in a mine in Harlan County, Kentucky,[3] but subsequent experience has shown that it did not take into account two important factors—avoidance of pillar-line points and maintenance of adequate development in advance of the pillar-line abutment area.

For ten years after Rice's retirement the USBM did little investigation and research on bumps, chiefly because so few were occurring that there was not much cause for alarm. But in 1951 there were three occurrences involving fatal injuries, and the Bureau began a statistical survey in that year. C. T. Holland, head of the department of mines at Virginia Polytechnic Institute, was retained as a consultant.

E. THOMAS, Member AIME, is Chief, Roof Control Research Group, Bureau of Mines, U. S. Department of the Interior, Pittsburgh, Pa.

TP 4768F. Manuscript, April 21, 1958. New York Meeting, February 1958.

The resulting study[4] of 117 case histories brought out these important conclusions:

1) Almost invariably the bump occurred in a locality affected by the abutment zones of one or more pillar lines.

2) In most cases the locality of the bump was influenced by the abutment zones of more than one pillar line. The term *pillar-line point* has been used for many years in the Appalachian region for such a situation. *Point* is used in the geographical rather than the mathematical sense.

3) In pillar-line extraction the following practices are safest in preventing bumps:

a. The mine layout should provide for pillars of uniform size and shape along the extraction line.

b. The mine layout should be planned so that no development need be done in the abutment zone of a pillar line.

c. The layout should permit open-end extraction of pillar lines from the next goaf, so that it will not be necessary to resort to pocket mining, splitting pillars, or any practice that will involve driving in the direction of the goaf within the abutment zone.

d. Pillars should be large enough to support area without undue roof and floor convergence before establishment of a pillar line.

These are, of course, generalities, and while they are useful in laying out areas where bumps can be expected, they are of limited help in many mines that were committed to a system of mining before it was realized that they were subject to bumps. Under such conditions it becomes necessary to choose between the following alternatives:

1) Abandon the territory, except for pillars that offer no extraction problems.

2) Through experience select the pillars that are most heavily loaded, and, by augering, induce bumps from a safe vantage point so that impinged loads are relieved. This method was first developed at the Gary, W. Va. mines of U. S. Steel Corp. and later adapted to mining thick coal beds at Kaiser Steel's Sunnyside mine in Utah. No scientific method is available to determine where to drill within a loaded pillar.

Although this method of unloading has worked very successfully at Gary—with one exception—

loaded pillars cannot always be pinpointed so readily, and no effective instrumentation has yet been devised to determine relative loading on various parts of a given pillar or the extent of relief obtained within the pillar after bumps have been triggered by drilling. There is a possibility of utilizing the microseismic equipment developed by Leonard Obert of the USBM, used with some success to predict rock bursts in deep ore mines. However, such use entails drilling holes for inserting geophones, and this might be extremely hazardous in a heavily loaded pillar.

Another possibility—one the Bureau intends to explore soon—is closer correlation of surface features, faulting, bedding, and other aspects with the loading and relief of pillars. At the same time an attempt will be made to measure minute differential movements along fault planes and correlate them with these data.

References

[1] G. S. Rice: *AIME Trans.*, 1934, vol. 19 (Coal Division).
[2] F. L. Gaddy: A Study of the Ultimate Strength of Coal as Related to the Absolute Size of the Cubical Specimens Tested. Department of Mining Engineering, Virginia Polytechnic Institute.
[3] J. F. Bryson: *AIME Trans.*, 1936, vol. 19 (Coal Division).
[4] C. T. Holland and E. Thomas: Coal Mine Bumps: Some Aspects of Occurrence, Cause, and Control. *USBM Bull. 535*, 1954.

Discussion of this article sent (2 copies) to AIME before Sept. 30, 1958, will be published in MINING ENGINEERING.

Ground Stress Investigations in Canadian Coal Mines

by A. Brown

RAPIDLY rising world demand for mineral products has accelerated depletion of the more readily accessible ores, particularly those of premium grade. Operations must proceed at a faster rate to deeper horizons, where there are problems of ground control that restrict economic recovery of the mineral and introduce new hazards to mine personnel. For some of the new Canadian mining fields severe problems of ground stress are still in the future, but much of Canada's mineral output comes from well established mines that have reached considerable depths.

It must also be anticipated that the depletion of premium grade ores will eventually necessitate mining low grade material at competitive cost, and unsolved problems of ground control can materially increase costs. Studies of ground stress phenomena in underground workings are therefore considered a present-day necessity, especially since these investigations must be a long-term effort owing to the highly complex nature of the problem and the difficulty of making full-scale observations.

In recent years the Mines Branch of the Department of Mines and Technical Surveys in Canada has conducted such an investigation. This report of the work is primarily concerned with stress problems in some Canadian coal mines and, in particular, with mine bumps.

Mines Branch investigations of this and related problems are carried out by a small team of mining engineers and physicists who, with assistance from geologists, pool their special skills in an integrated program. These Canadian investigations combine a field and laboratory approach. Since data obtained under contrasting mining conditions allow useful comparisons of ground behavior under stress, this article will present data gathered under a wide range of Canadian coal mining conditions. Two contrasting longwalls in eastern Canada will be discussed and two dissimilar pillar extraction operations in western Canada.

A. BROWN is Senior Mining Engineer, Fuels Division, Mines Branch, Department of Mines and Technical Surveys, Ottawa.

TP 4769F. Manuscript, Sept. 1, 1957. New York Meeting. February 1958.

Locale of Observations

In eastern Canada observations are being made in the collieries at Springhill, Nova Scotia. The district's No. 2 mine, which has a history of bump occurrences dating back to 1917, is currently being worked at a depth of 4200 ft. The mining method is longwall retreating along the strike and the practice is to retreat three walls in line, each about 350 ft long. There is no machine cutting or shooting—the coal is hand-picked and hand-loaded onto face conveyors.

There are three rows of hardwood chock block supports parallel to the coal face. These supports are built during the two daily coal loading shifts, and the rear line is withdrawn during the midnight shift. The goaves are partially packed by stone midwalls 12 ft wide which are built forward daily in step with the face advance. The seam dips at 15° and averages 9 ft of strong, well cleated bituminous coal enclosed in competent beds of shales, sandy shales, and sandstones of Carboniferous age. The bumps rarely disturb the retreating longwall faces but manifest themselves as violent upthrusts of pavement in the levels leading to the walls.

Observations have also been made in Springhill's No. 6 mine, which operated in a 5-ft seam of coal at a depth of about 2500 ft. Although No. 6 mine was

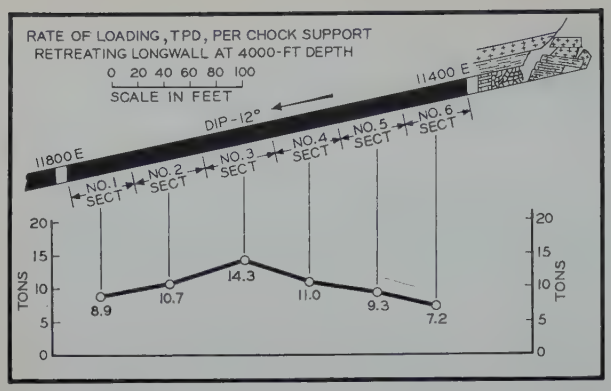

Fig. 1—Side view of longwall face in Springhill No. 2 mine, with graph showing rate of loading on artificial supports in different sections of the face.

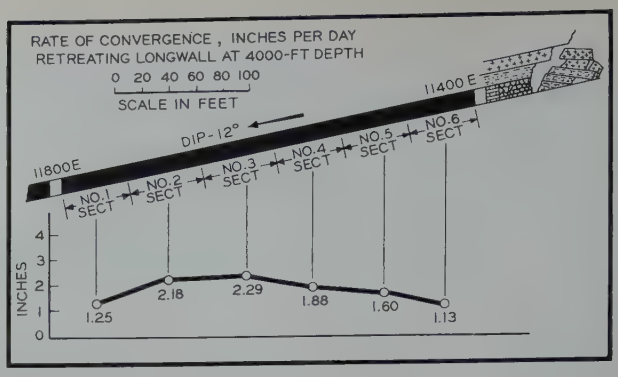

Fig. 2—Side view of longwall face in Springhill No. 2 mine, with graph showing observed rates of closure.

not as seriously affected by bumps as the No. 2, it was possible to make valuable comparisons regarding ground behavior in two dissimilar operations in the same coal field. As indicated, seam height and overburden were significantly different. Also, the wall faces in No. 6 mine were advancing, not retreating, and they operated on a daily cycle of undercutting, shooting, and loading. Lastly, the face observed in No. 6 mine was worked as a single unit and not in a combination of three as in the deeper operation. Face and gob supports were similar in both mines.

In western Canada, investigations into mine bumps have been conducted in the Rocky Mt. region in the Crowsnest Pass coal field, which has been affected by incidents of violent stress relief since 1907. The mining method generally employed in these thick, pitching seams is a retreating pillar extraction, but a modified form of longwall is used in a few mines where pitches are moderate. No packing is built in the goaves in either method and total caving is practiced. The enclosing strata, of Lower Cretaceous age, have been heavily faulted by mountain building forces and metamorphosed into unusually competent beds of shales, sandstones, and conglomerates. The orogenic stresses have also upgraded these Lower Cretaceous coals to medium volatile rank, but the accompanying processes of intense folding and extrusion have weakened them structurally and destroyed practically all evidence of bedding planes and cleat. Strata deformations ahead of extraction faces are of much less magnitude than those observed in the carboniferous measures of eastern Canada, and the less orderly advance of extraction lines tends to obscure trends in strata behavior. Even well to the rear of the extraction lines, ground falls are usually limited to the immediate roof beds, and it appears likely that long, flat arches are established that extend for considerable but as yet unknown distances into the goaves. A further interesting point of rock behavior is that although the strata are highly faulted careful measurements have failed to indicate any slippage across such discontinuities even at and behind the extraction faces.

The bumps are characterized by a violent upheaval of the floors and generally occur on or near the extraction line. There have been, however, early incidents in the Fernie area of the Crowsnest coal field where multiple roadways leading to large areas of total extraction were affected at greater distances. Usually the bumps are associated with broad, totally extracted areas under competent roofs that are able to sustain wide unsupported spans. In some of the earlier occurrences they have been attributed to the failure, over broad areas, of inadequate coal pillars.

To obtain a comprehensive understanding of ground behavior associated with longwall and pillar extraction methods, it is considered essential to attempt observations in the three zones represented by the extracted area, the production face, and the solid coal into which the face is advancing. It is also considered advisable, in order to obtain comparative data, to conduct such observations in both *bumping* and *non-bumping* mines. Observations in the open workings, as represented by the production face and its servicing roadways, usually include measurements and the loads imposed on artificial supports. For such purposes a number of reasonably reliable devices are available. The greatest difficulties lie in designing apparatus for observing stress changes in the solid strata and for remote measuring of closure and the re-establishment of ground loads in totally extracted and inaccessible areas. Since a knowledge of what transpires in these two zones is considered essential to further progress in ground stress investigations, considerable importance is attached to stress analysis studies leading to instrument development. A serious handicap in the selection and design of measuring techniques is created by the necessarily strict mining laws governing the use of electrically operated devices in coal mines. For mutual benefit, the Mines Branch promotes close liaison with research groups contesting with similar problems in other countries.

Within the limitations of this discussion it is possible to indicate briefly the object of various underground and laboratory programs and to present some examples of what has been observed.

Ground Behavior at Extraction Perimeters

To deal first with what may be broadly classified as *open workings,* observations have been concerned primarily with ground behavior on the edges of solid coal bordering totally extracted areas of the seam. Knowledge of wall closures and support loads along these edges gives some indication of how the ground loads are imposed on the solid coal and also the manner in which strata equilibrium is being restored in extracted areas. Hydraulic dynamometers of the telescoping prop variety and the flat cell type have been found useful. For closure observations a dependable recorder is on the market which can be supplemented with simple telescopic convergence rods for large-scale studies. These rods are particularly useful where rapid closure is occurring and frequent readings are being taken. In

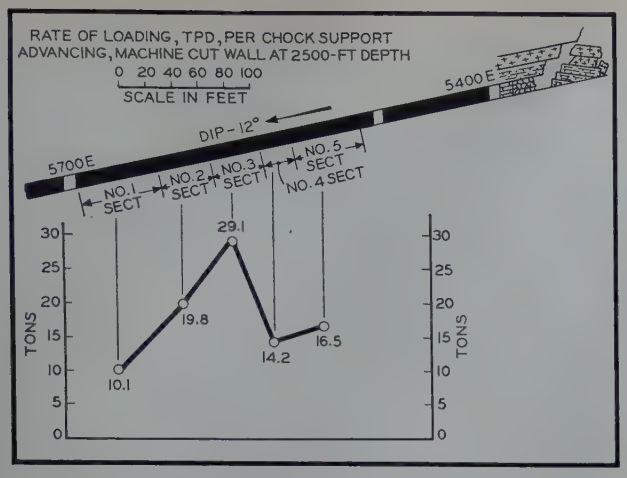

Fig. 3—Side view of longwall face in Springhill No. 6 mine, with rates of loading.

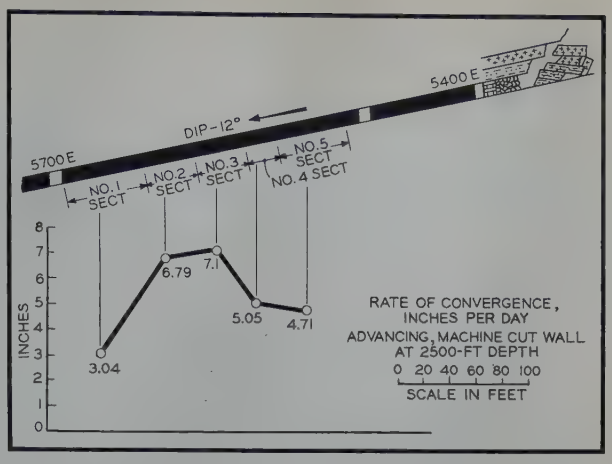

Fig. 4—Side view of longwall face in Springhill No. 6 mine, with graph showing observed rates of closure.

longwall operations the units are usually installed not only along the extraction face, but also in the levels servicing these walls. In a pillar extraction the instruments are deployed in grid fashion in rooms and levels ahead of the extraction line. As may be expected, underground conditions often prevent placing such apparatus in the most desirable positions. Also, the operations being studied may later be changed to an extent that will nullify or impair the value of the observations.

Fig. 1 is the side view of a longwall face in the Springhill No. 2 mine, with a graph showing rate of loading on the artificial supports in different sections of the face. It will be noted that the maximum values occurred approximately 100 ft above the lower end of the wall. Fig. 2 is the same side view illustrating the observed rates of closure in these same sections. Fig. 3 is a side view of a longwall face in the No. 6 mine, with a graph showing rates of loading on the supports. Fig. 4 illustrates the rates of closure in these same sections along the face. It is interesting to observe that in both mines the highest rate of support loading and the highest rate of convergence occurred in approximately the same position on the working face.

Conceivably the dominant common factor that would bring about such a similar result under widely different operating conditions is significant similarity in the strength of the rocks enclosing both seams. If rocks are not too dissimilar in characteristics they can be expected to fail in somewhat the same way in extracted areas and to set up a recognizably similar pattern of stress in the coal bordering the goaves. Since the total pitch length of the coal block in each mine was approximately the same, about 350 ft, it is also interesting to note that the distance from the edge of the older goaf (which lies on the rise side of the block) to the zone of maximum stress is nearly the same in each case. This distance may indicate the position of an abutment zone set up through the combined influence of the older goaf above and the new void being created by current extraction. The point of particular interest is that the increased depth apparently did not significantly modify the position of maximum loading on the exposed edge of a massive coal block. Of some significance also is the proximity of such an active zone to the level leading to the foot of the upper wall in No. 2 colliery, where three walls are operated in line. It is in this uppermost haulage level that almost all bumps in the active workings occur.

A striking parallel to this observed pattern of stress on long extraction faces in Springhill is reported[1] in the Champion Reef mine of the Kolar gold fields where a modified form of rill stope is employed with advance along the strike. It is reported that crushing of the upper portion of the block being mined will throw the pressure of the enclosing rock walls onto the bottom of the stope, which may then build up a tremendous amount of strain energy before failing.

Although such face observations were undertaken primarily to study ground behavior along the perimeter of massive coal blocks, the data also indicate the effects produced by individual mining operations at the coal face. Fig 5 illustrates the development of total convergence and the growth of support loading in No. 2 mine. It will be observed that convergence increases in a fairly linear fashion and indentations in the curve are due to decreased rate during shifts not producing coal. It is apparent that convergence proceeds in unison with coal removal and is promptly retarded when production ceases. Examination of the curve depicting growth of support load shows a reasonably linear relationship up to about 30 tons. Thereafter the rate of loading decreases. This lowered rate is considered due to yielding of the supports and floor rock rather than to a decrease of load.

Similarly, the results of face observations in the shallower No. 6 mine are illustrated in Fig 6. It will be observed that convergence proceeds in a generally linear fashion between the coal face and the caving line, with appreciably increased rates occurring during the coal loading shifts. The loading curve is reasonably linear up to a load of 50 tons and thereafter decreases.

Further reference to Figs. 5 and 6 reveals that the conditions observed in No. 6 mine, working at a depth of 2500 ft, were more severe than those observed in No. 2 at about 4000 ft of cover. It is therefore evident that under Springhill conditions depth is not a controlling factor in establishing the rate of closure and support loading on a longwall face. It would appear that a more significant factor is the type of face operations. In regard to speed of advance, the shallower, machine-cut wall advanced 6 ft per day while the deeper, hand-pick face advanced about 4 ft. On the basis of convergence per foot of daily advance the machine cut wall converged, on the average, 0.75 in. per ft of advance; the corresponding figure for the deeper operation

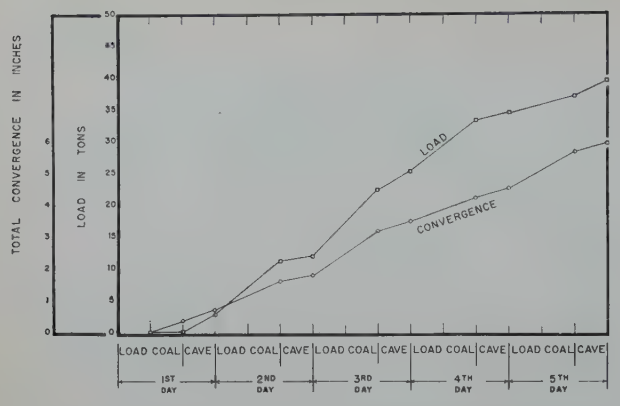

Fig. 5—Development of total convergence and the growth of support loading in No. 2 mine.

was 0.3 in. It is useful to compare such values with those obtained by Schwartz[2] in French mines for longwall operations using metal props and by N. S. Stephenson and S. Lewis[3] in United Kingdom collieries. Schwartz reports a daily convergence of 0.44 in. per ft of daily advance; a value of 0.62 in. was obtained by Stephenson and Lewis. These were for *non-bumping* mines and represented reasonably good face conditions.

The above observations at Springhill indicate that the loads effectively borne by the face supports can be imposed by the first 20 ft or so of strata immediately above the seam. It is therefore apparent that the bulk of the strata loading above the working area must be borne by the rock beds at no great distance from the seam. Their ability to perform this function depends on the care taken to preserve their strength, particularly when mining operations of undercutting and shooting are employed, as these can seriously deteriorate face conditions by weakening nearby rock beds. A speedy installation of adequate face supports under newly exposed roof can appreciably preserve the self-sustaining nature of the immediate strata.

Observations in the levels servicing such longwalls seek to determine the pattern of ground loading along these exposed edges of the large coal blocks being mined. It is hoped that these fringe studies in the *open*, in conjunction with observations made at the extraction faces, will clarify and support information obtained with borehole instruments in the *solid*. Elevation surveys were originally employed to differentiate between roof and floor movements, but results were not accurate enough to warrant continuing with this method, chiefly because there is no dependable base station within reasonable distance of the observation points. In the pitching seams of western Canada it was found impossible to attain acceptable accuracy in the inclined workings. In these western mines some trials were made with water-level devices in pitching rooms, but the long lengths of flexible tubing required were cumbersome and liable to damage in the coal chutes. Insofar as strata movements are concerned, therefore, much dependence is being placed on total convergence measurements, as these are direct measurements and quite reliable if taken carefully. In the case of the Springhill mines all evidence to date indicates that most of the convergence in roadways is due to floor lift.

Fig. 7 illustrates the closure observed at typical roadway stations plotted against distance to the wall face. For comparison, two samples are given of convergence observed in a Pennsylvania mine[4] and in a longwall operation in France.[5] These mines, particularly the Pennsylvania mine at 600 ft of cover, are substantially shallower than those at Springhill. The much greater amount and rate of convergences and distance affected in the Springhill roadways may be typical not only of coal mines operating under exceptionally deep cover but particularly of those possessing competent enclosing strata.

Reference to Fig. 7 will also reveal that two of these typical Springhill stations were chosen from among those with relatively narrow spans of gob (300 and 500 ft) while the other two were selected from those with wider spans (1500 and 1800 ft). There is no great difference between the 500, 1500, and 1800-ft spans, indicating that at Springhill the rate of closure on the levels does not progressively increase with growth of gob spans. Further information from continuing studies may possibly reveal that beginning at very short spans of 100 to 200 ft, there is a pattern of increasing convergence with increasing span up to a certain maximum width of gob and that thereafter the relationship does not change materially.

Fig. 8 illustrates the closure, with time, at a roadside station that was very close to two destructive bumps occurring within 16 days of each other. The decreased rate of convergence in the period preceding these bumps may indicate a temporary decrease in ground stress at this point or, equally, the existence in this part of the roadway of strong pavement strata more resistant to yielding under increasing load and thereby able to store energy and release it violently. Because of the marked heterogeneity of rock beds it is conceivable that such stronger zones can exist in the roadways, perhaps at irregular intervals, and serve as potential *loci* for bumps. More extensive study of the behavior of floor rocks in roadways is certainly warranted.

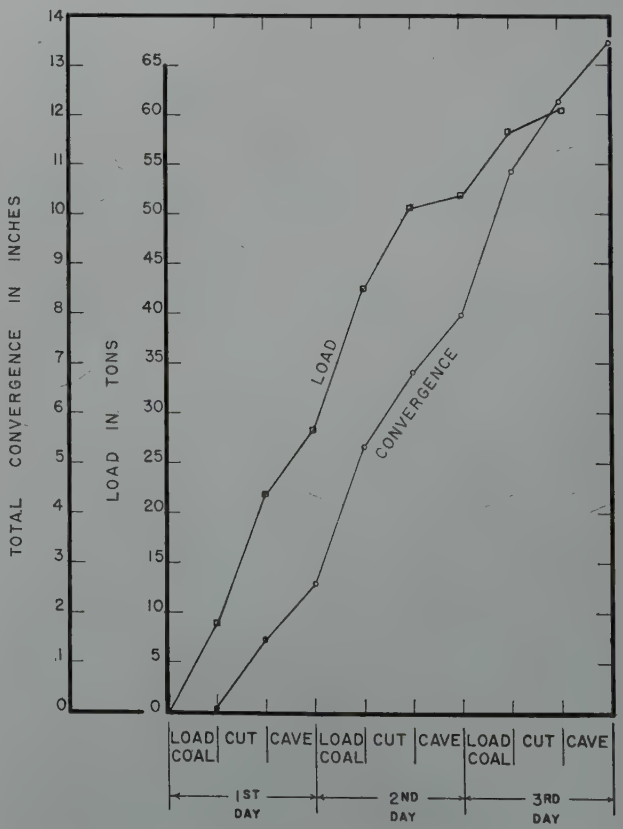

Fig. 6—Results of face observations in No. 6 mine.

Of the mines observed in western Canada only two—in Coleman, Alberta—will be considered. The McGillivray mine operates in a 9-ft coal seam at 2000 ft and the International mine operates in this seam at 2400 ft, at a point where the coal averages 17 ft thick. The McGillivray mine is subject to severe bumps; there have never been any occurrences in the International mine. The strata enclosing both mines are, on the whole, massive and competent, but in International the rock beds in immediate contact with the seam are relatively weak shales, whereas in McGillivray mine the rocks in immediate contact are more competent sandy shales, sandstones, and conglomerates. Although many faults intersect both workings, the strata are more severely folded in the McGillivray area, pinching out the seam in some locations and causing variations of 30° to 60° in the dip. With some local changes, usually at faults, the pitch in the International mine is fairly uniform at 30°.

Both mines use pillar extraction on the retreat. The practice is to drive a two-place level entry from the main haulage slope for several thousand feet along the strike to a predetermined boundary. Rooms are then driven up pitch to an older level above to begin pillar development at the inside end. Pillar extraction follows closely on pillar development and the two operations retreat toward the main slope. The panel of coal under exploitation extends the full length of the level entry and 400 ft along the pitch. To the rise side of this panel the totally extracted area extends for several thousands of feet towards the outcrop. Although there are some variations in size of pillars in each mine, those in International are approximately 85-ft square blocks and in the McGillivray mine 85 ft on the strike and 50 ft on the pitch.

In the thicker seam of International mine all development work is done in the top 7 ft of coal; the full height of the seam is subsequently mined at the pillar extraction line. In the McGillivray mine development work proceeds in the full thickness of the seam.

Bumps in the McGillivray mine have occurred on the pillar extraction line and also for distances up to 200 ft ahead, where they are usually associated with pillar splitting operations. Although International mine has never been affected by bumps, there is a slow but heavy extrusion of the bottom 10 ft of coal into the rooms and crosscuts that frequently closes them completely and necessitates re-driving. This extrusion is observable for several hundred feet ahead of the pillar extraction line.

Fig. 9 illustrates the closures observed on level roadways servicing the extraction lines in these two collieries. To complete the comparison an equivalent record is included for a roadway leading to a retreating longwall in No. 2 mine at Springhill. This figure shows the closure that occurred during a 500-ft advance of each of these three extraction faces. At the end of this advance, the extraction lines had arrived at the observation points. The horizontal axis of the graph indicates the length of time required to advance each extraction line the 500 ft. This method of comparing results over a long period and for a large advance was adopted because of the very irregular nature of the pillar extraction lines and the virtual impossibility of deciding, from pillar plans, just what the true shape and successive positions of the pillar line were during short intervals. All three operations progressed at normal

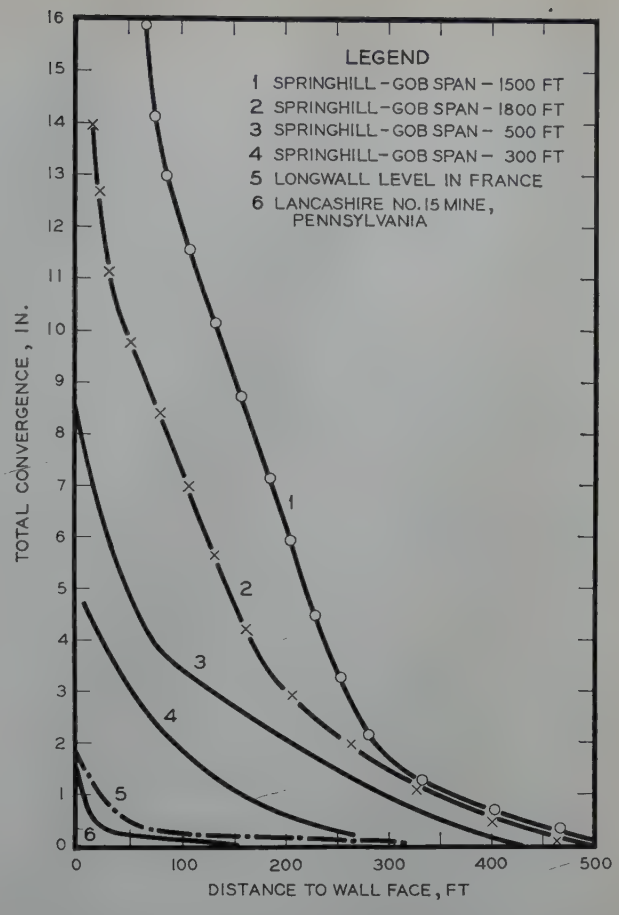

Fig. 7—Closure observed at typical roadway stations plotted against distance to wall face.

speed during their selected periods, but the effect of an annual holiday period at Springhill is revealed by a flattening graph about 50 days before the end of these observations.

The rigidity of ground in McGillivray mine is apparent from this record, especially in comparison with the adjoining International. It is reasonable to assume from the ground behavior observable in both mines that the freedom from bumps in International operations, under the same massive cover as its immediately adjacent neighbor, is due to the more yielding characteristics of the seam and its immediate roof and floor rocks. Such strata cannot, apparently, store up enough strain energy for violent release. However, it should not be inferred that the seam in the McGillivray is a strong coal capable of large resistance to converging rock walls, for it is quite characteristic of the sheared and friable coals of the Rocky Mt. region. It is not, for instance, as strong a coal as that of Springhill. Nevertheless, it will be observed from Fig. 9 that closure at McGillivray is markedly less than in Springhill. The answer must lie in the greater strength of the McGillivray rock beds, which are able to sustain long spans across yielding pillars and totally excavated areas. It is suggested, therefore, that in the pillar development area ahead of the McGillivray extraction line, the roof and floor strata may already be largely self-supporting but converging slowly enough, as indicated in Fig. 9, to maintain the enclosed pillars in a high state of stress for applicable periods before crushing. Experience at the mine indicates that pillars directly on or adjacent to the pillar extraction line are still highly stressed and

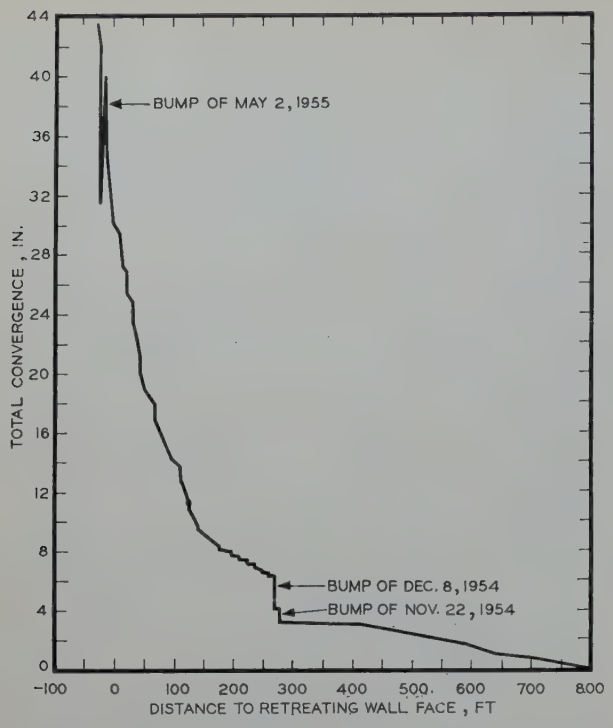

Fig. 8—Closure, with time, at a roadside station close to two bumps occurring within 17-day period.

generally can be mined safely only by taking successive slices off the destressed edges. An improved practice based on this concept would be to encourage greater yield in pillars by making them originally of reduced size, thus lowering their capacity for storing strain energy. Similarly, large pillars already formed could be split well in advance of the extraction line and before they come under the influence of the forward abutment pressure zone.

Measurements in the Solid

Further significant understanding of the mechanics of ground failure depends on the application of all available knowledge of stress analysis and the degree to which this knowledge can be utilized when operations are dealing with such heterogenous and aeolotropic materials as mine rock, which exhibit both elastic and plastic deformations under stress. In such studies due consideration must be paid to the phenomena of time strain and the influence of constraint on the behavior of rocks under stress. In this direction of continuing exploration into the largely unknown field of ground mechanics, it is encouraging that very substantial progress has been made during the last quarter-century in the allied field of soil mechanics. As an outgrowth of current studies at the Mines Branch, a beginning has been made in developing apparatus to observe stress changes *within the solid*, in the hope of gathering basic data related to stress conditions remote from open workings. To date, fairly extensive field tests have been conducted with a borehole load cell incorporating electric resistance strain gages, an electrical resistivity device, and ultrasonic apparatus. The load cell has been tested in both coal and metal mines, but the resistivity device was specifically designed for coal mines subject to gas outbursts and the ultrasonic equipment was designed for metal mines. For the sake of brevity only load cells will be discussed here.

With regard to borehole cells in general, it was initially considered that valuable preliminary information might be obtained by employing a simple hydraulic type as a scouting device pending development of a more precise unit. Consequently a number of hydraulic cells, molded from rubber, 3 ft long and 1½-in. diam, were installed inside boreholes drilled 50 ft deep into large coal blocks in the Coleman mines. The cells were grouted in with a mixture of coal dust and gypsum cement, then raised to initial pressures of 60 to 75 psi. Observations were continued for more than a year and until the pillar extraction line had reached the cells. Fig. 10 is a graph of the pressures observed with one cell as the extraction line progressed more than 1100 ft to meet it. Although it would be inadvisable to interpret much from this record, it does indicate that mining-induced stresses are detectable inside large coal pillars at appreciable distances ahead of an extraction line and that pressure on the embedded cell kept increasing as the extraction approached. Pending further trials with hydraulic units of improved design no explanation will be attempted for sudden changes in observed pressures such as that indicated at 650-ft distance in Fig. 10. As a borehole unit this simple type of hydraulic cell can be used in highly deformable materials only, such as the mountain coals of western Canada and possibly the soft clays of the Prairie mines.

When the Mines Branch began development of more precise types of borehole load cells, it was decided that observations of stress in a single direction should be extended to include the two principal stresses and their orientation. Also, since the units were intended for underground mines, they must retain a satisfactory degree of accuracy and reliability over long periods. A further requirement is that any such device must comply with strict mines regulations regarding safety. The development of a device embodying all these requirements presents unique difficulties.

Initial attempts have been to develop a strain-gage load cell incorporating electric resistance strain gages bonded to a strain-sensitive member of known elastic constants. Such efforts have been adequately reported in earlier papers,[6-8] and only the essentials will be given here. The main component is a metallic load-bearing disk of 2-in. diam and 3/16 in. thick, as designed for anticipated ground stress conditions at Springhill, with a rectangular rosette electric resistance strain gage bonded to each face. This type of gage has three separate strain-measuring elements mounted in horizontal, vertical, and 45° positions.

Stress in the disk is calculated from the formulas:

$$\sigma_1 = \frac{E}{2(1-\mu)}(e_1 + e_3) + \frac{E}{2(1+\mu)}\sqrt{\left[2e_2 - (e_1 + e_3)\right]^2 + (e_1 - e_3)^2}$$

$$\sigma_2 = \frac{E}{2(1-\mu)}(e_1 + e_3) - \frac{E}{2(1+\mu)}\sqrt{\left[2e_2 - (e_1 + e_3)\right]^2 + (e_1 - e_3)^2}$$

$$\theta = 1/2 \tan^{-1}\left[\frac{2e_2 - (e_1 + e_3)}{e_1 - e_3}\right]$$

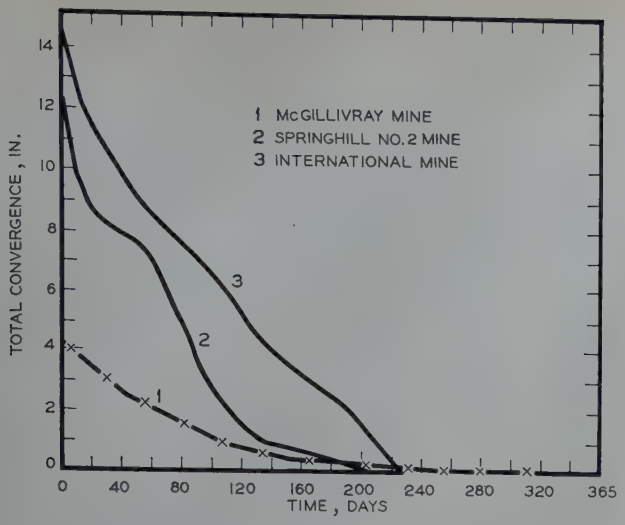

Fig. 9—Closures observed on level roadways servicing extraction lines at McGillivray and International mines. For comparison, a similar record is shown for roadway leading to retreating longwall in No. 2 mine at Springhill.

where σ_1 = maximum principal stress.
σ_2 = minimum principal stress.
θ = angle from direction of e_1 to σ_1.
e_1, e_2, e_3 = strains measured from rosette gages.
E = elastic modulus of disk material.
μ = Poisson's ratio of disk material.

In practice, the angle θ defining the direction of the maximum principal stress is expressed counterclockwise from the horizontal. Originally, the load-bearing disk was made of magnesium to take advantage of its low modulus of elasticity and thus obtain a high strain sensitivity to change in applied stress. Later, because of a possible sparking hazard associated with light alloys, the disk was made of steel but sufficiently decreased in section to retain enough sensitivity to changes in stress. In the earlier magnesium cell, the load-bearing disk was mounted inside a thin-walled cylindrical steel shell, but the later steel models were machined out of solid stock so that the disk became an integral part of the outer shell. The cylindrical shell has tightly fitted end caps to help exclude moisture and dust. Other essential components are a dummy gage for compensation of apparent strain due to temperature changes and a leveling device for proper orientation of the rosette grid at the back of the boreholes. Ancillary apparatus includes special inserting rods and a plunger device for depositing at the back of the borehole the desired quantity of grouting material, into which the cell is subsequently embedded. A five-conductor cable, usually in 50-ft lengths, is carefully connected on surface to the active and dummy gages and led out of the cell through a tight waterproofed gland. Readings may be taken with any satisfactory strain gage bridge, but because of the safety requirements in coal mines a specially designed low-current bridge, battery-operated, was constructed at the Mines Branch. Laboratory tests with this type of cell embedded in blocks of concrete and coal gave a repeatable relationship between load applied to the unconfined blocks and the observed stress changes in the disk. It will be readily appreciated, however, that the observed stress in such a metallic inclusion does not represent the magnitude of the stress in the enclosing medium, and while laboratory tests to date give some idea as to

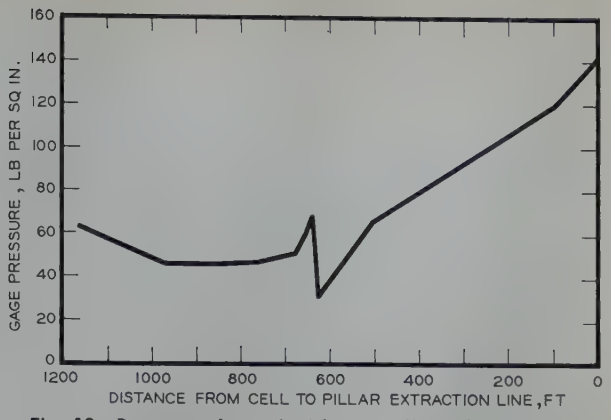

Fig. 10—Pressures observed with one cell as the extraction line progressed more than 1100 ft to meet it.

the ratio between the two under some specific conditions, much more testing remains to be done. To illustrate what has been observed at depth in the longwall workings at Springhill, Fig. 11 is the record of a cell over a three to four-month period as the wall face progressed from 380 ft to approximately 200 ft from the cell. This unit was installed in the coal 50 ft above the lower roadway in Fig. 1. As may be noted, the increase in stress in the cell is fairly gradual but proceeds in a series of jogs; this is quite typical of what has also been observed in the open workings during current and earlier[9] investigations. The principal stress is dilational and the shear stress is of small magnitude.

The shortcomings of the strain-gage load cell are caused to some extent by the rugged underground conditions under which it must be applied and by the problems of making strain gages stable over extended periods. Damage to cells has ranged from crushing of the cell bodies and straining of the load-bearing disk beyond the elastic limit—under what must be abnormally high stresses in the coal—to rupture of the electric cable by great extrusions of the coal seam toward the mine openings as the extraction face nears the installed cells. Another serious difficulty is encountered in drilling the required boreholes in highly stressed areas of the seam. In such areas, holes have readily been drilled into the coal for distances of 20 to 30 ft using light hand-held rotary drills, but immediately beyond these distances the holes collapse, jamming the rods and effectively preventing any further progress even with the heaviest drilling equipment available at the property. It is also considered that moisture has an important effect on the breakdown of cells despite very careful waterproofing. It is appreciated, of course, that this type of unit is essentially a strain-sensitive strut that indicates deformation of the borehole. In this respect its behavior is doubtful when the disk does not lie in the plane of applied stress. But even with these drawbacks, this type of borehole cell can provide useful data in underground observations.[7]

From theoretical considerations it can be shown that if the load cell has a modulus of elasticity at least three to four times greater than the surrounding media, then it is possible to relate changes of stress in the cell to those in the media. This method offers the advantage of not requiring an accurate knowledge of the modulus of the surrounding media.[10]

On the basis of this theory the Mines Branch is also developing an inclusion type of cell. Ideally

Table I. Mean Values of Elastic and Failure Characteristics for Some Canadian and European Mine Rocks under Uniaxial Stress at Room Temperature

Location	Rock Type	Aggregate Thickness Sampled, Ft	N	E_c	P_u	u	W	B	Type of Violent Stress Relief
Canmore, Alberta	Shale (slatey) †	Random samples	11	4.3x10⁶	49x10³	0.09	280*		Outbursts of gas and coal
	Shale (slatey) †		7	3.2	27	0.13	113*		
	Shale (slatey) †		3	5.5	55	0.13	275*		
Coleman, Alberta International mine	Shale	99	24	4.1	19	—	40	29	None
	Sandy shale	42	32	5.0	22	—	56	30	
	Sandstone	37	21	5.9	34	—	108	32	
	Conglomerate	45	10	4.9	26	—	72	28	
Coleman, Alberta McGillivray mine	Shale	108	33	3.9	15	0.09	14	25	Bumps
	Sandy shale	60	6	3.4	21	0.09	67	—	
	Sandstone	260	153	4.3	31	0.08	113	33	
	Conglomerate	4	5	3.6	32	—	167	30	
Cape Breton coal fields, Nova Scotia	Shale †	Random samples	2	1.8	11.3	0.22	36*		None
	Shale (clay) †		2	0.7	6.3	0.25	28*		
	Sandy shale		38	5.0	27.0	0.13	73*		
	Sandstone		13	1.6	8.5	0.48	23*		
Fernie, B. C. Elk River and Coal Creek mines	Shale †	240	12	5.6	25	—	56*		Bumps and outbursts of gas and coal
	Shale †		7	4.4	32	0.11	116*		
	Sandy shale	—	10	5.4	31	—	86*		
	Sandstone	85	35	6.0	25	—	52*		
	Conglomerate †		14	5.7	26	—	59*		
	Conglomerate †	61	1	4.8	37	0.12	142*		
Springhill, N. S. No. 4 mine	Shale	107	30	4.0	20	0.10	55*		Bumps
	Sandy shale	137	100	4.0	30	0.10	112*		
	Sandstone	64	105	4.5	25	0.10	69*		
Springhill, N. S. No. 2 mine	Shale	70	18	5.1	18	0.17	32*		Bumps
	Sandy shale	76	175	6.4	24	0.15	45*		
	Sandstone	46	110	4.6	22	0.11	53*		
Brodsworth, England Barnsley seam	Shale	Random samples	4	4.5	20	0.18	45*		None
Kilnhurst, England Parkgate seam	Sandstone	Random samples	12	2.7	16	0.20	47*		Bumps
Lorraine Collieries, France	Shale	Random samples	9	3.0	12	0.25	24*		None
	Sandy shale		6	3.5	22	0.10	70*		
	Sandstone		5	1.2	6	0.35	15*		
	Conglomerate †		4	2.0	9	0.34	20*		
	Conglomerate †		4	3.2	18	0.13	51*		
Neumehl, Germany	Sandstone †	Random samples	13	2.2	15.7	0.21	56*		Bumps
	Sandstone †		18	3.5	23.9	0.09	82*		

N = number of test specimens.
E_c = compression modulus, lbs/in.²x10⁶.
P_u = ultimate compressive strength, lbs/in.²x10³.
u = Poisson's ratio, dimensionless.
$W = \frac{1}{2}\frac{P_u^2}{E_c}$ strain energy at failure, in.-lbs/in.³
B = fracture angle, degrees.

† Groups of the same material with appreciably different characteristics or obtained from a different location in the area.
* Values calculated from mean values of compression modulus and ultimate compressive strength as listed in table.

this cell should take the form of a solid cylindrical metal inclusion, but a compromise must be reached in the design, as there is the problem of measuring the stresses inside this inclusion. It is also desirable to be able to measure stress in an arbitrary direction. This requirement is met by splitting the metal cylinder along the axis and sandwiching between these two halves a thin metal flat-jack filled with oil. The stresses exerted on this oil are recovered by a diaphragm type of recorder using electrical resistance strain gages. Work along much the same lines is being conducted in the United Kingdom. With this method it is essential to use the minimum volume of oil in order to maintain the effective elasticity of the load cell at a high enough level. It is also proposed to locate the diaphragm recorder in the roadway, so that if the electrical strain gage fails it can be replaced with minimum loss of readings.

In conjunction with the development of this cell, another type of cell is being developed to measure the magnitude and direction of two principal stresses. For this it is proposed to use a thick-walled steel tube. It is hoped to measure the stresses in this tube by an air-gaging technique that has many interesting possibilities for coal mines, where the use of electrical apparatus is so restricted.

With both these cells it is desirable, during installation, to pre-stress them as nearly as possible to the stress conditions of the enclosing media. An installation method for attaining the required stress level is being developed.

Seismological Observations

In collaboration with the Seismological Division of the Dominion Observatory,[11] there has also been considerable effort to learn whether or not minor earthquakes are occurring in the coal fields under study in eastern and western Canada and whether any such manifestations of regional geological activity are associated with mine bumps. These studies are also intended to supply a better record of the bumps occurring in each field, many of which are not noticeable and hence not reported by the mines concerned. Continuous recording of such events would make it possible to relate their incidence more closely to the mining operations.

For initial exploration of the problem two seismographs were installed in the coal mining centers at Fernie and Coleman in the Crowsnest Pass coal field of western Canada. A third was installed in the prairie region at Turner Valley, well distant from any mining operations. Earthquakes were recorded at all three stations and, in addition, many small disturbances were recorded at the mine sites, especially at the Coal Creek collieries of Fernie. A closer network of radio-linked seismographs was then installed in the Fernie area. The records of these seismographs established that the small disturbances were occurring in the mine workings. Later, in eastern Canada, a single seismograph was installed in the Springhill coal field to record the tremors occurring in the area and to study their association with the mining operations.

To summarize very briefly the findings of this study, there seems to be no correlation between earthquakes and bumps. Following an earthquake tremor the number of recorded bumps did not increase. There does appear to be a definite relation between the rate of mining activities and the frequency of local tremors, since it was observed—both in the East and in the West—that cessation of mining operations, even for a weekend, substantially reduces the number of tremors recorded. This would also indicate that the ground tremors observed are principally caused by strata readjustments associated with the current working faces and much less by long-term ground stress relief in older extracted areas of the underground workings.

Rock Mechanics

Complete understanding of the action of stress on a material necessitates laboratory investigation into the elastic and failure properties of that material. Investigations are being conducted along three distinct but related paths, namely, short-period uniaxial compression, long-period uniaxial compression (time-strain), and triaxial compression.

Studies have been carried out to determine a number of the elastic and failure properties of mine rock under short-period uniaxial compression, including the following: compression modulus, Poisson's ratio, ultimate compressive strength, strain energy at failure, and fracture angle.

These tests were conducted on right cylindrical specimens prepared from diamond drill cores varying from 7/8 to 1/8-in. diam. Longitudinal and transverse stress-strain relationships were obtained for stress increments of 1000 psi up to a maximum stress of 20,000 psi, and from such data the tangent values of compression modulus and Poisson's ratio at 6000 psi were obtained by graphical means. Each specimen was then loaded at a constant stress rate of 200 psi per sec until failure took place, and ultimate compressive strength, strain energy at failure, and fracture angle were determined.

Table I illustrates some results of tests carried out on specimens obtained from a number of Canadian mines. These results indicate the wide variation in elastic and failure properties between individual rock types and between similar rock types obtained from different mines. For comparison, results obtained from tests at the Fuels Division on a number of European mine rocks are also included. From the limited number of tests conducted so far, it would appear that rocks obtained from mines with a history of violent stress relief have a higher ultimate compressive strength and are capable of releasing more stress energy at failure than those obtained from mines not so affected.

Tests on the rocks from Springhill No. 2 mine do not support the view that a particular type of rock or individual bed is significantly stronger than the rest and therefore a possible single cause of bumps. It would appear rather that all rock beds in Springhill are quite competent.

It was recognized from the outset that the influence of time on the elastic and failure properties of mine rock must also be investigated. It was also appreciated that—as compared to short-period uniaxial compression testing—a study of time-dependent properties would be more difficult, necessitating the design of special apparatus and technique. Development in this direction has been carried out during the last two years, and a time-strain apparatus is now being completed in which the time-dependent characteristics of three separate specimens may be studied simultaneously at loads up to 25,000 lb.

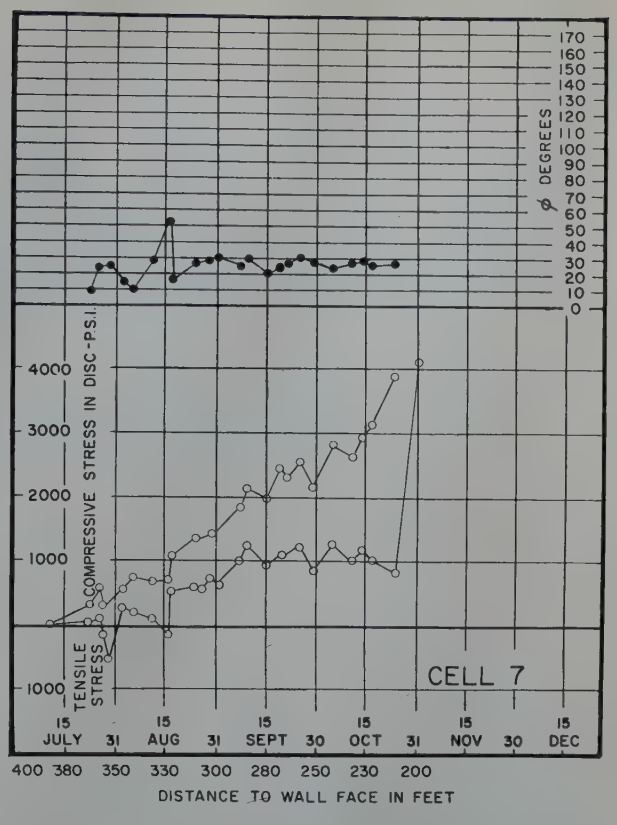

Fig. 11—Record of cell over period of several months as wall face progressed from 380 ft to about 200 ft from cell.

The third stage of study into the physical properties of mine rocks necessitates investigation into the behavior of these materials under conditions of triaxial stress. A few initial experiments have already been conducted, principally to secure information required for design of apparatus. A triaxial stressing unit is now being constructed at the Mines Branch. When it is completed a program of triaxial testing will be initiated.

References

[1] E. de St. Q. Issacson: Mining Conditions on the Kolar Gold Fields. *Kings College Mining Society Journal*, 1956, pp. 85-101.

[2] B. Schwartz: Measurement of Ground Pressure and of Movements at Longwall Faces in French Coal Mines. *CIMM Trans.*, 1954, vol. 57, pp. 259-261.

[3] N. S. Stephenson and S. Lewis: A Strata Control Survey. *Colliery Guard*, 1955, vol. 191, pp. 65-70.

[4] A. J. Barry and J. J. Wojciechowski: Roof Movement Study of Mechanized Retreating Longwall Operation, Lancashire No. 15 Mine, Bakerton, Cambia County, Pa. *USBM R. I. 5028*, 1954, 13 pp.

[5] B. Schwartz: Strata Movements in Coal Mines. *Kings College Mining Society Journal*, 1956, pp. 51-72.

[6] A. Ignatieff et al.: Current Investigations of Stress Relief in Canadian Coal Mines. *CIMM Trans.*, 1954, vol. 57.

[7] J. G. Buchanan et al.: Measurement of Stress Changes during Mining Operations. *Canadian Mining Journal*, 1955, vol. 12, pp. 49-55.

[8] A. Brown et al.: Rock Pressure Studies in the Mines at Springhill, Nova Scotia. A Progress Report. *CIMM Trans.*, 1956, vol. 59, pp. 242-251.

[9] T. L. McCall: Further Notes on Bumps in No. 2 Mine, Springhill, Nova Scotia. *AIME Trans.*, 1934, vol. 108, pp. 41-70.

[10] A. Coutinho: Theory of an Experimental Method for Determining Stresses Not Requiring an Accurate Knowledge of the Modulus of Elasticity. International Association for Bridge and Structural Engineering, *Pub.* 7, 1949, pp. 83-103.

[11] W. G. Milne and W. R. H. White: A Seismic Investigation of Mine Bumps in the Crowsnest Pass Coal Field. *Dominion Observatory*, Department of Mines and Technical Surveys, Ottawa, Canada. In Press.

Discussion of this article sent (2 copies) to AIME before Sept. 30, 1958, will be published in MINING ENGINEERING.

Control of Mountain Bumps in the Pocahontas No. 4 Seam

by Woods G. Talman and John L. Schroder, Jr.

EXPERIENCE has shown that certain known natural conditions and other indefinite characteristics combine to make a mining area vulnerable to mountain bumps. Some of the known conditions are heavy overburden, an overlying stratum of strong non-elastic rock, a structurally strong coal seam that does not crush easily and yet is the weakest stratum in the series, and a floor stratum of more than ordinary firmness.

The indefinite characteristics could include resistance of top or bottom of a coal seam to lateral flow, effect of immediate top and bottom strata, nature of the coal seam, and other factors about which very little is known. It is in this area that exhaustive study is needed to achieve positive control of the dreaded mountain bump hazard.

In the Gary district, West Virginia, two of the five operating mines have areas known to be vulnerable to mountain bumps.These are the No. 2 and 6 mines, which are working the Pocahontas No. 4 coal seam. In this area the seam is overlain at a zero to 10-ft interval by the massive Eckman sandstone, which is about 100 ft thick in the vulnerable areas. Total overburden, consisting of shale, coal seams, and sandstones, ranges from 700 to 1400 ft where bumps have occurred (Fig. 1). The coal seam is 4 to 8 ft thick and has a weak columnar structure of very soft and spongy or *woody* coal. The immediate top is either the Eckman sandstone or hard shale, both of which provide generally good roof conditions for mining operations. The bottom ranges from medium to hard gray shale.

The incidence of bumps in the Gary district dates from about 1930 and can be correlated to some degree with the increased rate of extraction attained with mechanical mining. During early years of operation at the No. 2 and 6 mines, most of the work was development and under comparatively light cover. As overburden became heavier, together with an increasing percentage of coal coming from pillar extraction, mountain bumps began to occur. Before 1945 they were much less severe than in later years, and because there were no injuries or fatalities, no records were kept. But by 1951 the incidence of bumps had increased to such extent that it became evident a mining system would have to be designed to eliminate or at least minimize these occurrences.

Drawing on experience with modified versions of old systems and certain characteristics peculiar to the Pocahontas No. 4 coal seam, the district mining engineer, Martin Hayduk, outlined the essential factors for bump control in the Gary district. These control factors indicated:

1) The highly stressed area, which lies within the limits of convergence effects, moves at approximately the same rate as the retreating pillar line.

2) There is a decided softening of the periphery of blocks which is greatest and deepest on the gob side.

3) Blocks less than 45 ft wide never have been known to bump in the Pocahontas seams.

Fig. 2 shows the mining plan based on these observations—a thin-pillar system with a minimum of secondary development.

It was recognized from the start that the Hayduk system had certain limitations. When pillar work backed up to an inevitable surrounded block it was no longer applicable; also, *burnt* bottom and/or unknown factors reduced the system's effectiveness in certain headings.

Since there was no way to eliminate the loaded block, it was decided to experiment with auger drilling to attain controlled release of this stored-up energy. The decision to auger was made after consideration of three separate plants, which were:

1) To cut the solid block into pillars of maximum size by driving away from the fracture line and at such a distance outby that development

W. G. TALMAN, Member AIME, is Assistant Vice President, Coal Staff, U. S. Steel Corp., Coal Div., Pittsburgh, Pa., and J. L. SCHRODER, JR., is Acting General Superintendent, Lynch District, Lynch, Ky.

TP 4771F. Manuscript, April 21, 1958. New York Meeting, February 1958.

would be active only in the area outside the abutment zone.

2) To induce a bump in the large block by blasting.

3) To drill enough holes through the large reserve blocks to effect a gradual crushing action, or induce a series of light bumps to release the stored energy.

Plan 1 was tried with only moderate success—bumps were minor, but still serious—and this approach was discontinued. Plan 2 was not tried because of the obvious safety hazard and violation of State and Federal regulations. Plan 3, adopted as an experiment in August 1953, proved three main criteria:

1) Coal pillars known to be heavily stressed can be drilled successfully.

2) Without jeopardizing the workmen's safety, mountain bumps can be triggered by drilling into loaded pillars.

3) Loaded pillars can be stress-relieved by drilling large-diameter holes with underground auger units. The pillars remaining can be mined normally without danger of reloading and bumping and also without so much pre-weakening that a general squeeze is induced.

Experience in the drilling program since 1953 has led to spotting holes opposite break-throughs, using two rows of cribs to protect the workmen and rig. There are lagging boards across one row of cribs. The details of a bump and the effectiveness of the barricade are shown in Fig. 3. If precautions had not been taken to crib and board between the mouth of the hole and the rig, the workmen would have suffered serious injuries or worse.

On the basis of drilling experience to date, *thumb rules* have been established to guide plans for probing or stress-relieving vulnerable blocks in the Pocahontas No. 4 seam:

1) Pre-weakening holes must be projected on room centers.

2) After a hole is drilled, room development is to follow the auger hole regardless of the direction it takes.

3) The drill rig shall not be positioned less than 35 ft from the mouth of the hole being drilled.

4) Drilling and section mining operations shall not be conducted on the same shift.

5) A section loading operation shall not be conducted less than two blocks away from a vulnerable block while augering is in progress.

6) Mine development shall stop 35 ft outby end of auger holes in cases where all stresses have not been released. With proper protection and specified distance from face, the hole may be extended.

7) No rooms or openings are to be driven without a protection hole on the vulnerable side.

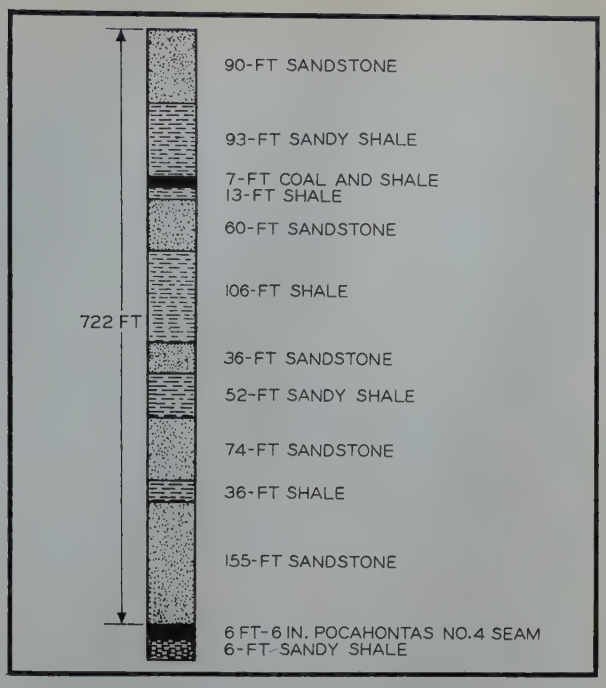

Fig. 1—Typical stratigraphic section overlying Pocahontas No. 4 seam. Cover ranges from 700 to 1400 ft.

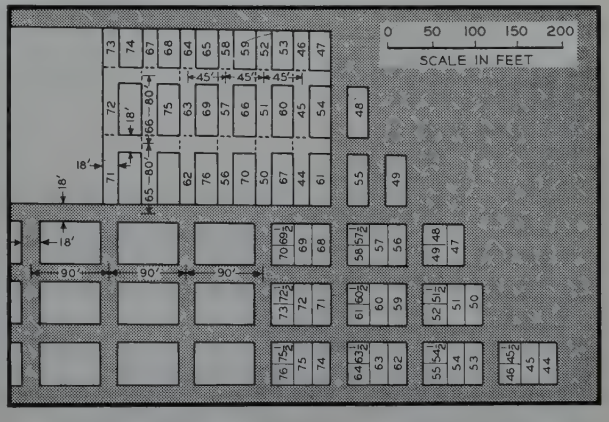

Fig. 2—Typical mining sequence utilizing the thin-pillar system.

8) When there is any doubt as to whether a hole has been closed by subsidence and/or bumps, it must be re-drilled before it is used as a protection hole.

9) It must be verified that auger holes have cut through bottom bone and coal to the mine floor.

10) There must be as few men as possible at the face at all times.

Figs. 4-8 show an actual drilling and mining sequence for stress-relieving one of the large blocks in No. 2 mine. During the course of the job there was a heavy bump, from which additional knowledge was gained.

Investigation of the bump shown in Fig. 7 resulted in the following conclusions:

1) Previous augering experience indicated stresses had been relieved in the area so that room advance and a break-through to room 2 could be accomplished with no difficulty.

2) The approved augering plan and subsequent room development were being carried out by mine management and workmen in exact detail.

3) The room advanced in a highly stressed area, resulting in a bump of medium intensity that was unpredictable.

A Joy crawler-mounted underground auger unit (Model AD-10) was received Aug. 15, 1957, complete with accessories and features custom-built to the specifications derived from two years of experimental work. This unit incorporates caterpillar mounting, dual controls, instantaneous reverse, integral roof jacks, two winches, 12-in. and 24-in. auger sections, a separate portable elevating conveyor, and various safety features. Face equipment receives power through a circuit breaker at the power source. This breaker is arranged so that a ground in the auger circuit or a severe overload—such as that caused by a bump stalling the auger—will trip it and remove power from the entire section.

A 25,000-cp, six-cell spotlight now facilitates inspection of auger holes, minimizing the danger in performing this important phase of the job.

Since 1953 several improvements in the drilling program have resulted from modifying the equipment and procedures. To help prevent fouling of the auger in light bumps and to control auger drift, Roy Parsons, mine foreman, designed an auger protective device. The first unit (core barrel) was made of ⅜-in. steel sheeting with 10-in. perforations. The diameter was 26 in., and the 7-ft length encased the first auger section and three-quarters of the second section. Since the 10-in. perforations of the initial design did not admit large lumps of coal, these openings were enlarged. Another improvement was shortening the unit to 4 ft. This permitted the device to follow sudden grade changes, whereas the 7-ft length did not.

The diameter of the new device has been reduced to 24 in. and the auger section in the barrel trimmed to fit. Originally the diameter was 2 in. larger than that of the outby augers, and when the hole outby the barrel closed to the minimum 24 in. it was difficult to retrieve the barrel after the hole was completed.

After three years of drilling in vulnerable blocks, much has been learned about the type of auger section used. The standard auger is 4 ft long, 24 in. diam, and 24 in. between ribbons with a 45° pitch. Spacing of ribbons and degree of pitch have been improved by using auger sections with ribbons 8 in. apart. Five augers—20 ft of this type of section—are used immediately behind the protective device or barrel. These closer-spaced augers perform two major functions:

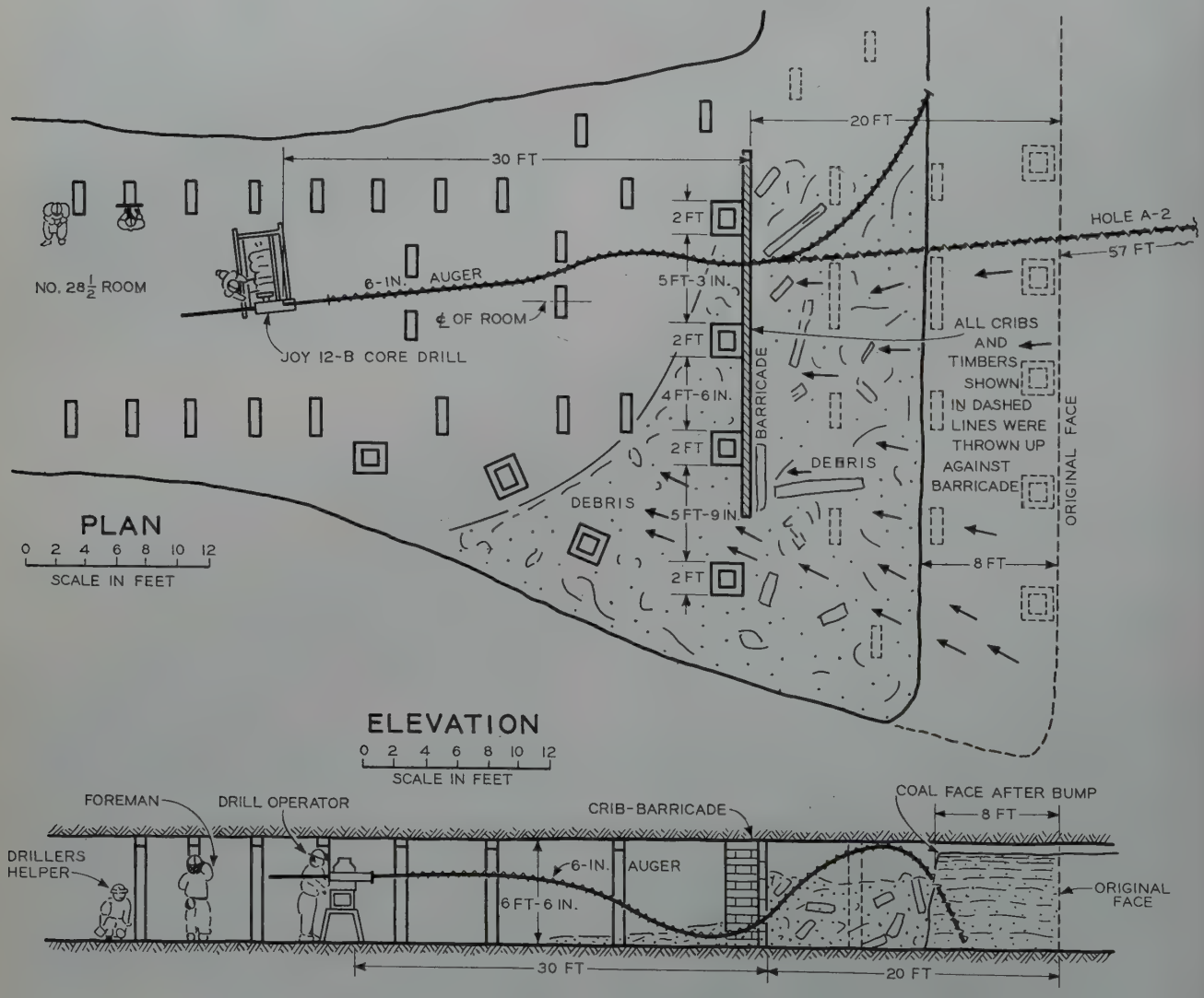

Fig. 3—Details of a bump in Pocahontas No. 4 seam and effectiveness of safety measures.

Fig. 4—Original plan for drilling and developing the block: Drill holes *A*, *B*, and *C* while extracting No. 1 pillars and then develop rooms 1 and 2 up to and including the first break-through. Hole *D* is to be drilled along with holes *F* and *G* in room 2. On completion of hole *G*, room 1 is to be cut through into the airway and No. 2 pillars extracted. Holes *H* and *I* are then to be drilled, room 2 cut through into the airway, and No. 3 pillars mined. On completion of hole 1, No. 4 pillars are to be extracted and rooms 3 and 4 developed through, at which point the block will be considered sufficiently developed to permit orderly extraction of pillars to a line to be established by indicated conditions as the pillar line moves outby.

Holes are to be drilled in alphabetical sequence, with drilling and mining conducted on opposite shifts.

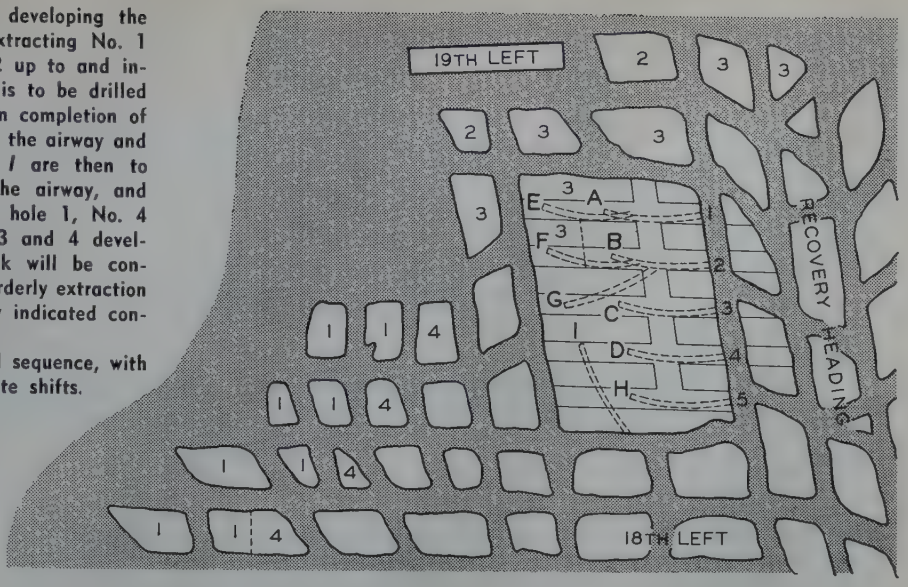

Figs. 5-8 (below)—FIRST: Shows progress on the large block with a revision to the original plan dictated by initial results with drilling and mining. Holes *A*, *B*, and *C* were drilled to their projected depths only after light medium bumps had continuously interrupted drilling operations by fouling and damaging the augers. Most of this trouble was attributed to light bumps and right-hand rotation of the drill, which caused sections to operate on curve alignment. SECOND: It was evident that the major stress in the block was not relieved by inby drilling and that further activity on that end of the block might cause a major bump, with injury to workmen. It was decided to try to activate a major bump by drilling from the outby end of the block. Hole *D* was drilled to the projected depth, and hole *E* set off a bump at 55 ft. THIRD: After hole *E* had induced a major bump, hole *F* was drilled only to reduce the size of the corner block. Hole *G* was drilled to ascertain remaining pressure. Since no pressure was found in hole *G*, loading operations were activated in the room following hole *C*, which had been drilled to a depth of 75 ft. Beginning at the mouth, loading operations had advanced 52 ft, or within 23 ft of the end of the hole, when a medium bump occurred. FOURTH: Here the vulnerable block is shown completely relieved of stress. Holes *I* and *J* were drilled in proper sequence as protection holes from room development.

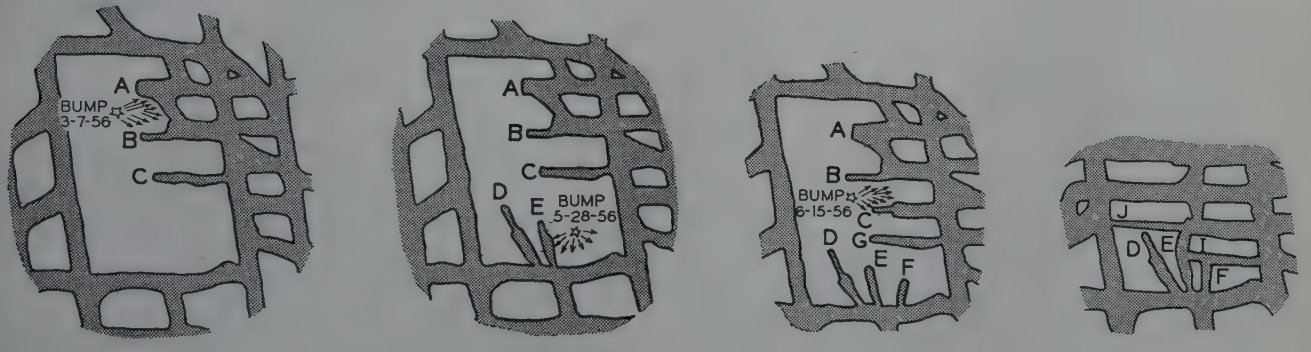

1) In the event of a bump, they limit the load on the outby augers so that the entire string is not completely loaded. This helps prevent fouling of the augers.

2) Owing to the steeper pitch of the 8-in. spacing between ribbons, the augers tend to stay on the bottom instead of riding up on top of the bottom bone as the 24-in. spaced ribbons do.

Originally the auger sections were held together with ¾-in. pins slipped into ¾-in. holes. This did not prove entirely satisfactory, as occasionally the pins slipped out and it was difficult to retrieve the augers. The problem was solved by enlarging the holes to 1 in. and using a 1-in. steel bolt. No augers have been lost since the change-over.

The major problem of keeping the auger on the bottom has been solved by establishing a drilling rate of approximately 10 in. per min.

Bits on the earlier cutting head were welded directly to the frame. This assembly has been improved by lugs on the cutting head, for faster bit changes.

Summary

In the course of drilling operations over the past four years, there has been considerable progress in controlling bumps in the Pocahontas No. 4 seam. This has been achieved by a trial and error approach to a safe and workable drilling plan, careful analysis of all bumps, and consultation with roof control specialists. Because men's lives are involved, many experiments have been restricted, and it has been necessary to find answers to the problem via the negative approach of "things not to be done in vulnerable areas."

The U. S. Bureau of Mines has initiated a program for exhaustive study of this subject and is now collecting field data. Part of the analysis involves correlating all experiences and data available from the various companies affected, and this alone will provide some interesting and helpful observations.

Discussion of this article sent (2 copies) to AIME before Sept. 30, 1958, will be published in MINING ENGINEERING.

Fine Grinding at Supercritical Speeds

by R. T. Hukki

(MINING ENGINEERING, page 581, May 1958, AIME Trans., vol. 211)

John F. Myers *(Consulting Engineer, Greenwich, Conn.)*—Since the art of comminution has lain practically dormant for many years, it is very interesting that R. T. Hukki approaches the subject with a new concept.

One is reminded of the research carried on by A. W. Fahrenwald of Moscow, Idaho, a few years ago. Fahrenwald mounted a steel bowl on a vertical shaft. The balls and ore placed in the bowl were rotated at fast speeds, thus simulating the supercritical speeds used by Hukki. The rolling action of the balls against the smooth shell liner has pretty much the same effect. The action is horizontal in one case and vertical in the other. Both researchers report good grinding activity.

It is also constructive that such able investigators give to the students of comminution their interpretation of their laboratory results in terms of large-scale operation. History shows that it takes a lot of time for such radically new ideas to be absorbed by the industry. Typical of this is the present-day activity of cyclone classification in primary grinding circuits. The idea of cyclone classification has been kicking around for 30 or 40 years.

Certainly we all suspect that the ponderous grinding mills of today, and their accessory apparatus, large buildings, etc., will ultimately give way to small fast units, just as this has occurred in other industries over the past 50 years.

At the moment there is no evidence that ball and liner wear is prohibitively high. In fact, at the time Fahrenwald was demonstrating his high-speed horizontal machine at the meeting of the American Mining Congress, several years ago, he assured this writer that the balls retained their shape much longer than they do in conventional tumbling mills. Rods and balls that slide (as some operators in uranium plants are experiencing) get flat. Apparently the balls have a rolling action.

Mr. Hukki's references to the processing capacity of the Tennessee Copper Co. mills is adequate. Those studying this subject will be greatly interested in the paper presented by Richard Smith of the Cleveland-Cliffs Iron Co. at the annual meeting of the Canadian Institute of Mining and Metallurgy in Vancouver April 24, 1958. This paper will be published during the latter part of 1958 in the *Canadian Institute of Mining and Metallurgy Bulletin.*

Hukki's pioneering spirit is to be commended.

R. T. Hukki *(author's reply)*—It has been heartening to read the objective discussion by J. F. Myers. The sincerity of his opinions is further strengthened by the fact that the article he has discussed contradicts in a major way the parallel achievements of his life work.

Myers is right in his opinion that in general it takes a long time before new ideas are accepted by the industry. On the other hand, revolutions usually take place at supercritical speeds. There are many indications at present that both the unit operation of grinding and the related subject of size control are now just about ripe for a revolution. In grinding, brute force must ultimately give way to science. Rapid progress can be anticipated in the following fields:

1) Autogenous fine grinding at supercritical speeds will be the first advance and the one that will gain recognition most easily on industrial scale. At this moment, little Finland appears to be leading the world. Crocker recently made a statement that in nine cases out of ten, your own ore can be used as grinding medium more effectively and far more economically than steel balls. This is true. The present author would like to introduce a supplementary idea: In eight cases out of the nine cited above, it can be done at the highest overall efficiency in the supercritical speed range. Fine grinding must be based on attrition, not impact. The path of attrition may be vertical, horizontal, even inclined.

2) In coarse grinding, the conventional use of rods is sound practice. However, even the rods can be replaced by autogenous chunks large enough to offer the same impact momentum as the rods. To obtain the momentum, the chunks must be provided with a free fall through a sufficient height in horizontal mills operated at supercritical speeds. Coarse grinding must be based on impact. Detailed analysis of the subject may be found in a paper entitled "All-autogenous Grinding at Supercritical Speeds" in *Mine and Quarry Engineering,* July 1958.

3) All conventional methods of classification, including wet and dry cyclones, are inefficient in sharpness of separation. Continuous return of huge tonnages of finished material to the grinding unit with the circulating load is senseless practice. In the near future the present methods will be either replaced or supplemented by precision sizing.

These three fields are also the ones to which J. F. Myers has so admirably contributed in the past.

Correction

Fine Grinding at Supercritical Speeds. By R. T. Hukki (MINING ENGINEERING, May 1958). Eq. 9, page 588, should be as follows:

$$T = c_4\,(\delta - \delta')\,n^{1.4}\,D^{2.7}\,L \text{ tph}$$

On page 584 of the article the captions for Figs. 4 and 5 have been placed under the wrong illustrations and should be interchanged.

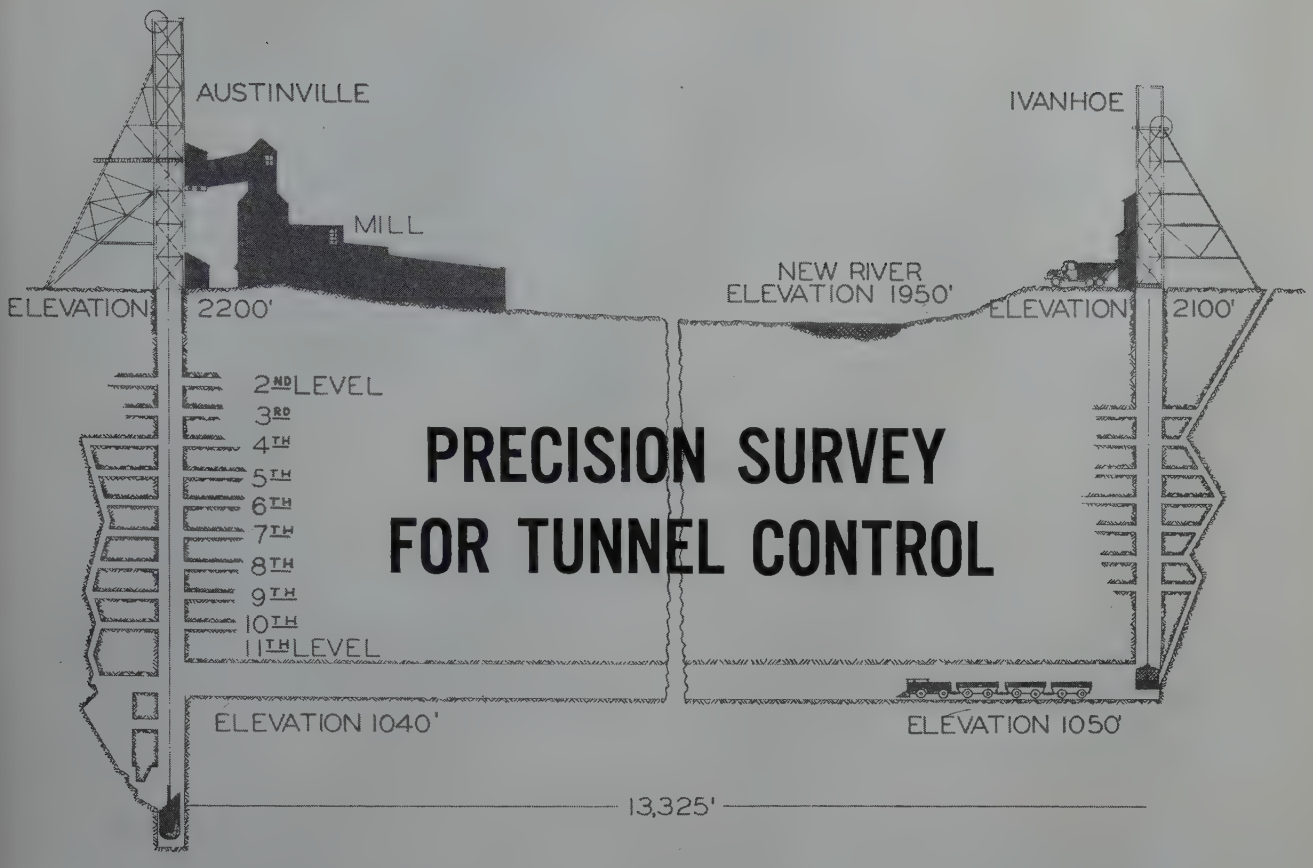

PRECISION SURVEY FOR TUNNEL CONTROL

by DOUGLASS D. DONALD

The New Jersey Zinc Co. successfully holed through a 2½-mile haulage tunnel connecting its new Ivanhoe shaft with the Van Mater Shaft at Austinville, Va. This 8 x 10-ft cross-section tunnel was driven from both ends and met at a point approximately a mile from one shaft and a mile and a half from the other. In order to make certain that the faces met accurately on line and grade it was necessary to refine conventional mine surveying practices.

The mines that are serviced by these shafts are located in the southwestern part of Virginia approximately midway between Roanoke and Bristol at the west foot of the Blue Ridge. While the presence of lead-zinc sulfide ores has been known in this area for more than 200 years, it was in 1902 that New Jersey Zinc Co. acquired the Austinville property, which has been in constant operation since that time. About ten years ago the company undertook an extensive diamond drilling program at Ivanhoe several miles to the southwest. This program was successful in locating sufficient ore to justify the purchase of a number of the properties in this area and plans were made to develop the new orebodies. The discovery of this ore as well as substantial additional reserves at Austinville resulted in a decision by the company to increase its daily milling capacity to 3000 tons, of which about 1000 tons would be supplied from the Ivanhoe mine.

After careful consideration of all possible methods of transporting this volume of ore from Ivanhoe to the mill, it became evident that diesel locomotive haulage through a 2½-mile tunnel between the two mines would best suit prevailing conditions. Since the lowest operating level, known as the 1100 level, of each mine would be at approximately the same elevation, it was obvious that such a tunnel should be driven on this level. Not only would this tunnel facilitate feeding Ivanhoe ore into the underground crusher and skip loading installation at Austinville, but it would also open up a known orebody 5000 ft southwest of the Van Mater shaft. In addition it would provide a valuable diamond drilling base from which a large and a potentially favorable but untested block of ground might be explored. In order to hasten the completion of the tunnel, it was felt that it should be driven from both ends.

ENGINEERING CONTROL PROCEDURES

It was vital that the tunnel junction be made accurately on line and grade; thus it was felt that engineering control of an unusually high degree of reliability was required to prevent an accumulation

DOUGLASS D. DONALD is associated with Behre Dolbear & Co., New York. TP 4778A. Manuscript, June 6, 1958.

This page of Mining Transactions AIME follows p. 892. The intervening non-Transactions pages appeared in MINING ENGINEERING.

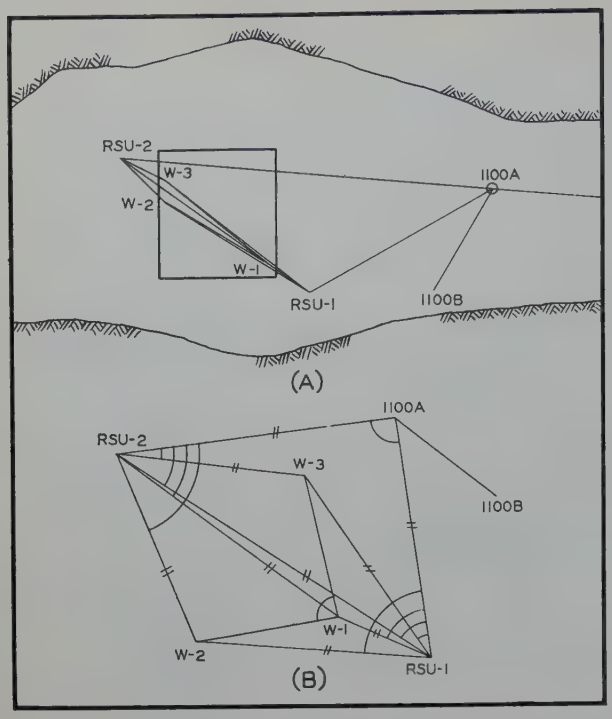

Layout sketch shows setup at 1100 level of Ivanhoe Shaft. Lower diagram shows details of triangles used for taking control off at the station level. Arcs show observed angles and the double barred lines were taped.

of errors. Otherwise a sloppy tunnel closure if not a very embarrassing situation could result. A review of preexisting surface and underground engineering control showed small but significant discrepancies which could seriously affect the whole project. It was, therefore, decided that only by establishing a whole new control system would it be possible to have confidence in the success of the tunnel closure. Since there was no room for blunders or systematic errors in the primary control circuit it was important that all segments of the circuit be designed so that they could be easily checked for accuracy and precision. Thus the triangulation net was laid out so that all stations could be occupied in order to close each triangle. Triangles having an angular error of closure in excess of 5" were resurveyed. Actually the maximum angular error that was distributed in any single triangle was 2".

Elevation control was carried as a series of closed traverses and a maximum error of closure of 0.01 ft was considered acceptable, although in practice the error was usually 0.005 ft or less. Horizontal control in the tunnel was carried as a series of overlapping closed traverses ranging in length from 1500 to 4000 ft. Minimum standards of precision for linear closure were taken as 1 part in 30,000 and 15" for angular closure. The errors in all acceptable traverses were distributed.

In order to meet these standards it was necessary to adopt certain procedures for taking the necessary measurements. All angles were measured using a mining transit with a 5½-in. horizontal circle graduated to 30'. Using a vernier direct readings could be made to 1', although with a certain amount of care readings could be estimated to 15". In triangulation work and shaft plumbing each angle was turned 12 times, 6 times to the right followed by 6 times to the left, alternate shots being taken with the telescope inverted. In order to fully benefit from the increased precision obtained by repetition, the plate was not reset after taking the first angle. Underground angles were turned four times, twice right and twice to the left again, inverting the telescope on alternate shots.

The commonest systematic error that might creep into the engineering control system could result from improper tape calibration or correction factors. Although catenary and tension corrections could be arrived at on a theoretical basis, it was felt that greater accuracy would be achieved by obtaining these corrections experimentally. It was therefore decided to establish a tape standardization range in an inactive part of the mine. A series of nine spads 25 ft apart were set in line in the back of the drift, with an extra spad placed midway between the 100 and 125-ft spads. Using a tape which had recently been standardized over a distance of 100 ft at 10-lb tension using end suspension by the U. S. Bureau of Standards, the distance between the spads from 0 to 100 ft and between 100 and 200 ft was very carefully determined. Once having determined these true distances, it was very easy to determine experimentally the combined catenary and tension corrections to be applied to a specific tape for measurements ranging from 12½ to 200 ft. The practice of applying 10-lb tension on distances up to 100 ft and 20-lb tension for distances from 100 to 200 ft was adhered to at all times, see figures on pages 980 and 981.

The first high precision taping traverse was measuring a 1000-ft base line for the surface triangulation net. Initially this was done according to U. S. Coast and Geodetic Survey specifications using the ventional four or five-man crew, but due to lack of experience it was found very difficut to hold the tape steady long enough at exactly the proper tension to obtain good readings. It was then decided to substitute two adjustable taping stands for the human tape holders in order to insure that the tape would be completely steady while measurements were being taken. One stand merely held the tape while the tension was applied at the other stand by means of a calibrated weight acting over a relatively large diameter sheave, thus reducing friction effects. The tape was read directly to 0.01 ft and estimated to 0.001 ft and readings were always taken at random on the tape rather than starting with a specific setting at one end of the tape. Two separate sets of readings were taken with different tape settings before moving to the next course and each reading was taken independently by each of the engineers carrying out the traverse. Comparison of the results of the two sets of tapings was made and if they corresponded closely enough they would move on to the next course.

Once this procedure had been adopted the base line measurements were carried out quite rapidly and a precision of somewhat better than 1 part in 800,000 was obtained. This was considerably more precise than the minimum requirements, which had been set at 1 part in 500,000.

Since this procedure worked so well on the surface, it was adapted to use for taping along the 1100 level. Track-mounted taping stands were made and worked especially well, since one of the permanent rails was laid directly beneath the engineering control points. Recording procedure was simplified by

having single readings made on each of three tape settings in order to reduce the probability of transposition of figures. If the spread of the three measurements did not exceed 0.003 ft their average was accepted.

It was found that underground control was best carried in three steps, one during which only the angles were turned, another measuring the distances and a third carrying vertical control. Since the ends of the tape were leveled when measuring distances, it was usually found convenient to combine taping and vertical control in a single step. The use of self-illuminated plumb bobs was a great help in expediting the angular traverses and the new taping methods enabled the engineers to measure distances precisely and rapidly. Once the procedures had been worked out it was possible for two engineers to complete about 500 ft of traverse per day.

SHAFT PLUMBING

Shaft plumbing has long been one of the most challenging problems to be faced by the mining engineer. There have been a great many ingenious methods devised for transferring engineering control down a vertical shaft, and one of the most complete summaries of different methods is contained in a series of articles by W. H. Wilson.[1] Peele's Handbook,[2] one of the more readily available reference books, briefly describes many of the basic plumbing methods.

For purposes of simplification, shaft plumbing may be resolved into two basic elements—first, transferring two or more points from the surface to underground and second, tying these points into the control system. Optical methods of transferring points down a shaft have long been used but are limited to relatively shallow shafts where the level to which the control is being taken can be clearly observed from the collar. The 1100 level in the Van Mater and Ivanhoe shafts was approximately 1050 ft below the collar and there was considerable water falling in each shaft, so optical plumbing was not feasible. Thus it became apparent that control points would have to be transferred by plumbing wires, but this method posed the problem of how to obtain accurate observations on wires that were constantly affected by the falling water and unavoidable air currents. Due to these factors it was felt that only by multiple observations on a swinging wire could a point be accurately established underground. Simple damping of the wire oscillations by immersing a medium weight plumb bob in a bucket of water was thought to be most effective, since more elaborate methods would only lengthen the required observation time.

In plumbing a South African shaft[3] a simple device used for steadying the plumb wire seemed suited to the problem at hand. Accordingly the Engineering Staff at Austinville drew up the plans for the Bertha shaft plumbing device using some of the principles of the South African device plus modification and refinements to better suit conditions that would be encountered in plumbing the Van Mater and Ivanhoe shafts. The Research Dept. of New Jersey Zinc Co. modified these plans and fabricated the instrument as shown in the accompanying photograph.

Once a satisfactory method of transferring control points underground had been determined, it was not too difficult to decide how to tie these points to the surface and underground control system. Coplaning, or "jiggling in" as it is more commonly referred to, was considered, but it was not felt to be sufficiently accurate. A direct method of incorporating one of the control points in the triangulation net and setting the transit over this point to survey directly in the other control points proved most effective as a means of tying the control points at the surface to the triangulation net. For reasons to be discussed later, this method was also used to take control off on the 1100 level at the Van Mater shaft. The use of Weisbach triangles seemed to be the best underground method for Ivanhoe. The late Professor Henry Briggs presented a mathematical analysis of the Weisbach triangle,[4] in which he demonstrated that the effects of linear errors of measuremnt are not as critical in obtaining accurate results as the angular error provided that the triangle is established to conform to the following conditions insofar as possible: The distance between the two wires is large, the ratio of the distance between transit and the near wire to the distance between wires is as small as possible and the acute angle at the transit between the two wires is small, preferably less than 25′.

A method of using three wires in the conformation of two Weisbach triangles back to back was described in an article by I. M. Marshall,[5] and had the added advantage of providing an excellent check on the accuracy of the plumbing. It was thus decided to use this three-wire method and add to it a second transit set-up as shown in the layout sketch.

Plumbing the Ivanhoe Shaft—Surface Control: Referring to the layout, W-1 is a station in the surface triangulation net. It consists of a small hole drilled in the top deck of the Ivanhoe headframe selected so that a wire could be passed to the 1100 level clear of all projections. From this station a triangulation station in the Van Mater headframe could be sighted some 13,154 ft to the northeast. The location of W-1 was transferred from the top of the headframe to the collar of the shaft where a notched steel trap was welded in place, thus giving a point from which a plumbing wire might be suspended. From this collar position of W-1, W-2 and W-3 were carefully surveyed. These points were also steel straps welded to shaft collar steel from which wires could be suspended. In practice W-2 and W-3 were only about 2 in. apart and about 12 ft from W-1, and the angle W-2, W-1, W-3 was found to be 0°-37′-56″ accurate to plus or minus 3″.

Transferring Points Underground: Plumbing wires were lowered, one near W-1 and the other

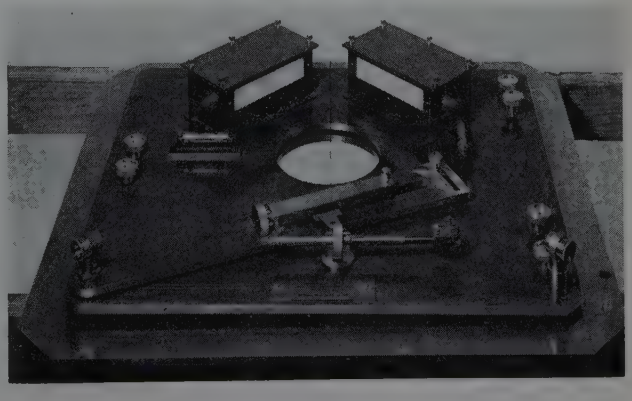

near W-2. No. 10 gage (0.024-in. diam) piano wire was used with a light weight attached to the end of each wire. After the wires reached the 1100 level the wire reels were secured in the headframe and the wires were placed in the notches of the plumbing straps. The light weights were replaced with 20-lb plumb bobs (each consisting of a short piece of I-beam with a hole drilled through the center of the web) after the plumb wire was cut so that the heavy bobs would hang in a damping bucket filled with water and set on the floor of the level.

About 4 ft above the level two 2x4's were securely nailed, one on each side of W-1 and approximately horizontal. The plumbing device was set on these beams so that W-1 passed through approximately the center of the large hole and the device was secured to the beams and leveled using screws provided for that purpose.

The procedure was to steady W-1 and start observing its oscillations on Scales A and B through the two peep sights. With a man reading each scale and one timing and recording, simultaneous readings were taken of the wire position every 12 sec for 5 min. After at least 5 min wait the procedure was repeated and the averages of the two sets of readings had to check to closer than half a scale division; otherwise a third set of readings was taken. If consistent sets of readings are not obtained after three or four repetitions the wire must be examined throughout its length to see if any outside influence is responsible for the erratic results.

After it was felt that a satisfactory average reading had been obtained on each scale, plumbing wire was removed and a tarpaulin rigged above the plumbing instrument to deflect the water. The arm of the device was then moved over the hole in the device and the pointer accurately set at the observed mean position of the plumb wire as determined from the average of the scale readings. The pointer has a small center hole in its base so that a short plumb line may be suspended beneath it to facilitate surveying this point from either above or below the device. Once this point has been so transferred to the plumbing device it may then be very accurately transferred to a securely anchored spad above the device and/or a zinc strip beneath it and the device may then be removed.

The same general procedure was repeated for W-2 except that care was taken so that observations could also be made on the wire when hung from W-3 without readjusting the instrument. After determining the mean position for W-2 the plumb wire was then moved to the W-3 position and its mean position determined. The wire was then removed, temporary roofing built over the instrument, and the pointer set on the mean position of either wire. After all angular and linear measurements were made for one setting, the pointer was moved to the second position. Transferring these points to spads or zinc strips is not worthwhile as a rule and is merely an avoidable source of potential error.

Trying-in to Underground Control: Once the three points had been transferred underground two random set-ups, RSU-1 and RSU-2, shown in the diagram, were selected so that W-2 fell to one side of W-1 and W-3 fell to the other and so that the distance from each random set-up to the near wire was as short as possible (in practice about 6 ft). The angle at each random set-up between W-1 and each of the other wire positions did not exceed 15′ and was usually closer to 10′. Thus an effort was made to utilize the strongest possible Weisbach triangle as mathematically demonstrated by Briggs.

Permanent control stations were established under and/or over each random set-up and at each set-up the angles were turned from 1100A to each of the wire positions and to the other random set-up. All distances as shown by solid lines in the diagram were taped. In effect control was obtained by means of the solution of four Weisbach triangles and tied in to triangle RSU-1, RSU-2, 1100A. The average azimuth resulting from the four solutions appears to be accurate ±6″ as determined from Peters' formula for determining the approximate value of the probable error of the arithmetic mean.

Plumbing the Van Mater Shaft: Three points were transferred from the collar of the Van Mater shaft to the 1100 level the same way as at Ivanhoe. Control was taken off underground by setting up the transit directly beneath the W-1 wire position and the angles were turned from the W-2 and W-3 positions to permanent level control. The angle W2-W1-W3 as observed underground corresponded

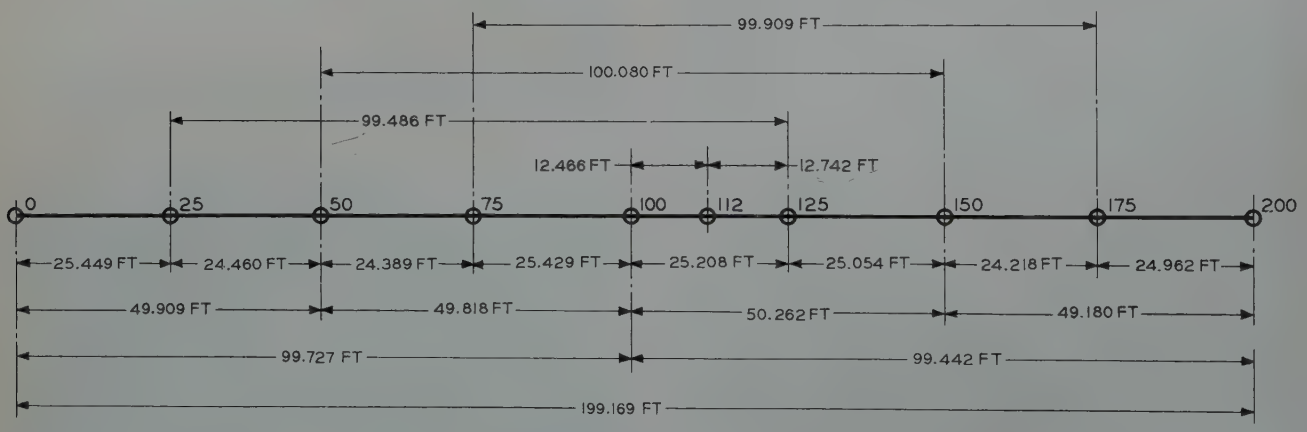

Details of tape standardization range established in an inactive part of the mine. Nine spads were set at 25-ft intervals in back of drift and distances then determined with tape already checked by the U. S. Bureau of Standards.

to that angle as observed on the surface to 9". This method was used instead of the Ivanhoe system for several reasons. For one thing, the distance between W-1 and the other two curves was 22 ft in the Van Mater shaft and only 12 ft in the Ivanhoe shaft. Thus it was less difficult to obtain accurate results by the direct method at Austinville than would have been possible in the Ivanhoe shaft. Furthermore, due to the nature of the rock excavation around the station at the Van Mater shaft, the positioning of W-1 in order to use Weisbach triangles could only have been about 7 ft from W-2 and W-3. Such an arrangement would result in a relatively weak Weisbach triangle according to Briggs' analysis. Incidentally, this direct method was far simpler than that used at Ivanhoe in that it required fewer observations, calculations and adjustments.

THE DEGREE OF PRECISION

It may appear to some that the degree of precision that was obtained in this project was considerably in excess of the requirements. This is true, but let it be stated that the cost of such excess precision should be considered as relatively cheap insurance that the tunnel junction would be accurately made. Actually the formulation of the surface control system and plumbing methods and the application of these elements of the engineering control net were carried out over a period of about three years so that much of it was done at times when the engineering staff was not overloaded with other tasks. Furthermore, once procedures were developed to obtain the desired minimum degree of precision, it was possible to obtain considerably more than minimum requirements with very little added time and care. For example, the use of the second random set-up in taking control off on the 1100 level at Ivanhoe was not essential, but since it could be done while observations were being taken from the first random set-up it only required one additional engineer and no extra time. It certainly contributed to the reliability of the results that were thus obtained.

Previous plumbing experience in the wet shafts at Austinville had made it clear that only by the use of an instrument such as the plumbing device described here could minimum standards be obtained. Once the device had been designed and fabricated, there was no sense in not using it to the limits of its capabilities.

Taping by hand held methods using a tension scale as recommended by the U. S. Coast & Geodetic Survey would ordinarily be required to assure minimum accuracy, but this necessitates a four- or five-man crew and requires a certain amount of skill to hold the tape steady enough for good readings. The use of taping stands with tension applied by means of a weight reduced the crew size to two men and permitted reading on an absolutely steady tape. Tape readings were repeated primarily in order to avoid blunders such as transposition of figures or unintentional reading to the wrong tape markings. Such a precaution reduced the probability that a traverse would not close accurately enough and would have to be re-run.

The procedures described above did result in an accurate tunnel closure. The triangulation net

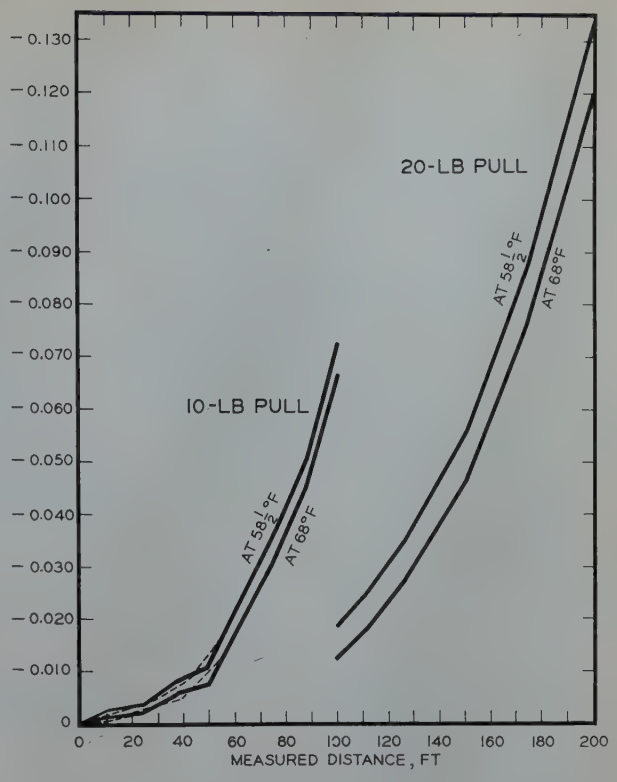

Correction curves for one tape, No. F 1684, show typical data derived from use of tape standardization range. Nine stations were used in arriving at calibration curve.

checked out with an old 2150 ft base line at Ivanhoe to 0.029 ft, actually within the limits of accuracy of the original taping of this base line. Since the triangulation stations on the Van Mater and Ivanhoe headframes were mutually visible, the bearing of the line between them was checked by turning angles from each end and comparing with the calculated bearing based on the newly established coordinate system. The observed bearings corresponded with each other exactly and differed from the calculated bearing by 3".

As previously stated, the engineering control system was carried out for a period of three years. As a result, more than a dozen engineers and technicians participated in the project so that credit for the work rests generally with the Mines Engineering Dept. at Austinville.

The author wishes to express his appreciation to C. G. Morgenstern, superintendent of the Bertha Mineral Div. and to A. R. Flinn, eastern manager of mines, for their suggestions and help in the preparation of this article. He also thanks New Jersey Zinc Co. for permission to publish the article.

REFERENCES

[1] W. H. Wilson: Devices for Plumbing of Vertical Shafts, *Mine & Quarry*, vol. 4, no. 2, Feb. 1939, p. 41-47; vol. 4, no. 3, March, p. 77-83; and April, p. 113-119.

[2] Robert Peele: *Mining Engineers' Handbook*, Third Edition, John Wiley & Sons, Inc., New York 1941.

[3] L. D. Browne: Movements of Freely Swinging Plumb Lines in Deep Vertical Shafts, Chem., Met. & Min. Soc. of S. Africa, vol. 49, no. 11, May 1949, pp. 445-450.

[4] Henry Briggs: *The Effects of Errors in Surveying*, Charles Griffin & Co., Ltd., London, 1912.

[5] I. M. Marshall: A Three-Wire Method of Plumbing a Shaft, *CIM Trans.*, 1938, vol. 41, pp. 237-245.

Discussion of this article sent (2 copies) to AIME before Oct. 31, 1958, will be published in MINING ENGINEERING.

Rock strata above coal seams. Note the massive sandstone beds above the portal.

by JOHN PEPERAKIS

MOUNTAIN BUMPS AT THE SUNNYSIDE MINES

Coal mine bumps are normally associated with pillar mining under moderate or deep cover. Severe bumps at Sunnyside, however, have not been confined to pillar lines. Many have occurred in virgin development and in localities a long way from active pillar workings. As early as 1918 bumps in virgin territory were attributed to the faulted structure in the Sunnyside area.[1]

Sunnyside is an old property, mined for more than 60 years. Both man-made and natural conditions contribute greatly to bump occurrences, and loss of life and great destruction of workings have resulted from some unusual bumps in recent years.

Before Kaiser Steel acquired the Sunnyside Mines in 1950, about 21 million tons of coal had been extracted. Large areas had been worked out and equally large areas first-mined. As demand for coking coal gradually diminished, extensive blocks were shut down, and during the low production period of the 1930's mining on a very limited scale was confined to a section of the property close to the coal tipple. Following purchase of the property Kaiser Steel developed the mines into a fully modernized operation.

The worked out and first mined areas covered about four square miles extending five miles along the strike and up to one and a half miles down dip from the outcrop. The sections with favorable mining conditions and clean coal had been largely extracted under the selective mining system imposed by economic conditions and the lack of cleaning plant facilities.

Large reserves remained on the fringes of the worked out sections and in areas under deep cover and difficult roof. There were also considerable reserves in first-mined areas. In recent years much of Sunnyside's daily output of 7000 to 8000 tons has been derived from the partially mined localities. Many bumps have occurred when pillars have been pulled within the first-mined areas and on the fringes. The bumps have been associated with retreating pillar lines backing up against old workings and pillar lines in old first-mined areas backing up against highly stressed oversized barrier pillars surrounded by smaller pillars.

In some parts of the property the upper Sunnyside seam was extensively worked in the past, and sizable areas of old works overlie the present lower seam workings. Abutment pressures from barrier pillars and pillar remnants are transmitted to the lower seam, contributing to bumps and squeeze conditions.

Cover: The terrain is exceedingly rough, and cover varies considerably over relatively short horizontal distances. For example, at No. 1 mine the 2000-ft cover line is ony 2700 ft from the coal outcrop, and at No. 2 mine the cover over the main hoisting slope increases from 1000 to 2000 ft in a horizontal span of 1200 ft. Cover over the present mining sections ranges from several hundred feet in the valleys to 2500 ft under the crest of the divides. A short distance ahead of Sunnyside's deepest development down dip the cover reaches 3000 ft or more.

J. PEPERAKIS, Member AIME, is Manager, Sunnyside Coal Mines, Kaiser Steel Corp., Sunnyside, Utah. TP 4770F. Manuscript, April 21, 1958. New York Meeting, February 1958.

Sunnyside mines 1, 2, and 3. Solid areas, mined out lower seam; stippled, mined out upper seam.

Worked out and first mined areas covered 4 sq miles. The main Sunnyside fault zone.

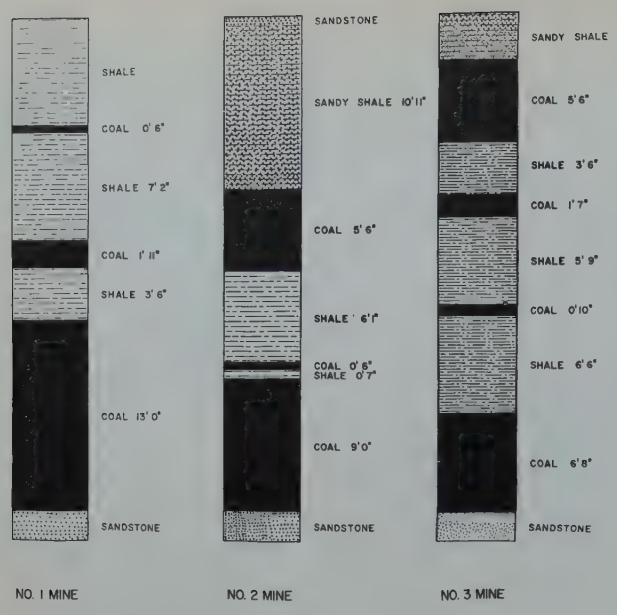

Cross section in vicinity of Sunnyside seams.

Over the coal the cover is predominantly massive sandstone, some beds reaching a thickness of several hundred feet. One massive bed of sandstone 200 ft thick is 150 ft above the coal seam. Failure or loading of this sandstone or other massive beds above it by subsidence movements is bound to create widespread disturbances in active sections around the periphery of a worked out area.

Immediate Roof Over Seam: Although the overlying formation is predominantly sandstone, the immediate roof over the coal is generally very poor, being composed of shales, sandy shales, thin laminations of sandstone and shale, and rider seams. This roof condition does not cause bumps, but it seriously increases the effect when they occur. Major bumps are usually accompanied by roof falls, some very extensive, and extraordinary roof support measures are needed to protect men and property.

Floor of Seam: Underlying the coal seam is a strong massive sandstone bed 20 to 50 ft thick, separated from the coal by a thin shale ranging from a few inches to several feet. It is believed that this sandstone member contributes greatly to bump occurrences.

GEOLOGY AND FAULT STRUCTURE

The Lower and Upper Sunnyside seams are the only workable seams outcropping along the Book Cliffs, a prominent escarpment in southeastern Utah lying on the northeastern flank of the San Rafael Anticline and the southern flank of the Uinta Basin Syncline. The strata dips under the cliffs to the northeast at 3° to 11°, the steeper dip generally prevailing near the outcrop. Except for a few localities, all present mining is carried on in the Lower Sunnyside, which ranges from 5½ to 16 ft in thickness. Separation between the lower and upper seam varies from 1 to 45 ft. The upper seam attains a maximum thickness of 6 ft, and in the past it was mined extensively because of more favorable top conditions and cleaner coal. At present it is mined in conjunction with the lower seam in localities where the separation is thin enough to warrant handling in the coal washery. In some localities, particularly in No. 1 mine, the upper seam splits into a number of thin rider seams. The nearest split, 2 to 3 ft above the lower seam, results in an exceedingly difficult roof control problem.

Faulting is very extensive. One prominent fault zone extends roughly along the strike through No. 1 and No. 3 mines, then swings down across the pitch and fans out into the No. 2 mine. Maximum displacement runs up to 33 ft; more commonly displacements range from 2 to 24 ft. There are also a few faults in the No. 2 and No. 3 mines running at right angles to the strike, one having a maximum displacement of 90 ft at the outcrop. The displacement diminishes toward the dip or away from the outcrop, so this type of fault does not pose undue problems in crossing with strike development. However, in one instance a dip fault contributed to the extraordinary caving of a slope.

Relation of Fault Structure to Bumps: It is not known whether tectonic movements due to the fault structure have some relation to the cause of bumps or whether the bumps cause movement along fault planes. The possibility that the unusual type of bump originates at the fault structure cannot be discounted, as the following instances will show:

1) In 1918, during the driving of a slope in No. 2 mine, there was considerable trouble from bumps, which could not be explained by commonly accepted theories concerning occurrences in other parts of the mine and in other mines of the same district. Previously there had been heavy bumps in pillar workings under heavy cover, but in this instance the workings were in virgin territory 1500 ft from the nearest pillar operations. Trouble was first encountered soon after the slopes penetrated a fault having an 18-ft displacement. As the slopes were driven

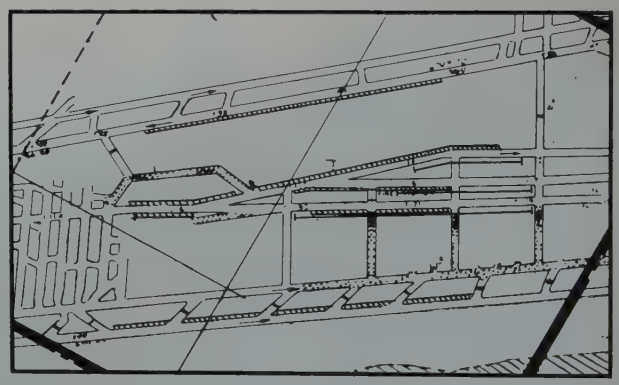

Bump of Jan. 24, 1957.

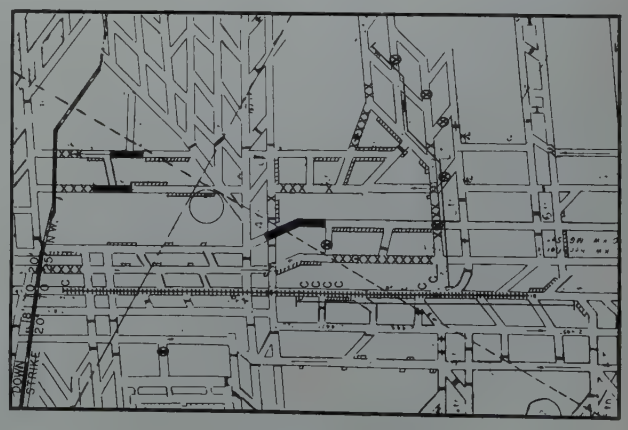

Bump of Jan. 27, 1957.

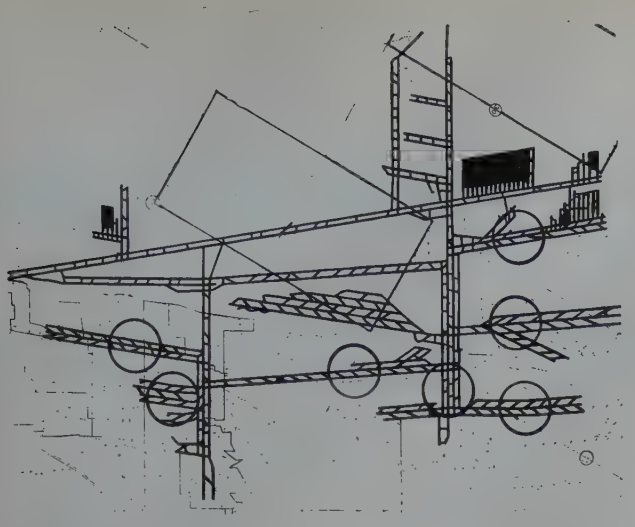

Bumps experienced in virgin coal on development.

downward, the frequency and force of the bumps increased, and the operating company resorted to heavy concrete wall construction and heavy timbering and lagging to protect personnel. Despite the obstacles presented, the slopes were finally driven 840 ft, where a 17-ft fault was encountered. After the fault was crossed and the slopes continued to advance no further bump disturbances were noted.

2) In 1951 an 1800-ft tunnel, the main haulage entrance into No. 1 mine, was being driven through a rock formation to intersect the coal seam. As the tunnel face approached to within 30 ft of a dip fault the face became active and fragments of rock flew out when the face was disturbed by barring down and drilling operations. As soon as the tunnel penetrated the fault no further disturbance was noted. At the time, the nearest active pillar work was 4500 ft away.

3) At the Range Creek pumping station, some distance from the mines, a number of earth tremors have been noted. The nearest mine working is 15,000 ft from the station. The coal lies 3000 ft below surface at the pumping station and 3500 ft below the divide separating Range Creek from Sunnyside. Tremors have also been felt in the townsite several miles from the mines, sometimes without any known occurrence of mine bumps.

4) Following a very extensive occurrence Jan. 24, 1957, the rock strata immediately adjacent to the main Sunnyside fault plane was violently shattered.

5) On Dec. 13, 1957, a violent bump manifested itself along a distance of 7000 ft. It was simultaneously recorded by men working at four points along three different fault planes in No. 2 mine. The epicenter of the bump could not be determined.

6) Disturbances have been noted in the vicinity of the main fault zone along slopes and haulageways, the most recent occurring on Nov. 21, 1957, in No. 1 and No. 2 mines. On this date indications of movement were discernable at the inby end of the No. 1 mine rock tunnel where it intersected a block formed by a strike and a dip fault. Along the same fault zone 13,000 ft distant in No. 2 mine where the faults cross the main slopes, disturbance was noted in the form of rib sloughage immediately adjacent to the fault planes. In both localities cover is less than 500 ft.

7) Most of the really severe bumps that have struck the workings in recent years have taken place close to the main Sunnyside fault.

UNUSUAL BUMP OCCURRENCES

In addition to these occurrences, there have been extremely violent bumps near the intersection of the main slopes of No. 1 mine with the main Sunnyside fault. These slopes first penetrated the fault in the early 1940's, and since that time there have been four major bumps in the area:

December 1944 Occurrence: The mine was almost entirely on development at this time, and except for one 700x300-ft section the nearest pillar area was more than a mile away. This small pillared area was about 2000 ft from the center of the bump. The slope entries had been advanced some 1000 ft below the Sunnyside fault zone, and cover over the area was approximately 1500 ft at the time of the bump, which centered over the main slope about 400 ft below the fault. Immediately following this occurrence a 350-ft section of roof over the main slope started to work, caving in about 45 min. The other slopes in the area were badly shaken but did not cave.

November 1952 Occurrence: At 11:40 a.m. on November 11 there was a bump of such magnitude that it was felt through most of the mine and at least two points on the surface. The areas most intensely affected were the outby end of the new partings, the Motor Road Extension, and the outby end of the old Motor Road parting. Extensive rib sloughage occurred at all these locations, and many crossbars

Airway reinforced by cribs.

Yieldable arch support on main haulage slope.

were knocked out on the old Motor Road. Rib sloughage in one aircourse extended clear to the surface, and outcrop openings being driven at the time were shaken up.

January 1957 Occurrences: Starting January 24, a series of bumps caused great damage to the main slope area between the fault and the 7th Left. The first of these, at 5:50 p.m., was the most severe of the series. Damage to the main slopes was very extensive; a heavily bolted section of roof in the track slope settled on the bolts throughout 500 linear feet of the entry, and the 80-lb track on the same slope was heaved and thrown out of line for a distance of 1300 ft. A concrete sill, used as a base for timber, was also thrown out of alignment for a distance of 175 ft, and six concrete stoppings and one overcast were damaged. Caves resulting from these bumps were all in the left side slopes and amounted to a total of 550 linear feet of entry. There was roof breaking over the entire bump area, both in areas with a bolted rock roof and in entries where top coal had been left. In the vicinity of the 5th Left parting 2000 linear feet of top coal roof was shattered. This had to be dropped and the exposed rock bolted.

Another severe occurrence in this series was recorded on January 27, centering in the vicinity of the main parting. Like the bump above the fault in 1952, it was very general and not as centralized as those that have occurred below the fault. This bump induced one small cave and generally shook up the main parting area. The seismograph at the University of Utah 120 miles away recorded a local tremor at the exact time.

Both the January 24 and 27 occurrences were felt throughout the towns of Sunnyside and Dragerton.

December 1957 Occurrence: At 10:08 a.m. on December 4 one of the main slope pillars, between the manway and return above 4th Right, bumped with extreme violence and the entire left side of the pillar burst for a distance of 220 ft, filling the manway with rock.

This entry had caved previously, and the cave had been used as fill and graded over, with only a ventilation area left open in the rock strata overlying the coal. This bump, therefore, was a rock burst rather than a coal failure. Roof and ribs in this entry had been bolted in 1954 with 8-ft bolts on 2-ft centers or less.

The parallel main slope was also badly shaken and had it not been for extensive roof bolting, 12x12-in. crossbars, and cribs, there would have been considerable caving on the haulage slope and nearby aircourses.

The tremor from this bump was felt throughout Sunnyside townsite. The seismograph at the University of Utah again registered a local tremor at the exact time of the occurrence.

Bumps in Development Work: In the early 1940's during initial development of No. 1 mine there were many bumps in development headings in virgin coal. These were not of the type normally associated with popping of coal from the face, as is the case in most deep work; they were of such magnitude as to break the top, knock out timber support, and cause roof falls, some very extensive.

The same type of occurrence prevailed at No. 2 mine. Slope and entry headings in virgin development bumped violently, although the nearest pillar workings were 1500 to 2500 ft away.

Cover over the development work thus affected ranged from 700 to 2100 ft.

MEASURES TO MINIMIZE HAZARD

1) In any section subject to bounces, long holes of 2¾-in. diam, up to 20 ft long, are drilled into the face and into the side of pillars having a tendency to bump. A relatively small charge of explosives is used. Many violent bumps have been triggered by this means. The load-carrying capacity of large blocks or pillars has also been reduced by long-hole shooting.

Although this system has not worked in all instances, it has proved one of the best means of triggering bumps while the men are in a safe place; its use is continuing and will be expanded. If manufacturers were to perfect a good long-hole drilling and tamping method, this system would be greatly improved.

2) Large blocks have been cut into smaller, more uniform pillars ahead of the retreating pillar line. This is especially important in areas cut up by old works where large barrier pillars are surrounded by many small ones. Long-hole shooting is used in cutting up these blocks, which cause more trouble at Sunnyside than anything else encountered along a pillar-line point.

This method is certainly no cure-all, since in many cases these large blocks are already stressed and violent bumps may be triggered as they are being cut up. Also, cutting up blocks too far in advance of the pillar line may induce an uncontrollable squeeze on the area.

3) In developing room blocks it has been found wiser not to drive connecting rooms through the block from one entry to another. At Sunnyside there are always violent bumps when a retreating pillar line backs up near an old opening. It is far better to leave the block solid in development.

4) In sections where the top will stand, it has helped considerably to break up entry blocks into pillars of uniform size ahead of pillar mining, but where roof conditions are poor the block system has not worked very well.

5) Maximum roof support is stressed in all areas subject to bumps, regardless of the means used to reduce the severity. Roof bolts are widely used in combination with cribs, crossbars on cribs, and 16-in. diam props.

6) In slope areas and haulageways where the unusual type of bump is likely to occur, the steel yieldable arch type of support is used extensively to minimize roof falls following a bump. Roof bolting and wooden support has been found lacking in this respect.

7) In one locality Sunnyside has resorted to hydraulic backfilling in extensive areas of old workings to obtain some relief from the burden imposed by bumps.

It is unlikely that bumps can be eliminated completely in mines operating under deep cover, especially where they occur even in development openings, but the effects can be minimized by the practices enumerated and by the use of proper roof and rib support.

Reference

[1] A. C. Watts: An Unusual "Bounce" Condition. *Coal Age*, Dec. 5, 1918.

Discussion of this article sent (2 copies) to AIME before Oct. 31, 1958, will be published in MINING ENGINEERING.

by WILLIAM F. CAMPBELL

DEEP COAL MINING IN SPRINGHILL NO. 2 MINE

One of the deepest coal operations today is the Springhill No. 2 mine of Cumberland Railway & Coal Co., subsidiary of Dominion Coal Co. Ltd. Mining is now conducted at a slope distance of 14,000 ft, with 4400 vertical ft of cover. The record of Springhill No. 2 can be said to contain the history of bumps in the Province of Nova Scotia.

The Springhill coal field forms part of the Cumberland field of Carboniferous age. There are seven mineable fields in the area, numbered in the order they were discovered. Mining has been carried on in all but the No. 4 and 5 seams, but present operations are confined to the No. 2. Fig. 1 shows a vertical section through the seams.

Opened in 1873, No. 2 mine was first worked from parallel slopes driven from the outcrop of No. 2 seam down to the 7700 level. As the mine went deeper, a two-place auxiliary slope was driven from the 6900 level to the present workings. A transfer level at the 7800 connects the main haulage with the auxiliary haulage slope. The No. 2 mine plan is shown in Figs. 2 and 3.

The seam is bituminous, averaging 8.5 to 9 ft thick. There is a well defined parting 14 to 16 in. from the roof, and this roof coal is harder than the rest of the seam.

Average pitch at the outcrop is 30°; at the 6500 level, 20°; at the 7900 level, 16°; and at the 13,800 level, 10°.

Immediate roof and floor strata consist of beds of variable thicknesses of shales, grading to arenaceous shales to shaly sandstones to sandstones. A characteristic of the strata is the appearance and disappearance of sandstone bands, of considerable thickness, over distances of several hundred feet.

MINE HISTORY

Entrance to No. 2 mine is obtained by three parallel slopes, separated by 100-ft pillars except in the upper portion of the mine where the pillars are smaller. Main haulage levels were originally driven 600 ft apart for room and pillar extraction. A parallel drainage and intake airway was driven below each haulage level and a parallel return airway (counter level) above. Pillars 80 to 100 ft wide separated these two servicing entries from the center haulage level. Inclines up to 700 ft apart were driven off the levels up pitch to the upper levels, and at 40-ft centers level rooms 12 ft wide were driven off each side of the inclines, separated by crosscuts every 50 to 100 ft. The rooms were driven up to 350 ft or until they were *holed* into the room from the adjoining incline—a plan followed until the level reached its boundary. When the entire area between two levels had been divided into pillars, the pillars were extracted from the boundary back to the slope pillars.

As depth of cover increased, mining conditions required larger pillars, and at the 3300 level, where

NECESSARY PRECAUTIONS FOR MINING AT DEPTH

In Room and Pillar Extraction:

1) Pillars must not be too small.

2) Pillar size must be uniform.

3) Extraction lines must be kept as straight and as uniform as possible. If they are irregular they should be brought back into line slowly.

4) Peninsulas of coal surrounded by gob must be avoided.

5) Pillars should not be disturbed after they have been formed. If it is necessary to increase the width of an opening, stripping or ribbing should be done gradually over a long distance. If increased width of openings is necessary at certain locations and can be anticipated, the openings should be widened during development.

6) Under no conditions should small pillars be left in the gob that would interfere with caving.

In Longwall Operations:

1) Pillars formed during development for retreating longwalls should be uniform in size and shape.

2) Pillars should not be split after development, but if pillar splitting does become necessary it should not be carried out within the zone influenced by the working faces.

3) Width of levels should not be increased after the levels have been developed. If it does become necessary to widen a level it must be done gradually over a long distance by stripping or ribbing the coal ribs.

4) Extraction lines should remain uniform. If several walls are worked together—one behind the other—a uniform distance must be maintained between them and the wall faces must be kept as straight as possible. If the walls do get out of line, they must be brought back into line gradually to allow for a gradual change in the stress distribution over the area.

5) Stumps of coal, roof supports, etc. must not be allowed to remain in the gob to interfere with caving.

6) Midwalls should be built as rigidly as possible and properly maintained.

W. F. CAMPBELL is Resident Superintendent, Cumberland Railway & Coal Co., Springhill, Nova Scotia. TP 4774F. Manuscript, April 21, 1958. New York Meeting, February 1958.

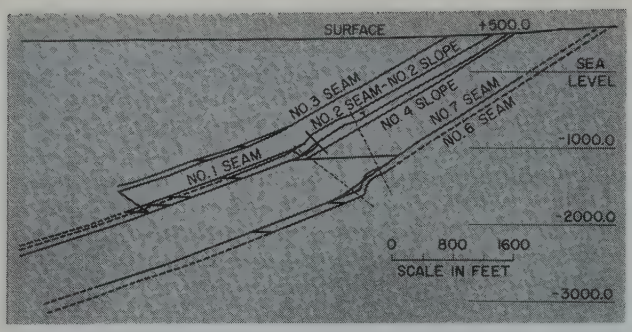

Fig. 1—*Vertical section through No. 2 slope.*

Fig. 2—*Photograph of No. 2 mine plan.*

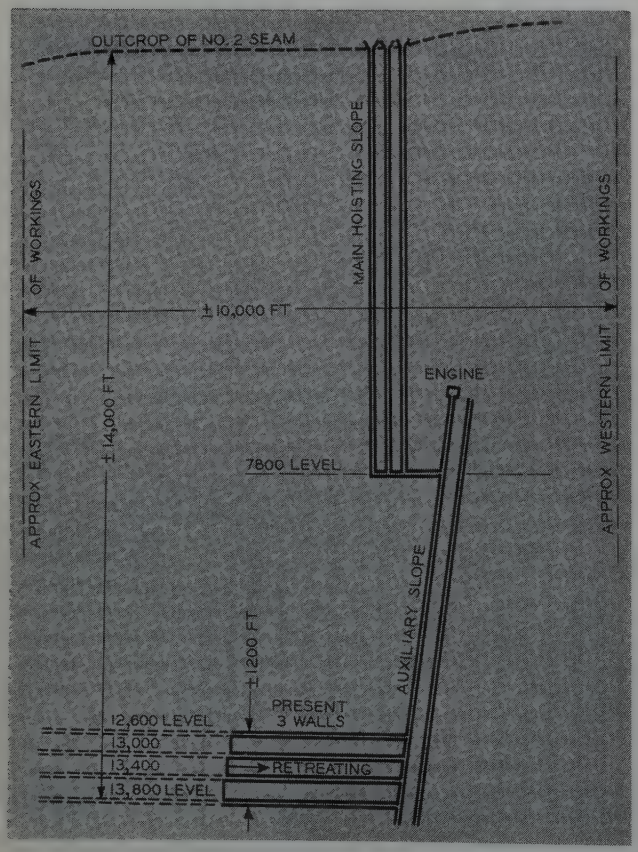

Fig. 3—*Simplified No. 2 mine.*

cover was 1600 ft, room pillars were driven on 50-ft centers and width of rooms and crosscuts was decreased from 12 to 10 ft. Even with these changes, excessive pavement heaving and roof falls required the additional work of cleaning up, and in many cases new rooms had to be driven on the high side of the old ones before the pillars could be extracted. When operations had to be suspended for a time, the entire section off the 3300 level had to be re-divided.

Change in Method: This led to a change in working method. On the 4000 levels, at 1800 ft of cover, rooms were not broken off the inclines until the levels had reached their boundaries. Room pillars were increased to 60x90 ft. This change did not correct the pavement heaving. In many cases when pillar extraction was started immediately after the room reached its limit, ribbing was necessary before the pillar was completely extracted.

After much consideration another change in method was adopted (see Fig. 4). The three-level entry system was maintained, and the levels were driven to their boundaries with inclines approximately 500 ft apart. When the level reached its boundary three rooms were driven from each side of the inside incline, and when pillar extraction began, rooms on the adjoining incline were started until three inclines were in operation. Pillars were 35 ft wide, the face of the advancing room was kept at least 40 ft ahead of the one below, and each pillar was brought back 40 to 50 ft ahead of the pillar below. Not more than three inclines and three rooms off each side of an incline were to be in operation at any one time. When the upper room pillar was brought back to the incline a new room was started off each side. The procedure was repeated until the level was reached and the area between levels was extracted to the slope pillars. This method proved satisfactory for the 4700 levels.

Early Occurrence of Bumps: The first recorded bump (Fig. 5) occurred July 1917 at the No. 3 incline, 4700 level, accompanied by a heavy fall of roof stone. Damage was confined to the empty turnout, where the high road was heaved and broken for 150 ft. Shortly before the bump occurred the high side coal had been ribbed 10 to 12 ft to allow for a spare road. Subsequently several other high side bumps occurred on this level at locations where it had been widened for spare roads.

Several coal bumps were experienced in rooms off the inclines of the 4700 West level, usually in those being driven toward the gob and in their last 50 ft or so of driving. After the room reached its boundary there were no further stress troubles during pillar extraction.

On the 5400 West level there were a great many bumps at the turnout or spare road locations, where the high side coal had been stripped for 10 to 12 ft. Many coal bursts and bumps occurred in rooms that were being driven, especially in those being driven to the waste, and on several occasions pillar bursts completely closed them with coal. These bumps occurred off inclines 2, 3, and 4 and were severe when the rooms got out of line. When the extraction line was maintained as shown in Fig. 4 the room bumps were not as serious.

The 5400 East level, under 2200-ft cover, was not seriously affected until the district bump of Dec. 6, 1924, at 11:40 a.m. The position of the workings and extent of damage are shown in Fig. 6. There was a

Continued on page 990

Fig. 4—*Room and pillar extraction adopted in an early attempt to lessen the danger of occurrence of bump.*

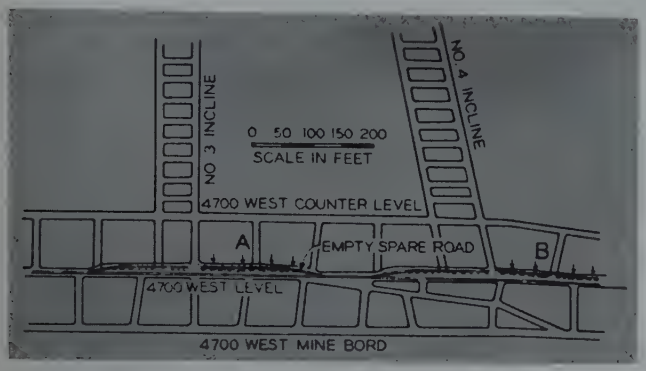

Fig. 5—*Bump of July 1917 on 4700 West level.*

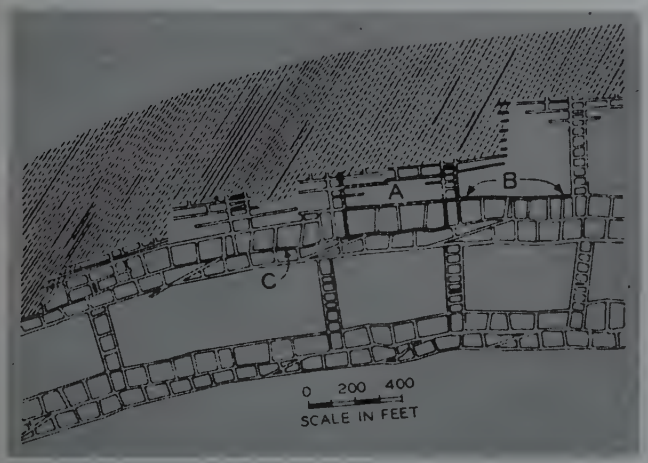

Fig 6—*This bump occurred on Dec. 6, 1924, at 11:40 a.m. The areas affected are shown cross-hatched.*

Fig. 7—*Plan showing bump locations during 5400 East longwall operations. Bumps numbered in order.*

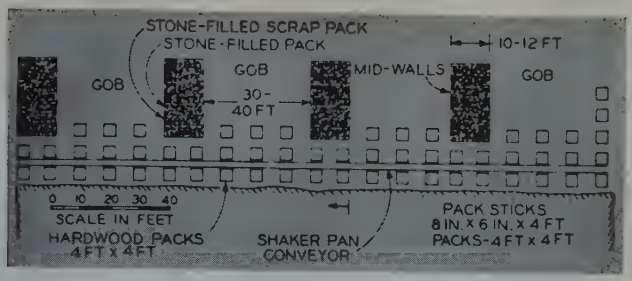

Fig. 8—*System of room support on longwall faces.*

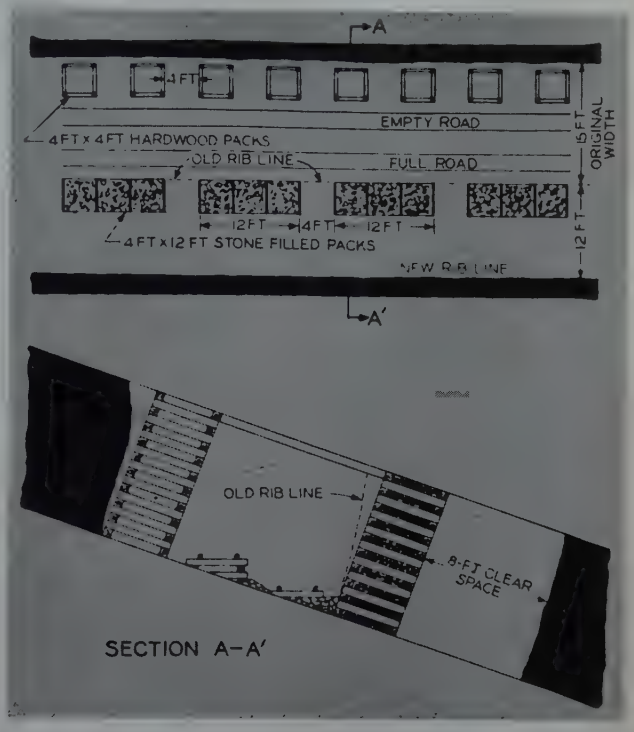

Fig. 9—*Plan showing widened levels.*

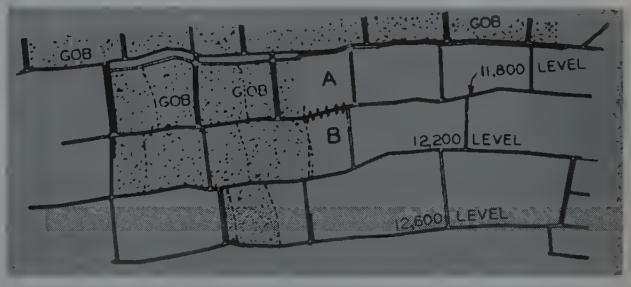

Fig. 10—*Position of faces and location of bumps on March 3 and 4, 1949. A) Bump March 3, 1949, completely filled this incline. B) Level bump March 4.*

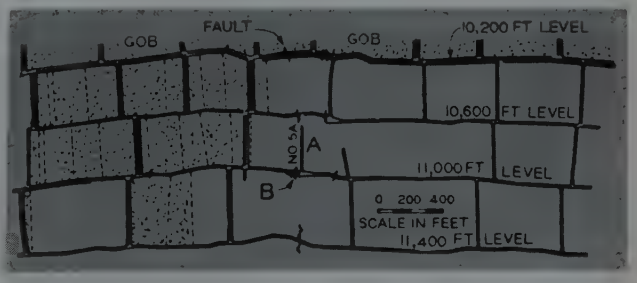

Fig. 12—*Position of walls and extent of damage caused by bumps of November 22 and December 8, 1954. A) thrust from high side. B) thrust from low side.*

second bump at 3:30 p.m. The morning bump completely closed the level between No. 3 and 4 inclines; the rails were thrown up against the roof by the ejected coal and pavement strata. No. 4 incline was partially closed from the level to the counter level, and the pavement was thrown up to the roof at the center of the incline with enough space for a man to crawl up either rib. The remainder of the incline was badly damaged. No. 3 incline was closed up to the counter level, and from here on it was blocked by heavy falls of stone. The bump at 3:30 p.m. caused a fall outby No. 5 incline.

On the 5400 East level there were two bumps prior to Dec. 6, 1924. These occurred as rooms were being driven toward the waste off No. 4 incline.

At the time of the district bump, coal was being mined off five inclines. The extraction line was irregular; in fact, it could be described as a stepped extraction line, the extraction faces off No. 3, 4, and 5 inclines forming a wide second step and the steps running parallel to the strike of the seam.

It was apparent to mine officials that the critical depth of cover for room and pillar extraction in No. 2 mine was being approached. Very little was known about other methods of extraction, but after much discussion with government consultants and prominent engineers, a system of longwall mining was introduced. Working out a longwall system that would reduce bump occurrence was a major operation, complicated by the fact that the 4700 and 6500 levels had already been developed for room and pillar extraction. During the changeover to a satisfactory system, production dropped from 1900 to 600 tpd.

The No. 6 to 8 inclines, 5700 West level, were started by the room and pillar method, but mining was abandoned because of pavement heaving and several severe bumps.

Longwall Operations Begun: The first form of retreating longwall mining began January 1925 on the 5900 West level when the 90-ft counter pillar was started from No. 6½ incline. This short wall was lengthened at the No. 6 incline up to the 5700 halfway level, and the 5700 West wall was started at No. 6 incline. Several bumps were encountered, and a break in the roof strata allowed 200 gpm of water to flow from the abandoned No. 3 mine. In December 1926 the area was vacated because of the danger that the volume would increase if there were more bumps in this section.

Similar longwall operations were started on the 5400 East and West levels in September 1925. At first only the counter pillars were extracted, but when halfway level openings had been driven between the 4700 and 5400 levels, the walls were extended to these halfway levels.

Many bumps occurred in the 5400 East and West longwall areas, especially on the levels. These sections of the mine had been cut into small pillars for room and pillar extraction, and to afford greater protection against bumps, a coal area to the high side and inby these longwalls was left unmined. Fig. 7 shows the area mined by the 5400 East longwall and the location of the bumps recorded during this mining. Most level bumps occurred shortly after the level was widened and cleaned up for spare roads.

Roof Support: The longwall roof support finally adopted is shown in Fig. 8. Not more than three lines of packs are on the walls at the end of the loading cycle; the third line is drawn and the conveyor pans advanced during the maintenance shift. Coal is mined on two shifts with hand picks and chipper picks driven by compressed air—the third shift is for maintenance. At first no midwalls were built, but it was noted that if the roof stood 20 to 30 ft in the gob and then caved the face was severely damaged. To eliminate these face bumps continuous rigid lines of stone walls, 10 to 12 ft wide, were built on 40 to 50-ft centers, extending into the gob and allowing the roof to break between them. The midwalls proved very successful.

The 5900 and 6500 East levels had been developed for room and pillar extraction, and before retreating longwall mining could be introduced in this area, halfway levels (the 5700 and 6300) had to be driven.

In August 1926, when the 5900 level room and pillar workings had reached No. 8 incline, the 5700 and 5900 East longwalls were started. There were a number of difficulties, and many face bumps were caused by the small pillars that had been developed on the 5900 level for room and pillar extraction. Several level bumps caused considerable damage, and on July 3, 1928, a district bump claimed one life and injured two men. The 5700 East level outby No. 3 incline was severely damaged for 190 ft, and the force ejected coal and pavement from the low side of the level. This bump was distinctly felt on surface.

Most Dangerous Locations: Review of the bumps showed that those at the face were not severe and that the most dangerous zone was on the levels for a distance of several hundred feet from the face. To afford greater protection in this zone it was decided to strip the low side rib to provide an extra width of 12 ft and build substantial stone-filled packs in this space (see Fig. 9). An 8-ft clear space was left between the coal rib and the low side of the packs. It was believed that the clear space would provide a void for any low side coal or strata that would be disturbed during a bump, giving men working in the level a chance to escape. This widening of the level was to extend some 800 ft ahead of the retreating wall faces.

The 5700 East level had been widened in this manner (from 100 ft outby No. 3 incline to No. 1 incline) and also the 5900 East level (from the wall face to 200 ft outby No. 2 incline) when a severe district bump occurred, on Oct. 12, 1928, injuring four men. The wall faces were just inby the No. 3 incline. The 5700 level was damaged for 1350 ft starting 150 ft outby No. 3 incline. Portions of the 5900 level were damaged and coal was thrown from the high sides of the 6300 and 6500 East levels. One minor bump occurred on the 5700 level and three on the 5900 level during the time they were being widened.

Effect of Widening Levels: Although it was not recognized at the time, in the writer's opinion widening the levels had an important bearing on bumps that followed in this area. Drilling in the roof and pavement strata disclosed a 60-ft sandstone bed in the near roof. The irregular-shaped pillars, the severe bump, and the discovery of sandstone in the near roof led to abandonment of this district after the roadways were cleaned up.

Frequency of Bumps Increased: In October 1928 the 6300 and 6500 East longwalls were started. The 6500 East level had been developed for room and pillar extraction, with the three levels driven inby No. 8 incline. After the walls retreated past No. 8 incline the rate of bumping increased. This area contained pillars 80 to 200 ft wide. A great number of

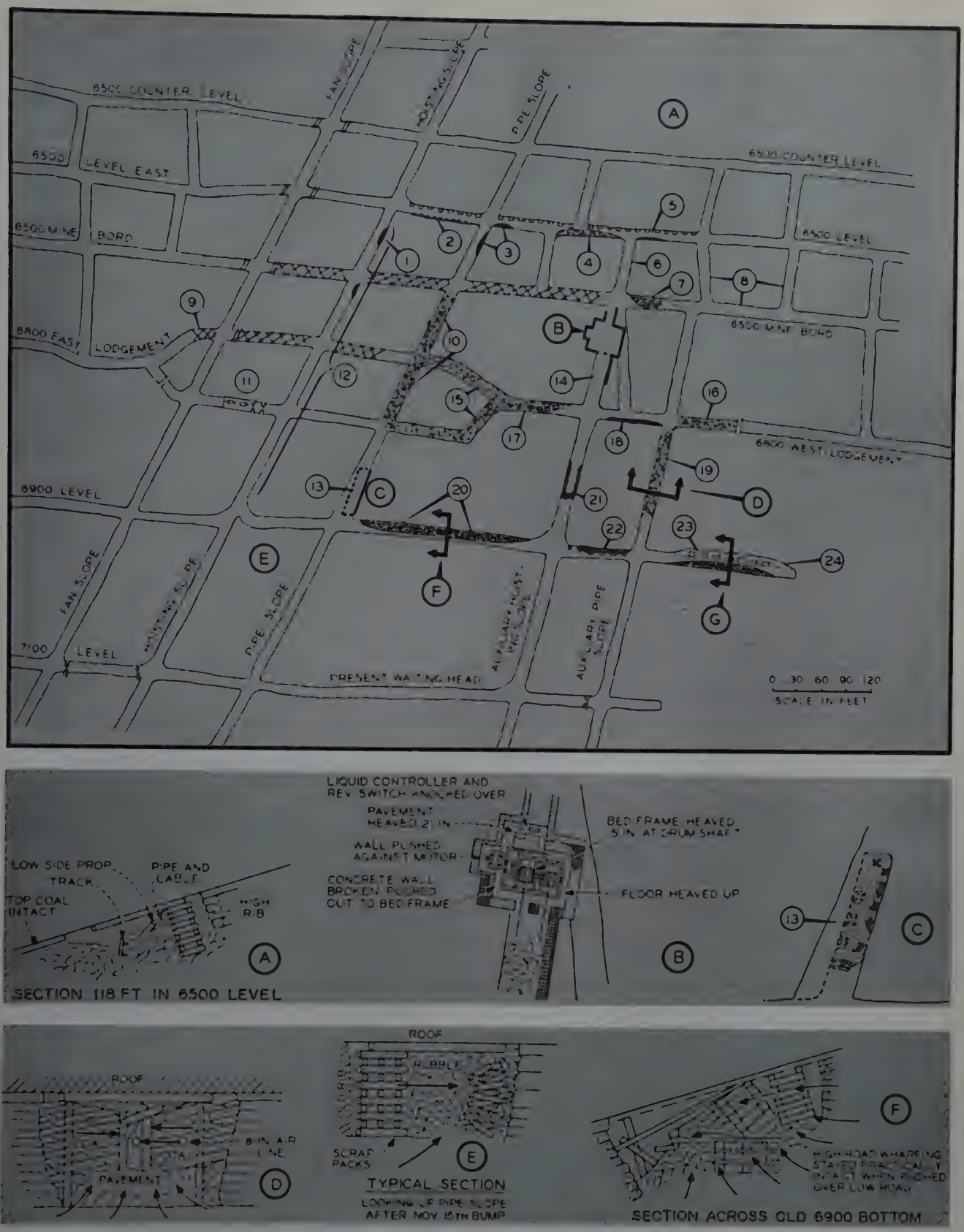

Fig. 11—District bump of Nov. 6, 1952—*1) Six west side props, rib kicked out. 2) Loose coal off low rib. 3) Eight west side props, rib kicked out. 4) Rib, props pushed to pack line, track coped to high side. 5) Broken water line, damaged low rib. 6) Ribs shaken, three I-beams down. 7) Ribs, packs pushed downhill; closed in. 8) Probably closed in. 9) Closed in by June 8 bump. 10) Pipe slope closed, some line breaks. 11) Airlock doors warped. 12) 300-ft track heave; line breaks. 13) Packs pushed to west rib; mine car smashed. 14) Pavement heaved; east rib kicked out. 15) Air, column line routes kicked in. 16) Packs pushed down, rib up; closed in. 17) High rib, packs kicked to low side; closed in. 18) Low rib coal knocked off. 19) West, east rib props pushed to east rib, closed in. 20) High rib kicked down, wharfing out, pavement heaved, track coped. 21) Pavement heaved, but ribs unaffected. 22) High rib, packs kicked downhill. 23) Low side props and coal kicked uphill, pavement heaved. 24) Drive for new lodgement.*

bumps occurred from No. 1 incline and inby for 1200 ft. Boreholes indicated that there were massive sandstone beds in the near roof, thickening in a westerly direction. Under these circumstances the area was abandoned 800 ft inby No. 1 incline in March 1932.

The 6900 and 7100 East levels were driven for longwall extraction. A very successful operation was carried out, and when the walls retreated to within 1700 ft of the main slope they were stopped because of the increased danger of bumps from heavy sandstone in the roof strata.

The 7400 and all subsequent east side levels were developed for retreating longwalls, and relatively successful operations were carried out on the east side of No. 2 mine. Level loaders were installed on the 9800 East, whereas previously coal had been loaded directly from conveyor pans into mine cars. The level loader consisted of a chain conveyor up to 300 ft long which carried the coal on the level from the face to a mine car loader. This installation lowered the height of level required at the face for mine car loading, reducing the amount of brushing done on the levels.

Effect of Small Pillars: In the 1930's, for experimental purposes, the 8600, 9000, 9400, and 9800 West levels were driven off the auxiliary slope. Inclines were driven off the 9000 and 9400 West levels at 100-ft intervals, and four rooms were driven off one of the inside inclines of the 9000 West level. A severe bump followed the driving of these rooms and two pillars burst outwards, completely demolishing three rooms. The roof was not affected. As the pillars between rooms proved to be too small, this district was abandoned.

Beginning in 1925, the main slope and its subsidiary roadways were affected by bumps. These were attributed to the small pillar size and to the fact that the coal pillars were disturbed during necessary re-timbering and pavement brushing. When operations in the overlying No. 1 seam became extensive the frequency of bumps on the main slopes increased, affecting these main entrances between the 3300 and the 6900 levels. Because of this increased bump activity, operations in No. 1 seam were stopped in 1954, and a decrease in the frequency of bumps on the main slopes followed.

A successful operation, relatively free from bumps in the extraction areas, was achieved from the 6900 East level, but on March 3, 1949, a severe bump occurred in faulty ground on No. 5A incline off the 11,000 East level, 300 ft from the wall face (see Fig. 10). This new incline was being driven outby a fault and had progressed 290 ft at the time of the bump, which threw the pavement up against the roof for the entire length of the incline. Twenty-four hours later a high side bump occurred on the level, damaging the level from the incline and inby 150 ft. The 10,600 East wall was 100 ft in advance of the 11,000 wall at this time.

At the time of this bump:

1) A pillar was in the process of being split.
2) No. 5A incline was being driven too close to the longwall faces.
3) The 11,000 East level had been widened at No. 5A incline.
4) The 10,600 East level had been widened inby the top of No. 5 incline, 11,000 East level.

As a result of this experience of one bump following another within 24 hr, an order was issued that no clean-up work was to be attempted for at least 24 hr following a bump.

In June and November, 1952, there was a series of bumps in the mine section between the 6500 and 6900 ft levels. The bumps in June were confined to the main slope and eastward from the 6500 to 7100 ft levels. On June 8 the 6800 East lodgement was badly damaged, and on November 6 a district bump occurred (see Fig. 11). The damage was extensive. Coal pillars burst outwards and coal and pavement strata were hurled into the openings. The nearest working places were in the 6900 West level, which was being driven for a lodgement, and the pipe slope was being ribbed above the 6900 level. While the 6900 West level was being driven it had previously bumped from the high side outby the auxiliary pipe slope, and on November 6 the low side bumped at the same location. The face was not affected by the low side bump. The pipe slope ribbing was not affected by the district bump on November 6, but this ribbing area bumped on November 8, and one miner was killed at the face.

This section of the mine had been split into small pillars of various shapes and sizes. These pillars were highly stressed. The driving of the 6900 West logdement, the ribbing on the pipe slope, or even the re-timbering and pavement brushing operations that had to be carried out could have triggered this district bump.

In 1954 two severe bumps occurred on the 11,800 level under 3800 ft of cover. On November 22 a high side bump completely destroyed the level from No. 4 incline to the face. The level was cleaned up. On December 8, a low side bump caused further severe damage to the level from No. 4 incline to the wall face. The position of the wall faces and the location of these bumps are shown in Fig. 12.

During the clean-up work after the first bump the 12,200 and 12,600 walls continued in operation. On November 22 the top of the 12,200 wall lagged far behind the bottom. On December 8, only a few feet separated the two walls and the top of the 12,200 wall no longer lagged behind the bottom.

To facilitate mining operations the 11,800 level was widened to allow a pack to be built between the track and the level chain conveyor. This level widening could have had a bearing on the high side bump. The relatively fast rate of change in the direction of the 12,200 wall face could have had an important bearing on the low side bump.

Three retreating longwalls—the 13,000, 13,400, and 13,800 walls—are in operation today.

To date some 500 bumps have been recorded in No. 2 mine. Many miners have been injured, and too often lives have been lost. It has been fortunate that in most cases bumps have occurred when men were absent from the affected areas.

It is strongly recommended that any precautionary measures against bumps be carried out solely by members of the mining engineering departments, for in the battle of winning coal at depth, underground officials are apt to be more concerned with daily, weekly, and monthly outputs.

The writer acknowledges indebtedness to H. Zorychta, mining engineer, Fuels Division, Mines Branch, Department of Mines and Technical Surveys, for assistance in preparing this article.

Discussion of this article sent (2 copies) to AIME before Oct. 31, 1958, will be published in MINING ENGINEERING.

by H. E. MAUCK

COAL MINE BUMPS CAN BE ELIMINATED

The many factors that control bumping must be carefully studied for each coal seam where bumps occur, and specifications known to exclude bumping should be incorporated in the mining plans. This calls for complete knowledge of the seam's characteristics and its adjacent strata, and in many instances these characteristics are not revealed until the seam is actually mined.

Pressure and shock bumps, the two general types, occur jointly and separately. In this discussion no differentiation will be made. Whether pressure or shock, they are treated as bumps, and both must be eliminated.

Bumps in mines have occurred in several places throughout the coal fields of the world. A study of many of these occurrences indicates that geologic characteristics, development planning, and mining procedure have contributed. But more specifically, there are conditions usually associated with bumps: thickness of cover, strong strata directly on or above the seam, a tough floor or bottom not subject to heaving, mountainous terrain, stressed and steeply pitching beds, and the proximity of faults and other geologic structures.

Mine planning should incorporate these known factors (not necessarily in order of importance):

1) Main panel entries should be limited to those absolutely necessary to ventilate and serve the mine. This reduces the span over which stresses may be set up that will later throw excessive pressures on barrier and chain pillars when they are being removed.

2) Barrier pillars should be as wide as practicable so that they will be strong enough to carry the loads thrown on them when final mining is being carried out.

3) Pillars should never be fully recovered on both sides of a main entry development if the barrier and chain pillars are to be removed later. The excessive pressures placed on the main chain and pillar barriers by arching of the gob areas can result in bumping when these barriers are being removed.

4) Full seam extraction is better accomplished by driving to the mine boundary and then retreat-drawing all pillars. If there are natural boundaries in the mine—such as faults, want areas, and valleys —retreat should be started there.

5) Pillars should be uniform in size and shape. The entire development of the mine should call for uniform blocks with entries driven parallel and perpendicular. Only angle break-throughs should be driven when necessary for haulage, etc.

6) For better distribution of rock stresses and reduction of carrying loads per unit area, both chain and barrier pillars should be developed with the maximum dimensions.

7) Pillars should be open-ended when recovered. If they are oblong, the short side should be mined first. Both sides of a block should not be mined simultaneously, but under no circumstance should the *lifts* be cut together.

8) Pillar *sprags* should not be left in mining. If they are not recoverable, they should be rendered incapable of carrying loads.

9) Pillar lines should be as short as practicable. (Three or four blocks are adequate). Experience has shown that rooms should be driven up and retreated immediately. The longer a room stands, the more unfavorable the mining conditions. This contributes to bumping.

10) Pillars should not be split in abutment zones (high stress areas lying close to mined out areas) and if slabbing is necessary, it should be open-ended.

11) Pillars should be recovered in a straight line. Irregular pillar lines will allow excessive pressures thrown on the jutting points. Experience has shown that the lead end of the pillar line can be slightly in advance.

12) Pillar lines should be extracted as rapidly as possible. This appears to lessen pressures on the line and render abutment zones less hazardous.

13) Extraction planning should call for large, continuous robbed out areas. Robbing out an area too narrow to get a major fall of the strata above the seam tends to throw excessive pressures on a pillar line.

14) Timbering in pillar areas should be adequate but not excessive. Too heavy timbering or cribbing is likely to retard roof falls and throw excessive weight on the pillar line.

15) Experience has shown that when pillar lines have retreated 800 to 1000 ft from the solid, bumps can occur. Because this distance may vary in different seams, impact stresses should be studied for each individual condition. In any event, extra precautions should be taken against bumps in this area.

This list of controlling factors may or may not be complete. It probably is not, but it covers most of the problem's significant aspects. The question is whether or not bumping can be eliminated. The answer is that bumping can be minimized and possibly eliminated if these and other established factors are thoughtfully considered and incorporated in the mining and extraction plans. If a mine has already been developed or the pattern set so that little change can be made, then it will be necessary to adjust to the most nearly practicable system that can incorporate the known factors.

H. E. MAUCK, Member AIME, is General Superintendent, Olga Coal Co., Coalwood, W. Va. TP 4772F. Manuscript, April 21, 1958. New York Meeting, February 1958.

Discussion of this article sent (2 copies) to AIME before Oct. 31, 1958, will be published in MINING ENGINEERING.

CAUSE AND OCCURRENCE OF COAL MINE BUMPS

by CHARLES T. HOLLAND

This discussion is concerned with those comparatively infrequent bumps that eject material from the failed mass with enough energy to wreck heavy machinery and seriously injure or kill people. In such cases there is a loud report, and the pressure waves set up in the mine atmosphere wreck ventilation controls several hundred feet from the site of the failure. Vibrations are induced in the earth's crust which may be detected several miles from the point of origin, and explosive gases may be released in large quantities.* Usually a dense suspension of dust is produced from the failed mass, together with dust placed in suspension by the resulting air blast.

These rock bursts or bumps have also been called *mountain shots, bounces, pillar bursts,* and *crumps.* Such occurrences, when extensive, are serious catastrophes, and may force abandonment of the mine.[1]

CAUSES OF ROCK BURSTS

Rock bursts in coal mines have occurred in several places under diverse geological conditions, mining methods, and/or practices. A study of many such occurrences indicates that they depend on the following conditions: 1) cover thickness of 500 ft or more, 2) cover composed of strong members and having a strong member lying close to or on the coal bed, and 3) a floor that does not readily heave.

The minimum thickness of cover under which coal mine rock bursts occur is based on observation. Under unusual circumstances involving very strong roof members and/or mining systems, and/or practices especially likely to induce bursts, a burst conceivably could occur under less roof. Under special circumstances rock bursts have occurred in marble quarries almost at the surface.[2] Furthermore, under very heavy cover it is likely that controlling roof members need not be as strong and as close to the coal bed to cause bumps.

Just what constitutes a strong roof or roof member is open to question. Obviously the strength of a roof member is determined by its thickness, the distance between bedding planes across which little or no bond exists, the spacing and development of joints, and the inherent strength of the rock material. Strata sections showing roofs under which rock bursts in coal mines have developed are illustrated in Fig. 2. In several instances the strength of rocks composing the roof of mines developing bumps has been tested. The tests (Table I) show that these rocks develop considerable strength in compression, bending, and shear and that in some cases the strengths are very high. No quantitative data are available concerning joints in roof members over coal beds where rock bursts have occurred, but the author has examined many mines subject to bursts and has received the impression that joints in the shales immediately over the coal beds are always present and well developed. In the main sandstone or conglomerate members themselves, however, where observed, he has yet to see a fracture system indicating well developed joints. Undoubtedly joints are present, but the evidence indicates that they are few, poorly developed, and widely spaced. In a mine subject to bumps, moreover, actual measurements of roof spans up to 225 ft between supports under a cover of about 800 ft have been made before roof failure occurred. Such spans signify strong roof.

In coal beds subject to rock bursts, the bottom rock is usually a sandy shale. A few tests (Table I) have been made on the floor rock of coal beds. Observations in mines indicate that they are usually weaker than roof rocks and that under load they show more plastic effects. Observation in ground subject to bursts invariably indicates a relatively strong floor highly resistant to heaving, although some heaving may occur.

Other factors listed as favorable to rock bursts are: 1) mountainous surface; 2) steeply dipping beds; 3) proximity of faults, folds, and other similar geologic structures. Many bursts have occurred in mines under mountainous country, although many bursts in mines under a surface with little relief indicate that thickness of cover, not relief, is the essential factor. In steeply dipping beds, many bursts occur in mines that are essentially flat, and rock bursts have been recorded in beds dipping as much as 35°.[1] Most rock bursts in the U. S. occur in beds that dip less than 10 pct. It is also true that most U. S. coal is produced from beds dipping less than 10 pct. Geologically, faults are regarded as providing stress relief, but in the vicinity of faults, as well as sharp folds, it would seem that residual stresses could be present. The fact that rock bursts occur in areas remote from faults and sharp folds suggests that their presence is not necessary for this phenomenon to take place. There have been many bursts close to faults and folds, and it may be assumed that occasionally such structures accentuate their occurrence.[3]

The conditions and circumstances under which they occur, coupled with the effects produced, leave

C. T. HOLLAND, Member AIME, is Professor and Head, Department of Mining Engineering, Virginia Polytechnic Institute, Blacksburg, Va. TP 4773F. Manuscript, April 21, 1958. New York Meeting, February 1958.

* In the Crowsnest Pass coalfield, British Columbia, a rock burst is estimated to have released 1.8 million cu ft of methane.

little doubt that the fundamental cause of coal mine bumps is failure of brittle material (coal and adjacent rock) from excessive stress. This being so, knowledge of the following factors is essential if the origin of rock bursts is to be understood and if measures to prevent them are to be successful: 1) cause of the excessive stresses, 2) reaction of coal pillars to load, 3) capacity of rocks to store and release strain energy, and 4) effects of mining methods on the cause of the burst. Although knowledge of these factors is not complete, each will be discussed briefly.

STRESSES ABOUT MINE OPENINGS

Consider a small cube of coal (Fig. 1) situated in a bed within the earth's crust, the faces of the cube perpendicular and parallel to the earth's radius. It will be recognized that the coal is loaded by the rocks lying between the cube and the earth's surface. Assuming that the rocks are homogeneous, isotropic, and perfectly elastic, it has been shown—for cover up to several thousand feet thick—that the load per unit of area on the horizontal faces of the cube is wd and the load on the vertical face is

$\frac{wd}{m-1}$. W, d, and m, respectively, are the weight of the earth's crust per unit volume, distance between the surface and the cube considered, and Poisson's number (Ref. 4, p. 199). If there are no crustal disturbances, and if the coal bed is thin in relation to its distance from the surface, it may be assumed with negligible error that this load is uniform throughout the bed.

Now, if the coal bed is penetrated by an opening, it will be found that stress concentrations are produced in the rocks forming the sides (pillars), roof, and floor of the opening. Assuming that the depth of the opening is more than three or four times its width and that the rocks are perfectly elastic, homogeneous, and isotropic, the following statements are theoretically true.

1) For a single opening the magnitude of the critical stress concentration in adjacent pillars depends on the following factors:[5]

a) Width of the opening divided by height of the opening. Variation of the critical stress at locations X with this ratio is shown by graphs in Fig. 3.*

b) Maximum stress depends on the geometric shape of the opening, that is, whether it is round, elliptical, rectangular, or square, and on the orientation of the axes of the opening with the force producing the stress.

c) The significant increase in stress extends into the solid rock or coal parallel with the opening for a distance about equal to the long width of the opening.

d) Maximum stress occurs in the plane of the wall of the opening (see Fig. 3).

e) Magnitude of the stress is affected by the value of Poisson's ratio of the rocks at the location considered.

2) In the case of multiple openings in the same bed, the maximum stress is not significantly affected if adjacent openings are farther apart than the sum of their widths.

* The stress values shown in Fig. 3 for R/H as related to S_t/S_v are the maximum at location X but are not necessarily the theoretical maximum stress on the opening.

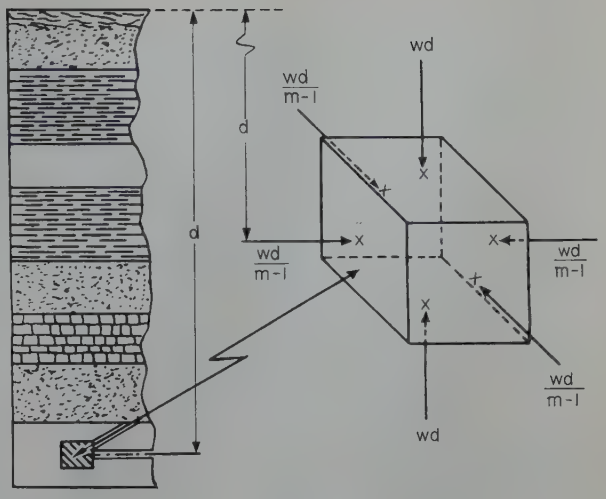

Fig. 1 (above)—*Stress conditions that prevail in coal beds before mining.*

Fig. 2 (below)—*Diamond drill logs showing roof strata over coal beds in which bumps have occurred.*

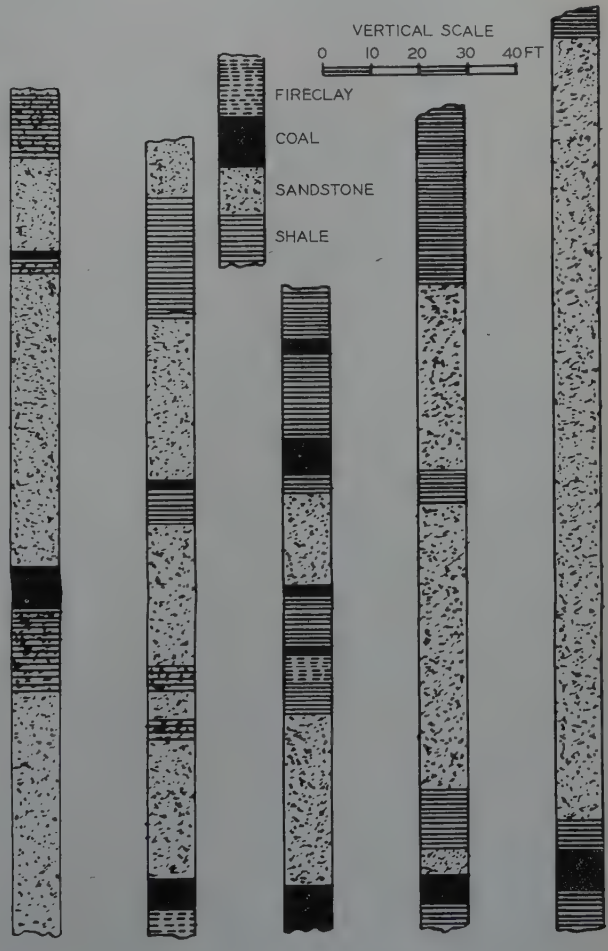

Table I. Physical Properties of Coal and Associated Rock from Beds in Which Bumps Have Occurred

Name of Bed and Location	Description of Rock Tested: Position	Type	Condition	Compressive Strength, Psi*: Normal to Bedding	Probable Error ±	Parallel to Bedding	Probable Error ±	Young's Modulus of Elasticity Normal to Bedding, Psi*: Secant Modulus‡	Probable Error ±	Shear Strength Normal to Bedding, Psi**: Strength	Probable Error ±
Upper Banner, Virginia	Roof	Sandstone	Dry	17860	367	16250	388	2,980,000	135350	4686	109
	Coal bed	Coal	Dry	3011	147			680,000	29000		
	Floor	Siltstone	Dry	3488	105	2073	242	1,709,000	471000	1353	74
	Floor	Siltstone	Wet	1250	22	909	42			1354	29
Pocahontas No 4, West Virginia	Roof	Sandstone	Dry	14741	254			5,290,000	407000	6653	305
	Roof	Sandstone	Wet					3,708,000	456000	5106	264
	Coal bed	Coal	Dry	2743	84			370,000	27000		
	Floor	Siltstone	Dry	7016	203	6647	306			2169	99
	Floor	Siltstone	Wet	4191	198	3972	211			1734	86
Harlan, Kentucky	Roof	Sandstone	Dry	13892	700	9519	195	3,000,000	592000	4833	233
	Roof	Sandstone	Wet							2615	155
	Coal bed	Coal	Dry	5138	224			567,000	38000		
	Floor	Siltstone	Dry	9003	529	7862	666	6,200,000	540000	2666	102
	Floor	Siltstone	Wet	5392	183	5389	421	4,600,000		2037	177
"C" or Taggart, Kentucky, and West Virginia	Roof	Sandstone	Dry	15550	528			3,670,000	371000	6233	261
	Coal bed	Coal	Dry	3122	314			580,000	81000		
	Floor	Siltstone	Dry	7587	1187			4,416,000	984000	3948	792
	Floor	Siltstone	Wet	6298	273	4740	608	6,466,000	330000	3786	168
Warcreek, West Virginia	Roof	Sandstone	Dry	19000	583			7,200,000	262000	4510	549
	Coal bed	Coal	Dry	2178	117			274,000	20600		
Lower Sunnyside, Utah	Roof	Siltstone	Wet	3869	564						
	Coal bed	Coal	Dry	4541	420	3660	380	487,000	34300		
	Floor	Sandstone	Wet	8987	355	6861	489				
Phalen, Nova Scotia	Roof	Sandstone	Dry	7700	540			7,548,000	86500	2660	251
	Coal bed	Coal	Dry	2197	305			259,000	59000		
Kenilworth, Utah	Coal bed	Coal	Dry	3642	140	4030	506	654,000	21000		
Marker, Virginia	Coal bed	Coal	Dry	5862	237						

* All rock specimens 2x2x4 in. or 1.5 diam x 3.0 in. All coal specimens 3-in. cubes.
** All specimens 1½x½ in. and 6 in. long approximately. Load applied normal to bedding.
† All specimens approximately 2x2x4 in.
‡ Secant drawn between zero stress and a point on the stress-strain curve at one-half ultimate strength.

3) If the openings are closer together than this, maximum stress occurs at the walls of the pillar forming the center of the group of openings, and this maximum stress is reached when the number of multiple openings is equal to or greater than five.[6]

4) In actual operations—because rocks are not perfectly elastic, homogeneous, nor isotropic and because local yield does occur—the maximum stress, as demonstrated by Phillips (Ref. 22, pp. 64, 65) and indicated by much experience in mining, does not occur at the walls of the opening but at a short distance inside the pillar. Furthermore, the maximum stress does not reach as great a value as theoretical considerations and laboratory experimental methods indicate.*

Actual distance inside the pillar, measured from the wall at which the maximum stress exists, has not been determined. Observations in many mines, however, indicate that this distance could have a minimum value of 1 to 6 or 8 times the bed thickness and that it is probably affected by width and height of the opening, depth of cover, and relative values of the elasticity and plasticity of materials comprising the roof, floor, and coal seam. The actual value of the stress produced probably lies between the theoretical maximum and the average stress concentration that would be produced if the weight of the strata above the unsupported opening were evenly distributed over the pillars for a distance equal to the opening width. In Fig. 3 an estimate of the actual stress distribution is shown by the dotted line. *This high stress area lying close to a mined out area is referred to as an abutment area or zone.*

Maximum stress in a pillar, as well as the stress distribution, as shown in Fig. 4, is influenced also by the width of the pillar relative to the width of the openings on each side of it. It should be noted that as long as the pillar is as wide as the opening the maximum stress is not materially lowered by making the pillar wider. However, making the pillar wider relative to the opening somewhat decreases the maximum stress and results in more of the pillar being under a lower stress. This is a factor that should be considered where the pillar, after being blocked out, will be subjected to the abutment loads of an advancing pillar line or longwall face.

In mining operations under heavy cover, it is not only necessary to realize that high stress areas are parallel to the mine openings and to have some idea of the intensity of the stress in the areas; it is also necessary to estimate how far these zones extend from the mined out areas. In the case of passageways, this can be done roughly by the rule given above. In the case of a goaf caused by pillar extraction or longwall operations, it cannot be done because it is not usually possible to measure the effective width of the goaf. However, it is recognized that increasing pressure will cause the rate of com-

* For example, the Pocahontas No. 4 coal bed in southern West Virginia is mined under cover up to 1800 ft thick. Development openings are driven 18 to 20 ft wide, and the bed is about 6 ft thick. According to the work of Panek, the tangential wall stress at mid-bed height under these conditions would reach values between 4000 and 5000 psi. Actual tests of 3-in. cubes of this coal show its compressive strength would be much less than this, perhaps as low as 400 psi. Yet the pillars usually show no evidence of failure in these headings.

In this same bed at a depth of 800 ft, the author has seen an opening 225 ft between supports lying between two old goaves approximately 1100 ft apart. According to theoretical considerations, the stress in the pillar walls would have been about 18,000 psi, yet the pillars showed little or no evidence of weight. In view of these observations, it is clear that the wall stress does not attain the maximum values indicated by theory.

Table I (Continued)

Modulus of Rupture, Psi**		Energy Stored, Lb per Cu In.		Poisson's Number† at		
Strength	Probable Error ±	At ½ Ultimate Strength in Compression	At Ultimate Strength in Compression	⅛ Ultimate Strength	¼ Ultimate Strength	½ Ultimate Strength
2984	104	14	53			
		See Fig. 9	See Fig. 9			
858	86					
379	37					
2167	55	5	21	21	19	13
1730	57					
		See Fig. 9	See Fig. 9			
2922	187	83	33	9	6	4
2339	299					
		See Fig. 9	See Fig. 9			
1216	350					
958	127					
2846	108	88	33.1			
		See Fig. 9	See Fig. 9	3.4	3.2	3.1
2178	328					
1733	208					
4230	310	6.4	24.7			
		See Fig. 9	See Fig. 9			
		See Fig. 9	See Fig. 9	3.9	3.4	2.8
1120	34	3.0	11.8			
		See Fig. 9	See Fig. 9			
		See Fig. 9	See Fig. 9	3.7	2.9	2.4
		See Fig. 9	See Fig. 9	4.0	3.4	3.1

pression of pillars to increase. So by determining the distance ahead of a pillar line or longwall face at which an increased convergence rate starts, it is possible to obtain an estimate of the width of the abutment zone. Several investigations of this kind have been made.[7-16] A careful study of these indicates that the minimum width of abutment area adjacent to an extensive goaf varies from 200 to 300 ft when the cover is 800 to 2000 ft. It is also probable that the abutment area extends over a greater width in room and pillar work than in retreating longwall, and over a greater width in retreating longwall than in advancing longwall. In room and pillar work it probably extends over a greater width where the ratio of least lateral pillar dimension to pillar thickness is small than where this ratio is large.

From the foregoing discussion it is clear that in the average mine two or more abutment loads from mined out areas may be superimposed. In areas where this occurs, very high stresses in the pillars may result. Two such conditions are shown in Fig. 5.

Relief Induced by Drilling Holes: As explained above, an opening made into a stressed area multiplies the existing stress at and near the surface of the opening. Consequently the walls of a hole drilled into a highly stressed pillar area could be stressed two or three times as much as the pillar itself. Such a stress, therefore, probably would cause the walls to fail, resulting in a bump or a slow squeeze of material near the hole. The unit value of the stress generated in the walls of the hole is independent of the size of hole—a drilled hole of any size should cause bumping or squeezing. However, tests on coal specimens indicate that large specimens fail at a lower unit stress than small ones. Because of this, a large hole drilled into a pillar is more likely to cause stress release than a small one. This is borne out in practice. It should also be pointed out that coals vary markedly in compressive strength (see Table I), and for this reason the size and spacing of holes drilled for stress release purposes is likely to vary for different coals.

INFLUENCE OF PILLAR SIZE

The compression (e_1) a cube of coal undergoes when under constraint is given by Eq. 1:[17]

$$e_1 = \frac{P_1}{E} - \frac{P_2}{mE} - \frac{P_3}{mE} \qquad [1]$$

in which P_1 is the compressive force producing the strain e_1, P_2 and P_3 are forces acting perpendicular to each other and to P_1, E is Young's modulus, and m Poisson's number. In the mine pillar the force P_1 will be the load imposed by the overburden. Under this force the pillar will tend to expand in a plane perpendicular to the force. The expansion will be resisted by the frictional forces induced between the coal pillar and the floor and top rock as well as by the frictional forces between various members of the coal bed itself. These forces will provide constraint to the central part of the pillar, and under a given set of conditions the constraining forces will increase as the size of the pillar increases. Consequently, up to a pillar size in which these forces, P_2 and P_3, produce perfect constraint, the compression e_1 caused by a given value of P_1 will decrease with increasing pillar size. After the pillar size increases to the point where perfect constraint exists, e_1 will no longer be affected by pillar size but only by the physical properties of the coal in the pillar. Therefore, above this critical size under a given value of P_1, all pillars composed of coal having the same physical properties will compress the same small amount.

Pillars that have uniform physical properties and are less than this critical size under a given P_1 will compress by an amount inversely proportional to the size of the pillar. A stiff unbending roof such as overlies coal pillars in mines that develop rock bursts tends to compress all pillars by the same amount. Under these conditions the larger pillars carry more than their share of the load and become highly stressed. Therefore, mining practices that allow large pillars to be blocked out surrounded by smaller ones create situations that are favorable for the occurrence of rock bursts in the large pillars unless all pillars are above the critical size. Actual mining experience demonstrates that in a situation of this kind it is usually the large pillars that develop the rock bursts.

In addition to the constraint that develops because of pillar size, variation in the value of E and m can cause load concentrations. Actual tests[10] prove that there is considerable variation in the value of E within comparatively small distances in a given coal seam, and stress concentration can therefore be expected from this cause. Little information is available concerning the values of Poisson's number for coal or how it varies in a coal bed. Because it is reasonable to assume considerable

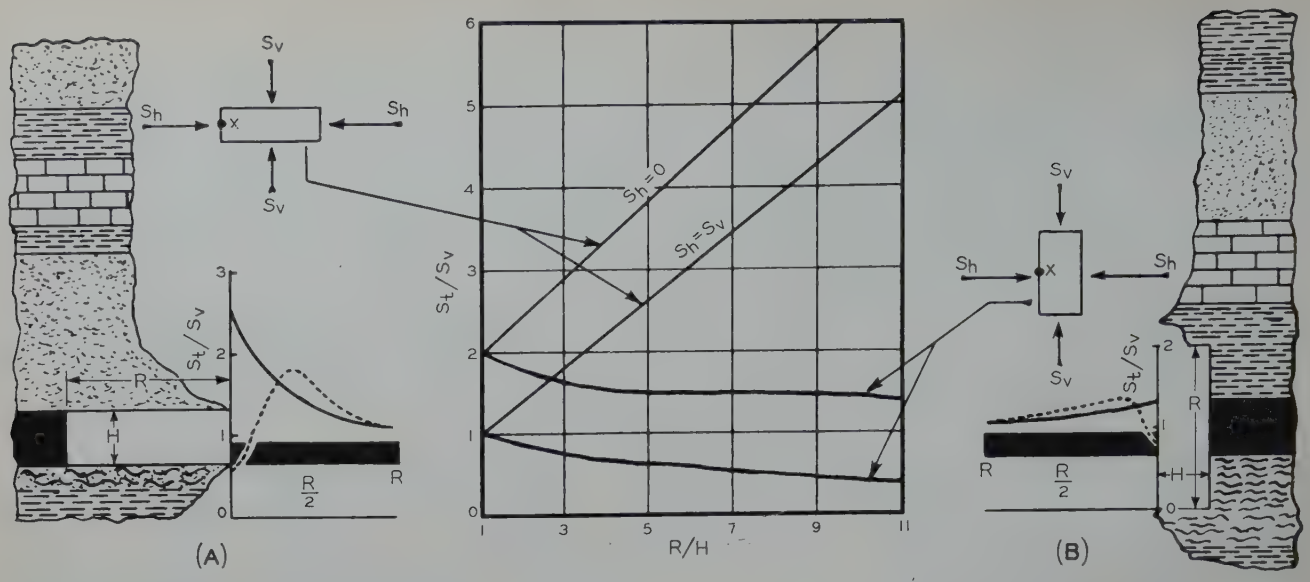

Fig. 3 (above)—*Stress conditions at mid-pillar height (X) in pillars adjacent to openings in coal beds. The graph showing the relation between S_t/S_v and R/H is based on experimental and mathematical investigations. The curves (A,B) showing the stress distribution (S_t/S_v as related to R) are estimated for the conditions $S_h = 1/3S_v$. Estimated distribution of theoretical stress is shown by the solid lines, for which the maximum and minimum values are theoretically correct and the values in between estimated. Estimated actual stress distribution is represented by the dotted curves showing the relationship between S_t/S_v and R. S_t = the tangential stress per unit area after the opening is made. S_v = weight of the overburden on the bed per unit area before the bed is disturbed by mining. S_h = horizontal stress in the bed before mining. R and H have the meanings shown. The information is based on Panek's work.*[5]

variation from place to place, stress concentrations are to be expected, increasing the probability of bursts. Any pillar or part of a pillar showing marked difference in hardness or physical structure is a likely location for a burst.

Impact Loading: Another factor, never proved to exist, that may cause high stress in mine pillars is impact loading,[18,19] which comes about because stratified mine roof spans an opening by acting as a series of beams or plates. Such structures impose high stress in support areas and perhaps relieve stress in areas behind the support. Then, as illustrated in Fig. 6, the failure of such a beam or plate or a failure of its support (such as a pillar or pillar remnant) can cause a high impact load on the pillar adjacent to the failed support, or, if the roof beam actually fails, on an area behind this pillar. Action such as this may cause a rock burst at the pillar line or at a place considerably removed from a pillar line.

Stress from Mined Areas: Stress concentration in an overlying or an underlying seam may be reflected in a bed being mined. Such concentrations in the overlying or underlying beds can come about from the various causes discussed above. A bed being mined can be affected, therefore, by abutment zones paralleling pillar lines or longwall faces or old goaves, or by stresses at unmined pillars in goaves in overlying or underlying beds. Whether or not the stress concentrations will have a serious effect depends on the distance between beds as well as the cover on the beds, and to a lesser extent, perhaps, on composition of the rocks between the beds concerned. Studies in the north of England indicate that the stresses induced by a goaf as wide as the " maximum pressure arch"* will extend a distance equal to twice the width of this arch above and below the seam in which the goaf exists. The width (see Fig. 7A) of the maximum pressure arch (W, expressed in yards) is given by Eq. 1:

$$W = \frac{d}{20} + 20$$

where d is the depth in feet from the surface to the bottom of the seam in which the width of the pressure arch is being computed.[20] That is, a bed lying at 800 ft would have a maximum pressure arch of 180 ft. This arch would produce stress concentration at its abutments for a distance of about 360 ft above and below the seam. The area affected in the seam being mined, however, would not necessarily be directly over or under the abutment of the arch in the seam above or below but would be located as illustrated in Fig. 7B. It will be apparent that many combinations of abutment loads can occur when more than one bed is mined. As illustrated in Fig. 11D, such concentrations can have serious results. Examples are shown in Fig. 7B. To these possible combinations should be added the stress multiplications that can occur owing to interaction of pillar lines and other causes when only one bed is mined.

* Maximum pressure arch is the widest opening in a mined bed across which the main roof load can be transferred to supports at the perimeter of the opening.

STRAIN ENERGY AND ROCK BURSTS

Coal and associated rock are highly elastic under load (see Fig. 8) and when stressed have the capacity to store elastic strain energy. When these materials are not constrained, the amount of energy stored varies approximately as the square of the stress in the rock or coal and inversely as Young's modulus of elasticity for the material. Fig. 9 shows the energy coal is estimated to store at various ultimate strengths when not constrained. These curves present the result of tests that have been run on coal from seams that have and have not developed bursts. It will be noted that these seams do not differ discernibly in their capacity to store energy. It will also be observed that unconstrained coal can store comparatively large amounts of strain energy when

highly stressed. At low stresses, however, the amount of strain energy stored per unit volume is small. When the coal is stressed to failure the violence of the failure, as well as actual measurements, indicates that a large proportion of this strain energy is released.[21]

When a rock is perfectly constrained and stressed in compression or tension, it stores strain energy as indicated by Eq. 2 (Ref. 22, p. 58):

$$W=\frac{1}{2E}\left\{P_1^2+2\left(\frac{P_1}{m-1}\right)^2-\frac{2}{m}\left[\left(\frac{2P_1^2}{m-1}\right)+\left(\frac{P_1}{m-1}\right)^2\right]\right\} \quad [2]$$

where W = strain energy stored per unit volume, E = Young's modulus of elasticity, m = Poisson's number, and P_1 = the principal stress acting.

Study of this equation shows that when the value of Poisson's number is 2, no energy is stored in the material stressed. Fig. 10 shows that when stressed at 2500 to 4000 psi and above coal has a Poisson's number of 2.* Consequently when perfectly constrained up to a stress of some 3000 psi, coal stores energy. When stressed above this figure, however, it stores no additional energy because of the increased stress. Therefore, pillars in which the constraint is small (when the ratio of pillar width to pillar thickness is less than 3 or 4) usually store energy nearly as an unconstrained body. When the pillar is large, the coal in the central part of the pillar is subject to high constraint and cannot store large amounts of energy, but the coal relatively close to a free face (for example, within four to six times the seam thickness) can store large amounts of energy. This is the part of the pillar, however, that is subject to high stresses (Figs. 3-5), and in this area the amount of energy stored is large. Consequently, if such a pillar is split or slabbed, mining may penetrate the highly stressed area storing large amounts of energy, and a severe burst may result. Also, when large pillars are surrounded by smaller ones, and the abutment area of an advancing pillar line moves over the large pillar, the resultant stress may become great enough to fail a part or all of the pillar containing this high-energy coal and a very serious burst can result.

As pointed out before, coal which can develop only comparatively low stress stores only small amounts of strain energy and should fail nonviolently. Thin-pillar mining systems therefore have been devised in the hope of eliminating bursts. Although they have not accomplished this, some of these systems have been successful enough to justify further experiment. In this connection it should be kept in mind that 3-in. test cubes of strong coal usually fail violently, and in several instances pillars only two or three times as wide as the bed is thick have failed with enough violence to injure workmen seriously (see Fig. 11B). At present it seems wise to limit these experiments to weaker coals such as the low and medium volatile seams, and even here the system should not be used to extract large pillars surrounded by smaller ones or in other conditions where the coal bed may be under unusually high stress.

Roof rocks when stressed can store energy in addition to that stored by seams. Tests indicate that under the same compressive strength as coal, these beds do not store as much energy per cubic inch of volume (see Table I). But these rocks also store

* Note that coals tested and listed in Table I do not attain a Poisson's number of 2 at this stress, although some are close.

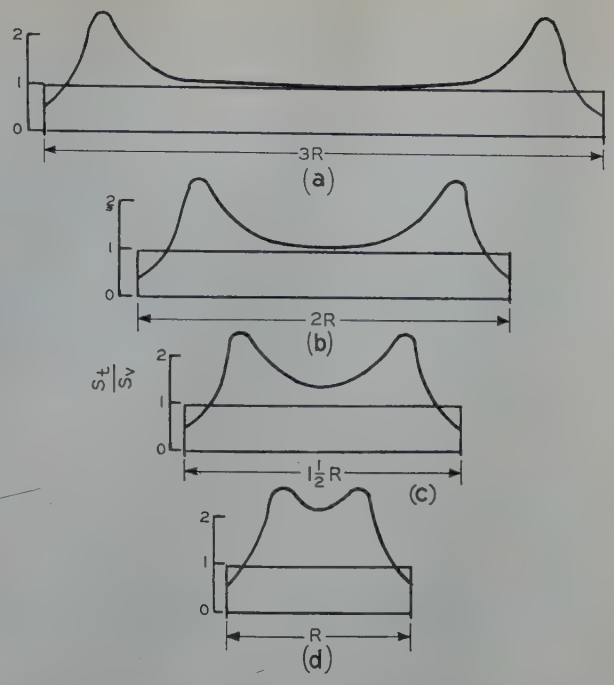

Fig. 4 (above)—*Pillar stress magnitude and distribution as affected by width of the pillar relative to width of opening (R). As the width of the pillar varies from one to three times the width of the opening it supports, the maximum stress decreases very little, but the stress distribution is changed.*

Fig. 5 (below)—*Abutment zones paralleling passageways and extensive goaves in a coal mine. In abutment zones the closest spaced lines indicate areas of highest stress. Area within the dotted line is defined as a pillar-line point and is that area lying within 200 to 300 ft of two or more goaves. The abutment zones from two or more openings may be superimposed, resulting in very high stress areas. Room C is being driven in such an area.*

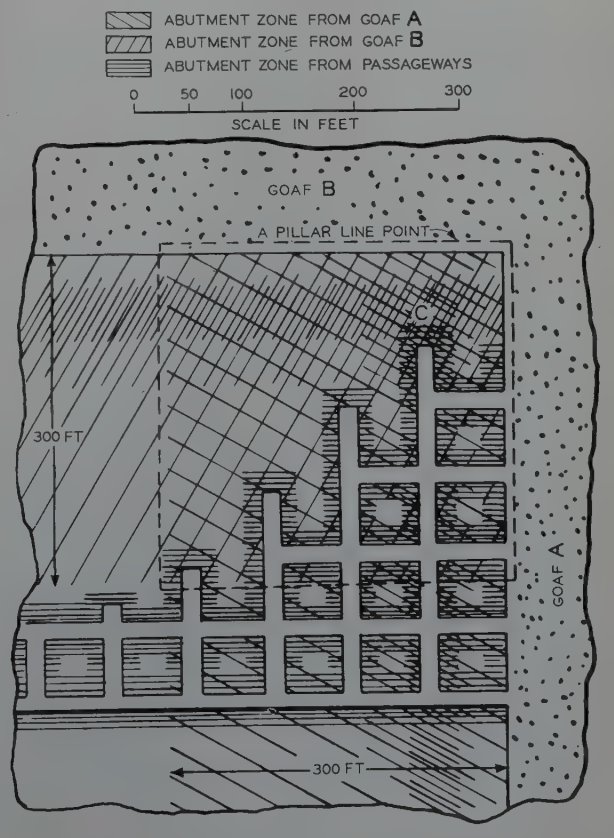

energy when stressed as plates or beams when spanning mined out areas. The amount of energy stored varies as the fifth power of the span developed. Also a cantilever beam can store about 36 times as much energy for the same span as a beam supported at both ends (Ref. 22, p. 59). These beams when they rupture probably release a great amount of this energy, which forms part of the energy that causes the impact loads discussed previously. For this reason it is important to prevent the formation of long spans acting either as beams or plates of unsupported roof, especially if the span is of a cantilever type. If the formation of long roof spans cannot be avoided, measures should be taken to prevent their instantaneous failure.

STRENGTH OF MINE PILLARS

Many investigations of the strength of coal in small specimens (2 to 4-in. cubes) reveal a strength of 1500 to 8000 psi. As the size of the test specimen increases, however, the unit strength drops. For example, as a 5-ft cube the Pittsburgh seam near Bruceton, Pa., has a strength of 695 psi, but as a 2½-in. cube its strength is 2486 psi (Ref. 23, pp. 1, 12). Gaddy[24] investigated the strength of cubical coal specimens and found that the ultimate strength of the cubical specimen tested varied inversely as $\sqrt{\text{dimension}}$ and that the general equation for the strength of a cubical specimen is

$$S \frac{K}{\sqrt{D}} \qquad [3]$$

in which K is a coefficient depending upon the physical characteristics of the coal bed and D is the dimension of the cube in inches.

Mueller[25] has demonstrated that a comparatively small confining stress greatly increases the strength of coal. The Scranton Engineers' Club[26] determined that the strength of anthracite varies as $\sqrt{\frac{1}{\text{thickness}}}$ of the pillar, other things being equal. The author[21] has demonstrated experimentally that for small laboratory specimens of bituminous coal the strength varies as $\sqrt{\frac{\text{width of specimen}}{\text{thickness of specimen}}}$ and Greenwald[23] and others have demonstrated experimentally that essentially the same relationship holds true for much larger specimens tested under mine conditions. Furthermore, the present writer's experiments[21] demonstrated that, under laboratory conditions, after the ratio width of specimen to thickness of specimen increased above 4.9 the weaker coals, such as the low volatile bituminous coals, did not fail abruptly but squeezed. The ratio was increased to 8 or higher before the stronger high volatile coal squeezed rather than failed abruptly. This increase in strength as the ratio width to thickness increased was undoubtedly due to the effects of a confining pressure such as noted by Mueller. The confining pressure builds up in laboratory specimens as well as in mine pillars, because of the friction between the coal and the top and bottom rocks and the tendency of coal to expand horizontally under a vertical load.

The strength of coal pillars in mines, however, is not given by tests of small cubical specimens or by tests of cubical specimens having edge dimensions equal to bed thickness. On the basis of laboratory experiments and studies of loads supported by pillars in coal mines for periods up to 40 years, Holland and Gaddy[31] have suggested that the average ultimate strength of a coal mine pillar can be represented by Eq. 4:

$$S = \frac{k\sqrt{L}}{T} \qquad [4]$$

where S = ultimate strength of coal pillar, psi.
k = coefficient depending on the coal bed.
L = least width of the pillar in inches.
T = thickness of pillar in inches.

The exact $\frac{\text{least width}}{\text{thickness}}$ ratio over which this equation applies is not known, but it seems likely that it would apply for values between 0.75 and 15. Above a ratio of about 15 the pillar probably becomes indefinitely strong and fails only by squeezing, i.e., plastic flow, but it should not be assumed that a pillar having an average stress below the ultimate value given above will not fail abruptly. Such a failure may be explained by the rim stress in a pillar (Fig. 4). This concentration of stress may cause a pillar to fail at the edge even though the main body of the pillar does not. In the low volatile seams of southern West Virginia three pillars approximately 150 ft on a side and 6½ ft thick failed abruptly and with great violence under an overburden of 800 to 1200 ft, but it is believed that these failures were initiated by rim failures. Coeuillet[27] places the minimum width of a pillar that will not fail abruptly at greater than 150 ft.* The actual strength of coal pillars is still in doubt, but it may be safe to make the following assumption:

1) For ratios of $\frac{\text{least width}}{\text{thickness}}$ between 0.75 and 15 the unit strength of a coal pillar may be given by the equation $S = \frac{K\sqrt{L}}{T}$.

2) It should not be assumed that any pillar less than 250 to 300 ft on a side in a bed 6 to 8 ft thick under an excessive load, concentrated or otherwise, will gradually fail by squeezing rather than by shattering in whole or in part.

Actual size of pillars to be used depends as much on loading conditions as on strength of pillars. Fig. 3 shows the theoretical loading as well as an estimate of the probable loading of the pillar immediately adjacent to the passageway. It will be noted that the zone of disturbed stress about a passageway is estimated to extend a distance into the pillar about equal to the width of the excavation. Consequently, if two passageways driven in a bed are separated by a distance equal to their combined widths, their zones of disturbed stress should not influence each other (see Fig. 4). In consideration of this fact, Panek (Ref. 5, p. 39) has suggested that pillars should have a minimum width equal to the combined widths of the passageways that delineate the

* The key to this situation may be the coefficient of friction, under extremely high loading conditions, between the coal and the roof and floor rock or within the coal itself. The coefficient when the coal is loaded beyond a critical unit load, or following a very small movement of the coal relative to the top and bottom rocks, may suddenly decrease and permit an instantaneous decrease of the constraining force, thereby permitting a pillar burst to occur. In this connection the brown stains on the roof, common to all burst areas, indicate relative motion between the coal and top rock under high stress conditions at the interface. More research is warranted on this phase of bursts.

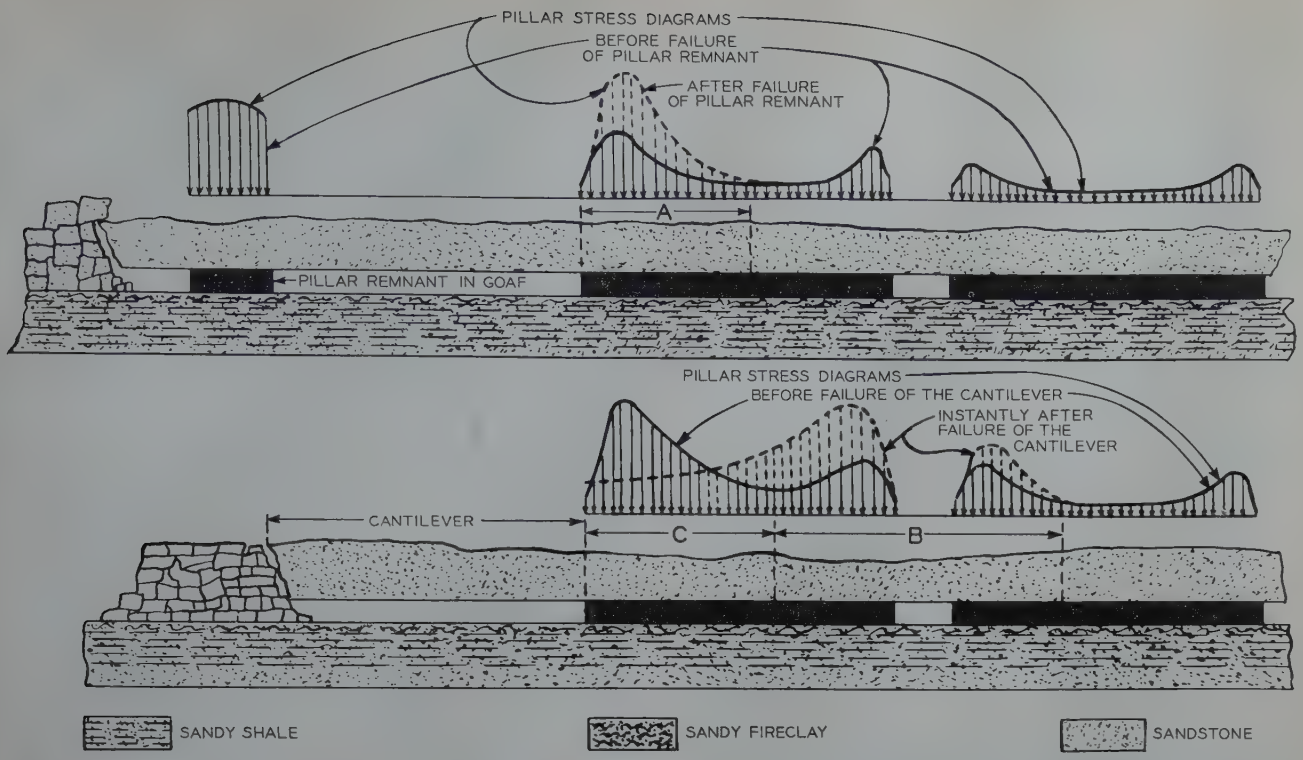

Fig. 6—*Impact stress in coal beds. If the pillar remnant fails suddenly, part or all the load it supported is instantly transferred to the pillar at A and may produce a high impact stress that might cause a shock bump at A, see upper drawing. As the span of the cantilever increases due to mining, the stress at C also increases as shown in lower drawing. If the span becomes long, a pressure bump may occur at C. If the cantilever fails suddenly, the stress at C is decreased, but a high impact stress may be caused in the area B and could result in a shock bump in this area.*

Fig. 7—*Abutment areas adjacent to the maximum pressure arch. Part A shows the general properties of the arch. DE is the high stress area in the abutment. Note that it is acting in all beds across which the arch extends. CD is a low pressure area, and in EF the stress in the coal bed is only a little greater than that which prevailed before the middle seam was mined. Part B illustrates how abutment loads from areas mined in overlying and underlying beds may be superimposed. At IJ three abutment loads act, resulting in a very high stress in the rocks. At GH point two abutment loads are superimposed. There are many other possible combinations.*

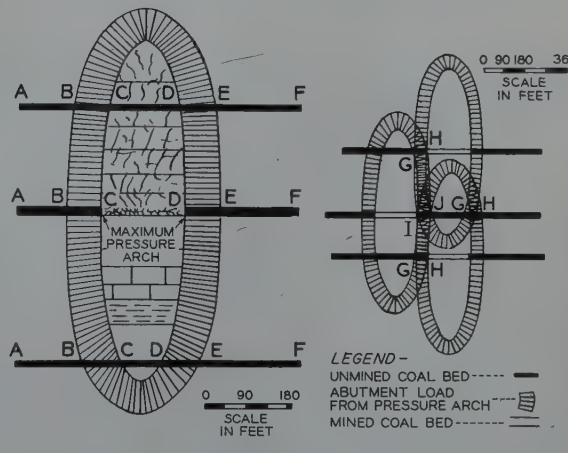

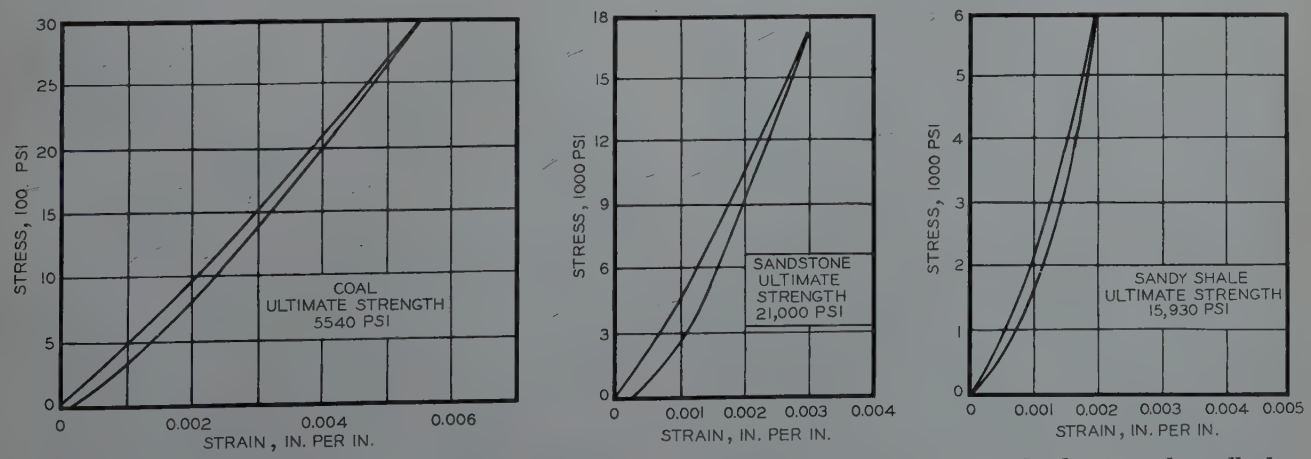
STRESS, 100 PSI
COAL ULTIMATE STRENGTH 5540 PSI
STRAIN, IN. PER IN.
STRESS, 1000 PSI
SANDSTONE ULTIMATE STRENGTH 21,000 PSI
STRAIN, IN. PER IN.
STRESS, 1000 PSI
SANDY SHALE ULTIMATE STRENGTH 15,930 PSI
STRAIN, IN. PER IN.

Fig. 8—*Typical stress-strain curves for shale, sandstone, and coal under a compression load. Note that all three show high elasticity under a load applied for a short time, although strengths range from 5,540 to 15,930 psi.*

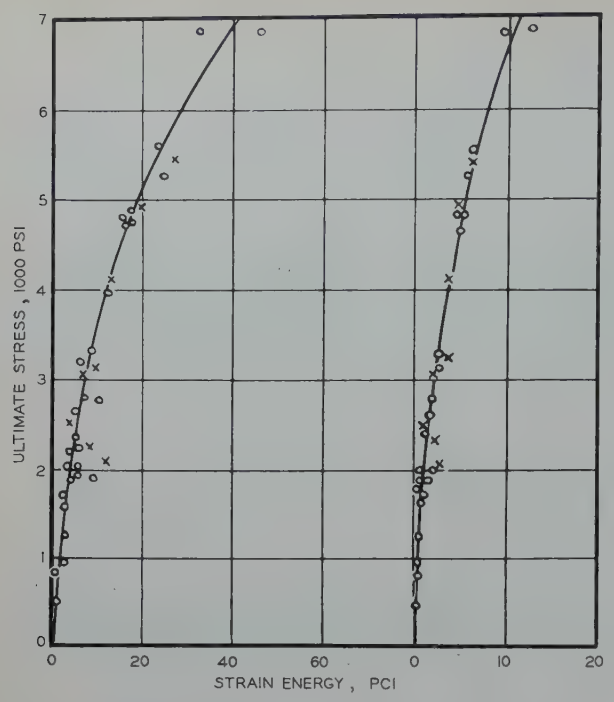

Fig. 9—*Energy stored by coal when stressed and unconstrained. Circles represent coal from beds that have not developed bumps and crosses the coal from beds that have. Curve A shows the energy estimated to be stored at the ultimate strength of the coals tested. Curve B (at right) shows the energy stored when the coal is stressed to one half its ultimate strength.*

pillars. Actually, the minimum width of pillars should be somewhat more than this, as the coal at the edge usually is destressed and sometimes failed for a distance of one to three times the thickness of the bed. Furthermore, the pillar is liable to be subject to the zone of very high stress advancing ahead of a pillar line. Pillars should be designed to take care of this increased stress, and pillars loaded as A and B of Fig. 4 are loaded will be able to carry this increased stress better than pillars loaded as C and D are.

Since there is no certainty that small pillars will give protection against bursts, it seems wise at present, because of the factors listed above, to make them as large as possible. In most cases, legal requirements of practical considerations will limit room pillars to a maximum side dimension of 80 to 100 ft. A square pillar is the best shape. Because of the tendency of pillars to load up when larger than surrounding pillars, all should have the same dimensions. Furthermore, since the maximum stress on a pillar increases as the width of the passageways that cut it out, passageways should be kept as narrow as practicable. Certainly in beds up to 6 or 8 ft thick, the passageway should not be more than 14 to 16 ft wide.

The manner in which the pillar is recovered is important. It should be kept in mind that under heavy cover the edge of the pillar next to an extensive goaf is usually crushed and/or destressed for a considerable distance into the pillar. Recovery lifts therefore should be taken off the goaf side. Also, for a given area of recovery per lift this practice decreases the unit strength of the pillar the least. Pillars should not be split, as this causes the greatest decreases in unit strength for a given area of recovery (Ref. 28, p. 60). In addition, a place driven through the pillar must pass through the areas of highest stress and greatest stored energy content where burst probabilities are the largest. The pillar should not be slabbed on the side away from the goaf, because here the area of destressed coal paralleling the passageway is narrower, and it is highly probable that mining operations will penetrate it before the stresses have been dissipated. Even in open end operations, the slab taken from a pillar should be no wider than 12 to 14 ft in beds up to 6 or 8 ft thick.

Under some conditions it would considerably promote safety if the destressed area of a pillar next to an extensive goaf could be made wider. Experiments in South Africa indicate that in the hard rock of the gold mines on the Witwatersrand blasting can be used to widen the destressed area.[29,30] In this case the destressing is done by boring deep holes into and normal to the face and blasting them with just enough explosive to fracture the rock without shooting it down. These destressing holes are drilled 3 to 5 ft apart and 10 ft deep. To date the practice seems to have reduced the number and severity of the rock bursts that occur. Limited experience in coal mines with similar operations suggests that bumps can be controlled and induced at opportune times. Solid shooting in coal mining is fraught with danger, but in some cases where the bump hazard is high the practice might be justified if adequate precautions were taken.

WHERE ROCK BURSTS OCCUR

In a survey of the occurrence of coal mine bumps fairly complete data have been gathered on 163 pillar bursts.* This information has been analyzed to find out where and under what mining practices bursts occur. Results of the analysis are presented in Tables II and III.

* This has continued the survey made by the U. S. Bureau of Mines and reported in *Bull. 535*.[32]

Examination of Table II will reveal that about 80 pct of all bursts studied were located definitely or probably on a pillar-line point (see Figs. 5 and 11 A and C). To appraise properly the significance of the large proportion of bursts occurring on points, it would be necessary to know the proportion of

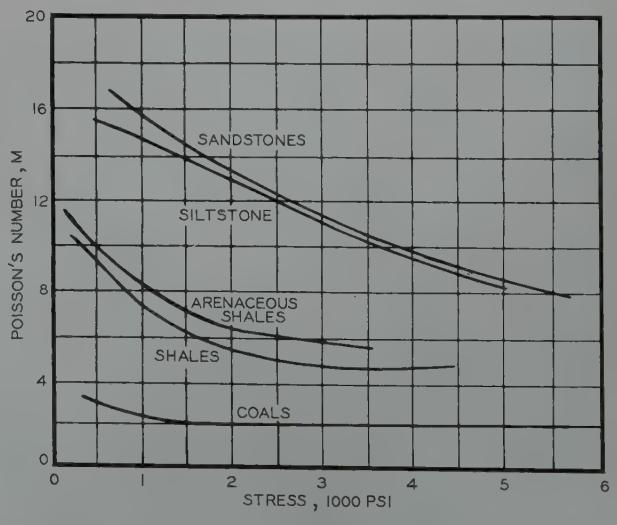

Fig. 10—*Poisson's number for various coal-measure rocks, varying stresses. (After Phillips, Ref. 22, p. 62).*

coal produced from these areas. This information is not available, but inspection of a great many mine plans indicates that much less than half the coal was produced from the areas classed as pillar-line points. It is therefore readily apparent that the likelihood of bursts occurring on points is much higher than the probability in other areas. These points or projections, as explained above, are the areas in which mine pillars are subjected to the greatest loads and highest stresses. Furthermore, nearly all the bumps studied occurred in or close to areas where pillars were being extracted.

Table III presents results of the analysis of the bursts as related to mining operations. To develop the full significance of the results, it is also necessary to know the relative amount of coal produced from each operation. As in the case of pillar-line points, this information is not available, but some general estimates can be made. For example, 19 pct of the bursts occurred in open end pillar extraction. Apparently this operation is often associated with bursts. When it is realized, however, that in mines subject to rock bursts most pillars are recovered by open end methods and that such methods probably account for 50 pct of the coal produced, it will be seen that the operation is relatively safe. Operations other than open end—such as slabbing and splitting in the abutment area, development in abutment areas, and pillar-and-stall recovery—account for 45 pct of the bursts, although such operations probably produce less than 25 pct of the coal. It should also be noted that fewer than 1 pct of the bursts studied occurred in development that was done out of the pillar-line or goaf-line abutment area. This development was done under cover just as heavy as that which prevailed over the abutment areas of pillar lines and goaves and probably accounted for at least 25 pct of the coal produced.

Table II. Location of Bumps

Location	Number	Percent of Total
On pillar line points	111	68
Probably on pillar line points	23	14
Probably not on pillar line points	7	4
Definitely not on pillar line points	19	12
Insufficient information to classify	3	2
Total	163	100

The rock bursts classified as district bursts in Table III are those that affect several pillars simultaneously (see Figs. 11C and 12B). Such bursts in the past usually have been called *shock* bumps. It is important to note that 80 pct of these occurred in the area defined as a pillar-line point. While in many cases these probably are rightly named shock bumps, it should be observed that all were in areas where pillars are subject to very high static loading. The chances are quite high that some of these actually were not shock bumps as usually defined, but pressure bumps. It is also possible that failure of one pillar from excessive pressure may have caused stress disturbances resulting in failure of other pillars that were stressed close to the point of failure—a kind of chain reaction.

PREVENTION OF ROCK BURSTS

Rock bursts in coal mines are best prevented if the mine is planned from the beginning to eliminate their occurrence in every way possible. This involves thorough study of the natural conditions, especially cover thickness and the make-up of that cover with regard to strong strata as well as the rocks forming the floor. The following points should be given particular attention:

1) In complete-extraction operations all the coal should be recovered. The all too frequent practice of leaving pillars or pillar remnants in the goaf should be eliminated. The load-supporting capacity of those that cannot be recovered should be destroyed insofar as possible, to lessen the danger of bursts from failure of beam or plate support areas.

2) Pillar lines should be orientated with the natural fracture system of the roof to promote caving in the goaf, so that long spans will not form over goaf areas. If the formation of long spans cannot be avoided, steps should be taken to prevent their rupture. Cribs used judiciously have been employed successfully to do this.

3) Development in abutment areas of pillar lines or old goaves should be avoided. This can be done by keeping active development more than 200 to 300 ft ahead of the pillar line or from the goaf edge. Furthermore, places making development in abutment areas should not be driven toward pillar lines or old goaves. This means that development places are always being advanced toward areas of lower stress. Fig. 13 shows one method that will avoid both mining on points and development in the abutment zone of old goaves.

4) Extraction should be planned to eliminate points formed by converging pillar lines or pillar lines on an old goaf and advancing parallel to the old goaf (see Fig. 13). It is particularly important to eliminate, whenever possible, the practice of leaving a set of entries protected by heavy barrier pillars 200 to 300 ft wide between mined out areas.

5) Pillars should be recovered by open end methods, and the *lift* removed in each cycle should

Continued on page 1004B

Table III. Mining Operations Being Performed or Conditions Existing When Bumps Occur in Coal Mines

Mining Operation Being Performed (Col. 1)	Number of Bumps (Col. 2)	Percent of Total (Col. 3)	Bumps that Occurred on Pillar-Line Points	
			Number* (Col. 4)	Percent Number in Col. 4 is of Number Listed in Col. 2 (Col. 5)
Open end pillar extraction	31	19	20	65
Slabbing pillars in abutment areas	35	21	26	74
Developing in abutment areas	30	18	24	80
Splitting pillars in abutment areas	9	6	9	100
Pillar not being mined and back from extraction line	16	10	9	56
District bumps	10	6	8	80
Pillar and stall pillar recovery	7	4	4	57
Pillar being mined, bump not at face	2	1	2	100
Recovery of pillars surrounded by goaf and small pillars or partly mined pillars	3	2	3	100
Pillar on completed goaf line and not being mined	5	3	5	100
Miscellaneous	4	3	2	50
Insufficient information to classify	11	7	8	73
Total	163	100		

* Only part of the bumps classed as probably on pillar line points are included in this count.

Fig. 11

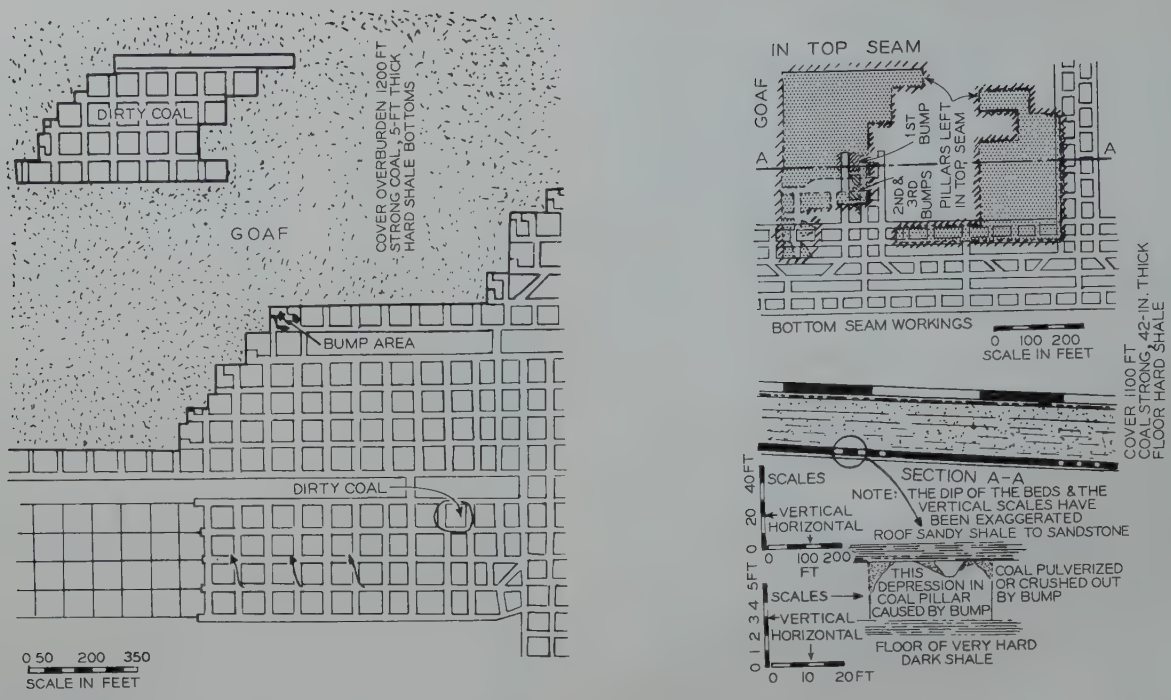

A. (ABOVE)—Occurrence in pillar in a point area where two abutment loads impinged on the pillar, which was being recovered by open end lifts driven parallel to first one goaf and then the other. B. (BELOW)—This bump in a pillar only 12 ft wide resulted in fatal injuries. In many coal beds a thin pillar may bump. C. (RIGHT)—A district bump, which affected 14 pillars. Note that part of the pillars that bumped were in a point area. Bump may have been set off by driving the place shown (in which a cut had been completed a few minutes before failure occurred) into the large pillar. An estimated 2000 to 3000 tons of debris were produced by the failure. D. (UPPER RIGHT)—This bump occurred as development places in a lower bed were being driven under a pillar in a mined out upper bed. Pillar in upper bed was carrying multiple abutment loads.

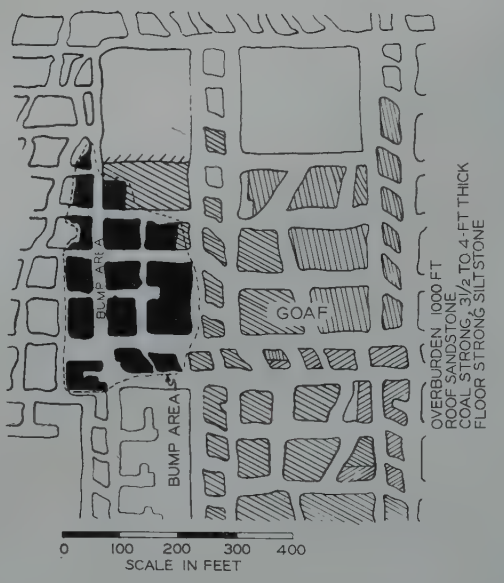

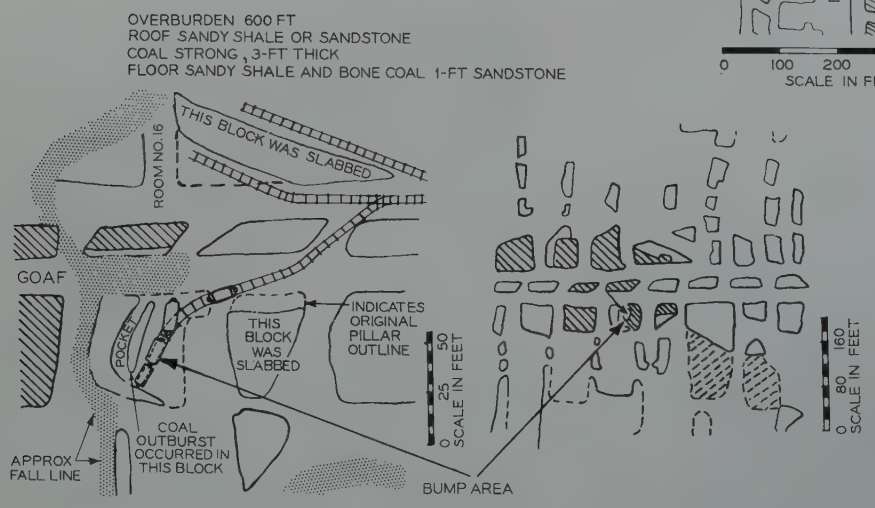

A. Bump occurred as rooms were being developed in point area. This point carried two heavy abutment loads and may have carried a third lighter abutment load from the area developed by entries.

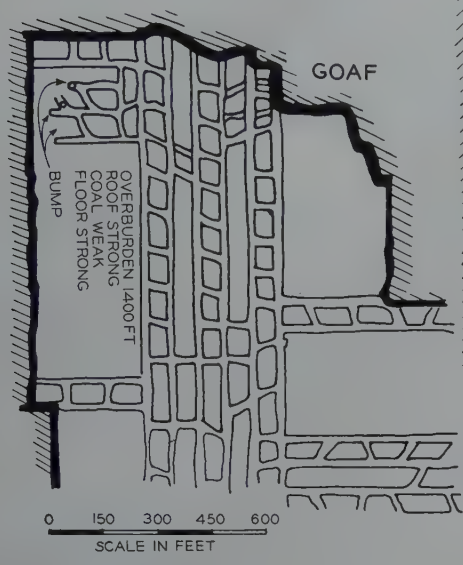

B. A very large district bump. The pillar line had several point areas, but bump occurred outside goaf abutment zone. Burst seems to have been an impact bump. Several thousand tons of debris were produced.

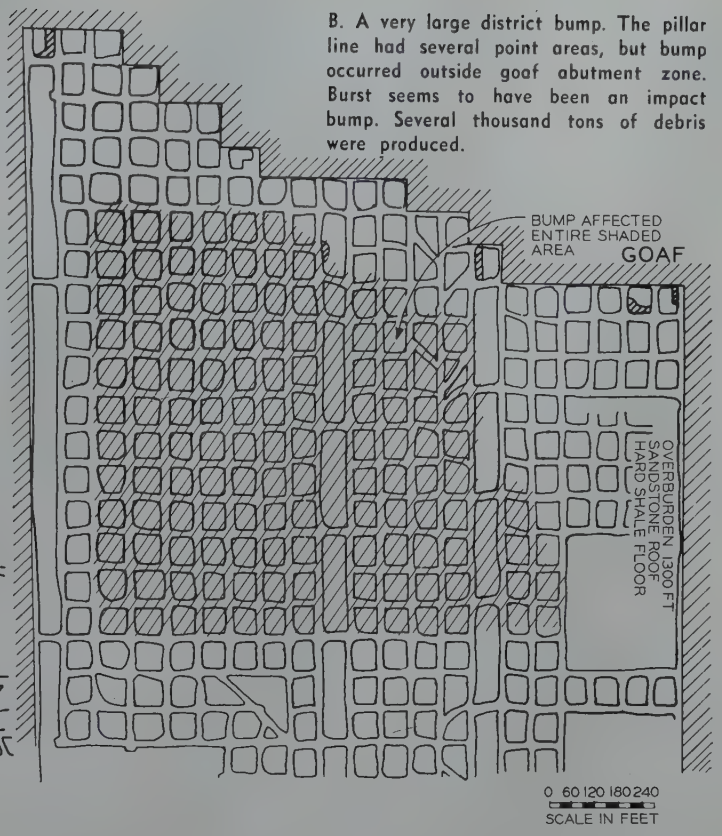

C. Bump occurred as pillar in a point area was being slabbed from the outby side toward the goaf. Three abutment loads probably impinged on this pillar, two from goaf and one from large area developed by slabbing.

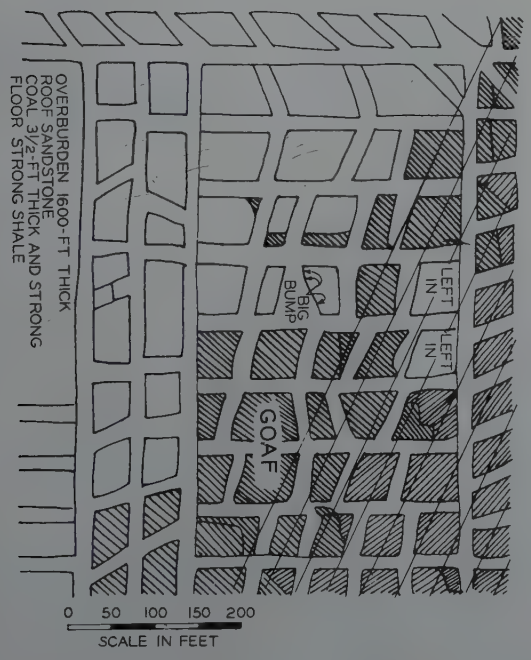

D. The bump failures of these pillars were separated by three days. These pillars may or may not have been in a point area. The fact that these two bumped and others adjacent to them did not may be accounted for by variations in the physical properties of coal in the pillars which resulted in these pillars carrying excessive load.

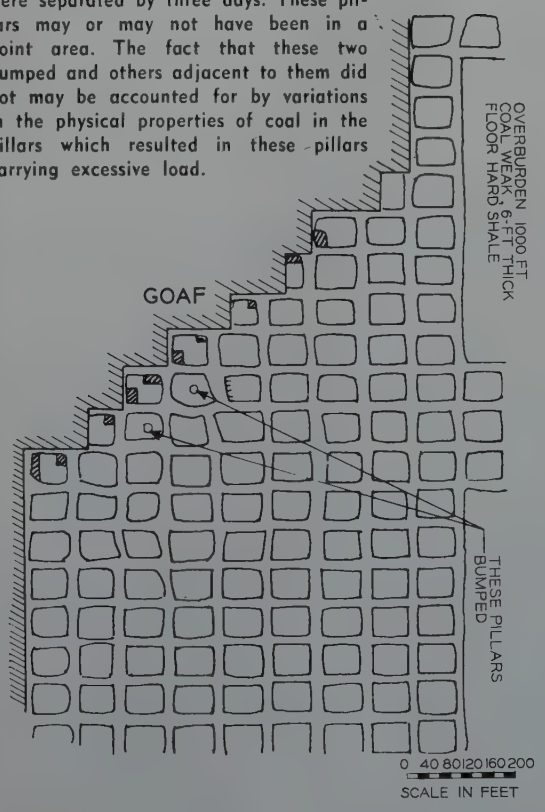

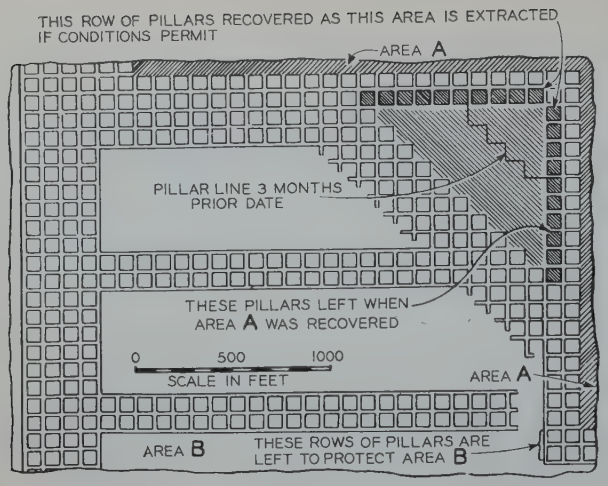
THIS ROW OF PILLARS RECOVERED AS THIS AREA IS EXTRACTED IF CONDITIONS PERMIT
AREA A
PILLAR LINE 3 MONTHS PRIOR DATE
THESE PILLARS LEFT WHEN AREA A WAS RECOVERED
0 500 1000
SCALE IN FEET
AREA A
AREA B
THESE ROWS OF PILLARS ARE LEFT TO PROTECT AREA B

Fig. 13—*Planned extraction provides a mining system to be used under conditions that cause bumps.*

not be more than 12 to 14 ft wide. The loose end of the lift (the end next the goaf) should be kept ahead of the tight end (next the pillar) and not more than one lift should be worked on any pillar at the same time.

6) To give the support needed, pillars should be as large as practicable. Also, large pillars provide great resistance to abrupt failure as well as less face through which highly stressed areas, due to variations in physical properties of coal, can fail abruptly.

7) Pillars should be uniform in size and shape (see Fig. 13) to prevent concentration of excessive loads on large pillars or pillars of different shape.

8) Pillars should not be split in abutment zones nor slabbed except on the goaf side in areas of high stress. If rock falls in existing passageways necessitate splitting or slabbing a pillar, slabbing offers less chance of a burst. Slabs should be driven as narrow as possible, and special precaution should be taken to protect the miners, especially the cutting machine crew.

9) In areas where overstressed pillars are known to exist, they can be drilled with large-diameter drills to induce a bump and relieve stress in the pillar. Again, it is important to give adequate protection to the drill crew. It should also be noted that this method does not give protection against a shock bump or district bump, illustrated in Figs. 11 C and 12 B.

10) In mining where the bump hazard is great and where only pillar-and-stall recovery can be used, drilling and blasting the solid side of the pillar could increase the safety of driving the next stall. This practice should be attempted only where is conforms to legal requirements and adequate safety precautions are adopted against the hazards of solid shooting.

Finally, our understanding of rock bursts is by no means complete. More research is needed, especially with regard to stress distribution in coal seams and adjacent rocks as influenced by mining methods or practices. Better means are needed to predict accurately the time and place of rock bursts. As matters stand now, it is possible only to point out locations where rock bursts are most likely to occur. A comprehensive research program would do much to clear up some of the mystery surrounding this problem of deep mining.

It should be emphasized that for mining under deep strong cover, no absolute preventative of rock bursts in coal mine is known, but the measures listed above should greatly lessen the probability of their occurrence and decrease the severity of rock bursts that do occur.

Discussion of this article sent (2 copies) to AIME before Oct. 31, 1958, will be published in MINING ENGINEERING.

REFERENCES

[1] G. W. Evans: Discussion of Bumps in No. 2 Mine, Springhill. *AIME Trans.*, 1930, vol. 88, p. 194.

[2] M. K. Hubert: Discussion on Causes of Rock Bursts. *Rock Bursts* (Symposium), 1942. *AIME TP 1468*, p. 26.

[3] R. F. Pescod: Rock Bursts in the Western Portion of the South Wales Coalfield. Institution of Mining Engineers, *Trans.*, 1947-48, vol. 107, pp. 512-536.

[4] D. W. Phillips: Tectonics of Mining. *Colliery Engineering*, June 1948, p. 199.

[5] L. A. Panek: *Stresses About Mine Openings in a Homogeneous Rock Body*, 1951. Privately published.

[6] W. I. Duvall: Stress Analysis Applied to Underground Mining Problems, Part II. Stress Analysis Applied to Multiple Openings and Pillars. *USBM R. I. 4387*, 1949, pp. 2-6.

[7] H. P. Greenwald et al.: Studies of Roof Movement in Coal Mines. 1. Montour 10 Mine of the Pittsburgh Coal Co. *USBM R. I. 3355*, 1937.

[8] E. R. Maize and H. P. Greenwald: Studies of Roof Movement in Coal Mines. 2. Crucible Mine of Crucible Fuel Co. *USBM R. I. 3452*, 1939.

[9] E. R. Maize, E. Thomas, and H. P. Greenwald: Studies of Roof Movement in Coal Mines. 3. Gibson Mine of the Hillman Coal & Coke Co. *USBM R. I. 3506*, 1940.

[10] C. T. Holland: Pillar Deformation in a Bituminous Coal Mine. *AIME Trans.*, 1938, vol. 130, pp. 333-357.

[11] T. L. McCall: Further Notes on Bumps in No. 2 Mine, Springhill, Nova Scotia. *AIME Trans.*, 1934, vol. 108, pp. 41-70.

[12] D. W. Phillips and T. J. Jones: Strata Movement Ahead of and Behind Longwall Faces. Institution of Mining Engineers, *Trans.*, 1941-42, vol. 101, pp. 348-349.

[13] J. Brass et al.: Fifth Progress Report of the Safe Working in Mines Committee, Method of Working and Roof Support in the Parkgate Seam. Institution of Mining Engineers, *Trans.*, 1933-34, vol. 86, pp. 231-263.

[14] J. F. Bryson: Further Developments in Preventing Bumps in Harlan County Coal Mines. *AIME Contribution 107*, 1937, pp. 3-4.

[15] A. Winstanley: Longwall Roof Control. Institution of Mining Engineers, *Trans.*, 1930-31, vol. 81, p. 384.

[16] H. M. Hudspeth: Ground Movements in Advance of Longwall. *Iron and Coal Trades Review*, Jan. 6, 1933, pp. 1-3.

[17] H. M. Hudspeth and D. W. Phillips: The Forces Induced by the Extraction of Coal and Some of Their Effects on Coal-Measure Strata. Institution of Mining Engineers, *Trans.*, 1932-33, vol. 85, p. 38, Eq. 1.

[18] E. H. A. Joseph: Rock Bursts: The Mechanism of Crush Bursts. *Journal of the Chemical, Metallurgical, and Mining Society of South Africa*, 1938-39, vol. 39, pp. 114-134.

[19] G. S. Rice: Bumps in Coal Mines—Theories of Causes and Suggested Means of Prevention or of Minimizing Effects. *AIME Trans.*, 1936, vol. 119, pp. 11-39.

[20] Divisional Strata Control Research Committee, National Coal Board, Durham and Northern (N & C) Divisions: Report on Effects of Working an Adjacent Seam upon New Developments. Institution of Mining Engineers, *Trans.*, 1953-54, vol. 107, p. 389.

[21] C. T. Holland: Physical Properties of Coal and Associated Rock as Related to Causes of Bumps in Coal Mines. *AIME Trans.*, 1942, vol. 49, pp. 84-85.

[22] D. W. Phillips: Rock Bursts or Bumps in Coal Mines. Institution of Mining Engineers, *Trans.*, 1944-45, vol. 104.

[23] H. R. Greenwald, H. C. Howarth, and I. Hartman: Experiments on Strength of Small Pillars of Coal in the Pittsburgh Bed. *USBM TP 605*, 1939, pp. 1, 12.

[24] F. L. Gaddy: A Study of the Ultimate Strength of Coal as Related to the Absolute Size of the Cubical Specimens Tested. Virginia Polytechnic Institute Engineering Experiment Station, *Bull 112*, 1956, p. 56.

[25] O. Mueller: Investigation of Carbon Rocks as an Explanation of Pressures in Mines. *Gluckauf*, 1930, nos. 22 and 29. German text translated by J. Billeter.

[26] W. Griffith and E. T. Connor: Mining Conditions under the City of Scranton, Pa. *USBM Bull. 25*, 1912, p. 77 et seq.

[27] R. Coeuillet: Existence or Absence of Bumps. An Attempt to Determine the Cause of Bumps by Comparison with a Mine Free From This Phenomenon. *International Conference about Rock Pressures and Support in the Workings*, 1951, p. 427. English Text.

[28] C. T. Holland: Some Aspects of Violent Failures in Coal Mine Pillars and Adjacent Strata. West Virginia Coal Mining Institute, *Proc.*, 1943, p. 60.

[29] A. J. A. Roux, E. R. Leeman, and H. G. Denkhouse: The Conception of Destressing and the Results Obtained from Its Application. Part I. *Journal of the South African Institute of Mining and Metallurgy*, 1957, vol. 58, pp. 101-119.

[30] F. G. Hill and R. P. Plowman: Destressing, with a Discussion on the Results so far Obtained. *Journal of the South African Institute of Mining and Metallurgy*, 1957, vol. 58, pp. 120-127.

[31] C. T. Holland and F. L. Gaddy: Some Aspects of Permanent Support of Overburden on Coal Beds. West Virginia Coal Mining Institute, *Proceedings*, 1956, p. 55.

[32] C. T. Holland and E. Thomas: Coal Mine Bumps. Some Aspects of Occurrence, Cause and Control. *USBM Bull. 535*, 1953.

APPLICATION OF ELECTROSTATICS TO POTASH BENEFICIATION

by I. M. LeBARON and W. C. KNOPF

In the Carlsbad area potash is dry-mined and wet-concentrated. Wet concentration involves recirculation of saturated brines, with resultant difficulties of brine disposal and inherent losses in recovery through solution of the KCl.

A dry beneficiation process for potash minerals would offer many advantages over present methods. International Minerals & Chemical Corp. has been working on development of a dry process for some time. This article is a progress report.

Potash ores available in this country are largely mixtures of halite and sylvite contaminated with slimes and often with many sulfate and magnesium minerals. Electrostatic concentration of KCl when the contaminating minerals are in low percentage has been accomplished. Continuous production of better than 60 pct K_2O concentrate from high potassium sulfate ores has not been demonstrated at the present time.

Laboratory Procedure: Laboratory work on electrostatic beneficiation of potash minerals has been carried out using both pure crystals and mined ore. Electrostatic separation of the two main components of potash ore, sylvite (KCl) and halite (NaCl), is accomplished by first heat-treating the ore to allow for electric charging of the particles. Preferential exchange of electrical charges between different mineral particles through surface contact is the principal mechanism involved.

After proper conditioning of the particle surfaces, the oppositely charged minerals are dropped vertically into a horizontal electric field having a field gradient from about 5000 to 15,000 v per in. The particles are free-falling in the field. A suitable power supply is used to produce the proper total voltage for the electric field. Total required voltage is, of course, a function of electrode spacing. A typical electrode arrangement with power supply is shown in Fig. 1. In general, the total voltage on any system is 75,000 to 90,000 v. Power consumption is negligible, as leakage at insulators and corona discharge are the main losses in the system.

Optimum preheat temperatures for pure material components generally are not the same as for mined minerals. Fig. 2 shows clearly that maximum recovery on a 50 pct pure KCl, 50 pct pure NaCl mixture occurs at a preheat temperature of about 600°F. In this test the preheat mixture was allowed to cool to about 225°F before dropping through the electric field. The optimum temperature for separation is practically never the optimum temperature of preheat.

Optimum separation for mined Carlsbad potash ores occurs when a preheat temperature closer to 900°F is used, as shown by Fig. 3, which plots percent sylvite (KCl) in the concentrate and tails as a function of preheat temperatures. Here again the ore was allowed to cool to about 225°F before separation. It should be noted that efficiency of separation increases continuously with increasing preheat temperatures until incipient fusion of the ore takes place at about 950°F.

The increase in optimum preheat temperature for Carlsbad ores over the pure minerals can be traced to the effect of the clay slimes intimately associated with the mined potash. If the slimes associated with the ore are removed by washing with alcohol or other non-aqueous material, the necessity of preheating to the high temperature is removed. This temperature range has been proved critical within these limits during continuous pilot plant operation.

Concentrate and tailings grade and optimum recovery also are functions of the temperature of the potash mineral particles during separation in the electric field. Fig. 4 presents data indicating that feed to the rougher pass should range between 150°F and 275°F for best results. It has been found by subsequent pilot plant work that these temperatures can be maintained in actual operation.

Table I. Typical Mineral Composition of Products

	Weight Pct				
	Phase I Conc.	Phase I Tails	Final Conc.	Phase II Tails	Final Tails
Sylvite	80.99	3.01	93.64	38.28	5.35
Halite	12.33	91.09	2.09	47.30	88.98
Langbeinite	3.95	4.29	2.79	11.31	3.40
Other Sulfates	0.78	0.13	0.21	0.27	0.50
Insoluble	1.94	0.60	1.29	2.83	0.75
Pct K_2O as KCl	51.16	2.31	59.15	24.18	3.30
Total K_2O	52.06	3.29	59.78	26.74	4.01

Table II. Effect of Sulfate Removal on Final Concentrate

	Pilot Plant Concentrate (No Correction)				Pilot Plant Concentrate (Assuming SO_4 Removal)			
Run	Tons	K_2O, Pct	Ind. Rec.	Act. Rec.	Tons	K_2O, Pct	Ind. Rec.	Act. Rec.
A	219	58.8	84.0	72.5	209	60.7	83.7	71.5
B	185	59.5	77.4	64.7	177	61.0	77.1	63.7
C	179	58.3	86.8	80.3	168	60.8	86.6	78.0
D	193	59.3	77.9	62.8	185	60.8	77.6	61.6
E	194	59.8	91.4	68.3	101	61.1	91.4	67.6
Total	880	59.1	82.4	69.2	840	60.9	82.1	68.1

I. M. LeBARON, Member AIME, is Vice President of the Research Division and W. C. KNOPF Assistant Director of Research, International Minerals & Chemical Corp. Central Research Laboratory, Skokie, Ill. TP 4761H. Manuscript, Dec. 2, 1957. New Orleans Meeting, February 1957.

This page of Mining Transactions follows p. 1004B. The intervening non-Transactions pages appeared in MINING ENGINEERING.

Pilot plant process and process equipment fall into two major sections, preparation and concentration.

Preparation Section: Run-of-mine ore is first crushed to —14 mesh for liberation. This is accomplished by a primary crusher reducing the ore to —1 in. and by a secondary crusher operating in closed circuit with vibrating screens. It is desirable to produce a minimum of fines in the crusher circuit to improve recovery and efficiency of concentration. This will be discussed later.

Crushed ore is fed to a 10x90-ft rotary kiln and heated to 800° to 900°F. This deactivates the slimes that coat the particles and allows a differential electric charge to form on particle surfaces on cooling. The kiln is gas-fired and operation is countercurrent. The hot ore then is fed to a cascade-type cooler and cooled by a countercurrent flow of air to about 250°F. The heated cooler discharge air is utilized as secondary air in the kiln. Ore is now ready for separation into its components in an electric field.

Concentration: Conveyor belts and elevators send the cooled ore at 225°F to the rougher pass in the concentration building, see Fig. 5. This is the phase I section of the concentration operation, consisting of a rougher and a scavenger pass. Each of these units contains three pairs of electrodes arranged as indicated. The products to be recycled from each unit are caught in hoppers, conveyed to an elevator and re-combined with the feed to that unit.

Tailings from the upper half of phase I rougher and from the phase I scavenger are sent to waste. However, a portion of the tailings approaches 99 pct NaCl in purity and can be utilized as industrial salt without further processing. A d-c potential of about 90,000 v is required to operate the concentrating sections, but very little power is required to maintain a suitable electric field between the electrodes. These 500 to 600 watts are needed primarily because of corona losses.

Many variables pertaining to this rougher operation have been studied in the pilot plant. Sulfate minerals associated with the sylvinite ore—such as langbeinite, leonite, kainite, and polyhalite—affect the efficiency of beneficiation; so does the amount of slimes adhering to the surfaces of particles to be separated. The duration and degree of agitation during processing; cooling methods and times of cooling; retention time of the ore in the kiln; recycle loads; excessive fines and many other operating conditions have also been studied.

The rougher scavenger flowsheet (indicated in Fig. 5) operating on ores of 10 to 19 pct K_2O produced a rougher concentrate consistently analyzing 48 to 54 pct K_2O. Operation to this point is simple and straightforward. Ores that are high in slimes and difficult to treat may be concentrated to 48 to 54 pct K_2O inexpensively and with resultant deactivation of slimes. For ores that are difficult to concentrate, it may well be economic to operate through this rougher stage at 50 pct K_2O concentrate, following it with wet concentration to obtain final 60 pct K_2O saleable grade. Concentration to this point has been quite successful.

On clean ores low in sulfate running above 20 pct K_2O the rougher concentrate will run about 55 pct K_2O and can be run through a cleaner and recleaner stage in closed circuit to produce a final 60 pct K_2O concentrate. This has been demonstrated on a

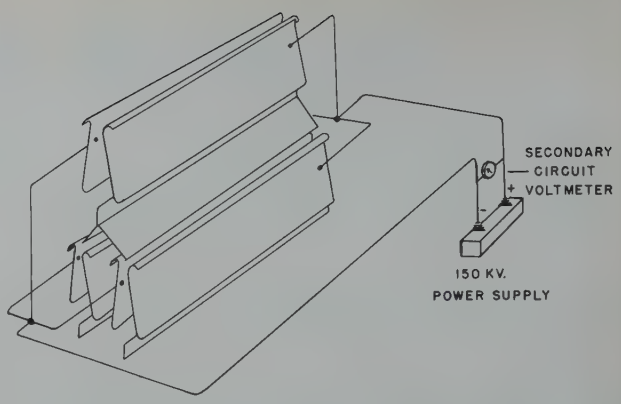

Fig. 1—Typical electrode arrangement.

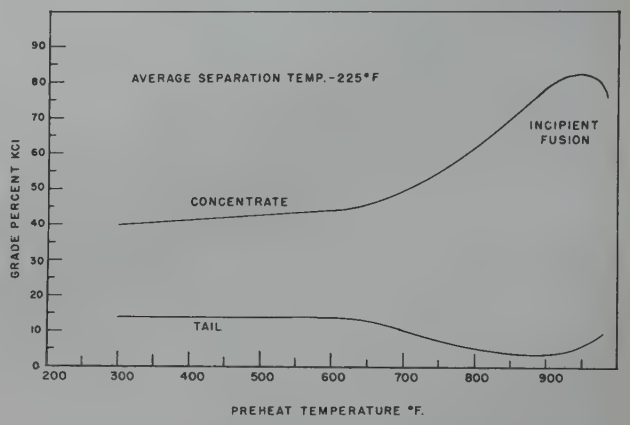

Fig. 3—Preheat temperature vs percent KCl, potash ore.

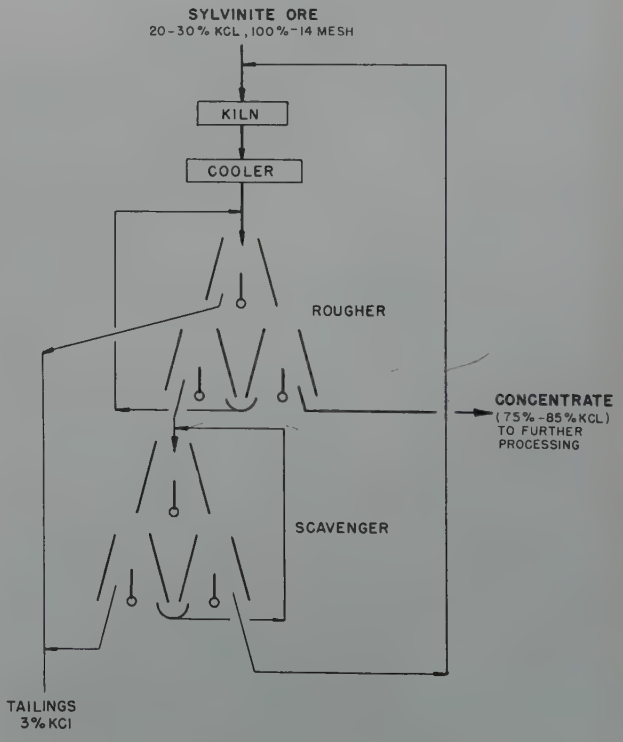

Fig. 5—One-stage electrostatic concentration, potash ore.

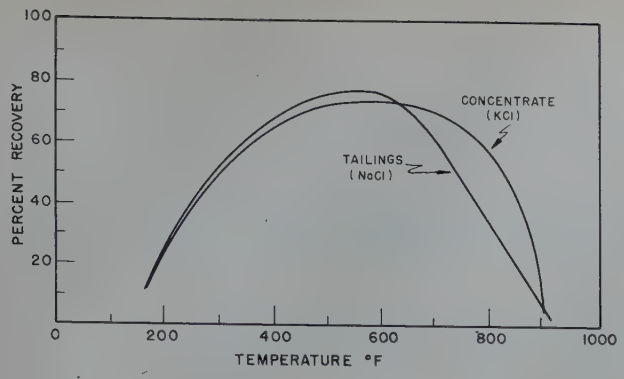

Fig. 2—Preheat temperature vs percent recovery.

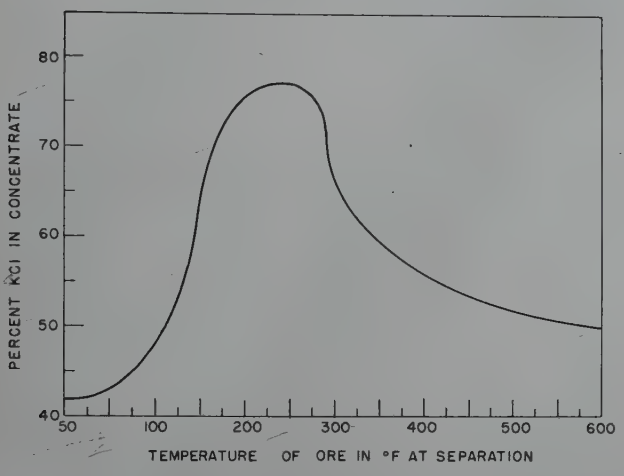

Fig. 4—Rougher feed separation vs temperature.

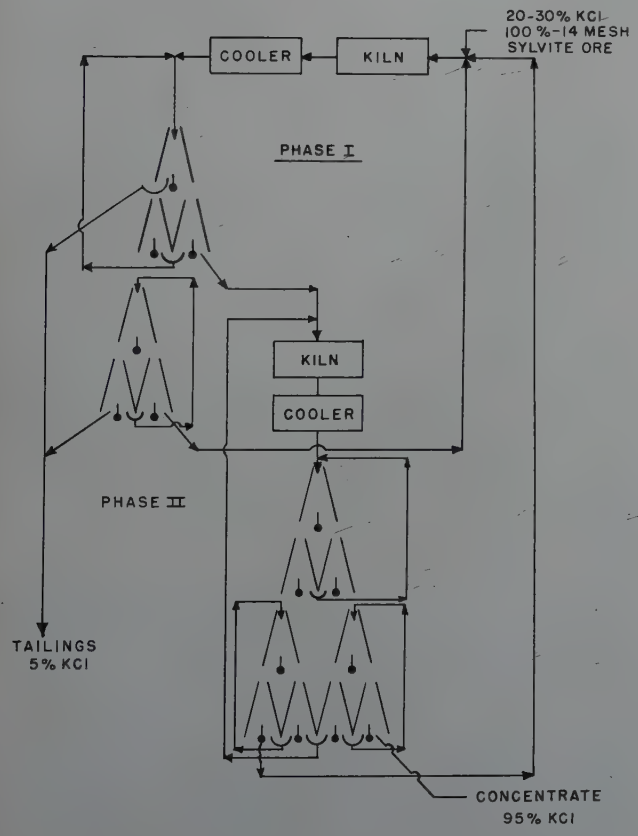

Fig. 6—Two-stage electrostatic concentration, potash ore.

sub-pilot plant scale with rates running about 1 tph. However, on ores high in sulfate such cleaner and recleaner operations result in very little increase in K_2O concentration.

For further dry concentration the rougher concentrate is reheated before cleaning and recleaning. A typical flowsheet is shown in Fig. 6. To determine its operating characteristics, the dry concentration pilot plant at Carlsbad has recently operated continuously on sylvite ore using this flowsheet. Concentrate grades produced during this period have varied from a low of 56.3 pct K_2O to a high of 60.2 pct K_2O, with an average for the period of 59.1 pct K_2O. Saleable grade concentrate analyzed 60 pct K_2O. The biggest single reason for not turning out a 60 pct K_2O product consistently is that the sulfate minerals tend to report to the concentrate. Table I gives a typical mineral composition of various products in the flowsheet shown in Fig. 6.

Table II shows the effect of sulfate on the grade of concentrate for various runs. Langbeinite was the chief sulfate mineral found during these runs. Removal of the sulfates allows the concentrate grade to approach 61 pct K_2O. Table II also lists the indicated and actual recoveries for various tonnage runs using the Fig. 6 flowsheet. High concentrate grades with indicated recoveries above 90 pct were unusual. K_2O had to be bled to the tails to remove enough sulfate to produce high grade. This affects the recovery of the operation materially.

The difference between actual and indicated recovery is largely a loss of fines. In the kiln operation fines swept to the dust collector were not returned to the circuit. At least 10 pct of the feed was lost in this way.

Fines of less than 150 mesh cannot be efficiently concentrated at the same time the coarser material passes through the electrode system. About half the loss in fines was in this screen mesh fraction. Through efficient dust collection and air separation the other 50 pct of the loss could have been returned to the circuit.

These data indicate the importance in this type of processing of reducing the percentage of fines produced in feed preparation.

FUTURE PROGRAM

To develop the present dry operation into a complete unit for concentration of potash ores under 20 pct K_2O and high in sulfate, at good recovery producing better than 60 pct K_2O concentrates, the following difficulties must be overcome:

1) Losses in the fines must be decreased. This can be done by handling fines in a separate circuit and by better air sizing.

2) Sulfate removal and concentration must be improved in the circuit. There are indications that with the proper flowsheet sulfate can be produced as a separate concentrate. This is being studied.

It is estimated that the cost of concentrating 5000 tpd of ore to a 50 pct K_2O product by using the Fig. 5 flowsheet will be 60¢ to 80¢ per ton of ore fed. This includes amortization of capital but is only plant level expense. The cost for concentration using the flowsheet in Fig. 6 is estimated at 75¢ to $1.25 per ton of ore fed.

Work is continuing at International's Research Division to perfect this process for use on potash ores.

Discussion of this article sent (2 copies) to AIME before Nov. 30, 1958, will be published in MINING ENGINEERING.

APPLICATION OF ELECTROSTATICS TO CONCENTRATION OF COARSE PEBBLE PHOSPHATE

by E. NORTHCOTT and F. N. OBERG

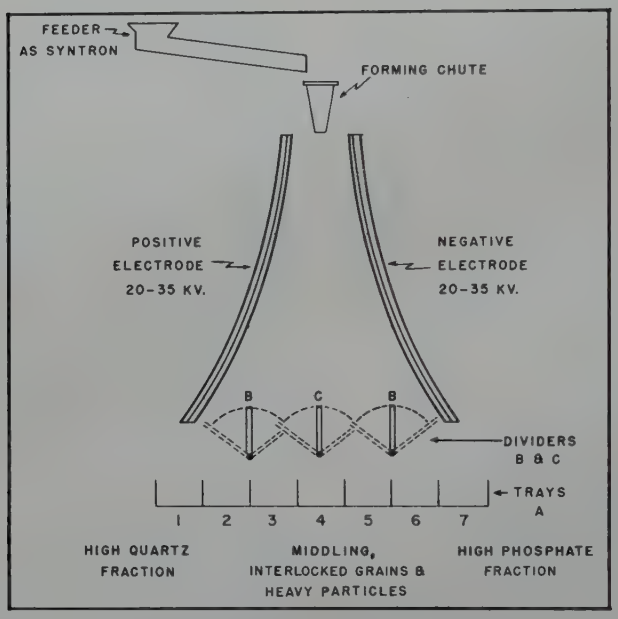

Fig. 1—Single LeBaron-Lawver electrode set showing feeder and the product dividers for batch A and for the pilot plant (B and C) operation.

By electrostatic separation, coarse Florida pebble phosphate, too low-grade to find a ready market, can be upgraded to a satisfactory saleable product. Pebble running from 60 pct bone phosphate of lime may be upgraded to 73 to 77 pct BPL depending on the mineralogical structure of the pebble and the nature of the silica impurity.

High-grade concentrates from Florida pebble phosphate deposits have long been recovered by wet methods. When work was begun in the field, only the coarse pebble (generally +1 mm) was recovered. In the 1920's a froth flotation process was developed to separate quartz from the finer phosphate fractions, but this method proved unsatisfactory for treating the intermediate fraction (—1 mm +35 mesh). Consequently various other processes were adapted, including agglomerate tabling and spiral separation of reagentized feed. Today the three processes are used—washing and screening for coarse pebble, tabling or spiraling for intermediate sizes, and flotation for —35 mesh material.

E. NORTHCOTT, Member AIME, is Manager of the Florida Experiment Station, Research Div., International Minerals & Chemical Corp., Mulberry, Fla. F. N. OBERG, Member AIME, formerly with the Research Div., is now with Homestake Mining Co., New Mexico Partners, Grants, N. M. TP 4762H. Manuscript, Dec. 2, 1957. New Orleans Meeting, February 1957.

These wet concentration methods yield high-grade products from the finer fractions of the ore, but the coarse pebble is not beneficiated further than removal of the fine particles. The grade of the coarse product is its natural grade, and when this is low the product has a limited market. The trend of grade in the Florida deposits is downward. High-grade ore has been selectively mined and depleted, but extensive areas of lower grade ore remain. To obtain a desirable product from this ore, beneficiation will be required.

The wet processes used to concentrate fine material follow naturally the mining and wet ore transporting methods used in the Florida fields. For this reason, and because wet process plants are well established in the area, the dry electrostatic separation process has not been extensively applied even though it has proved practicable. To treat the finer size materials by dry methods would involve drying large tonnages of silica. However, +1 mm pebble, which is higher grade and contains less silica, can be dry concentrated for less cost per unit of phosphate. It is dried according to standard practice. To treat it electrostatically would not involve changing present plants or installing more drying capacity. The advantages of dry-crushing and prevention of slime loss make the dry concentration of the coarse pebble attractive. A valuable concentrate can be made from inexpensive pebble by simple crushing to liberate silica at about 14 mesh, moderate heating, and electrostatic treatment.

International Minerals & Chemical Corp. operated an electrostatic pilot plant in which raw ores and spiral and flotation feed were concentrated. The plant used the LeBaron-Lawver free-fall process, which requires no contact between electrodes and ore particles. The principle involved in this process is based on the fact that particles of different minerals are charged differently by various phenomena and will react differently when subject to an induced high-voltage electric field. In practical application the charge is developed, during and after heating, by particle-to-particle contact, or by contact with a metal surface. Temperatures to which ores are heated and cooled before separation vary with the specific minerals to be separated. The optimum preheat temperature for pebble phosphate is 300° to 350°F, followed by cooling to 200° to 250°F before the ore is dropped through a free-fall of 6 to 9 ft between oppositely charged electrodes.

These electrodes (Fig. 1) are connected to a potential differential of 40 to 70 kv. In phosphate beneficiation the quartz and phosphate, bearing negative and positive charges respectively, are deflected in opposite directions by the external electric field. Ore particles not freed by crushing, too heavy to be sufficiently deflected by the electrodes, or prevented from deflection by other particles, fall into a central position as a middling fraction. For testing purposes in a batch process, the ore is ordinarily split into a number of portions as represented by the seven fractions shown at *A* in Fig. 1. Table I shows typical results obtained by a batch concentration test on a low-grade +1 mm Florida pebble sample. It will be noted that the percentage of BPL* (bone phosphate of lime, or tricalcium phosphate) in the fractions increases as the negative electrode is approached, and conversely the silica or quartz content decreases. The center portion is near feed grade.

* 1 pct of BPL is equivalent to 0.45762 pct P_2O_5.

By selecting and combining the individual portions, it is possible to make products that can be called concentrates, tailings, and middlings. For example, if portions 5, 6, and 7 (Table I) are combined, a concentrate assaying 75.6 pct BPL and 2.8 pct SiO_2 will be obtained. Likewise portions 1, 2, and 3 will produce a fraction containing 30.2 pct BPL and 55.1 pct SiO_2. Portion 4 will then be left for recycle or for further treatment.

Using this established test procedure, a large number of batch tests have been performed on samples of coarse phosphate pebble products. It was found that a high-grade concentrate could be produced, generally with high phosphate recovery. Table II shows the amount of 75 pct BPL concentrate produced in a number of tests. With pebble feeds ranging from 67.2 to 70.1 pct BPL, 62 to 92 pct of the phosphate was recovered as a 75 pct BPL concentrate, and the silica content was dropped from over 10 pct to less than 6 pct. These results were obtained by a single pass of LeBaron-Lawver concentration. It is stressed that in this tabulation no credit is taken for further recovery by middling recycle. Such recycle is unusual in plant practice.

In plant practice, where a middling is made and recycled, the division into the three products is not done by splitting into seven fractions and then recombining but is performed automatically by adjustable splitters installed between the electrodes (Fig. 1, at *B* if three products are to be made or at *C* if only two products are desired with no middling).

It can be demonstrated by calculation from Table I that the electrostatic fractions forming the low BPL product (portions 1, 2, and 3) cannot be called true tailings by acceptable metallurgical standards. Although this product contains only 11.7 pct of the phosphate values, its grade is not as low as throwaway tailings made by wet concentration processes.

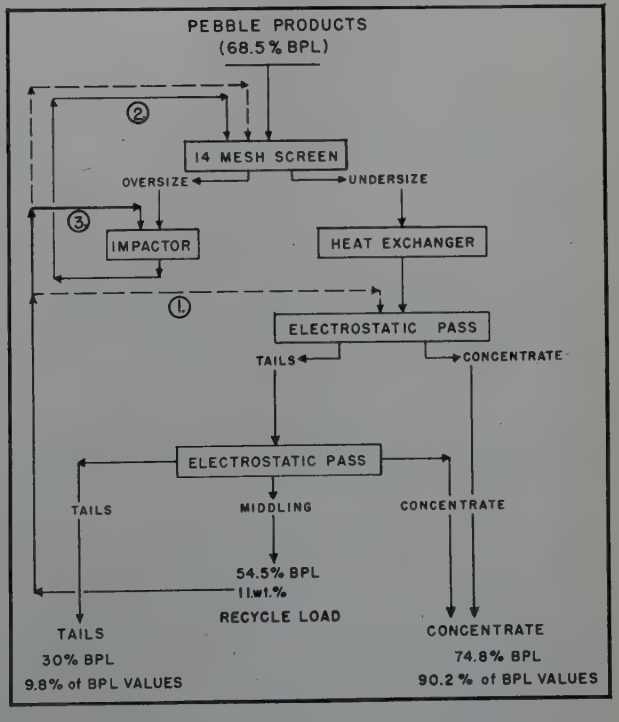

Fig. 2—A flowsheet and bone-phosphate-of-lime balance of two-stage electrostatic sub-pilot plant.

Table I. Electrostatic Concentration of Crushed Coarse Pebble-Quartz-Phosphate Rock System

Electrode	Feed: +1 mm crushed through 14 mesh Portion	Wt, Pct	BPL, Pct	SiO_2, Pct
Positive	1	4.3	19.5	72.3
	2	7.8	27.4	59.2
	3	12.3	35.7	46.5
	4	16.9	65.2	20.3
	5	23.0	74.8	3.8
	6	25.8	75.9	2.3
Negative	7	9.9	77.0	1.5
	Feed	100.0	62.8	18.5

However, if the low-grade product is treated by another step of electrostatic beneficiation, the quality of the high-silica fraction will compare favorably with that of tailings produced by flotation or spiral beneficiation. This additional step of separation is analogous to scavenger flotation.

This step was incorporated in a double pass sub-pilot plant (capacity, 600 lb per hr) designed and constructed to treat +1 mm pebble products. It is represented by the flowsheet, Fig. 2, which also shows a typical BPL balance.

In this plant the coarse pebble is fed to an 18-in. Sweco separator with a 14-mesh screen deck, in closed circuit with an impactor. Undersize from the screen enters a vertically-baffled muffle-type heat exchanger, where the temperature of the ore is raised to 300° to 400°F. The heated feed is then elevated to the top of a 30-ft enclosed tower containing two sets of LeBaron-Lawver electrodes. The upper electrode is fed at a constant rate by a Syntron feeder. The ore is spread evenly to fall in a ribbon parallel to the electrodes. In this particular plant the forming chute directly above and between the electrodes is 4 in. wide, and the electrodes are 12 in. wide. They are mounted 10 in. apart at the top and spread to 36 in. at the bottom. The height of the electrodes is approximately 9 ft. A conventional product divider (Fig. 1, *C*) splits a concentrate from the stream. This stream is removed from the tower by a suitable chute. The tailings from the upper pass form the feed for the lower and final pass. They are collected in a hopper and reformed by a chute directing them between the lower electrodes. Material at the bottom of the lower electrodes is divided by adjustable splitters (at *B*, Fig. 1) into concentrates, tailings, and middlings. The lower concentrates and tailings are removed as finished products, while the middlings are recycled to process. During sub-pilot plant runs, various points of middling return were tested, as shown at 1, 2, and 3 of Fig. 2. It was found that recycle to the impactor produced the most satisfactory results.

Other variables that might affect the separation have been investigated during the batch and sub-pilot plant test runs. Among these are: 1) degree of crushing; 2) preheat temperatures of the ore at separation and of the surrounding atmosphere; and 3) electrode voltage. Test results have proved that the ranges given in this article produce satisfactory separation.

Most of the tests, both batch and sub-pilot plant, were performed on *pebble fines*. This product is removed from dried coarse pebble to improve the size quality and provide a more uniform feed to electric furnace plants. Some of the fine material results from inefficient removal of small particles in washing plants and from breakdown of soft and agglomerated particles during drying. It represents 50 to 60 pct of the entire pebble when screened at 8 or 10 mesh. Its grade is inferior to other fine phosphate materials, averaging about 68.5 pct BPL compared to over 75 pct BPL for flotation and spiral concentrates. With large amounts of wet concentrates available, the off-grade product does not find a ready sale. Concentration is required to make a desirable product.

Enough testing was also done on the oversize pebble to show its amenability to electrostatic concentration. Beneficiation of this product should be seriously considered because of the depletion of high-grade ore reserves and a steady decline in grade of pebble being mined. Large areas of low grade ore are available in the Florida deposits, but this pebble cannot command a premium price in the electric furnace burden market. Electrostatic beneficiation of pebble products is more advantageous than wet methods for a number of reasons. It can be dried in facilities already installed and operating. It can be dry-crushed for electrostatic separation without the slime loss that would accompany wet grinding for flotation or spiral concentration.

Preliminary cost estimates are of doubtful value when based on such small-scale units as a 600-lb per hr sub-pilot plant, but it is indicated that an electrostatic plant to treat 500,000 tons of low grade pebble per year will cost about $600,000. This amount would provide for the crushing, screening, heating, and separating equipment, with such necessary auxiliaries as conveyors, elevators, dust collectors, and surge bins. It has been assumed that drying and storage facilities will not need enlarging but that those currently in use will be adequate for use with the electrostatic plant.

On the basis of amortization of this capital as well as current labor and material costs, it is further estimated that plant will produce 380,000 tons of concentrates for about $0.50 per ton, plant level cost not including raw material charges. This figure allows no credit for tailings or for dust, which will undoubtedly have some value. As stated, these figures are based on small-scale tests, and pilot plant operation on a larger scale is now indicated.

Table II. Yield of 75 Pct BPL Concentrate from Low Grade +1 MM Phosphate Pebble. Results of Batch Testing with No Middling Recycle

Test	BPL, Pct Head	BPL, Pct Concentrate	BPL, Recovery, Pct	SiO_2, Pct Head	SiO_2, Pct Concentrate
1	69.0	75.0	80	13.3	4.7
2	70.0	75.0	80	11.2	4.2
3	67.8	75.0	82	12.6	3.9
4	69.7	75.0	76	11.1	5.4
5	70.0	75.0	70	11.2	4.2
6	68.4	75.0	89	12.0	4.0
7	69.3	75.0	62	11.4	4.5
8	68.0	75.0	80	12.1	3.9
9	70.1	75.0	73	10.1	4.2
10	67.2	75.0	70	13.4	4.0
11	70.0	75.0	92	11.5	4.7
12	67.4	75.0	85	12.1	3.7
13	67.7	75.0	85	12.1	3.5
14	68.0	75.0	86	11.9	4.8
15	69.7	75.0	90	10.9	4.3
Average	68.8	75.0	80	11.8	4.3

Discussion of this article sent (2 copies) to AIME before Nov. 30, 1958, will be published in MINING ENGINEERING.

APPLICATION OF ELECTROSTATICS TO FELDSPAR BENEFICIATION

by E. NORTHCOTT AND I. M. LeBARON

Before describing the electrostatic processing of feldspar, it might be well to review some of the basic definitions and terminology of feldspars. The feldspar minerals constitute a group of aluminosilicates of potassium, sodium, and calcium. Barium feldspar sometimes occurs naturally but is very rare. Hardness varies between 6 and 6.5 and specific gravity between 2.5 and 2.8. Color is generally white or pale shades of red, yellow, or green. The approximate chemical composition of the principal feldspars is given in Table I.

The albite (sodium aluminum silicate) and an-

E. NORTHCOTT, Member AIME, is Manager of the Florida Experiment Station, Research Div., and I. M. LeBARON, Member AIME, is Vice President, Research Div., International Minerals & Chemical Corp. TP 4763H. Manuscript, Dec. 2, 1957, New Orleans Meeting, February 1957.

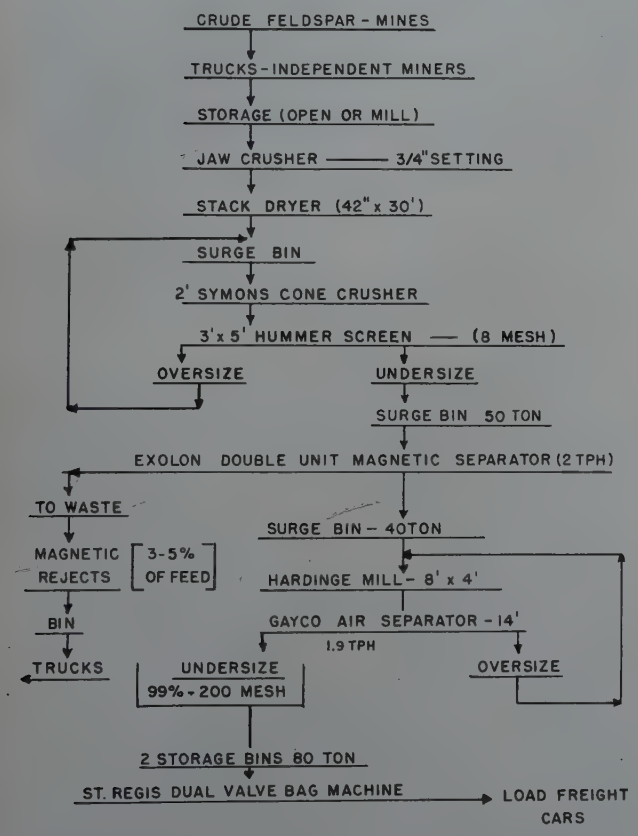

Fig. 1—Flowsheet of International's operation at Topsham, Me., prior to installation of electrostatic unit.

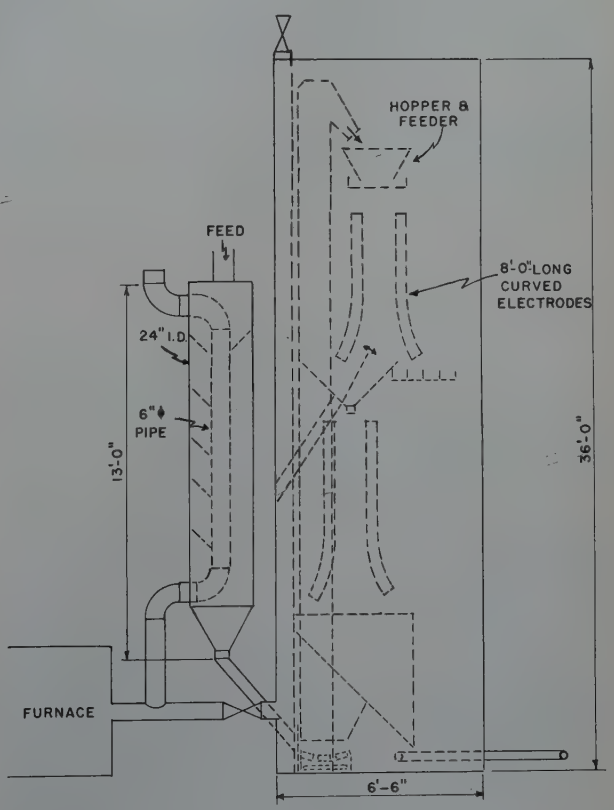

Fig. 2—Pilot plant flowsheet at Florida Experiment Station, where tests were performed on 1000-lb lots.

Table I. Approximate Chemical Composition of Principal Feldspars

Feldspar	Formula	Composition, Pct				
		K_2O	Na_2O	CaO	Al_2O_3	SiO_2
Orthoclase	$KAlSi_3O_8$	16.9	—	—	18.4	64.7
Microcline	$KAlSi_3O_8$	16.9	—	—	18.4	64.7
Albite	$NaAlSi_3O_8$	—	11.8	—	19.4	68.8
Anorthite	$CaAl_2Si_2O_8$	—	—	20.1	36.6	43.3

orthite (calcium aluminum silicate) feldspars are the end members of a series called plagioclase. These two molecules form a complete solid solution series ranging from pure soda feldspar at one end to the pure lime feldspar at the other end. Intermediate solid solutions are known as oligoclase, andesine, labradorite, and bytoconite. The general structure throughout this series is the same. Sodium and calcium may replace each other and silicon and aluminum may replace each other in the structure.

Orthoclase and albite are completely miscible at high temperatures but are miscible only to a limited extent at low temperatures. For this reason potash feldspar usually contains a little soda and, conversely, soda feldspars usually contain a little potash in the lattice. Alkali feldspar (K and Na feldspar mixtures) of medium composition separates into two phases upon cooling; one is rich in potash feldspar, the other in soda feldspar. The two form an intergrowth of oriented lamellae known as perthite. Typical analyses of a few commercial feldspars are shown in Table II.

Table II. Typical Analyses of Some Commercial Feldspars

No.	Ignition Loss	SiO_2	Al_2O_3	Fe_2O_3	CaO	MgO	K_2O	NaO_2
1	0.20	73.9	14.6	0.10	0.3	Tr	7.9	3.0
2	0.20	69.6	17.4	0.08	1.4	Tr	6.5	5.1
3	0.30	66.5	18.4	0.08	0.10	Tr	12.0	2.7
4	0.10	71.6	16.3	0.07	0.40	Tr	7.8	3.7
5	0.30	68.8	17.1	0.09	0.20	Tr	10.4	3.0
6	0.30	68.1	17.5	0.09	0.20	Tr	10.9	2.8
7	0.30	68.5	17.5	0.07	0.20	Tr	10.5	3.1

Many pegmatites contain feldspar, but in impure form or uneconomical concentration. In the early days rich streaks were hand-mined and then hand-cobbed, with a waste of some 80 pct of the rock mined. Effort was made to maintain purity and uniformity, but there were complaints about fluctuations in alkali content and impurities such as tourmaline, mica, and iron oxides. (Alkali content is defined as the sum of K_2O and Na_2O present in the feldspar; the alkali ratio is the ratio of K_2O to Na_2O in the ore.)

In recent years the pottery industry has utilized more and more of the flotation grades of soda spar, but there is still a strong demand for a high-potash feldspar where purity can be controlled. The object of the investigation on electrostatic beneficiation of Maine feldspar was threefold: 1) A reduction in the free quartz content of the final product, 2) perhaps even more important, an increase in the alkali ratio so that the ore could qualify completely as a high-potash feldspar, and 3) more uniformity of product without expensive selective mining.

The ore discussed in this article came from the Consolidated Feldspar operations of International Minerals & Chemical Corp. at Topsham, Me. It is a coarse-grained microcline-perthite pegmatite averaging 74 pct feldspar and 23 pct quartz. About 2 pct muscovite and trace amounts of biotite, tourmaline, garnet, and iron oxide are present. The mineral composition is as shown in Table III.

FORMER PLANT FLOWSHEET

Fig. 1 presents a flowsheet of the Maine operations before installation of the electrostatic unit. This has been retained, with insertion of the electrostatic step, which is sandwiched between the magnetic purification and the final (Hardinge) grind. Crude feldspar is delivered to the plant by truck and dumped into storage, either in the mill building or in the area surrounding the plant. From storage it is fed manually into a 10x18-in. jaw crusher set to reduce to ¾ in. The ore is then fed by bucket elevator to a stack dryer powered by fuel oil. After drying, it is again elevated and stored in a 50-ton surge bin, from which it is fed to a 2-ft Symons cone crusher, and reduced to −8 mesh. The cone crusher is in closed circuit with a 4x5-ft Hummer screen. The oversize is recycled to the cone crusher, while the undersize (−8 mesh) is delivered to another 50-ton surge bin. (During operation of the eletrostatic plant the cone crusher is set to 14 mesh.) From the surge bin the ore is fed to a double Exolon magnetic separator at about 2 tph. Magnetic rejects from this separator average 3 to 5 pct of the feed and are conveyed to a bin for ultimate disposal by truck. After leaving the magnetic separator, the nonmagnetic portion is again binned prior to being fed into a 8x4-ft Hardinge mill utilizing flint pebbles. Discharge from the Hardinge mill is separated by a 14-ft Gayco air separator into ±200 mesh products. The +200 mesh recycles to the mill and the −200 mesh is stored in 80-ton bins. From these final product storage bins the 99 pct −200 mesh feldspar is bagged in a St. Regis dual-valve machine or loaded in boxcars as the customer demands.

APPLICATION OF LeBARON-LAWVER PROCESS

Although beneficiation of Maine feldspar by the LeBaron-Lawver process had already been investigated for several years, it is in the last five or six years that considerable technological improvement has been made.

A pilot plant flowsheet, shown in Fig. 2, was set up at the IMC Florida Experiment Station in Mulberry, and sub-pilot plant tests were made on 1000-lb lots. Prior to the pilot plant work numerous batch tests were made with results approximating those given in Table V.

Table III. Mineral Composition, Topsham Ore

From Optical Data, Pct		From Chemical Analysis, Pct	
Microline-perthite	71	Orthoclase	46
Free albite	3 to 4	Albite	24
Quartz	23	Anorthite	2
Muscovite	2	Quartz	24
Others*	trace to ½	Others*	4
	100		100

* Includes biotite, tourmaline, garnet, and iron oxides.

IMC's pilot plant at Mulberry, Fla.

Batch Testing Method: The material is ordinarily heated in an oven and manually placed into a Syntron feeder from which the ore is fed between the electrodes and collected in eight pans at the bottom of the electrodes. These pans are of equal width and the method of reporting is usually by pan number, running from left to right, or from positive to negative electrode (see Fig. 3) followed by suitable analyses. Data obtained from both the batch testing and the sub-pilot plant work indicate that given a feed of approximately 8 pct K_2O and 74 pct SiO_2 a product can be produced consistently with a K_2O content of 10.4 to 10.6 pct and a SiO_2 content of 69 to 69.5 pct. These values are at a weight recovery of 72 to 75 pct and a feldspar recovery of 93 to 95 pct. On the basis of these results, a pilot plant was installed at the Topsham plant. After demonstration runs, the pilot plant was taken over by the operating plant personnel and became an integral part of their operation.

ELECTROSTATIC PILOT PLANT

A flowsheet of the electrostatic plant is shown in Figs. 4 and 5. The equipment utilized in this pilot plant operation in order of material flow is as follows:

A.	Screw conveyor	2 hp	9-in. diam, 8½ ft long,
B.	No. 1 elevator	¾ hp	26 ft high, 4 tph
C.	Feed bin		maximum capacity (estimated)
D.	Table feeder	1 hp	26 ft high, 8 tph max-
E.	No. 2 elevator	3 hp	imum capacity
F.	Heat exchanger		
G.	No. 3 elevator	3 hp	38½ ft high, 15 tph maximum capacity
H.	Syntron feed spreader	2 kw-hr	Above 15 tph
I.	High voltage system	2 kw-hr	100 kv at 8 ma
J.	Concentration tower unit		
K and L.	Two vibratory conveyors	2 hp (total)	
M.	Hot gas supply (fire-box and oil burner 3¼ hp)		

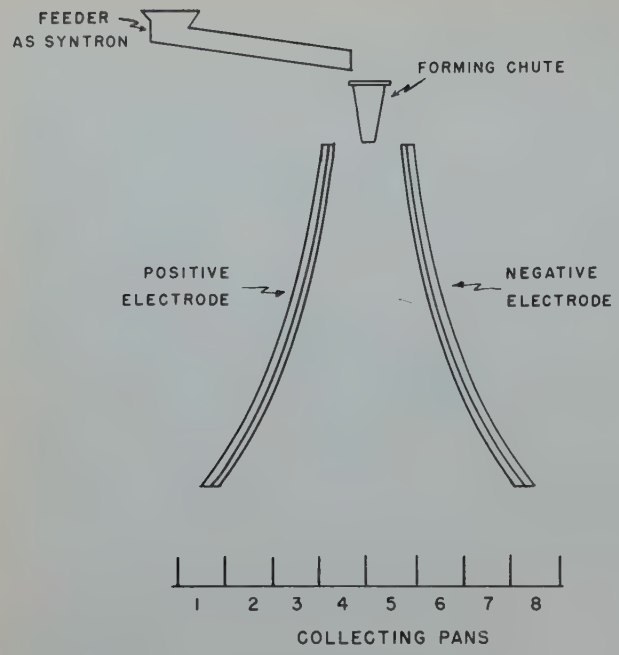

Fig. 3—A batch-type laboratory unit.

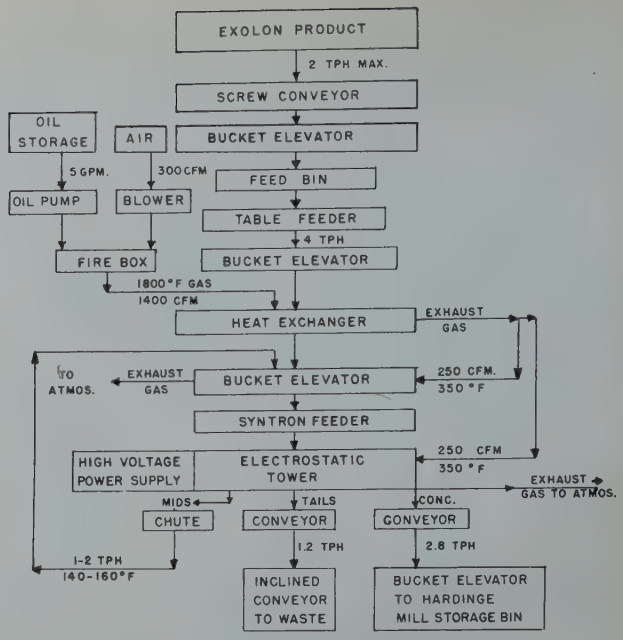

Fig. 4—Complete plant section for electrostatic process. Feed bin is surge point ahead of one-shift section.

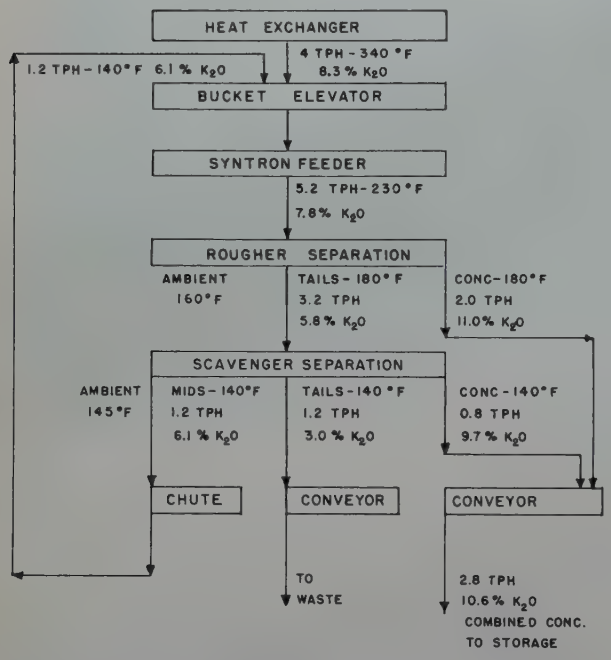
HEAT EXCHANGER
1.2 TPH - 140°F 6.1 % K2O
4 TPH - 340 °F 8.3 % K2O
BUCKET ELEVATOR
SYNTRON FEEDER
5.2 TPH - 230 °F
7.8% K2O
ROUGHER SEPARATION
AMBIENT 160°F
TAILS - 180° F 3.2 TPH 5.8 % K2O
CONC - 180° F 2.0 TPH 11.0% K2O
SCAVENGER SEPARATION
AMBIENT 145°F
MIDS - 140°F 1.2 TPH 6.1 % K2O
TAILS - 140 °F 1.2 TPH 3.0 % K2O
CONC - 140°F 0.8 TPH 9.7 % K2O
CHUTE
CONVEYOR
CONVEYOR
TO WASTE
2.8 TPH
10.6% K2O
COMBINED CONC. TO STORAGE

Fig. 5 (above)—Concentration section, electrostatic process. This section runs one-shift a day.

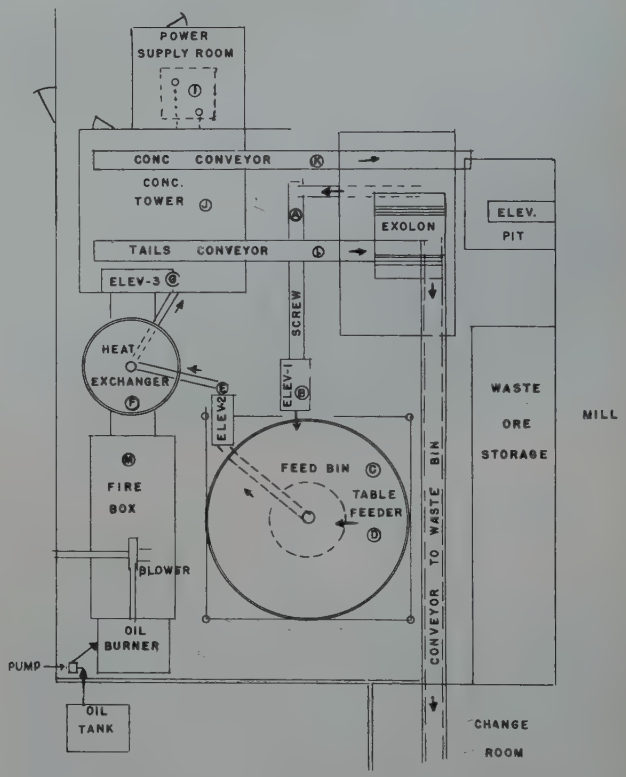

Fig. 6 (right)—Arrangement of equipment in pilot plant.

Figs. 6, 7, and 8 indicate the equipment arrangement and location of the pilot plant in relation to the Topsham mill.

Feed to the pilot plant is the —14 mesh nonmagnetic product of the Exolon magnetic separator. With reference to Fig. 6, the feed is chuted to the screw conveyor (A) and thence to the No. 1 elevator (B) and is stored in the feed bin (C). During pilot plant operation, rate of feed from the bin is controlled by a variable depth cutter blade on the constant speed table feeder (D). This material is chuted to the No. 2 elevator (E) and then fed to the heat exchanger (F). The heat exchanger discharges by gravity to No. 3 elevator (G) and the hot feed is elevated to the top of the concentration tower (J), where the ore is separated into concentrates, tailings, and middlings. The middlings are recycled to the No. 3 elevator (G) while the other products are collected on the two vibratory conveyors (K and L). Hot gases are supplied from the oil

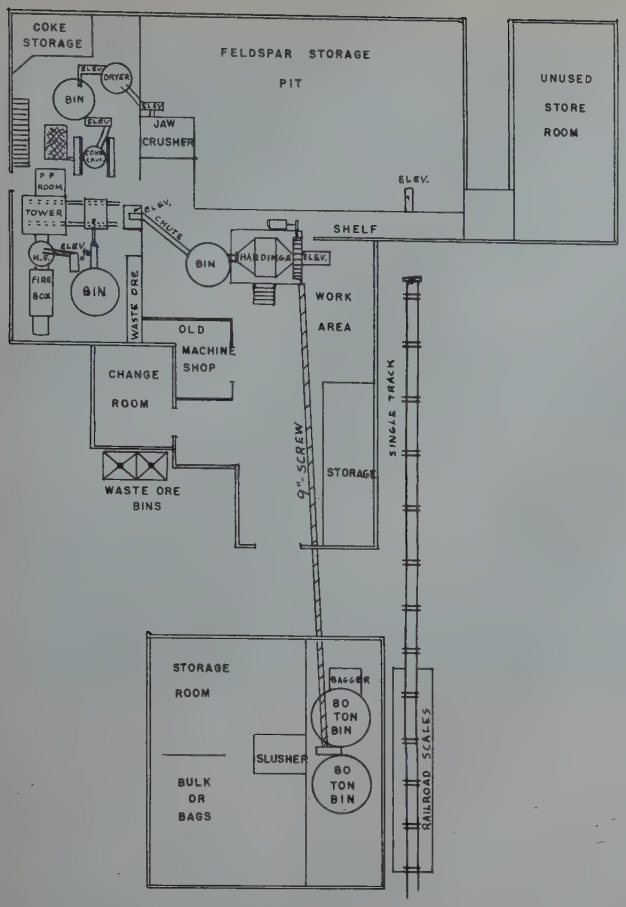

Fig. 7–Equipment arrangement, Topsham feldspar mill.

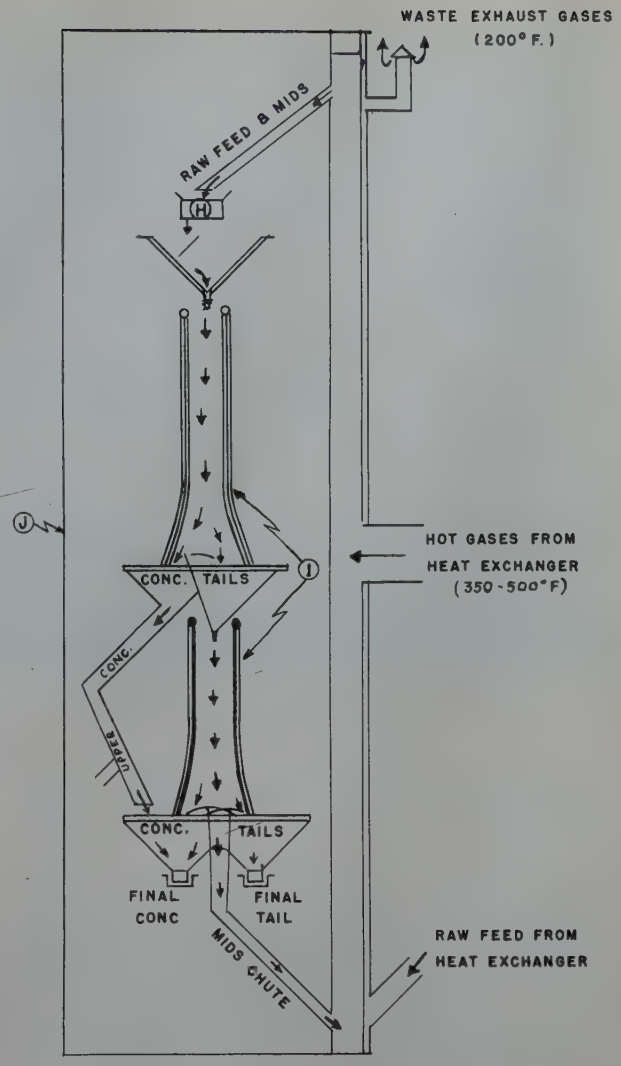

Fig. 8–Equipment arrangement, concentration tower.

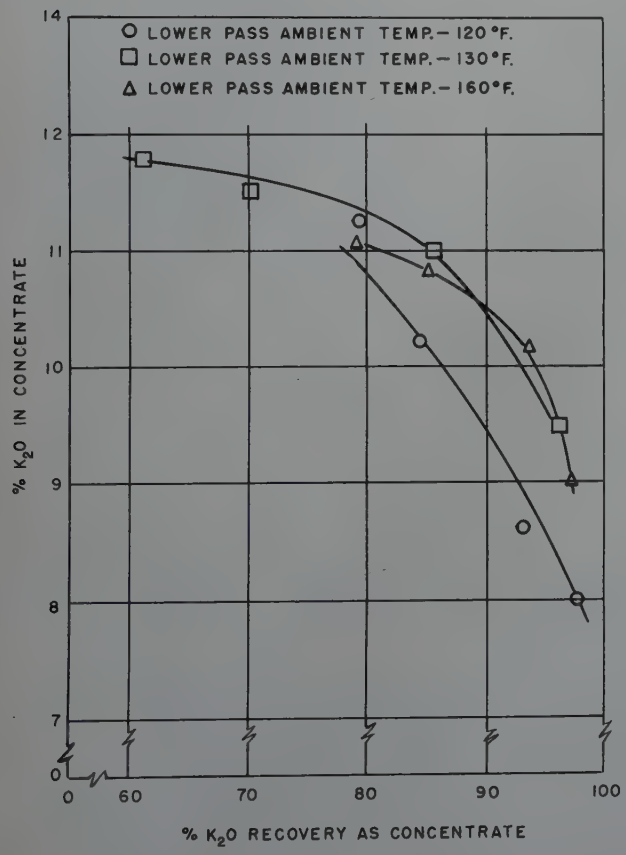
LOWER PASS AMBIENT TEMP.– 120 °F.
LOWER PASS AMBIENT TEMP.– 130 °F.
LOWER PASS AMBIENT TEMP.– 160 °F.
% K_2O IN CONCENTRATE
% K_2O RECOVERY AS CONCENTRATE

Fig. 9–Upper pass temperature in tower is 155°F.

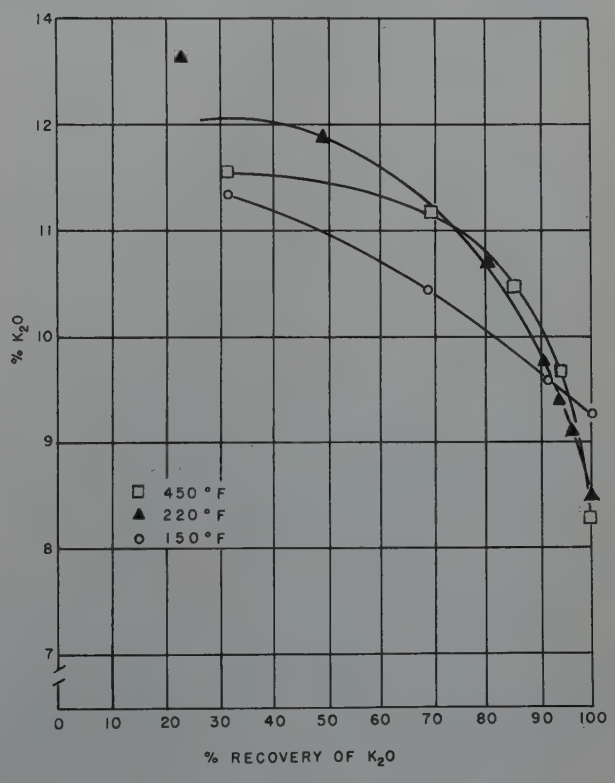

Fig. 10 (right)–The static separation of Topsham ore when it was heated to listed temperature.

A section of the International Minerals & Chemical Corp. Florida Experiment Station.

burning firebox (M) to the bottom of the heat exchanger (F).

Ore flow within the concentrating unit (J) is shown in Fig. 5. The heated ore is fed to a 5-ft Syntron spreader. From the Syntron a forming chute deflects the curtain of ore midway between the upper pass electrodes. A concentrate is withdrawn by means of an adjustable splitter and the residue is collected in another forming chute and fed to the lower electrodes. Here in the lower pass another concentrate is produced which joins the upper concentrate to form the high potash feldspar product. In the lower pass a second adjustable splitter produces a middling and final tail. The middling fraction is gravity-fed back to the elevator, which conveys raw feed to the Syntron, while the tailing fraction joins the plant magnetic rejects for disposal.

Heat Exchanger: This baffled-fall heat exchanger is 66 in. diam and 15 ft high (including conical sections). The hot exhaust gases enter the bottom and leave the top, passing through the stainless steel duct. They do not come in contact with the ore being heated. The gases enter the heat exchanger at approximately 1800°F and leave at 500°F; the ore enters at 30° to 60°F, depending upon the ambient conditions, and leaves at 250° to 300°F.

Syntron Feed Spreader: The model FC-44 Syntron feeder can handle more than 15 tph and spread feed through a 5-ft opening in a continuous, relatively even curtain of falling feed. It is rated 18 amp at 200 v.

Table IV. Chemical Analysis, Topsham Ore

Element	Pct
SiO_2	73.4
Al_2O_3	15.0
Fe_2O_3	0.07
CaO	0.5
MgO	Trace
Na_2O	2.8
K_2O	8.2
LOI	0.2
	100.2

Table V. Representative Batch-Test Electrostatic Separations on Topsham Ore

Batch Test or Pan No.	Wt, Pct	K_2O, Pct	Na_2O, Pct	Al_2O_3, Pct	SiO_2, Pct
1	10.8	2.2	2.9	8.4	85.1
2	17.6	2.8	3.0	9.2	83.0
3	20.3	6.3	3.1	12.1	78.2
4	21.2	11.0	3.3	16.9	69.0
5, 6, 7, 8	30.1	12.7	3.0	18.5	65.1
Head	—	8.3	3.0	14.0	74.1

Table VI. Screen Assay of Feed, Concentrate, and Tailing

Tyler Mesh	Wt, Pct			K_2O, Pct			SiO_2, Pct		
	Feed	Conc.	Tail	Feed	Conc.	Tail	Feed	Conc.	Tail
+20	8.7	9.4	6.9	8.3	9.8	3.4	76.1	72.4	82.6
20x35	32.4	35.5	24.4	8.4	9.8	2.9	76.5	71.0	85.6
35x48	14.4	13.8	16.0	8.4	10.8	2.8	72.5	66.8	87.5
48x65	10.5	9.8	12.3	8.5	11.2	2.8	71.9	66.3	87.7
65x100	9.9	9.3	11.3	8.2	11.1	2.8	71.5	66.1	84.3
100x200	12.0	12.2	11.6	8.3	11.1	2.7	70.4	66.4	81.0
−200	12.1	10.0	17.4	8.2	10.0	4.2	69.2	68.0	78.1
Head	—	—	—	8.3	10.4	2.9	73.5	69.5	84.0

Table VII. Percentage Chemical Composition of Feed, Concentrate, and Tailing

Element	Feed	Concentrate	Tailing
SiO_2	73.5	69.5	84.0
Na_2O	3.0	2.9	2.8
K_2O	8.3	10.4	2.9
CaO	0.4	0.2	0.4
Fe_2O_3	0.08	0.06	0.10
Al_2O_3	14.3	16.6	8.3
LOI	0.4	0.4	0.4

High Voltage System: This includes the 0 to 100-kv Beta Electric Corp. power supply and control unit, the high voltage insulators and high voltage wiring system, and the electrodes. The high voltage wiring system includes some 100 ft of wire (premium spark-plug wire), 16 Lapp post insulators, and two choke coils of approximately 5000 Henrys each suspended from the ceiling of the power supply room by 20-lb test nylon line. The high voltage electrodes consist of two sets of electrodes, 5 ft in horizontal dimensions and 8 ft high. The electrodes are spaced 10 in. apart at the top and 36 in. at the bottom. Individual electrodes are made up of 3-in. aluminum tubes (the lower 4 ft bent on a 10-ft radius) spaced 1 in. apart and hung from a 4½-in. O. D. Lucite header. All tubes are joined electrically. A potential of 70,000 v is applied to the electrodes.

Concentration Tower Unit (Fig. 8): The 10-gage steel shell, which is covered on the outside with ½ in. of insulation, houses several chutes and hoppers. Rougher (upper pass) concentrate and tailings are collected by hoppers that form a chute to allow an even curtain of falling ore in the rougher and scavenger (lower pass) section. There are also chutes that combine rougher and scavenger concentrate (as a final concentrate) and scavenger middling chutes that combine with raw feed from the heat exchanger to form rougher (or Syntron) feed. Supports are also included for the Syntron feed spreader, electrodes, and vibratory conveyors, which handle the pilot plant products to waste or to storage.

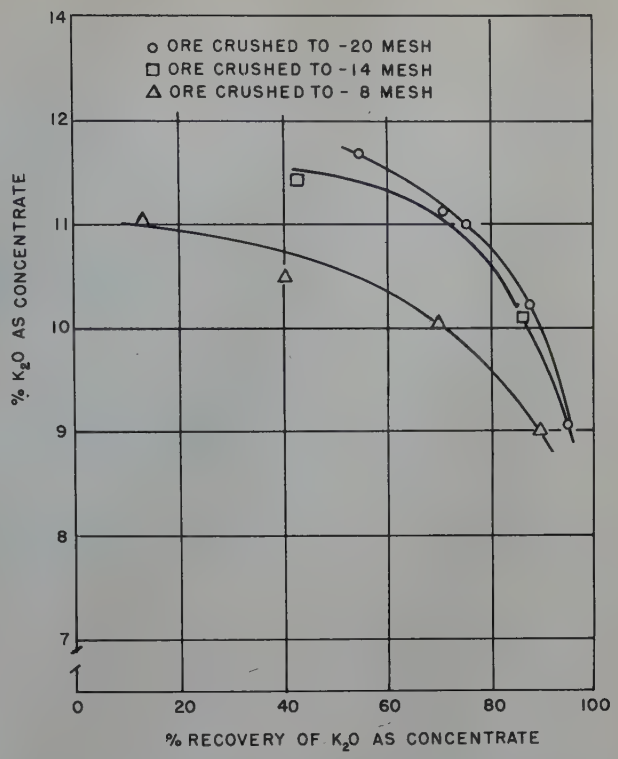

Fig. 11—Static separations of Topsham ore crushed to 8, 14, and 20 mesh. The 14-mesh grind was selected.

PROCESS FEATURES

Separation efficiency of the electrostatic section of the Topsham feldspar mill is unaffected by variations of feed rate from 1.5 to 7.5 tph. Because of the limited feed bin capacity and the capacity of conveying equipment away from the electrostatic unit, an extended plant run in excess of 7.5 tph has not been made.

Voltage Requirements: After extensive tests at Topsham it was found that the high voltage power supply, which was adequate for test purposes at Mulberry, was not rugged enough to operate in the dust-filled atmosphere of the feldspar mill and withstand the ever-present vibration. These power supplies were essentially heavy-duty laboratory models with the high voltage produced by a delicately tuned radio frequency oscillator and a light duty RF rectifier (1B3 electronic tube) in a voltage tripler circuit. The alternative was to install, if possible, a stronger and more mechanically rugged power supply with more current available at higher voltages. Following installation of Beta Electric Corp. model 2068, 0 to 100 kv, there was no further difficulty in maintaining the necessary potential of 70 kv at the electrodes.

Temperatures: During operations the firebox exhaust temperature ranged from 1850°F to a maximum of 1900°F. This produced an ore temperature of 240°F (plus or minus 15°) at the Syntron feeding the electrostatic unit. A portion of the firebox exhaust gases was introduced into the elevator feeding the electrostatic unit, and the remainder was introduced directly into the electrostatic tower itself. The result was a relatively constant temperature of 155°F in the top of the tower and 135°F in the lower portions of the tower within half an hour after start-up. These temperatures were varied by introducing cold air at the bottom of the tower and also by adding space heaters. However, the temperatures mentioned (155°F in the top, 135°F at the bottom, and 240°F ore temperature) were found to be optimum. (Refer to Figs. 9 and 10).

Mesh of Grind: To determine the maximum mesh grind for most efficient operation, several tests were made on 8, 10, 14, and 20 mesh. The best metallurgical results were obtained from a 20-mesh grind, but going this fine on the Symons cone crusher presented tonnage problems and raised too much dust, and the next best grind (14 mesh) was adopted as optimum. The relationship between the various grinds is presented in Fig. 11.

Process Control: Process control is attained by use of a geiger counter to determine the K_2O value as a function of the K^{40} isotope. In many instances the variation in geiger K_2O analysis has proved less than corresponding chemical analysis for K_2O.

After the burner is lighted and the conveying equipment and feeders are started, the only attention necessary is to take a sample every half hour and place it in a geiger tube for counting. No extra labor is needed—the two men ordinarily required to run the mill can also operate the electrostatic unit. If any variations from standard grade of concentrate are indicated by the geiger counter, the unit can be realigned by a simple movement of divider setting.

Representative data for the electrostatic process are presented in Tables VI and VII.

REFERENCE

[1] R. B. Ladoo: *Nonmetallic Minerals*, 2nd ed., p. 205, McGraw-Hill Book Co. Inc., New York, 1951.

Discussion of this article sent (2 copies) to AIME before Nov. 30, 1958, will be published in MINING ENGINEERING.

THE GEIGER COUNTER AS A CONTROL TOOL IN PROCESSING POTASSIUM-BEARING ORES

by W. C. KNOPF and G. SAMSEL

For several years International Minerals & Chemical Corp. has used a radiation method to assay potassium content of products from potash and feldspar beneficiation. The procedure is rapid, accurate, and inexpensive and is easily handled, if necessary, by nontechnical personnel. Data are presented to show the accuracies that may be expected if the technique is used for control of pilot plants or large-scale plants.

Natural potassium is composed of three isotopes —K^{39}, K^{40}, and K^{41}. Five other isotopes, artificially produced, have been detected. In natural potassium only the K^{40} isotope, with a half life of 1.4×10^9 years, is radioactive. Its modes of decay are beta and gamma rays, positrons, and x-rays. Only the more abundant beta rays, however, are important in radiation measurements using geiger tubes.

Barnes and Salley[1] measured radiation of potassium salts in solution in 1943. Gaudin and Parnell[2] first reported the use of solid salts arranged in a vessel surrounding the β counter in 1948. Later, Scheel[3] used the method to assay potassium content of various crude and finished potash salts.

Experimental: Dip-type Geiger-Muller tubes (TGC-5) supplied by Tracerlab Co. were used in all radiation counting measurements. The tube was encompassed by a glass container about ½ in. larger in diameter than the tube. This container, which served as a sample holder, was closed at the bottom with a rubber stopper to facilitate removing the samples. Samples were not weighed, but about 40 g of sample were needed for each test.

Electrical impulses from the tube were counted on either a Tracerlab scaler or a rate meter. To obviate the need for constant attendance, preset features were incorporated into the scalers, so that at a predetermined time or count the units were automatically deactivated. When rate meters were used, counting rates were read directly from instrument or from a recorder used in conjunction with the rate meter.

Each tube was calibrated, according to the manufacturer's instructions, to determine the correct operating voltage to insure reproducible results. A linear calibration plot of percent K_2O vs counting rate was also obtained for each tube by recording the counting rate plus background count of several standards of different K_2O content chemically analyzed by the chloroplatinate method.[4] These standards were of approximately the same particle size distribution as samples to be assayed. Specific background count caused by cosmic rays and other surrounding radiation was checked periodically by counting a sample of pure NaCl. Fig. 1 is a representative calibration plot. Assays were determined directly from the standard plot or calculated by subtracting the background count from the counting rate, then multiplying by the slope of the line.

Chemical assays of the test samples were made by the Sherril method,[5] a flame photometric technique, or the chloroplatinate method.

Data: The radiation assay method has been used for three years by International Minerals & Chemical Corp. in the laboratory and in pilot plants processing ores containing potassium. These dry concentration plants process sylvinite and langbeinite ores at Carlsbad, N. M., and feldspar ores at Topsham, Maine.

Sylvinite ore is predominantly a mixture of sylvite (impure KCl) and halite (impure NaCl). Contaminants include sulfates, such as langbeinite ($2MgSO_4 \cdot K_2SO_4$), kieserite ($MgSO_4 \cdot H_2O$), polyhalite ($MgSO_4 \cdot K_2SO_4 \cdot 2CaSO_4 \cdot 2H_2O$), and slimes. Langbeinite ore is predominantly langbeinite and halite with small amounts of sylvite, sulfates other than langbeinite, and slimes.

Several variables, in addition to correct calibration and standardization of tubes, were found to be important in obtaining reproducible results. Particle size distribution of standard samples should be

W. C. KNOPF, Member AIME, is Assistant Director of Research and G. SAMSEL is Senior Research Chemist, Central Research Laboratory of International Minerals & Chemical Corp., Skokie. Ill. TP 4764H. Manuscript, Dec. 2, 1957. New Orleans Meeting, February 1957.

During a three-year period 1000 measurements of laboratory and pilot plant operations were recorded comparing chemical assays on potassium-bearing ores with those using radiation techniques. Results show that the radiation technique can be readily adapted as a control tool. Variables affecting radiation measurements are discussed.

approximately the same as samples to be assayed. Data in Table I show the effect obtained by assaying samples of different mesh size. The −48+65 mesh fraction was considered a standard with zero error. Measurements using pure KCl vary by as much as 18 pct when different mesh fractions are assayed. Fortunately errors due to particle size distribution can be minimized in practice by calibrating the tube with standard samples of approximately the same particle-size distribution as samples to be assayed in the plant.

Radiometric counting techniques should be recognized strictly as a statistical method. Probable accuracy is a function of the number of counts. The larger the count, the more accurate the results. A useful relationship is the *percent probable error*, which is equivalent to $\frac{67.45}{N}$. Thus if the number of counts for a given sample is increased from 200 to 2000, the probable error drops from 4.8 to 1.5 pct. In the analysis of a 60 pct K_2O potash concentrate, this reduces the probable error from 3 pct K_2O to 0.9 pct. Obviously, the total number of counts should be selected to achieve the desired accuracy. This can be shown clearly by Table II, which gives the spread of actual error as a function of counting time. This data was obtained on a sylvinite concentrate counted ten times at each of the three periods of time. It is apparent that increased counting time improved accuracy of the results.

Wide variation in temperature of the sample during radiation counting can result in erratic data. As an illustration, Table III shows data obtained by repeatedly counting a feldspar concentrate as it cooled from 200°F to room temperature. Counting time for each assay was about 2 min. It can be seen that at first as the sample cooled counting rates increased until the tube and the sample temperatures were approximately in equilibrium. Counting rates then decreased as temperatures approached ambient to reach the 15 pct K_2O value obtained by chemical assay. In addition to the undesirable temperature effect, tube life is shortened by exposure to high temperatures, and after exposure, tubes can rarely be depended on for normal operation. Counting should be done, therefore, with feeds at ambient temperature.

During the three-year period, more than 1000 tests were made in these pilot plants comparing radiation assays with chemical assays. Results of these comparisons are summarized in Table IV. Chemical assays were taken as the basis of comparison in determining deviations. Results were derived from raw data with maximum differences as high as 7.9 pct K_2O recorded for sylvinite concentrates, and as high as 3.9 pct K_2O for tailings of 1 to 5 pct K_2O, overall range. In spite of this, the arithmetic mean difference for all tests was 0.8 pct K_2O and the algebraic mean difference was 0.21 pct K_2O. These differences would have been less except for the fact that values for sylvinite rougher concentrates and feed, Table IV, were exceptionally high. These large values may be accounted for in part by some laxness of personnel, since the importance of accurate assays for control at these

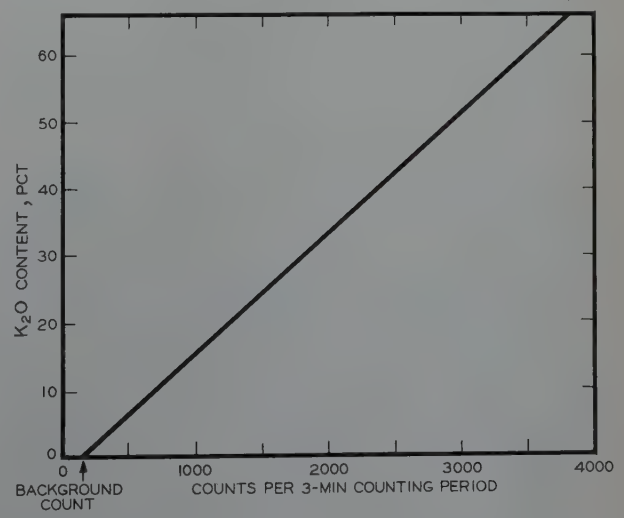

Fig. 1—Counts observed vs K_2O content of ore assayed.

Table I. Effect of Particle Size of Pure KCl on Measured Radiation Activity

Mesh	Cpm*	K_2O by Count, Pct	Error, Pct
−45+65	1040	63.2	0
−28+48	1010	61.4	2.8
−18+28	960	58.3	7.8
−12+18	860	52.0	17.7

* Counts per minute.

points in the pilot plant circuit has not been stressed.

Arithmetic mean differences for all sylvinite fractions was 1.4 pct K_2O, and the algebraic mean difference was −0.6 pct K_2O. Arithmetic mean differences for langbeinite and feldspar fractions were 0.8 pct K_2O and 0.5 pct K_2O, respectively. The increased accuracy obtained with feldspar is attributed to a longer counting time. Feldspar was counted for 10 min, whereas Carlsbad samples were counted for 3 min. This shorter period was necessitated by a shortage of operating personnel. Algebraic mean differences for langbeinite and feldspar products were −0.1 pct and +0.2 pct K_2O, respectively.

Table II. Effect of Counting Time on K_2O Assay of Sylvinite Concentrate

	K_2O, Pct					
	Radiation Assay	Deviation from Chemical Assay*	Radiation Assay	Deviation	Radiation Assay	Deviation
	1 Min		4 Min		16 Min	
Arithmetic mean	60.7	1.8	60.9	0.9	61.4	0.3
Algebraic mean	—	−0.7	—	−0.5	—	−0.02

* Chemical assay 61.4 pct K_2O.

Comparison of probable error with experimental error, Table IV, shows the two values to be fairly close for concentrates, particularly sylvinite final concentrates. This substantiates theory in that more accurate results are obtained where more counts were recorded. Total counts for sylvinite concentrates, for example, were 3000 to 4000, whereas counts for sylvinite tail fractions were 300 to 500. Although experimental error values appear extraordinarily high for tailing fractions, a 25 pct error of a 2 pct K_2O product would only be 0.5 pct K_2O.

SUMMARY

Assays were made on approximately 1000 samples ranging from 1 to 61 pct K_2O by chemical methods and by radiation methods. These pilot plant results show that the radiation technique is satisfactory for control purposes as well as for research or analytical laboratories where a rapid method of analysis is required.

Even with a counting time of 3 min or a total elapsed time of 5 min for each sample, results were accurate enough for control of the pilot plants. Since radiation counting is a statistical method, accuracies could have been improved by increasing the counting time. Even with a substantially longer counting time, the assay technique would be faster than chemical methods, since samples do not have to be weighed or put into solution.

In general it can be expected that the arithmetic mean difference of 0.8 pct K_2O obtained in these tests will be equaled or decreased, as present data include some preliminary results obtained before all the variables were recognized. The arithmetic mean difference of 0.5 pct K_2O assays of feldspathic materials ranging from 3 to 11 pct K_2O indicates the accuracy that might be obtained with a 10-min counting period. This accuracy would be even better, for example, if sylvinite concentrates, which ranged from 55 to 61 pct, were counted for the 10-min period.

Some sources of errors encountered with the radiation method of assay were:

1) Incorrect standardization and calibration of geiger tubes.

2) Variation of particle-size distribution of the test sample with samples used for calibration.

3) Variation of temperature of sample during counting period.

4) Insufficient number of counts to give accurate results.

These variables must be taken into consideration if accurate results are to be obtained with the technique.

Table III. Effect on K_2O Assay of Cooling Sample from 200°F to Room Temperature

Temperature, °F	Cpm	K_2O, Pct
200	344	19.2
—	355	19.8
—	326	17.8
—	322	17.6
—	307	16.8
—	292	15.8
75	281	15.0

Table IV. Summary of Results Obtained From Comparison of Assays by Radiation and by Chemical Methods

Product	Range, Pct K_2O	Probable Error, Pct	Experimental Error, Pct	Mean Difference, Arithmetic Pct K_2O	Algebraic Pct K_2O	Maximum Difference, Pct K_2O
Sylvinite						
Final concentrate	55 to 61	1.2	1.5	0.9	−0.6	7.9
Rougher concentrate	45 to 52	1.3	4.0	1.9	−1.7	4.3
Feed	12 to 19	2.5	9.2	1.4	−0.7	4.4
Tailings	1 to 5	4.5	25.1	0.9	−0.5	3.9
Langbeinite						
Concentrate	18 to 22	1.8	3.8	0.8	−0.1	4.3
Feldspar						
Concentrate	9 to 11	1.5	5.2	0.5	−0.2	1.8
Feed	6 to 9	1.8	6.3	0.5	−0.04	1.5
Tailings	3 to 5	2.1	10.7	0.5	−0.07	1.3

REFERENCES

[1] R. B. Barnes and D. J. Salley. Analyses for Potassium by its Natural Radioactivity. *Industrial Engineering Chemistry*, 1943, vol. 15, pp. 4-7.

[2] A. M. Gaudin and J. H. Pannell: Radioactive Determination of Potassium in Solids. *Analytical Chemistry*, 1948, vol. 20, p. 1154.

[3] K. C. Scheel: Rapid Determination of Potassium in Potash Salts by Radiation Measurement. *Angew. Chem.*, 1954, vol. 66, pp. 102-106.

[4] N. H. Furman: *Scott's Standard Method of Chemical Analysis*. New York, Van Nostrand Co., Inc., 1939.

[5] E. Sherril: U.S. Patent 1,849,960, 1932.

Discussion of this article sent (2 copies) to AIME before Nov. 30, 1958, will be published in MINING ENGINEERING.

LINEAMENT TECTONICS AND SOME ORE DISTRICTS OF THE SOUTHWEST

This study examines the structural framework of the Southwest for evidence of the four principal trends of lineament tectonics. It attempts to classify their intersections and compares the positions of those trends that appear most favorable with the positions of the presently known mining districts.

by EVANS B. MAYO

This is a controversial topic. The author, in presenting his analysis, is aware that the study of lineament tectonics and relation of ore districts to regional structure is complicated by insufficient data and, unavoidably, by personal bias.

The development of lineament tectonics has been summarized by Umbgrove.[1] Early attempts to fit ore districts into the Cordilleran framework were made by Billingsley and Locke,[2,3] who do not refer to lineament tectonics, although their approach is similar; they observe that heat and fluids, including the ore-depositing fluids, are most likely to rise at or near intersections of major structures where the crust is fractured, or weakened, to great depth.

As a result of studies distributed over the earth—including ocean basins as well as continents—some tectonists recognize four dominant structural trends: 1) northwest; 2) northeast; 3) nearly east-west, or equatorial; and 4) nearly north-south, or meridional. Baker[4] proposed a theory to account for these trends and Sonder[5] called their world-wide arrangement the regmatic shear pattern. Moody and Hill[6] proposed a much more complicated shear network which, although fascinating and perhaps ultimately useful, will not be followed here. In a recent review of deformation within the Cordillera, Wisser[7] mentioned the four fundamental directions.

The fact that many geologists deny the existence of the regmatic shear pattern implies that the fundamental structures are far from obvious. It may mean, also, that some geologists are not accustomed to examine regional and world maps analytically. The maps require much study, and certain features should be isolated on overlays. Even so, with the present limited knowledge, uncertainties remain. The following analysis is a qualitative experiment, subject to change as information accumulates, and should be supplemented by the western sheet of the Tectonic Map of the United States.[8]

E. B. MAYO is Professor of Geology, University of Arizona, Tucson, Ariz. TP 4776 I. Manuscript, April 8, 1958. New York Meeting, February 1958.

LINEAMENT FRAMEWORK, SOUTHWESTERN U.S.

Many have probably gained the impression that the Cordillera of the West is oriented northwest-southeast and from this, unless experience rules otherwise, it is natural to assume that the structure likewise trends northwest-southeast. To an important extent this is true, yet anyone tracing off the western sheet of the Tectonic Map all the recorded northwest-southeast structures may be surprised to see what a small part of the entire area they occupy. In southwestern U. S. (Fig. 1) the northwest-southeast structures are mostly restricted to the eastern, southern, and western parts. The eastern margin of the Cordillera from northern Colorado to the International Boundary near El Paso, Tex., is obviously determined by some structure other than northwesterly ones. In eastern Nevada and far southward toward the Gulf of California many mountain ranges, valleys, and faults are meridional. In the Rocky Mts. of Colorado, and at many places in southern Arizona, the crystalline Pre-Cambrian is foliated northeast-southwest. The Uinta Mts. of Utah trend approximately east-west, in much the same way as a broad belt of transverse, west-northwest structures—the Texas lineament of Hill[5,9] and Ransome[10] in southern Arizona, southwestern New Mexico, and southern California.

It seems, then that there are four regmatic shear directions in the Southwest, but at many places they are discontinuous, and their projections must be inferred. To clarify these trends the four sets have been isolated into two systems: 1) northwest-northeast and 2) east-west-north-south (Figs. 2 and 3).

Northwest-Northeast System: A number of prominent northwest-trending zones of structure are easily recognized. They are designated by circled Roman numerals, the northeast-trending structures by circled capital letters.

Perhaps no two geologists would agree completely on the positions of all these belts. Names given below are for convenience only, and may be discarded where other names have priority.

(I) The Sierra Nevada-Lower California belt contains the Jurassic-Cretaceous granitic massifs of the Sierra Nevada and Lower California. These

This page of Mining Transactions AIME follows p. 1096. The intervening non-Transactions pages appeared in MINING ENGINEERING.

EXPLANATION OF STRUCTURE SYMBOLS

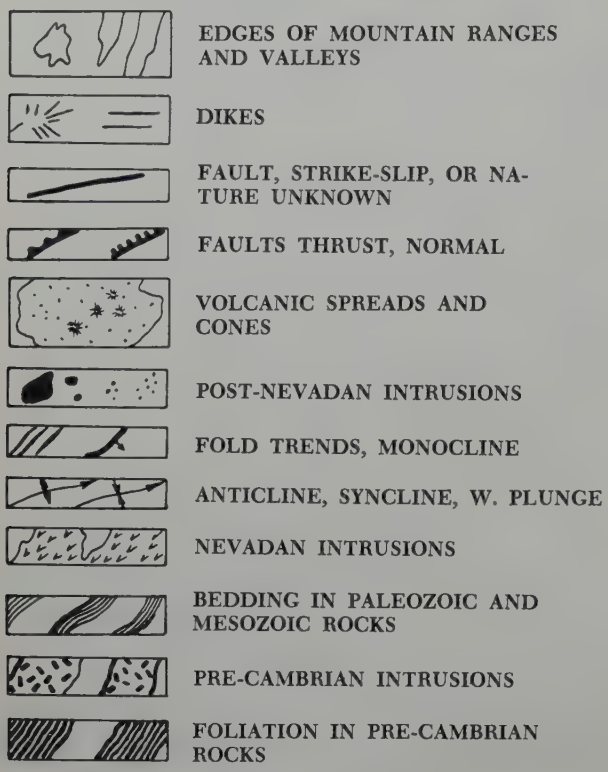

Symbols used on Figs. 1-3

crystalline masses form a barrier between the Pacific coastal region, dominated by northwest trends, and the interior where other structural trends are prominent.

(II) The Walker zone seems to extend from the northern end of the Sierra Nevada, southeastward into northwestern Sonora. Billingsley and Locke,[3] who proposed the name *Walker line*, suggested that this zone curved into southeastern Arizona. It is believed, however, that the line they defined includes several different structural belts.

(III) The southwest Arizona belt is parallel to the Walker zone and reaches from the Patagonia and Santa Rita Mts. of southern Arizona northwestward into southern Nevada.

(IV) The central Arizona belt extends northwestward from the Chiricahua and Mule mountains of southeastern Arizona to the San Francisco volcanic field.

(V) The southwestern New Mexico belt reaches from the International Boundary near Columbus, N. M., toward the Grand Canyon in Arizona. This belt is obscure in the Datil volcanic field and Colorado Plateau and possibly does not cross these features.

(VI) The New Mexico-Utah zone extends from the Guadalupe Mts. in trans-Pecos Texas and New Mexico, past Mt. Taylor, through the high Plateaus volcanic field to the Gold Hill district in Utah. The continuity of this zone, although locally interrupted, seems obvious.

(VII) The southwestern Colorado zone, beginning west of Tucumcari, N. M., extends past Taos and along the southwest side of the San Juan volcanic field and beyond to Bingham, Utah.

(VIII) The central Colorado belt begins in the area of the Spanish Peaks in southern Colorado and trends through Leadville and Climax toward the Washakie Basin in southern Wyoming.

(XI) The Laramie zone trends acutely across the Front Range of Colorado and along the western side of the Laramie Basin, Wyoming.

The following zones appear to be complementary to the above northwesterly trends:

(A) The northeast-trending Santa Rita belt is vaguely shown by faults, aligned intrusions, and the southeastern margin of the Datil volcanic field. It begins southwest of Bisbee, Ariz., and reaches past Tyrone and Santa Rita, N. M., to the northern end of the Tularosa Basin.

(B) The Morenci belt is also vaguely defined and may not extend as far as indicated (Fig. 2). It passes through the Datil volcanic field, its course revealed by alignments of the San Agustin plain, New Mexico, and the modifications at the northwestern ends of valleys at Mogollon, N. M., and Morenci, Ariz. The extension of this zone east of the Rio Grande is marked by faults and by the northeast trend of foliation in Pre-Cambrian rocks.

(C) The Jemez zone, beginning with a southwest-trending trough in southern Colorado, passes through the Jemez caldera and the Mt. Taylor area and along the northwestern border of the Datil volcanic field. The existence of this zone in the Globe-Miami district is suggested by the alignment of post-Nevadan intrusions and other structural features. Between Globe and Ajo, the Jemez zone seems concealed by the overprint of the Texas lineament (1-1, Fig. 3) and other structures. It may extend across southern Arizona to the Pinacate volcanos of northwestern Sonora, and beyond to the little cluster of cones on the Pacific Coast.

Zones (A), (B), and (C) form a broad northeast-trending belt that includes most of the Datil volcanic field as well as many other volcanic features. The broad belt, therefore, seems to have been tectonically active in later geologic time.

South of zone (C) the eastern front of the Cordillera trends somewhat east of north, whereas north of zone (C) the trend is about north-south, or even a little west of north. In the Spanish Peaks region near zone (C), therefore, there is a definite turn in the Cordilleran front, and apparently zones (A), (B), and (C) have had some part in modifying the course of the border between the Great Plains and the Rocky Mts. The broad belt of zones (A), (B), and (C) is obviously of great importance in the regional structure; should it cross some equally important belt of structures, intersections of great interest would be expected.

(D) The Front Range zone is named for the Front Range porphyry belt of Colorado, which forms the eastern part of the zone. The zone appears to extend southwestward along the northwest edge of the San Juan volcanic field to the Carrizo Mts. in northeastern Arizona. It may continue farther, through the San Francisco volcanic field to the area of northeast-trending foliation in the Pre-Cambrian rocks east of the Colorado River.

(E) and (F), two northeast-trending zones, occupy essentially the position of the Wyoming lineament of Ransome (Ref. 10, p. 294). There may exist in the southwestern part of this Wyoming belt a

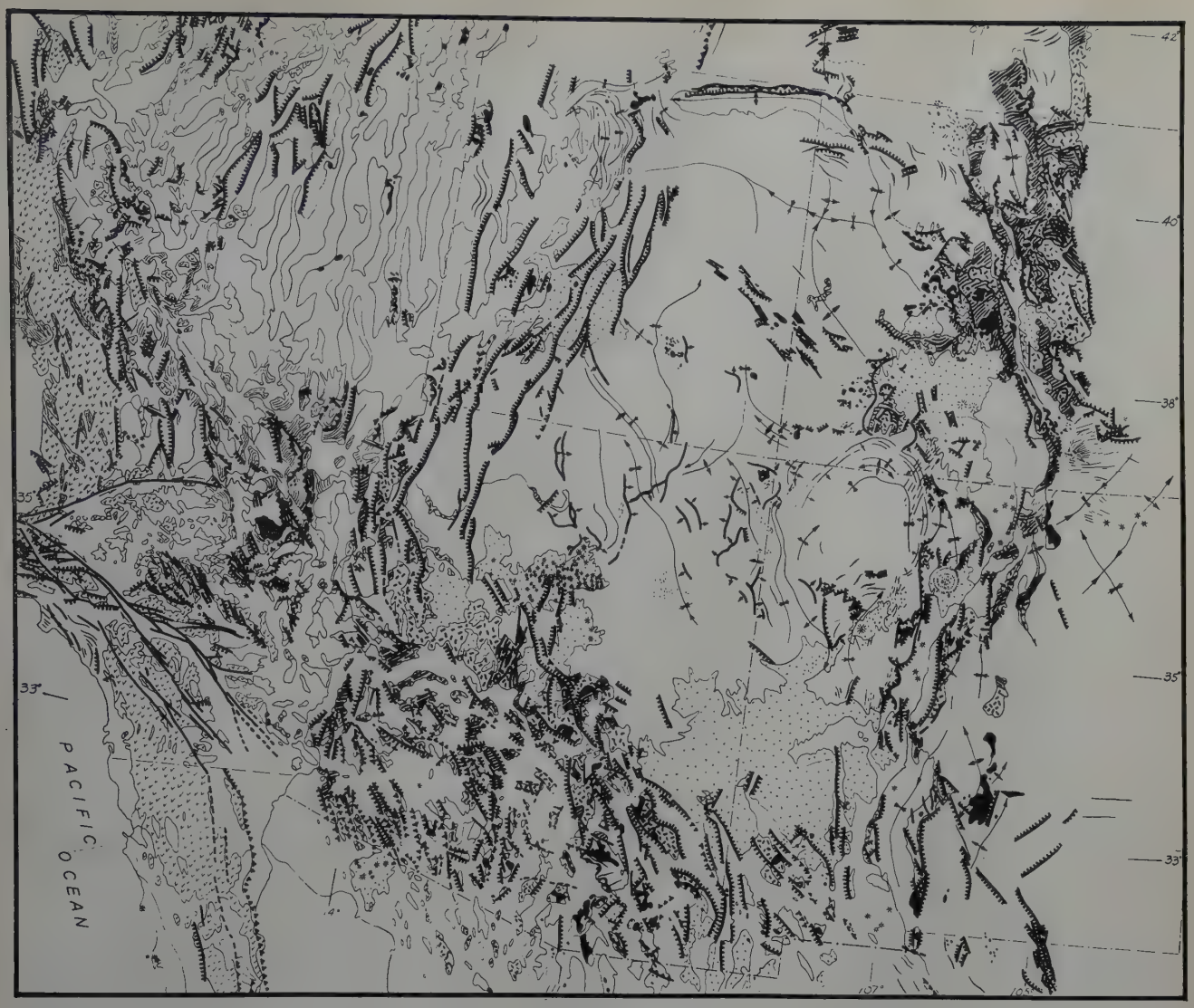

Fig. 1

very broad area of northeasterly trends, partly indicated by foliation in Pre-Cambrian rocks and partly by bedding trends in Paleozoic sediments. Traced northward out of Colorado, the Rocky Mt. ranges end in the northeastern part of this belt, in southern Wyoming. Broad passes intervene between these ranges and the more northern Rockies of Wyoming. The southwestern end of the belt is aimed toward the gap between the granitic massifs of the Sierra Nevada and Lower California.

(G) The southern Nevada zone is mostly shown by the trends of mountains and intervening valleys, and to a lesser extent by aligned intrusions. It should impinge on the eastern front of the Sierra Nevada between Lone Pine and Independence, Calif. Possibly this zone reaches northeastward to the vicinity of Bingham, Utah.

(H) The central Nevada zone is definitely indicated by aligned faults, yet exact position and orientation are uncertain. The structures seem to impinge on the Sierra Nevada in the Mammoth embayment, northwest of Bishop, Calif. This trend is considered largely responsible for the great reentrant in the Sierra front and may be partly responsible for the abrupt broadening of the granitic core southwest of the embayment.

(J) The Carson zone meets the Sierra front near Carson City, Nev. Toward the northeast the course of this belt of structures is suggested by the trends of valleys and mountains, by aligned intrusions, and by faults. To the southwest it may be the reason for some of the granitic prongs along the western edge of the Sierra Nevada batholith.

Although only two sets of lineaments have been examined, it already seems obvious that important geologic features are located at places where these two sets of trends cross. Some of these features, indicated in Fig. 2, are as follows:

1. (1) and (G, H, J), not exclusive—Sierra Nevada batholith.
2. (I) and (C,D,E,)—broadest part of the batholith of Lower California.
3. (II) and (C)—Pinacate volcanos.
4. (II) and (E,F)—large intrusions in Mohave Desert of California.
5. (II) and (G,H,J)—granitic intrusions east of Sierra Nevada.
6. (IV, V) and (D)—San Francisco volcanic field.
7. (V, VI) and (A,B,C)—Datil volcanic field and associated intrusions.
8. (VI) and (F)—High Plateaus volcanic field and intrusions.
9. (VII) and (C)—Jemez Caldera.
10. (VII) and (D)—San Juan volcanic field and intrusions.
11. (VII) and (G?)—Intrusions at and near Bingham, Utah.

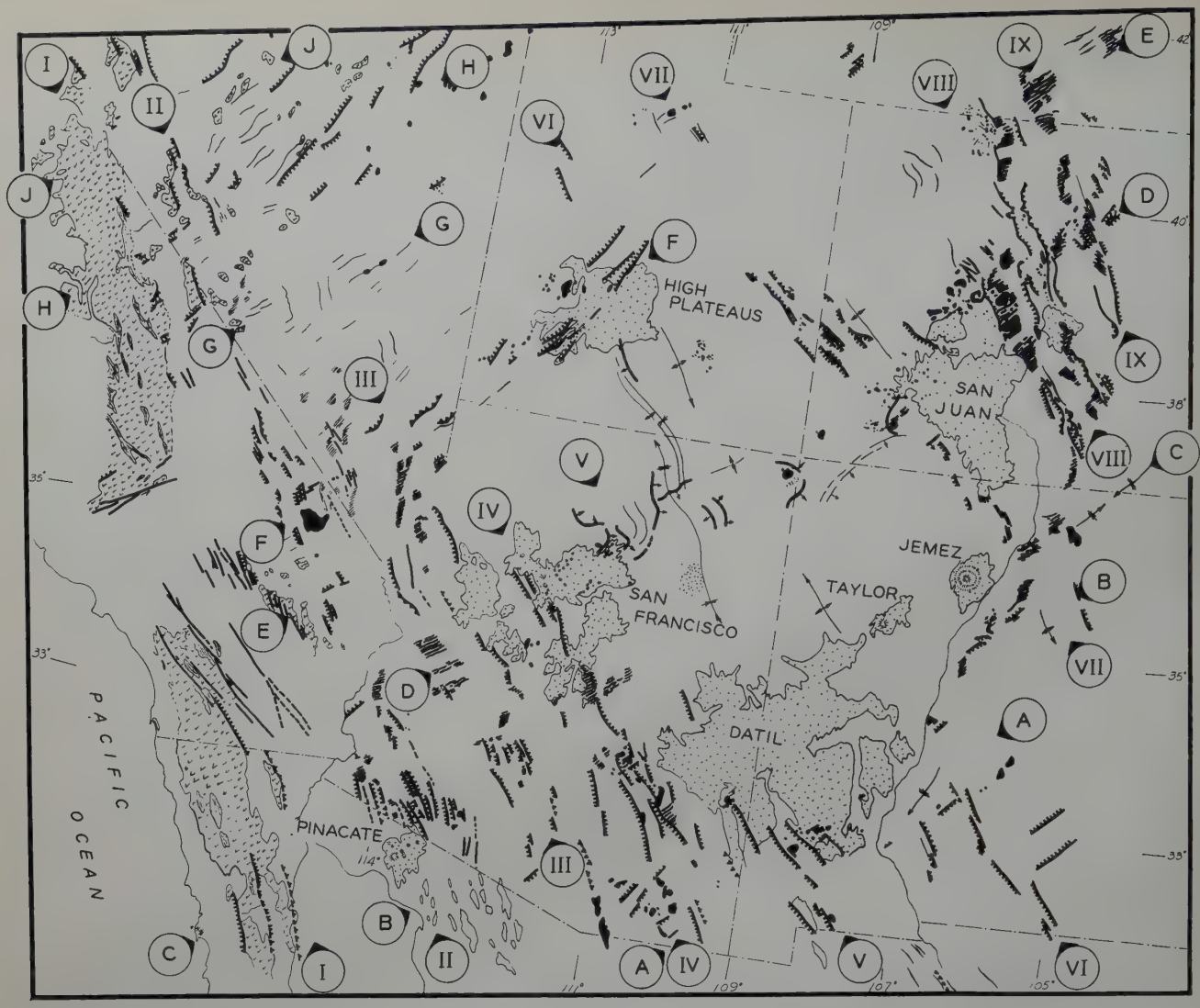

Fig. 2

12. (VIII) and (D)—large area of porphyry intrusions north of San Juan volcanic field, Colorado.

13. (VIII) and (E)—group of intrusions along Colorado-Wyoming border.

14. (IX) and (D)—Front Range porphyry belt, Colorado.

These examples suggest how intersecting weak zones in the crust may have localized the phenomena of intrusion and volcanism. The suggestion is further strengthened by consideration of the east-west-north-south lineament system.

East-West-North-South System: The structures belonging to this system are locally obvious, but in large areas they are either lacking or have not yet been mapped. This is particularly true of the east-west set. As a rule the two sets only approximately follow the east-west or north-south directions. The north-south set is usually oriented somewhat east of north, and the east-west set somewhat north of west. On the basis of information traced from the Tectonic Map,[8] there appear to be the following nearly east-west structures (Fig. 3):

(1) Texas lineament (with a possible branch, 1′). This great belt of transverse structures forms the southern border of the tectonic framework of the western U.S. In the region of Fig. 3, the Texas lineament is by far the most pronounced transverse belt. It can be traced from trans-Pecos Texas on the east to the Transverse Ranges of Southern California on the west. Strands within the belt, as in southern Arizona, are marked by nearly east-west faults and elongated or aligned intrusions. The entire zone, in southern Arizona, may be more than 150 miles wide.

(2) The San Francisco zone is not satisfactorily revealed by the assembled data. The best evidence for its existence is in eastern California and southern Nevada, where trends of intrusive contacts, elongated intrusions, west-northwest faults, and curves in thrusts and in the trend of bedding suggest a transverse disturbance. Some of the cones in the San Francisco volcanic field are arranged in transverse rows; possibly this trend extends into east-central New Mexico where foliation in Pre-Cambrian is oriented west-northwest. If this is the case, there are broad gaps with no evidence, and the supposed San Francisco zone is poorly defined. Perhaps it is valid only where supporting evidence has been mapped.

(3) The Spanish Peaks belt trends from southern Colorado past the San Juan volcanic field and into southern Utah. Groups of intrusions seem to continue this trend across Utah, and faults, intrusions and a belt of thrusts indicate its path across Nevada. This zone apparently reaches the Mother Lode of California near Plymouth.

(4) The Cripple Creek zone reaches from the southern end of the Front Range, Colorado, west-

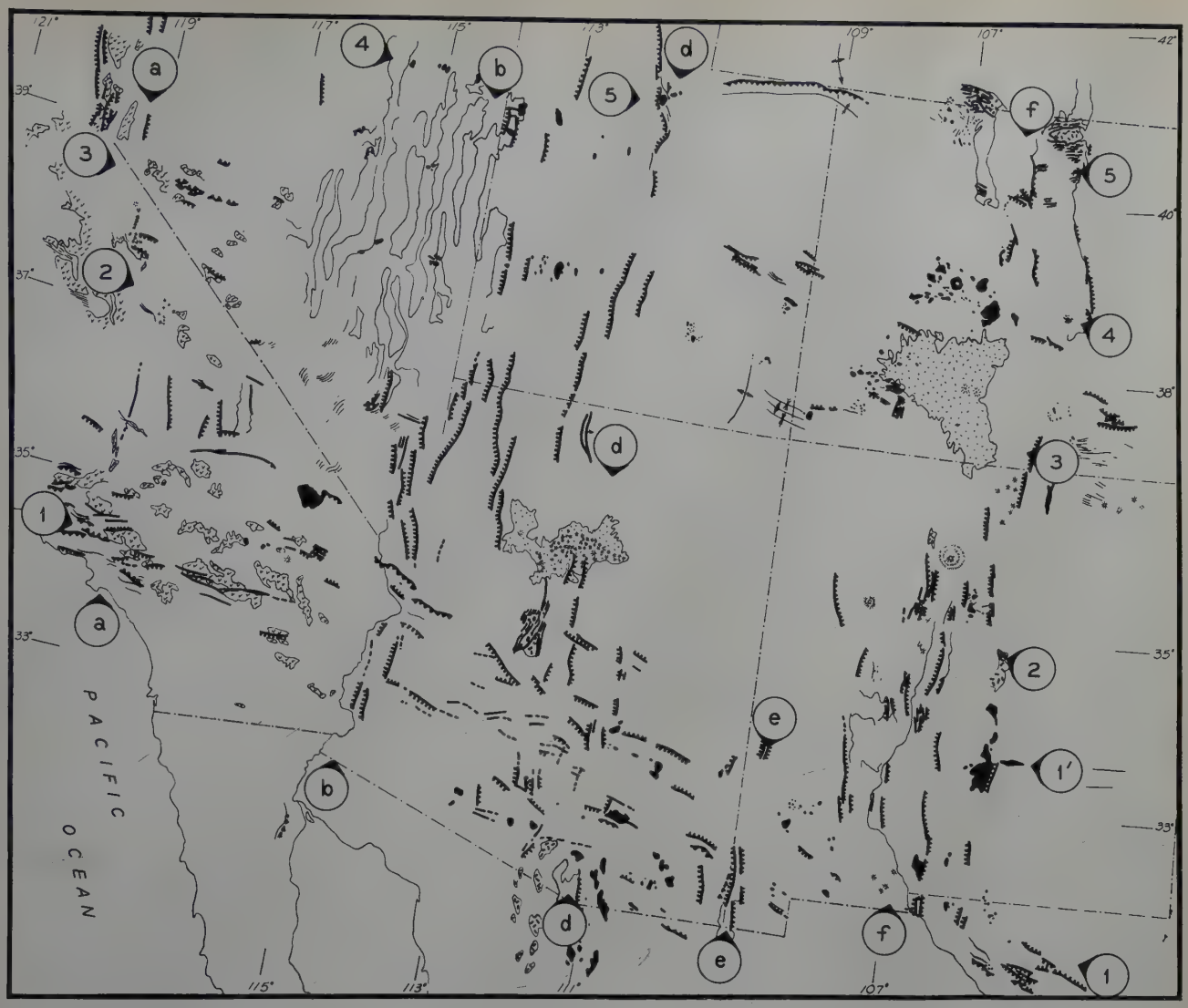

Fig. 3

ward to the great group of porphyry intrusions, and on into eastern Utah. This structure may extend across Utah to the Gold Hill district and westward into eastern Nevada.

There is some evidence (Fig. 3) in eastern Nevada that a transverse structure exists midway between zones (3) and (4).

(5) The Uinta belt begins in northern Colorado and follows along the Uinta axis to Bingham, Utah. Perhaps this is a branch structure, related to the Cripple Creek zone as (1′) is related to the Texas lineament.

Crossing the above structures are the nearly north-south lineaments, of which the following are recognizable:

(a) The Sierra Nevada belt is indicated at the north by north-south faults that at first merely border the Sierra, then slice obliquely into it and across it (e. g., Kern Canyon fault). Perhaps this meridional zone does not cross the Transverse Ranges of southern California.

(b) The Colorado River zone is very broad at the north, in eastern Nevada, and narrows southward along the Colorado River. It reaches the northern end of the Gulf of California.

(d) The Utah-Arizona belt trends north-south through central Utah and Arizona. In Utah and in northern Arizona it forms a boundary between the plateaus to the east and the Basin and Range province to the West.

(e) The Pelonicillo belt parallels the interstate boundary in southeastern Arizona and southwestern New Mexico.

(f) The Cordilleran Front belt, a very broad zone of meridional structures, parallels the eastern margin of the Rocky Mts. in Colorado and New Mexico.

Comparison of Figs. 2 and 3 suggests that most if not all the 14 features listed above are localized not only on intersections of structures belonging to the northwest and northeast sets, but also on north-south-east-west crossings. For example, the Sierra Nevada batholith seems somewhat related to transverse zones (2) and (3) and to north-south zone (a), as well as to the structures already mentioned; the San Francisco volcanic field occupies the intersection of zones (2?) and (d); Datil volcanic field is on the northern margin of the Texas lineament where this is crossed by the north-south structures (e) and (f); the intrusions near Bingham, Utah, occupy the intersection of lineaments (5) and (d), and so on.

It has been noted that some of the structural trends are marked by aligned intrusions, and possibly these intrusions occupy minor intersections on the trends. If this is so, the evidence quite eludes the present analysis. It is otherwise, however, with cer-

tain groups of intrusions, with granite masses of regional dimensions, and with some of the most arresting volcanic phenomena. These features occupy the intersections indicated, or at least suggested, by data on the maps.

The above relation suggests that some of the major intersections, having been unusually weak places in the crust, were the sites of especially pronounced and long-continued igneous activity. This repeats Billingsley's and Locke's idea[11] that escape of heat and fluids is particularly favored on the structural intersections.

THE STRUCTURAL INTERSECTIONS

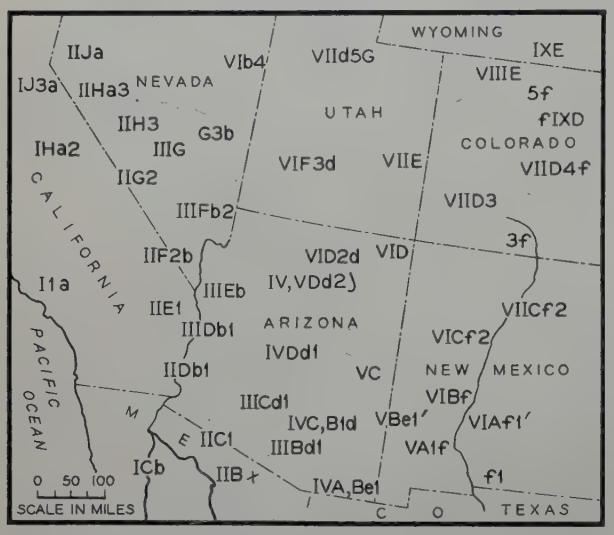

The *geologic crossroads* were located on a tracing (Fig. 4, above) first placed over Fig. 2, then over Fig. 3. There are many intersections, and it is disconcerting to realize that the entire region will be covered, provided the structural zones selected are numerous enough and broad enough. No doubt every place is an intersection of some kind, but this fact is of no aid in selecting areas of special geologic or economic interest, so it becomes necessary to establish guides to selection. This brief inquiry cannot approach a complete list of guides, but a few seem promising:

1. Crossings of the most pronounced structure belts—such as the Texas lineament and zones (A), (B), and (C)—should be of greatest interest.
2. The structural trends concerned should be fairly obvious, suggesting that the trends have been active in later geologic time.
3. More than two directions should meet at the intersection.
4. One or more of the directions should be accompanied by evidence of igneous activity.
5. Small or moderate-sized post-Nevadan intrusions should occupy the intersection, or:
6. If Nevadan granites of regional dimensions are present, the areas of interest should be marginal to the granite.

It is realized that areas of great importance from the viewpoint of exploration may be concealed and may therefore lack some or all of the above characteristics. This is of no importance in the present study, in which the objective is correlation with known ore districts.

With the guides listed above, selections can be made from the intersections in Fig. 4. These intersections are considered according to the transverse belts on which they are located.

INTERSECTIONS, TEXAS LINEAMENT

This broad, transverse belt is crossed by structures that follow the other three regmatic shear directions. Most important of these, apparently, is the northeast bundle of zones (A), (B), and (C). Next in order seem to be northwest zones (III), (IV), and (V); northeast zones (D), (E), and (F); and northwest zones (I) and (II). All the north-south belts reach or cross the Texas lineament.

Structural crossings were arranged into four classes. Intersections that involve the Texas lineament and zones (A), (B), or (C) and at least one other direction, and likewise have small or moderate-sized intrusions, are rated first class. An intersection involving four directions plus intrusions is also rated first class. If four directions are present but there are no intrusions, the intersection is second class, and if there are three directions plus intrusions but zones (A), (B), or (C) are not represented it

Table I. Intersections On and Near Texas Lineament

I	la	(2nd class)	II	El	(2nd class)
III	Eb	(3rd class)	III	Dbl	(2nd class)
II	Dbl	(2nd class)	I	Cb	(3rd class)
II	Cl	(1st class)	II	B	(4th class)
IV	Ddl	(1st class)	III	Cdl	(2nd class)
III	Bdl	(1st class)	IV	C,Bld	(1st class)
V	C	(4th class)	IV	A,Bel	(1st class)
V	Bel'	(1st class)	VI	Bf	(2nd class)
V	Alf	(1st class)	VI	Afl'	(1st class)
	fl	(4th class)			

Table II. Lineament Intersections and Mining Districts

First Class Intersections		Mining Districts
II	Cl	Ajo
IV	Ddl	Jerome-Bradshaw-Bagdad
III	Bdl	Twin Buttes-Silver Bell
V	Bel'	Morenci-Mogollon
V	Alf	Santa Rita-Tyrone
VI	Afl'	Capitan iron—no important district known
IV	A,Bel	Bisbee-Tombstone-Courtland-Gleeson
IV	C,Bld	San Manuel, Ray, Miami, Superior, Globe, Mammoth, etc.

Second Class Intersections		Mining Districts
I	la	No important district known
II	El	Eagle Mountains, iron
II	Dbl	No important district known
III	Dbl	Artillery Mountains, manganese
III	Cdl	No district known
VI	Bf	Magdalena

Table III. Intersections On and Near Transverse Zone (2)

First Class Intersections		Mining Districts
I	Ha2	Southern end of Mother Lode on west; Bishop tungsten on east
VII	Cf2	Pecos
VI	Cf2	Mt. Taylor-Grants region, uranium
II	Fb2	Goodsprings-Searchlight, Nevada; Mountain Pass, California
VI	D2d	Monument No. 2—White Mesa

Second Class Intersections		Mining Districts
II	G2	Silver Peak-Goldfield-Rhyolite-Bullfrog
VI	D	Carrizo Mountains, uranium

Table IV. Intersections on Transverse Zones (3), (4) and (5)

First Class Intersections		Mining Districts
I	J3a	Mother Lode
II	Ha3	Aurora—Candelaria
VII	d5G	Bingham-Park City-Tintic, etc.
VI	F3d	Marysvale-Silver Reef-Iron Springs
VII	D3f	San Juan districts
VII	4Df	Cripple Creek

Second Class Intersections		Mining Districts
II	Ja	Virginia City (Comstock Lode)
II	H3	Tonopah
	G3d	Pioche
VI	b4	Gold Hill
	f IX D	Front Range Mineral Belt, Leadville, Climax

is second class. If three directions are present without intrusions the intersection is third class; if only two directions are represented it is fourth class. The localities and structural trends represented are shown in Fig. 4 and listed in Table I. The first and second class intersections only are listed, together with the associated mining districts, in Table II.

The contrast between the first and second class intersections is revealed in the relative number and importance of the *hits* scored in each class—seven out of eight in the first class, but no better than three out of six, and probably no major ore district, in the second class.

Intersections On and Near Transverse Zone (2): This vaguely defined, apparently weak or inactive zone compares very unfavorably with the Texas lineament, and its intersections have had to be classified somewhat differently. Where four trends cross and intrusions are present, the crossing is considered first class, but if intrusions are absent it is considered third class, even though important volcanic phenomena are present. Where two or three trends cross and intrusions are present the crossing is second class. All other cases are relegated to third or fourth class and eliminated. Locality VI Dd2 attains to first class because small, ultrabasic intrusions not shown on the map are present, whereas locality IV, V Dd2 is assigned to third class because the surface is mostly covered by volcanic rocks. Even so, uranium has been mined near Cameron, Ariz.

Few places in this transverse zone can be considered major ore districts. Most important, perhaps, are Bishop tungsten in California and Monument No. 2 in Arizona.

Intersections in Zones (3), (4), and (5): Parts of these zones are not satisfactorily revealed by the data on the Tectonic Map, but in general these structures are more obvious than transverse zone (2). It may be that over certain intervals, particularly in Utah and Nevada, the continuity of zones (3) and (4) will never be established. The first and second class intersections are listed in Table IV.

As selected above there are 19 first class intersections and 13 second class intersections. Ore districts are found on 18 of the first class, 10 of the second class. Furthermore, most—but not all—the major ore districts are on the first class crossings.

At first the correlation between intersections and ore districts seems remarkable—about 94 pct for the first class, 77 pct for the second. But these figures take no account of districts that were missed. Excepting some uranium-bearing areas, most of these are of lesser importance. If there is an additional transverse zone between zones (3) and (4), Ely and Eureka may occupy crossings on this zone.

The personal factor is, of course, a disturbing source of error. With all good intentions, the structural trends and their crossings were probably not selected without bias. In spite of many uncertainties, however, it is believed that a systematic relation does exist between the crossings of certain elements of the regional framework and the most important occurrences of ore.

IMPROVING CONTROL

Better maps will provide one answer to present imperfections in correlating ore faci with structure. Fortunately the maps continue to improve, and it should gradually become possible to deal more confidently with two-dimensional geometry. But two dimensions are not enough.

If hypogene ore has come from *below*, something must be known of conditions at depth, and probably the greater the depth the better. Three-dimensional control of ore is best disclosed by mine workings and natural sections. Billingsley and Locke in their second paper[2] offered a few examples, and many more are available. Whatever indirect knowledge is gained of the third dimension—beyond the depth of mines, drillholes, and erosion—must be won by the geophysicist.

Every geological problem, however, is four-dimensional, that is, it involves time. The structural history of any region under investigation holds the answer to the relative importance of various structural trends. Which structures were the longest active and when were they active? Where were the sedimentary basins of the past and when were they deformed? What was the sequence of intrusion, extrusion, differentiation,[10] and alteration? These features have been discussed and shown on maps, but the writer knows of no regional study involving all of them. If such complete data were available the mineral districts might be fitted into the regional framework like jewels into their settings. In that case a proper setting without its jewel would be subject to the most earnest inquiry.

This generalized account can only suggest a direction for further work. Obviously, regional structure is the essential framework for all geological studies, including investigations of ore deposits. It seems, then, that the methods and theory of lineament tectonics should be important in future explorations for economic minerals. The structural framework of the Southwest may prove to be different in many respects from the one proposed here, yet that framework should become more obvious as information accumulates. As the framework becomes more definite it should clarify the positions of known ore districts, reveal localities where new ore might reasonably be searched for, and outline those places where exploration would probably be wasted.

This article was written at the invitation of W. C. Lacy, who generously aided in its preparation. Although the author is acquainted with the geology of parts of the region discussed, the material presented here is mostly compilation. The American Association of Petroleum Geologists kindly granted permission to use information shown on part of the Tectonic Map of the United States.[8] Information was taken, also, from Vincent Kelley's tectonic map of the Colorado Plateau.[13]

REFERENCES

[1] J. H. F. Umbgrove: *The Pulse of the Earth*, pp. 304-308, Martinius Nijhoff, The Hague, 1947.
[2] P. Billingsley and A. Locke: *AIME Trans.*, 1941, vol. 44, pp. 9-64.
[3] R. T. Hill: *AIME Trans.*, 1902, vol. 32, pp. 163-178.
[4] C. L. Baker: *Pan American Geologist*, 1933, vol. 59, pp. 19-32.
[5] R. A. Sonder: American Geophysical Union, *Trans.*, 1947, vol. 28, pp. 939-945.
[6] J. D. Moody and M. J. Hill: Geological Society of America, *Bull.*, 1956, vol. 67, pp. 1207-1246.
[7] E. Wisser: *Quarterly of the Colorado School of Mines*, 1957, vol. 52, no. 3, pp. 54-73.
[8] P. B. King and Map Committee: *Tectonic Map of the United States*, American Association of Petroleum Geologists, Tulsa, 1944.
[9] R. T. Hill: Geological Society of America, *Bull.*, 1928, vol. 39, p. 265.
[10] F. L. Ransome: *Problems of American Geology*, pp. 287-376. Yale University Press, 1913.
[11] P. Billingsley and A. Locke: *AIME Trans.*, 1933, vol. 501, pp. 2-12.
[12] W. C. Lacy: *AIME Trans.*, 1957, vol. 209, pp. 559-562.
[13] V. C. Kelley: University of New Mexico Publication in Geology, 1955, No. 5.
[14] V. C. Kelley: *USGS Prof. Paper No. 300*, pp. 171-178.
[15] C. L. Baker: University of Texas, *Bull.*, 1934, No. 3401, pp. 206-214.

Discussion of this article sent (2 copies) to AIME before Dec. 31, 1958, will be published in MINING ENGINEERING.

U. S. GOVERNMENT SUPPORT TO MINERAL INDUSTRIES OF LATIN AMERICA

by SUMNER M. ANDERSON

Any discussion of outside support to Latin American mineral industries must concede at once the pre-eminent role of U. S. industry and business. American capital has developed the great copper resources of Chile and Peru, the lead-zinc of Peru and Mexico, the bauxite of Surinam and Jamaica, the petroleum and iron ore of Venezuela. American consumers have provided the market for their products. U. S. companies operating south of the border have trained Latin American geologists, engineers, chemists, and skilled labor—including metal, mineral, and fuel technicians—to new and greater competence.

The industrial demands of World War II drastically altered world economics and concepts of U. S. foreign mineral requirements. In this country discovery of vital mineral resources fell far behind the alarming depletion rates, and there was new appreciation of the actual and potential importance of the world's less extensively explored areas. During the war and afterward, the task of supplying the nation's mineral requirements became greater than private industry could carry alone, and the Government assumed a position of continuing support.

In Latin America, as elsewhere, this support applies in three categories: banking, procurement, and technical assistance. The first two are now generally accepted as necessary Government functions; the third has often been misunderstood and misinterpreted, although it has given rise to legitimate controversy. There have been major accomplishments in all three categories, as well as some errors of judgment.

Since the beginning of World War II, U. S. Government financing, procurement, and technical assistance have been applied on a large scale to a wide range of commodities and services throughout the free world. The present discussion—under the separate headings mentioned—will concern only the support related to a single industrial group in a single geographic area.

S. M. ANDERSON, Member AIME, is Chief Latin American Specialist, Division of Foreign Activities, U. S. Bureau of Mines, Washington, D. C. TP 4730A. Manuscript, May 16, 1957. New Orleans Meeting, February 1957. Updated by author to June 30, 1958.

FINANCING FOREIGN MINERAL PROJECTS

During the War Federal banking was conducted on an emergency scale by temporary agencies created to meet the abnormal circumstances. Unfortunately, there are no readily available data on these activities that would permit evaluating loans and credits extended for mineral projects in Latin America. The only agency operating in this field since World War II is the Export-Import Bank, under its own authority and to some extent from credits authorized by the Office of Defense Mobilization. The Bank can offer more capital—on more favorable terms—than is available from most Latin American banks, and its staff of engineers evidently can appraise loan applications more favorably than commercial banks in this country are willing to do. The risks seem to be justified, as defaults have been well under 1 pct of total loans.

From V-J day 1945 to the end of 1957, mineral loans to Latin America have been authorized for projects totaling $541.63 million in eight countries. In order of magnitude of credits, they have been made to Brazil, Peru, Chile, Mexico, Argentina, Venezuela, Guatemala, and Bolivia. In order of magnitude by industries, they are for development and expansion of steel mills, copper, manganese, nitrate plants, iron ore, zinc plants, sulfur plants, cement plants, tungsten, coal, and lead.

Loan Distribution: By far the largest loans have been $307.9 million for iron and steel projects in Brazil, Chile, Mexico, Argentina, and Peru; $100.4 for developing the great low-grade copper deposits of southern Peru; and $55.3 million for developing manganese deposits in the Territory of Amapa, Brazil. Others range from $20.8 million for a zinc smelter in central Peru to $19 thousand for iron-mine trucking equipment in Chile. It has been noted that 59 pct of the loans have been to foreign companies, 14 pct to companies of mixed foreign and American capital, and 27 pct to American mining companies. About 40 pct of the total authorizations has been disbursed so far.

In addition to these amounts, the Strategic Materials Division of the Economic Cooperation Admin-

"All aspects of this aid are based on the belief that U. S. freedom, military and industrial strength, and prosperity cannot be preserved in isolation from the rest of the world and that the nation's continued progress and security are inseparably integrated with the economic growth of the Western Hemisphere."

istration agreed in 1950 to advance up to $5.963 million in Marshall Plan funds and 1.8 million from ECA counterpart funds in Britain to develop extensive bauxite resources in Jamaica, with repayment over a period of 20 years in aluminum ingot for the National Strategic Stockpile. French and Netherlands possessions in the Latin American area were also eligible to receive loans from this source.

World Bank and Subsidiary: The Export-Import Bank performs only the functions of a bank. However, the International Bank for Reconstruction and Development—a U. N. institution better known as the World Bank—has recently established an organization that can not only lend money but can also participate in management on a shareholder or partnership basis. This new subsidiary, called the International Finance Corp., has been capitalized with approximately $100 million by more than 30 member nations of the World Bank. Private industrial projects will be considered for either IFC financing or participating loans from private investors in member nations, or both, with expectation of increasing the international flow of capital. Financing in the mineral field will be confined initially to projects in metal and mineral processing but eventually may be extended to mining. As a participating member, the U. S. Government has contributed $35,168,000, or 35 pct of the organization's capital.

Investment Insurance: The International Cooperation Administration has made some foreign loans, but none to American mineral projects. However, to encourage new American investment abroad that will promote the purposes of the Mutual Security Act the ICA, acting through the Export-Import Bank, has offered two types of investment insurance since Oct. 15, 1954, each at a cost to the insured of 0.5 pct per year of the face amount of the contract. One type insures the investor against inability to convert into dollars the capital invested in a foreign country and the earnings derived from this capital. The other insures the investor for a specified maximum amount against expropriation or confiscation of property.

As of mid-1958, a single guarantee of $3 million against expropriation had been written on new mineral investments in Bolivia,* but several million dollars' worth of applications from Latin America were pending. At present both types of insurance are available for investments in Bolivia, Costa Rica, Cuba, Equador, Guatemala, Haiti, Honduras, Paraguay, the British West Indies and British Guiana, the French West Indies and French Guiana, and the Netherlands Antilles and Surinam; convertibility insurance only is available in Colombia and Peru. Those interested in applying for investment insurance may obtain further details by writing the Investment Guaranties Branch, International Cooperation Administration, Washington 25, D. C.

PROCUREMENT

Federal procurement is a business conducted to provide materials and equipment essential to normal Government operations and—on a larger scale—the defense and security of this country and the free world. The function of security includes purchase of reserve stocks of strategic minerals and other raw materials. Procurement is not designed or ordinarily administered to benefit the foreign supplier of material; nevertheless, the seller, his community, and the country where he operates prosper and are strengthened in accordance with the economic laws of business in a capitalistic system. Thus procurement of minerals from foreign sources is not aid in the usual sense of the word, but the type of support that any business supplier receives from his customers. Latin America is the largest foreign provider of essential minerals to the U. S. and consequently the chief recipient of mineral-bought dollars and their equivalent in American goods. Of course the suppliers individually determine the extent to which their profits are used for further mineral development.

Before World War II authority for Federal purchasing was vested in the Treasury Department's Procurement Division. But the start of World War II began an unprecedented demand for arming the nation and its allies, and from 1940 to the present,

* A gold-dredging operation of South American Placers Inc., wholly-owned subsidiary of South American Gold & Platinum Co.

purchasing authority has been disbursed and reconsolidated through a succession of special-purpose agencies. Certain types of purchases today are controlled by the AEC, but the bulk of metal and mineral purchasing for the minimum and long-term objectives of the military stockpile and for the supplemental stockpile is the delegated responsibilty of the Defense Materials Service of the General Services Administration. However, some of these supplies are augmented through procurement services of other agencies, such as the International Cooperation Administration, which buys with counterpart funds, and the Commodity Credit Corp., which barters with surplus agricultural products.

It is difficult to ascertain how much the Federal Government has spent, during or since World War II, for ores, concentrates, metals, and minerals from Latin America—to say nothing of crude petroleum and petroleum products, which are not stockpile items. Probably these purchases are in the low billions of dollars.

In a few items purchase contracts alone have not been enough to insure adequate flow of supply. For this reason the Defense Plant Corp., a warborn subsidiary of the Reconstruction Finance Corp., was created to put the U. S. Government in the production business. Initial authorizations in 1942 to invest $4 million for vanadium-production facilities in Peru and $5 million for copper-production facilities in Chile involved the Government in management control during the war period only, but two other ventures have lasted much longer—the Longhorn tin smelter and the Nicaro nickel project.

Tin Smelter Project: Construction of the Longhorn tin smelter at Texas City was begun in October 1941 by Ford, Bacon & Davis, in accordance with plans designed by the Tin Processing Corp., subsidiary of the Billiton Co. Production started in April 1942 and continued under Government contract through 1956. Initial cost of building the smelter was about $6.3 million, but investment in property, plant, and equipment had reached $13.059 million by mid-1956, when the net value, after deduction for depreciation, was listed at $5.445 million. The plant was sold Jan. 3, 1957, by the Federal Facilities Corp. of the Treasury Department* to the Wah Chang Corp. for $1.35 million, plus $2 million contingent on certain defined results of operation.

Billiton Co. believes the smelter cannot compete successfully with tin smelters operating elsewhere in the world, partly because of higher labor costs. The accounting procedures used by the Government report an average operating loss of $721,000 a year for the six-year period since 1950, but a responsible official of the Federal Facilities Corp. has stated that the entire Government tin program, which involved marketing transactions in addition to smelter operation, was conducted without financial loss to the Government. In any event, the purpose of insuring a continuous flow of tin to this country during the war and until the stockpile objectives were reached was realized. During its 15 years of operation the smelter produced 447,312 long tons of refined tin from about 970,000 tons of concentrate—practically all the tin concentrate imported into the U. S. Smelter receipts from Bolivia amounted to about 741,000 long tons of concentrate containing 273,400 tons or 36.9 pct Sn. This concentrate had to be blended with 71.9 pct concentrates from other sources—chiefly Indonesia, Thailand, and the Belgian Congo—to make high-quality tin.

The effect on Bolivia's economy was perhaps an exception to the rule of beneficial support. Although the purchase program substantially subsidized Bolivian small and medium-scale producers of substandard concentrates and prolonged their industrial existence, it is doubtful that any general improvement in the country's economic condition has resulted since the revolution of April 1952.

Nicaro Nickel Project: The other Defense Plant Corp. venture that survived the war is the Nicaro nickel plant on Levisa Bay, Oriente Province, Cuba. In rounded figures capital investment, starting in 1942 with $19.3 million, reached $31.7 million by 1949, when it was taken over by the GSA. Under that agency $56.6 million has been added, and by June 30, 1958, investment totaled $88.3 million, before amortization and depletion amounting to $17.8 million. The plant was operated between December 1943 and March 1947 on a fee basis by Nicaro Nickel Co., subsidiary of Freeport Sulphur, with funds supplied by the Reconstruction Finance Corp. Freeport Sulphur Co. owns or controls much of the deposits supplying the ore.

The plant was idle from April 1, 1947, to Jan. 30, 1952, and was transferred first to the War Assets Administration and later to the GSA, after that organization had been established by law in mid-1949 as a permanent management agency of Government property and records.

When the Korean War again created a nickel shortage, resumption of Nicaro's operations became a factor of national security. The plant was rehabilitated on contract by the Frederick Share Corp., which had constructed it, and since Jan. 31, 1952, it has been operated on a fee basis by the Nickel Processing Corp., of which National Lead Co. owns 60 pct and Fomento de Minerales Cubanos S. A., 40 pct. As of June 30, 1958, nine years and ten months of total operation have produced approximately 134,000 short tons of nickel, plus cobalt in 168,000 tons of oxide derived from some 109 million dry short tons of ore containing 1.38 pct Ni.

The plant is reported to have operated without Government subsidy or loss to the taxpayers since 1952. Established at a time when private enterprise could not be induced to venture capital in this commercially untested process, it has added substantially to the National Stockpile and has brought an important, growing industry to Cuba. Now that the plant has proved successful the Government, following its usual policy, hopes to sell or lease it to private industry.

TECHNICAL ASSISTANCE

Technical assistance in minerals for Latin American programs consists largely of teaching, training, and exchange and development of information. It provides only the supplies and equipment necessary for effective education. Usually technical assistance programs do not supply capital for economic development, but attempt to create or improve conditions and local skills that will encourage private investment.

The field of mineral resources is only one area in which technical assistance is offered—there are programs for agriculture, industry, transportation,

* To which control had passed when the Reconstruction Finance Corp. was liquidated in 1954.

Table I. Export-Import Bank Loans* Authorized (Less Cancellations and Expirations) to Metal and Mineral Development Projects in Latin America, Sept. 2, 1945 to Dec. 31, 1957

Metals and Minerals	Thousands of Dollars								
	Total, Latin America	Argentina	Bolivia	Brazil	Chile	Guatemala	Mexico	Peru	Venezuela
Ferrous Metals									
Iron ore	26,043	—	—	12,274	2,769	—	—	11,000	—
Iron and steel mills	281,858	60,000	—	68,279	77,550	—	76,029	—	—
Manganese**	57,885	—	—	55,341	1,150	—	745	649	—
Tungsten ore	3,363	3,000	363	—	—	—	—	—	—
Total	369,149								
Nonferrous Metals									
Copper***	101,239	—	—	—	800	—	—	100,439	—
Lead ore	500	—	—	—	—	500	—	—	—
Zinc plants	21,138	—	—	—	—	—	338	20,800	—
Total	122,877								
Nonmetallic minerals									
Cement plants	6,358	—	—	3,056	—	—	290	—	3,012
Nitrate plants	29,090	—	—	—	27,851	1,239	—	—	—
Sulfur plants	11,414	2,000	—	—	—	—	9,414	—	—
Total	46,862								
Fuels									
Coal	2,740	—	—	—	—	—	2,740	—	—
Total Metals and Minerals	541,628	65,000	363	138,950	110,120	1,739	89,556	132,888	3,012

Source: Compiled by Federal Bureau of Mines from Export-Import Bank of Washington semi-annual reports to Congress.
* Including credits from DPA funds ($16,634 thousand) and guarantees of loans from commercial banks ($691 thousand).
** To Brazil and Mexico for manganese ore development; to Chile for ferromanganese plant.
*** To Chile for copper wire plant; to Peru for copper ore mining.

health, education, labor, public administration, and community development. At present about 25 pct of all technical assistance funds is allocated to Latin America; 75 pct is divided among countries of the Near and Far East, Europe, and Africa. The U. S. spends about $1.5 million a year for Latin American mineral projects, or 4 pct of the Latin American technical cooperation expenditures.

All mineral projects are conducted by specialists of the sponsoring agency, working jointly with counterpart personnel of the host countries, along three general lines of procedure: 1) the specialist, by instruction and demonstration, directs the approach to problems presented by his hosts; 2) the specialist and his co-partners join in completing a project; 3) qualified candidates of the host countries are selected for specific periods of advanced training in the U. S.

Before, during, and for a short time after World War II technical assistance in various forms for Latin American mineral projects was sponsored or provided by the State Department's Interdepartmental Committee on Scientific and Cultural Relations and Institute of Inter-American Affairs and by subsidiary agencies of the Office of Emergency Management and the Reconstruction Finance Corp. For the past several years technical assistance has been the direct responsibility of both the UN and the AEC, and principally of the State Department's International Cooperation Administration and predecessor agencies.

Since 1950 the UN has administered a worldwide technical assistance program to which the U. S. contributes about $15 million a year, or 54 pct of the cost. It is estimated that not more than $100,000 of this goes to mineral projects in Latin America. The UN recruits staff and field specialists from all member countries, including those behind the Iron Curtain, and has occasionally borrowed from the U. S. Department of the Interior. It grants fellowships for professional training in any country that can supply the type of training desired.

Since 1951 the AEC has conducted projects varying from a month to several years' duration in Bolivia, Brazil, Colombia, Peru, and Venezuela. These projects include brief preliminary investigations of known and potential uranium areas; supply of technical reports on uranium geology, exploration, and ore recovery; and training of foreign scientists in those subjects in their own countries and the U. S. The AEC assigns specialists from its own staff and from the USGS to countries with which it makes independent agreements.

On June 5, 1950, President Truman signed the Act for International Development, making active foreign policy of the famous Point IV of his 1949 inaugural address, in which he stated: "The material resources which we can afford to use for the assistance of other people are limited. But our imponderable resources in technical knowledge are constantly growing and are inexhaustible. . . . Greater production is the key to peace. And the key to greater production is a wider and more vigorous application of modern scientific and technical knowledge."

Technical Assistance Program: On September 8, 1950, by Executive order, the Point IV Program became the primary responsibility of the Department of State, which brought together all fields of technical assistance, including the minerals field but excluding uranium, under the Technical Cooperation Administration newly created for that purpose. However, the U. S. Department of the Interior retained a share of technical control of the mineral program specialists assigned by its agencies. In 1953 the Technical Cooperation Administration was merged with other related agencies to become eventually the present International Cooperation Administration; the Point IV Program came to be known alternatively as the Technical Assistance Program, but the nonpartisan principles of the program were endorsed by President Eisenhower and continued without fundamental change. The International Cooperation Administration contracts for the services of American consultants and consulting firms and recruits specialists from private industry when this is practicable, but it more regularly retains, on special assignment, personnel supplied and technically administered by the U. S. Department of the Interior. During the fiscal year 1958 ICA expenditures for mineral projects in Latin America amounted to $591 thousand, distributed, in

Table II. Latin American Specialists Trained by U. S. Department of the Interior in Geology, Chemistry, Engineering, and Metallurgy, 1946 to June 30, 1958

From	By USGS	By USBM	Total
Middle America			
Cuba	1	3	4
Haiti	1	—	n 1
Mexico	29	13	42
Costa Rica	1	—	1
Total, Middle America	32	16	48
South America			
Argentina	4	—	4
Bolivia	3	—	3
Brazil	21	15	36
Chile	9	—	9
Colombia	5	4	9
Ecuador	1	—	1
Paraguay	1	—	1
Peru	6	9	15
Uruguay	—	1	1
Venezuela	2	—	2
Total, South America	52	29	81
Total Latin America	84	45	129

order of magnitude, to Brazil, Chile, Peru, Mexico, Cuba, Colombia, and British Guiana.

Semi-independently and under most of the shifting sponsorships and administrative ties summarized here, the U. S. Department of the Interior has been involved in technical cooperation with 14 Latin American countries, in addition to other foreign areas, continuously since 1940 through its Geological Survey, and since 1942 through both its Geological Survey and Bureau of Mines. The two agencies operate similarly in regard to their trainee programs, carefully screening candidates for advanced training in the U. S. These candidates must have had fundamental academic education in geology, chemistry, engineering, or metallurgy to qualify for specialized advanced study, usually of one year's duration, at Government laboratories and field stations throughout the U. S., and in some instances at American universities. More mature and fully trained professionals occupying positions of importance, such as the heads of foreign Government mineral agencies, receive "leader grants" of one to three months, visiting Government research stations and industrial operations in the U. S. to observe the latest techniques and practices of possible application to problems in their own countries.

Since 1946, when the trainee program started, the USGS and USBM have returned to responsible mineral positions in Latin America 129 trainees and leaders from 14 countries. This does not include the many foreign engineers, geologists, metallurgists, and chemists who are trained on the job with American field parties in their home countries.

Twelve years is a short period by which to evaluate a training program. Accomplishments have not been spectacular, but they have been steady and in some areas are showing signs of compounding with time. Definite progress has been made against the old Spanish tradition that physical work is degrading to a professional man.

Many Latin American countries are seriously short of candidates with the basic technical education to qualify for advanced training and equally short of technical schools offering adequate courses in mining engineering and earth sciences. The technical assistance cooperative program is being adjusted to improve this situation where possible. One of the most frustrating obstacles is that Government service offers small economic incentive in the upper brackets and none in the lower brackets, so that working hours must permit employes to make a living in private part-time employment. The situation will have to be corrected from within the countries themselves; Mexico and Venezuela are among those showing progress in this direction.

Role of U. S. Geological Survey: In field programs abroad the USGS and USBM pursue the same training objectives but operate independently of each other and by somewhat different methods. The USGS, in close cooperation with its counterpart agency in the host country, undertakes long-term mapping and reconnaissance projects or detailed geological study of specific areas and the simultaneous bilingual publication of results as official documents. Since 1942, 56 such studies have been published, documenting work in 15 countries. Fifty-one of these cover economic mineral resources of thirteen metals and seven industrial minerals, including ground water, and five are academic studies of volcanism and stratigraphy. All contribute to the knowledge of mineral resources and geological processes, to the competence of those engaged in their preparation, and to the effectiveness of national geological agencies. Some may have influenced the decision of investors in developing resources. The largest single project, still in progress, is the determination of iron ore reserves in the State of Minas Gerais, Brazil, which will assume world importance if and when transportation outlets to the coast are established. M. A. Hanna Co. is studying this problem in relation to the extensive holdings of the St. John del Rey Mining Co.

The USGS now has technical representation in Mexico, Brazil, Chile, and Peru. Past projects have also been conducted in British Guiana and in all the Latin American republics except Uruguay.

Role of U. S. Bureau of Mines: USBM specialists work in an advisory and instructional capacity with and through their counterpart agencies—which may be equivalent technical agencies, government-controlled operating organizations, or development banks—with less emphasis on full-time participation in integrated projects than on special phases of established operations. Results of such projects as the coal studies of southern Brazil have been reported in USBM publications, but most of these accomplishments do not lend themselves to constructive publication.

Metallurgists advise on establishment and operational improvement of Government metallurgical laboratories that serve the domestic mining industry. They also extend direct aid to small and medium-sized mineral operators on appropriate techniques of ore treatment, which often make the difference between marginal and profitable operations. Large-scale operators are entitled to this service but usually rely on their own technical staffs. Examples are too numerous and varied to list here, but one that is outstanding is the establishment in 1950 of Brazil's first profitable lead-refining industry by reducing from 8 days to 5 hr the process time for eliminating antimony.

Government development banks stimulate domestic mining ventures by making capital loans, and USBM mining engineers help the banks to evaluate investment risks and guide the applicants on efficient organization and operating procedure. These services are not restricted to loan applicants but apply also to projects endorsed by the counterpart agency to which the specialists are attached. In Colombia, USBM engineers are helping to expand

the national coal industry, and in Mexico they have inaugurated a badly needed health and safety program. The engineer assigned to Peru has successfully promoted the establishment of a department of metallurgy at the Universidad Nacional de Ingenieria in Lima, under joint sponsorship of the University, the governments of Peru and the U. S., and mining companies operating in Peru.

At present the USBM has representatives in Brazil, Colombia, Cuba, Mexico, and Peru. A project in Bolivia was terminated in 1951.

U. S. Department of the Interior expenditures for technical assistance before 1946 were nominal. From 1946 through 1950 they averaged $70,000 a year and from 1951 through 1958 about $200,000 a year, almost entirely from funds supplied by other agencies. Every representative sent on a foreign assignment, whether by the Geological Survey or the Bureau of Mines, is fully supported by the specialized facilities of his agency at home.

Occasionally the Bureau of Mines provides technical services by direct contract to foreign governments, which pay the total cost. The largest of these projects has been the successful development of an oil-shale treatment process in cooperation with the Brazilian Oil Shale Commission, which expanded its pilot plant at Taubate to semi-commercial operation, turned over in 1957 to Petroleo Brasileiro, S. A. (Petrobras).

CRITICISMS OF FOREIGN AID PROGRAM

The foreign aid program, of which technical assistance is only a part, rests on the fact that this country and other free nations are mutually dependent for their welfare and long-term security. Yet the most persistent criticism of foreign aid is the accusation that the program is a giveaway. The Bureau of Mines and the Geological Survey have not conducted their missions gratuitously. Latin America is contributing to joint technical assistance projects of all types at a ratio of $2.70 for every $1.00 from the U. S.

One unique diagnosis is noteworthy only because it was postulated by someone who was then executive secretary of the UN Economic Commission for Europe. In a speech delivered in December 1956 at the New School for Social Research, the Swedish economist, Gunnar Myrdal, said that foreign aid is extended to atone for practicing the selfish principles of ordinary business. He believes the U. N. should control expenditure of all U. S. foreign aid funds.

Latin American government leaders praise the quality of U. S. aid to countries in this hemisphere but commonly complain that expenditures have been a trickle compared with the total billions distributed since World War II. This must be conceded, but it ignores two highly pertinent facts: By far the greatest proportion of aid to Europe and Asia has been directed toward recovery from war devastation and building military defenses against the Soviet threat, while virtually all the aid to Latin America, which has been spared the necessity for that type of help, has been in the form of technical assistance and economic programs.

Segments of the American mining industry have suggested that their Federal Government is fostering the competition of foreign industries with American interests abroad, despite the traditional doctrine that private enterprise thrives under competition. Actually, in the field of small to medium operations, technical assistance has been concentrated on developing resources that American capital has ignored as being too small or of no investment interest for other reasons.

One example may be cited of the effect of Government support in the field of large operations. Regular mining of the Serra do Navio manganese ores, Territory of Amapa, Brazil, was formally inaugurated Jan. 5, 1957, at an annual shipping rate of 600,000 tons and capacity of 1 million tons. All three elements of U. S. Government support have contributed in developing this operation. Technical assistance collaborated in early examination and evaluation of the discovery; the Export-Import Bank lent $55.3 million in development capital; and the GSA secured the loan with a Government procurement agreement. The list of beneficiaries is long. The U. S. Government will profit by interest on the loan and assurance of a steady supply of ore for the stockpile. U. S. security will be strengthened by the easing of dependence on Eastern Hemisphere sources for manganese. Three companies will profit directly—the Brazilian Industria e Comerico de Minerios S. A.; Bethlehem Steel Co., co-owner and operator with the Brazilian company; and Foley Bros., the contractor for plant, railroad, and docking installations. The city of Macapa on the Amazon will become an important international port, and thousands of inhabitants of the Territory will enjoy a higher standard of living. At the port inauguration the manganese project was lauded by a Brazilian official as "an example of what may be done by national private initiative when aided by the Brazilian Government in collaboration with foreign financial and technical aid."

FUNDAMENTAL CONCEPTS

Banking and procurement are immediate economic assets to the U. S., and the annual interest on outstanding loans of the Export-Import Bank to Latin American mineral projects is far greater than the cost to the American taxpayer of Federal expenditures for technical assistance in the same area.

All aspects of this aid are based on the belief that U. S. freedom, military and industrial strength, and prosperity cannot be preserved in isolation from the rest of the world and that the nation's continued progress and security are inseparably integrated with the economic growth of the Western Hemisphere.

In promoting this growth, we are meeting sincere cooperation from professional and industrial people of the member nations. The same is not always true of their governments, many of which maintain barriers to capital investment in highly restrictive legislation, taxation, exchange controls, and the historically demonstrated threat of expropriation. But the outlook is hopeful. Progressive reforms have been adopted in several countries, and the tangible results in mineral industrial growth can not be ignored indefinitely by their neighbors. Acceptance of the continued role of Latin America solely as a source of raw materials for American conversion to finished goods is regarded as a serious underestimate of the future. Latin America has already started an industrial revolution that may well match, in the next fifty years, the growth pattern of this country during the past fifty. We contribute to that growth that we may continue to share its rewards.

Discussion of this article sent (2 copies) to AIME before Dec. 31, 1958, will be published in MINING ENGINEERING.

SCALE-UP RELATIONSHIPS IN SPODUMENE FLOTATION

Flotation feed was held constant for batch laboratory tests and continuous pilot and commercial plant tests on a spodumene ore to determine the relationship between flotation behavior and the size and type of flotation machine. Results showed that additional retention time would be needed in the plant flotation circuit to duplicate laboratory or pilot plant performance when operating variables of the plant flotation machines remained unchanged.

by W. E. HORST

During the past few years of operation at Kings Mountain, N. C., full-scale flotation has generally yielded poorer metallurgical results than those obtained in the laboratory or pilot plant. After 2 min in each size of Denver flotation machine in the spodumene rougher circuit, pilot recovery (41.7 pct) was almost three times that of the plant (13.6 pct) and about twice that of the laboratory (21.0 pct). Pilot and commercial plant data are based on continuous operation, and laboratory results on batch testing of rougher performance. The ore is a pegmatite containing spodumene, feldspar, quartz, mica, and amphibolite.

Data were accumulated to evaluate the scale-up relationships between laboratory, pilot plant, and plant flotation cells. Flotation rate constants and dimensional analysis were used to define the relationship existing between flotation behavior and scale of operation.

Measuring Flotation Rates: Efficiency of the rougher stage was measured by flotation rate, defined as the recovery that can be attained within a given time.*

* The problem of measuring flotation rates has been studied by many investigators, whose methods have varied. Published studies on flotation kinetics have been summarized recently by Gaudin.[1]

When comparing flotation rates, it is more satisfactory to compare straight line relationships between recovery and flotation time than exponential curves resulting from plotting cumulative recovery vs cumulative flotation time. To convert the exponential curves into straight line relationships, rate equations were applied similar to those used in chemical kinetics to study the velocity of chemical reactions.

Two rate equations have been used in this investigation to measure efficiency of the various cells:

1.5 Order Rate Equation

$$\frac{dR}{dt} = k(A-R)^{1.5} \qquad \text{[Eq. 1]}$$

Second Order Rate Equation

$$\frac{dR}{dt} = K(A-R)^{2} \qquad \text{[Eq. 2]}$$

Upon integration Eq. 1 becomes:

$$\frac{1}{(A-R)^{1/2}} = \frac{k}{2}t + \frac{1}{A^{1/2}} \qquad \text{[Eq. 3]}$$

and Eq 2 becomes:

$$\frac{1}{A-R} = Kt + \frac{1}{A}$$

or

$$\frac{t}{R} = \frac{1}{A^2K} + \frac{t}{A} \qquad \text{[Eq. 4]}$$

where R = cumulative recovery [percent recovery of total value (spodumene) in flotation feed].
A = initial concentration, pct (100 pct of mineral to be separated).
t = flotation time (minutes).
k = flotation rate constant for 1.5 order rate equation [units: 1/(percent) 0.5 (min)].
K = flotation rate constant for second order rate equation [units: 1/(percent) (min)].

W. E. HORST, Junior Member AIME, is Metallurgical Engineer for Foote Mineral Co., Research and Development Dept., Berwyn, Pa. TP 4779B. Manuscript, Nov. 7, 1957. Southeastern States Mining Conference, Tampa, Fla., October 1957.

Application of Dimensional Analysis: Use of dimensional analysis for a particular application is based on the assumption that certain variables are independent, and all others dependent or irrelevent. In the flotation process the following variables were assumed to be independent—flotation rate, length (measurement of flotation machine), impeller speed, horsepower, and pulp density. Other variables were assumed to be dependent or irrelevant. For example, capacity is dependent on flotation rate and aeration on impeller speed and horsepower.

The five independent variables can be expressed by a dimensionally homogeneous equation as follows:

$$f\,(K, L, N, H.P., \rho) = 0 \text{ where}$$

K = flotation rate constant (second order rate equation).
L = length, measurement of flotation machine.
N = impeller speed.
$H.P.$ = horsepower.
ρ = pulp density.

In accordance with Buckingham's theorem, the above equation can be reduced to the form:

$$f\left(\frac{K\rho L^3}{N}, \frac{\rho N^2 L^5}{H.P.}\right) = 0 \qquad \text{[Eq. 5]}$$

or

$$\frac{K\rho L^3}{N} = f\left(\frac{\rho N^2 L^5}{H.P.}\right) \qquad \text{[Eq. 6]}$$

The dimensionless groups described by Eq. 6 were used in this investigation to correlate flotation scale-up and flotation behavior.

Operating Data: The spodumene rougher circuit products from continuous plant and pilot plant operations and batch laboratory tests were sampled to determine the flotation rate for each scale of operation. During the sampling periods, surface treatment and chemical conditions (reagent consumption and pH) were held constant, as they were the same for each scale of operation. The same was true for particle size of flotation feed. For all practical purposes the only variables in each operation were cell design and capacity.

Relationship Between Laboratory, Pilot Plant, and Plant Flotation Performance as Described by Second Order Rate Equation: The *integrated* form of the second order rate equation was used to correlate the flotation rates between the continuous operation of plant and pilot plant cells and batch operation of laboratory cell. This equation was selected because it best fitted the data from the three sizes of cells. Fig. 1 plots flotation time/recovery vs flotation time for each type of cell; corresponding flotation rate constants are tabulated below:

Flotation Cell Size	Flotation Rate Constant, K
Plant	0.09
Pilot plant	0.83
Laboratory	0.50

On the basis of these rates, ratios were calculated for the various flotation cells. Under the operating conditions during testing, for example, 9.2 times as much flotation time would be required in the plant cells to achieve a recovery equal to that obtained in the pilot plant:

Scale of Operation	Flotation Rate Ratio
Pilot plant:plant	9.2:1
Laboratory:plant	5.6:1
Laboratory:pilot plant	0.6:1

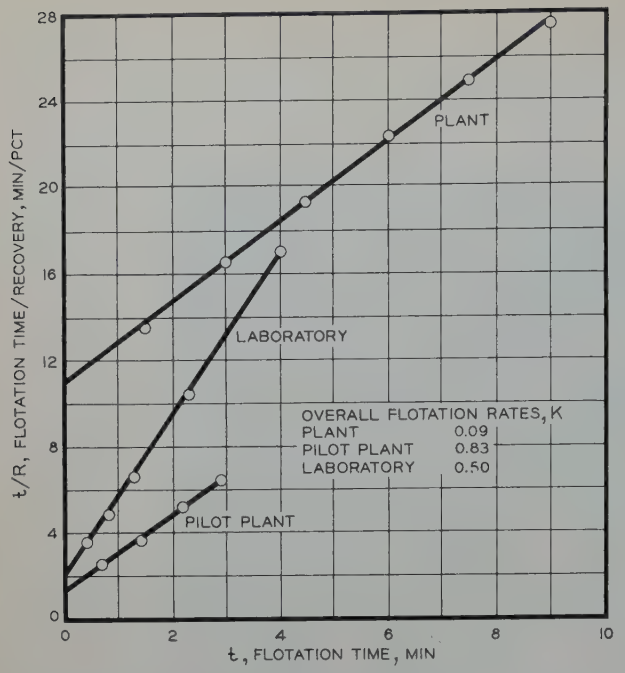

Fig. 1—Flotation time vs flotation time/recovery.

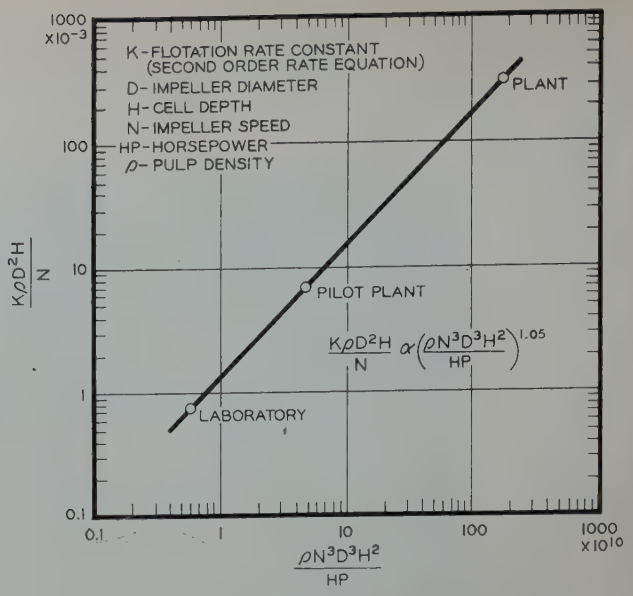

Fig. 2— $\frac{K\rho D^2H}{N}$ *vs* $\frac{\rho N^3D^3H_2}{H.P.}$

Reasons for the varying rates between flotation machine sizes may be numerous and complex. However, on the basis of operating data and flotation rates, a relationship was developed as shown in Fig. 2 which correlates operating variables with flotation rates. Using dimensionless groups the relationship $(K\rho D^2H/N) \propto (\rho N^3D^3H^2/H.P.)^{1.05}$ was found to exist. Although three sets of operating data (scales of operation) are admittedly insufficient to determine an equation involving the two dimensionless groups cited above, the data as shown in Fig. 2 suggest that such a method would make it possible to use laboratory, pilot plant, or plant data to predict results (for one or each scale of operation) for various operating conditions. Undoubtedly other dimensionless groups could be employed to describe existing scale-up relationships for other flotation processes; however, in this application (spodumene flotation) the above relationship satisfied existing conditions based on available data.

Dimensional analysis is an additional tool for predicting plant-scale flotation performance on the basis of laboratory or pilot plant results.

Plant Flotation Circuit Behavior as Described by 1.5 Order Rate Equation: The 1.5 order rate equation was used for this phase of the investigation because it best fitted data for the plant rougher flotation circuit, as shown in Fig. 3, for the various size fractions of spodumene from —30 mesh through 325 mesh. Similarly the 1.5 order rate equation fitted the plant flotation results for the gangue minerals carried over in the rougher concentrate. Flotation rate constants for the various size fractions of spodumene and gangue minerals are recorded in Table II. Data for spodumene are plotted in accordance with the integrated form of the 1.5 order rate equation in Fig. 3.

Data plotted in Fig. 4 illustrate the spodumene content of the plant rougher circuit tailings vs particle size. It may be observed that actual and predicted tailing assays occurring when the rougher circuit retention time was doubled are in excellent agreement in the size range below 80 mesh (see Fig. 3). These size fractions comprise the major portion of the plant flotation tailings. The predicted tailing assays were calculated by using the flotation rate constants (Table II) and assuming a rougher retention time of $2y$. Such an increase in retention time could be achieved by doubling the number of rougher cells or by decreasing the pulp flow one half. The latter method was practiced to attain continuous plant performance data operating with a retention time of $2y$.

Generally in the flotation process it is desirable to collect the concentrate over a minimum period in order to achieve maximum grade. But data in Table III show that there was little difference (74.0 to 77.5 pct spodumene) in the rougher concentrate grade from cells No. 1 through No. 6 (continuous operations).

Flotation rates of the various size fractions of gangue minerals (Table II) were determined to predict the spodumene content of the rougher concentrate resulting from a retention time of $2y$. On the basis of calculated rougher concentrate grade (71.5 pct spodumene) with retention time $2y$, it appears that the counter effect of coarse and fine material would not remain in balance (that is, hold the grade constant) if the retention time were doubled $(2y)$. Therefore it would be expected that the rougher concentrate grade would decrease with increased flotation time. However, the finished concentrate was not down-graded when the rougher circuit retention time was doubled (from y to $2y$). On this basis it is evident that a change in flotation time can result in equal or increased concentrate grades with increased recovery even though the rougher circuit retention time is increased. The major source of gangue minerals in the rougher float may be mechanical entrapment and therefore independent of retention time. In any case increased retention time was not detrimental to grade.

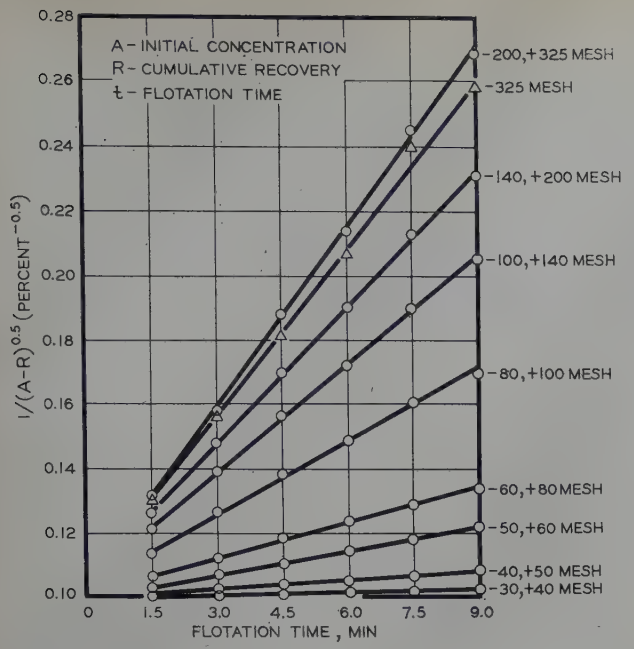

Fig. 3—The continuous plant results, t vs $1/(A-R)^{0.5}$, are plotted here for the various particle sizes.

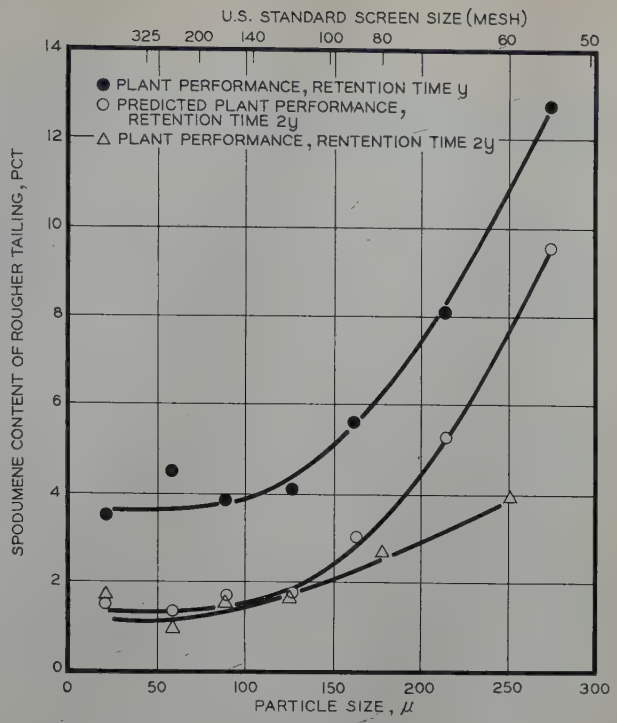
U.S. STANDARD SCREEN SIZE (MESH)
PLANT PERFORMANCE, RETENTION TIME y
PREDICTED PLANT PERFORMANCE, RETENTION TIME 2y
PLANT PERFORMANCE, RENTENTION TIME 2y
SPODUMENE CONTENT OF ROUGHER TAILING, PCT
PARTICLE SIZE, μ

Fig. 4—Above graph presents plant results for the spodumene content of rougher tailing vs particle size.

CONCLUSIONS

Flotation rates and dimensional analysis were used to develop the relationship $(K\rho D^2H/N) \propto (\rho N^3D^3H^2/H.P.)^{1.05}$, which correlates the operating variables with flotation rates as experienced in spodumene flotation. This relationship provides a means for using laboratory, pilot plant, or plant data to make an intelligent prediction of expected results for various operating conditions and flotation cell sizes. Although other dimensionless groups may be utilized to describe existing scale-up relationships for other flotation processes, this procedure presents an additional engineering tool for predicting plant-scale performance based on laboratory or pilot plant test results.

The spodumene content of the rougher tailings produced when the retention time was doubled substantiated predicted results in the size range from 80 mesh down based on calculations using flotation rate constants for the various size fractions. These size fractions comprise the major portion of the flotation tailings.

Although this investigation does not provide reasons for the differences in flotation rates or efficiencies between sizes of cells, it does demonstrate how flotation rate constants (as determined from rate equations) and dimensional analysis can be used as tools for measuring the relative magnitude of these differences.

The writer wishes to thank the Foote Mineral Co. for permission to publish this article, and D. B. Coghlan, assistant director of research, and N. A. Arbiter, consultant, for their interest and constructive criticism.

REFERENCES

[1] A. M. Gaudin: *Flotation*, pp. 384-387, McGraw-Hill Book Co., New York, 1957.
[2] W. E. Horst and T. M. Morris: Can Flotation Rates be Improved? *Engineering and Mining Journal*, 1956, vol. 157, no. 10, pp. 81-83.
[3] R. L. Kidd and W. L. Wall: Effect of Particle Size on Flotation of Sphalerite. *Mining and Metallurgy*, 1933, vol. 14, pp. 421-422.
[4] H. L. Langhaar: Dimensional Analysis and Theory of Models. John Wiley & Sons Inc., New York, 1954.
[5] S. C. Sun: The Mechanism of Coarse Coal and Mineral Froth Flotation. *AIME Trans.*, 1950, vol. 187, pp. 616-622.

Discussion of this article sent (2 copies) to AIME before Dec. 31, 1958, will be published in MINING ENGINEERING.

Table I. Operating Variables

Flotation Machine	Plant	Pilot Plant	Laboratory
Denver cell no.	No. 24 Sub-A	No. 5 Sub-A	500 g
Cell depth	3.38 ft	0.917 ft	0.708 ft
Rated cell volume	50 cu ft	0.248 cu ft	0.106 cu ft
Power intensity	0.059 hp per cu ft	0.125 hp per cu ft	0.563 hp per cu ft
Impeller speed	265 rpm	1200 rpm	1900 rpm
Impeller diameter	1.83 ft	0.375 ft	0.229 ft
Pulp density	81.0 lb per cu ft	77.4 lb per cu ft	80.5 lb per cu ft

Table II. Flotation Rate vs Particle Size, Kings Mountain Plant Rougher Flotation Circuit

Screen Fraction	Average Particle Size, μ	Flotation Rate Constant $(k)\,1/(A-R)^{0.5}\,t$ Spodumene	Gangue Minerals
−30, +40	505	0.07×10^2	0.34×10^4
−40, +50	359	0.18×10^2	1.0×10^4
−50, +60	274	0.50×10^2	1.0×10^4
−60, +80	214	0.75×10^2	1.7×10^4
−80, +100	163	1.56×10^2	2.7×10^4
−100, +140	127	2.22×10^2	3.3×10^4
−140, +200	90	2.82×10^2	5.0×10^4
−200, +325	59	3.73×10^2	8.0×10^4
−325	22	3.20×10^2	11.7×10^4

Table III. Plant Rougher Circuit Concentrate Grade

Cell	Rougher Concentrate, Spodumene, Pct
1	76.1
2	74.2
3	75.6
4	76.6
5	74.0
6	77.5
Combined	75.5

RUBEANIC ACID FIELD TEST FOR COPPER IN SOILS AND SEDIMENTS

In normal soils there are usually 10 to 50 parts of copper in every million parts of soil. Only 0.2 to 5 pct of this copper can be found by any simple cold chemical attack. Now, with rubeanic acid reagent paper, a prospector or field geologist can detect as little as 4 ppm of readily available copper in soil. This degree of sensitivity is enough to determine the presence of copper anamalous areas and, eventually, to discover copper mineralization.

By HARRY V. WARREN and ROBERT E. DELAVAULT

Circumstances determine whether it is better to make analyses in the field or in a permanent laboratory. The rubeanic acid test described in this article has been designed primarily for field use: it is simple and virtually foolproof, and it requires a minimum of field kit.* It is sensitive, easily detecting 4 ppm of readily extractable copper in a soil. This is by no means a quantitative test, but it is accurate enough to provide a valuable indicator of copper anomalous areas for both prospectors and field geologists.

* **Ed. Note:** Persons interested in purchasing kits suitable for rubeanic acid prospecting can obtain information by writing Eldrico Geophysical Sales Ltd., 633 Hornby Street, Vancouver 1, B.C. The University of British Columbia does not produce these kits for sale and has no financial interest in their production.

The easiest method for detecting metal deposits that do not produce visible float or stains is to make a simple chemical test for the metal in overlying soil, or in the silt of a stream that may have picked up metal farther upstream.

In Brief: Testing for copper may be done easily by shaking a soil sample with strong acetic solution in a small test tube and pouring the mud into a small filter, the tip of which rests upon a strip of reagent paper impregnated with rubeanic acid (dithio-oxamide).

When copper is present—and only when it is—a blue spot develops. The more copper, the darker the spot. If the copper content is merely the small amount present everywhere, there is a pale blue or hardly visible spot; if it is abnormally high, the spot will be dark. There are, of course, intermediate cases where the experienced geochemist cannot tell offhand whether a medium-strength spot represents rich agricultural soil, weak copper mineralization, or distant rich copper mineralization. Reagents and material are inexpensive; the test may be readily done on the spot with a simple kit easy to pack and handle.

Anyone interested in general problems of soil sampling as applied to prospecting may refer to an article recently presented to the AIME.[1] In exploration work it is the contrast between the metal content of anomalous and background areas that is important; absolute values become of greater interest when an anomalous area is being investigated in detail. With specific reference to copper, it has been the authors' experience that the amounts of metal extracted from anomalous and normal soils with buffer solutions of decreasing pH show better contrast if an acid reagent is used. This contrast tends to increase with increasing acidity until 3 to 4 pH is reached. Using a short cold attack on unheated soil, it has been found that further increases in acidity do not produce better results, and only increase the hazards involved in carrying strong acids.

An acidity of about pH 4 is satisfactory for direct determination of copper by dithizone. But dithizone itself introduces some problems: it must be made up fresh at frequent intervals, and with some soils, notably those with much ferric iron, oxidation may take place before all the copper has reacted with the dithizone. Rubeanic acid keeps its strength unimpaired for long periods, is unaffected by oxidation, and is practically specific for copper at pH 4. Consequently it seems an ideal reagent to use in prospecting for copper.

History and Background: Rubeanic acid (systematic name: dithio-oxamide $(SC\text{-}NH_2)_2$) has long been known as a spot test reagent for some heavy metals with which it gives a number of compounds. Only copper and some metals of the platinum family are believed capable of providing any rubeanate compounds under conditions of moderate

H. V. WARREN, Member AIME, and R. E. DELAVAULT are, respectively, Professor and Research Associate, Department of Geology and Geography, University of British Columbia, Vancouver, Canada. TP 4783L. Manuscript, May 7, 1958. Northwest Regional Meeting, Spokane, 1958.

acidity (pH 4 to 5) and under the conditions of dilution to be expected in extractants derived from cold soils. Careful tests with as much as 50 micrograms of cobalt or nickel, or 500 micrograms of iron in 1 ml of solution, have produced no reaction on rubeanic reagent paper at a pH near 5. However, it should be noted that rubeanic acid reacts poorly with copper in the presence of large concentrations of ammonium ions.

The use of rubeanic acid for copper prospecting was first introduced in North America by Stevens and Lakin,[2] who advocated a soil extractant of 10 pct acetic acid. They suggested that the spot test be made under controlled and restricted conditions and used a chromograph,[2, 3] which passes a known volume of filtered solution through a strip of reagent paper at a controlled speed. By this technique the spots are reproducible and semi-quantitative determinations are possible.

The above technique is admirable, and, in the authors' opinion, deserves wider recognition. However, the technique is at its best when used in a laboratory. With the modest modifications hereafter described, rubeanic acid can become a potent and reliable tool in the field kit of every prospector.

REAGENTS AND PROCEDURE

Rubeanic Acid Paper: Dissolve 1 g of rubeanic acid (dithio-oxamide) in 100 ml of reagent-grade acetone. Place the resulting solution in a shallow glass or porcelain dish, and pass through it strips of filter paper ½ in. wide and 3 to 4 ft long. (Such strips are sold in rolls for chromatography.) Alternatively the strips can be stretched horizontally and drops of the reagent solution deposited about 1½ in. apart. The reagent is harmless, but it will stain fingers an unsightly black. This, however, may serve as a reminder that the utmost cleanliness is necessary throughout this operation. These strips will dry in a few minutes and, once dried, this rubeanic paper can be wrapped up and stored in any suitable container for months.

Extracting Solution: To make a quantity of solution, take 1 lb (500 g) of hydrated sodium acetate, and 1 qt (1 liter) of acetic acid respectively, and enough copper-free water to make up 1 gal. Both the acetate and acetic acid should be of reagent grade. Should the solution not give a satisfactory blank, when tested with rubeanic paper, the copper can readily be removed by shaking the solution with 50-ml portions of a solution of dithizone, 50 to 100 mg in 1 liter of carbon tetrachloride or chloroform. Rather than spend time removing copper from solutions, it may be easier merely to obtain another source of supply. Actually another batch of chemicals from the same supply house may be found to be copper-free.

Procedure: Place a piece of filter paper about 1 in. square on the bottom of a beaker. Take a strip of the reagent paper 1 to 1¼ in. long, write on one end the identifying assay number, and lay it on the filter paper. Fold a filter paper so that it fits into the beaker. With the pyrex beaker commonly used, 50 ml, the filter must be folded into a cone a little sharper than would be the case if it were being prepared for a funnel. The tip of this filter must be as sharp as possible, and it must just touch the reagent paper. Any twisting or crushing of the filter will cause any spot to be blurred. If polyethylene containers are used, small tabs may be cut in the polyethylene at suitable heights and these may be

EQUIPMENT

Beakers:
Pyrex 50-ml Griffin-shape beakers are good, as are the lower parts of polyethylene bottles that have been cut in two. (See below.)

Test Tubes:
Either glass or polyethylene may be used. The 12-mm size cut 60 mm long is satisfactory.

Test Tube Stoppers:
These may be either of cork or polyethylene and should be soaked in 50 pct acetic acid and carefully rinsed before initial use.

Measuring Spoon:
For the quarter-teaspoon sample required (equal to about 1 g of dry soil) a plastic or aluminum teaspoon or measuring spoon serves.

Glazed Onion Skin Paper:
Cut one 2-in. square piece for each assay.

Filters:
Flat circles, 9 cm, acid-washed, are best. Whitman No. 1 porosity is satisfactory. Some grades or brands, although excellent for ordinary gravimetric work, may be found to contain too much copper, as may be evidenced by unsatisfactory blank tests when the other reagents are known to be metal-free.

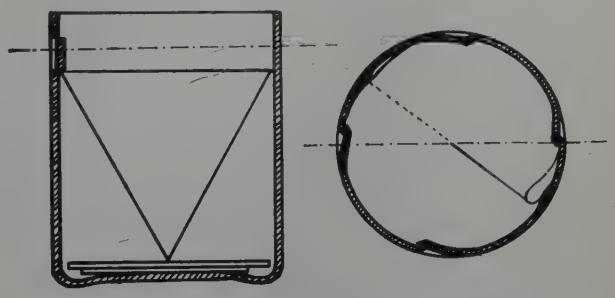

Fig. 1A—Cross sections of apparatus showing how the filter and papers are placed in the polyethylene beaker.

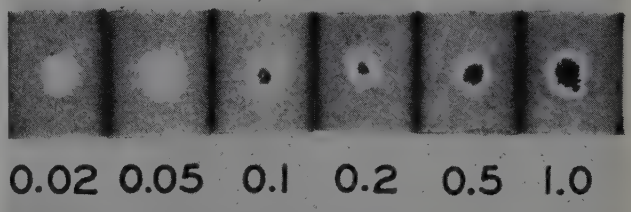

Fig. 1B—These spot tests on the right have been made with absolute amounts indicated in micrograms.

Fig. 1C—Top line, spot tests made recently with 1 g of soil. Approximately 5 pct of the soluble copper contents appears on spot.

Second line, spot tests made with the same soils nearly two years previously, under field conditions.

No. 1, 3, 5, 7, 8, 9, 11 samples taken in immediate vicinity of mineralization. No. 2, 4, 6, 10 samples taken at various short distances from mineralization. All of the above samples were taken from glacial drift that varied in depth from only a few inches up to 40 ft.

pushed in so that the filter paper will be held exactly in place, Fig. 1*a*.

Then on an onion skin paper square place a heaping measuring spoon of the soil to be tested. Using the spoon, sort out any roots or coarse material. Collect a spoonful of as fine and even-grained material as may be practical and transfer to a test tube, using the onion skin paper, the clean side of which may then be wrapped around the stopper. This prevents unnecessary contamination of the stopper if copper-rich samples are encountered.

Add 1 to 2 ml of extracting solution, depending on the dryness of the soil. Just enough extractant should be added to make a thick slurry of the sample, which can then be shaken and poured on to the bottom of the filter. The extractant may be added from a squeeze bottle or a measuring scoop built into the stopper of a pyrex bottle if this is used for carrying the solution. After a short apprenticeship, most operators soon learn to judge closely the amount of extractant that must be added to achieve good and consistent results. After the test tube is stoppered it should be shaken vigorously, some 70 strokes for about 15 sec, and the resultant mixture of soil and extractant poured into the tip of the filter.

Obviously there will be some variations in the amount of the extractant and its contained copper which will pass through the filter on to the rubeanic acid paper. The size and intensity of any resulting spot will indicate the amount of copper present in available form in the sample. As a crude approximation it can be assumed that some 5 pct of the solution will pass on to or through the reagent paper. Nevertheless, this 5 pct seems adequate to indicate even modest copper anomalies in soil once the normal background for an area has been established.

Unless the test tube mixture has been made too liquid and the beaker itself is wetted by a sample rich in copper, the beaker is ready to be used again. Otherwise it must be wiped clean with filter paper. Fortunately any salting from this source is improbable, but should it occur, it can readily be recognized by a general darkening of the reagent paper instead of a normal spot.

Standardization: Under average conditions it can be assumed that 5 pct of the liquid from the extractant passes through the reagent paper. If the sample slurry is not dilute enough less liquid will pass, but it will, of course, be more concentrated. If the sample slurry is too dilute, more solution will pass, but it will be less concentrated than normal. For semi-quantitative work, therefore, it is acceptable to compute the amount of extractable copper in the soil, expressed in parts per million, by multiplying by 20 the absolute amount of copper (in micrograms) appearing on the spot, always assuming that a 1-g sample of soil has been taken. It may be remembered that one microgram per gram represents one part per million.

Spots of known copper content can be obtained by passing extractant solutions containing known amounts of copper through reagent paper under as nearly similar conditions of speed and dilution as might be encountered under field conditions. This last point is very important, because only spots of the same color intensity and size are really equivalent. Fig. 1*b* shows a series of standard spots.

In practice it is possible to identify copper anomalies merely by visual inspections of the spot tests after determining empirically the normal background of the area in which the work is being done.

It may be useful to remember that the drainage status of a particular soil sample can influence the metal content of a soil; low swampy or poorly drained ground is likely to accumulate more copper than corresponding ground that is well drained. Likewise good agricultural land is usually richer than uncultivated land in the same area.

Fig. 1*c* shows spot tests that were obtained 20 months before being photographed, together with their corresponding tests recently made. It can be seen that the tests may be kept a considerable period for reference purposes.

In taking soil samples it is prudent to try to take all samples from one horizon. The horizon just below the layer of organic litter, referred to as the A_1, is recommended. This is the horizon that a non-specialist can most easily be trained to recognize and sample without error. Sampling too high or too low usually obtains too much or too little organic material, errors that can often be observed if the soil is later examined in a laboratory.

The visible intensity of the spots speaks for itself, but aside from the warnings already given, when results are interpreted the limitations involved in any soil sampling technique must be kept in mind. In particular it is well to remember: 1) a soil does not necessarily represent the underlying rock; 2) the amount of heavy metal in a soil may depend more on the ease with which the mineralization weathers than on its grade; and 3) a pattern of high values may represent the spreading of a halo rather than the pattern of any underlying mineralization.

Other Uses: It is possible to test any green or rusty weathering stain for copper. All that is necessary is to soak a strip of reagent paper in the extractant and apply the wet test paper to the material to be tested. If any sizable amount of copper is present, the tell-tale blue-black stain will appear on the back of the paper. Indeed, any rusty gossan or iron-rich residual soil can be tested roughly by sprinkling it on the test paper wetted with the extractant solution and then examining the other side of the test paper.

Stream sediments can be examined in the same manner as soils, although new backgrounds must be established, of course, for each set of new circumstances.

This method was first tried out extensively in the field by Grant Sawyer, of Kennco Explorations (Canada) Ltd., under whose auspices this technique was developed. The authors also extend their gratitude to Northwestern Explorations Ltd., Trisides Mining Co. Ltd., Cardiff Mining Co. Ltd., and H. H. Heustis of Bethlehem Cooper Ltd., for permission to collect samples on Bethlehem ground in the Highland Valley area of British Columbia.

The Defence Research Board of Canada (Grant No. DRB 7510/06), The Geological Survey of Canada, Kennco Explorations (Canada) Ltd., and the Brock Chair provided the bulk of the funds for the laboratory aspect of this project.

REFERENCES

[1] H. V. Warren and R. E. Delavault: Soils in Geochemical Prospecting. MINING ENGINEERING, October 1956, vol. 8, pp. 992-996.
[2] R. E. Stevens and H. W. Lakin: The Chromograph, a New Analytical Tool for Laboratory and Field Use. USGS Circ. 63, 1949.
[3] L. E. Reichen: Geochemical Field Test for Determination of Nickel in Plants. *Analytical Chemistry*, 1951, vol. 23, pp. 727-729.

Discussion of this article sent (2 copies) to AIME before Dec. 31, 1958, will be published in MINING ENGINEERING.

ADVANCES IN MAGNETIC SEPARATION OF ORES

Magnetic separation of iron ores is one of the fastest-growing segments of the minerals beneficiation industry. The tonnage of taconite ores processed annually by magnetic separation will, in a few years, reach 100 million.

by L. A. ROE

Magnetic separation occupies an attractive position in the field of ore beneficiation. It is a simple yet effective method, used for some 150 years and steadily growing more important. This type of beneficiation orginated in 1792, when William Fullarton was issued a British patent covering the separation of iron ore by magnetic attraction.

What is magnetism, and why are some materials capable of being magnetized and others not? The study involves many unknowns, and even a partial answer to these questions would be a dissertation in solid state physics and perhaps other fields of science. But the last two decades have revealed basic facts as to why certain materials are magnetic and what happens to them when they are magnetized.

Some of the newer studies in solid state physics have developed a theory that can be applied to studies of magnetism. It is claimed that magnetism stems fundamentally from the spin of electrons in atoms that tend to go in pairs, spinning in opposite directions. The atom as a whole can act as a magnet only when there is an imbalance of electronic spin. Whenever an atom has an odd number of electrons, therefore, this imbalance exists. This neutralizing effect explains why a piece of material that contains atomic magnets is not necessarily magnetic. The physicists tell us that iron is composed of many small magnetized regions called *domains*, which consist individually of millions of atoms. The piece of iron becomes magnetized when an external force lines up these *domains* in the same direction.

L. A. ROE, Member AIME, is Director of Central Engineering, International Minerals & Chemical Corp., Skokie, Ill. TP 4781B. Manuscript, May 28, 1958.

Fundamental data developed by physicists working in fields far removed from minerals beneficiation are now available for developing better magnetic separators for ore processing.

More Data Needed on Magnetic Properties of Minerals: There is less information on magnetic properties of minerals than there is for certain aspects of magnetic separator design. When the data on magnetic properties is available, it is often directed toward the study of powders for tape recorders and other highly scientific endeavors that are of little use to the beneficiation engineer. W. R. Crane's table of tractive forces, published in 1902, is still a guide in the study of magnetic minerals. Bits of other information regarding electrostatic conductivity, dielectric constant values, and permeability of various minerals have also appeared but are of small practical value in magnetic separation of ore.

It is extremely important to obtain pure mineral specimens for making investigations and to record results that may be of use in studies of magnetic processes. Reference to the large volume of data developed by those concerned with analysis and design of permanent magnets soon reveals that these people have extensively evaluated the effect of various *impurities* on magnetic properties. Much of the science of the ferrite industry is based upon spinel-type structures which are varied by substitution of selected elements or even subtraction of elements, leaving vacant sites in the space lattice.

Magnetic separators are used to beneficiate a wide variety of industrial minerals. In this application the relatively large volumes of nonmagnetics are usually the commercial products. The amount of mag-

This page of Mining Transactions AIME follows p. 1188. The intervening non-Transactions pages appeared in MINING ENGINEERING.

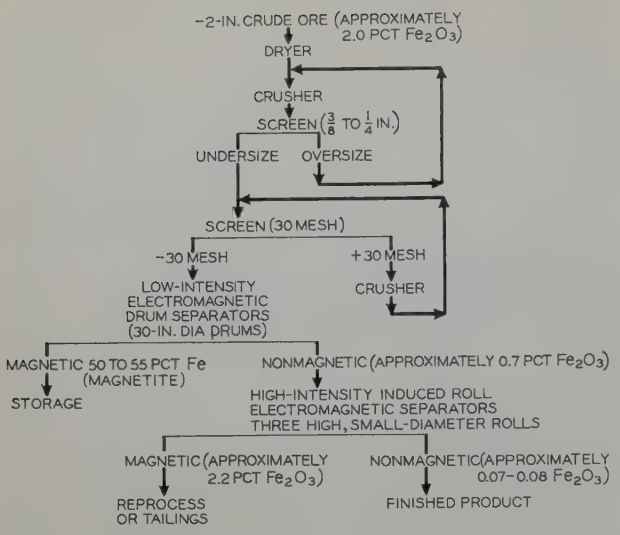

Fig. 1–Dry magnetic processing of nepheline syenite.

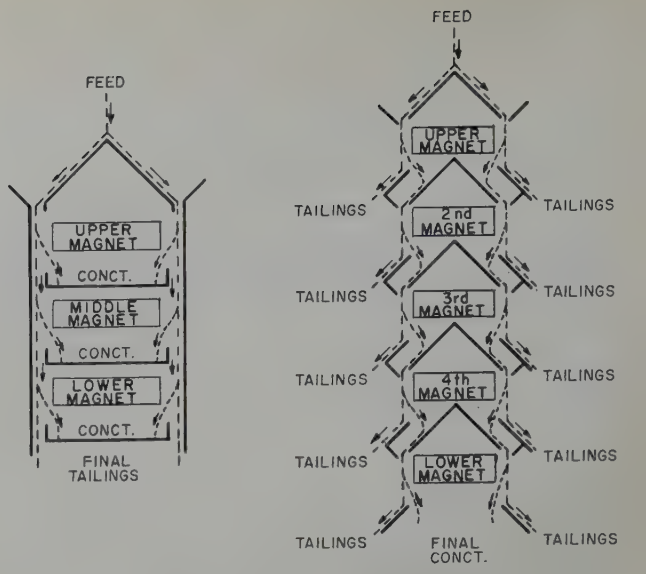

Fig. 2–No. 1 (left) and No. 3 Edison separators, 1890.

netic material removed is quite small, and dry separation is the general rule.

Magnetic separation is also important in processing phosphate, titanium, chrome, manganese, tungsten, molybdenum, nickel, niobium, and tantalum ores.

Pioneer Work on Dry Separation: It is interesting to note that much of the pioneer work in magnetic processing of ores was done on dry material. In spite of the disadvantages of dusty, uncomfortable plants, the dry method has produced acceptable concentrates in most cases.

No definite date can be given for the change in emphasis from dry to wet processing of iron ore, but the wet processing method is treating by far the largest tonnage at the present time. In the past two or three years many advances in the science of magnetic separation of iron ore have been in the field of dry processing, where a major revolution in iron ore beneficiation may be taking place. But now consider an area of magnetic separation where dry methods have never lost their attractiveness.

Table I. Iron Analysis of Crude and Beneficiated Minerals Used in the Ceramic Industry

Mineral	Crude Ore, Fe_2O_3, Pct	Beneficiated Product, Fe_2O_3, Pct
Aplite	0.60 to 1.30	0.30
Glass sand	0.15 to 0.20	0.01 to 0.03
Feldspar	0.15	0.05 to 0.07
Nepheline syenite	1.7 to 2.1	0.07 to 0.08

Table II. Typical Results Obtained with Edison Dry Magnetic Separator

Feed	20 pct Fe (0.7 to 0.8 pct P)
No. 1 machine concentrate	40 pct Fe (tails 0.8 pct Fe)
No. 2 machine concentrate	60.0 pct Fe
No. 3 machine concentrate	68.0 pct Fe
Total concentrate	68.0 pct Fe, 2 to 3 pct SiO_2
Total tail	1.12 pct Fe
Finished Briquettes	
Fe, 67 to 68 pct	Mn, 0.05 to 0.10 pct
SiO_2, 2 to 3 pct	P, 0.028 to 0.33 pct
Al_2O_3, 0.4 to 0.8 pct	Traces of CaO, Mgo, and S

Importance to Industrial Minerals Production: Several industrial minerals used in manufacturing ceramics have long been processed by dry magnetic separation—kyanite, quartz, aplite, feldspar, and nepheline syenite, which is currently processed in considerable quantities in Canada and Russia.

Extensive deposits of nepheline syenite occur in Russia, Scandinavia, India, the U. S., and Canada. The Canadian deposit that is commercially exploited, near Nephton, Ont., is unique in its uniform quality and low percentage of iron-bearing minerals. This orebody, known as Blue Mountain, is more than five miles long and up to a mile wide. Located by Norman Davis in 1912, it has long been known to be one of the world's most extensive deposits of this material. Before the Blue Mountain ore was considered for use in the ceramic industry, it was studied as a possible source of aluminum and also as a source of potash.

Instead of bauxite, according to a recent Russian announcement, the Volkhov Aluminum Works near Leningrad is successfully using nepheline, which comes from the extensive apatite deposits of the Kola Peninsula. Besides aluminum, the Russians are recovering gallium, sodium and potash salts, and constituents of Portland cement.

With the formation of Canadian Nepheline Syenite Ltd. in 1935, the Canadian deposit was seriously investigated as a feldspar substitute for the ceramic industry.* Feldspar that has a relatively high alkali and alumina content has also been preferred by the glassmakers to the less readily available potash feldspar. The search for a substitute that might be even better in some cases than feldspar led to investigation of the nepheline syenite deposits in Canada. The first test sample, weighing 30 tons, was concentrated by high-intensity magnetic separation and distributed to ceramic plants in Canada and the U. S. for test purposes. It soon appeared that nepheline syenite would be a useful substitute for feldspar, and the market has grown steadily until now it is considered one of the major minerals used in the ceramic industry. Among the companies now oper-

* Feldspar has been used in China as a ceramic material since 621 A. D.

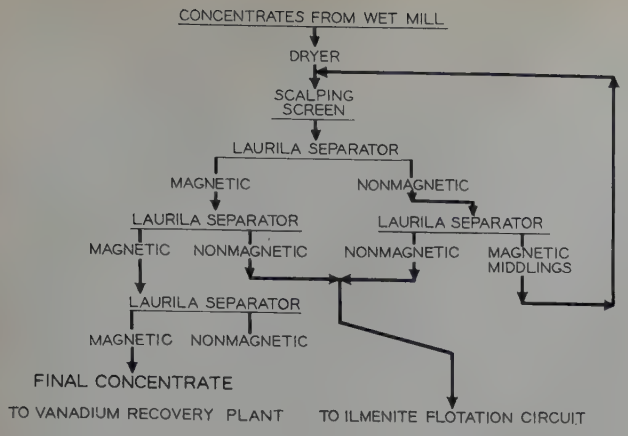

Fig. 3 (above)—Otanmaki dry magnetic separation plant.

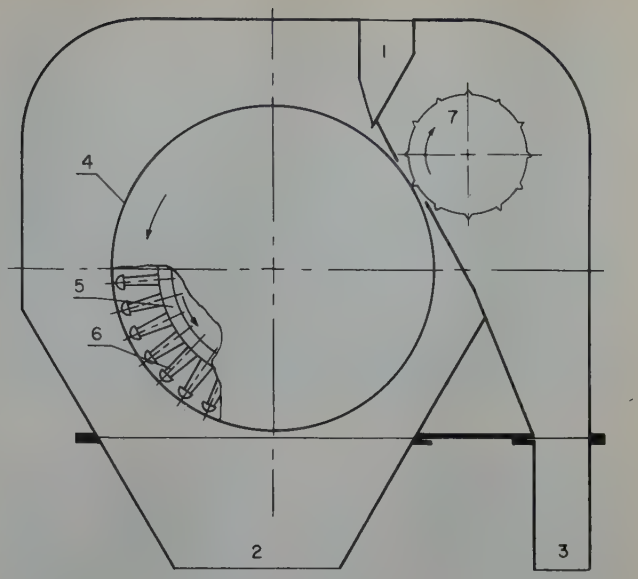

Fig. 4 (right)—Laurila separator: 1) feed introduction, 2) tailing discharge, 3) concentrate discharge, 4) drum, 5) magnet carrying wheel, 6) permanent magnet, 7) induction roller. (Also see Figs. 5A and B, p. 1264.)

ating in Canada are American Nepheline Co., successor to Canadian Nepheline Syenite Ltd., and International Minerals & Chemical Corp. (Canada) Ltd. For purposes of this article the overall flowsheets of these plants will not be discussed, but the magnetic separation features will be described.

Dry Magnetic Separation of Nepheline Syenite: The first equipment used in magnetic separation of nepheline syenite is a low-intensity, large-diameter drum separator to remove highly magnetic minerals —primarily magnetite or mixtures of magnetite and other elements. The magnetics removed by this electromagnetic separator are placed in a storage pile or sold as byproduct magnetite. The magnetite concentrate analyzes 50 to 55 pct Fe. The nonmagnetic product from the first separator is stored in surge bins, from which it is drawn for distribution to high-intensity induced-roll magnetic separators, which remove feebly magnetic minerals.

Generally about 25 pct of the ore fed to a nepheline syenite plant is lost as waste during crushing, drying, grinding, and reduction of iron content, which is usually lowered from 2.0 to 0.08 pct. Table I compares iron analyses of several crude and beneficiated ceramic raw materials that undergo dry magnetic separation.

Dry Magnetic Separation of Iron Ore: There are many inherent advantages in processes that utilize dry magnetic separation to beneficiate iron ore. Wet concentration of magnetite ore, in comparison, requires 500 to 1000 gal of water per ton of concentrate produced. This means extensive use of water resources, as well as disposal systems and sometimes complicated water reclamation systems. Some of the new low grade iron ore discoveries in Canada are in areas where the climate encourages use of dry processing methods.

Production of superconcentrates also favors these methods for iron ores. As Thomas Edison demonstrated more than 50 years ago, it is not difficult to produce large tonnages of concentrates containing 68 pct Fe and only 2 to 3 pct SiO_2 when dry magnetic separation procedures are used. One of Edison's pilot plants consistently produced concentrates of more than 71 pct Fe.

Edison devoted eight years, at a cost of more than $2 million, to inventing a magnetic process and constructing a plant for concentrating low grade iron ore into desirable furnace feed. In the 1890's, recognizing the iron industry's dependence on the somewhat limited ore supplies in the East, Edison developed a method of separating iron minerals from the iron-bearing sand he had observed along the shore of Long Island. After preliminary small-scale tests with these sands, he constructed a large plant near Lake Hopatcong, N. J., to beneficiate a low grade magnetite ore and founded the town of Edison, N. J., to provide homes for the workers. Among the plant's many innovations were new crushers, belt conveyors, dryers, and briquetting machines, as well as inventions in magnetic separation.

Edison's developments in magnetic separation, which have not been widely publicized, were characterized by simple construction. The separators he finally installed in his commercial plant consisted of several electromagnets arranged one above the other, utilizing a free-fall principle to separate gangue from magnetite. The commercial plant in New Jersey used four separators, which he designated Nos. 1 through 4. It is significant, with reference to the data for this plant listed in Table II, that ore containing only 12 to 20 pct Fe was upgraded to concentrate containing 68 pct Fe. Present-day proponents of the smelting advantages of extremely high grade iron ore concentrates will be interested in the outcome of tests made with Edison high grade iron ore concentrate at Catasauqua, Pa. Results of a five-day test were spectacular. On the regular ore charge this furnace produced 100 to 110 tons of pig iron per day. When briquetted concentrates from Edison's plant were used, furnace output rose to more than 138 tpd. Altogether, 477 magnetic separators were installed in the New Jersey plant.

After Edison's New Jersey plant failed, U. S. interest in large-scale magnetic separation of iron ore decreased. Edison's failure was caused primarily by the sudden drop in the iron ore market following discovery of the great Mesabi Range. The New Jersey deposit, moreover, was inadequately prospected and of lower quality than anticipated.

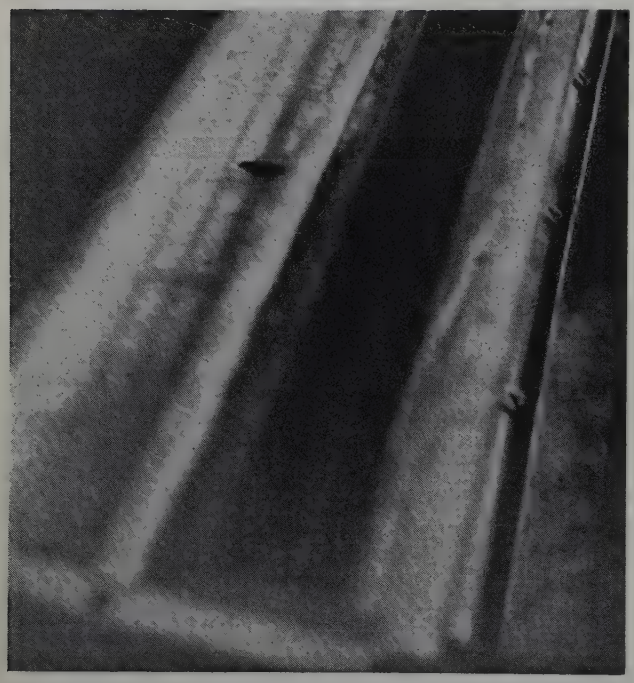

Figs 5A and 5B—Laurila separator in the Otanmaki Co. shop. Lower view is close-up of the drum.

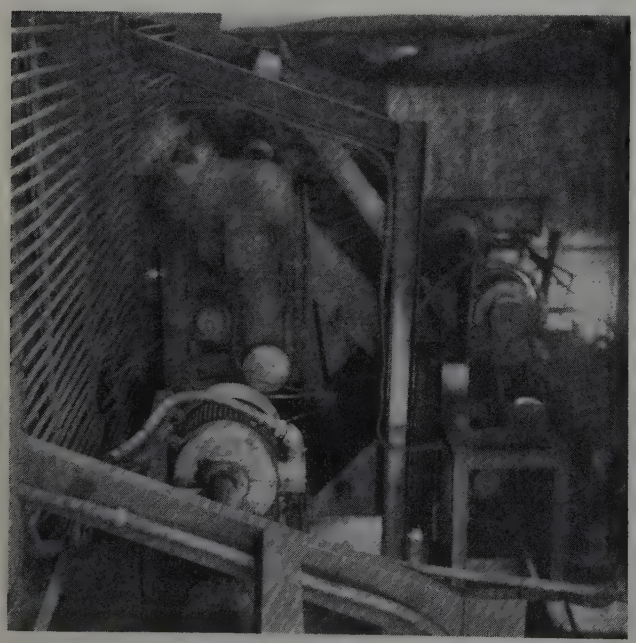

Fig. 6—The Laurila separators in commercial operation.

Now there is renewed interest in dry magnetic separation of iron ores. Some of the more recent studies of dry separation methods have been undertaken in: 1) the Ontario Research Foundation; 2) the Finland Institute of Technology, Helsinki, and the Otanmaki Co; 3) the ore dressing laboratory of the Royal Institute of Technology in Stockholm, Sweden; 4) Carpco Research & Engineering Div., Carpco Mfg. Co., Florida; and 5) various German laboratories and the Salzgitter Co.

Otanmaki Commercial Plant Operations: The Otanmaki Co. in Finland is processing, in considerable tonnages, ilmenite-magnetite-pyrite ore similar to that mined at Tahawus, N. Y. As this article is concerned chiefly with new developments in dry magnetic separation, no description will be given of the wet mill, but it should be mentioned that a highly efficient wet magnetic separation circuit is used to remove a very large percentage of magnetite from the ilmenite. This is important, since any magnetite going to the ilmenite flotation circuit is lost to the ilmenite and downgrades the ilmenite product.

Fig. 3 is a flowsheet of the dry magnetic separation plant at Otanmaki. Wet filtered magnetic concentrate is picked up by a magnetic pulley from a conveyor belt and fed into a drum dryer. The dried concentrate is fed by elevator to the dry magnetic separation section.* Here a scalping screen removes tramp oversize prior to the dry separation step. The dried concentrate is then fed to Laurila separators, where centrifugal force separates the nonmagnetic or weakly magnetic particles from the magnetic. Invented by Erkki Laurila of the Finland Institute of Technology, this drum-type separator incorporates permanent magnets made of Alnico V or similar material. The machine is undergoing further development, both at the Institute and at Otanmaki. It is now manufactured by Maschinen-und Stahlbau, Krupp Rheinhausen, Germany.

* It should be realized that the ilmenite-magnetite operation at Otanmaki involves a separation that could not be made economically by wet magnetic methods.

At Otanmaki the rougher concentrate is cleaned twice by dry separators. The rougher tailing is sent over a cleaner separator operating at lower speed, and the final tailing containing ilmenite is sent back to the ilmenite flotation section.

Operating conditions in the dry separator section are difficult. Separator design includes an oil mist lubrication system to spray the bearings, since the dry magnetite concentrate is at 120° to 140°C. Thermal expansion of the separator shells has also caused trouble.

During the period covered by the Otanmaki commercial plant results listed in Table III, the magnet wheel was stationary and the drum speed was 230 rpm on the rougher and 180 rpm on the scavenger separator. These results show that 11 pct of the

Table III. Otanmaki Plant Results with Dry Magnetic Separation

	Fe, Pct	TiO_2, Pct	Fe_3O_4, Pct	Distribution, Wt, Pct
Feed	65.5	5.7	86.9	100.0
Magnetite concentration	68.6	2.15	95.6	89.0
Middlings	60.5	8.3	75.8	10 to 15
Tailing	36.2	36.9	7.5	11.0

Magnet wheels stationary. Drum speeds 230 rpm, except scavenger separator at 180 rpm.

Table IV. Types of Magnetic Separators Used in Swedish Iron Ore Mills

Mill	Separator, Type	Size, In. Diam x Length	Drum, Rpm	Power, Kw
Balsjo, Sweden	Lowenhielm in (rougher) (2) series		39	
	Lowenhielm in cleaners (3) series		52 52 65 75	2.5
Carl Shaft mill, Striberg, Sweden	Lowenhielm	24x35	40	2.1
Hematite HMS plant	(8) magnetic circuit			
Stripa mill	(19) Lowenhielm	24x35	64	3.7
	Lowenhielm			1.45
	Rougher, two in parallel cleaner			1.45
Haksberg mill	(2) Vulcanus countercurrent cobber	37x34	35	3.7
	(2) MF2, Morgardshammer cobber	28x33	36	—
Persberg	(26) Lowenhielm	24x34	46 to 50	1.25
	(1) Jeffrey rubber covered counter-current drum	35x36		1.5 hp
	(25) Lowenhielm	24x34	44 to 60	1.4 hp
	(3) Thunes (three-drum) (perm magnets)	24x69		
Bodas mill	(9) Lowenhielm 3-mm thick rubber-covered drum	24x34	50	1.9 hp
Kallfallet	(9) Grondal	31x35	45	1.5 hp
Langnas	(20) Lowenhielm	24x34	54 to 62	2
Dannemora	(6) Morgardshammer GW617P (perm magnets) rubber-covered (three in series)	25x68	103	1
Bastkarn	Lowenhielm	24x34	75	2.5 ph
Kantorp	(5) Lowenhielm (2) Allians			
Grangesberg	Allians	30x32		
	Thunes (perm magnets)	24x69		
Blotberget	Thunes (perm magnets)	24x71		2
Tuolluvaara	(15) Drum (perm magnets)	24x67		
Malmberget	(70) Harden	32x32	30 to 32	
	(8) Thunes (perm magnets)	24x67	30 to 32	

Note: Number of separators installed noted in parentheses. Power in kilowatts unless otherwise specified.

original feed is removed as a tailing product. Examination of the middlings has shown that no reasonable amount of regrinding will liberate the minute veinlets of magnetite in this fraction.

Early work on the Otanmaki dry magnetic process indicated that fatty acid materials added during drying operations were beneficial in the dry separation of this ore. Materials such as oleic acid, fuel oil, sulfuric acid, tall oil, and caustic soda were added prior to the drying stage. The fatty acid reagents formed a coating on individual particles which apparently helped disperse the mineral particles. Despite these initial successes, however, the commercial plant has stopped using fatty acids and is obtaining satisfactory results without adding chemicals to the magnetite.

Salzgitter Separator: In Germany the 30-in. dry magnetic separator* manufactured by Erzbergau Salzgitter A. G. is now commercially treating 5 to 6 tph of hematite and goethite ores at about 1 kw-hr per ton of feed. This unit uses a maximum field intensity of 23,000 gausses, which can be compared to a maximum of 14,000 gausses in a laboratory Davis tube separator. The magnetic circuit is energized by two air-cooled d-c coils. The four induced rolls have corrugated surfaces and the spacing between the pole pieces and the rolls is considered critical.

* Designed by A. Goltz of the Salzgitter Co.

The Ontario Research Foundation has developed several new dry magnetic separators designed for ore beneficiation, each for a specific particle size range, though as yet there are no commercial installations. For several years this institution has used dry concentration methods to produce the superconcentrates needed for sponge iron tests. Recent investigations have developed a complete dry magnetic separation flowsheet, which has been used upgrade on ore from 25 pct Fe to more than 63 pct Fe.

Wet Magnetic Separation of Iron Ore in Sweden: In Europe, especially Scandinavia, the drum-type wet magnetic separator is very popular, both the electromagnetic and permanent magnet types. A major difference as compared to U. S. separators is that the drum is near the surface of the pulp. In other words, the pulp level is very low, as it was in the early Grondal separator, used successfully since the turn of the century.

In general, it can be said that foreign plants favor large numbers of lower-capacity machines. At the same time, they often produce a higher grade concentrate, which is in much demand for sponge iron and powdered iron production.

It is highly important to the iron ore industry that more efficient magnetic separators be developed. A speaker at the American Mining Congress in September 1957 stated that the steel industry is shifting emphasis from cost of ore to cost of steel in the ladle. Further, it was claimed that steel costs can be reduced 26¢ per ton for each percentage point reduction in silica content of concentrates such as taconite pellets.

Recent success in new designs of dry magnetic separation machines points up the impending production of higher-quality iron ore. This trend will be accelerated by the growing sponge-iron industry's demand for superconcentrates. And in the industrial minerals field more efficient removal of iron-bearing minerals can be expected as developments encouraged by the iron ore industry are adopted by industrial minerals operations.

Discussion of this article sent (2 copies) to AIME before Jan. 31, 1959, will be published in MINING ENGINEERING.

LUCKY FRIDAY MINE: HISTORY, GEOLOGY, AND DEVELOPMENT

By WILLIAM T. FOLWELL

The Lucky Friday mine east of Mullan, Idaho, is an outstanding example of a property in the Coeur d'Alene district where a small and insignificant-appearing silver-lead-zinc vein at the surface has changed at depth into a large vein of great importance. The Lucky Friday vein has little if any surface expression and above the 1200 level the ore shoots are small and discontinuous. Between the 1200 level and 2450 level, the lowest developed level, the main ore shoot has shown remarkable improvement on each succeeding lower level, and today the mine is one of the major lead-silver producers in the Coeur d'Alene district.

History: The Lucky Friday property is on the north side of the South Fork of the Coeur d'Alene River in sections 25, 26 and 35, T. 48 N., R. 5 E., Hunter mining district, Shoshone County, Idaho. This is about one mile east of the town of Mullan, which serves the eastern portion of the Coeur d'Alene district. The southern part of the property is crossed by a branch line of the Northern Pacific Ry. and by U. S. Highway 10. This highway is the principal road crossing the panhandle of Idaho and connects the district with Spokane, Wash., on the west and Missoula, Mont., on the east. The main portal and surface plant of the Lucky Friday mine is at an elevation of 3365 ft, only a short distance above the valley floor and a few hundred feet from U. S. Highway 10, so the mine is readily accessible for year-round operation.

The property is comprised of six claims, known as the Lucky Friday group, owned outright by the Lucky Friday Silver-Lead Mines Co. There are four patented claims, Good Friday, Lucky Friday, Northern Light, and Lucky Friday Fraction No. 2 (Mineral Survey No. 3028), and two unpatented claims, Hunter and Creek.

In addition, Lucky Friday owns an undivided one-half interest in the Hunter Creek property, which adjoins the Lucky Friday group on the north; a 90 pct interest in the mineral rights in the Jutila Ranch (160A), which adjoins the Lucky Friday group on the east; and a 60 pct interest in the Lucky Friday Extension claim group, which adjoins the Lucky Friday group on the west. The company also has a long-term mining lease on the Hunter Ranch, which adjoins the Lucky Friday group on the west.

The claims of the Lucky Friday group were located between 1899 and 1906. The Lucky Friday Mines Co. was organized in 1906 and did considerable exploration work by surface trenching and shallow underground workings, only to see the property sold by the Shoshone county sheriff to satisfy labor claims totaling $2000 in 1912. Another firm, Lucky Friday Mining Co., bought the claims in 1914 and spent 12 years driving what is now known as the tunnel level crosscut. This tunnel intersected a vein previously exposed in a higher tunnel, but it was only a few inches wide. The vein was followed a short distance westerly but was so unpromising that the work was discontinued in favor of extending the main crosscut tunnel several hundred feet north. No ore was found and all work was discontinued. The property was held in such low esteem by the firm that it let taxes amounting to less than $15 a year go delinquent for nine years.

Then the property lay idle for two more years until in 1938 John Sekulic, a Mullan service station operator, took a lease, with a $15,000 purchase option, on the advice of an old miner who had worked in the mine. Sekulic re-opened the tunnel level crosscut and explored the vein with an easterly drift for about 200 ft. The vein was too narrow to be of commercial value but was believed interesting enough to warrant further exploration at depth. Lacking funds to explore the vein at depth, Sekulic tried to get the district's larger operating companies to take over his lease and option. They were not interested because of the lean tunnel level showing and the fact that the property lay between the White Ledge fault on the north and Osburn fault on the south, an area which geologists always considered unworthy of exploration.

Sekulic then organized the present company and assigned his lease and option to it for stock. This was in 1939. Enough stock was sold locally to finance sinking of a shaft 100 ft from the tunnel level east drift. The vein at this additional depth still was not commercial but showed some improvement. Treasury stock was offered at 5 to 10¢ a share

W. T. FOLWELL, Member AIME, is Mining Engineer and Geologist, Lucky Friday Silver-Lead Mines Co., Wallace, Idaho. TP 4780A. Manuscript, June 3, 1958. AIME Pacific Northwest Regional Meeting, April 1958.

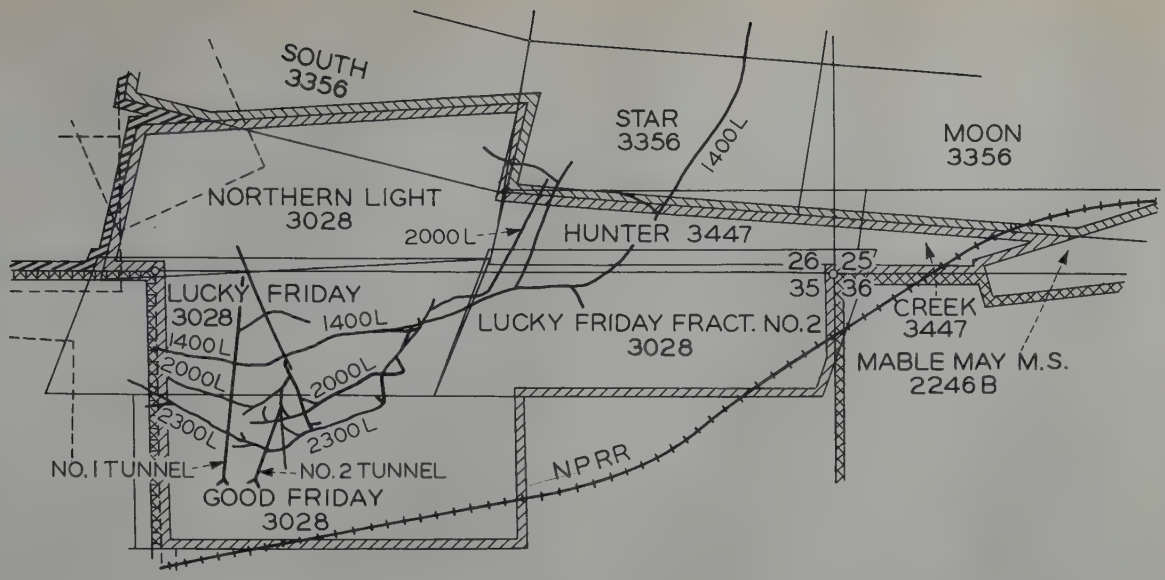

to finance deeper work, but few buyers were found.

Finally, the late Judge Albert H. Featherstone of Wallace, then president and manager of Golconda Lead Mines, and his son, John A. Featherstone, financed deeper development. Part of the cost was raised through a bank loan; directors also loaned the company money. The vein did not yield commercial ore until a depth of 300 ft was reached, and there the vein was narrow and the ore shoot only 25 ft long. Since the start of the present company operations the net smelter returns have been nearly $8 million and the company has paid $1.5 million in dividends.

Development: The mine is developed through two vertical internal shafts, both collared on the tunnel level at an elevation of about 3365 ft. The original shaft was sunk to the 2000 level and was used to explore the vein at 200-ft intervals to that depth. The new three-compartment shaft, 325 ft south of the original one, extends to a depth of 3142 ft and is used as the main hoisting shaft. This new shaft was raised from the 2000 level to the tunnel level and sunk from the 2000 level to the 3050 level. Below the 2000 level the vein is developed by crosscutting and drifting from the new shaft at 150-ft intervals. The crosscut distance from the shaft to the vein on the 2450 level is 200 ft and the distance to the vein on the 3050 level is expected to be about 475 ft. The vein has not been explored below the 2600 and 3050 levels. A large sump and primary pumping station has been installed on the 3050 level, so except for station enlargements and pockets, the major facilities for deeper exploration and development of the mine are completed.

Most of the mining is cut-and-fill. As a whole the ground stands well and very little timbering is required in the drifts until development raises have been driven and the stope sections are prepared for mining. Until recently two-cap, timbered raises with a combined slide and manway and joker compartments on each side have been used in most development work but now three-cap raises with separate slide and manway compartments or a modification of this type are being used on the new development work. The raises are driven approximately 100 ft apart and the intervening blocks of ground are mined cut-and-fill with little timbering. Waste fill, usually obtained from exploration headings, is transferred to the stopes through the raises.

The ore is milled on a custom basis at a 200-tpd flotation plant 5 miles away owned by Golconda Lead Mines.

Geology: The Coeur d'Alene district is principally underlain by metamorphosed sedimentary rocks of the Pre-Cambrian Belt Series. In the district, the Belt series, aggregating more than 20,000 ft in thickness, has been divided into six formations by the U. S. Geological Survey. These are, in ascending order, the Prichard, Burke, Revett, St. Regis, Wallace and Striped Peak formations.

Bedding: Most of the sedimentary rocks are of shallow water origin and have been regionally metamorphosed so that the prevailing rocks of the district are quartzites, argillites, slates, calcareous shales, and rocks of intermediate composition. Because of the common origin and similarity in composition few sharp transitions occur in the sequence and in many places the transition from one formation to another is poorly defined and the contact can only be approximated. In areas of extreme folding and faulting, and especially in structurally complex areas of intense bleaching and alteration the division between formation is even less certain.

Folding: The rocks of the district have been intimately folded into a complex system of anticlines and synclines. In many of the folds the beds are sharply contorted and crumpled, and some of the folds are overturned; thus throughout much of the district the strata are inclined at angles greater than 45° and in many places are vertical. The axes of the major folds of the district have a general east-west trend.

Faulting: In this district faulting is as pronounced and as complex as the folding. The most noteworthy fault is the Osburn, which crosses the district in a west-northwesterly direction and has been traced for many miles east and west of the district. The apparent vertical displacement along the Osburn fault is as much as 10,000 ft and the horizontal displacement is thought to be as much as 12 to 15 miles, with the south block moving west relative to the north block. North of the Osburn fault many of

the major faults trend northwesterly or northerly, while in the southerly part of the district the larger faults have trends more nearly parallel to the Osburn fault. Most of the east-west trending faults, both major and linking structures, are normal with steep southerly dips, but some are reverse faults of considerable displacement.

Ore Occurrence: The principal ore shoots occur within bleached or hydrothermally altered zones as a result of fissure filling and replacement along faults and fracture zones. Although irregular in detail, the large orebodies are lenticular in outline and are noted for their great vertical extent and continuity. The outstanding example of this great vertical range is the Morning Star vein near Mullan which has been stoped continuously from the surface for a vertical depth of more than 6500 ft.

The Lucky Friday mine area is within a block of ground bounded on the south by the Osburn fault and on the north by a parallel westerly-striking structure mapped by the USGS as the White Ledge fault. The rocks within this block are strongly folded but in general strike east and dip steeply towards the south.

Locally, and particularly in the vicinity of the vein, the bedding is highly contorted and warped. The principal rocks in the vicinity of the mine are argillites and quartzites of the St. Regis and Revett formations. Some purplish-gray argillite of the St. Regis formation is exposed in the footwall of the vein on the 1400 level, but for the most part the original colors of the rock have been destroyed by intense alteration and the rocks in the vicinity of the vein throughout most of the mine area are light greenish-gray, light tan to buff, or white.

The Vein: The Lucky Friday vein has been followed horizontally on the 2000 level and lower levels for about 1400 ft and developed through a vertical range of 2700 ft from the surface to the 2450 level. The main portion of the vein has an average strike of N 65° E that is remarkably constant from the tunnel level to the lowest levels of the mine. Below the 1600 level, however, the vein lengthens both easterly and westerly and these extensions deviate from the general strike. The westerly portion strikes about N 65° W and the easterly extension of the vein strikes north to N 30° E. The vein is locally irregular in strike, particularly in the northeasterly part where it is offset by numerous southeasterly-trending cross faults. The horizontal displacement of the vein by these faults is generally less than 5 ft and the greatest displacement is about 100 ft on a fault near the easterly end of the vein on the 1800 level. Little if any displacement on the same fault was noted on the 2300 level, however.

The vein dips southerly, the dips ranging from vertical to as flat as 45°, with an average dip of 78° from the tunnel level to the 2450 level. Below the 1800 level in the easterly section of the mine the vein dips steep to vertical and reverses dip.

The vein is characterized by a single persistent fault fissure that has been variably replaced by galena and quartz with subordinate amounts of tetrahedrite, sphalerite, pyrite, chalcopyrite, and siderite. Small amounts of pyrargyrite (ruby-silver) and jamesonite have been found in the westerly section of the vein and in a small hanging wall vein. The main strand of sulfide, usually high-grade galena, varies in width from less than an inch to more than 8 ft. Irregular stringers and pods of galena and other sulfides usually accompany the main strand in one or sometimes both walls of the vein. In places of intense fracturing and silicification very fine-grained galena and tetrahedrite are disseminated in the wallrock for several feet on either side of the vein. Similar disseminations of galena and tetrahedrite are present as a replacement of certain favorable quartzite beds for distances of tens of feet away from the vein.

In the upper levels of the mine the vein was explored and developed for lengths of 300 ft or less and the ore shoots above the 1200 level were generally less than 100 ft long. (On the 500 level the orebody was 50 ft long.) The shoots were very persistent in vertical range, however, and below the 1400 level the orebody lengthened horizontally with each successively lower level to a total mineable length of 1113 ft on the 2300 level. This includes an ore shoot 168 ft long on the westerly extension of the vein and the 945-ft long orebody on the main vein. As of January 1958, drift development on the 2450 level had opened a continuously mineable section of ore 1195 ft long and the easterly limit of the orebody had not yet been reached. The westerly extension of the vein has not yet been completely developed on the 2450 level, and a new level, the 2600, is being developed.

Development work in the lower levels of the mine has shown considerable improvement in width and grade as well as in the length of the orebody as compared with the shorter ore shoots in the upper part of the mine. The average stoping width in the main portion of the vein below the 2000 level is about 7 ft, while narrow widths of 4 to 6 ft are maintained in parts of the westerly and easterly extensions of the vein. The average tenor of ore for the past three years based on mill head assays was 17.9 oz Au, 8.8 pct Pb, and 1.4 pct Zn.

Ore reserves have been estimated to provide 19.2 years of operation beyond February 1958 based on the average yearly production of 40,000 tons maintained at the present time. This ore reserve is based on the recent development work completed on the 2450 level.

Many favorable geologic factors point to a promising future for the Lucky Friday mine. Most significant, perhaps, in a general way, are the deep-seated characteristics of the Coeur d'Alene district orebodies. The major orebodies of the district range in strike length from 1000 to as much as 4000 ft and are noted for their great vertical extent and continuity. In applying this generalization to the Lucky Friday mine, it is of particular interest to note:

First, the strike length of the ore shoot has lengthened on each succeeding deeper level; on the lowest developed level, the 2450, the ore shoot is more than 1000 ft long and drifting has not as yet reached the limits of this shoot.

Second, the bleached argillaceous and quartzitic rocks of the Revett formation exposed in the bottom levels of the Lucky Friday mine are among the most favorable host rocks for ore in the district. The relationship of the attitude of the bedding and vein is such that favorable host rock can be expected to great depth.

Third, the Lucky Friday ore has an excellent silver-lead ratio and is not exceptionally high in zinc. Work thus far has shown no appreciable mineralogical zoning in the orebody and no increase in the iron-zinc ratio with depth.

Discussion of this article sent (2 copies) to AIME before Jan. 31, 1959, will be published in MINING ENGINEERING.

• *Magnetic separation was first applied commercially to Mesabi Range taconite at Babbitt, Minn.,*[1] *in 1922. The venture was premature, and development lapsed until 1940-1945, when the Erie and Reserve mining companies and the Oliver Iron Mining Div. of U. S. Steel sponsored 1 and 2-tph pilot investigations, directed by E. W. Davis at the Minnesota Mines Experiment Station.*

• *This was followed by Erie's 2000-ton preliminary taconite plant at Aurora, Minn., in 1948; Reserve's 3000-ton pilot plant at Babbitt in 1952;*[2,3] *and Oliver's 6000-ton Pilotac operation at Mountain Iron in 1953. (These capacities are nominal and are expressed in long tons of crude ore per day.) Magnetic separation technology and machine designs were adopted from operations in eastern U. S.*[4] *and Scandinavia.*[5,6]

• *The pilot plant investigations led to construction of two commercial taconite plants. The E. W. Davis Works of Reserve Mining Co., with a nominal capacity of 3.75 million tons of pellets per year, got under way in 1955,*[7] *and Erie's 7.5-million ton plant began operation two years later.*[8]

MAGNETIC SEPARATION FOR MESABI MAGNETITE TACONITE

By J. E. FORCIEA, L. G. HENDRICKSON, and O. E. PALASVIRTA

All pilot and commercial plants working with Mesabi Range taconite employ wet magnetic separation. Progress is being made with a dry magnetic process,[9-11] but this has not yet been applied to taconite except in the laboratory and pilot plants.

Flowsheets in all five plants are similar, including multiple stages of grinding, each followed by magnetic separation, which rejects a finished tailing. The flowsheet in Fig. 1 is used in the preliminary and commercial plants of the Erie and Reserve mining companies and in Unit C of Oliver's Pilotac plant. At Erie the desliming operation is omitted. In the Reserve plants two ball mills are used with each rod mill. Pilotac uses flowsheet 2 in Unit A-B and has also tested flowsheet 3. Principal differences in the three flowsheets are the number of grinding stages and the type of roughing. The terms *open-circuit roughing* and *closed-circuit roughing* are best defined by the diagrams.

Special Test Data Given in Table I: For the Erie and Reserve commercial plants, Table I reflects routine conditions. Pilotac, the experimental plant, has been run with several flowsheets, including those followed at Erie and Reserve's commercial operations. Pilotac data for these last two flowsheets are similar to commercial plant results and are not repeated in Table I; statistics are given, however, for special test conditions, using other flowsheets, when the objective was to produce extra-grade concentrate.

Variations Among Taconites: Although crude ore tributary to these plants is generally classified as taconite, there are important differences in mineralogy and fineness of dissemination.

J. E. FORCIEA, L. G. HENDRICKSON, and O. E. PALASVIRTA, Members AIME, are, respectively, Development Engineer, Oliver Iron Mining Div., U. S. Steel Corp., Pilotac Plant, Mountain Iron, Minn.; Supervisor of Field Development, Pilotac Plant, Mountain Iron, Minn., and Development Engineer, Research Laboratory, Duluth.
TP 4777B. Manuscript, April 30, 1958. N. Y. Meeting, February 1958.

Table I. Magnetic Separation

Flowsheet	Erie Mining Co. Commercial Plant — Two-Stage Grinding, Closed-Circuit Roughing with No Desliming (See Fig. 1)			Reserve Mining Co., E. W. Davis Works — Two-Stage Grinding, Closed-Circuit Roughing with Desliming (See Fig. 1)		
Service designation	Cobbing	Roughing	Finishing	Cobbing	Roughing	Finishing
Grinding machine preceding	Rod mill	Ball mill	Ball mill	Rod mill	Ball mill	Ball mill
Sizing device preceding:						
Type	Screen	Trommel	Cyclones	Trommel	Trommel	Cyclones
Size opening	¼ in.	¼ in.	—	⅝ in.	—	—
Feed:						
Source	Rod mill disch.	Ball mill disch.	Cyclone o'flow	Rod mill disch.	Ball mill disch.	Deslimer u'flow
Size	14 pct +8M; 30 pct −100M	1 pct +14M; 55 pct −100M	1 pct +100M; 75 pct −325M	−¼ in.	—	85 to 90 pct −325M
Solids, pct	55.5	60	22	—	—	—
Ltph/foot magnet width	12.5	18 to 20	2.5	18 to 20	12-14	3 to 3.5
Concentrate solids, pct	72	65	55	—	—	—
Magnetite iron, pct:						
In feed	22.0	49.5(B) (38.0) (C)	51.0	24.5	—	—
In concentrate	38.0	52.0(B) (51.0) (C)	64.0 (Total Fe)	40	— (53) (C)	64.5(Total Fe)
In tails	1.8	0.8(B) (0.8) (C)	1.2	—	—	—
Recovery	96.3	99.9(B) (99.5) (C)	99.5	—	—	—
Machine, general description (D)	Concurrent drums Spigot tails disch.	Countercurrent drum Spigot tails disch.	Semi-cntrcrnt. drums O'flow tails disch.	Concurrent drums Spigot tails disch.	Linney belt	Semi-cntrcrnt. drums O'flow tails disch.
Number of stages	2	1	3	2	1	2
Manufacturer	Memco	Jeffrey-CPS564	Jeffrey-3SPC-464	Jeffrey	Dings	Dings XW6
Magnet:						
Width, in.	48	60	60	48	48	36
Number of poles	5	5	4	6	10	6
Electro or permanent	Electro	Permanent	Permanent	Electro	Electro	Electro
Field strenth, gauss (A)	700	600	400	—	—	—
D-C excitation:						
Volts	230	None	None	—	—	—
Amperes	40 max	None	None	—	—	—
Field strength control	Rheostats	None	None	By voltage control	Rheostat	By voltage control
Drum or belt speed, fpm	189	189	251—1st; 180—2nd and 3rd	—	—	—
Drum:						
Diam, in.	36	36	30	36	Belt	30
Bearing type	Ball bearing	Ball bearing	Ball bearing	Ball bearing	Belt	Ball bearing
Shell cover material	Rubber	Rubber	Rubber	Endless rubber belt	Belt	None
Head material	Cast aluminum	Cast aluminum	Cast aluminum	—	Belt	—
Drive, installed horsepower per stage	3	2	1.5	—	—	—

* Steffensen type. **Notes:** 1) Average of middle of pole and middle of gap readings taken 12 in. from end of pole and 2 in. from drum surface. 2) Figures apply to separator feed, which is a circulating load.

Twofold Achievement of Magnetic Separation: Because of the nature of magnetic separation and the characteristics of Mesabi Range taconite, the process has a dual effect—it is the sole method of concentrating, and it greatly reduces grinding costs.

Table I shows that in cobbing −¼ in., about 40 pct of the feed can be rejected as final tailing, and that in roughing an additional 12 to 15 pct is rejected, thereby reducing the load on the fine grinding stages. Additional smaller benefits accrue from maximum rejection of gangue early in the flowsheet. It has been found that magnetite lost to tailings is more finely disseminated and would require finer grinding to make grade than average material. Also, the more gangue rejected in cobbing and roughing, the higher the grade of final concentrate for a given finisher separator efficiency and fineness of grind. Finally, it is obvious that if upgrading efficiency is improved in the final separation stage, the required concentrate grade can be produced at a coarser grind.

Variables in Rejection Efficiency: The following discussion will emphasize high rejection efficiency of separation, which is more difficult to achieve than high recovery efficiency.

It is generally held that in a drum-type magnetic separator, almost all separation takes place in the zone where magnetics migrate to the magnet face. As the particles of solids come within the field, the magnetics flocculate, and some nonmagnetics become entrained with them. It is believed that as the magnetics are transported along the magnet face there is very little additional rejection. Some further rejection of very fine gangue particles can be achieved by producing as dry a concentrate as possible or by drawing the collected concentrate through clean water.

Significance of Particle Size: When the magnetic separator and operating conditions are being selected, the principal factor is particle size of feed. As particle size decreases, feed rate must decrease and feed be diluted; magnetic field intensity may be lowered. Particle size also dictates the type of tank that can be used. For example, if the feed contains appreciable quantities of +20-mesh, spigot discharge is generally provided for tailings.

Conditions Governing Rate of Feed: For material of given screen analysis and magnetics content, feed rate is limited by two factors—quantity of solids and volume of pulp. One or the other will become limiting, depending on the desired feed pulp density. Table II shows ranges for feed rates at which satisfactory metallurgical results are achieved at Pilotac, as well as data for maximum feed rates that have been investigated. As feed rate of solids is increased while feed pulp density is held constant, concentrate grade decreases, but iron recovery is almost unaffected. As the volumetric feed rate of pulp is increased while feed rate is held constant

Data from Operating Plants

Flowsheet	Oliver Iron Mining Div., U. S. Steel Corp. — Three-Stage Grinding, Open-Circuit Roughing with Desliming (See Fig. 2)				Pilotac Plant — Three-Stage Grinding, Closed-Circuit Roughing with Desliming (See Fig. 3)		
Service designation	Cobbing		Roughing	Finishing	Cobbing	Roughing	Finishing
Grinding machine preceding	Rod mill		Ball mill	Ball mill		Ball mill	
Sizing device preceding:							
Type	Trommel		Cyclones	Cyclones		Trommel	
Size opening	½ in.		—	—		½ in.	
Feed:							
Source	Rod mill disch.		Cyclone o'flow	Deslimer u'flow		Ball mill disch.	
Size	50 pct −20M		50 pct −270M	85 pct −270M		20 pct −270M	
Solids, pct	35		40	25		50	
Ltph/foot magnet width	20		13	2.5		22	
Concentrate solids, pct	70		55	55		55	
Magnetite iron, pct:							
In feed	23		38	61		45 (B) (38) (C)	57
In concentrate	38		58	65.7		48 (B) (49) (C)	65.7
In tails	2.0		0.8	1.5		1.5 (B) (1.5) (C)	1.5
Recovery	96.5		99.3	99.8		99.7 (B) (99.0) (C)	99.5
Machine, general description (D)	Concurrent drums		Semi-cntrcrnt. drums	Semi-cntrcrnt. drums*		Countercurrent drums*	
Number of stages	Spigot tails disch. 2		O'flow tails disch. 3	O'flow tails disch. 3		Spigot tails disch. 1	
Manufacturer	1st Stage Jeffrey-C740	2nd Stage Dings XW3	Memco DA	Memco DA		Jeffrey-CS551	
Magnet:							
Width, in.	36	48	72	72		48	
Number of poles	7	3	4	4		5	
Electro or permanent	Electro	Electro	2 electro, 1 permanent	2 electro, 1 permanent		Electro	
Field strength, gauss (A)	600	550	600 500	600 500		700	
D-C excitation:							
Volts	230	230	230 —	230 —		230	
Amperes	31	11	19 —	19 —		43	
Field strength control	None used	None used	None used	None used		None used	
Drum or belt speed, fpm	200	200	200	200		200	
Drum:							
Diam, in.	36	24	30	30		36	
Bearing type	Sleeve	Ball bearing	Sleeve	Sleeve		Sleeve	
Shell cover material	⅛-in. stainless	⅛-in. stainless	⅛-in. stainless	None		⅛-in. stainless	
Head material	Cast aluminum	Bronze	Bronze	Bronze		Cast aluminum	
Drive, installed horsepower per stage	3	2	5	5		2	

(Same as for three-stage grinding, open-circuit roughing flowsheet, Fig. 2.)

(Same as for three-stage grinding, closed-circuit roughing flowsheet, Fig. 3.)

3) Figures apply to new ball mill feed and show overall performance of the closed-circuit roughing.
4) Where spigot tails discharge is stated, overflow facilities are also provided.

(i.e., by reduction of pulp density) concentrate grade tends to rise, but iron recovery falls somewhat owing to increased losses in fine sizes.

IMPROVING CONTROL

Multiple-Stage Separation: Concentrate grade is improved by multiple stages of separation in series. All Mesabi Range taconite plants employ two stages of cobbing; in the second stage, 7 to 15 pct of the first stage concentrate weight is rejected to tailing. Reserve Mining Co. is installing a third stage of cobber magnetic separators. In the case of the closed-circuit roughing flowsheet, only single-stage separators are used, but since the feed includes the ball mill circulating load, three to four stages of separation are actually performed. Three stages of separation are desirable for open-circuit roughing and for finishing.

Gains and Losses with Pulp Dilution: As the percent solids in feed decreases, grade of concentrate improves, but iron losses tend to increase in the finer sizes. This increase occurs because: 1) higher shearing forces act against the magnetic pull on the particles and 2) in a dilute pulp there is less chance of magnetic flocculation, which is essential to recovery of fine particles. At high pulp density of feed, concentrate grade decreases because nonmagnetic or weakly magnetic particles are mechanically entrained in the matte of magnetic particles that forms at the separator collecting surface. With regard to concentrate grade and recovery, feed pulp densities of 20 to 25 pct would be most desirable, but because of other factors such as water consumption and separator volumetric capacity, higher densities are used in separations on coarse materials. Table II shows feed densities that have been found satisfactory at Pilotac.

Field Strength Tested at Pilotac: As indicated earlier, higher field intensity is required for coarser feed. Field intensities found satisfactory at Pilotac are given in Table II. These values are averages of center of pole and center of gap readings taken at least 12 in. from the end of the magnet and 2 in. away from the shell. For a 5-pole magnet, this would be the average of nine readings.

Field intensities specified apply to unoxidized magnetite taconite. If some of the magnetite has been converted to hematite by oxidation, higher field strengths are required. If as much as 20 pct of the magnetite is oxidized, recovery is noticeably reduced.

Provisions have been made for varying the field intensity of cobbers and roughers in the Reserve plant and cobbers in the Erie plant. The field intensity is decreased at times in order to reject to tailings more of a weakly magnetic middling. This improves concentrate grade, possibly with some small loss in iron recovery. When field intensity is

reduced at Pilotac, the same result is not achieved, possibly because of differences in mineralogy.

Effect of Belt or Drum Speed: Satisfactory results can be achieved with belt or drum speeds varying from 150 to 250 fpm. High speeds produce wetter and therefore dirtier concentrate. Low speeds reduce machine capacity.

SEPARATOR DESIGN

To a great extent feed particle size governs the type of separator tank that can be used, but within these limitations, the following design features are generally applicable.

Overflow discharge of tailings is desirable, as it insures positive drum submergence, but if the feed is coarser than about 20 mesh, there is a tendency for the tank to sand up, and spigot as well as overflow discharge must be provided for tailings.

Pulp must be presented to the magnet so that all magnetics come very close to the magnet poles. It should therefore be in a state of turbulence as it reaches the pick-up zone. This problem, which is most serious in concurrent-type drums, is overcome by installation of rubber vanes or a step on the feed pan at right angles to the flow at the point where pulp enters the magnetic field. With countercurrent and semi-countercurrent tanks like the Steffensen, this problem does not arise, since tailings must pass a considerable magnet arc before discharging. All types should be designed to prevent flow of pulp around the end of the magnet.

Underwater sprays should be avoided. It is difficult to keep them open and to see whether they are functioning.

Tank designs favored at Pilotac are shown in Figs. 4-6. Fig. 4, showing a concurrent separator suitable for cobbing, illustrates a step on the feed pan to produce turbulence at the point of pick-up. Rubber vanes are equally effective. Fig. 6 shows a semi-countercurrent separator suitable for open-circuit roughing or finishing.

The drum diameter must be large enough to contain a magnet that will produce the required field strength. For cobbers and closed-circuit roughers, 36-in. diam drums are used. However, indications are that 30-in. diam may be sufficient for second and third stages of cobbing and also for closed-circuit roughers. Reasonably good results are achieved with 24-in. diam drums as second-stage cobbers at Pilotac. For open-circuit roughers and finishers 30-in. diam drums are satisfactory. Some cost saving can be effected with smaller drums. In Scandinavian practice, 24-in. drums are now used almost exclusively.

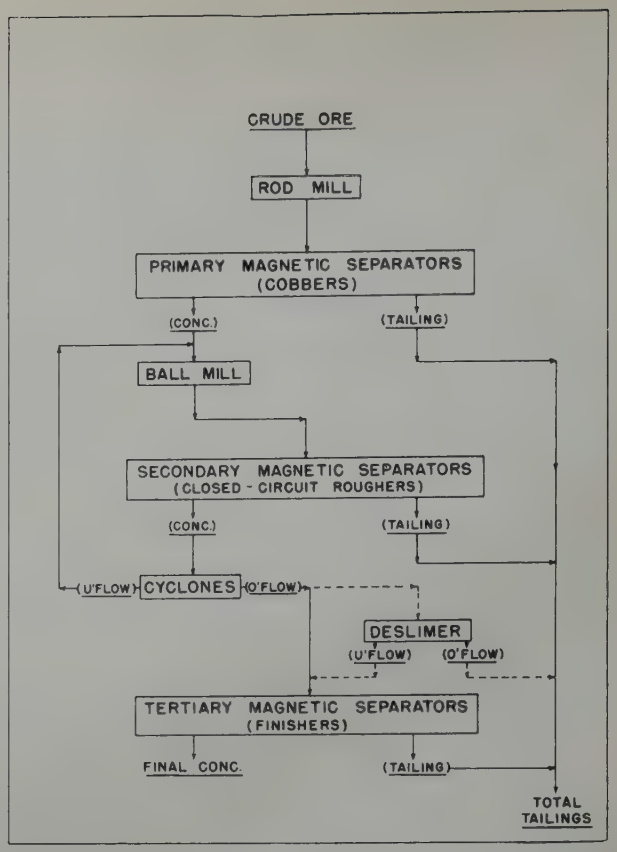

Fig. 1—Two-stage grinding with closed-circuit roughing.

Drums may be at least 6 ft wide (magnet width). Six-foot cobbers of 36-in. diam have been operated at Pilotac for two years, and now that initial bearing trouble has been eliminated performance is satisfactory. A finisher 6 ft x 30 in. has operated a year without trouble. With machines 6 ft wide, results are better when feed is introduced at two points.

The number of poles in the magnet is not important as long as the desired field is developed over the arc required for transportation of magnetics in a tank of the type selected.

Permanent magnets have been proved practical and can be used instead of electromagnets when field strengths of 600 gausses or less are required, but they are not applicable if field intensity must be varied. The principal advantage is that electrical maintenance of magnets is eliminated.

The foregoing remarks apply to metallurgical aspects of separator design. However, because of the vital role of separators, features affecting the operation and maintenance are equally important. Such

Table II. Satisfactory Conditions That Apply at Pilotac Plant

Type of Service	Properties of Feed		Feed Rate Per Foot of Magnet Width				Satisfactory Feed, Solids, Pct	Recommended Tank Design	Satisfactory Field Strength, Gausses
			Pulp, Gpm		Feed, Ltph				
	Size	Mag. Fe, Pct	Maximum	Satisfactory	Maximum	Satisfactory			
Cobbing	50 to 60 pct −20 mesh	22 to 24	150	75 to 125	20	12 to 18	30 to 40	Concurrent, spigot discharge	600 to 700
Roughing (closed circuit)	50 to 60 pct −100 mesh	48 to 52	125	75 to 100	25	12 to 18	50 to 55	Countercurrent or counter rotation—spigot discharge	600 to 700
Roughing (open circuit in three-stage grinding flowsheet)	40 to 50 pct −270 mesh	38 to 42	125	75 to 100	20	8 to 12	35 to 40	Steffensen type, semi-counter —current-overflow	500 to 600
Finishing	80 to 90 pct −270 mesh	50 to 60	100	40 to 60	6	2 to 3	20 to 25	Steffensen type, semi-counter —current-overflow	400 to 500

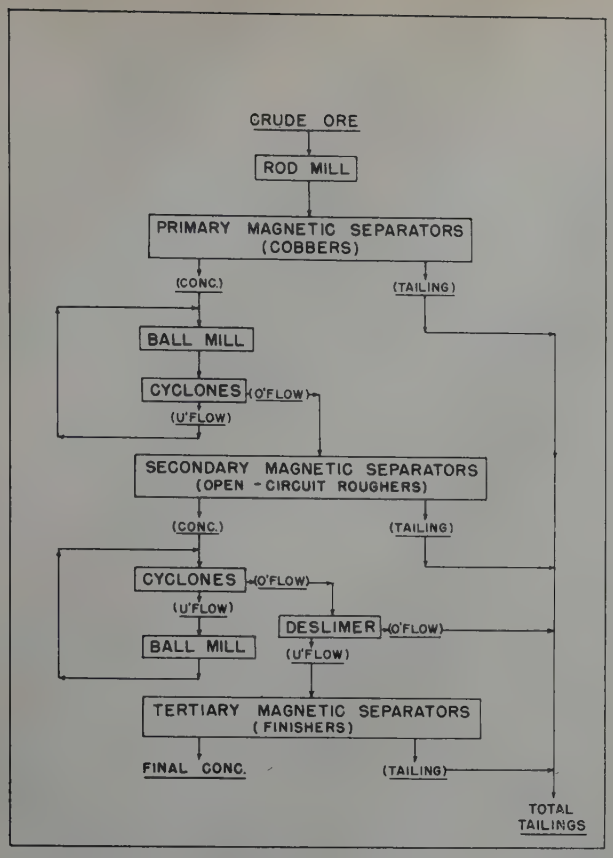

Fig. 2—Three-stage grinding with open-circuit roughing.

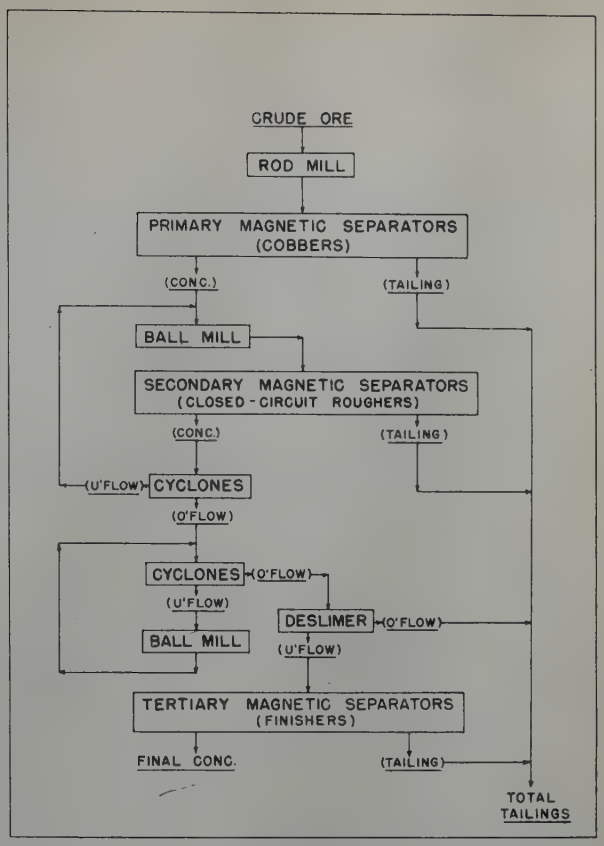

Fig. 3—Three-stage grinding with closed-circuit roughing.

matters could well be the subject of another article and are dealt with very briefly here from the viewpoint of Pilotac experience.

Features Affecting Operation and Maintenance: All wearing parts, such as feed and concentrate pans, should be readily replaceable, and design should provide for positive location of these parts. Drum bearings should be carefully designed, especially with regard to sealing against dirt, and replacement should be possible without removal of drum heads. Sleeve-type bearings with replaceable sleeves on drum and shaft are favored over roller or ball bearings because there is less danger of damaging head and shaft if failure occurs. There is practically no difference in power required to drive sleeve-type and ball-bearing drums.

Stainless steel of the 18-8 type, which is nonmagnetic and corrosion-resistant, is desirable for shell and tank construction throughout, including feed boxes.

Cobber and rougher drum shells at Pilotac are protected with ⅛-in. stainless steel butt-welded covers. Rubber is also satisfactory for roughers and is generally used for finishers.

Drives and bearings should be thoroughly protected against spill and splash.

For drum head construction, bronze is better than aluminum because it corrodes less easily; it is preferred, too, for cobbers and roughers because it resists abrasion.

Desliming, a Phase of Separation: Desliming in this instance may be considered a type of magnetic separation carried out in a hydroseparator. Cyclone overflow is passed through magnetizing coils to flocculate the magnetite, which then settles very rapidly in the hydroseparator, while nonmagnetic gangue may be rejected as overflow.

It is important to maintain the deslimer underflow at maximum density to eliminate as much of the slime-containing liquid as possible. If the

Table III. Davis Tube Test Procedures

Name of Test	Davis Tube −200 Mesh Test	Davis Tube *As Is* Test	Cobber Davis Tube *As Is* Test	Davis Tube −20 +65 Mesh Test
Abbreviation	D.T. −200M	D.T. *As Is*	Cobber D.T. *As Is*	D.T. −20 +65M
Origin of sample	Any material	Any material	Cobber concentrate	Crude ore crushed through ¼ in.
Preparation of sample	Pulverize all through 200 mesh screen.	No preparation. Use *As Received* or *As Is*.	Discard +4 and mesh fraction and run test on −4 mesh. Otherwise *As Is*.	Screen out −20 +65 mesh fraction and use this fraction for test.
Sample size	Use sample size that will insure magnetics in tube are not over 10 g. Usually 50 g for tails and 10 g for conc.	Same as for D.T. −200M test.	60 g run in four 15-g batches.	50 g
Testing time, min	2 to 4 min or until tube is clear.	Same as for D.T. −200M test.	2 min	Same as for D.T. −200M test.
Magnet current, amps, d-c	1.7	1.7	1.2	1.7
Tube speed, strokes per min	90	90	100 to 110	90
Water rate, gpm	0.4	0.4	0.6	0.4

Table IV. Use of the Davis Tube *As Is* Test in Analyzing Finisher Performance

Line		Pct
1	Total iron in Davis tube *as is* concentrate made of finisher feed	66.9
2	Total iron in finisher concentrate	66.4
3	Total iron in Davis tube *as is* concentrate made of finisher concentrate	67.2
1-2	Overall difference between the performance of the Davis tube and the plant finisher	0.5
3-2	Amount of free gangue and/or slime (rejectable) left in finisher concentrate	0.8
3-1	Amount of upgrading achieved by finisher through rejection of low-grade middling particles	0.3

Table V. General Specification of Conditions Assumed for Prediction Calculations

Magnetic Separation	Fineness of Grind Preceding	Stages of Separation	Type of Machines
Cobbing	50 pct −20 mesh in cobber conc.	2	Concurrent
Roughing (open circuit)	45 pct −270 mesh in rougher feed	3	Semi-countercurrent, Steffensen type
Finishing	To be determined	3	Semi-countercurrent, Steffensen type

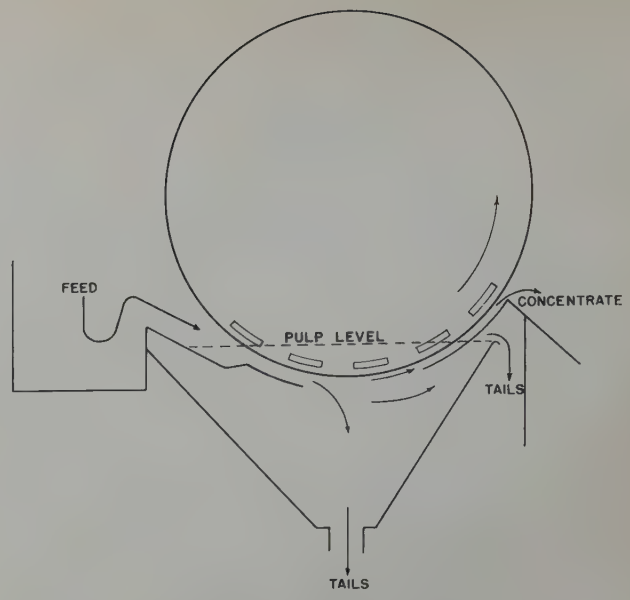

Fig. 4—Tank design in use at Pilotac plant. Concurrent spigot discharge, drum magnetic separator. (Cobber).

underflow is not demagnetized, magnetization of deslimer feed must be carefully controlled. When magnetization is too strong it impairs finisher performance, probably because the magnetic flocs will not release entrained gangue.

Pilotac experimenters found it impractical to control the magnetizing force to suit the needs of both the deslimer and the finishers. The problem was solved by demagnetizing the deslimer underflow, so that feed magnetization could be freed from requirements of the finishers. Demagnetization also greatly improved fluidity of the underflow, which discharged by gravity.

The chief benefit of desliming is thorough rejection of fine gangue. If succeeding finishers are inefficient or overloaded the iron content of finisher concentrate may be increased 1 to 3 pct, but efficient finishers lessen the effect. Rejection of some middling particles can also be achieved by high overflow rates, but some fine magnetite is then lost.

As normally operated at Pilotac, the deslimer underflow is 5 to 8 pct higher in magnetite iron than deslimer feed. The overflow assays about the same in magnetite iron as finisher tails.

SEPARATOR PERFORMANCE

The Davis magnetic tube tester is used extensively to evaluate and predict magnetic separator performance. The procedures for four types of tests, as used at Pilotac, are described in Table III. The essential difference between these tests lies in the origin of samples and the preparation prior to treatment in the Davis tube.

The following quantitative data are obtained:

1) "The percent weight recovery of Davis tube concentrate," a measure of the amount of magnetic material retained in the tube.

2) "The percent weight rejectable," found by subtracting the percent concentrate weight recovery from 100 pct.

3) The percent total iron in the Davis tube concentrate.

Use of the Davis tube is based on the assumption of perfect magnetic separation, that is, retention of all particles containing magnetite and rejection of all particles free of magnetite. The first of these assumptions is not strictly true, but in practice the error has little significance.

Since Mesabi Range taconites commonly contain iron silicates and carbonates, and sometimes hematite, the assay for total iron is not equivalent to that for magnetite iron. It is therefore desirable to determine magnetite iron recoveries by a method that reports magnetite iron only. Pilotac feed, for example, assays 30 pct total Fe, but only 23 pct magnetite; recovery calculations based on total iron would be misleading as to efficiency of magnetic separation.

All taconite plants on the Mesabi Range determine magnetite by the same method. A sample ground to pass 200 mesh is treated in the Davis tube and the concentrate assayed for total iron. The magnetite content is obtained by multiplying the total iron assay by the Davis tube concentrate weight recovery. This method contains certain sources of error, but since the same method is applied to feed, concentrate, and tailing, their effects tend to cancel out in calculations of magnetic iron recovery.

An error of a different type results if the magnetite grains are partially oxidized. In this instance, as the Davis tube has a higher field strength than commercial separators, it will retain as concentrate partially oxidized grains that will be lost in commercial separators. In such cases the magnetite iron content must be determined by chemical means.

Davis tube *as is* tests are used to indicate the ultimate separation possible with a particular size

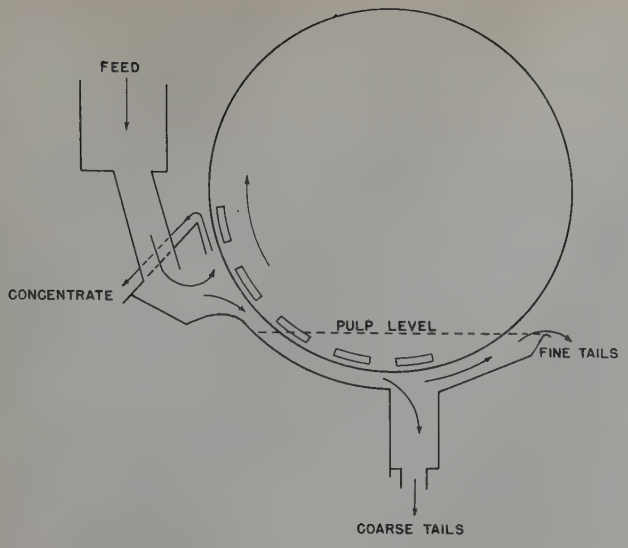

Fig. 5—Design of Pilotac's countercurrent spigot discharge, magnetic separator. (Closed-circuit rougher).

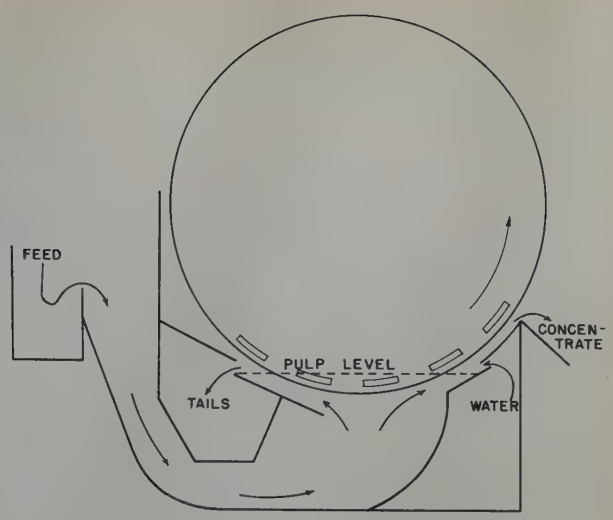

Fig. 6—Semi-countercurrent, full-overflow drum magnetic separator. Suitable for open-circuit roughing or finishing.

consist. Tests of this type also provide a standard of efficiency for commercial separation and reveal the nature of inefficiencies in commercial separators.

The cobber Davis tube *as is* test is usually applied on cobber concentrate to show how much rejectionable material is left in the concentrate by separator inefficiency. Fig. 7, based on data from these tests, indicates that the coarser the cobber feed, the easier it is to produce clean concentrate. This effect could not be illustrated by comparison of concentrate grades only, because better mineral liberation at finer sizes would offset the effect of poorer magnetic separation.

In analyzing rougher performance, the Davis tube *as is* method determines the number of stages needed for effective cobbing.

Finisher performance is judged by essentially the same method. Since it is reasonable to assume that the Davis tube retains practically all magnetite and middling particles, but rejects all slime and liberated gangue, the following conclusions can be drawn:

1) If a given finisher concentrate can be upgraded by treatment, *as is*, in the Davis tube, the difference in total iron assay between finisher concentrate and Davis tube *as is* concentrate can be considered a measure of the amount of fully liberated gangue and/or slime that was retained in the finished concentrate.

2) If the assay of Davis tube *as is* concentrate made from finisher concentrate is higher than the assay of a Davis tube *as is* concentrate made from the finisher feed, the difference is a measure of the amount of upgrading that the finisher achieved by rejecting, presumably, low grade middling particles.

Since these differences are small (see Table IV) conclusions can be drawn only after several tests, but reference to Fig. 8 shows that 1 pct increase in iron assay can save 3 to 4 pct —270 mesh in fineness of grind.

Rejection of low grade middling by cobbers and roughers makes possible a final concentrate of a required grade with less grinding than predicted on the basis of a Davis tube test on a ground crude ore

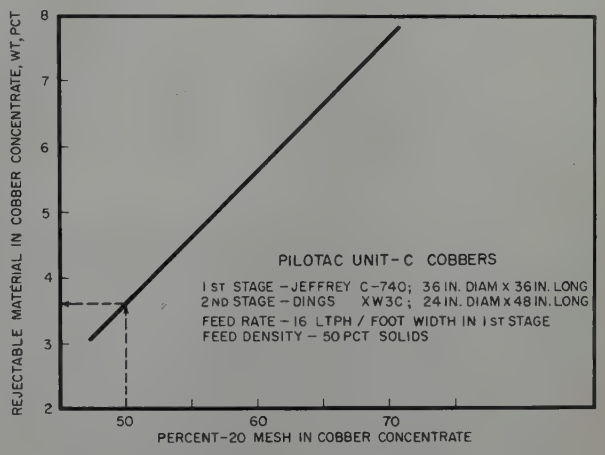
REJECTABLE MATERIAL IN COBBER CONCENTRATE, WT. PCT
8
7
6
5
4
3
2
PILOTAC UNIT-C COBBERS
1 ST STAGE – JEFFREY C-740; 36 IN. DIAM X 36 IN. LONG
2 ND STAGE – DINGS XW3C; 24 IN. DIAM X 48 IN. LONG
FEED RATE – 16 LTPH / FOOT WIDTH IN 1 ST STAGE
FEED DENSITY – 50 PCT SOLIDS
50
60
70
PERCENT-20 MESH IN COBBER CONCENTRATE

Fig. 7—Plotted test results show that the coarser the cobber feed, the easier it is to produce clean concentrate.

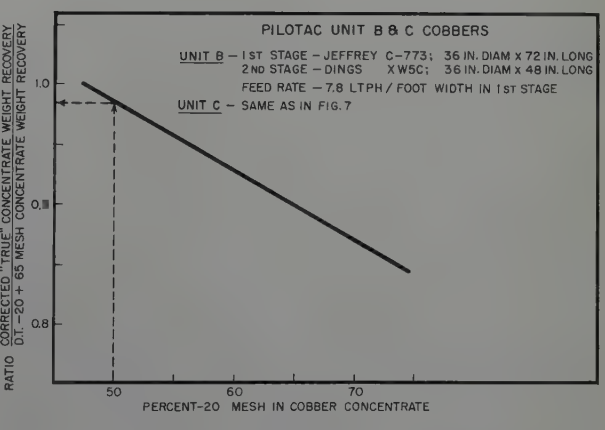
RATIO CORRECTED "TRUE" CONCENTRATE WEIGHT RECOVERY / D.T. -20 + 65 MESH CONCENTRATE WEIGHT RECOVERY
1.0
0.9
0.8
PILOTAC UNIT B & C COBBERS
UNIT B – 1 ST STAGE – JEFFREY C-773; 36 IN. DIAM X 72 IN. LONG
2 ND STAGE – DINGS XW5C; 36 IN. DIAM X 48 IN. LONG
FEED RATE – 7.8 LTPH / FOOT WIDTH IN 1 ST STAGE
UNIT C – SAME AS IN FIG. 7
50
60
70
PERCENT-20 MESH IN COBBER CONCENTRATE

Fig. 7A—Liberation characteristics for predicting cobber performance are determined from a Davis tube test on the —20 +65 mesh fraction of the crude. Graph shows the relationship that has been established, for Pilotac ore, between these results and the actual plant performance.

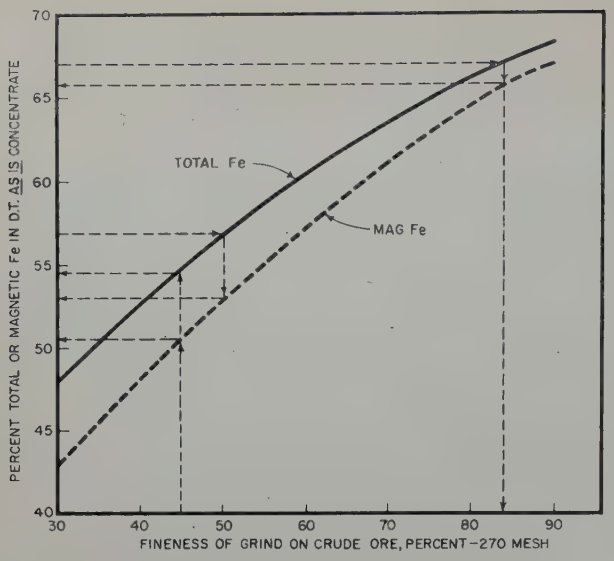

Fig. 8—Liberation characteristics of Pilotac ore sample.

sample. This effect approximately offsets the difference in separation efficiency between the Davis tube and a plant finisher, working on the same feed. For prediction purposes, therefore, the fineness of finisher feed required to produce a certain grade of finisher concentrate may be taken as the grind on crude ore required to produce the grade in the Davis tube.

A somewhat generalized example will illustrate the Pilotac method for predicting performance of a given plant on a given material. The example is based on the following conditions:

1) Flowsheet as in Fig. 2.
2) General conditions as given in Table V.
3) Final concentrate grade required: 67 pct Fe.
4) The assumption (on basis of plant experience) that the magnetite iron recoveries will be 96.5, 99.5, and 99.7 pct in cobbers, roughers, and finishers, respectively.

Liberation characteristics for predicting cobber performance are determined from a Davis tube test on the −20 +65 mesh fraction of the crude. With Pilotac ore, a relationship has been established between these results and actual plant performance. Actual plant weight recovery is corrected by dividing by the magnetite iron recovery and multiplying by the percent weight recovery in the Davis tube *as is* test to give a so-called *corrected true concentrate* weight recovery. The ratio of this to the Davis tube −20 +65 mesh concentrate weight recovery is plotted against the percent −20 mesh in cobber concentrate as shown in Fig. 7A.

If the Davis tube −20 +65 mesh concentrate weight recovery is 60 pct and the cobber concentrate 50 pct −20 mesh, using Fig. 7A, the *corrected true concentrate* weight recovery becomes $0.985 \times 60 = 59.1$ pct. From Fig. 7, the percent rejectable expected in cobber concentrate is found to be 3.6 pct (or 96.4 pct cobber Davis tube *as is* weight recovery). Therefore expected weight recovery becomes

$$59.1 \times \frac{96.5}{96.4} = 59.2 \text{ pct}$$

Assuming that the crude ore assays 23 pct Mag. Fe and the percent magnetite iron recovery is 96.5 pct, then cobber concentrate (rougher feed) will assay

$$\frac{0.965 \times 23}{59.2} = 37.5 \text{ pct Mag. Fe}$$

Liberation data for predicting rougher and finisher performance are developed by controlled grinding tests on crude ore and Davis tube *as is* tests on the ground crude ore. For each product, the total iron and the magnetite iron contents are determined and then liberation curves are drawn, as shown in Fig. 8. According to these curves, the total and magnetite iron assays, corresponding to a grind of 45 pct −270 mesh, are 54.5 pct and 50.5 pct respectively. A correction is again made, allowing for the fact that the plant roughers are capable of rejecting some low grade middling material. Using a corrected figure of 53 pct Mag. Fe for the rougher concentrate, a figure of $0.995 \times \frac{37.5}{53.0} = 70.4$ pct for weight recovery (on basis of rougher feed) is obtained.

From Fig. 8, it is observed that a Davis tube concentrate assaying 67 pct iron can be produced by grinding the crude ore to 84 pct −270 mesh. This, then, is the required grind. Using the magnetite iron assay of 65.7 pct, finisher weight recovery becomes $\frac{0.997 \times 53.0}{65.7} = 80.4$ pct of finisher feed. Overall magnetite iron recovery is $\frac{99.7}{100} \times \frac{99.5}{100} \times 96.5 = 95.7$ pct. Overall weight recovery is $\frac{80.4}{100} \times \frac{70.4}{100} \times 59.2 = 33.5$ pct.

The authors are indebted to F. D. DeVaney of Pickands Mather & Co. for data on the Erie Mining Co. commercial plant. Preparation of this paper was facilitated by the cooperation of all companies engaged in taconite beneficiation. Finally, appreciation is expressed to R. J. Morton and R. L. Bennett of Oliver Iron Mining Div., U. S. Steel Corp., under whose direction the work was done.

REFERENCES

[1] A. B. Parsons: Operations of the Mesabi Iron Company, *Engineering and Mining Journal*, February 1924, p. 202.
[2] Oscar Lee: Taconite Beneficiation Comes of Age at Reserve's Babbitt Plant, MINING ENGINEERING, May 1954, p. 484.
[3] E. F. Furness and T. Maki: Types of Commercial Wet Magnetic Separators and Their Application to Minerals Dressing. Presented at Annual Meeting of AIME, February 1955.
[4] R. S. Dean and C. W. Davis: Magnetic Separation of Ores. *Bull. 425*, U.S. Dept. of Interior, 1941.
[5] J. K. Johanssen: Iron Ore Concentration at Sydvaranger, Norway. *Journal of the Iron and Steel Institute*, May 1949, p. 4.
[6] The Sydvaranger Story. *Mining World*, October 1953, p. 49.
[7] Reserve's New Taconite Project. *Engineering and Mining Journal*, December 1956, p. 75.
[8] R. H. Ramsey: Teamwork on Taconite. *Engineering and Mining Journal*, March 1955, p. 71.
[9] E. Laurila: A Theory of Dry Magnetic Separation of Fine Grained Strongly Magnetic Materials. *Suomalaisen Tiedeakatemian Tuomituksia*, Helsinki, 1954.
[10] P. E. Cavanagh and E. W. Williams: Dry Magnetic Concentration, *Canadian Mining and Metallurgical Bulletin*, September 1957, p. 558.
[11] Urmas Runolinna: Dry Magnetic Separation of Finely Ground Magnetite. Paper presented at International Mineral Dressing Congress, Stockholm, Sweden, September 1957.

Discussion of this article sent (2 copies) to AIME before Jan. 31, 1959, will be published in MINING ENGINEERING.

TRANSACTIONS

January-December 1958, Vol. 211

Society of Mining Engineers of AIME

A

Advances in Magnetic Separation of Ores ....Dec 1261
aluminum, Hall process ....Apr 496
American Metal Climax Corp., in Peru Jan 104
American Smelting & Refining Co., geology of Toquepala, Peru ....Feb 262
Discussion ....June 669
Anderson, S. M.: *U. S. Government Support to Mineral Industries of Latin America* ....Nov 1176
Application of Electrostatics to Concentration of Coarse Pebble Phosphate ....Oct 1084
Application of Electrostatics to Feldspar Beneficiation ....Oct 1087
Application of Electrostatics to Potash Beneficiation ....Oct 1081

B

Barker, R. A., and Ward, S. H.: *Case History of the Juniper Prospect* Jan 100
Beneficiation (see also comminution, hydrometallurgy, flotation, magnetic separation):
comminution, heating ....Apr 490
feldspar, electrostatics ....Oct 1087
Florida pebble phosphate electrostatics ....Oct 1084
geiger counter in processing potassium-bearings ores ....Oct 1094
instrumentation, Ideal Cement Co. Feb 266
magnetic separation of iron ores ..Dec 1261
magnetic separation of Mesabi taconite Dec 1269
potash, electrostatics ....Oct 1081
Rotobelt filter ....Feb 253
sink-float separation ....July 788
spodumene flotation ....Nov 1182
Bond, F. C.: *Grinding Ball Size Selection* ....May 592
Bonini, W. E., and Hickok, E. A.: *Seismic-Refraction Method in Ground-Water Exploration* Apr 485
Brisse, A. H., and McMorris, W. L., Jr.: *Convertol Process* ....Feb 258
Brown, A.: *Ground Stress Investigations in Canadian Coal Mines* ....Aug 879
Brown, J. H., et al.: *Intergranular Comminution by Heating* ....Apr 490
Bump Symposium—Progress in Control Aug 877
Butler, B. S.: *Mineralizing Solutions That Carry and Deposit Iron and Sulfur.* Discussion ....May 595

C

Campbell, W. F.: *Deep Coal Mining in Springhill No. 2 Mine* ....Sep 987
Canada, kyanite flotation ....Jan 111
Cananea Consolidated Copper Co., contact metasomatic deposits ....Mar 365
Case History of the Juniper Prospect Jan 100
Cause and Occurrence of Coal Mine Bumps ....Sep 994
Charles, R. J.: *Energy-Size Reduction Relationships in Comminution.* Discussion ....Apr 481
Citron, E. H.: *Cleaning Fine Coal with Newly Developed Jig* ....Apr 488
Cleaning Fine Coal with Newly Developed Jig ....Apr 488
Coal:
bump symposium, part I ....Aug 877
bump symposium, part II ....Sep 982
Coal preparation:
Convertol process ....Feb 258
jig for cleaning ....Apr 488
Rotobelt filter ....Feb 253
Coal Mine Bumps Can Be Eliminated Sep 993
Comminution: (See also Beneficiation)
grinding at supercritical speeds ....May 581
Discussion ....May 589, Aug 892
grinding ball size selection ....May 592
intergranular by heating ....Apr 490
Control of Mountain Bumps in the Pocahontas No. 4 Seam ....Aug 888
Convertol Process ....Feb 258
Copper:
contact metasomatic deposits ....Mar 365
Cuajone porphyry copper deposit Jan 104
rubeanic acid field test ....Nov 1186
Cornell, C. F., et al.: *Filtration and Control of Moisture Content on Taconite Concentrates.* Discussion ....May 596
Cornell, C. F., et al.: *The Rotobelt Filter* ....Feb 253
Courtright, J. H., and Richard, K.: *Geology of Toquepala, Peru* ....Feb 262
Discussion ....June 699

D

Dahlstrom, D. A., et al.: *Filtration and Control of Moisture Content on Taconite Concentrates.* Discussion ....May 596
Dahlstrom, D. A., et al.: *The Rotobelt Filter* ....Feb 253
Deep Coal Mining in Springhill No. 2 Mine ....Sep 987
Delavault, R. E., and Warren, H. V.: *Rubeanic Acid Field Test for Copper in Soils and Sediments* Nov 1186
dewatering, Rotobelt filter ....Feb 253
Distribution Curves for Sink-and-Float Separation of Iron Ores ....July 788
Douglas, T. B.: *Instrumentation in Ideal's New Houston Cement Plant* ....Feb 266
Douglas, D. D.: *Precision Survey for Tunnel Control* ....Sep 977
Dunyon, A. F., et al.: *Filtration and Control of Moisture Content on Taconite Concentrates.* Discussion ....May 596

E

economics, U. S. Government support to Latin American mineral industries ....Nov 1176
Eimco Corp., Rotobelt filter ....Feb 253
education, Latin America under U. S. foreign aid program ....Nov 1176
Effect of Chemical Reagents on the Motion of Single Air Bubbles in Water ....June 694
Emmett, R. C., et al.: *The Rotobelt Filter* ....Feb 253
Energy-Size Reduction Relationships in Comminution. Discussion ....Apr 481
Equipment:
cleaning fine coal ....Apr 448
Rotobelt filter ....Feb 253
Exploration:
ground-water ....Apr 485
Lucky Friday mine, Idaho ....Dec 1266
soil testing ....July 781
structure frameworks ....Nov 1169
Toquepala, Peru ....Feb 262
Discussion ....June 699

F

feldspar, electrostatics for beneficiation Oct 1087
Filtration and Control of Moisture Content on Taconite Concentrates. Discussion ....May 596
Fine Grinding at Supercritical Speed May 581
Discussion ....May 589, Aug 892
Foote Mineral Co., spodumene flotation Nov 1182
Flotation:
air bubbles in water affected by chemical reagents ....June 694
iron oxide slime coatings ....July 792
kyanite ....Jan 111
measuring aeration in flotation cells July 796
nonmetallics with sodium silicates June 691
spodumene, plant scale-up from test results ....Nov 1182
Flotation of a Canadian Kyanite ....Jan 111
Folwell, W. T.: *Lucky Friday Mine: History, Geology, and Development* ....Dec 1266
Forciea, J. E., et al.: *Magnetic Separation for Mesabi Magnetite Taconite* ....Dec 1269
Fuerstenau, D. W., et al.: *Iron Oxide Slime Coatings in Flotation* July 792
Fuerstenau, D. W., and Wayman, C. H.: *Effect of Chemical Reagents on the Motion of Single Air Bubbles in Water* ....June 694

G

Gaudin, A. M., et al.: *Intergranular Comminution by Heating* ....Apr 490
Iron Oxide Slime Coatings in Flotation ....July 792
Gayle, J. B.: *Improved Method for Measuring Aeration in Flotation Cells* ....July 796
Geiger Counter as a Control in Processing Potassium-Bearing Ores Oct 1094
Genesis of Titaniferous Magnetites and Associated Rocks of the Lake Sanford District, New York. Discussion ....Jan 379
Geochemistry:
distribution trends in soil ....July 781
rubeanic acid field test for copper in soils ....Nov 1186
Geology:
Cuajone porphyry copper deposit Jan 104
ground-water exploration ....Apr 485
lineament tectonics and ore districts of Southwest ....Nov 1169
Lucky Friday mine, Idaho ....Dec 1266
mineralized cretaceous horizons in northeastern Mexico ....Jan 108
Peruvian Cordillera ....Mar 365
Toquepala, Peru ....Feb 262
Discussion ....June 699
Geology of Toquepala, Peru ....Feb 262
Discussion ....June 699
Geophysics:
Juniper Prospect, New Brunswick Jan 100
seismic-refraction method, ground-water exploration ....Apr 485
Gillson, J. L.: *Genesis of Titaniferous Magnetites and Associated Rocks of the Lake Sanford District, New York.* Discussion Jan 379

gold, Homestake Mining Co. ....June 685
Goodman, J. E., and Lewis, F. M.: *Grinding Practice at Tennessee Copper Co.'s Isabella Mill.* Correction ....Jan 107
Graphical Representation of Theoretical Soluble Losses by CCD ....July 786
Greenwalt, R. B., and Sollenberger, C. L.: *Relative Effectiveness of Sodium Silicates of Different Silica-Soda Ratios as Gangue Depressants in Nonmetallic Flotation* ....June 691
Grinding Ball Size Selection ....May 592
Grinding Practice at Tennessee Copper Co.'s Isabella Mill. Correction Jan 107
Ground Stress Investigations in Canadian Coal Mines ....Aug 879

H

Henderson, A. F., et al.: *Filtration and Control of Moisture Content on Taconite Concentrates.* Discussion ....May 596
Hendrickson, L. G., et al.: *Magnetic Separation for Mesabi Magnetite Taconite* ....Dec 1269
Hickok, E. A., and Bonini, W. E.: *Seismic-Refraction Method in Ground-Water Exploration* Apr 485
Holland, C. T.: *Cause and Occurrence of Coal Mine Bumps* ....Sep 994
Homestake Mining Co., underground mining ....June 685
Horst, W. E.: *Scale-Up Relationships in Spodumene Flotation* ....Nov 1182
Hukki, R. T.: *Fine Grinding at Supercritical Speed* ....May 581
Discussion ....May 589, Aug 892
Hydrometallurgy:
aluminum, Hall process ....Apr 496
continuous countercurrent decantation July 786

I

Ideal Cement Co., instrumentation ..Feb 266
Improved Method for Measuring Aeration in Flotation Cells ....July 796
Industrial minerals:
beneficiation by electrostatics ....Oct 1087
beneficiation of Florida pebble phosphates ....Oct 1084
flotation of ....June 691
geiger counter in processing potassium-bearing ores ....Oct 1094
instrumentation, Ideal Cement Co. Feb 266
potash beneficiation at Carlsbad, N. M. ....Oct 1081
pyrophyllite ....Jan 97
spodumene flotation plant scale-up from test results ....Nov 1182
Instrumentation in Ideal's New Houston Cement Plant ....Feb 266
Intergranular Comminution by Heating Apr 490
International Minerals & Chemical Corp.:
feldspar beneficiation ....Oct 1087
concentration, coarse pebble phosphate ....Oct 1084
potash beneficiation ....Oct 1081
processing potassium-bearing ores, geiger counter as control tool Oct 1094
Interpretation of the Literature on the Mechanism of the Hall Process. Abstract ....Apr 496
Iron ore:
magnetic separators ....Dec 1261
Mesabi taconite, beneficiation ....Dec 1269
sink-float separation ....July 788
Iron Oxide Slime Coatings in Flotation July 792

J

Jackling, Daniel C., Lecture 1958, A. H. Shoemaker ....June 685

K

Knopf, W. C., and LeBaron, I. M.: *Application of Electrostatics to Potash Beneficiation* ....Oct 1081
Knopf, W. C., and Samsel, G.: *The Geiger Counter as a Control in Processing Potassium-Bearing Ores* ....Oct 1094
kyanite, flotation of ....Jan 111

L

Lacy, W. C.: *Porphyry Copper Deposit, Cuajone, Peru* ....Jan 104
lead (see also lead-zinc), Lucky Friday mine, Idaho ....Dec 1266
lead-zinc (see also lead), mineralized Cretaceous horizons in northeastern Mexico ....Jan 108
LeBaron, I. M., and Knopf, W. C.: *Application of Electrostatics to Potash Beneficiation* ....Oct 1081
LeBaron, I. M., and Northcott, E.: *Application of Electrostatics to Feldspar Beneficiation* ....Oct 1087
Lewis, F. M., and Goodman, J. E.: *Grinding Practice at Tennessee Copper Co.'s Isabella Mill.* Correction ....Jan 107
Lineament Tectonics and Some Ore Districts of the Southwest Nov 1169
Loeb, C. M., Jr.: *Intergranular Comminution by Heating* ....Apr 490
Lucky Friday Mine: History, Geology, and Development ....Dec 1266

M

magnetic separation, mineral composition and magnetic susceptibility Mar 373
marketing, pyrophyllite ....Jan 99
Magnetic Separation for Mesabi Magnetite Taconite ....Dec 1269
Mauck, H. E.: *Coal Mine Bumps Can Be Eliminated* ....Sep 993
Mayo, E. B.: *Lineament Tectonics and Some Ore Districts of the Southwest* ....Nov 1169
McMorris, W. L., Jr., and Brisse, A. H.: *Convertol Process* ....Feb 258
Mexico, mineralized Cretaceous horizons in northeastern ....Jan 108
Miaw, H. L., et al.: *Iron Oxide Slime Coatings in Flotation* ....July 792
Mineralized Cretaceous Horizons in Northeastern Mexico ....Jan 108
Mineralizing Solutions That Carry and Deposit Iron and Sulfur. Discussion ....May 595
mineralogy, magnetic susceptibility of minerals ....Mar 373
Mining methods:
control of bumps in Pocahontas No. 4 seam ....Aug 888
stoping at Homestake ....June 685
tunnel control ....Sep 977
Mitchell, D. R., and Spokes, E. M.: *Relation of Magnetic Susceptibility to Mineral Composition* ....Mar 373
Mitchell, D. R., and Spokes, E. M.: *Relation of Magnetic Susceptibility to Mineral Composition.* Discussion ....Apr 489
Mountain Bumps at the Sunnyside Mines ....Sep 982

N

New Brunswick, Canada, electromagnetic survey, Juniper Prospect Jan 100
New Jersey Zinc Co., The, Ivanhoe mine ....Sep 997
Northcott, E., and LeBaron, I. M.: *Application of Electrostatics to Feldspar Beneficiation* ....Oct 1087
Northcott, E., and Oberg, F. N.: *Application of Electrostatics to Concentration of Coarse Pebble Phosphate* ....Oct 1084

O

Oberg, F. N., and Northcott, E.: *Application of Electrostatics to Concentration of Coarse Pebble Phosphate* ....Oct 1084

P

Palasvirta, O. E., et al.: *Magnetic Separation for Mesabi Magnetite Taconite* ....Dec 1269
Peperakis, J.: *Mountain Bumps at the Sunnyside Mines* ....Sep 982
Peru:
contact metasomatic deposits ....Mar 365
Cuajone porphyry copper deposit Jan 104
geology at Toquepala ....Feb 262
Discussion ....June 699
Petrologic Methods for Application to Solid Fuels of the Future. Discussion ....May 591
Planning Deep Mining at Homestake (1958 Jackling Lecture) ....June 685
Porphyry Copper Deposit, Cuajone, Peru ....Jan 104
Potash:
electrostatics for beneficiation ....Oct 1081
electrostatics for concentration, coarse pebble phosphate ....Oct 1084
potassium-bearing ores, processing, geiger counter as control tool Oct 1094
Precision Survey for Tunnel Control Sep 977
pyrophyllite, in North Carolina ....Jan 97

R

Relation of Magnetic Susceptibility to Mineral Composition ....Mar 373
Relation of Magnetic Susceptibility to Mineral Composition. Discussion ....Apr 489
Relative Effectiveness of Sodium Silicates of Different Silica-Soda Ratios as Gangue Depressants in Nonmetallic Flotation ....June 691
Research:
control of bumps in Pocahontas No. 4 seam ....Aug 888
ground stress, coal mines ....Aug 879
Resources and Utilization of North Carolina Pyrophyllite ....Jan 97
Richard, K., and Courtright, J. H.: *Geology of Toquepala, Peru* ....Feb 262
Discussion ....June 699
Roe, L. A.: *Advances in Magnetic Separation of Ores* ....Dec 1261
Rotobelt Filter, The ....Feb 253
Rubeanic Acid Field Test for Copper in Soils and Sediments ....Nov 1186

S

Samsel, G., and Knopf, W. C.: *The Geiger Counter as a Control in Processing Potassium-Bearing Ores* ....Oct 1094
Sanchez-Mejorada, P.: *Mineralized Cretaceous Horizons in Northeastern Mexico* ....Jan 108
Scale-Up Relationships in Spodumene Flotation ....Nov 1182
Schopf, J. M.: *Petrologic Methods for Application to Solid Fuels of the Future.* Discussion ....May 591
Schroder, J. L., Jr., and Talman, W. G.: *Control of Mountain Bumps in the Pocahontas No. 4 Seam* Aug 888
Seismic-Refraction Method in Ground-Water Exploration ....Apr 485
Shafts, shaft sinking:
development at Homestake ....June 685
plumbing ....Sep 977
Shoemaker, A. H.: *Planning for Deep Mining at Homestake* (1958 Jackling Lecture) ....June 685
Significance of Geochemical Distribution Trends in Soil ....July 781
silver, Lucky Friday Mine, Idaho ....Dec 1266
Sollenberger, C. L., and Greenwalt, R. B.: *Relative Effectiveness of Sodium Silicates of Different Silica-Soda Ratios as Gangue Depressants in Nonmetallic Flotation* ....June 691
spodumene, flotation ....Nov 1182
Spokes, E. M., and Mitchell, D. R.: *Relation of Magnetic Susceptibility to Mineral Composition.* Discussion ....Apr 489
Stokes, J. J., Jr.: *Interpretation of the Literature on the Mechanism of Hall Process.* Abstract ....Apr 496
Structural Control of Contact Metasomatic Deposits in the Peruvian Cordillera ....Mar 365
Stuckey, J. L.: *Resources and Utilization of North Carolina Pyrophyllite* ....Jan 97
Study of Thorium and Uranium Minerals by X-Ray Microscopy ....June 689

T

Talman, W. G., and Schroder, J. L., Jr.: *Control of Mountain Bumps in the Pocahontas No. 4 Seam* Aug 888
Terrones, L., A. J.: *Structural Control of Contact Metasomatic Deposits in the Peruvian Cordillera* Mar 365
thorium, X-ray microscopy ....June 689

U

Underground mining:
bump control ....Sep 993
cause, occurrence of coal mine bumps Sep 994
control of bumps in Pocahontas No. 4 seam ....Aug 888
Lucky Friday mine, Idaho ....Dec 1266
Springhill No. 2 mine ....Sep 987
stress investigations in Canadian coal mines ....Aug 879
Sunnyside mines ....Sep 982
uranium, X-ray microscopy ....June 689
U. S. Bureau of Mines Investigations and Research on Bumps ....Aug 878
U. S. Government Support to Mineral Industries of Latin America Nov 1176

W

Ward, S. H., and Barker, R. A.: *Case History of the Juniper Prospect* Jan 100
Warren, H. V., and Delavault, R. E.: *Rubeanic Acid Field Test for Copper in Soils and Sediments* Nov 1186
Wayman, C. H., and Fuerstenau, D. W.: *Effect of Chemical Reagents on the Motion of Single Air Bubbles in Water* ....June 694
Woody, R. J.: *Graphical Representation of Theoretical Soluble Losses by CCD* ....July 786
Wuerker, R. G.: *Distribution Curves for Sink-and-Float Separation of Iron Ores* ....July 788
Wyman, R. A.: *Flotation of a Canadian Kyanite* ....Jan 111

Y

Yamaguchi, S.: *Study of Thorium and Uranium Minerals by X-Ray Microscopy* ....June 689
Yardley, D. H.: *Significance of Geochemical Distribution Trends in Soil* ....July 871